SPECTROCHIMICA ACTA

Founder Editor

A. GATTERER S.J. +

Editors

U.S.A.

V. A. FASSEL *Ames, Iowa*

F. A. MILLER *Pittsburgh*

UNITED KINGDOM

H. W. THOMPSON *Oxford*

EDITORIAL ADVISORY BOARD

B. Bak, *Copenhagen*
N. S. Bayliss, *Perth, W. Aust.*
L. J. Bellamy, *Waltham Abbey*
Wallace R. Brode, *Washington, D.C.*
C. G. Cannon, *Pontypool*
C. G. Carlsson, *Stockholm*
B. L. Crawford, *Minneapolis*
G. Duyckaerts, *Liège*
C. Feldman, *Oak Ridge*
H. Friedman, *Washington*
W. Gordy, *Durham, N.C.*
D. Hadži, *Ljubljana*
D. F. Hornig *Princeton, N.J.*
R. N. Jones, *Ottawa*
H. Kaiser, *Dortmund*
M. Kasha, *Tallahassee*
J. A. A. Ketelaar, *Amsterdam*
J. Lecomte, *Paris*
E. Loeuille, *Paris*
R. C. Lord, *Cambridge, Mass.*
S. L. Mandelstam, *Moscow*
A. Mangini, *Bologna*
J. R. McNally, *Oak Ridge*
R. Mecke, *Freiburg*
A. C. Menzies, *London*
S. Mizushima, *Tokyo*
R. L. Mitchell, *Aberdeen*
G. Porter, *Sheffield*
W. C. Price, *London*
R. E. Richards, *Oxford*
H. Schüler, *Hechingen-Hohenzollern*
B. F. Scribner, *Washington, D.C.*
N. Sheppard, *Cambridge*
H. Shull, *Bloomington, Indiana*
D. M. Smith, *Wembley*
E. H. S. van Someren, *Broxbourne*
H. Stammreich, *São Paulo*
B. Vodar, *Bellevue, S. et O.*
A. Walsh, *Melbourne*
H. L. Welsh, *Toronto*
M. Kent Wilson, *Medford, Mass.*
N. Wright, *Midland (Mich.)*

VOLUME XIII

1959

PERGAMON PRESS

NEW YORK · LONDON · PARIS · LOS ANGELES

VOL. 13 958/59

Spectrochim. Acta

SPECTROCHIMICA ACTA

CONTENTS OF VOLUME XIII

Nos. 1/2

F. F. Bentley, E. F. Wolfarth, N. E. Srp and W. R. Powell: Analytical applications of far infrared spectra—I 1

S.-I. Mizushima, I. Nakagawa, M. J. Schmelz, C. Curran and J. V. Quagliano: Infra-red absorption spectra of inorganic co-ordination complexes—XVII . . . 31

D. C. McKean: Force constants, interbond angle and solid state spectrum of disiloxane 38

H. Bevan, S. V. Dawes and R. A. Ford: The electronic spectra of titanium dioxide . 43

O. Botschkowa, S. Frisch and E. Schreider: Quantitative spektralanalyse von gasgemischen 50

L. J. Bellamy: The origin of group frequency shifts—I 60

D. B. Powell and N. Sheppard: Infrared spectra and vibrational frequencies of co-ordinated ethylene 69

F. Meda: Infrared absorption spectra of α-halogenated keto-steroids 75

M. Tsuboi, T. Shimanouchi and S-I. Mizushima: Analysis of P- and R-branches of the 950 cm^{-1} band of $^{14}NH^3$ 80

A. L. Bluhm: The infrared spectra and the structure of some homophthalimides . . 93

T. P. Schreiber and D. L. Fry: Spectral character as a function of spark source parameters 99

P. Tarté: Recherches sur les fréquences de déformation OH—I 107

B. Bak, D. Christensen, L. Hansen-Nygaard and J. Rastrup-Andersen: The structure of vinyl fluoride 120

A. D. E. Pullin: The variation of infrared vibration frequencies with solvent . . 125

M. N. Oganov and A. R. Striganov: Quantitative analysis, by a spectrographic method, of the isotopic composition of hydrogen, deuterium and tritium mixtures . . . 139

Research Notes

J. Romand, G. Balloffet and B. Vodar: Application of the vacuum sliding spark to the spectrochemical analysis in the far ultraviolet 150

K. Nagaraja Rao and A. B. Biswas: An infrared absorption study of *n*-alkyl malonic acids and their diethyl esters 151

Report of Meeting

9th Annual Conference of the American Association of Spectrographers . . . 154

Book Review

"Absorption Spectrophotometry", Second Edition, by G. F. Lothian (reviewed by W. C. Price) 159

Papers to be published in future issues 160

No. 3

A. Miyake, I. Nakagawa, T. Miyazawa, T. Shimanouchi and S-I. Mizushima: Infra-red and Raman spectra of dichloroacetyl chloride in relation to rotational isomerism . 161

D. A. Sinclair and R. N. Whittem: Apparent rectification in Tesla sparks . . 168

A. Danti and R. C. Lord: Rotational analysis and upper-stage transitions of parallel absorption bands in benzene, *sym*-benzene-d_3, benzene-d_6 and pyridine . . . 180

VOL.
13
1958/5

H. Stammreich, D. Bassi, O. Sala and H. Siebert: The vibrational spectrum of the dichromate ion 192

D. M. Shaw, O. Wickremasinghe and C. Yip: A simple device for the spectrochemical analysis of minerals in an inert atmosphere using the Stallwood jet 197

E. A. V. Ebsworth, J. R. Hall, M. J. Mackillop, D. C. McKean, N. Sheppard and L. A. Woodward: Vibrational spectra and structure of trisilylamine and trisilylamine-d_9 202

G. L. Caldow and H. W. Thompson: Vibrational bands of *iso*thiocyanates, thiocyanates and *iso*cyanates 212

J. P. Jesson and H. W. Thompson: Vibrational band intensities of the C≡N group in aliphatic nitriles 217

P. E. B. Butler, D. R. Eaton and H. W. Thompson: Vibration–rotation bands of keten 223

H. W. Thompson and D. A. Jameson: Vibrational frequency and band intensity of the carbonyl group 236

C. Gual, R. I. Dorfman and H. Rosenkrantz: The infrared absorption spectra of ring-*D* steroid lactones—I. Intense hydrogen bonding in estrololactone 248

Research Notes

C. G. Cannon and B. C. Stace: νOH of trifluoroethanol and the Kirkwood–Bauer relation 253

H. W. Thompson and D. J. Jewell: Effect of solvent upon vibration bands . . 254

L. W. Daasch: Infra-red group frequencies vs. electronegativity 257

Report of Meeting 260

Erratum 260

OL.
13
3/59

No. 4

E. A. V. Ebsworth and N. Sheppard: The infrared spectra of some methylammonium iodides: angle deformation frequencies of $\overset{+}{N}H$ and $\overset{+}{N}H_2$ groups 261

K. Laqua and U. Lucto: Ein thyratrongesteuertes Schaltgerät für Wechselstromabreissbögen 271

R. G. Snyder and J. C. Decius: The infrared spectra of $N_2H_6Cl_2$ and $N_2H_6F_2$ . . 280

H. Rosenkrantz and C. Gual: The infrared absorption spectra of ring-*D* steroid lactones—II. Structure absorption correlations 291

E. Lieber, C. N. R. Rao and J. Ramachandran: The infrared spectra of organic thiocyanates and *iso*thiocyanates 296

R. N. Kniseley, V. A. Fassel, R. W. Tabeling, B. G. Hurd and B. B. Quinney: Quantitative spectrographic analysis of the rare earth elements—X. Determination of rare earth impurities commonly associated with purified thulium, ytterbium, lutetium and scandium 300

L. H. Ahrens and R. A. Edge: Observations on the use of LaO bands for d.c. arc spectrochemical analysis 304

D. A. Dows: Torsional vibrations in CO_2 and N_2O crystals 308

Z. Hainski et P. Herman: Essais d'enregistrements à énergie d'émission contrôlée . 311

Research Note:

J. A. A. Ketelaar, C. J. H. Schutte and B. L. Schram: Infrared absorption spectrum of the nitrite ion in alkali halide solid solutions 336

Book Reviews:

R. G. Parr: Molecular Electronic Bibliography (L. Kasha and M. Kasha) . . 338

J. K. Hurwitz: Proceedings of the Colloquium Spectroscopicum Internationale VI. (Edited by W. van Tongeren and F. Freese) 339

R. L. Mitchell: Chemische Spektralanalyse (W. Seith und K. Ruthardt, Fünfte Auflage von Walter Rollwagen) 339

Papers to be published in future issues 340

VOL.
13
1958/5

SUBJECT INDEX TO VOLUME XIII

Absorption spectrum of titanium oxide 43
Alkyl malonic acids and esters, infra-red spectra 151
Ammonia, band at 950 cm^{-1} 80

Benzene and deuterobenzenes, rotational analysis of infra-red bands 180

Book Reviews:
'Absorption Spectrophotometry' by G. F. Lothian 159
'Chemische Spektralanalyse' by W. Seith and K. Ruthardt 339
'Molecular Electronic Bibliography, Vol. I, by L. & M. Kasha 338

Carbonyl group:
vibrational frequency and intensity 236
solvent effects on 254
Co-ordination complexes, of platinum and palladium, with:
ammonia 31
ethylene 69
Copper salts (basic), infra-red spectra 107

Dichloroacetyl chloride 161
Disiloxane, vibrational spectrum of 38

Emission spectrographic analysis:
controlled emission, recording of 311
gaseous mixtures 50
hydrogen, deuterium and tritium mixtures 139
lanthanum 304
rare earths 300
spectral character and spark-source parameters 99
Stallwood jet method 197
thyratron-regulated a.c. arc 271
vacuum sliding spark for far ultra-violet 150

Far infra-red spectra, a review 1
Force constants in:
bonds involving silicon or carbon 211
dichromate ion 192
siloxane 38

Group frequency shifts:
correlation with electronegativities 257
multiple bonds 60

Halogenated keto-steroids, infra-red spectra 75
Hydrazine dihydrohalides, infra-red spectra 280
Hydrogen bonding in:
basic copper salts 107
estrololactone 248
Hydroxyl group, vibration frequency of 107

Hydroxyl group:
vibration frequency of 107
in different solvents 253
Homophthalimides, infra-red spectra 93

Instrumentation:
controlled emission, recording of 311
far infra-red 1
high-frequency discharge in gases 50
Tesla sparks 168
thyratron-regulated a.c. arc 271
vacuum sliding spark 150
Infra-red spectra beyond 15 μ 1
Infra-red spectra of:
alkyl malonic acids and esters 151
basic copper salts 107
benzene, deuterobenzenes and pyridine 180
carbon dioxide and nitrous oxide crystals 308
dichromate ion 192
dichloroacetyl chloride 161
disiloxane 38
α-halogenated keto-steroids 75
homophthalimides 93
hydrazine dihydrochloride and dihydrofluoride 280
keten 223
methylammonium iodides 261
nitrite ion in alkali halide solid solutions 336
platinum and palladium, ammine complexes 31
platinum and palladium, ethylene complexes 69
steroid lactones 248, 291
thiocyanates, isothiocyanates and isocyanates 212, 296
trisilylamine and deutero derivatives 202
vinyl fluoride 120
Intensities of vibration bands, nitriles 217

Keten, vibration–rotation bands 223

Lanthanum, emission spectrographic analysis 304

Meeting, report of:
American Association of Spectrographers, Chicago, 1958 154
Methylammonium iodides, infra-red spectra 261

Nitriles, vibrational band intensities 217
Nitrite ion, infra-red spectra of 336

Palladium ammines, infra-red spectra of 31
Palladium ethylene complexes, infra-red spectra of 69
Platinum ammines, infra-red spectra of 31
Platinum ethylene complexes, infra-red spectra of 69
Pyridine, rotational analysis of infra-red bands 180

Raman spectra of:
dichloroacetyl chloride 161
dichromate ion 192

VOL.
13
1958/5

Rare earths, emission spectrographic analysis 300
Rotational isomerism, in dichloroacetyl chloride 161

Solvent, effect on:
carbonyl group frequency 254
hydroxyl group frequency in trifluoroethanol 253
vibration frequencies 125
Steroid lactones, infra-red spectra 248, 291

Tesla sparks, apparent rectification in 168
Thiocyanates, isothiocyanates and isocyanates, infra-red spectra of 212, 296
Titanium dioxide, electronic spectrum of 43
Torsional vibrations in CO_2 and N_2O crystals 308
Trifluoroethanol, hydroxyl frequency in 253
Trisilylamine and deutero derivative, infra-red spectrum 202

Vibrational frequencies, effect of solvent 125
Vibrational frequencies and electronegativity of attached groups 257
Vibrational frequencies of:
carbonyl groups 236
CO_2 and N_2O crystals 308
lactones 291
multiple bonds 60
NH^+ and NH_2^+ groups 261
$N_2H_6^{++}$ ion 280
nitrite ion 336
thiocyanates and isothiocyanates 212, 296
Vinyl fluoride, microwave spectrum of 120

DL.
3
3/59

AUTHOR INDEX TO VOLUME XIII

(B.R.) indicates a Book Review

Ahrens L. H. 304
Bak B. 120
Balloffet G. 150
Bassi D. 192
Bellamy L. J. 60
Bentley F. F. 1
Bevan H. 43
Biswas A. B. 151
Bluhm A. L. 93
Botschkowa O. 50
Butler P. E. B. 223
Caldow G. L. 212
Cannon C. G. 253
Christensen D. 120
Curran C. 31
Daasch L. W. 257
Danti A. 180
Dawes S. V. 43
Decius J. C. 280
Dorfman R. I. 248
Dows D. A. 308
Eaton D. R. 223
Ebsworth E. A. V. 202, 261
Edge R. A. 304
Fassel V. A. 300
Ford R. A. 43
Frisch S. 50
Fry D. L. 99
Gual C. 248, 291
Hainski Z. 311
Hall J. R. 202
Hansen-Nygaard L. 120
Herman P. 311
Hurd B. G. 300
Hurwitz J. K. (B.R.) 339
Ichishima I. 161
Jameson D. A. 236
Jesson J. P. 217
Jewell D. J. 254
Ketelaar J. A. A. 336
Kniseley R. N. 300
Laqua K. 271
Lieber E. 296
Lord R. C. 180
Lucoto U. 271
Mackillop M. J. 202
McKean D. C. 38, 202
Meda F. 75
Mitchell R. L. (B.R.) 339
Miyake A. 161
Miyazawa T. 161
Mizushima S-I. 31, 80, 161
Nakagawa I. 31, 161
Oganov M. N. 139
Parr R. G. (B.R.) 338
Powell D. B. 69
Powell W. R. 1
Price W. C. (B.R.) 159
Pullin A. D. E. 125
Quagliano J. V. 31
Quinney B. B. 300
Ramachandran J. 296
Rao C. N. R. 296
Rao K. Nakaraja 151
Rastrup-Andersen J. 120
Romand J. 150
Rosenkrantz H. 248, 291
Sala O. 192
Schmelz M. J. 31
Schram B. L. 336
Schreiber T. P. 99
Schreider E. 50
Schutte C. J. H. 336
Shaw D. M. 197
Sheppard N. 69, 202, 261
Shimanouchi T. 80, 161
Siebert H. 192
Sinclair D. A. 168
Snyder R. G. 280
Srp N. E. 1
Stace B. C. 253
Stammreich H. 192
Striganov A. R. 139
Tabeling R. W. 300
Tarté P. 107
Thompson H. W. 212, 217, 223, 236, 254
Tsuboi M. 80
Vodar B. 150
Whittem R. N. 168
Wickremasinghe O. 197
Wolfarth E. F. 1
Woodward L. A. 202
Yip C. 197

VOL. 13 1958/59

Spectrochimica Acta, 1958, Vol. 13, pp. 1 to 30. Pergamon Press Ltd., London

Analytical applications of far infrared spectra—I*

Historical review, apparatus and technique

F. F. Bentley, E. F. Wolfarth, Nora E. Srp and W. R. Powell
Wright Air Development Center, Wright-Patterson Air Force Base, Ohio, U.S.A.

(*Received* 2 *January* 1958)

Abstract—A review of some of the analytical applications of far infrared spectra is presented in this paper, and most of the available literature is cited. A double beam double pass spectrophotometer for use in the 15–35 μ region is described briefly, and some of the special techniques of obtaining infrared spectra in the cesium bromide region are discussed. Spectra in the cesium bromide region are particularly useful in material characterization. Slight changes in structure produce considerable changes in the spectra, giving a more specific "fingerprint" of a molecule. Furthermore, group correlations in the cesium bromide region are capable of giving information of value in structural determinations and serve as a complement to the rocksalt spectra. Many common solvents such as carbon disulfide, furan, benzene and dioxane, have large "open windows" in the 15–35 μ region, and the infrared spectra of these and other solvents are given. Some of the advantages of far infrared spectra in structure analysis are discussed.

Introduction

The far infrared spectral region is considered to be that part of the spectrum between the KBr prism cut off (about 20 μ) and the wavelengths at which microwave techniques may be successfully employed (about 2000 μ). When considered in terms of wave numbers the far infrared region covers only about 10 per cent as much of the spectrum as the fundamental region (2–20 μ). Consequently the number of systems to be studied and the nature of the information to be gained from the 16–35 μ region is limited. This is one reason for the small amount of experimental work conducted in the far infrared, particularly for use in analysis. It must be acknowledged, too, that many investigators think that the information needed in analytical applications could be obtained more easily from more accessible regions of the spectrum or from Raman spectra.

Although most analytical problems can be solved through the use of spectra obtained in the 2–16 μ region, there are many cases where the additional information that could be obtained from the 16–35 μ region would give a more complete answer. Infrared spectra in the far infrared region give a more specific "fingerprint" and should be particularly useful in solving analytical problems where the molecules differ only slightly in structure. Furthermore, there are problems that would be difficult to solve through the use of spectra obtained in the rocksalt region alone.

The use of cesium bromide spectra as a physical method of analysis has not,

* Presented at the Conference on Analytical Chemistry and Applied Spectroscopy in Pittsburgh, Pennsylvania, 3 March 1955.

until recently, found widespread application. This has been due, primarily, to the instrumental difficulties in obtaining useful spectra in this region in a short period of time. Low energy, atmospheric absorption and stray radiation are the greatest difficulties in the design of fast recording double beam instruments for the far infrared.

This paper presents a review of previous work in the far infrared region and discusses the apparatus and techniques used in obtaining the spectra in the cesium bromide region. Subsequent papers in this series will discuss group correlations, material characterization, and specific qualitative and quantitative applications of far infrared spectra.

Although the apparatus described in this paper may be used for investigating only a small portion of the far infrared region, namely between 20 and 35 μ, it covers the region which is of the most interest in analytical applications. This is true because most of the low lying vibrational frequencies occur in this region. Furthermore, the interesting possibility of using a cesium bromide prism to cover the entire region from 15 to 35 μ exists. The dispersion of the cesium bromide prism is not markedly inferior to that of potassium bromide from 15 to 20 μ, and the convenience of a single prism for the whole 15–35 μ region is obvious [263].

In many respects the far infrared picture today, at least from the standpoint of analytical applications, is analogous to the status of infrared spectroscopy in the fundamental region after World War II. At that time infrared techniques were being used to a limited extent on single beam instruments to solve analytical problems. It was not until the development of double beam spectrophotometers, however, that a tremendous amount of spectral data were amassed, and infrared spectroscopy as a physical method of analysis found widespread application. Today the bulk of the infrared spectra between 15 and 40 μ are obtained on single beam instruments equipped with potassium bromide, cesium bromide and thallium bromide–iodide (KRS-5) optics. Although a considerable amount of spectral data are available as far out as 20 μ, it is widely scattered in the literature, and in many instances is not presented in a form best suited for qualitative analysis. Very few spectra of compounds other than the simple molecules are available in the 20–40 μ region [450]. With the recent development of interchange units for potassium bromide and cesium bromide prisms of existing double beam instruments, and with means of eliminating stray radiation, as is done on the double beam double pass spectrophotometer discussed in this paper, or by filters, it appears that the region between 15 and 50 μ, like the fundamental region a few years ago, is on the threshold of a new era in analytical applications.

Many molecules have low-lying vibrational frequencies [493]. These are potentially useful for identifying such substances as substituted benzenes, heterocyclics and aliphatic hydrocarbons. Similarly, stretching and bending vibrations for heavy atoms in molecules (bromine, iodine, sulphur, silicon) often are observed in the far infrared region. Spectra here are also particularly useful in material characterization. Slight changes in structure produce considerable changes in the spectra, giving a more specific "fingerprint" of the molecule. Far infrared spectra appear to be more sensitive to crystal structure, and molecules that differ by only a CH_2 group are readily distinguished by their spectra in the solid state. In most

VOL.
13
1958/5

instances the solid molecules that exhibit this sensitivity to crystal lattice vibrations possess entirely different spectra in solution. As a consequence the physical state in which molecules are studied is more critical in the far infrared.

Historical

Our first knowledge of the far infrared region of the electromagnetic spectrum came from the classical experiments of RUBENS and co-workers [412]. Using reststrahlen techniques they were able to study the absorption and reflection spectra of various materials far into the long wavelength region. As a result of these studies and those of many investigators to follow, there are today five main methods available for far infrared investigations: prism and grating spectrometry, focal isolation [410, 411] total reflection [199] and the method of residual rays [318, 446, 335]. Although the last three methods are used for specific reasons, prism and grating spectrometry are today the accepted means of investigating the far infrared. With recent developments prism spectrometry has been extended in the far infrared region to 50 μ, but for investigations beyond this the instrument of choice is a grating spectrometer equipped with echelette gratings [335, 373].

Early far infrared investigations made use of the reststrahlen technique introduced by RUBENS and NICHOLS [409]. Many of the long wavelength spectra were obtained on the apparatus built by CZERNY and described by BARNES [36, 39, 68, 69, 98, 99]. Using the reststrahlen bands observed by SCHAEFER and MATOSSI [414], the method of residual rays was employed by STRONG [446] in the early thirties, and more recently by O'LOANE [335] to study the infrared spectra of certain inorganic and organic substances beyond 20 μ. BARNES used the reststrahlen apparatus of CZERNY in combination with wire gratings to study the long wavelength infrared region from 20 to 135 μ.

The introduction of the echelette grating by R. W. WOOD in 1910, and the subsequent development of these gratings by RANDALL and co-workers [395] was an important contribution to far infrared spectroscopy. In 1918 RANDALL and his students [399] built the first effective prism-grating spectrometer, which was an adaptation of the one used by LANGLEY in 1880 to study the spectrum of the sun. Since there were no prism materials at that time which were transparent beyond 15 μ this instrument was limited by the opacity of rocksalt. Potassium bromide prisms, which extended the spectral region to almost 30 μ, were fashioned in 1930, and sensitive thermopiles and amplifiers became available around 1935 [395, 450]. With these components the construction of a far infrared spectrometer that would give spectral data of the same quality as that obtained in the fundamental region became a reality.

Several grating spectrometers for the far infrared have been constructed in the past. Two that gave excellent spectral data in the region between 25 and 200 μ were built at the University of Michigan [393, 394]. Two were constructed at Johns Hopkins University for investigating the spectral region between 100 and 700 μ [290, 292, 450] and one at Ohio State University to cover the region between 25 and 400 μ [334]. Recently PITZER and co-workers [53] used a grating spectrometer of the type described by RANDALL in the 22–77 μ region. For the most part these instruments have been used to determine the transmission

of various crystalline and filter materials, and to study the spectra of simple molecules.

Using a sylvine (KCl) prism Rubens studied the infrared region almost to 20 μ in 1895. It was not until 1930, however, that prisms became available which extended the spectral region beyond 20 μ. As a graduate student at the University of Michigan, Strong [450] grew the first large KBr crystal in the U.S.A., fashioned it into a prism and, with Randall, constructed one of the first recording prism spectrometers which extended the spectral region almost to 30 μ. The last war gave us two important new infrared optical materials, AgCl and KRS-5. The latter is a thallium bromide–iodide single crystal material from which lenses or prisms, which are transparent to 40 μ, may be fashioned. Using one of the first commercially available prism spectrometers [38], a Model 12 Perkin–Elmer, Plyler and co-workers [361, 471] demonstrated the usefulness of this material in the spectral region between 24 and 40 μ. Recently Plyler and co-workers demonstrated the usefulness of CsBr [367] and CsI [1, 368, 273] as prism materials for the 24–54 μ region. Although other materials, such as crystalline quartz, have been considered to extend the spectral region beyond 50 μ, the problem is now being approached by placing a grating in a spectrometer in place of the Littrow mirror [373, 373a]. The prism is removed and the stray radiation reduced by reflection gratings and reststrahlen plates, or by blackened silver mirrors which are first roughened with a fine emery cloth.

There are several commercially available double beam infrared spectrophotometers, other than the double beam double pass Perkin–Elmer Model 21 Spectrophotometer described in this paper, which are currently being used to obtain spectral data in the 15–40 μ region. The Baird Infrared Spectrophotometer, Model 4-55, may be equipped with a KBr prism and interchange unit to extend the spectral region to approximately 25 μ [381]. The single pass Perkin–Elmer, Model 21, Infrared Spectrophotometer [78] is being used to provide accurate absorption spectra in the 2–37 μ region. Special filters are used in the latter instrument to reduce stray radiation. Several Perkin–Elmer, Model 321, Broad Range Infrared Spectrophotometers are currently being used to obtain spectra in the 2–33 μ region [350]. This instrument is a modified version of the double beam double pass spectrophotometer described in this paper. The primary difference is in the frequency of beam switching and the manner of coding. The Hilger and Watts [317] Recording Infrared Spectrometer may be equipped with the appropriate optical materials to obtain infrared spectra in the far infrared region. Two features of the Beckman IR-3 Spectrometer [47] makes it particularly adaptable to the far infrared region. The double monochromator principle serves to eliminate stray radiation and increases the resolution. Since the instrument operates under vacuum conditions energy losses due to atmospheric absorption is removed. Although no spectral data are yet available on the new Beckman IR-4 Spectrophotometer [313] in the far infrared region, it embodies the double monochromator principle, and should be capable of recording useful spectral data in the 16–36 μ region using cesium bromide optics.

The usefulness of the far infrared spectral region has been discussed by Randall [392, 398, 399]. He has shown in several survey articles that this region may

VOL. 13 1958/5

Table 1. References to spectral data in the far infrared region

A. *Aliphatic hydrocarbons:*

1. Alkanes: [10, 11, 90, 120, 143, 162, 192, 212, 214, 223, 224, 280, 355, 372, 374, 422, 436, 443, 444, 456, 504]
2. *cyclo*Alkanes: [26, 117, 227, 228, 241, 242, 255, 338, 362, 403, 496]
3. Alkenes: [8, 9, 10, 24, 44, 56, 125, 145, 168, 175, 183, 215, 233, 254, 261, 265, 304, 335, 400, 401, 402, 423, 458, 459, 472, 475, 494]
4. Alkynes: [44, 92, 94, 95, 109, 154, 173, 302, 303, 314, 396, 406]

B. *Aromatic hydrocarbons:*

1. Benzene ring systems: [1, 15, 16, 17, 18, 19, 33, 40, 121, 147, 148, 149, 150, 151, 152, 193, 232, 234, 235, 243, 244, 280, 300, 301, 316, 341, 348, 356, 372, 418]
2. Polynuclear ring systems: [27, 153, 221, 222, 237, 246, 248, 256, 352, 354]
3. Heterocyclic ring systems: [5, 25, 76, 84, 111, 160, 161, 187, 196, 226, 236, 245, 255, 268, 297, 306, 307, 353, 424, 431, 500, 509]

C. *Alcohols:*

[35, 55, 64, 335, 419, 455, 469]

D. *Ethers:*

[33, 93, 180]

E. *Carbonyl compounds:*

1. Aldehydes: [57, 108, 144, 179, 296, 335, 417, 428, 467]
2. Ketones: [24, 56, 103, 125, 183, 239, 247, 248, 249, 296, 382]
3. Acids: [420]
4. Esters: [114, 29]
5. Salts: [122, 129, 130, 131, 132, 134, 135, 136, 202]

F. *Halogenated compounds:*

[1, 2, 28, 31, 33, 34, 50, 51, 52, 53, 58, 60, 61, 62, 65, 74, 75, 82, 89, 101, 103, 109, 113, 121, 126, 141, 142, 147, 148, 149, 150, 151, 152, 153, 175, 190, 206, 207, 218, 220, 228, 231, 232, 267, 269, 271, 272, 273, 274, 275, 276, 277, 278, 285, 294, 312, 315, 316, 322, 323, 324, 325, 326, 327, 328, 329, 330, 331, 333, 335, 341, 347, 348, 357, 358, 363, 364, 365, 366, 371, 375, 377, 379, 380, 406, 407, 415, 427, 429, 432, 433, 434, 435, 440, 447, 466, 469, 470, 473, 475, 480, 481, 490, 501, 502, 503, 505, 508]

G. *Nitrogen compounds:*

1. Amines: [23, 30, 33, 49, 91, 311, 477, 483]
2. Amides: [46, 110, 308]
3. Nitriles: [33, 34, 127, 184, 225, 302, 421, 478, 479]
4. Nitro compounds: [33, 238, 257, 462, 487, 496]
5. Amino acids: [129]
6. Cyanate: [146]
7. Miscellaneous: [3, 12, 14, 65, 67, 80, 84, 96, 112, 115, 119, 146, 169, 170, 253, 332, 386, 404, 452, 461, 465]

H. *Sulfur compounds:*

[21, 22, 45, 46, 58, 76, 97, 116, 131, 160, 177, 187, 196, 359, 360, 476]

I. *Polymers:*

[1, 309, 370, 468, 486]

Table 1. (*Contd.*)

J. *Metallo-organics:*

1. Boron compounds: [6, 88, 91, 158, 260, 383, 384, 441, 442, 445]
2. Silicon compounds: [73, 82, 174, 188, 289, 338, 405, 430]
3. Phosphorous compounds: [100, 102, 104, 156, 298, 453, 454, 482]
4. Germanium compounds: [124, 208, 262]
5. Selenium compounds: [299, 343, 413]

K. *Inorganic compounds:*

[13, 20, 22, 38, 41, 43, 45, 54, 63, 66, 68, 70, 71, 77, 80, 81, 85, 86, 87, 98, 118, 128, 133, 137, 138, 139, 155, 156, 157, 158, 163, 164, 165, 166, 169, 170, 171, 176, 177, 185, 189, 191, 194, 195, 197, 200, 201, 203, 209, 213, 216, 219, 252, 258, 259, 260, 265, 266, 270, 281, 282, 283, 286, 288, 294, 310, 311, 320, 321, 332, 334, 335, 336, 337, 339, 340, 342, 344, 345, 346, 351, 378, 383, 386, 387, 388, 389, 390, 391, 395, 397, 404, 408, 413, 414, 416, 420, 437, 438, 447, 449, 452, 453, 454, 457, 463, 464, 465, 484, 495, 497, 498, 499 507]

L. *History, instrumentation and general references:*

[1, 4, 7, 32, 36, 37, 39, 42, 47, 48, 53, 59, 69, 72, 78, 79, 83, 99, 105, 106, 107, 123, 159, 167, 172, 178, 181, 182, 186, 198, 199, 204, 205, 206, 210, 211, 217, 229, 240, 251, 263, 266, 279, 284, 287, 290, 291, 292, 295, 305, 313, 317, 318, 319, 334, 350, 361, 367, 368, 369, 370, 376, 381, 385, 392, 393, 394, 398, 399, 409, 410, 411, 412, 425, 432, 439, 446, 448, 450, 451, 460, 471, 474, 485, 488, 489, 491, 492, 493, 506]

provide information of great value not found elsewhere, or at least, not easily obtained from more accessible regions of the spectrum. Although the contribution of far infrared to the knowledge of molecular structure, revealed through detailed analysis of band spectra, was Professor Randall's primary interest, he surmised the importance of this region for the identification of molecules closely related in structure. Several other general articles dealing with the experimental difficulties, techniques and advantages of far infrared spectroscopy have appeared in the literature [1, 39, 53, 79, 290, 319, 334, 361, 367, 373, 376, 393, 395, 397, 446, 448, 450, 492]. Matossi and co-workers [284] studied the reflection spectra of a large number of silicates out to 25 μ, and Weniger [488] gave a summary of the reflection and transmission studies in the far infrared with a bibliography up to 1921.

A number of articles describing the applications of infrared spectroscopy to chemical research and analysis have touched briefly the far infrared region. Colthup's [83] spectra structure correlations extend out to 25 μ, and Bellamy [48] has discussed many of the fundamental vibrations which occur in the potassium bromide region. Just recently Jones and Sandorfy [205] devoted Chapter 4 of the Weissberger Series, Volume IX, to the application of infrared and Raman spectroscopy to the elucidation of molecular structure. The assignments for vibrational frequencies of many molecules in the far infrared region, which were not covered by Bellamy, are included in this work. Yoshinaga and Oetjen [506] discussed the sampling techniques for transmission measurements in the far infrared region.

In much of their earlier work European spectroscopists contributed a great deal to the potassium bromide region. Thompson, Torkington and Sutherland of England, using sylvine optics, worked out to 20 μ giving the spectra of polymers, chemicals and commercial solvents [474]. Lecomte and co-workers have studied

VOL. 13 1958/5

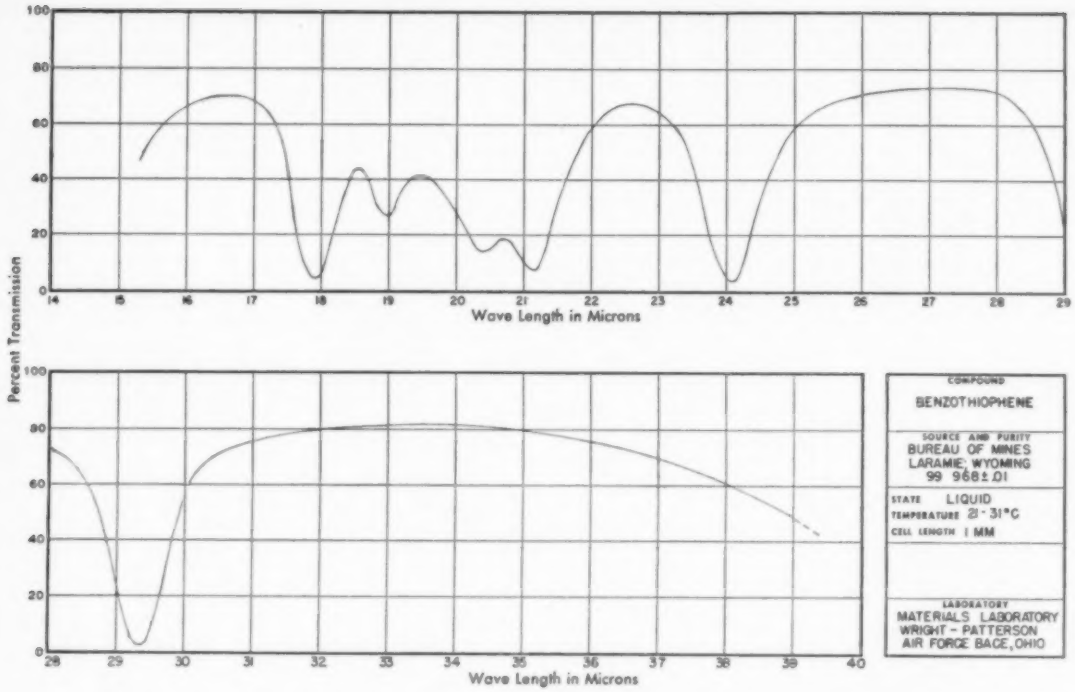

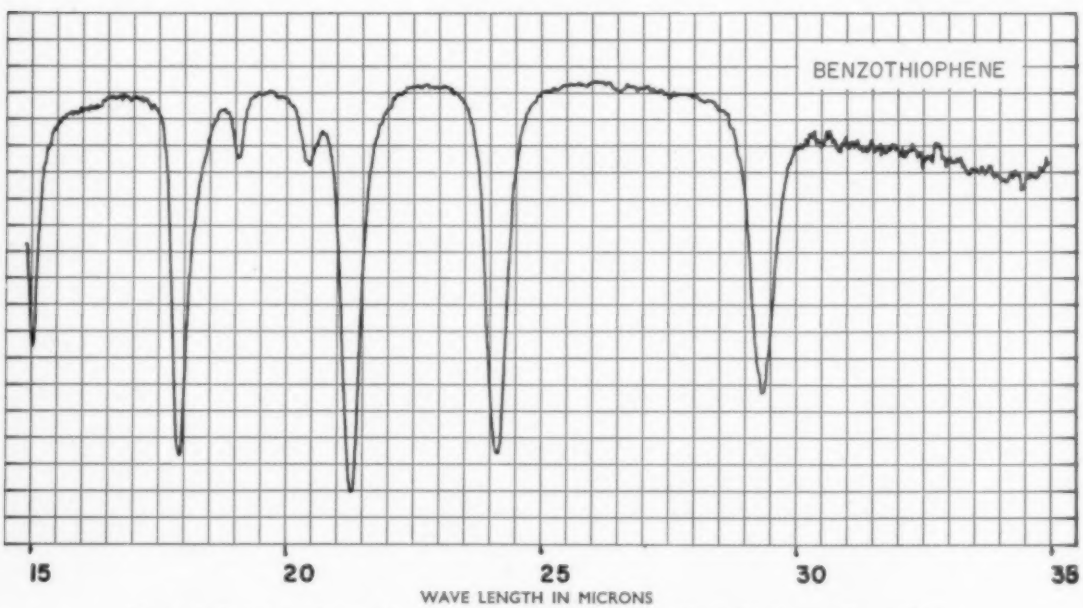

Fig. 1. Infrared spectrum of benzothiophene from 15–35 μ. Top: Spectrum of benzothiophene obtained on a single beam instrument using a KRS-5 prism. Bottom: Spectrum of benzothiophene obtained on the double beam double pass spectrophotometer.

hundreds of organic and inorganic compounds out to 20 μ [229–251]: Recently Lecomte and co-workers have gathered data on the absorption of inorganic and organic substances in the region beyond 20 μ. An effort has been made to give references for a large part of the far infrared spectra that has been obtained for various classes of organic and inorganic molecules. The list of references, shown in Table 1, are by no means complete, but they should be of some value to the analyst and the research worker who may have need of spectral data in the long wavelength region.

Apparatus and procedure

The instrument used in these studies was a special double pass Perkin–Elmer Model 21 Spectrophotometer equipped with cesium bromide optics. It is essentially a conventional Model 21 double beam optical null spectrophotometer modified to include a double beam double pass system developed by Vincent J. Coates and Larkin Scott of the Perkin–Elmer Corporation. The Perkin–Elmer, Model 321, Broad Range Infrared Spectrophotometer is a slightly modified version of the instrument described here. The primary difference is in the frequency of beam switching and the manner of coding. An optical diagram of the Model 321 is given in the Perkin–Elmer Instrument News [350]. The instrument was described by Siegler and Flynn [425] at the Columbus Symposium in June 1956.

The advantages of the double beam double pass spectrophotometer are evident. It eliminates stray radiation, which is appreciable in this region, and the resolution is only slightly less than that of the single pass Perkin–Elmer Model 21. Some loss in energy, which is already low in the far infrared is the most serious disadvantage of this instrument over single pass double beam spectrophotometers.

The advantage of the double beam double pass spectrophotometer over single beam double pass instruments is the great savings in time required to obtain an infrared spectrum. The data from a single beam instrument are merely a spectral record of the energy transmitted by the substance under examination. The absorption bands are superimposed on a highly variable background and a considerable amount of time is needed to convert the modified energy curve into a true spectrum by calculating the percentage absorption at a very large number of key points along the record. Moreover special filters to reduce stray radiation and careful drying and flushing to remove the strong atmospheric water bands in the far infrared are also essential in obtaining useful spectra on a single beam instrument. A comparison of the spectra obtained by the two systems is shown in Fig. 1. The spectrum of benzothiophene (top), recorded on a Perkin–Elmer Model 12C Spectrometer using KRS-5 optics and plotted on a standard API form, required several hours to obtain. The spectrum of the same material (bottom), however, was recorded on the instrument used in these studies in 30 min.

The optical changes made in the Perkin–Elmer Model 21 Spectrophotometer to convert it to a double pass instrument are shown in Fig. 2. The major changes involve the addition of an intercept mirror (A), corner mirror (B) and coding shutter (C). The coding shutter is located at the intermediate slit image of the monochromator and acts on the wanted second pass radiation, but not on the stray or first pass radiation. It is held accurately in place with the rotation of the

VOL. 13 1958/5

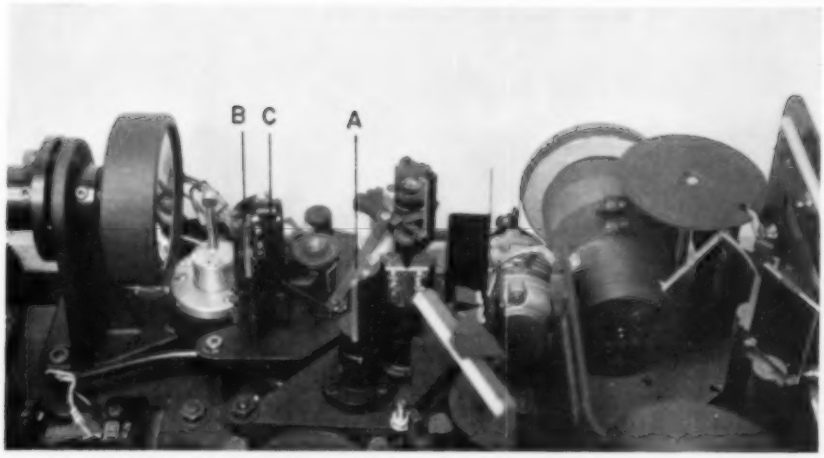

Fig. 2. Inside view of the double beam double pass spectrophotometer with the cesium bromide prism removed.

OL.
.3
3/59

VOL.
13
1958/5

beam switching mirror. The coding shutter's optical position is adjusted for the cesium bromide prism.

The wavelength scale of the spectrophotometer is calibrated using atmospheric carbon dioxide and water vapor absorption bands in this region. The position of the carbon dioxide band at 14·98 μ serves as an excellent calibration reference point for each measurement. The accuracy of the wavelengths recorded is probably better than $\pm 0{\cdot}05$ μ, which in this region of the spectrum is equivalent to about 1·5 cm^{-1}.

Curves for the 100 per cent and zero are shown in Fig. 3(A). Most of the absorption due to atmospheric water vapor [Fig. 3(C)] can be removed by flushing the instrument with dry nitrogen and using drying agents such as magnesium perchlorate or phosphorus pentoxide. The double beam double pass spectrophotometer is capable of resolving the atmospheric water vapor bands at 28 μ [Fig. 3(B)] which are separated by 4 cm^{-1}. A scanning speed of 4 min/μ in the 27·9–29 μ regions was used. The region from 15 to 27 μ is normally covered at a speed of 1 min/μ and that from 29 to 34 μ in 2 min/μ. The spectral slit widths, obtained with a spectral slit width schedule of 1000, range from 6·2 to 3·3 cm^{-1} in the 16–34 μ regions. The natural widths of a vibrational band of the average size molecule is rarely less than 5 cm^{-1}. Although it would be desirable to use spectral slit widths less than 5 cm^{-1}, it has been pointed out by other workers [492] that better than 95 per cent of the work can be handled with spectral slit widths of 5–7 cm^{-1}.

The deviation in percentage transmittance due to noise does not exceed 2 per cent from 15 to 35 μ under normal operating conditions. Curves showing the reproducibility of the double pass double beam spectrophotometer are shown in Fig. 3(D). This curve of 1-*iso*propylnaphthalene represents two successive runs taken 30 min apart. The response characteristics are shown in Fig. 4(A). With the double pass optical system in the Perkin–Elmer Model 21 Spectrophotometer, the scattered light is less than 1 per cent in the 15–35 μ region. The percentage transmission is, for all practical purposes, zero at 31 μ when a rock salt shutter is placed in the sample beam. This is shown in Fig. 4(A).

Solvent and sampling techniques for the far infrared

Special sampling techniques

Conventional infrared techniques are used, and in some instances simplified in obtaining far infrared spectra. Many common solvents can be used, and since nujol has no significant absorption bands in this region it serves as a mulling agent for solid materials. The spectra of greases, high polymers, and samples which are corrosive to cesium bromide plates can be obtained by using cells of polyethylene and KRS-5 to support the materials. Although suitable solvents can be found for most organic solids, cesium bromide pellets are easily prepared and can be used in qualitative and quantitative analysis of solids in this region.* Transparent cesium

* Scrap pieces of cesium bromide can be purchased from the Harshaw Chemical Company, Cleveland, Ohio. The material is quite soft and difficult to grind into a powder suitable for pellet work by mechanical means. Powdered cesium bromide can be obtained by dissolving a 5 g crystal of cesium bromide in approximately 20 ml of distilled water and grinding the solution in an agate mortar until the water evaporated leaving a powder of very small particle size. The powder was dried thoroughly in an oven at 120°C before using. Pellets prepared from cesium bromide treated in this manner were clear and durable. They can be used in the fundamental and far infrared region.

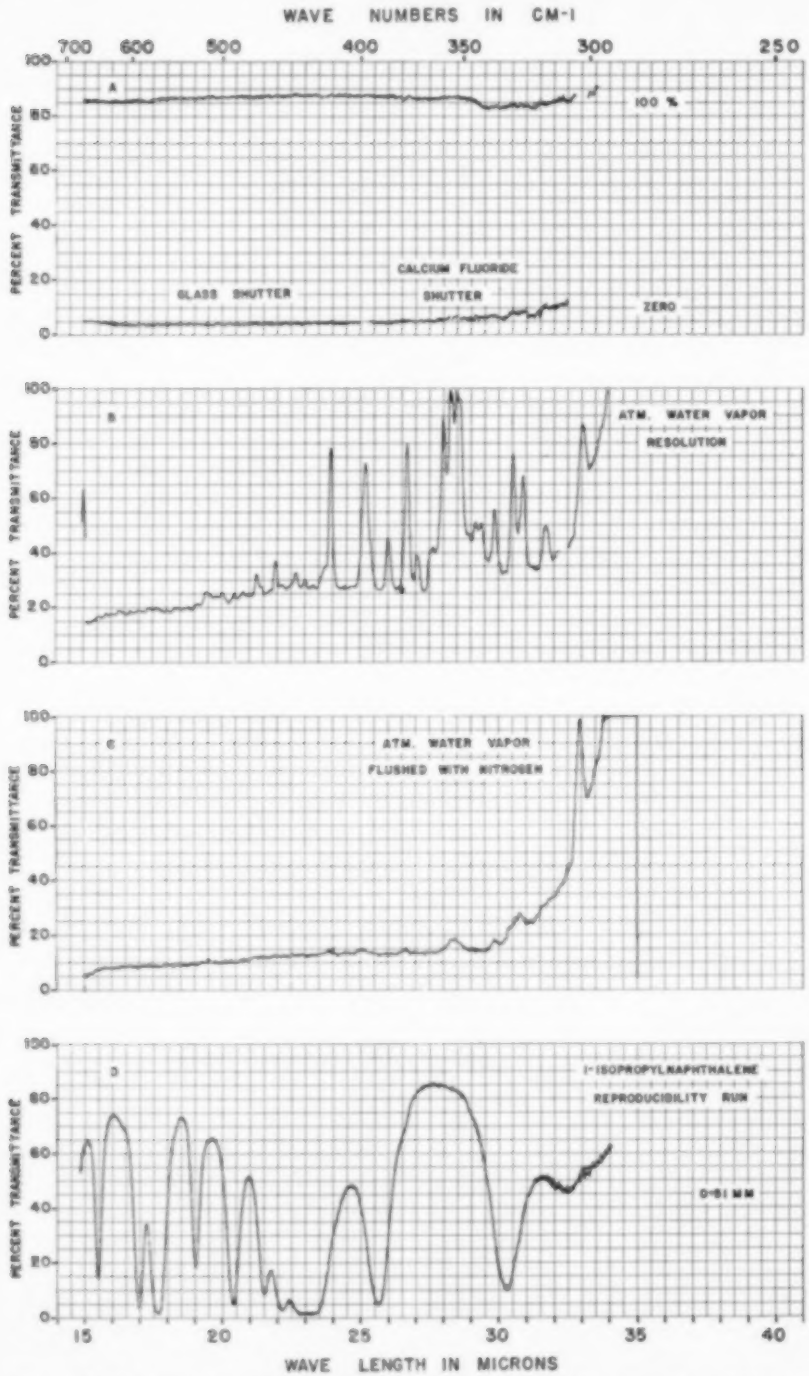

Fig. 3. Performance data obtained on the double beam double pass spectrophotometer: A—The 100 per cent and zero. B—Resolution of atmospheric water vapor. C—Removal of atmospheric water vapor by flushing instrument with dry nitrogen. D—Spectra of 1-*iso*-propylnaphthalene showing the reproducibility of the instrument.

VOL. 13 1958/5

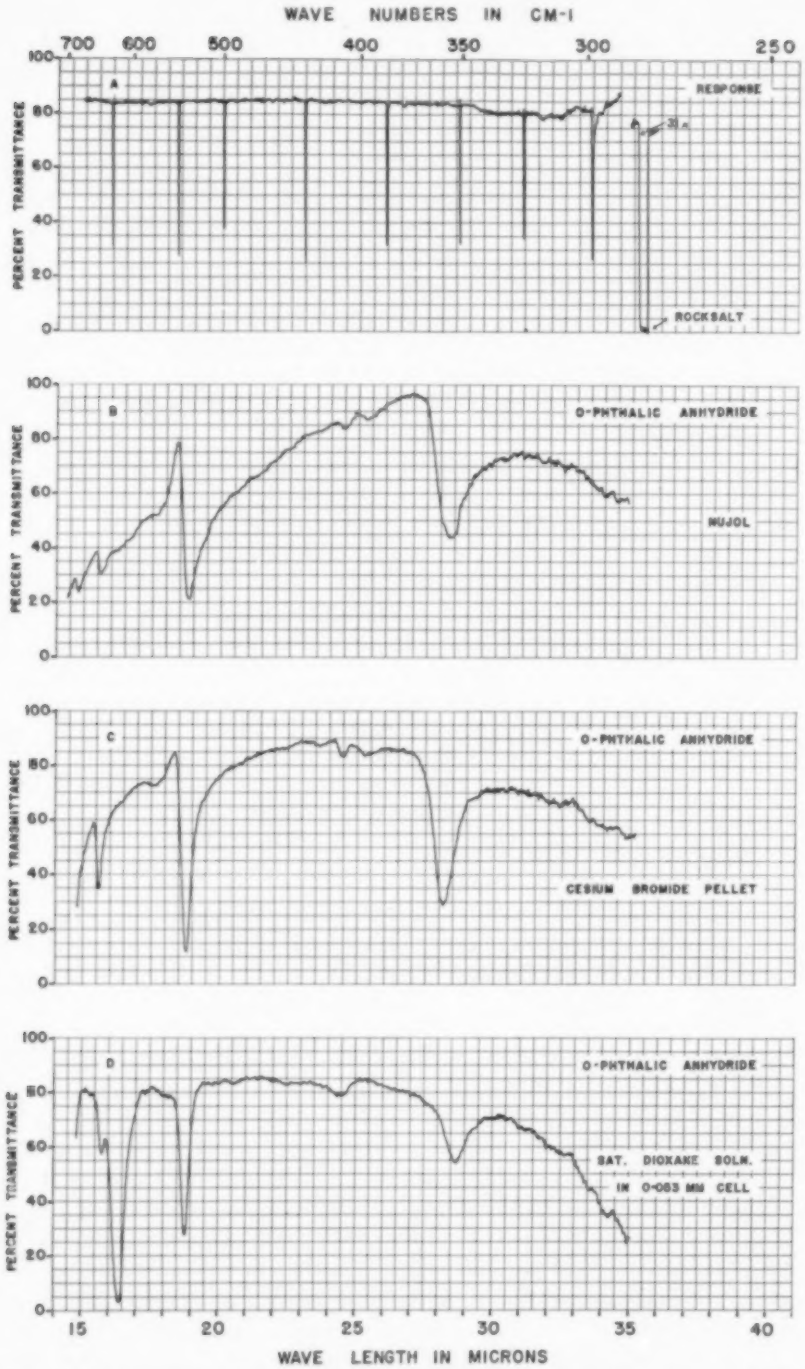

Fig. 4. Performance data on the double beam double pass spectrophotometer: A—Deflexions of pen produced by placing an opaque shutter in the sample beam, and a stray radiation check at 31 μ with rocksalt in the sample beam. B—Infrared spectrum of *o*-phthalic anhydride in nujol. C–Infrared spectrum of *o*-phthalic anhydride in a cesium bromide pellet. D—Infrared spectrum of *o*-phthalic anhydride in dioxane solution.

bromide disc, prepared in pellet dies without a sample, can be used as demountable cells to support materials while obtaining their spectra.

The spectra of *o*-phthalic anhydride, shown in Figs. 4(B), 4(C) and 4(D) as a nujol mull, cesium bromide pellet and a dioxane solution, are typical of the spectra of solid materials in the long wavelength region of the spectrum, and illustrate the effect of light scattering and wavelength shifting due to the different mediums. The Tyndall scattering is rather pronounced in the nujol spectrum. This is indicated by the fall off in energy at shorter wavelengths. The sudden increase in absorption on the shorter wavelength side of the absorption bands can be attributed to the Christiansen filter effect. Although the Tyndall scattering is more pronounced at shorter wavelengths it is interesting to note that the effect is quite appreciable at longer wavelengths.

In the far infrared region, shifts in wavelengths due to the physical state of the sample appear to be greater than in the fundamental region of the spectrum. As seen in the spectrum of *o*-phthalic anhydride, Figs. 4(B), 4(C) and 4(D), the absorption band at 28 μ shifts as much as 0·5 μ to longer wavelengths in going from the cesium bromide pellet to a solution in dioxane. The wavelength position of this band in nujol is intermediate between its position in the cesium bromide and solution spectra.

Polymeric materials such as rubber, resins and plastics were recorded as pyrolyzates, films, or in solution. In some instances the pyrolyzates were dissolved in benzene and their infrared spectra recorded in solution. The spectra of liquid samples were recorded in cesium bromide and KRS-5 cells. Since the latter cells give interference patterns and reflect approximately 30 per cent of the incident beam at each surface, cesium bromide cells are more desirable for work in the long wavelength region. The cesium bromide plates are soft and easily polished with paper towels. In an air conditioned room corrosion by atmospheric water vapor is not very serious, and with careful handling the cesium bromide cells are as easy to work with as potassium bromide or sodium chloride cells. For the most part a cell with a longer pathlength is required for the cesium bromide region than for the rocksalt region of the spectrum. Although the most useful cell is 0·50 mm thick, the highly polar materials require cells as thin as 0·05 mm and the less polar materials require cells as thick as 2 mm.

Although commercial solvents were used to obtain the infrared spectra shown here, an effort was made to use those that were chemically pure whenever possible. In some instances the compounds were of high purity, but in other cases technical grade chemicals were used. The grade of purity and the manufacturer, whenever possible, are indicated on the spectra.

Solvents

The solvent situation in the cesium bromide is more encouraging than in the sodium chloride region [204, 385, 460]. Many aliphatic and aromatic hydrocarbons which are outstanding solvents for paints, varnishes, waxes, resinous materials, oils, greases, silicones, etc., can be used in the 15–35 μ region. Solvents such as hexane, *cyclo*hexane, 2:4:4-trimethylpentane, nujol, benzene, thiophene, furan and 1:4-dioxane have large windows and can be used. The transmission of

VOL. 13 1958/5

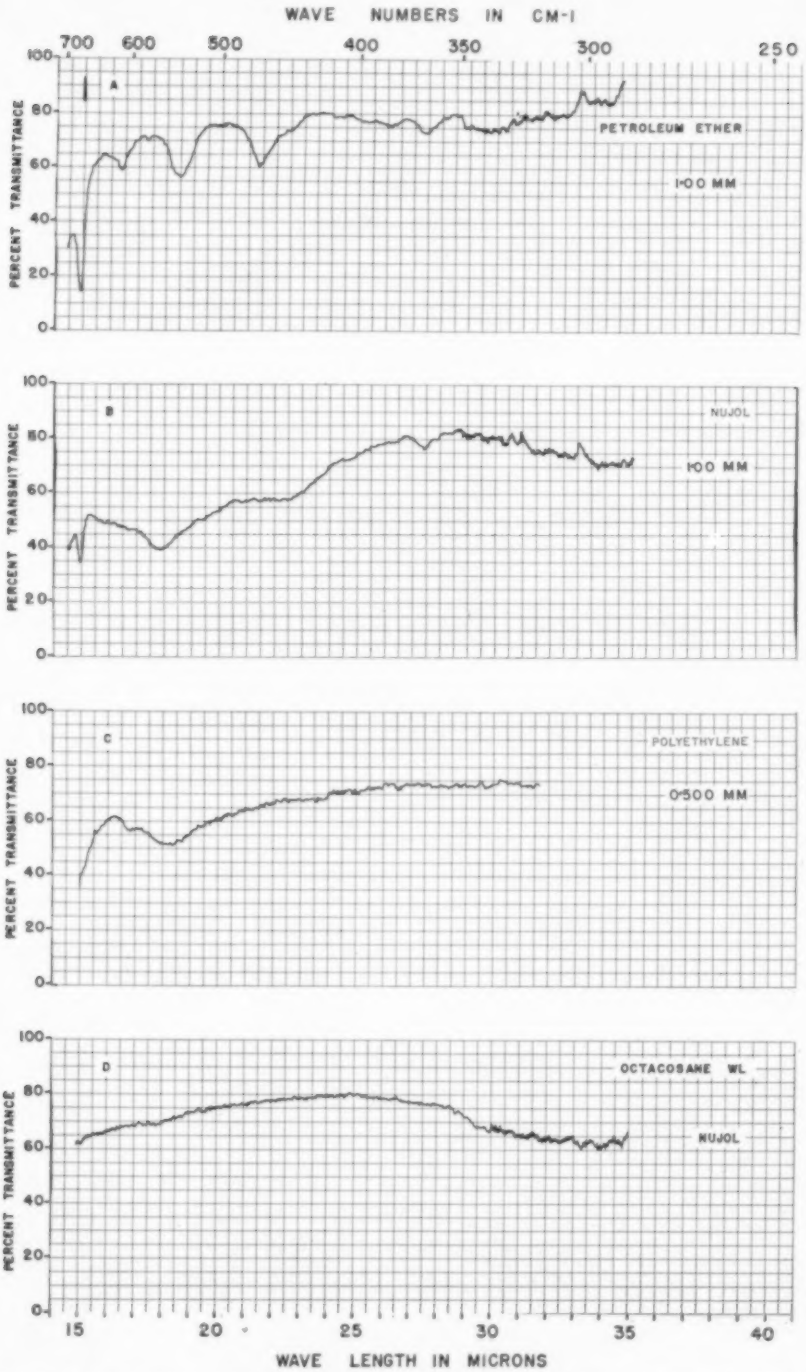

Fig. 5. Infrared spectra from 15–35 μ of organic solvents: A—Petroleum ether. B—Nujol. C—Polyethylene (transparent material). D—Octacosane.

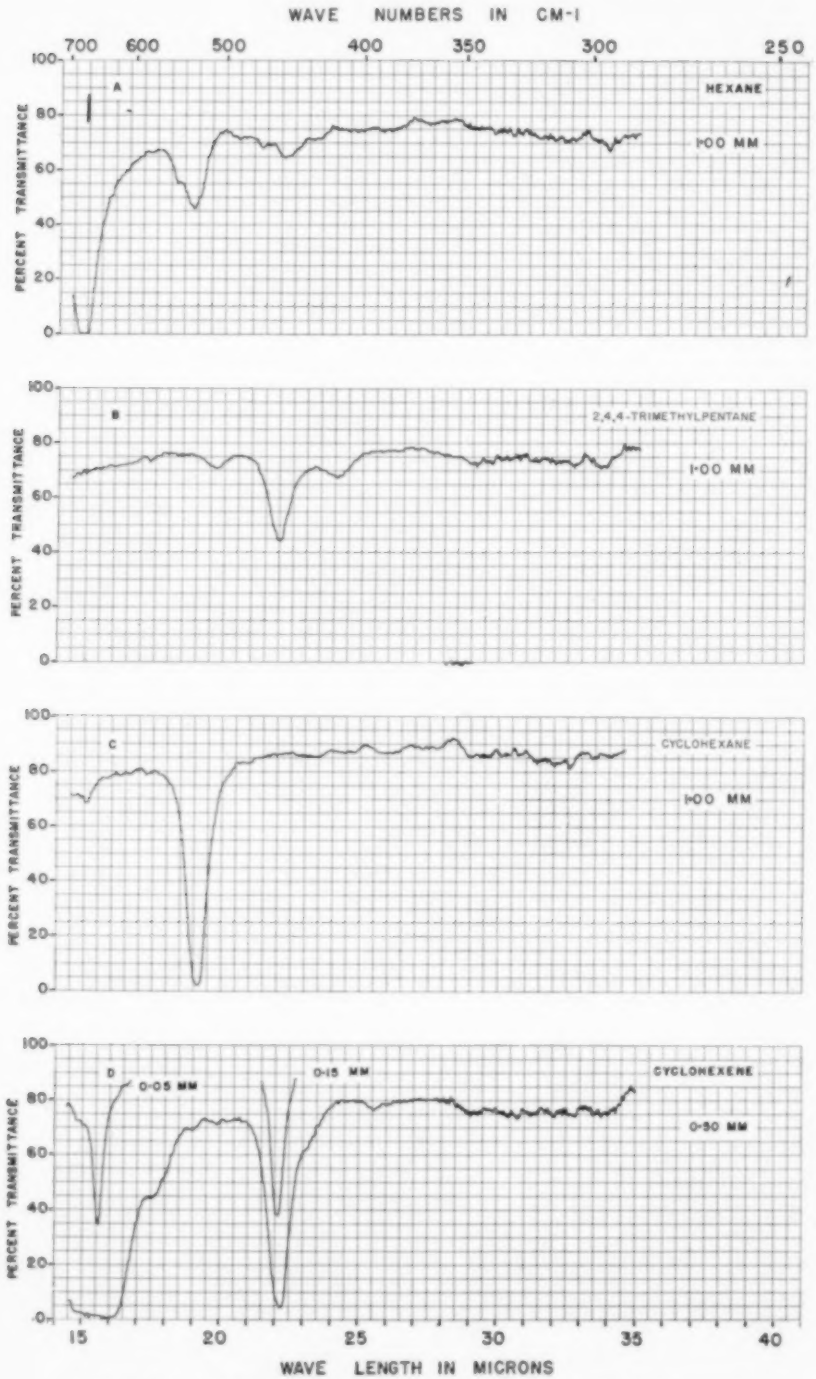

Fig. 6. Infrared spectra from 15–35 μ of organic solvents: A—Hexane. B—2:4:4-Trimethylpentane. C—*cyclo*Hexane. D—*cyclo*Hexene.

VOL. 13 1958/5

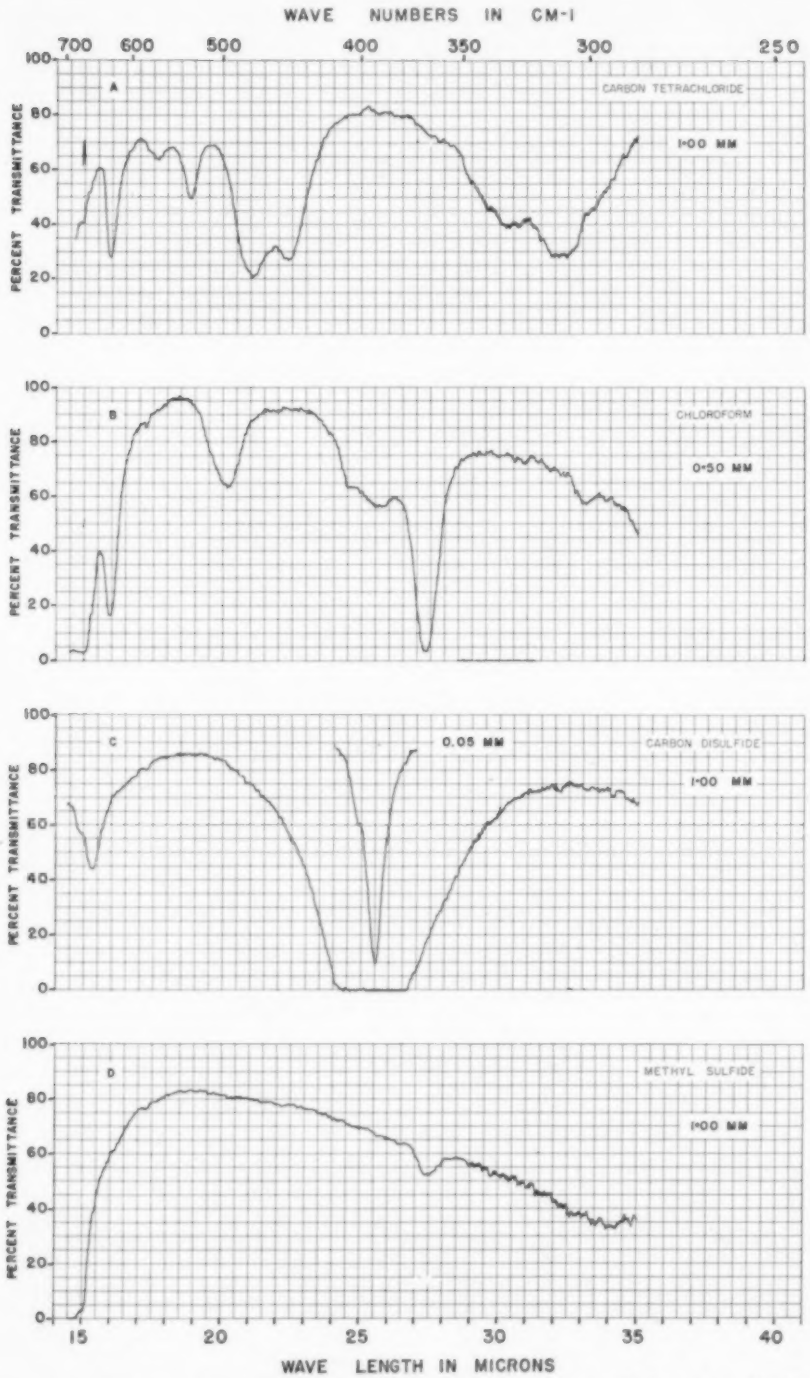

Fig. 7. Infrared spectra from 15–35 μ of organic solvents: A—Carbon tetrachloride. B—Chloroform. C—Carbon disulfide. D—Methyl sulfide.

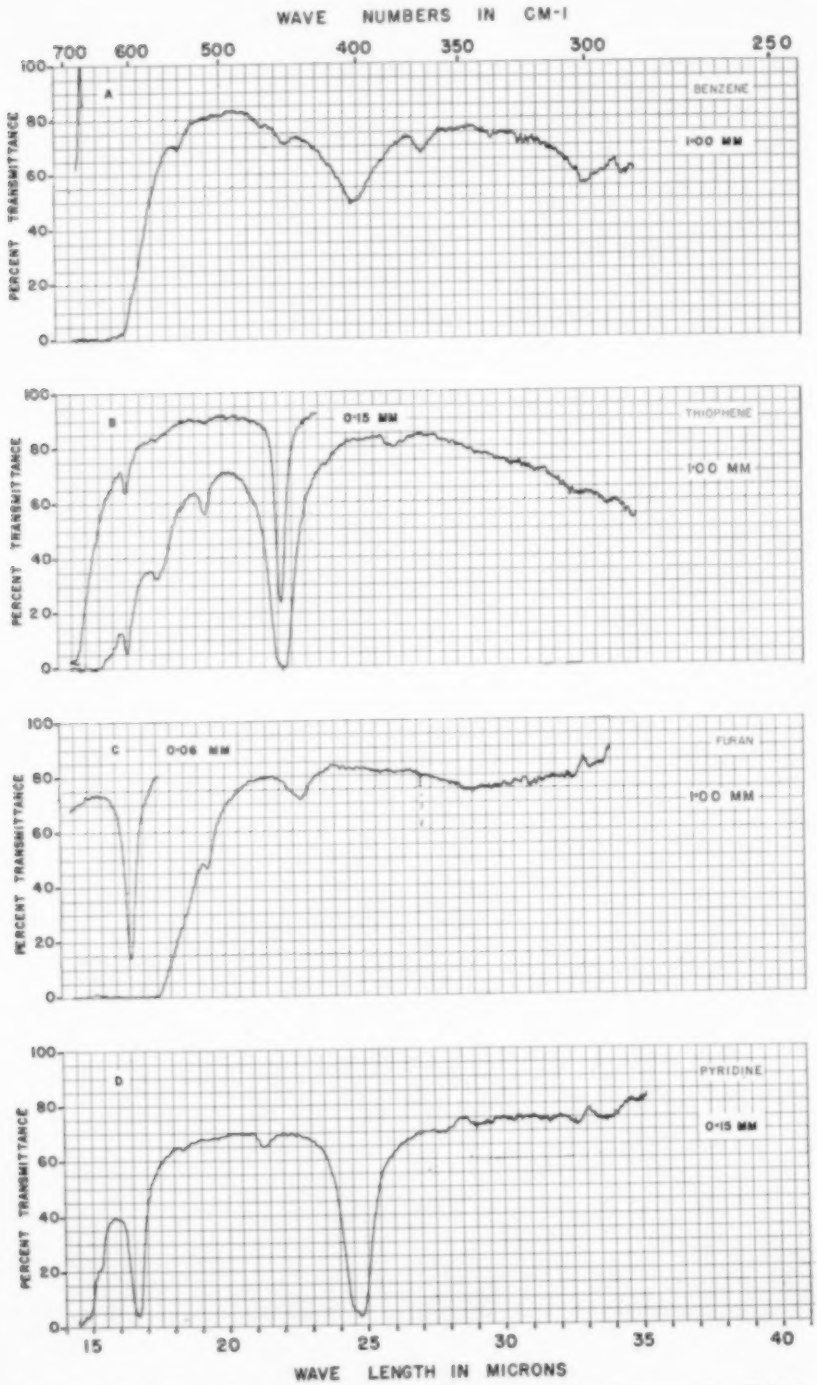

Fig. 8. Infrared spectra from 15–35 μ of organic solvents: A—Benzene. B—Thiophene. C—Furan. D—Pyridine.

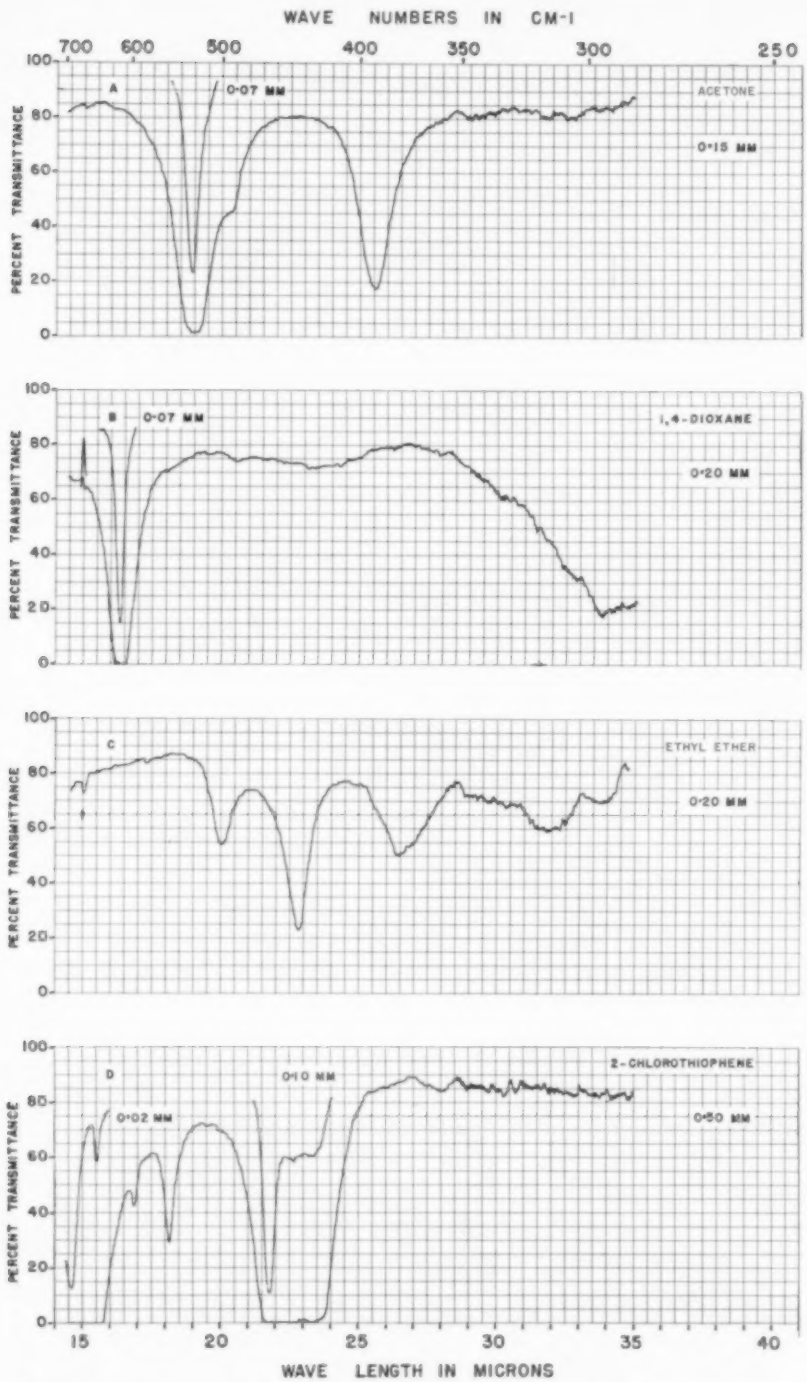

Fig. 9. Infrared spectra from 15–35 μ of organic solvents: A—Acetone. B—1:4-Dioxane. C—Ethyl ether. D—2-Chlorothiophene.

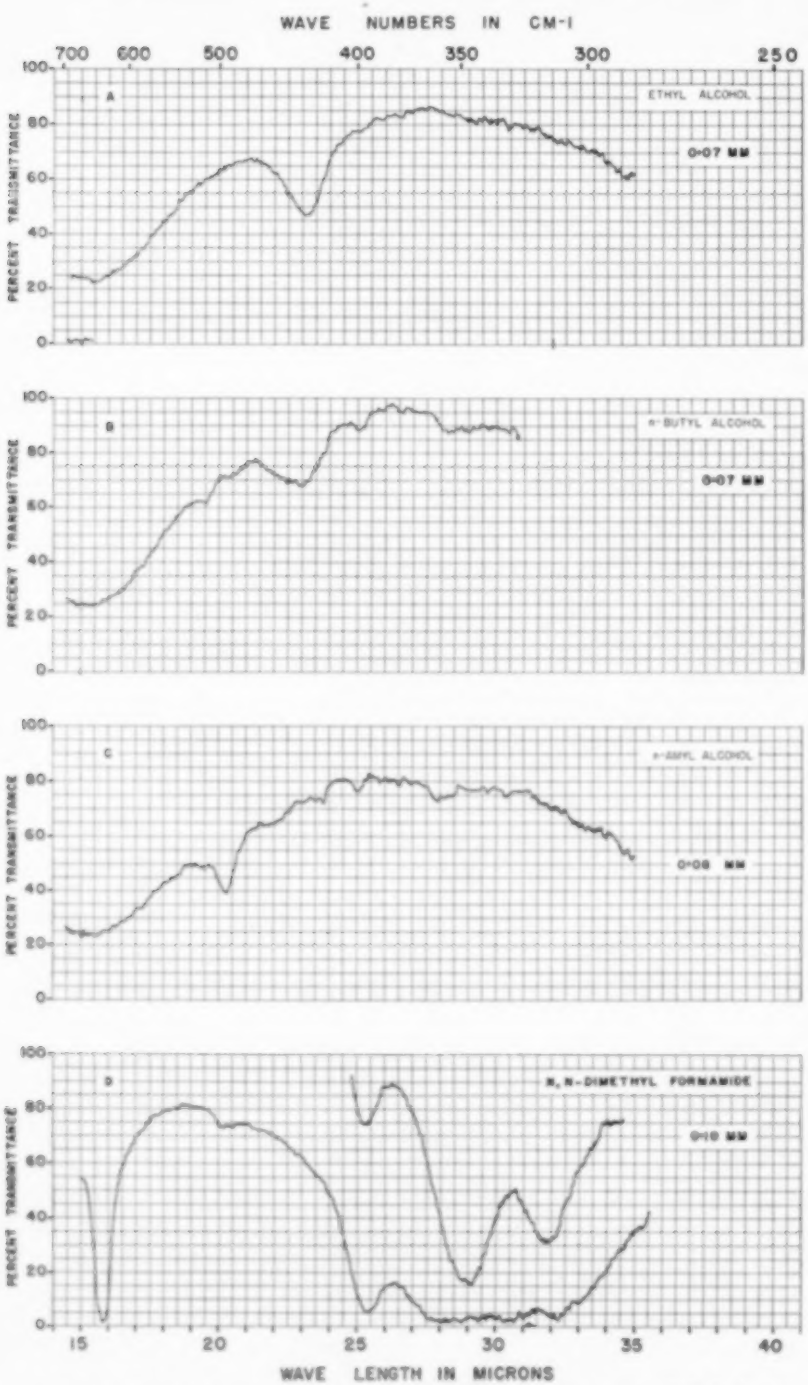

Fig. 10. Infrared spectra from 15–35 μ of organic solvents: A—Ethyl alcohol. B—n-Butyl alcohol. C—n-Amyl alcohol. D—N:N-dimethyl formamide.

VOL.
13
1958/5

benzene is greater than 40 per cent throughout the 18–35 μ region in 1·00 mm cells. The spectrum of 1:4-dioxane has an open window from 18 to 31 μ. This is an outstanding solvent because of its great dissolving power and large region of transmission. Acetone and ether have appreciable absorption in the far infrared, but these solvents have windows where dioxane absorbs. The whole region between 15–35 μ can be covered by using a combination of the last three exceptionally good solvents. Nujol has no appreciable absorption bands in this region and can be used as a mulling agent to obtain the spectra of solid materials.

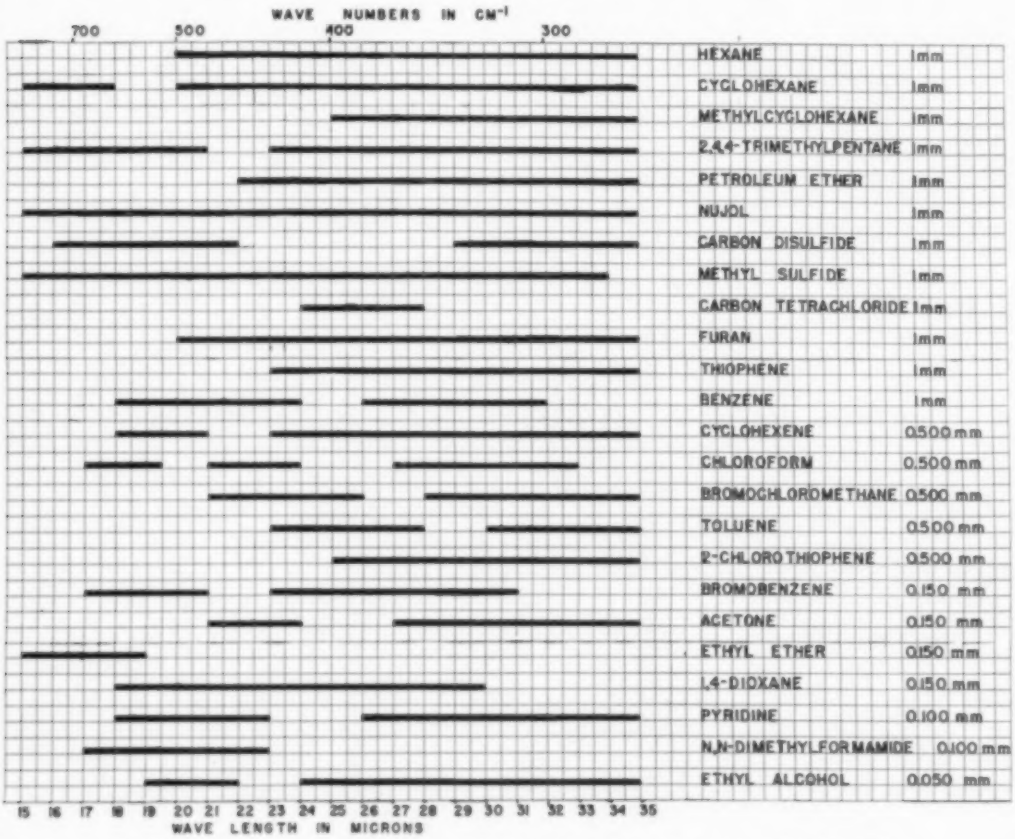

Fig. 11. Pictorial diagram of solvents for the cesium bromide region. The black lines represent useful regions.

Several years ago TORKINGTON and THOMPSON recommended a number of solvents for use in the infrared out to 20 μ [474] and more recently MARRISON [279] investigated 60–70 organic liquids for solvents in the 15–25 μ region. The infrared spectra of a number of readily available solvents in the 15–35 μ region are shown in Figs. 5–10. The less polar solvents can be used in cells as thick as 2 mm, while solvents as polar as acetone can be used in 0·2 mm cells. This is an advantage in both qualitative and quantitative work. Polar compounds

such as esters and silicone are usually highly soluble in benzene and dioxane, and since very little solvent is needed to dissolve these compounds, thin cells can be used to record their spectra with very little masking from the solvent.

A list of the more commonly used organic solvents is shown in Fig. 11. The black lines indicate the wavelength regions in which these solvents are most useful. The transmission of these solvents in the indicated range is greater than 40 per cent of the incident energy at the thickness shown. In general the less polar solvents are listed at the top of the chart and the more polar ones at the bottom.

Acknowledgement—The authors would like to acknowledge Dr. Alvin Kosak, formerly of the University of Cincinnati, for suggesting as a graduate thesis problem a group correlation study of some organic sulfur compounds in the 15–40 μ region. Work along these lines led to this study on analytical applications of far infrared spectra. The special double beam double pass spectrophotometer used in these studies was designed and manufactured by the Perkin–Elmer Corporation on Contract AF 33(616)-1199. The authors wish to express their appreciation to Mr. Vincent Coates of Perkin–Elmer for the key role he played in designing the instrument and for his encouragement and assistance in making this project a success. They would like to acknowledge the assistance of Dr. Horace Ziegler, Mr. Richard LeClair and Mr. Larkin Scott of the Perkin–Elmer Corporation. The authors would also like to thank Mr. George Rappaport, formerly of this Center, for his assistance in preparing the performance specifications desired in an instrument to cover the 16–40 μ region, and First Lt. Gordon Oshesky for his assistance in obtaining the spectral data used in this article.

References

[1] Acquista N. and Plyler E. K., *J. Opt. Soc. Amer.* 1953 **43** 977.
[2] Adel A. and Barker E. F., *J. Chem. Phys.* 1934 **2** 627.
[3] Adel A. and Barker E. F., *Rev. Mod. Phys.* 1944 **16** 236.
[4] Allard G., *Helv. Chim. Acta* 1936 **19** 1270.
[5] Anderson F. A., Bak B., Brodersen S. and Rastrup-Anderson J., *J. Chem. Phys.* 1955 **23** 1047.
[6] Anderson W. E. and Barker E. F., *J. Chem. Phys.* 1950 **18** 698.
[7] Applications of infrared spectra to chemical problems. *Trans. Faraday Soc.* 1945 **41** 171.
[8] Aston J. G., Isserow S., Szasz G. J. and Kennedy R. M., *J. Chem. Phys.* 1944 **12** 336.
[9] Aston J. G., Szasz G. J., Woolley H. W. and Brickwedde F. G., *J. Chem. Phys.* 1946 **14** 67.
[10] Avery W. H. and Ellis C. F., *J. Chem. Phys.* 1942 **10** 10.
[11] Avery W. H. and Morrison J. R., *J. Appl. Phys.* 1947 **18** 960.
[12] Badger and Cartwright, *Phys. Rev.* 1929 **33** 692.
[13] Bailey C. R. and Hale J. B., *Phil. Mag.* 1938 **25** 98.
[14] Bailey C. R. and Carson S. C., *J. Chem. Phys.* 1939 **7** 859.
[15] Bailey C. R., Hale J. B., Ingold C. K. and Thompson J. W., *J. Chem. Soc.* 1936 931.
[16] Bailey C. R., Carson S. C. and Ingold C. K., *J. Chem. Soc.* 1946 252.
[17] Bailey C. R., Hale J. B., Herzfeld N., Ingold C. K., Leckie A. H. and Poole H. G., *J. Chem. Soc.* 1946 255.
[18] Bailey C. R., Carson S. C., Gordon R. R. and Ingold C. K., *J. Chem. Soc.* 1946 288.
[19] Bailey C. R., Gordon R. R., Hale J. B., Herzfeld N., Ingold C. K. and Poole H. G., *J. Chem. Soc.* 1946 299.
[20] Bailey C. R., Cassie A. B. D. and Angus W. R., *Proc. Roy. Soc.* 1930 **130** 133.
[21] Bailey C. R. and Cassie A. B. D., *Proc. Roy. Soc.* 1931 **132** 236.
[22] Bailey C. R. and Cassie A. B. D., *Proc. Roy. Soc.* 1932 **135** 375.
[23] Bailey C. R., Carson S. C. and Daly E. F., *Proc. Roy. Soc.* 1939 **173** 339.

VOL. 13 1958/5

[24] Bak B. and Anderson F. A., *J. Chem. Phys.* 1954 **22** 1050.
[25] Bak B., Brodersen S. and Hansen L., *Acta Chem. Scand.* 1955 **9** 749.
[26] Baker A. W. and Lord R. C., *J. Chem. Phys.* 1955 **23** 1636.
[27] Barca D. and Galateanu, *Bull. soc. roumaine phys.* 1936 **37** 19.
[28] Barcelo J. R., *J. Res. Nat. Bur. Stand.* 1950 **44** 521.
[29] Barcelo J. R. and Martin C. S., *J. Phys. Radium* 1954 **15** 403.
[30] Barcelo J. R. and Bellanato J., *Spectrochim. Acta* 1956 **8** 27.
[31] Barchewitz P. and Parodi M., *J. Phys. Radium* 1939 **10** 143.
[32] Barchewitz P. and Parodi M., *C.R. Acad. Sci., Paris* 1938 **206** 1891.
[33] Barchewitz P. and Parodi M., *C.R. Acad. Sci., Paris* 1938 **207** 903.
[34] Barchewitz P. and Parodi M., *C.R. Acad. Sci., Paris* 1939 **209** 30.
[35] Barker E. F. and Bosschieter G., *J. Chem. Phys.* 1938 **6** 563.
[36] Barnes R. B. and Czerny M., *Z. Phys.* 1931 **72** 447.
[37] Barnes R. B., *Rev. Sci. Instrum.* 1934 **5** 237.
[38] Barnes R. B., McDonald R. S., Williams V. Z. and Kinnaird R. F., *J. Appl. Phys.* 1945 **16** 77.
[39] Barnes R. B., *Phys. Rev.* 1932 **39** 562.
[40] Barnes R. B., Benedict W. S. and Lewis C. M., *Phys. Rev.* 1935 **47** 129.
[41] Barnes R. B., *Phys. Rev.* 1935 **47** 658.
[42] Barnes R. B., Benedict W. S. and Lewis C. M., ibid 1935 **47** 918.
[43] Barrow G. M., *J. Phys. Chem.* 1955 **59** 987.
[44] Bartholome E. and Karweil J., *Z. phys. Chem.* B 1937 **35** 442.
[45] Bartunek P. F. and Barker E. F., *Phys. Rev.* 1935 **48** 516.
[46] Baxter J. N., Cymerman-Craig J. and Willis J. B., *J. Chem. Soc.* 1955 669.
[47] *Beckman Bull.* No. 237.
[48] Bellamy L. S., *The Infrared Spectra of Complex Molecules.* Wiley, New York 1954.
[49] Bellanato J., Sardina M. A. T. and Matutano, *Anales. real. soc. espan. fis y quim.* B 1955 **51** 271
[50] Bernstein H. J., *Canad. J. Res.* B 1950 **28** 132.
[51] Bernstein H. J. and Powling J., *J. Amer. Chem. Soc.* 1951 **73** 1843.
[52] Bernstein R. B., Zietlow J. P. and Cleveland F. F., *J. Chem. Phys.* 1953 **21** 1778.
[53] Bohn G. E., Freeman N. K., Gwinn W. D., Hollenberg J. L. and Pitzer K. S. *J. Chem. Phys.* 1953 **21** 719.
[54] Bonino G. B. and Fabbri G., *Atti. accad. nazl. Lincei, Rend. Classe sci fis, mat e nat.* 1955 **19** 386.
[55] Bordon A. and Barker E. F., *J. Chem. Phys.* 1938 **6** 553.
[56] Børge B. and Anderson F. A., *J. Chem. Phys.* 1954 **22** 1050.
[57] Brand J. C. D. and Minkoff G. J., *J. Chem. Soc.* 1954 2970.
[58] Brandt G. R. A., Emeleus H. J. and Haszeldine R. N., *J. Chem. Soc.* 1952 2549.
[59] Brattain R. R., *Phys. Rev.* 1941 **60** 164.
[60] Brown J. K. and Sheppard N., *Trans. Faraday Soc.* 1954 **50** 535.
[61] Brown J. K. and Sheppard N., *Trans. Faraday Soc.* 1954 **50** 1164.
[62] Brown J. K. and Sheppard N., *Proc. Roy. Soc.* A 1955 **231** 555.
[63] Burke T. G., Smith D. F. and Nielsen A. H., *J. Chem. Phys.* 1952 **20** 447.
[64] Burkhard D. G., *Dissertation.* Univ. of Mich. Ann Arbor, Mich. 1950.
[65] Burns W. G. and Bernstein H. J., *J. Chem. Phys.* 1950 **18** 1669.
[66] Cabannes-Ott C., *C.R. Acad. Sci., Paris* 1956 **242** 2825.
[67] Califano S. and Luttke W., *Z. phys. Chem.* 1956 **6** 83.
[68] Cartwright C. H. and Czerny M., *Z. Phys.* 1934 **90** 457.
[69] Cartwright C. H., *Z. Phys.* 1934 **90** 480.
[70] Cartwright C. H., *Nature, Lond.* 1935 **135** 872.
[71] Cartwright C. H., *Nature, Lond.* 1935 **136** 181.
[72] Cartwright C. H., *J. Chem. Phys.* 1936 **4** 413.
[73] Cerato C. C., Lauer J. L. and Beachell H. C., *J. Chem. Phys.* 1954 **22** 1.
[74] Cheng H. C. and Lecomte J., *C.R. Acad. Sci., Paris* 1935 **201** 199.

[75] Cheng H. C. and Lecomte J., *J. Phys. Radium* 1935 **6** 477.
[76] Chiorboli P. and Mirone P., *Atti. accad. nazl. Lincei. Rend. Classe sci. fis mat e nat.* 1954 **16** 243.
[77] Cilento G., Ramsay D. A. and Jones R. N., *J. Amer. Chem. Soc.* 1949 **71** 2753.
[78] Coates V., Miller T. and Savitzky A., *Appl. Spectroscopy* 1955 **9** 14.
[79] Coblentz W. W., *Sci. Monthly* 1949 **68** 102.
[80] Cohn H., Ingold C. K. and Poole H. G., *J. Chem. Soc.* 1952 4272.
[81] Cohn H., *J. Chem. Soc.* 1952 4282.
[82] Collins R. L. and Nielsen J. R., *J. Chem. Phys.* 1955 **23** 351.
[83] Colthup N. B., *J. Opt. Soc. Amer.* 1950 **40** 397.
[84] Corrsin L., Fox B. J. and Lord R. C., *J. Chem. Phys.* 1953 **21** 1170.
[85] Couture L., *C.R. Acad. Sci., Paris* 1944 **218** 669.
[86] Couture L., *C.R. Acad. Sci., Paris* 1946 **222** 495.
[87] Cowling T. G., *Reports on Progress in Physics* Vol. 9 p. 29. Physical Society, London.
[88] Cowan R. D., *J. Chem. Phys.* 1949 **17** 218.
[89] Cowan R. D., Herzberg G. and Sinha S. P., *J. Chem. Phys.* 1950 **18** 1538.
[90] Crawford B. L., Avery W. H. and Linnett J. W., *J. Chem. Phys.* 1938 **6** 682.
[91] Crawford B. L. and Edsall J. T., *J. Chem. Phys.* 1939 **7** 223.
[92] Crawford B. L., *J. Chem. Phys.* 1939 **7** 140.
[93] Crawford B. L. and Joyce L., *J. Chem. Phys.* 1939 **7** 307.
[94] Crawford B. L., *J. Chem. Phys.* 1939 **7** 555.
[95] Crawford B. L., *J. Chem. Phys.* 1940 **8** 526.
[96] Crawford B. L. and Fletcher W. H., *J. Chem. Phys.* 1951 **19** 406.
[97] Cymermen J. and Willis J. B., *J. Chem. Soc.* 1951 1332.
[98] Czerny M., *Z. Phys.* 1925 **34** 227.
[99] Czerny M., *Z. Phys.* 1927 **44** 235.
[100] Daasch L. W. and Smith D. C., *J. Chem. Phys.* 1951 **19** 22.
[101] Daasch L. W., Liang C. Y. and Nielsen J. R., *J. Chem. Phys.* 1954 **22** 1293.
[102] Daasch L. W., *J. Amer. Chem. Soc.* 1954 **76** 3404.
[103] Daasch L. W. and Kagarise R. E., *J. Amer. Chem. Soc.* 1955 **77** 6156.
[104] Daasch L. W. and Smith D. C., *Analyt. Chem.* 1951 **23** 853.
[105] Dadieu A. and Kohlrausch K. W. F., *J. Opt. Soc. Amer.* 1931 **21** 286.
[106] Dahlke W., *Z. Phys.* 1939 **114** 205.
[107] Dahlke W., *Z. Phys.* 1939 **114** 672.
[108] Davidson D. W., Stoicheff B. P. and Bernstein H. S., *J. Chem. Phys.* 1954 **22** 289.
[109] Davidson D. W. and Bernstein H. S., *Canad. J. Chem.* 1955 **33** 1226.
[110] Davies M., Evans J. C. and Jones R. L., *Trans. Faraday Soc.* 1955 **51** 761.
[111] Davis P. W., Univ. Microfilm, No. 12017. Ann Arbor, Mich.
[112] Decius J. C. and Pearson D. P., *J. Amer. Chem. Soc.* 1953 **75** 2436.
[113] Decker C. E., Meister A. G., Cleveland F. F. and Bernstein R. B., *J. Chem. Phys.* 1953 **21** 1781.
[114] Delay A., Duval C. and Lecomte J., *C.R. Acad. Sci., Paris* 1943 **216** 40.
[115] Delay A., Duval C. and Lecomte J., *Bull. Soc. Chim.* 1945 **12** 581.
[116] Dennison D. M. and Wright N., *Phys. Rev.* 1931 **38** 2077.
[117] Derfer J. M., Pickett E. E. and Boord C. E., *J. Amer. Chem. Soc.* 1949 **71** 2482.
[118] Dixon R. N. and Sheppard N., *J. Chem. Phys.* 1955 **23** 215.
[119] Dodd R. E., Rolfe J. A. and Woodward L. A., *Trans. Faraday Soc.* 1956 **52** 145.
[120] Donneaud M. T., *C.R. Acad. Sci., Paris* 1954 **239** 1480.
[121] D'Or L., Alewaeters R. and Collin J., *Rec. Trav. Chim.* 1956 **75** 862.
[122] Douville F., Duval C. and Lecomte J., *Bull. Soc. Chim.* 1942 **9** 548.
[123] Dowine A. R., Magoon M. C., Purcell T. and Crawford B., *J. Opt. Soc. Amer.* 1953 **43** 941.
[124] Dows D. A. and Hexter R. M., *J. Chem. Phys.* 1956 **24** 1029.
[125] Drayton L. G. and Thompson H. W., *J. Chem. Soc.* 1948 1416.
[126] Duchesne J., *Nature Lond.* 1937 **139** 288.

VOL. 13 1958/5

[127] Duncan N. E. and Janz G. J., *J. Chem. Phys.* 1955 **23** 434.
[128] Duval C. and Lecomte J., *Bull. Soc. Fr. Min.* 1943 **66** 284.
[129] Duval C. and Lecomte J., *Bull. Soc. Chim. Fr.* 1943 **10** 180.
[130] Duval C., Lecomte J. and Delay A., *Bull. Soc. Chim. Fr.* 1944 **11** 180.
[131] Duval C. and Lecomte J., *Bull. Soc. Chim. Fr.* 1944 **11** 376.
[132] Duval C. and Lecomte J., *Bull. Soc. Chim. Fr.* 1946 **13** 477.
[133] Duval C. and Lecomte J., *C.R. Acad. Sci., Paris* 1941 **213** 998.
[134] Duval C. and Lecomte J., *C.R. Acad. Sci., Paris* 1942 **215** 131.
[135] Duval C. and Lecomte J., *C.R. Acad. Sci., Paris* 1943 **217** 42.
[136] Duval C. and Lecomte J., *C.R. Acad. Sci., Paris* 1944 **219** 483.
[137] Duval C. and Lecomte J., *C.R. Acad. Sci., Paris* 1954 **239** 249.
[138] Duval C. and Lecomte J., *C.R. Acad. Sci., Paris* 1955 **240** 66
[139] Eberhardt W. H. and Burke T. G., *J. Chem. Phys.* 1952 **20** 529.
[140] Edgell W. F. and May C. E., *J. Chem. Phys.* 1952 **20** 1822.
[141] Edgell W. F. and Ultee C. J., *J. Chem. Phys.* 1954 **22** 1983.
[142] El-Saban M. Z., Meister A. G. and Cleveland F. F., *J. Chem. Phys.* 1951 **19** 855.
[143] Evans J. C. and Bernstein H. J., *Canad. J. Chem.* 1956 **34** 1037.
[144] Evans J. C. and Bernstein H. J. *Canad. J. Chem.* 1956 **34** 1083.
[145] Evans J. C. and Wilmshurst J. K., *Canad. J. Chem.* 1956 **34** 1139.
[146] Eyster E. H. and Gillette R. H., *J. Chem. Phys.* 1940 **8** 369.
[147] Ferguson E. E., Hudson R. L., Nielsen J. R. and Smith D. C., *J. Chem. Phys.* 1953 **21** 1457.
[148] Ferguson E. E., Hudson R. L., Nielsen J. R. and Smith D. C., *J. Chem. Phys.* 1953 **21** 1464.
[149] Ferguson E. E., Hudson R. L., Nielsen J. R. and Smith D. C., *J. Chem. Phys.* 1953 **21** 1470.
[150] Ferguson E. E., Hudson R. L., Nielsen J. R. and Smith D. C., *J. Chem. Phys.* 1953 **21** 1727.
[151] Ferguson E. E., Hudson R. L., Nielsen J. R. and Smith D. C., *J. Chem. Phys.* 1953 **21** 1730.
[152] Ferguson E. E., Hudson R. L., Nielsen J. R. and Smith D. C., *J. Chem. Phys.* 1953 **21** 1736.
[153] Ferguson J. and Werner R. L., *J. Chem. Soc.* 1954 3645.
[154] Ferigle S. M., Cleveland F. F. and Meister A. G., *J. Chem. Phys.* 1952 **20** 1928.
[155] Fock J., *Z. Phys.* 1934 **90** 44.
[156] Fung L. W. and Barker E. F., *Phys. Rev.* 1934 **45** 238.
[157] Fuson N., Randall H. M. and Dennison D. M., *Phys. Rev.* 1939 **56** 982.
[158] Gage D. M. and Barker E. F., *J. Chem. Phys.* 1939 **7** 455.
[159] Ganz E., *Helv. Phys. Acta.* 1945 **18** 551.
[160] Garach J. and Lecomte J., *Bull. Soc. Chim. Fr.* 1946 415.
[161] Garach J. and Lecomte J., *C.R. Acad. Sci., Paris* 1946 **222** 74.
[162] Gates D. M., *J. Chem. Phys.* 1949 **17** 393.
[163] Gaunt J., *Trans Faraday Soc.* 1953 **49** 1122.
[164] Gaunt J., *Trans. Faraday Soc.* 1955 **51** 893.
[165] Genzel L. and Klier M., *Z. Phys.* 1956 **144** 25.
[166] Genzel L., *Z. Phys.* 1956 **144** 311.
[167] Gershinowitz H. and Wilson E. B., *J. Chem. Phys.* 1938 **6** 197.
[168] Gershinowitz H. and Wilson E. B., *J. Chem. Phys.* 1938 **6** 247.
[169] Giguère P. A. and Liu I. D., *J. Chem. Phys.* 1952 **20** 136.
[170] Giguère P. A. and Liu I. D., *Canad. J. Chem.* 1952 **30** 948.
[171] Giguère P. A. and Harvey K. B., *Canad. J. Chem.* 1956 **34** 798.
[172] Gore R. C., *Proc. Opt. Soc. Amer.* 1944 **34** 349.
[173] Grisenthwaite R. J. and Thompson H. W., *Trans. Faraday Soc.* 1954 **50** 212.
[174] Gutowsky H. S. and Stejskal E. O., *J. Chem. Phys.* 1954 **22** 939.
[175] Guy J. and Lecomte J., *Bull. Soc. Chim. Fr.* 1947 977.

[176] Haccuria M., *Bull. Soc. Chim. Belges.* 1953 **62** 428.
[177] Hadni A., *C.R. Acad. Sci., Paris* 1953 **236** 1761.
[178] Hadni A., *C.R. Acad. Sci., Paris* 1954 **238** 573.
[179] Hadni A., *C.R. Acad. Sci., Paris* 1954 **238** 2150.
[180] Hadni A., *C.R. Acad. Sci., Paris* 1954 **239** 349.
[181] Hadni A., *J. Phys. Radium* 1954 **15** 417.
[182] Hadni A., *J. Phys. Radium* 1956 **17** 77.
[183] Halverson F. and Williams V. Z., *J. Chem. Phys.* 1947 **15** 552.
[184] Halverson F., Stamm R. F. and Whalen J. J., *J. Chem. Phys.* 1948 **16** 808.
[185] Hansler R. L. and Oetjen R. A., *J. Chem. Phys.* 1953 **21** 1340.
[186] Harris L. and Beasley J. K., *J. Opt. Soc. Amer.* 1952 **42** 134.
[187] Hartough H. D., *Thiophene and its Derivatives* p.106. Interscience, New York 1952.
[188] Hawkins J. A. and Wilson M. K., *J. Chem. Phys.* 1953 **21** 360.
[189] Hawkins N. J. and Mattrow H. C., KAPL–1041. U.S.A.E.C. 1954.
[190] Heisler J. *et al.* CRLR–310–ASTIAD–28828. Army Chem. Center, Maryland.
[191] Hellwege K. H., *Ann. Phys.* 1939 **34** 521.
[192] Herzberg G., *Infrared and Raman Spectra of Polyatomic Molecules.* Van Nostrand New York, 1945.
[193] Herzfeld N., Ingold C. K. and Poole H. G., *J. Chem. Soc.* 1946 316.
[194] Hettner G., Pohlman R. and Schumacher H. J., *Z. Phys.* 1934 **91** 372.
[195] Hettner G., Pohlman R. and Schumacher H. J., *Z. Phys.* 1935 **96** 203.
[196] Hidalgo A., *C.R. Acad. Sci., Paris* 1954 **239** 253.
[197] Hopf H., *Z. Phys.* 1940 **116** 310.
[198] Hyde W. L., *J. Chem. Phys.* 1948 **16** 744.
[199] Jentzsch F. and Laski G., *Geiger-Schiels Handbuch der Physik* Vol. XIX p. 802. Springer, Berlin 1926.
[200] Jones E. A., Parkinson T. F. and Murray R. B., *J. Chem. Phys.* 1949 **17** 501.
[201] Jones E. A., Kirby-Smith J. S., Woltz P. J. H. and Nielsen A. H., *J. Chem. Phys.* 1951 **19** 242.
[202] Jones L. H. and McLaren E., *J. Chem. Phys.* 1954 **22** 1796.
[203] Jones L. H., *J. Chem. Phys.* 1955 **23** 2448.
[204] Jones R. N. and Lauzon R., *Nat. Res. Council Bull.* No. 3.
[205] Jones R. N. and Sandorfy C., *Chemical applications of Spectroscopy* Vol. IX, Ch. 4. Weissberger Series, Interscience, New York 1956.
[206] Kagarise R. E. and Daasch L. W., *J. Chem. Phys.* 1955 **23** 113.
[207] Kagarise R. E. and Daasch L. W., *J. Chem. Phys.* 1955 **23** 130.
[208] Kaiser W., Collins R. C. and Fan H. Y., *Naturwissenschaften* 1953 **40** 479.
[209] Kaiser W. and Fan H. Y., *Phys. Rev.* 1955 **98** 966.
[210] Kellner L., *Z. Phys.* 1929 **56** 215.
[211] Kellner L., *Reports on Progress in Physics* Vol. 8 p. 200. Physical Society, London 1942.
[212] Kellner L., *Trans. Faraday Soc.* 1945 **41** 217.
[213] Ketelaar J. A. A. and Vedder W., *Rec. Trav. Chim.* 1955 **74** 1482.
[214] Kettering C. F. and Sleator W. W., *Physics* 1933 **4** 39.
[215] Kilpatrick J. E. and Pitzer K. S., *J. Res. Nat. Bur. Stand.* 1947 **38** 191.
[216] Klemperer W., *J. Chem. Phys.* 1956 **24** 353.
[217] Koch B., *Ann. Phys.* 1938 **33** 335.
[218] Kuratani K. and Mizushima S. I., *J. Chem. Phys.* 1954 **22** 1403.
[219] Lagemann R. T. and Jones E. A., *J. Chem. Phys.* 1951 **19** 534.
[220] Lagemann R. T., Jones E. A. and Woltz P. J. H., *J. Chem. Phys.* 1952 **20** 1768.
[221] Lambert P. and Lecomte J., *Ann. Combustibles Liquides.* 1934 **9** 979.
[222] Lambert P. and Lecomte J., *Ann. Combustibles Liquides* 1935 **10** 1077.
[223] Lambert P., *Ann. Phys.* 1938 **10** 503.
[224] Lambert P. and Lecomte J., *C.R. Acad. Sci., Paris* 1938 **206** 1174.
[225] Lambert P. and Lecomte J., *C.R. Acad. Sci., Paris* 1939 **208** 740.
[226] Lambert P. and Lecomte J., *C.R. Acad. Sci., Paris* 1939 **208** 1148.

VOL. 13 1958/5

[227] Lamneck J. H., Hipsher H. F. and Fenn V. O., *NACA Technical Note* No. 3154, 1954.
[228] Larnaudie M., *C.R. Acad. Sci., Paris* 1950 **230** 1756.
[229] Lecomte J., *C.R. Acad. Sci., Paris* 1933 **196** 1011.
[230] Lecomte J., *C.R. Acad. Sci., Paris* 1929 **189** 155.
[231] Lecomte J., *C.R. Acad. Sci., Paris* 1934 **198** 65.
[232] Lecomte J., *C.R. Acad. Sci., Paris* 1935 **201** 1340.
[233] Lecomte J., *C.R. Acad. Sci., Paris* 1936 **203** 1501.
[234] Lecomte J., *C.R. Acad. Sci., Paris* 1937 **204** 1186.
[235] Lecomte J., *C.R. Acad. Sci., Paris* 1938 **206** 1568.
[236] Lecomte J., *C.R. Acad. Sci., Paris* 1938 **207** 395.
[237] Lecomte J., *C.R. Acad. Sci., Paris* 1939 **208** 1636.
[238] Lecomte J., and Mathieu J. P., *C.R. Acad. Sci., Paris* 1941 **213** 721.
[239] Lecomte J., *C.R. Acad. Sci., Paris* 1945 **221** 49.
[240] Lecomte J., *Cahiers-Phys.* 1943 **17**.
[241] Lecomte J., Piaux L. and Miller O., *Bull. Soc. Chim. Belges* 1934 **43** 239.
[242] Lecomte J., Piaux L. and Miller O., *Bull. Soc. Chim. Belges* 1936 **45** 123.
[243] Lecomte J., *J. Phys. Radium* 1937 **8** 489.
[244] Lecomte J., *J. Phys. Radium* 1938 **9** 13.
[245] Lecomte J., *J. Phys. Radium* 1938 **9** 512.
[246] Lecomte J., *J. Phys. Radium* 1939 **10** 423.
[247] Lecomte J., *J. Phys. Radium* 1945 **6** 127.
[248] Lecomte J., ibid. 1945 **6** 257.
[249] Lecomte J., *Bull. Soc. Chim. Fr.* 1956 163.
[250] Lecomte J. and Duval C. L., *Bull. Soc. Chim. Fr.* 1945 **12** 91.
[251] Lecomte J., *Bull. Soc. Chim. Fr.* 1945 **12** 706.
[252] Lee E. and Wu C. K., *Trans. Faraday Soc.* 1939 **35** 1366.
[253] Le Fevre R. J. and O'Dwyer M. F., *Austr. J. Chem.* 1953 **6** 341.
[254] Linnett J. W. and Avery W. H., *J. Chem. Phys.* 1938 **6** 686.
[255] Linnett J. W., *J. Chem. Phys.* 1938 **6** 692.
[256] Lippincott E. R. and O'Reilly E. J., *J. Chem. Phys.* 1955 **23** 238.
[257] Lindermeyer P. H. and Harris P. M., *J. Chem. Phys.* 1953 **21** 408.
[258] Long D. A., Murfin F. S. and Williams R. L., *Proc. Roy. Soc.* A 1954 **223** 251.
[259] Lord R. C. and Wright N., *J. Chem. Phys.* 1937 **5** 642.
[260] Lord R. C. and Nielsen E., *J. Chem. Phys.* 1951 **19** 1.
[261] Lord R. C. and Venkateswarlu P., *J. Chem. Phys.* 1952 **20** 1237.
[262] Lord R. C. and Steese C. M., *J. Chem. Phys.* 1954 **22** 542.
[263] Lord R. C., McDonald R. S. and Miller F. A., *J. Opt. Soc. Amer.* 1952 **42** 149.
[264] Lord R. C. and Venkateswarlu P., *J. Opt. Soc. Amer.* 1953 **43** 1079.
[265a] Lord R. C. and McCubbin T. K., *J. Opt. Soc. Amer.* 1957 **47** 689.
[265] Lord R. C., *Phys. Rev.* 1952 **85** 140.
[266] Maar O., *Z. Phys.* 1939 **113** 415.
[267] Madigan J. R. and Cleveland F. F., *J. Chem. Phys.* 1951 **19** 119.
[268] Malherbe F. E. and Bernstein H. J., *J. Amer. Chem. Soc.* 1952 **74** 4408.
[269] Malherbe F. E., Allen G. and Bernstein H. J., *Canad. J. Chem.* 1953 **31** 1223.
[270] Malm J. G., Weinstock B. and Classen H. H., *J. Chem. Phys.* 1955 **23** 2192.
[271] Mann D. E., Acquista J. and Plyler E. K., *J. Res. Nat. Bur. Stand.* 1954 **52** 67.
[272] Mann D. E. and Plyler E. K., *J. Chem. Phys.* 1953 **21** 1116.
[273] Mann D. E., Acquista N. and Plyler E. K., *J. Chem. Phys.* 1953 **21** 1949.
[274] Mann D. E., Acquista N. and Plyler E. K., *J. Chem. Phys.* 1954 **22** 1199.
[275] Mann D. E., Acquista N. and Plyler E. K., *J. Chem. Phys.* 1954 **22** 1586.
[276] Mann D. E. and Plyler E. K., *J. Chem. Phys.* 1955 **23** 1989.
[277] Mann D. E., Acquista N. and Plyler E. K., *J. Chem. Phys.* 1955 **23** 2122.
[278] Mann D. E., Meal J. H. and Plyler E. K., *J. Chem. Phys.* 1956 **24** 1018.
[279] Marrison L. W., *J. Sci. Instrum.* 1952 **29** 233.
[280] Martin J. M., Johnston R. W. B. and O'Neal M. J. J., *Analyt. Chem.* 1954 **26** 1886.
[281] Martz D. E. and Lagemann R. T., *J. Chem. Phys.* 1954 **22** 1193.

[282] Maru R. T., Sutherland G. B. B. M. and Tyrell H. V., *Phys. Rev.* 1954 **96** 801.
[283] Matossi F. and Kruger H., *Z. Phys.* 1936 **99** 1.
[284] Matossi F. and Bluschke H., *Z. Phys.* 1938 **108** 295.
[285] Matutano J. R. B., *Anales real. soc. espan fis y quim* A 1949 **45** 315.
[286] Matutano J. R. B. and Otero C., *Anales real. soc. espan fis y quim* B 1955 **51** 223.
[287] Maybury R. E., Katz J. J. and Gordon S., *Rev. Sci. Instrum.* 1954 **25** 1133.
[288] Maybury R. H., Gordon S. and Katz J. J., *J. Chem. Phys.* 1955 **23** 1277.
[289] Mayo D. W., Opitz H. E. and Peake J. S., *J. Chem. Phys.* 1955 **23** 1344.
[290] McCubbin T. K. and Sinton W. M., *J. Opt. Soc. Amer.* 1950 **40** 537.
[291] McCubbin T. K. and Sinton W. M., *J. Opt. Soc. Amer.* 1952 **42** 113.
[292] McCubbin T. K., *Dissertation*. Johns Hopkins Univ. 1951.
[293] McCubbin T. K., *J. Chem. Phys.* 1952 **20** 668.
[294] McGee P. R., Cleveland F. F., Meister A. G. and Decker C. E., *J. Chem. Phys.* 1953 **21** 242.
[295] McGovern J. J. and Friedel R. A., *J. Opt. Soc. Amer.* 1947 **37** 660.
[296] McMurry H. L., *J. Chem. Phys.* 1941 **9** 231.
[297] Mecke R. and Spiesecke H., *Spectrochim. Acta.* 1956 **7** 387.
[298] Meyrick C. I. and Thompson H. W., *J. Chem. Soc.* 1950 225.
[299] Millazzo G. and Gerding H., *Rec. Trav. Chim.* 1953 **72** 957.
[300] Miller F. A. and Crawford B. L., *J. Chem. Phys.* 1946 **14** 282.
[301] Miller F. A. and Crawford B. L., *J. Chem. Phys.* 1946 **14** 292.
[302] Miller F. A. and Hannan R. B., *J. Chem. Phys.* 1953 **21** 110.
[303] Miller F. A. and Bauman R. P., *J. Chem. Phys.* 1954 **22** 1544.
[304] Miller S. I., Weher A. and Cleveland F. F., *J. Chem. Phys.* 1955 **23** 44.
[305] Mills I. M., Scherer J. R., Crawford B. and Youngquist M., *J. Opt. Soc. Amer.* 1955 **45** 785.
[306] Mirone P. and Bonino C., *Atti. accad. nazl. Lincei. Rend. Classe Sci. fis mat. e nat.* 1954 **17** 250.
[307] Mirone P., *Gazz. Chim. Ital.* 1956 **86** 165.
[308] Miyazawa T., *J. Chem. Soc. Japan* 1956 **77** 526.
[309] Mochel W. E. and Hall M. B., *J. Amer. Chem. Soc.* 1949 **71** 4082.
[310] Momin A. U., *Proc. Indian Acad. Sci.* A 1953 **37** 254.
[311] Moore G. E. and Badger R. M., *J. Amer. Chem. Soc.* 1952 **74** 6076.
[312] Mortimer F. S., Blodgett R. B. and Daniels F., *J. Amer. Chem. Soc.* 1947 **69** 822.
[313] Muller R. H., *Analyt. Chem.* 1956 **28** 73A.
[314] Murray M. J. and Cleveland F. F., *J. Chem. Phys.* 1940 **8** 133.
[315] Nakagawa I. and Mizushima S. I., *J. Chem. Phys.* 1953 **21** 2195.
[316] Narosimham N. A., El-Sabban M. Z. and Nielsen J. R., *J. Chem. Phys.* 1956 24 420.
[317] *News Letter*. Jarrell-Ash Co., Newtonville, Mass., May 1955.
[318] Nichols E. H., *Phys. Rev.* 1897 **4** 314.
[319] Nielsen A. H., *Recent Advances in Infrared Spectroscopy*. Tech. Mem. 53-2, Office of Ordance Research.
[320] Nielsen A. H., Burke T. G., Woltz P. J. H. and Jones E. A., *J. Chem. Phys.* 1952 **20** 596.
[321] Nielsen A. H. and Woltz P. J. H., *J. Chem. Phys.* 1952 **20** 1878.
[322] Nielsen J. R. and McMurry H. L., *J. Chem. Phys.* 1948 **16** 67.
[323] Nielsen J. R., Claassen H. H. and Smith D. C., *J. Chem. Phys.* 1950 **18** 1471.
[324] Nielsen J. R., Liang C. Y. and Smith D. C., *J. Chem. Phys.* 1952 **20** 1090.
[325] Nielsen J. R., Claassen H. H. and Smith D. C., *J. Chem. Phys.* 1952 **20** 1916.
[326] Nielsen J. R., Liang C. Y., Smith R. M. and Smith D. C., *J. Chem. Phys.* 1953 **21** 383.
[327] Nielsen J. R., Liang C. Y. and Smith D. C., *J. Chem. Phys.* 1953 **21** 1060.
[328] Nielsen J. R., Liang C. Y., Smith D. C. and Alpert M., *J. Chem. Phys.* 1953 **21** 1070.
[329] Nielsen J. R., El-Sabban M. Z. and Alpert M., *J. Chem. Phys.* 1955 **23** 324.
[330] Nielsen J. R., Claassen H. H. and Moran N. B., *J. Chem. Phys.* 1955 **23** 329.
[331] Nielsen J. R., Liang C. Y. and Daasch L. W., *J. Opt. Soc. Amer.* 1953 **43** 1071.

VOL. 13 1958/5

[332] Nightingale R. E. and Wagner E. L., *J. Chem. Phys.* 1954 **22** 203.
[333] Noether H. D., *J. Chem. Phys.* 1942 **10** 664.
[334] Oetjen R. A., Haynie W. H., Ward W. M., Hansler R. L., Schauwecker H. E. and Bell E. E., *J. Opt. Soc. Amer.* 1952 **42** 559.
[335] O'Loane J. K., *J. Chem. Phys.* 1953 **21** 669.
[336] O'Loane J. K. and Wilson M. K., *J. Chem. Phys.* 1955 **23** 1313.
[337] Osberg W. E. and Hornig D. F., *J. Chem. Phys.* 1952 **20** 1345.
[338] Oshesky G. D. and Bentley F. F., *J. Amer. Chem. Soc.* 1957 **79** 2057.
[339] Otero C. and Matutano J. R. B., *Anales real. soc. espan. fis y quim* B 1956 **52** 291.
[340] Pace E. L. and Pierce L., *J. Chem. Phys.* 1955 **23** 1248.
[341] Pajeau R. and Lecomte J., *Bull. Soc. Chim.* 1946 412.
[342] Palik E. D., *J. Chem. Phys.* 1955 **23** 217.
[343] Palik E. D., *J. Chem. Phys.* 1955 **23** 980.
[344] Parodi M. M., *C.R. Acad. Sci., Paris* 1937 **204** 1111.
[345] Parodi M. M., *C.R. Acad. Sci., Paris* 1937 **204** 1636.
[346] Parodi M. M., *C.R. Acad. Sci., Paris* 1937 **205** 607.
[347] Parodi M. M., *C.R. Acad. Sci., Paris* 1938 **207** 1196.
[348] Parodi M. M., *C.R. Acad. Sci., Paris* 1941 **212** 1138.
[349] Parodi M. M., *C.R. Acad. Sci., Paris* 1942 **214** 542.
[350] *Perkin–Elmer Instrument News* 1956 **7** No. 3 7.
[351] Perkins W. D. and Wilson M. K., *J. Chem. Phys.* 1952 **20** 1791.
[352] Person W. B., Pimentel G. C. and Schnepp O., *J. Chem. Phys.* 1955 **23** 230.
[353] Pickett L. W., *J. Chem. Phys.* 1942 **10** 660.
[354] Pimentel G. C. and McClellan A. L., *J. Chem. Phys.* 1952 **20** 270.
[355] Pitzer K. S., *J. Chem. Phys.* 1944 **12** 310.
[356] Pitzer K. S. and Scott D. W., *J. Amer. Chem. Soc.* 1943 **65** 803.
[357] Pitzer K. S. and Hollenberg J. L., *J. Amer. Chem. Soc.* 1953 **75** 2219.
[358] Pitzer K. S. and Hollenberg J. L., *J. Amer. Chem. Soc.* 1954 **76** 1493.
[359] Plyler E. K. *et al.*, *J. Res. Nat. Bur. Stand.* 1947 **38** 499.
[360] Plyler E. K., Stair R. and Humphreys C. J., *J. Res. Nat. Bur. Stand.* 1947 **38** 211.
[361] Plyler E. K., *J. Res. Nat. Bur. Stand.* 1948 **41** 125.
[362] Plyler E. K. and Acquista N., *J. Res. Nat. Bur. Stand.* 1949 **43** 37.
[363] Plyler E. K., Smith W. H. and Acquista N., *J. Res. Nat. Bur. Stand.* 1950 **44** 503.
[364] Plyler E. K. and Lamb M. A., *J. Res. Nat. Bur. Stand.* 1951 **46** 382.
[365] Plyler E. K. and Benedict W. S., *J. Res. Nat. Bur. Stand.* 1951 **47** 202.
[366] Plyler E. K. and Acquista N., *J. Res. Nat. Bur. Stand.* 1952 **48** 92.
[367] Plyler E. K. and Acquista N., *J. Res. Nat. Bur. Stand.* 1952 **49** 51.
[368] Plyler E. K., *Instrumentation for High Resolution.* Presented at the Columbus Symposium on Molecular Spectroscopy, June 1957.
[369] Plyler E. K., *J. Phys. Radium.* 1954 **15** 519.
[370] Plyler E. K., *J. Chem. Phys.* 1947 **15** 885.
[371] Plyler E. K., *J. Chem. Phys.* 1948 **16** 1008.
[372] Plyler E. K., *J. Chem. Phys.* 1949 **17** 218.
[373a] Plyler E. K. and Acquista N., *J. Res. Nat. Bur. Stand.* 1954 **56** 149.
[373] Plyler E. K. and Acquista N., *J. Res. Nat. Bur. Stand.* 1955 **23** 752.
[374] Plyler E. K., *J. Opt. Soc. Amer.* 1947 **37** 746.
[375] Plyler E. K., *J. Opt. Soc. Amer.* 1948 **38** 664.
[376] Plyler E. K. and Ball J. J., *J. Opt. Soc. Amer.* 1952 **42** 266.
[377] Polo S. R. and Wilson M. K., *J. Chem. Phys.* 1953 **21** 1129.
[378] Polo S. R. and Wilson M. K., *J. Chem. Phys.* 1954 **22** 900.
[379] Polo S. R., Palm A., Voelz F. L., Cleveland F. F., Meister A. G., Bernstein R. B. and Sherman R. H., *J. Chem. Phys.* 1955 **23** 833.
[380] Pontarelli D. A., Meister A. G., Cleveland F. F., Voelz F. L., Bernstein R. B. and Sherman R. H., *J. Chem. Phys.* 1952 **20** 1949.
[381] *Preliminary Tech. Bull.* 43A, Baird-Atomics, Cambridge Mass.

[382] Price D., *J. Chem. Phys.* 1941 **9** 725.
[383] Price W. C., *J. Chem. Phys.* 1949 **17** 1044.
[384] Price W. C., Fraser R. D. B., Robinson T. S. and Longuett-Higgins H. C., *Disc. Faraday Soc.* 1950 **9** 131.
[385] Pristera F., *Appl. Spectroscopy* 1952 **6** 29.
[386] Pulford A. G. and Walsh A., *Trans. Faraday Soc.* 1951 **47** 347.
[387] Ramdas A. K., *Proc. Indian Acad. Sci.* A 1952 **36** 55.
[388] Ramdas A. K., *Proc. Indian Acad. Sci.* A 1953 **37** 441.
[389] Ramdas A. K., *Proc. Indian Acad. Sci.* A 1953 **37** 451.
[390] Ramdas A. K., *Proc. Indian Acad. Sci.* A 1954 **39** 81.
[391] Raman C. V., *Nature, Lond.* 1948 **161** 165.
[392] Randall H. M., *Science* 1927 **65** 167.
[393] Randall H. M. and Firestone F. A., *Rev. Sci. Instrum.* 1938 **9** 404.
[394] Randall H. M., *Rev. Sci. Instrum.* 1932 **3** 196.
[395] Randall H. M., *J. Opt. Soc. Amer.* 1954 **44** 97.
[396] Randall H. M. and Barker E. F., *Phys. Rev.* 1934 **45** 124.
[397] Randall H. M., Dennison D. M., Ginsberg N. and Weber L. R., *Phys. Rev.* 1937 **52** 160.
[398] Randall H. M., *Rev. Modern Phys.* 1938 **10** 72.
[399] Randall H. M., *J. Appl. Phys.* 1939 **10** 768.
[400] Rao K. N. and Palik E. D., *J. Chem. Phys.* 1955 **23** 2112.
[401] Rasmussen R. S., *J. Chem. Phys.* 1943 **11** 249.
[402] Rasmussen R. S. and Brattain R. R., *J. Chem. Phys.* 1947 **15** 120.
[403] Rathjens G. W., Freeman N. K., Gwinn W. D. and Pitzer K. S., *J. Amer. Chem. Soc.* 1953 **75** 5634.
[404] Reding F. P. and Horning D. F., *J. Chem. Phys.* 1951 **19** 594.
[405] Richards R. E. and Thompson H. W., *J. Chem. Soc.* 1949 124.
[406] Richardson W. S. and Goldstein J. H., *J. Chem. Phys.* 1950 **18** 1314.
[407] Rix H. D., *J. Chem. Phys.* 1953 **21** 1077.
[408] Rix H. D., *J. Chem. Phys.* 1954 **22** 429.
[409] Rubens H. and Nichols E. F., *Ann. Phys. Chem.* 1897 **60**.
[410] Rubens H. and Woods R. W., *Berl. Ber.* 1910 1122.
[411] Rubens H. and Woods R. W., *Phil. Mag.* 1911 **21** 249.
[412] Rubens H. and Von Baeyer O., *Phil. Mag.* 1911 **21** 689.
[413] Sachsse H. and Bartholome E., *Z. phys. Chem.* B 1935 **28** 257.
[414] Schaefer C. and Matossi F., *Das Ultrarote Spektrum* p. 60. Springer, Berlin 1930.
[415] Schaefer C. and Kern R., *Z. Phys.* 1932 **78** 609.
[416] Schaefer C., Matossi F. and Wirtz K., *Z. Phys.* 1934 **89** 210.
[417] Schneider W. G. and Bernstein H. J., *Trans. Faraday Soc.* 1956 **52** 13.
[418] Shapiro C. V., Gibbs R. C. and Johnson J. R., *Phys. Rev.* 1931 **38** 1170.
[419] Shearin P. E. and Plyler E. K., *J. Opt. Soc. Amer.* 1938 **28** 61.
[420] Sheline R. K. and Pitzer K. S., *J. Amer. Chem. Soc.* 1950 **72** 1107.
[421] Sheppard N. and Sutherland G. B. B. M., *J. Chem. Soc.* 1947 453.
[422] Sheppard N., *J. Chem. Phys.* 1949 **17** 74.
[423] Sheppard N. and Sutherland G. B. B. M., *Proc. Roy. Soc.* 1949 **196** 195.
[424] Short L. N. and Thompson H. W., *J. Chem. Soc.* 1952 **168**.
[425] Siegler E. H. and Flynn T. F., *Abstract of Columbus Symposium on Molecular Spectroscopy*, June 1956.
[426] Simova P., *Izvest. Bulgar Adak. Nauk. Otdel. Fiz Mat. i Tekh. Nauki Ser. Fiz.* 1951 **2** 107.
[427] Simpson D. and Plyler E. K., *J. Res. Nat. Bur. Stand.* 1953 **50** 223.
[428] Singer W. E., *Phys. Rev.* 1947 **71** 531.
[429] Sleator W. W., *Phys. Rev.* 1931 **38** 147.
[430] Smith A. L., *J. Chem. Phys.* 1953 **21** 1997.
[431] Smith A. L., Unpublished work, Dow Corning Corp. 1955.
[432] Smith D. C., Nielsen J. R. and Claassen H. H., *J. Chem. Phys.* 1950 **18** 326.
[433] Smith D. C., Brown G. M., Nielsen J. R., Smith R. M. and Liang C. Y., *J. Chem. Phys.* 1952 **20** 473.

VOL. 13 1958/5

[434] Smith D. C., Saunders R. A., Nielsen J. R. and Ferguson E. E., *J. Chem. Phys.* 1952 **20** 847.
[435] Smith D. C., Ferguson E. E., Hudson R. L. and Nielsen J. R., *J. Chem. Phys.* 1953 **21** 1475.
[436] Smith L. G. and Woodward W. M., *Phys. Rev.* 1942 **61** 386.
[437] Sohm M., *Z. Phys.* 1940 **116** 34.
[438] Spitzer W. G. and Fan H. Y., *Phys. Rev.* 1955 **99** 1893.
[439] Stafford R. W. and Barnes R. B., *J. Opt. Soc. Amer.* 1944 **34** 348.
[440] Stewart H. B. and Neilsen H. H., *Phys. Rev.* 1949 **75** 640.
[441] Stewart J. E., *J. Res. Nat. Bur. Stand.* 1956 **56** 337.
[442] Stewart J. E., *J. Chem. Phys.* 1955 **23** 2204.
[443] Stitt F., *J. Chem. Phys.* 1939 **7** 297.
[443] Stitt F., 1939 **7** 297.
[444] Stitt F., *J. Chem. Phys.* 1940 **8** 56.
[445] Stitt F., *J. Chem. Phys.* 1941 **9** 780.
[446] Strong J., *Phys. Rev.* 1931 **37** 1565.
[447] Strong J., *Phys. Rev.* 1931 **37** 1661.
[448] Strong J., *Phys. Rev.* 1931 **38** 1818.
[449] Strong J. and Woo S. C., *Phys. Rev.* 1932 **42** 267.
[450] Strong J., *Phys. Today* 1951 **4** 4.
[451] Strong J., *Rev. Sci. Instrum.* 1932 **3** 810.
[452] Stroup R. E., Oetjen R. A. and Bell E. E., *J. Chem. Phys.* 1953 **21** 2072.
[453] Stroup R. E. and Oetjen R. A., *J. Chem. Phys.* 1953 **21** 2092.
[454] Stroup R. E., Oetjen R. A. and Bell E. E., *J. Opt. Soc. Amer.* 1953 **43** 1096.
[455] Stuart A. V. and Sutherland G. B. B. M., *J. Chem. Phys.* 1956 **24** 559.
[456] Sutherland G. B. B. M. and Simpson D. M., *J. Chem. Phys.* 1947 **15** 153.
[457] Sutherland G. B. B. M. and Penny W. G., *Proc. Roy. Soc.* A 1936 **156** 678.
[458] Szasz G. J., McCartney J. S. and Rank D. H., *J. Amer. Chem. Soc.* 1947 **69** 3150.
[459] Talley R. M. and Nielsen A. H., *J. Chem. Phys.* 1954 **22** 2030.
[460] Tarpley W. and Vitiello C., *Analyt. Chem.* 1952 **24** 315.
[461] Tarte P., *Bull. Soc. Chim. Fr.* 1951 **60** 227.
[462] Tarte P., *J. Chem. Phys.* 1952 **20** 1570.
[463] Taylor A. M., *Trans. Faraday Soc.* 1929 **25** 314.
[464] Taylor J. H., Benedict W. S. and Strong J., *J. Chem. Phys.* 1952 **20** 1884.
[465] Teranishi R. and Decius J. C., *J. Chem. Phys.* 1954 **22** 896.
[466] Thompson H. W. and Temple R. B., *J. Chem. Soc.* 1948 1422.
[467] Thompson H. W. and Harris G. P., *Trans. Faraday Soc.* 1942 **38** 37.
[468] Thompson H. W. and Torkington P., *Trans Faraday Soc.* 1945 **41** 246.
[469] Thompson H. W., *Trans. Faraday Soc.* 1946 **42** 432.
[470] Thompson H. W. and Torkington P., *Proc. Roy. Soc.* A 1945 **184** 21.
[471] Tilton L. W., Plyler E. K. and Stephens R. E., *J. Res. Nat. Bur. Stand.* 1949 **43** 81.
[472] Torkington P., *Proc. Roy. Soc.* 1951 **206** 17.
[473] Torkington P. and Thompson H. W., *J. Chem. Soc.* 1944 303.
[474] Torkington P. and Thompson H. W., *Trans. Faraday Soc.* 1945 **41** 184.
[475] Torkington P. and Thompson H. W., *Trans Faraday Soc.* 1945 **41** 236.
[476] Trotter I. F. and Thompson H. W., *J. Chem. Soc.* 1946 481.
[477] Ueno K., and Martell A. E., *J. Phys. Chem.* 1955 **59** 998.
[478] Venkateswarlu P., *J. Chem. Phys.* 1951 **19** 293.
[479] Venkateswarlu P., *J. Chem. Phys.* 1952 **20** 923.
[480] Venkateswarlu P., *J. Chem. Phys.* 1952 **20** 1810.
[481] Voelz F. L., Cleveland F. F. and Meister A. G., *J. Opt. Soc. Amer.* 1953 **43** 1061.
[482] Wagstaffe F. J. and Thompson H. W. *Trans. Faraday Soc.* 1944 **40** 41.
[483] Waldron R. D., *J. Chem. Phys.* 1953 **21** 734.
[484] Waldron R. D., *Phys. Rev.* 1955 **99** 1727.
[485] Walsh A., *J. Opt. Soc. Amer.* 1952 **42** 213.

[486] Wells A. J., *J. Appl. Phys.* 1940 **11** 137.
[487] Wells A. J. and Wilson E. B., *J. Chem. Phys.* 1941 **9** 314.
[488] Weniger W., *Rev. Sci. Instrum.* 1936 **7** 436.
[489] Weniger W., *J. Opt. Soc. Amer.* 1923 **7** 517.
[490] West W. and Farnsworth M., *Trans. Faraday Soc.* 1931 **27** 145.
[491] White J. U., *J. Opt. Soc. Amer.* 1947 **37** 713.
[492] Williams V. Z., *Rev. Sci. Instrum.* 1948 **19** 135.
[493] Williams V. Z., *Science* 1951 **113** 51.
[494] Wilson E. B. and Wells A. S., *J. Chem. Phys.* 1941 **9** 319.
[495] Wilson M. K. and Polo S. R., *J. Chem. Phys.* 1952 **20** 1716.
[496] Wilson T. P., *J. Chem. Phys.* 1943 **11** 361.
[497] Woltz P. J. H. and Nielsen A. H., *J. Chem. Phys.* 1952 **20** 307.
[498] Woltz P. J. H., Jones E. A. and Nielsen A. H., *J. Chem. Phys.* 1952 **20** 378.
[499] Wright N. and Randall H. M., *Phys. Rev.* 1933 **44** 391.
[500] Wright N., *J. Biol. Chem.* 1937 **120** 641.
[501] Wu T. Y., *J. Chem. Phys.* 1939 **7** 965.
[502] Wu T. Y., *J. Chem. Phys.* 1942 **10** 116.
[503] Wu T. Y., *Phys. Rev.* 1934 **46** 465.
[504] Wu V. L. and Barker E. F., *J. Chem. Phys.* 1941 **9** 487.
[505] Yoshinaga H., *J. Chem. Phys.* 1955 **23** 2206.
[506] Yoshinaga H. and Oetjen R. A., *J. Opt. Soc. Amer.* 1955 **45** 1085.
[507] Yoshinaga H. and Oetjen R. A., *Phys. Rev.* 1956 **101** 526.
[508] Yoshino T., *Bull. Chem. Soc. Japan* 1954 **27** 592.
[509] Zurcher R. F. and Gunthard H. H., *Helv. Chim. Acta.* 1955 **38** 849.

VOL.
13
1958/5

Spectrochimica Acta, 1958, Vol. 13, pp. 31 to 37. Pergamon Press Ltd., London

Infrared absorption spectra of inorganic co-ordination complexes—XVII*

Infrared spectra of platinum(II) and palladium(II) ammine complexes

San-ichiro Mizushima,† Ichiro Nakagawa, M. J. Schmelz,‡
C. Curran and J. V. Quagliano

(*Received* 19 *May* 1958)

Abstract—The infrared spectra of $[Pt(NH_3)_4]Br_2$, $[Pt(NH_3)_4]Cl_2$, $[Pd(NH_3)_4]Cl_2$, $Pt(NH_3)_2C_2O_4$, $Pd(NH_3)_2C_2O_4$, *cis*- and *trans*-$Pt(NH_3)_2Cl_2$, and *cis*- and *trans*-$Pd(NH_3)_2Cl_2$, have been measured in the 2–15 μ region. Assignment of the observed absorption bands is reported. Skeletal frequencies have been calculated and the nature of the ligand-to-metal bond is discussed.

Introduction

In light of previous investigations, many infrared absorption bands of metal ammine complexes can be explained. The H—N stretching vibrations in different types of ligands have been characterized [1] and a systematic study of the three deformation vibrations of NH_3 co-ordinated with a variety of metals has been reported [2]. The infrared spectra of many Co(II) and Co(III) ammine complexes have been examined and the NH_3 deformation frequencies have been assigned on the basis of the normal vibration calculations [3, 4]. Similar studies of chloro and oxalato ammine complexes of Pt(II) and Pd(II) are reported in this paper. Several of these complexes have also been investigated by Powell and Sheppard [5] who based their assignment of the hydrogenic vibrations on deuteration effects.

Experimental

Preparation of compounds

Tetrammineplatinum(II) chloride, $[Pt(NH_3)_4]Cl_2$, was prepared by the method of Keller [6].

Anal. Calcd. for $[Pt(NH_3)_4]Cl_2$: N, 16·76; H, 3·62. Found: N, 16·49; H, 3·74.

Tetramminepalladium(II) chloride, $[Pd(NH_3)_4]Cl_2$, was prepared by dissolving diamminedichloropalladium (II) in liquid ammonia and allowing the excess ammonia to evaporate.

Anal. Calcd. for $[Pd(NH_3)_4]Cl_2$: Cl, 28·97. Found: 28·71. *cis*-Diamminedichloroplatinum(II), $Pt(NH_3)_2Cl_2$, was prepared by the method of Jorgensen [7].

Anal. Calcd. for $Pt(NH_3)_2Cl_2$: Cl, 23·62. Found: 23·81. *trans*-Diamminedichloroplatinum(II), $Pt(NH_3)_2Cl_2$, was prepared by the method of Ramberg [8].

Anal. Calcd. for $Pt(NH_3)_2Cl_2$: Cl, 23·62. Found: 23·85. *cis*-Diamminedichloropalladium(II), $Pd(NH_3)_2Cl_2$, was prepared as described by Grinberg [9].

* For paper XVI in this series, see *J. Amer. Chem. Soc.* **80**, 5081 (1958).

† Visiting Professor, from the Faculty of Science, University of Tokyo.

‡ Sister Mary Judith, R.S.M. Supported in part under AEC Contract AT(11–1)–38, Radiation Project of the University of Notre Dame; Contribution from the Department of Chemistry, University of Notre Dame.

Anal. Calcd. for $Pd(NH_3)_2Cl_2$: Cl, 33·50. Found: 33·68. *trans*-Diamminedichloropalladium(II), $Pd(NH_3)_2Cl_2$, was prepared by the method of Mann *et al.* [10].

Anal. Calcd. for $Pd(NH_3)_2Cl_2$: Cl, 33·50. Found: 33·78. Diammineoxalatoplatinum(II), $Pt(NH_3)_2C_2O_4$, was prepared by the method of Grinberg [11].

Anal. Calcd. for $Pt(NH_3)_2C_2O_4$: NH_3, 10·72. Found: 10·43. Diammineoxalatopalladium(II), $Pd(NH_3)_2C_2O_4$, was prepared as described by Mann *et al.* [12].

Anal. Calcd. for $Pd(NH_3)_2C_2O_4$: C_2O_4, 38·47. Found: 37·98.

Absorption measurements. All spectra were obtained by means of a Perkin–Elmer Model 21 recording infrared spectrophotometer, using NaCl and CaF_2 prisms. Compounds were prepared in KBr discs and their spectra checked in Nujol mulls.

Results

Table 1 lists the frequencies and intensities of the observed infrared bands, and the assignment of these bands, to be explained in the discussion.

Discussion

(A) *The square planar complexes* $[Pt(NH_3)_4]^{++}$, $[Pd(NH_3)_4]^{++}$, cis *and* trans-$Pt(NH_3)_2Cl_2$, *and* cis *and* trans-$Pd(NH_3)_2Cl_2$. The frequencies of the NH_3 ligands present in the dichloro Pt(II) and Pd(II) complexes can be treated separately because they are much higher than those of nitrogen-to-metal and chlorine-to-metal frequencies.

The H—N stretching frequencies are observed in the 3μ region. The NH_3 deformation frequencies have been calculated according to the method described in previous papers [2, 13]. The deformation (H) and repulsive (F) force constants and the intramolecular tension (κ) used in this calculation are shown in Table 2. The values of these constants, except for H(HNM) and $F(H \cdots M)$, are the same as those of Co(II) and Co(III) complexes [3, 4]. Furthermore, the same values of H(HNH) and $F(H \cdots H)$ have been used successfully in the normal vibration calculation of NH_3 and NH_4^+ [13].

The calculated frequencies of the NH_3 deformation vibrations have been found to agree favourably with the observed frequencies as shown in Table 3. The calculation showed that the degenerate deformation frequency depends on H(HNH) and $F(H \cdots H)$, the rocking frequency on H(HNM) and $F(H \cdots M)$, and the symmetric deformation frequency on all four constants. Therefore it follows that differences in the nature of the central metal atom should be reflected very strongly in the value of the ammonia rocking frequency, considerably in the symmetric deformation frequency and very little in the degenerate deformation frequency. This is the case as shown in Table 3.

In the spectra of the dichlorodiammines of both Pt(II) and Pd(II) as seen in Fig. 1, doublets are observed for the *cis* complexes in the region of the NH_3 symmetrical deformation frequencies, whereas only a single peak is observed for each of the *trans* complexes.

From the above discussion the nature of the vibration appearing as infrared absorptions in the NaCl region can be explained. Furthermore, the values of the NH_3 rocking frequencies (in other words, the value of H(HNM), indicate considerable covalent character of the metal-to-nitrogen bond. The nature of this bond

VOL.
13
1958/5

Table 1. Observed frequencies (cm^{-1}) of Pt(II) and Pd(II) ammine complexes and their assignments

$[Pt(NH_3)_4]Cl_2$	$[Pd(NH_3)_4]Cl_2$	*c*-$Pt(NH_3)_2Cl_2$	*t*-$Pt(NH_3)_2Cl_2$	*c*-$Pd(NH_3)_2Cl_2$	*t*-$Pd(NH_3)_2Cl_2$	$Pt(NH_3)_2C_2O_4$	$Pd(NH_3)_2C_2O_4$	Assignment
3130 vs, b	3120 vs, b	3270 vs	3260 vs	3300 vs	3330 vs	3250 s	3250 s	ν(N—H)
—	—	3200 s	3185	3200 vs	3260 vs	3200 s	3150 s	ν(N—H)
—	—	—	—	—	—	1690 vs	1695 vs	ν(C=O)
—	—	—	—	—	—	1665 vs	1665 vs	ν(C=O)
1630 s, b	1620 s, b	1628 m	1645 m, 1594 m	1605 s	1615 s	1592 s	1630 s	$\delta(NH_3$ deg)
1570 s	—	1544 m	1540 m	—	—	1573 s	—	$\delta(NH_3$ deg)
—	—	—	—	—	—	1395 vs	1400 vs	ν(C—O)
1370 sh	1335 s	1315 s	1290 vs	1265 sh	1255 vs	1352 s	1335 sh	$\delta(NH_3$ sym)
1352 vs								
1333 sh	1310 vs, 1285 s	1303 s	—	1246 vs	—	—	1315 s	$\delta(NH_3$ sym)
—	—	—	—	—	—	1250 s	1250 s	ν(C—O)
—	—	—	—	—	—	900 vw	895 vw	ν(C—C)
—	—	—	—	—	—	832 s, 850 sh	823 s	δ(O—C=O)
840 s	840 s	796 s	819 s	745 m, b	757 s	792 s	779 m	$\delta(NH_3$ rock)
—	800 s	—	—	—	—	—	760 sh	$\delta(NH_3$ rock)

vs = very strong; s = strong; m = medium; w = weak; sh = shoulder; b = broad; vw = very weak;
c = *cis*; *t* = *trans*.
ν = stretching vibration; δ = deformation vibration; deg = degenerate; sym = symmetric; rock = rocking.

can be determined more directly from the values of the corresponding stretching frequencies (skeletal frequencies). But these frequencies lie beyond the NaCl region examined in this investigation. On the basis of the Raman frequencies in the low frequency region reported by Mathieu [14], however, we can calculate

Table 2. Force constants in 10^5 dyn/cm and intramolecular tension (κ) in 10^{-11} dyn/cm

$H(\mathrm{HNH}) = 0.540$,	$F(\mathrm{H}\cdots\mathrm{H}) = 0.060$,	$\kappa = -0.040$
$H(\mathrm{HNM}) = 0.12 \sim 0.18$ (variable),*	$F(\mathrm{H}\cdots\mathrm{M}) = 0.10$	

* See Table 3.

these skeletal vibrations. Considering the NH_3 group to be a dynamic unit, we can treat the skeletal vibrations of the $[Pt(NH_3)_4]^{++}$ ion as those of a five-body model of the point group D_{4h}.

Using the symmetry coordinates corresponding to each symmetry class, the

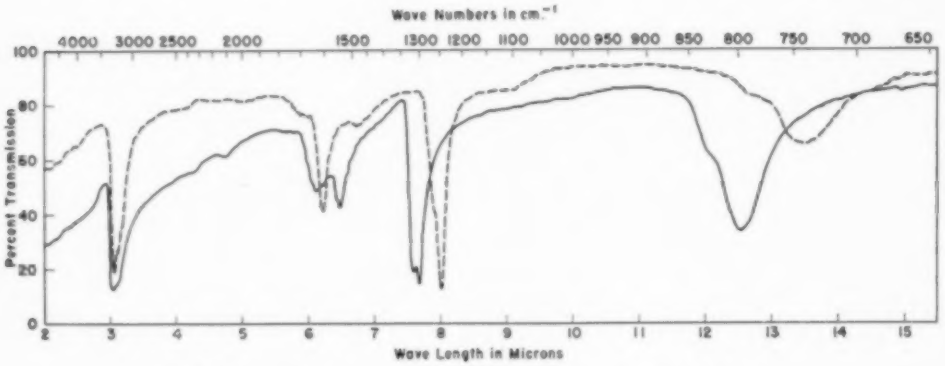

Fig. 1.——— *cis*-Diamminedichloroplatinum(II), $Pt(NH_3)_2Cl_2$
– – – – *cis*-Diamminedichloropalladium(II), $Pd(NH_3)_2Cl_2$

secular equation is set up according to Wilson's procedure [15]. The G and F matrices of this equation are calculated as:

$$G_{A_{1g}} = (\mu_B) \qquad F_{A_{1g}} = (K + 2F)$$

$$G_{B_{1g}} = (4\mu_B) \qquad F_{B_{1g}} = \left(H + \frac{11}{20}F\right)$$

$$G_{B_{2g}} = (\mu_B) \qquad F_{B_{2g}} = \left(K - \frac{1}{5}F\right)$$

$$G_{E_u} = \begin{pmatrix} \mu_B + 2\mu_A & 2\sqrt{(2\mu_A)} \\ 2\sqrt{(2\mu_A)} & 2(\mu_B + 2\mu_A) \end{pmatrix} \qquad F_{E_u} = \begin{pmatrix} K + \frac{9}{10}F & -\frac{9\sqrt{2}}{20}F \\ -\frac{9\sqrt{2}}{20}F & H + \frac{11}{20}F \end{pmatrix}$$

VOL. 13 1958/5

Table 3. The calculated and observed coordinated NH_3 deformation frequencies (cm^{-1})

	$[Pt(NH_3)_4]^{++}$		$[Pd(NH_3)_4]^{++}$			$Pd(NH_3)_2Cl_2$		
	Calculated	Observed $[Pt(NH_3)_4]Cl_2$	Calculated	Observed $[Pd(NH_3)_4][PtCl_4]$*	Observed $[Pd(NH_3)_2]Cl_2$	Calculated	Observed *cis*	Observed *trans*
Degenerate Deformation	1579	1630	1579	1632	1620	1579	1605	1615
Symmetric Deformation	1345	1370 sh 1352 1333 sh	1292	1283	1335 1310 1285	1268	1265 1246	1255
Rocking Deformation	860	840	785	785	840 800	748	745	757
Values of H(HNM) (10^5 dyn/cm)		0·177		0·142			0·127	

* For observed frequencies of $[Pd(NH_3)_4][PdCl_4]$, see reference [3].

Here μ_A and μ_B are the reciprocals of the masses of the Pt atom and the NH_3 group, K is the Pt—N bond stretching force constant, H is the force constant for the deformation of the N—Pt—N bond angle, and F is the force constant for the non-bonded N · · · N interaction [16].

Table 4. Force constants of $[Pt(NH_3)_4]^{++}$ (10^5 dyn/cm)

$K = 2{\cdot}804$	$H = 0{\cdot}147$	$F = 0{\cdot}05$

Using the force constants shown in Table 4, the values calculated according to the usual procedure are in good agreement with those observed as shown in Table 5, indicating that the values of these force constants are reasonable. From the value of the force constant K, it can be concluded that the nitrogen-to-metal bond should be fairly covalent in the $[Pt(NH_3)_4]^{++}$ complex ion.

(B) $Pt(NH_3)_2C_2O_4$ *and* $Pd(NH_3)_2C_2O_4$. These complexes can be considered to have a planar structure:

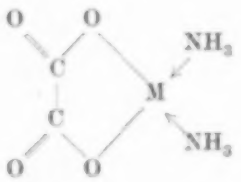

Therefore, the infrared spectra of these complex salts can be approximately explained by considering the superposition of the vibrations of ammine complexes described above and those of the structure:

assigned in a previous paper [17].

Table 5. Calculated and observed frequencies (cm^{-1}) of $[Pt(NH_3)_4]^{++}$ ion

Symmetry class	Vibrational mode	Calculated	Observed†
A_{1g}(R)	ν(Pt—N)	538	538†
B_{1g}(R)	δ(N—Pt—N)	270	270
B_{2g}(R)	ν(Pt—N)	528	526
E_u(IR)	ν(Pt—N)	577	Outside the observable region in the present IR measurements
	δ(N—Pt—N)	204	

* R = Raman active, IR = infrared active.
† See reference [14].

VOL. 13 1958/5

The assignment of the infrared spectra of these complexes can be made without ambiguity as shown in Table 1. The differences in the NH_3 rocking frequencies of these compounds from those of the ammine complexes explained above arise from the small change in force constants caused by the neighbouring groups.

Although we have not observed the ligand-to-metal frequencies in these complexes, we can conclude from the presence of the NH_3 rocking vibrations as shown in Table 1, that the nitrogen-to-metal bond is fairly covalent [4].

The nature of the oxygen-to-metal bond can be determined from the value of the C—O stretching frequency [17]. As this value is nearly equal to that reported for the tris-(oxalato)-metal complexes [17] we can conclude that ionic and covalent character contribute almost equally to the nature of the oxygen-to-metal bond.

References

[1] Svatos G. F., Curran C. and Quagliano J. V., *J. Amer. Chem. Soc.* 1955 **77** 6159.
[2] Svatos G. F., Sweeny D. M., Mizushima S., Curran C. and Quagliano J. V., *J. Amer. Chem. Soc.* 1957 **79** 3313.
[3] Mizushima S., Nakagawa I. and Quagliano J. V., *J. Chem. Phys.* 1955 **23** 1367.
[4] Bertin E. P., Nakagawa I., Mizushima S., Lane T. J. and Quagliano J. V., *J. Amer. Chem. Soc.* 1958 **80** 525.
[5] Powell D. B. and Sheppard N., *J. Chem. Soc.* 1956 3108.
[6] Keller R. N., *Inorg. Syn.* 1946 **2** 250.
[7] Jorgensen S. M., *Z. anorg. Chem.* 1910 **24** 181.
[8] Ramberg L., *Z. anorg. Chem.* 1913 **83** 35.
[9] Grinberg A. A., *C. R. Acad. Sci. U.R.S.S.* 1933 215; *Chem. Abstr.* **28** 1624.
[10] Mann F. G., Crowfoot D., Gattiker D. C. and Wooster N., *J. Chem. Soc.* 1932 1905.
[11] Grinberg A. A., *Helv. Chim. Acta* 1931 **14** 460.
[12] Mann F. G., Crowfoot D., Gattiker D. C. and Wooster N., *J. Chem. Soc.* 1935 1642.
[13] Nakagawa I. and Mizushima S., *Bull. Chem. Soc. Japan* 1955 **28** 589.
[14] Mathieu J. P., *J. Chim. Phys.* 1939 **36** 308.
[15] Wilson E. B., *J. Chem. Phys.* 1939 **7** 1047; 1941 **9** 76.
[16] Sweeny D. M., Nakagawa I., Mizushima S. and Quagliano J. V., *J. Amer. Chem. Soc.* 1956 **78** 889.
[17] Schmelz M. J., Miyazawa T., Mizushima S., Lane T. J. and Quagliano J. V., *Spectrochim. Acta* 1957 **9** 51.

Spectrochimica Acta, 1958, Vol. 13, pp. 38 to 42. Pergamon Press Ltd., London

Force constants, interbond angle and solid state spectrum of disiloxane

D. C. McKean
Department of Chemistry, University of Aberdeen, Scotland

(*Received* 9 *May* 1958)

Abstract—Force constants have been determined from the skeletal vibration frequencies of trisilylamine, $N(SiH_3)_3$, and disiloxane, $O(SiH_3)_2$. If the stretching interaction force constant involving two Si—X bonds is the same in the amine and in the ether, then the SiOSi angle is $<150°$.

An infrared spectrum of solid disiloxane at liquid air temperature has been obtained, which suggests that the ether is bent in the solid state.

A RECENT study of the vibrational spectra of disiloxane $[(SiH_3)_2O]$ and disiloxane-d_6, by LORD, ROBINSON and SCHUMB [1], revealed a conspicuous lack of coincidences between infrared and Raman frequencies, from which the authors concluded that the molecule of the ether has a linear skeleton. This conclusion is at variance with the evidence from electron diffraction measurements which indicate SiOSi angles of 141° in disiloxane [2] and $130° \pm 10°$ in hexamethyl disiloxane [3]. An alternative approach to the structure of these molecules has been employed by KRIEGSMANN [4], who has calculated an SiOSi angle of 150° from the skeletal vibration frequencies of the hexamethyl derivative, assuming a simple valence force field. In such a calculation, however, the neglect of interaction force constants can lead to serious error. In the present paper a more complete potential function is calculated for disiloxane based in part on the transfer of an interaction force constant from trisilylamine. A critical review of the errors likely to be involved leads to the conclusion that the SiOSi angle lies between 135 and 155°.

The potential function for trisilylamine will be considered first.

Potential function for trisilylamine

In the molecule of trisilylamine, the heavy atoms have been shown to be coplanar [5]. The vibrational spectra have been obtained recently [6] and the following assignments of the skeletal vibration frequencies made: $\nu_1(a_1')$ 496 cm^{-1}, $\nu_2(e')$ 996 cm^{-1}, $\nu_4(e')$ 204 cm^{-1}. In trisilylamine-d_9 ν_3 lies at 964 cm^{-1}. The notation is that employed by HERZBERG [7] for a planar XY_3-type molecule.

Since it is necessary to assume that no coupling between hydrogen or deuterium and skeletal motion occurs, it is preferable to choose the value of 964 cm^{-1} for ν_3, taken from the deuterated molecule, in view of the proximity of ν_3 to silyl deformation and rocking frequencies in the lighter molecule.

The effective mass of the silyl group was taken to be 31 units. G- and F-matrices were set up by the Wilson method: it is necessary to quote only the symmetry coordinates used in the E'-class:

$$S_{3a} = 1/\sqrt{6}(2d_1 - d_2 - d_3)$$

$$S_{4a} = 1/\sqrt{6}(\alpha_{23} - \alpha_{13} - \alpha_{12})$$

VOL. 13 1958/5

where d and α are bond stretching and angle bending displacement co-ordinates respectively, the subscripts referring to the various silyl groups.

The complete force field for the A_1'- and E'-classes contains four force constants F_{11}, F_{33}, F_{31} and F_{44} of which only F_{11} can be determined independently. If the potential function for stretching motion is written:

$$2V = k_1(d_1^2 + d_2^2 + d_3^2) + 2k_{12}(d_1d_2 + d_2d_3 + d_3d_1)$$

then

$$F_{11} = k_1 + 2k_{12}$$

$$F_{33} = k_1 - k_{12}$$

The signs of F_{34} and of k_{12} can be predicted from considerations of valence and this limits to a small range the possible values of F_{33}, F_{34} and F_{44}.

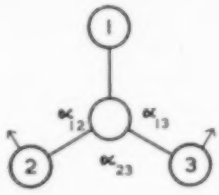

S_{4a}

Fig. 1. Skeletal configuration of trisilylamine and symmetry coordinate S_{4a}.

Figure 1 illustrates the motion represented by S_{4a}. If the orbitals of the nitrogen atom readjust themselves, by rehybridization, to follow the silicon atoms [8], it is to be expected that the bonds to atoms 2 and 3 will be strengthened and shortened, while the bond to atom 1 is weakened and lengthened, corresponding to the formation of two s–p and one p bonds. A motion involving inphase contributions from S_{3a} and S_{4a} will therefore occur more readily than if S_{3a} and S_{4a} are out of phase. Consequently the sign of F_{34} will be negative. The same result is obtained if it is assumed that non-bonding atom repulsions [9] are responsible for the presence of F_{34}.

Values of F_{33} and F_{34} have therefore been calculated for assumed values of F_{34} of 0, $-0{\cdot}5$ and $-1{\cdot}0$ mdyn/Å^2. These are shown in Table 1, together with the values of k_1 and k_{12} obtained therefrom.

In molecules in which there is appreciable resonance between adjacent bonds, or where non-bonding atom repulsions are important, k_{12} is positive. An upper limit to F_{34} of about $-0{\cdot}5$ mdyn/Å^2 is thereby established.

Potential function for disiloxane

Disiloxane is treated as a XY_2-type molecule, using the same effective mass of 31 for the silyl group as for the amine. The frequencies 606 and 1094 cm^{-1} are chosen for $\nu_1(a_1)$ and $\nu_3(b_1)$ respectively, the first being taken from the spectrum of $(SiH_3)_2O$ and the second from that of $(SiD_3)_2O$ in order to minimize the coupling between skeletal and hydrogen motion in ν_3. The skeletal bending vibration

frequency has not yet been located and must lie below 280 cm^{-1} [1]. The symmetry coordinates for the A_1 class are:

$$S_1 = 1/\sqrt{2}(d_1 + d_2)$$
$$S_2 = \alpha$$

The complete force field again contains four force constants F_{11}, F_{12}, F_{22} and F_{33}. In terms of the potential function for bond stretching, $2V = k(d_1^2 + d_2^2) + 2k_{12}d_1d_2$, $F_{11} = k_1 + k_{12}$ and $F_{33} = k_1 - k_{12}$.

In view of the fact that ν_2 has not yet been assigned, it is convenient to consider first the approximation in which F_{12} and F_{22} (and hence ν_2) are assumed to be zero. F_{11} and F_{33} may then be determined unambiguously from ν_1 and ν_3. The results are shown in Table 2, where it is seen that k_{12} is a sensitive function of the SiOSi angle.

If the force fields in the ether and the amine are similar, then the values of k_{12} in this table should be comparable with the value of k_{12} of 0·27 mdyn/Å, calculated for the amine, for the case where $F_{34} = 0$.

The assumption that k_{12} is a transferable constant therefore leads to the conclusion that the SiOSi angle is 150°. A variation of ± 50 per cent in k_{12} changes this angle by $\pm 4°$. A linear disiloxane molecule would require to have an interaction force constant four times greater than that of the amine and this seems most unlikely.

This treatment can now be improved by introducing an arbitrary bending frequency of 200 cm^{-1} and by allowing F_{12} to be other than zero. The sign of F_{12} can be predicted in an identical manner to that of F_{34} in the amine. With the symmetry coordinates listed above, it is readily shown that F_{12} must be positive.

The effects on k_1 and k_{12} are shown for a fixed SiOSi angle of 150°. The introduction of a bending frequency does not in itself alter the stretching force constants appreciably. The effect of the presence of F_{12} is to increase the value of k_{12} for a given SiOSi angle. Hence if k_{12} is to be the same in the amine as the ether, a lower SiOSi angle is required.

The effect of the undetermined parameter F_{34} in the amine lies in the same direction. If F_{34} is appreciable, the value of k_{12} is lower and the calculated SiOSi angle is also lower.

Another source of error in this calculation is due to the fact that the frequencies chosen will not represent purely skeletal motion. In the case of the antisymmetric skeletal stretching modes of the ether and the amine the frequency shifts on deuteration are small (1107–1094 and 996–964 cm^{-1}). By choosing the frequencies 1094 and 964 from the deuterated species the error is minimized and is unlikely to exceed 1° in the calculated SiOSi angle. It is harder to evaluate the amount of hydrogen motion in the symmetric skeletal stretching modes of these molecules. The proximity of the latter to the silyl deformation frequency is greater in the ether than in the amine (1009–606 cm^{-1}, 1011–496 cm^{-1}) so that the ether mode at 606 cm^{-1} will probably involve more hydrogen motion than the amine mode at 496 cm^{-1}. A higher value of ν_1 in the ether again leads to a higher value of k_{12} for a given angle and consequently to a lower SiOSi angle. It may therefore be concluded that if k_{12} is transferable from the amine to the ether

VOL. 13 1958/5

Table 1. Force constants for trisilylamine

A'_1 class	F_{11} (mdyn/Å)		4·49	
E' class	F_{34} (assumed) (mdyn/Å²)	0	−0·50	−1·00
	F_{33} (mdyn/Å)	3·64	4·43	5·11
	F_{44} (mdyn/Å³)	0·47	0·44	0·53
	k_1 (mdyn Å)	3·92	4·45	4·90
	k_{12} (mdyn/Å)	+0·27	+0·02	−0·21

Table 2. Force constants and interbond angle in disiloxane (assuming $F_{12} = F_{22} = 0$)

∠SiOSi	120°	125°	130°	135°	140°	145°	150°
k_1 (mdyn/Å)	4·50	4·53	4·59	4·68	4·78	4·90	5·03
k_{12} (mdyn/Å)	−1·09	−0·86	−0·63	−0·40	−0·16	+0·07	+0·29
∠SiOSi	155°	160°	165°	170°	175°	180°	
k_1 (mdyn/Å)	5·17	5·30	5·42	5·51	5·57	5·59	
k_{12} (mdyn/Å)	+0·51	0·70	0·87	1·00	1·08	1·11	

$\nu_1 = 606\ \text{cm}^{-1}$ $\nu_2 = 1094\ \text{cm}^{-1}$

Table 3. Force constants in disiloxane (assuming ∠SiOSi = 150°)

	(1)	(2)	(3)	(4)
ν_2 (assumed) (cm⁻¹)	0	200	200	200
F_{12} (assumed) (mdyn/Å²)	0	0	+0·50	+1·00
F_{11} (mdyn/Å)	5·32	5·19	5·82	6·20
F_{22} (mdyn/Å³)	0	0	0·28	0·38
F_{33} (mdyn/Å)	4·73	4·73	4·73	4·73
k_1 (mdyn/Å)	5·03	4·96	5·28	5·46
k_{12} (mdyn/Å)	+0·29	+0·23	+0·54	+0·73

$\nu_1 = 606\ \text{cm}^{-1}$ $\nu_2 = 1094\ \text{cm}^{-1}$

with an accuracy of only ±50 per cent, the maximum value of the SiOSi angle is 155°. Setting a probable upper limit to F_{12} and F_{34} of 0·50 mdyn/Å², the lower limit to the SiOSi angle is about 135°. The probable value lies between 140° and 150°.

While it is not necessary that disiloxane should have the same structure in the gaseous and solid states, it is interesting to note that the infrared spectrum of the solid ether at liquid air temperatures suggests a bent configuration.* The spectrum shown in Fig. 2 was obtained on a Hilger H-800 infrared spectrometer equipped with prisms of sodium chloride and potassium bromide, the sample being deposited as a film on a window cooled to liquid air temperatures in a conventional low temperature cell. The silyl rocking frequency at 764 cm⁻¹ in the gas, Fig. 2, is split into four components at 772, 744, 729 and 723 cm⁻¹ in the solid. The

* Stronger evidence for the bent structure has recently been obtained by R. F. Curl and K. S. Pitzer *J. Amer. Chem. Soc.* 1958 **80** 2371 from the infrared spectra of disiloxane in argon and nitrogen matrices.

most natural interpretation for these is that they originate from the two strongly infrared active modes of a nearly linear molecule, which would lie at 758 and 726 cm^{-1}, but which have been split each into two components of equal intensity by

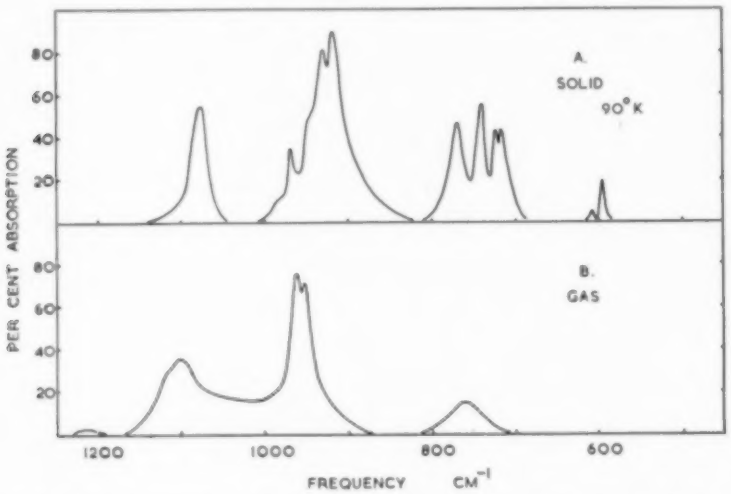

Fig. 2. Infrared spectra of disiloxane: A. Solid at liquid air temperatures B. Gas at room temperature.

the crystalline field. In addition, two peaks are observed in the solid near 600 cm^{-1} which indicate that the symmetric SiO stretching mode is infrared active.

Acknowledgement—I am indebted to Dr. B. J. Aylett for the sample of disiloxane and to Dr. L. A. Woodward for helpful criticism.

References

[1] Lord R. C., Robinson D. W. and Schumb W. C., *J. Amer. Chem. Soc.* 1956 **78** 1327.
[2] Ewing V. C. and Sutton L. E. Private communication.
[3] Yamasaki K., Kotera A., Yokoi M. and Ueda Y., *J. Chem. Phys.* 1950 **18** 1414.
[4] Kriegsmann H., *Z. fur. Electrochem.* 1957 **61** 1088.
[5] Hedberg K., *J. Amer. Chem. Soc.* 1955 **77** 6491.
[6] Ebsworth E. A. V., Hall J. R., MacKillop M. J., McKean D. C., Sheppard N. and Woodward L. A. *Spectrochim. Acta* to be published.
[7] G. Herzberg, *Infrared and Raman Spectra of Polyatomic Molecules.* D. Van Nostrand, Company, Inc., New York 1945.
[8] Linnett J. W. and Wheatley P. J., *Trans. Faraday Soc.* 1949 **45** 33, 39, 897.
[9] Heath D. F. and Linnett J. W., *Trans. Faraday Soc.* 1948 **44** 561.

VOL. 13 1958/5

Spectrochimica Acta, 1958, Vol. 13, pp. 43 to 49. Pergamon Press Ltd., London

The electronic spectra of titanium dioxide

H. Bevan, S. V. Dawes and R. A. Ford*
Research Department, British Nylon Spinners Ltd., Pontypool, England

(*Received* 26 *May* 1958)

Abstract—The absorption spectra of thin evaporated films of anatase and rutile have been recorded between 20,000 and 50,000 cm^{-1}. The intense absorption in this region is assigned to an exciton transition arising from the transfer of an electron from an oxygen to a titanium ion. The number and symmetry properties of the excited states associated with this configuration are discussed. The splitting of the exciton band observed in both anatase and rutile is related to the distortion of the TiO_6 octahedra in these crystals.

1. Introduction

The light absorption of titanium dioxide is of particular interest since this pigment photo-sensitizes the oxidation of various organic media. The "chalking" of paints and the photo-degradation of delustred synthetic fibres are practical examples of this problem. We report here on the absorption of anatase and rutile in the region 20,000–50,000 cm^{-1}, the measurements being made on thin evaporated films.

Early work by Goodeve [1] using the diffuse reflection method was inconclusive regarding the structure of the intense absorption of anatase below its onset near 25,000 cm^{-1}. Recently Treiber *et al.* [2], again using the diffuse reflection method have reported that anatase shows a shallow maximum around 28,500 cm^{-1}. Our results do not confirm this.

2. Experimental

Anatase films were prepared by the method of Barrell and Preston [3]. Reduced titanium oxide was vacuum evaporated from a coated tungsten spiral on to fused quartz slides which were subsequently baked in air. On heating to 450–500°C, these amorphous films change to anatase [4]. Rutile films were prepared by rapidly evaporating films of titanium metal which were subsequently oxidized at 400°C [5]. The thickness of the titanium films was determined from transmission measurements using the data of Hass [6]. Care was taken to study the films at a variety of thicknesses so that absorption and interference effects could be separated. Spectroscopic measurements were made using a Unicam S.P. 500.

3. Spectra

From Fig. 1 it is clear that anatase has two transitions of roughly equal intensity in the quartz ultraviolet, I at 40,000 cm^{-1} and II at 47,500 cm^{-1}. Rutile shows an intense band, I, at 36,400 cm^{-1} with a second transition forming a strong

* Present address: Mullard Research Laboratories, Salfords, Redhill, England.

shoulder at 45,500 cm^{-1}. In all cases the bands are broad, without structure at room temperature, and of high intensity. Calculated values of extinction coefficient are given in Table 1. Oscillator strengths have also been computed using the standard formula, $f = 4{\cdot}3 \times 10^{-9} \int \varepsilon \, dv$. The band contours of the anatase II and rutile II bands are insufficiently resolved to make calculation worthwhile.

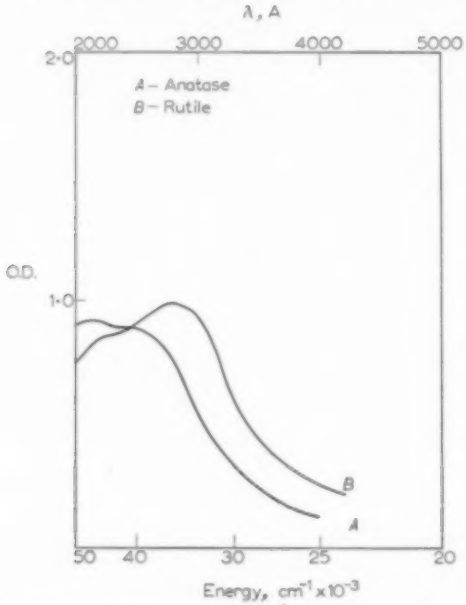

Fig. 1. Absorption spectra of thin films of anatase and rutile (approximate thickness, 100 Å).

A feature of particular interest is the apparent doublet structure of these spectra the respective splittings between the I and II bands in anatase and rutile being 0·94 and 1·13 eV. Similar splittings have been observed by Hilsch and Pohl [7] in the spectra of alkali halide crystals where they have been interpreted as due to spin-orbit coupling with the ^2P ground states of the halogen atoms. However, the small spin-orbit coupling on free oxygen, approximately 0·03 eV excludes this explanation here. Even if interaction with the ^2D state of the Ti^{3+} ion where the spin-orbit coupling amounts to 0·05 eV is included, the possible splitting is still an order too small.

Table 1

Transition	Energy (eV)	Splitting ($E - E_I$) (eV)	ε_{molar}	f
Anatase I	4·95		18,000	~1
II	5·89	0·94	18,500	
Rutile I	4·51		19,000	~1
II	5·64	1·13	16,000	

4. Discussion

In his work TREIBER concluded that the absorption of titanium dioxide above 25,000 cm^{-1} was due to oxygen anion vacancies and metal impurity centres, but the very high values of oscillator strength that we have found makes this most improbable. It seems more likely that we are concerned with an intrinsic lattice absorption. However, this cannot be due to excitation directly into the conduction band since CRONEMEYER [8] has shown, in the case of rutile, that the photoconductivity peaks around 25,000 cm^{-1} but falls off in the region of the intense absorption. The absorption must therefore represent an exciton transition in which a $2p$ electron from an oxygen ion (i.e. from the highest filled band in the crystal) is transferred to an adjacent titanium ion.

OVERHAUSER [9] has considered the excited states arising from a configuration of this type and shown that multiplet structure may be expected due to the breakdown of exciton degeneracy. In the case of transfer of an oxygen $2p$ electron into the $3d$ shell of titanium, the number of exciton states may be derived as follows. The $2p$ and $3d$ states are respectively three and fivefold degenerate leading to a fifteen-fold orbital degeneracy. Also there are three nearest neighbour titaniums around each oxygen and four possible spin states of the electron hole pair giving a total of $15 \times 3 \times 4 = 180$ exciton states. Then each of these states will itself be N-fold degenerate since the hole may be located on any of the N oxygen ions in the crystal. However, not all the 180 exciton states will be of importance in the optical spectrum because of symmetry restrictions. It may be readily shown that there are only seven allowed transitions between the $2p$ and $3d$ states involved [10] and since spin-orbit coupling is small in titanium dioxide we need only consider singlet states. This reduces the number of overlapping exciton transitions to $7 \times 3 \times 2 = 42$, of which 18 with their transition moment axes coincident with the inter-ionic axis, will be most intense. This multiplicity of possible transitions probably contributes to the broad structureless nature of the anatase and rutile bands at room temperature. More information on this should be obtained by work at low temperatures.

So far we have considered titanium dioxide to be purely ionic. However inspection of the Ti—O bond distances in anatase and rutile, which are significantly less than the appropriate ionic radii sums, shows that in both cases there is a small but definite covalent contribution to the lattice energy. In this case the permissible electron transfer transitions will be defined by the character of the covalent part of the ground state wavefunction. With titanium dioxide this will require us to consider the part played by the $4s$, $4p$ and $3d$ orbitals of the titanium if we are to obtain suitable octahedral coordination without resort to elaborate resonance between structures.

Electron transfer transitions in crystals

The appropriate description of a crystal lattice which is intermediate in type is by a wave function of the form:

$$\Psi_N = a\psi_1 + b\psi_2 \tag{1}$$

where ψ_1 describes an ionic structure and ψ_2 the covalent structure with an electron

transferred. The importance of this for the crystal spectra is that there will necessarily be excited states of the form;

$$\Psi_E = a^*\psi_2 - b^*\psi_1 \tag{2}$$

where

$$a^* \approx a; \quad b^* \approx b \text{ and } a^2 + b^2 + 2ab\int\psi_1\psi_2\,dt = 1 \tag{2a}$$

to which optical transitions will be allowed. Since we are dealing with crystals where b is small, it is clear from equation (2a) that such transitions may be considered as essentially inter-ionic electron transfers. However for coefficient b to

Table 2. Symmetry classification of orbitals in titanium dioxide

Titanium orbitals	Oxygen orbitals	Symmetry (O_h)	Bond type
$4s$	$+ N_1(\sigma_1 + \sigma_2 + \sigma_3 + \sigma_4 + \sigma_5 + \sigma_6)$	a_{1_g}	σ
$3d_{z^2}$	$+ N_2(2\sigma_1 - \sigma_2 - \sigma_3 - \sigma_4 - \sigma_5 + 2\sigma_6)$	e_g	
$3d_{x^2-y^2}$	$+ N_3(\sigma_2 - \sigma_3 + \sigma_4 - \sigma_5)$	e_g	
$4p_z$	$+ N_4(\sigma_1 - \sigma_6)$	t_{1_u}	
$4p_x$	$+ N_5(\sigma_2 - \sigma_4)$	t_{1_u}	
$4p_y$	$+ N_6(\sigma_3 - \sigma_5)$	t_{1_u}	
$3d_{xy}$	$+ N_7(\pi_{x_3} - \pi_{x_5} + \pi_{y_2} - \pi_{y_4})$	t_{2_g}	π
$3d_{yz}$	$+ N_8(\pi_{y_1} - \pi_{y_6} + \pi_{z_3} - \pi_{z_5})$	t_{2_g}	
$3d_{zx}$	$+ N_9(\pi_{z_2} - \pi_{z_4} + \pi_{x_1} - \pi_{x_6})$	t_{2_g}	

be finite the overlap integral $\int\psi_1\psi_2\,dt$ must also be finite. This sets certain restrictions on the mixing of ψ_1 and ψ_2. They must belong to the same symmetry species relative to the inter-ionic axis and be of the same spin type or spin-orbit species if jj coupling is operative.

Let us briefly consider the possible orbital combinations which will contribute to the covalent wavefunction, ψ_2 in anatase and rutile. Both these crystals may be considered to be built up from TiO_6 octahedra, (symmetry O_h), for which suitable bonding orbitals can be most readily obtained by using the $4s$ and $4p$ as well as the $3d$ orbitals of the titanium as we have mentioned above, (i.e. equivalent to d^2sp^3 hydridization). The possible combinations which yield suitable symmetry orbitals are given in Table 2.

Oxygens 1 and 6 are on the z-axis, 2 and 4 on the x-axis and 3 and 5 on the y-axis. Then $\sigma_{1\ldots6}$ represent oxygen $2p$ orbitals which point towards the titanium. $\pi_{x,y,z}$ represent other oxygen $2p$ orbitals which are directed along the x, y and z axes respectively. $N_{1\ldots9}$ are normalizing factors. Each combination of titanium and oxygen symmetry orbitals gives rise to a bonding M.O. and anti-bonding M.O. of the same symmetry, so producing an energy level scheme of the type shown in Fig. 2. In this we have shown the π bonding (t_{2_g}) to be zero since there is no evidence from the spectra of either $[Ti(H_2O)_6]^{3+}$ [11] or Ti^{3+} ions in oxide glasses [12] that it contributes to the structure. Only when the metal-ligand bonds are very short, as in certain metal carbonyls and such ions as MnO_4^-, CrO_4^- and ClO_4^-

VOL. 13 1958/5

[13] does it seem to become important. We have twelve electrons from our six oxygens to introduce so the six lowest M.O.s, the a_{1_g}, t_{1_u} and e_g bonding orbitals will be filled. The exact order of these orbitals is uncertain.

We may now consider the allowed transitions from these bonding M.O.s which are predominantly localized on the oxygen into anti-bonding M.O.s which are predominantly localized on the titanium. Since the ground states of anatase and rutile will be $^1A_{1_g}$ all the excited states will have symmetry $^1T_{1_u}$. The allowed transitions, are given in Table 3.

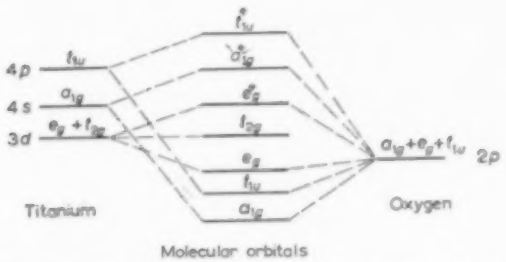

Fig. 2. Molecular orbital energy level scheme for titanium dioxide. (Asterisks are attached to anti-bonding orbitals.)

In assigning the bands we have observed in anatase and rutile, it is clear that excitation must be from the t_{1_u} orbital since the transitions from a_{1_g} and e_g will be of very high energy. Of the t_{1_u} excitation, we prefer $t_{1_u} \rightarrow t_{2_g}$ since no other strong bands have been observed at longer wavelengths with either crystal. Another reason that leads us to strongly prefer this assignment is that here excitation is to

Table 3. Allowed transitions in titanium dioxide

$a_{1_g} \rightarrow t^*_{1_u}$
$t_{1_u} \rightarrow t_{1_g}$
$t_{1_u} \rightarrow e^*_g$
$t_{1_u} \rightarrow a^*_{1_g}$
$e_g \rightarrow t^*_{1_u}$

an essentially non-bonding orbital which has little overlap with adjacent wavefunctions. The exciton nature of the observed band in rutile, which is unusual for an intense band in the ultraviolet, may therefore be understood. The very high intensity of the transitions must be associated with the large polarity change which occurs on electron transfer.

Exciton splitting

Since spin-orbit coupling cannot explain the splitting of the I and II bands in titanium dioxide, we must consider other causes. JÖRGENSEN [14] has suggested that the II bands should be assigned to $t_{1_u} \rightarrow e^*_g$ in which case the splitting from the $t_{1_u} \rightarrow t_{2_g}$, I bands should correspond to the crystal field splitting of the degenerate 3*d* orbitals of titanium in the octahedral field. However, inspection of the

$^2T_{2g} \rightarrow {}^2E_g$ transition of the Ti^{3+} ion, which should give an estimate of this splitting, shows it to be situated at 20,400 and 18,700 cm^{-1} in aqueous medium and oxide glasses respectively, giving splitting values of 2·55 and 2·33 eV. Bearing in mind the high lattice energies of anatase and rutile we should expect the splitting in these crystals to be at least as large as the latter value. However the observed splittings are around 1 eV so this assignment does not seem probable.

Under these circumstances it seems most probable that the splitting is associated with the small tetragonal distortions of the TiO_6 octahedra which have been found in these crystals [15]. In both crystals there are two Ti—O distances that are longer than the other four making up the octahedron. As a result the

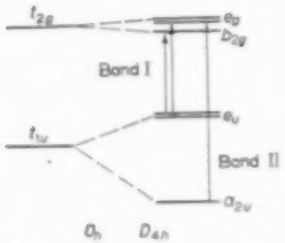

Fig. 3. Splitting of the t_{1u} and t_{2g} molecular orbitals of titanium dioxide by octahedral and tetragonal fields.

site symmetry of the titanium is reduced from O_h to D_{4h} with a consequent breakdown of the t_{1u} and t_{2g} degeneracies. Formally, t_{1u} becomes a_{2u} and e_u; and t_{2g} becomes b_{2g} and e_g. The allowed transitions between these orbitals are then $a_{2u} \rightarrow e_g$, $e_u \rightarrow b_{2g}$ and $e_u \rightarrow e_g$. Since the tetragonal distortion should cause only a slight splitting of the t_{2g} orbitals, the $e_u \rightarrow b_{2g}$ and $e_u \rightarrow e_g$ transitions may appear accidentally degenerate and both contribute to the anatase and rutile I bands. This is illustrated in Fig. 3. Then our assignments under D_{4h} become $^1A_{1g} \rightarrow {}^1A_{2u}$ and $^1A_{1g} \rightarrow {}^1E_u$ for the I bands and $^1A_{1g} \rightarrow {}^1E_u$ for the II bands.

The origin of the distortion in anatase and rutile crystals is of some interest. In fact it is more complex than we have suggested above, being composed of a rhombic as well as a tetragonal component. But the absence of any more detailed splitting in the spectra suggests that the effective symmetry is D_{4h} and not V_h. The rhombic component, giving rhombic angles of 80·8°, 90·0° and 99·2° in rutile, is entirely due to electrostatic crystal packing requirements. A regular octahedral structure requires each oxygen to be coordinated to three titaniums the angles between these bonds being 90°, 135° and 135°, whereas electrostatic equilibrium requires angles of 120°. Pauling [16] has shown that the actual angles are a compromise between this electrostatic requirement and anion–anion repulsion, since angles of 120° would require a minimum anion–anion distance of 2·40 Å which is much less than the appropriate ionic radii sum for two oxygens of 2·80 Å. On the other hand the tetragonal distortion is probably related to the covalent component of the ground state wavefunction. Orgel [17] and McClure [18] have recently related tetragonal phase formation in transition metal oxides to the operation of the Jahn–Teller effect. However with titanium dioxide no Jahn–

VOL. 13 1958/5

Teller splitting of the ground state is possible because there is no orbital degeneracy. The T_{1_u} excited states, on the other hand, are orbitally degenerate and may suffer tetragonal distortion due to Jahn–Teller splitting. If this is so, we suggest that the small amount of the excited state wavefunction that is mixed into the ground state function Ψ_N may cause a small distortion of the ground state although this state is not itself orbitally degenerate.

Acknowledgements—The authors wish to thank Professor M. H. L. Pryce for his continued interest in this work and for reading and commenting on this manuscript. They are also grateful to Mr. R. G. C. Arridge for many helpful discussions and British Nylon Spinners Limited for permission to publish this work.

References

[1] Goodeve C. F., *Trans. Faraday Soc.* 1937 **33** 340.
[2] Treiber E. *et al. Acta Chem. Scand.* 1954 **8** 1865.
[3] Barrell H. and Preston J. S., *Proc. Phys. Soc.* B 1951 **64** 97.
[4] Arnulf A., *Le Vide* 1946 **1** 129.
[5] Hammer K., *Optik.* 1948 **3** 495.
[6] Hass G., *Vacuum* 1952 **2** 231.
[7] Hilsch R. and Pohl R. W., *Z. f. Phys.* 1930 **59** 812.
[8] Cronemeyer D. C., *Phys. Rev.* 1952 **87** 876.
[9] Overhauser A. W., *Phys. Rev.* 1956 **101** 1702.
[10] Pryce M. H. L., Private communication.
[11] Hartmann H. *et al. Z. phys. Chem.* 1951 **197** 116 and 239.
[12] Dunitz J. D. and Orgel L. E., *J. Phys. Chem. Solids* 1957 **3** 318.
[13] Wolfsberg M. and Helmholz L., *J. Chem. Phys.* 1952 **20** 837.
[14] Jörgensen J. K., Private communication.
[15] Cromer D. J. and Herrington K., *J. Amer. Chem. Soc.* 1955 **77** 4708.
[16] Pauling L., *Nature of the Chemical Bond* p. 336 Oxford Univ. Press, 1948.
[17] Dunitz J. D. and Orgel L. E., *J. Phys. Chem. Solids* 1957 **3** 20.
[18] McClure D. S., *J. Phys. Chem. Solids* 1957 **3** 311.

Spectrochimica Acta, 1958, Vol. 13, pp. 50 to 59. Pergamon Press Ltd., London

Quantitative Spektralanalyse von Gasgemischen

O. Botschkowa, S. Frisch and E. Schreider
Physics Research Institute, A. A. Zdanov State University, Universityetskaya, Nabezgnaja 7/9, Leningrad, USSR

(*Received* 10 *June* 1957. *Revised* 8 *May* 1958)

Abstract—A method is described for the quantitative spectral analysis of gas mixtures. A high frequency discharge with external electrodes is used as light source. In the analysis of rare gases containing nitrogen, hydrogen, oxygen or carbon monoxide, using discharges in narrow capillaries at a pressure of 100 Torr, 10^{-4}–10^{-5} per cent of the added gas could be determined. For the analysis of small amounts of noble gases in others, specially favourable conditions of excitation occur in tubes 0·5 mm in diameter and with a pressure of about 1/10 Torr.

The analysis of molecules gas mixtures, e.g. N_2–CO_2, can also be carried out in a high frequency discharge. A method for analysing three component mixtures is described, for the case in which the intensity of the spectral lines is affected by a change of concentration of only one component.

An increase in sensitivity may be achieved by using other types of discharge.

1. Spektralanalyse von Gasgemischen in der Hochfrequenzentladung mit Aussenelektroden

Bekanntlich ist die quantitative Spektralanalyse von Gasen mit einer Reihe von Schwierigkeiten verbunden. Diese Schwierigkeiten können in zwei Gruppen aufgeteilt werden [1, 2, 3]: (a) Schwierigkeiten, die mit den Eigenheiten der Anregung der Spektren von Gasen verbunden sind: (b) Schwierigkeiten, die mit der Veränderung der Zusammensetzung des Gasgemisches im Prozess der elektrischen Entladung verbunden sind.

Trotz des prinzipiellen Charakters dieser Schwierigkeiten kann man doch Weg zu ihrer Gehebung andeuten. Zur Bestimmung der schwer anregbaren Komponenten muss man mit einer Lichtquelle von hoher Elektronentemperatur und möglichst grosser Elektronenkonzentration arbeiten. Für die leicht anregbare Komponenten wird eine hohe Konzentrationsempfindlichkeit bei der Beobachtung des Leuchtens in der positiven Säule der Glimmentladung beim hohen Druck und in weiten Entladungsröhren erreicht.

Die Schwierigkeiten, die durch die Veränderung der Zusammensetzung des Gasgemisches während des Entladungsprozess hervorgerufen werden, kann man auf zwei Wegen beseitigen: (a) beim langsamen Durchsaugen des Gemisches durch das Entladungsrohr, was bei grösseren Mengen des zu analysierenden Gemisches ist; (b) durch die Anwendung von Lichtquellen mit äusseren Elektroden.

In einer Reihe der von den Verfassern unternommenen Arbeiten [3, 4] wurde als Lichtquelle eine Hochfrequenzentladung mit Aussenelektroden benutzt. Die Entladung wurde durch einen Hochfrequenzgenerator angeregt, der nach dem Schema 1 gebaut ist. Die Leistung des Generators war 350 W. Der Generator arbeitete mit einer Frequenz von 6 MH2. Eine Änderung der Frequenz wurde nicht vorgesehen, da vielfache Untersuchungen [5, 6, 7] zeigten, dass der Charakter der Entladung bei der Frequenzänderung nicht bemerkbar verändert wird.

VOL. 13 1958/5

Der Schwingkreis des Generators wurde mit dem Entladungsrohr mittels einer speziellen Verbindungsspule verbunden, deren Enden mit den Aussenelektroden des Entladungsrohres verbunden wurden.

Bei des Entladung in einem Rohr mit Aussenelektroden ist die Gasabsorption

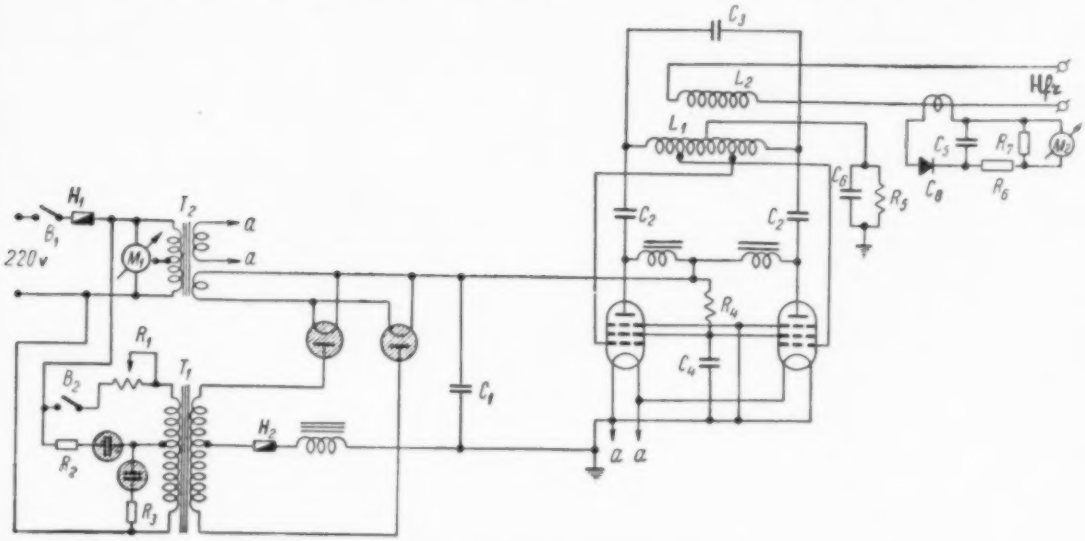

Abb. 1. Schema des Hochfrequenzgenerators.

bedeutend schwächer, als bei der Entladung in demselben mit Innenelektroden. Aber auch bei diesem Entladungstyp können schlecht reproduzierbare Analyseergebnisse erhalten werden, falls keine geeigneten Massnahmen getroffen worden sind. In Abb. 2 sind die Messresultate der Intensitätsverhältnisse der Linie He

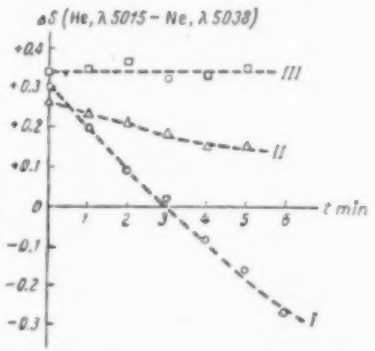

Abb. 2. Änderung der Intensitätsverhältnisse von He–Ne Linien in Abhängigkeit von der Röhrenleuchtzeit: (I)—Lang in Betrieb gewesenes Glasrohr. (II) Glasrohr nach dem Einlassen von Luft. (III) Quarzrohr.

λ5015 Å zur Linie Ne λ5038 Å im Gemisch Helium–Neon mit 7% Neon angeführt. Die Aufnahmen wurden mit ein und derselben Gasmenge bei ununterbrochenem Leuchten des Rohres mit Aussenelektroden gemacht, mit einer Zwischenzeit von 1 min. Die Angaben sind für 3 Fälle angeführt: (a) ein schon lange Zeit benutztes Glasrohr; (b) ein Glasrohr, in das vor der Aufnahme des zu analysierenden

Gemisches Luft eingelassen wurde; (c) ein Quarzrohr. Aus der Abbildung ersieht man die völlige Untauglichkeit des alten Glasrohres für die Analyse. Darin findet ein "Ausbrennen" von Helium statt. Dieser "Ausbrenneffekt" von Helium kann durch die Abscheidung des Wasserstoffs von den Wänden des Rohres erklärt werden, wobei der Wasserstoff die Intensität der Heliumlinien stark schwächt. In Quarzröhren gibt es kein "Ausbrennen" von Helium. Aber bei einer langwierigen Arbeit tritt auch in den Quarzentladungsröhren eine Änderung der

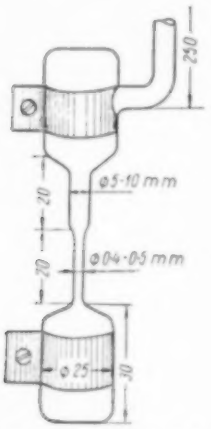

Abb. 3. Rohr mit veränderlichem Querschnitt aus Quarzglas.

Abb. 4. Kapillare als Entladungsrohr.

Zusammensetzung des Gemisches ein. Deswegen muss man neue Entladungsröhren benutzen, ohne dass sie durch Dämpfe beschmutzt wären. Vor der Aufnahme des zu analysierenden Gemisches ist es am besten, das Rohr von einem dem zu analysierenden Gemisch ähnlichen Gemisch durchströmen zu lassen.

Das Quarzentladungsrohr hatte die in der Abb. 3 angegebene Gestalt. Der mittlere Teil des Rohres hat zwei verschiedene Querschnitte. Der breitere Teil (mit einem Durchmesser von 10 mm) wird bei der Analyse von Zusätzen benutzt, die kleinere Anregungsspannungen haben, als die Grundkomponente. Der engere Teil des Rohres (mit einem Durchmesser von 0·5 mm) wird bei der Analyse schwer anregbarer Komponenten von Gemischen benutzt.

Bei sehr kleinen Mengen des zu analysierenden Gases kann als Entladungsrohr eine an einem Ende zugelötete und an eine Töplerpumpe angeschlossene Kapillare benutzt werden (Abb. 4). Mit der Hilfe der Töplerpumpe konnte die zu analysierende Gasmenge in die Kapillare gepresst werden.

Beim angegebenen Durchmesser der Kapillare wird die Konzentrationsempfindlichkeit der Analyse durch den Gasdruck wesentlich beeinflusst. Eine Erniedrigung des Gasdrucks hat die Erhöhung der Empfindlichkeit der schwer anregbaren Komponente des Gemisches zur Folge. Es ist aber nicht zweckmässig, die Analyse bei niedrigeren Drucken als 0·1 Torr durchzuführen, da der Einfluss der Gasabscheidung von den Wänden des Entladungsrohrs bei übermässig niedrigen Drucken stärker wird und ausserdem die gesamte Strahlungsintensität verringert

VOL. 13 1958/5

wird. Eine Drucksteigerung hat die Erhöhung der Empfindlichkeit der Analyse der leicht anregbaren Komponente des Gemisches zur Folge.

Die quantitative Analyse der Gase wurde wie üblich mittels Eichkurven durchgeführt, die nach Eichgemischen aufgebaut worden waren. Die Eichgemische wurden unmittelbar in der Apparatur hergestellt, mit der die Gefässe mit den reinen Gasen verbunden wurden. Der Prozentsatz der einzelnen Gemischkomponenten wurde nach ihren Partialdrucken bestimmt. Die Eichkurven wurden aufgezeichnet in Koordinaten—Logarithmus der Zusatzkonzentration—Schwärzungsdifferenz des analytischen Linienpaares. Für eine Reihe konkreter Aufgaben wurde ausser der photographischen Methode noch eine photoelektrische Methode der Intensitätsmessungen der Spektrallinien und in Fällen, wo eine halbquantitative Einschätzung der Zusätze genügte, die visuelle Methode mittels eines Spektroskops [8] angewandt.

Betrachten wir jetzt einige konkrete Beispiele von Analysen.

(a) *Analyse von Edelgasen auf Zusätze*

Bei der Bestimmung von solchen Zusätzen wie Stickstoff, Wasserstoff, Sauerstoff und Kohlenwasserstoffe in Edelgasen ist es für das Erreichen der maximalen Konzentrationsempfindlichkeit der Analyse notwendig, bei möglichst hohem Druck in dem Entladungsrohr zu arbeiten. Aber es erweist sich, dass in Entladungsröhren mit grösseren Durchmesser eine Drucksteigerung zu einer bedeutenden Abschwächung der Strahlungsintensität führt. Darum ist man gezwungen, bei der Verwendung von solchen Röhren sich auf den Druck zu beschränken, der 20 Torr nicht überschreitet. Die Konzentrationsempfindlichkeit der Analyse ist unter solchen Bedingungen nicht hoch, sie beträgt nicht mehr als Hundertstel eines Prozents. Jedoch senkt in engen Kapillaren eine Drucksteigerung bis zu 100 Torr nicht die Strahlungshelligkeit und erlaubt 10^{-4}–10^{-5}%-ige Zusätze zu bestimmen [8]. In Abb. 5 sind die Eichkurven zur Bestimmung von Stickstoff in Helium gegeben. Die Aufnahmebedingungen: Druck von 600 Torr, Durchmesser der Kapillare 0·5 mm, Stromstärke 300 mA. Unter diesen Bedingungen erscheint neben dem Linienspektrum des Heliums das Bandenspektrum des Heliummoleküls He_2. Im Stickstoffspektrum überwiegen die Banden N_2^+. Die Stickstoffbanden erscheinen im Spektrum bei der Konzentration von 10^{-5}% Stickstoff in Helium an. Bei Durchführung von Analysen auf solche kleine Mengen von Zusätzen ist es jedoch nötig, besondere Aufmerksamkeit der Vorbereitung des Rohres vor der Analyse zu widmen. Bekanntlich wird der Stickstoff während der Entladungszeit absorbiert. Wenn man deswegen in ein gut entgastes and in reinem Helium vorbereitetes Entladungsrohr das Gemisch einlässt, das kleine Zusätze von Stickstoff enthält, sind im Spektrum Stickstoffsbanden nur bei Konzentrationen von 10^{-3}% zu finden. Wenn man aber das Rohr einige Male mit einem 10^{-5}% Stickstoff enthaltenden Gemisch hat durchströmen lassen, dann verstärkt ein Zufügen von Stickstoff in der Menge von $2 \cdot 10^{-5}$% spürbar die Intensität seiner Banden.

Die Stickstoffanalyse in Neon ist mit Auswahlschwierigkeiten der analytischen Linienpaare verbunden. Das erste positive Bandensystem von N_2 wird nur bei Stickstoffskonzentrationen in der Ordnung von Zehnteln eines Prozents angeregt.

Bei kleinen Stickstoffkonzentrationen erhält man jedoch hauptsächlich N_2^+-Stickstoffbanden im Gebiet $\lambda = 4600$ Å, wo es unter diesen Bedingungen keine Neonlinien gibt. Die Stickstoffanalyse kann man entweder nach der absoluten N_2^+-Bandenintensität durchführen oder, wenn im Gemisch kleinere Mengen von CO_2

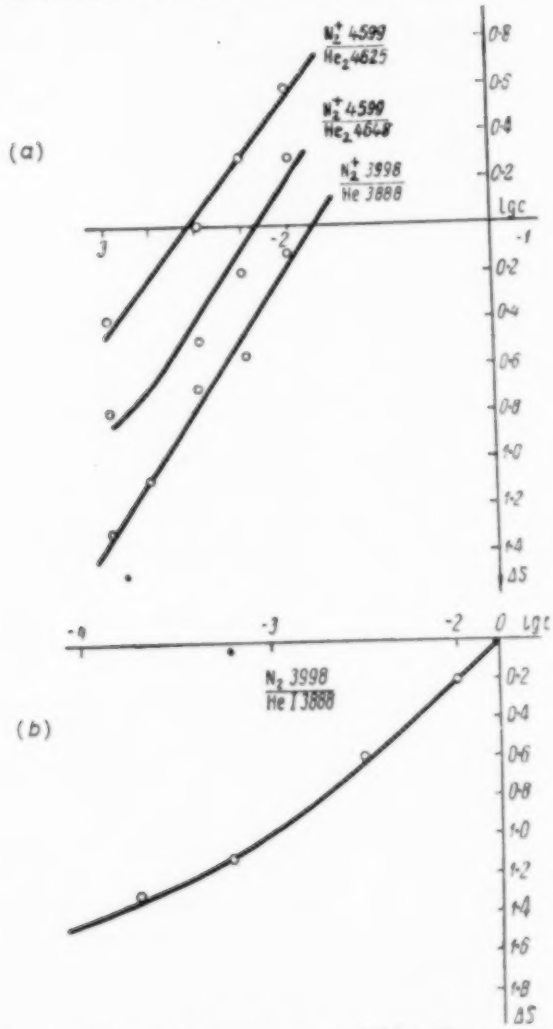

Abb. 5. Eichkurven für Stickstoffbestimmung in Stickstoffheliumgemisch. Stickstoffkonzentration: (A) 0·002–0·01%; (B) 0·0002–0·01%.

oder CO sind, so kann man die Analyse nach der CN-Banden-intensität durchführen, die sich linear mit der Stickstoffskonzentration ändert.

Sauerstoff in Helium and Neon kann nur in einer Konzentration von 10^{-4}% an bestimmt werden.

Sowie bei der Stickstoffanalyse als auch bei der Sauerstoffanalyse muss man

VOL. 13 1958/5

das Entladungsrohr vorher mit einem dem zu analysierenden Gemisch ähnlichen Gemisch durchströmen lassen, da Sauerstoff während der Entladung sogar stärker absorbiert wird als Stickstoff. Die Eichkurven für HO_2 und N_2 weisen kleine Neigung und eine merkliche Abweichung von der Geradlinigkeit; das kann sowohl durch das Vorhandensein eines Schleiers als auch durch die Anwesenheit kleinerer Mengen der von vorhergehenden Entladungen in dem Rohr zurückgebliebenen Zusatze erklärt werden.

Bei der Ausarbeitung der Methodik für die Wasserstoffanalyse in Edelgasen ist es vor allem erforderlich, die Arbeitsbedingungen des Entladungsrohrs auszuwählen, bei denen von den Wänden der Apparatur keine grössere Menge von Wasserstoff abgeschieden wird. Die H_α-Linie des Wasserstoffs ist im Spektrum eines beliebigen Gemisches intensiv, falls, in der Apparatur vor der Gemischzufuhr Luft vorhanden war, die Wasserdampfspuren enthalten hat. Die von den Wänden abgeschiedene Wasserstoffmenge ist bei der Arbeit mit hohen Entladungsströmen besonders gross. Folglich muss bei der Wasserstoffanalyse mit den minimal möglichen Strömen und nach einem langen Auspumpen der Anlage gearbeitet werden. Ausserdem ist in der Entladung das Vorhandensein von Quecksilberdampf zu vermeiden, da sich bei der Entladung von Quecksilber und Wasserstoff ein Quecksilberhydrid bilden kann, was zum Verschwinden des atomaren Wasserstoffs aus Entladung führt und die Analyseempfindlichkeit vermindert.

(b) *Analyse der Edelgaszusätze in Molekülgasen*

Die Analyse kleinerer Zusätze von Edelgasen in Molekülgasen ist das Beispiel einer Analyse auf schwer anregbare Gasgemischkomponente. Besonders günstige Anregungsbedingungen für sie werden in Röhren mit einem Durchmesser von 0·5 mm, bei einem Druck von Zehntel eines Torr erreicht.

Als Beispiel einer Analyse führen wir die Analyseergebnisse auf Zusätze von Krypton in Sauerstoff an. In diesem Falle können die Eichkurven nach einem analytischen Paar Kr, λ5870 Å–OI, λ5437 Å im Konzentrationsintervall 0·2–3% aufgetragen werden.

Bei der Auftragung der Eichkurven macht sich bemerkbar, dass die Kryptonlinien auf den ersten Aufnahmen nach der Gemischzufuhr in das Entladungsrohr viel intensiver sind, als auf den darauffolgenden. So z.B. war die Schwärzungsdifferenz ΔS für das analythische Paar Kr, λ5870 Å-OI, λ5437 Å bei 1·5% Krypton in Sauerstoff: 0·28; 0·11; 0·12; für 2·3% Krypton: 0·55; 0·34; 0·32. Wie man sieht, ist das Intensitätsverhältnis auf den ersten Aufnahmen grösser, als auf den übrigen; die zweite und die dritte Aufnahme geben Intensitätsverhältnisse, die miteinander gut übereinstimmen. Deswegen ist mit den Aufnahmen erst nach einer gewissen "Einbrennzeit" zu beginnen, die in diesem Falle nicht weniger als 5 min dauern soll.

(c) *Analyse von molekülaren Gasgemischen*

In einer Hochfrequenzentladung kann man auch die Analyse von Gasgemischen durchführen, in denen unter Einwirkung der Entladung chemische Reaktionen vor sich gehen. Als Beispiel betrachten wir die Analyse der Stickstoff- und Kohlendioxydgasgemische. Im Spektrum dieses Gemisches kann man bei der Entladung

die N_2, CO- und CN-Banden beobachten. Die CO-Moleküle entstehen aus der Dissoziation von CO_2-Molekülen. Beim Zusammenwirken von CO und N_2 bildet sich CN. Nachdem das Entladungsrohr einige Minuten geleuchtet hat, stellt sich ein Gleichgewicht ein und die Stickstoffmenge kann man sowohl nach den Stickstoffbanden, als auch nach den CN-Banden bestimmen. Dabei ist es notwendig die Spaltbreite des Spektrographen konstant zu halten, da von der Spaltbreite der Schwärzungsgrad der Photoplatte am Bandkopf abhängig ist. In Abb. 6 sind die Eichkurven für die Stickstoffbestimmung in CO_2 im Konzentrationsintervall von

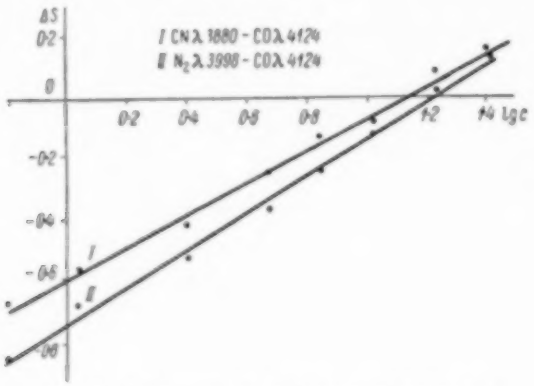

Abb. 6. Eichkurven für Stickstoffbestimmung in Stickstoffkohlendioxydgasgemisch.

0·5–25% angegeben. Aufnahmebedingungen: Durchmesser der Kapillare—0·5 mm, Druck—3·5 Torr, Strom—350 mA. Die Bestimmungsempfindlichkeit von Stickstoff kann durch Drucksteigerung erhöht werden.

2. Gasanalyse von Vielkomponentengemischen

Bei der Gasanalyse von Vielkomponentengemischen entsteht unvermeidlich die Frage nach dem Einfluss der im Gemisch vorhandenen zusätzlichen Gasen auf die Linienintensität. Ein solcher Einfluss kann durch zwei Ursachen hervorgerufen werden: (a) die Veränderung der Entladungsbedingungen (die Herabsenkung der Elektronentemperatur) beim Zusatz einer Komponente mit niedrigerer Ionisierungsspannung; (b) chemische Reaktionen in der Entladung.

Verschiedene Analyseverfahren sind beim Vorhandensein einer "dritten Komponents" möglich. Eines der möglichen Analyseverfahren von Dreikomponentengemischen wenden wir in dem Falle an, wenn die Intensität der Spektrallinien durch Konzentrationsänderung nur einer Gemischkomponente beeinflusst wird [9, 10]. Als Beispiel betrachten wir die Analyse vom Helium–Neon–Argongemisch. Zufügen von Neon ändert nicht die Intensitätsverhältnisse von Argon- und Heliumlinien. Zufügen von Argon aber ruft eine Veränderung der Intensitätsverhältnisse von Helium- und Neonlinien hervor. Das kann dadurch erklärt werden, dass sich Ionisierungs- und Anregungsspannungen von Helium und Neon weniger voneinander unterscheiden, als die von Helium und Argon. Deswegen ändert das Zufügen von Neon zum Gemisch die Elektronentemperatur nur wenig, da sie

VOL. 13 1958/5

schon durch das Vorhandensein von Argon im Gemisch stark herabgesetzt worden ist. In diesem Zusammenhang kann man für die Analysedurchführung in erster Linie die Eichkurven für die Bestimmung von Argon in Helium auftragen (Abb. 7). Gleichzeitig muss man kontrollieren, ob nicht doch das Zufügen von Neon auf das Verhältnis der Linienintensitäten Argon–Helium Einfluss hat. Zweitens werden Eichkurven für die Neonbestimmung in einem Neon–Helium–Argon-Gemisch für verschiedene Konzentrationen von Argon angetragen (Abb. 7B). Man erhält eine Reihe von Kurven, die parallel zu einander verschoben sind. Zuerst wird die

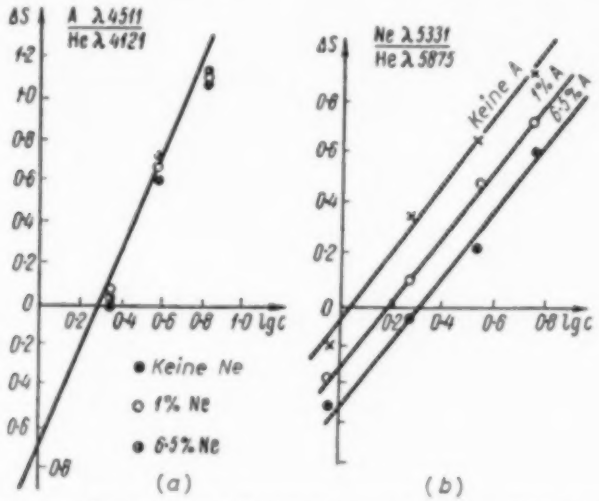

Abb. 7. Eichkurven für Argon- und Neonbestimmung in Helium–Neon–Argon-Gemisch: (a) Analyse auf Argon; (b) Analyse auf Neon.

Argonkonzentration nach der ersten Eichkurve bestimmt und damit wird fixiert, welche Kurve aus der zweiten Reihe der Eichkurven man zur Bestimmung der Neonkonzentration benutzen muss.

Eine Gemischanalyse mit mehr als drei Komponenten kann man auf die Analyse eines Dreikomponentgemisches durch die Einführung des "spektroskopischen Bufer" zurückführen. Das Verfahren besteht darin, dass in das Gasgemisch eine zusätzliche Komponente eingeführt wird, die eine niedrigere Ionisierungsspannung hat als die zu analysierende Komponente [13]. Bei bestimmter Konzentration wird diese Zusatzkomponente die Elektronentemperatur der Entladung völlig bestimmen, wodurch gleichzeitig der Einfluss der einzelnen Gemischkomponente auf einander beseitigt wird. Die Konzentration dieser Zusatzkomponenten kann unabhängig von den Relativkonzentrationen aller anderen Komponenten bestimmt werden. Die Untersuchungen zeigten, dass sie um eine Ordnung höher als die Summe der Konzentrationen aller zu analysierenden Komponenten sein muss.

Wenn also in einem Vielkomponentengemisch die Komponente mit der niedrigsten Ionisierungsspannung in genügend grosser Menge vorhanden ist, so hängt dadurch die Bestimmungsempfindlichkeit von der Konzentration aller anderen Gemischkomponenten nicht ab. Für schwerer anregbare Komponente wird die

Analysenempfindlichkeit nur durch diese leichter anregbare Komponente bestimmt werden.

3. Spektralanalyse bei der Impulsentladung

Die Konzentrationsempfindlichkeit einer Analyse auf schwer anregbare Komponenten liegt niedrig, sie überschreitet nicht 0·1%. Eine Erhöhung der Analyseempfindlichkeit kann durch die Anwendung von Impulslichtquellen erreicht werden [14]. Für die Impulsentladung ist eine hohe Stromdichte und ein hoher Ionisationsgrad der Gase kennzeichnend. Untersuchungen der Charakteristiken von Impulsentladungen in Edelgasen mit Hilfe der Methode der Spektralzeitauflösung [11] zeigten, dass die Funkenlinien eher als die Bogenlinien angeregt werden. Die Entladungsbedingungen verändern sich stark während des Impulsverlaufs. Wenn man deshalb mittels Zeitauflösung bestimmte Zeitabschnitte im Verlauf des Impulses selbst herausschneidet, so kann man einen solchen Zeitmoment wählen, wo die Entladungsbedingungen für Anregung der Linien des zu analysierenden Elements am günstigsten sind. Wenn man den gesamten Impuls photographiert, geht dieser Vorteil verloren. Im Vergleich zur Linie selbst vergrössert sich auch der Schleier stark. Aber auch ohne Spektralzeitauflösung gibt die Impulsentladung grosse Vorteile im Vergleich zu anderen Quellen, weil sie gleichzeitig die Anregung von Bogenlinien einer schwer anregbaren Komponente sowie die Anregung von Funkenlinien einer liecht anregbaren Komponente ermöglicht. Ausserdem, wie schon erwähnt, werden in der Impulsquelle wenig absorbierte Gase abgesondert, ungeachtet von Anwesenheit der Innenelektroden.

VOL.
13
1958/5

Zusammenfassung

Es wird eine Methode der quantitativen Spektralanalyse von Gasgemischen beschrieben. Als Lichtquelle wird eine Hochfrequenzentladung mit Aussenelektroden benutzt.

Bei der Analyse von Edelgasen auf Zusätze (N_2, H_2, O_2, CO), bei der Entladung in engen Kapillaren beim Druck von 100 Torr, können 10^{-4}–10^{-5}%-ige Zusätze bestimmt werden.

Bei der Analyse kleinerer Zusätze von Edelgasen in Molekülgasen werden besonders günstige Anregungsbedingungen in Röhren mit einem Durchmesser von 0·5 mm, bei einem Druck von Zehntel eines Torr erreicht.

In einer Hochfrequenzentladung kann auch die Analyse von molekülaren Gasgemischen durchgeführt werden, z.B. des N_2–CO_2-Gemisches.

Eine Methode der Analyse der Dreikomponentengemischen im Falle, wenn die Intensität der Spektrallinien durch Konzentrationsänderung nur einer Gemischkomponente beeinflusst wird, wird angegeben.

Die Erhöhung der Analysenempfindlichkeit kann durch die Anwendung von Impulslichtquellen erreicht werden.

Literatur

[1] Frisch, S. *Westnik Leningr. Univ.* 1950 **6** 26.
[2] Frisch, S. *Westnik Leningr. Univ.* 1954 **18** 57.
[3] Botschkowa, O. u. Schreider, E. *Spektralanalyse von Gasgemischen.* Gosisdat, Moskau 1955.

[4] Frisch, S. u. Schreider, E. *Izv. Akad. Nauk SSSR, Ser. fiz.* 1949 **13** 465.
[5] Bhatt *Proc. Ind. Acad. Sci.* 1935 **1** 891.
[6] Beck, H. *Z. Phys.* 1935 **97** 355.
[7] Noller, W. *Z. Phys.* 1938 **110** 320.
[8] Botschkowa, O. u. Schreider, E. *Westnik Leningr. Univ.* 1956 **16** 57.
[9] Schreider, E. *Sawodskaja Laboratorija* 1952 **18** 326.
[10] Wignen, J. u. Van Tiggelen, A. *Spectrochimica Acta* 1950 **4** 8.
[11] Bogdanow, S. u. Wulfson, K. *Dokl. Akad. Nauk SSSR* 1941 **30** 309.
[12] Botschkowa, O. u. Schreider, E. *Sawodskaja Laboratorija* 1955 **21** 311.
[13] Botschkowa, O. u. Rasumowskaja, L. *Izv. Akad. Nauk SSSR, Ser. fiz.* 1957 **21**.
[14] Botschkowa, O. u. Schreider, E. *Izv. Akad. Nauk SSSR, Ser. fiz.* 1955 **19** 75.

L.
3
/59

Spectrochimica Acta, 1958, Vol. 13, pp. 60 to 68. Pergamon Press Ltd., London

The origin of group frequency shifts—I

Abnormal frequencies in multiple bonds

L. J. Bellamy
E.R.D.E., Ministry of Supply, Waltham Abbey, Essex

(*Received* 27 *May* 1958)

Abstract—The data available on multiple bond frequencies in various intramolecular environments has been reviewed and further evidence is presented that the frequency shifts are directly related to the inductive and mesomeric effects of the substituents. Abnormal frequencies occur when the usual balance of these forces is upset and they can often be satisfactorily accounted for from a consideration of the potential energies of the competing canonical forms.

Introduction

There is now a good deal of evidence that the frequencies of multiple bonds are very little sensitive to the mass effects of the substituents, unless these happen to be hydrogen or deuterium atoms. Vibrational coupling effects are also relatively uncommon in this series. Nevertheless, the frequencies vary widely with the nature of the substituents, and Hartwell, Richards and Thompson [1] have suggested that this is due to the operation of inductive and mesomeric effects. This is borne out by the results of later workers [2–4] and by the many quantitative relationships which have been found between group frequency shifts and other physical properties which depend upon the same factors [2, 5–8]. In special cases, field effects can also give rise to frequency shifts but these are relatively small and will not be further considered here.

The relative incidence of inductive and mesomeric effects depends directly upon the differences in the potential energies of the separate canonical forms. In the following paper a number of cases are considered in which these differ widely or in which they can be systematically varied by known amounts, and it is shown that many abnormal group frequencies can be satisfactorily accounted for on this basis.

The operation of inductive and mesomeric effects on multiple bonds

Inductive effects can lead to either a rise or a fall in the frequency of a multiple bond depending upon its original polarity. In a compound such as acetone the electron cloud of the carbonyl link is displaced towards the oxygen atom giving the bond some polar character. The replacement of a methyl group by a strongly electronegative chlorine atom results in the attraction of this charge cloud back nearer to the geometric bond centre. The carbonyl link then becomes less polar and the frequency rises. In a non-polar compound such as but-2-ene however, the charge cloud of the double bond is initially central. Replacement of a methyl group by chlorine displaces the cloud away from the bond centre leading to a more polar bond of lower frequency. When mesomerism is absent, the frequency

VOL.
13
1958/5

shifts arising from induction will be a direct function of the electronegativities of the substituents, and a number of such cases are known [2, 9]. However when mesomerism occurs, the inductive effect also varies due to the alteration in the charge of the substituents. Contributions from ionic forms are usually too small to have any significant effect upon the frequencies of multiple bonds but special cases occur which are considered separately below.

Mesomerism of the group of R—C(=O)— to the polar structure $R\overset{+}{=}C\overset{}{-}\overset{-}{O}$ occurs through the donation of an electron from the lone pair of R. It will always increase the polarity of the multiple bond and lower its frequency. In the case of C=C links it follows that both induction and mesomerism will lead to lower frequencies, and this is supported by the fact that, in general no C=C frequencies are found at significantly higher values than that of the purely covalent but-2-ene. The only exceptions to this are fluorinated olefines which form a special group which is discussed below. The direct connexion between the frequency changes of normal olefines and the polarity of the double bond is well shown by the smooth relationship which connects the frequency shifts with the enthalpies of hydrogenation [10].

When the multiple bond is initially polar, as in the carbonyl group, the direction of frequency shift following substitution is less easy to predict as the inductive and mesomeric effects operate in different directions. In some cases however this is possible from potential energy considerations. For example, it is known that the energy difference between the two canonical forms of vinyl chloride is approx. 60 kcal [11]. Using this value it is possible to calculate the corresponding difference for acetyl chloride, making use of the known bond energies of the different C—C, C=O links, etc. The value obtained is 110 kcal which suggests that any contribution from the mesomeric form $Cl\overset{+}{=}C\overset{}{-}\overset{-}{O}$ is likely to be too small to have any appreciable effect upon the frequency. This is confirmed by the abnormally long C—Cl bond length (1·82 Å) and of course by the high carbonyl frequency.

Considerations of this kind therefore lead to a reasonable explanation of the fact that the substitution of a chlorine atom on to a C=O link raises the frequency by 90 cm^{-1}, whereas substitution at a C=C link lowers it by 70 cm^{-1}.

The reduction of mesomerism by opposed resonance

In amides, resonance contributions from forms such as $-\overset{+}{N}=C\overset{}{-}\overset{-}{O}$ lead to a substantial stabilization as measured by the resonance energy. The low carbonyl frequencies found in such systems have therefore been attributed to the predominance of this effect over induction which would result in a frequency rise [1]. However the contribution of mesomeric forms will be reduced in compounds in which the nitrogen atom forms parts of a cyclic system which itself possesses resonance energy derived from the lone pair electrons of the nitrogen. For example the pyrrole ring has a resonance energy of about 25 kcal derived from the resonance with an aromatic type canonical form. In N-acetyl pyrrole (I)

resonance to the canonical form (II) can only occur at the expense of the normal resonance of the pyrrole ring, as the same lone pair nitrogen electrons are required in each case and it is therefore less favoured than in normal amides to the extent of about 25 kcal. Otting [12] and Staab, Otting and Ueberle

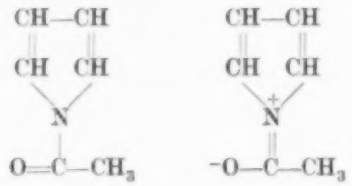

(I) (II)

[13] have already drawn attention to the remarkably high amide carbonyl frequencies of N-acetyl pyrroles, imidazoles and tetrazoles, and similar data has been given by Tanner [14]. Otting *et al.* associate the high frequencies with a reduction in the incidence of mesomerism, and this is strongly reinforced by a semiquantitative consideration of the energy changes involved. In the table, the

Table 1

Compound	ν_{CO} cm^{-1} ($CHCl_3$)	Resonance energy of patent ring (kcal)
$CH_3(CH_2)_nCO\ NH_2$	1679[a]	0
N-Acetyl indole	1711[b]	13[c]
N-Acetyl pyrrole	1732[b]	24·5[c]
N-Acetyl imidazole	1747[b]	38
N-Acetyl triazole	1765[b]	51·5
N-Acetyl tetrazole	1779[b]	65[d]
Acetyl chloride	1800	—

(a) Jones R. N. and Sandorfy C., *Chemical Applications of Spectroscopy* p. 522. Interscience 1956.
(b) Ref [13].
(c) Wheland G. W., *Resonance in Organic Chemistry* p. 99. Wiley, New York 1955. The value for indole represents the total resonance energy less that of benzene.
(d) McEwan W. S. and Rigg M. W., *J. Amer. Chem. Soc.* 1951 **73** 4725.

frequencies of a series of heterocyclic amides of this type are listed along with the resonance energies of the parent ring systems. The resonance energies quoted for imidazole and triazole are very approximate, having been obtained by interpolation between those of pyrrole and tetrazole, but in a regular series of this kind are probably adequate for the order of precision required. In the figure, the carbonyl frequencies are plotted directly against these energy values and a smooth progression is found. The curve is asymptotic at high energies and high frequencies, as is to be expected. The resonance energy of tetrazole (ca. 65 kcal) appears to be approaching a value at which the normal amide resonance would be precluded altogether. Any further increase in the resonance energy of the heterocyclic system would not then influence the carbonyl frequency, which would depend solely upon the electronegativity of the nitrogen atom. The curve suggests that

VOL. 13 1958/5

this limiting value for ν_{co} in amides is near 1810 cm^{-1}, which compares well with the carbonyl frequency of acetyl chloride in which mesomerism is also effectively absent (see above) and in which the electronegativity of the halogen substituent is the same as that of nitrogen.

At the other end of the curve the slope is much less steep, so that a change in the resonance energy of the cyclic system over the range ± 5 kcal corresponds to

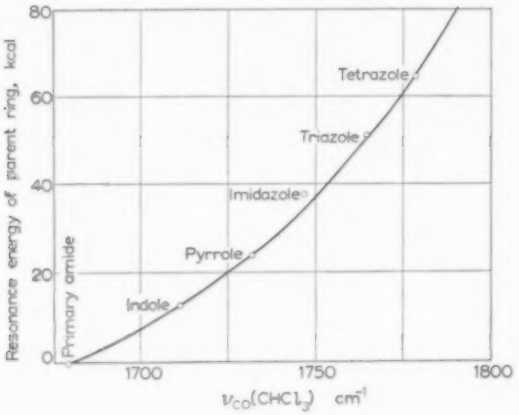

Fig. 1.

a frequency shift of 30 cm^{-1}. This may well explain the considerable carbonyl frequency shifts which accompany changes of state in normal amides, as energy changes of this order might well arise from intermolecular interactions.

It should be emphasized that the figure illustrates relative rather than absolute energy changes. As the carbonyl frequency rises from 1680 cm^{-1} to 1810 cm^{-1}, the resonance stabilization energy of the amide system itself falls from about 20 kcal to zero. At the same time the inductive effect of the nitrogen atom alters steadily as the contribution from positively charged forms is reduced. Neither of these effects is fully taken into account in the figure but both can be expected to show a smooth progression over the range. These findings therefore afford a further example of the direct dependence of the carbonyl frequency upon the inductive and mesomeric effects of the substituents and allow of a reasonable explanation of the very high amide frequencies which have been observed.

The increase of mesomerism by complementary resonance

The converse of the above cases must be sought in systems in which the occurrence of mesomerism at a carbonyl group will result in a substantial gain in the resonance energy of a cyclic system. Examples of this occur with 1:4-pyrones and thiapyrones. Mesomerism in 1:4-thiapyrone (III) does not lead to the form (IV) but to the more stable structure (V) and the additional resonance energy of the cyclic system has been assessed at 33 kcal in the case of 3:5-diphenyl 1:4-thiapyrone [15].

The additional resonance lowers the potential energy of the canonical form (V) below the normal value, and mesomerism is thereby increased, resulting in

low carbonyl frequencies. 1:4-Pyrone [16] absorbs at 1626 cm^{-1} and in the corresponding thiapyrone and its derivatives in which the resonance stabilization is greater, the carbonyl absorption [17] falls in the range 1609–1590 cm^{-1}. The direct dependence of these low values upon the heterocyclic ring resonance is well shown by the spectrum of the sulphone (VI) in which the ring resonance is eliminated by

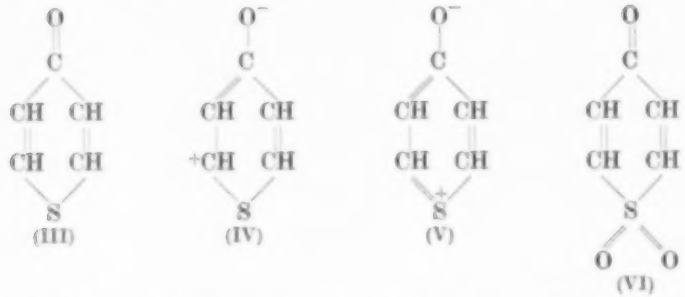

the removal of the lone pair electrons of the sulphur atom. The carbonyl frequency [17] then rises to 1657 cm^{-1} which is more normal for a cyclic $\alpha{:}\beta$, $\alpha'{:}\beta'$ unsaturated carbonyl group. It is probable that similar effects occur in the hydroxy pyridines and pyrimidines which exist in the ketonic form. The carbonyl frequencies appear to be unduly low compared with normal amides but they are difficult to recognize with certainty because of the accompanying bands from the heterocyclic rings.

VOL. 13 1958/5

The incidence of steric factors upon mesomerism

Conjugation and mesomerism both involve some degree of delocalization of the electrons over the atoms of the resonating group, and are therefore very sensitive to the planarity of the bonds concerned. Steric factors which decrease or increase the coplanarity of the systems will therefore lead to frequency shifts by alterations in the contributions of resonance forms.

An example of the first kind is found in the *o*-substituted acetophenones studied by Braude and Timmons [18]. By a gradual increase in the size of the *o*-substituent the carbonyl group can be progressively twisted out of the plane of the ring and the carbonyl frequency rises, reaching a limiting value near to that of saturated systems, when the *o*-substituent is very large. Braude *et al.* have assessed the potential energy changes which occur as the angle between the carbonyl group and the plane of the ring is increased. These are found to show a reasonably smooth relationship with the relative carbonyl frequency shifts over the whole range.

Examples of the opposite kind occur in systems such as (VII) which have been studied by Huisgen *et al.* [19].

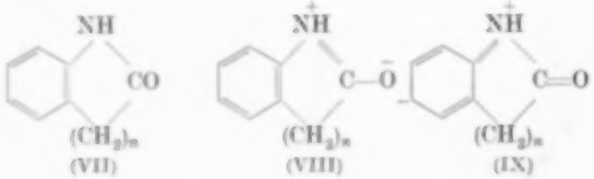

Here the degree of resonance to forms such as (VIII) is reduced by contributions from canonical forms such as (IX) which compete directly for the available lone pair electrons of the nitrogen atom. The extent to which competition occurs depends directly upon the number of (CH_2) groups in the ring. As these increase the heterocyclic ring becomes more puckered so that contributions from form (IX) are diminished and those from form (VIII) increased. The amide carbonyl frequency therefore falls progressively from $n = 1$(CO 1710 cm^{-1}) to $n = 5$(CO 1660 cm^{-1}). The first step is also due in part to the change of ring size from five to six members but the remainder can be attributed wholly to the steric effect. The observed frequencies for this series are directly parallel by the Pk_a values of the amide NH group.

Competition between alternative mesomeric forms

Systems such as (VII) and the N-acetyl pyrroles, are examples of molecules in which mesomerism affects the carbonyl group to a smaller extent than in normal amides because of competitive effects. However many simpler cases exist, and the high frequencies of acetanilides (ca. 1700 cm^{-1}) probably arise in the same way. One interesting case is that of the vinyl esters, R—CO—O—CH=CH_2, in which mesomerism to the form $CH_3—C(=O^-)—O^+—CH=CH_2$ is largely inhibited by the competition for the oxygen electrons of the alternative form $CH_3—C(=O)—O^+=CH—CH_2^-$. This is confirmed by the absence of resonance energy in vinyl acetate. The multiple bond frequencies are therefore controlled only by the inductive effect of the oxygen atom, and in accordance with the suggestions given earlier, the carbonyl frequencies rise (near 1800 cm^{-1}) and the olefinic frequencies fall. The N-nitrosoamides R—CO—N(—)—N=O afford an interesting contrast. Mesomerism is again inhibited by a competitive effect of the C=O, and N=O groups for the same lone pair electrons at the central nitrogen. However as both multiple bonds are now polar, the resulting inductive effect results in a frequency rise in both cases. The carbonyl absorptions in such systems occur [20] near 1740 cm^{-1} and the nitroso absorptions near 1525 cm^{-1}. Normal monomeric dialkylnitrosoamines absorb near 1450 cm^{-1}. It should be noted that anomalies of this kind arise only when a competitive substituent is attached to the electron donating group. They do not occur for example in a compound such as tetramethyl urea in which the attachment is to the carbonyl group. In such cases the degree of resonance is increased and the carbonyl frequency is lower than usual (1639 cm^{-1}).

Contributions from ionic forms

It has been suggested that aluminium trichloride complexes of acetyl chloride, and of nitrosyl chloride exist wholly in ionic forms, and this is strongly supported by the observed frequencies. Thus, the former absorbs [21] at 2300 cm^{-1} corresponding to the structure $[CH_3C{\equiv}O]^+AlCl_4^-$, whilst the latter absorbs [22] at

2236 cm^{-1} close to the frequency of the NO^+ ion. The likelihood of contributions from similar ionic forms in more normal structures can be roughly assessed from energy considerations. The potential energy difference between the covalent and ionic forms X—Y=Z and $X^-[Y{\equiv}Z]^+$ is given by $\Delta E = D_{xy} + I_y - E_x - D_{x^-y^+} + D_{x-y} - D_{x=y}$, where ΔE is the energy difference, D_{xy}, etc., the dissociation energies of the appropriate bonds, I_y the ionization potential of Y and E_x the electron affinity X. The dissociation energy of the ionic bond $D_{x^-y^+}$ is obtained from the relation $e^2/(r_{x^-} + r_{y^+})$. Calculations of this kind suggest that ΔE will normally be large and that contributions from ionic forms can be discounted. Exceptions occur however, as in the case of nitrosyl chloride. Only a rough estimate of ΔE is possible in this case, as although reasonably good values are available for most of the terms of the above equation $D(N{\equiv}O)$ can only be approximated from the known values of $D(N{-}O)$ and $D(N{=}O)$. Nevertheless the resulting value for ΔE is −15 kcal which suggests that there will be a considerable contribution from the ionic form $Cl^-(NO)^+$. This was originally suggested by Ketelaar [23] to account for the abnormally long Cl—N bond (1·96 Å), and is also strongly supported by studies of the exchange of isotopically labelled chlorine atoms of NOCl with those of the non-electrolyte $POCl_3$, from which an ionic product for $[NO]^+Cl^-$ of 10^{-16} g-ion^{2}l^{-2} has been derived [24]. This accounts for the high N≡O stretching frequency, which is 300 cm^{-1} higher than in nitrosobenezene. It probably also explains the unusual observation that the N≡O frequency of this compound is higher in polar solvents than it is in the vapour phase [25], as the contribution of the ionic forms would be increased in such solvents.

Ionic forms will not be favoured if alternative mesomeric structures of lower potential energy are available. They are therefore most likely to arise in compounds with fluorine substitution as this element alone combines a very high inductive power with a very limited capacity for mesomerism due to its high ionization potential. Contributions from the form $F^-(FC{\equiv}O)^+$ may therefore play some part in the very high carbonyl frequency [26] of COF_2 (1928 cm^{-1}), and it is suggested below that similar effects are responsible for the abnormal C=C frequencies of fluorinated olefines.

The influence of fluorine substitution in olefines

The behaviour of olefinic bonds with multiple fluorine substitution has long presented a major group frequency anomaly. Vinylidine fluoride [27] absorbs at 1728 cm^{-1}, and the frequency rises steadily with further substitution to 1872 cm^{-1} (Raman) [28] in perfluoroethylene. No other cases are known in which the C=C frequency rises significantly above the value of 1675 cm^{-1} for the covalent bond of but-2-ene, suggesting that some unique property of fluorine is involved. In vinylidine fluoride the strong inductive effect of the halogens must increase the polarity of the C=C link, and the negative end of the dipole produced will lie at the carbon atoms carrying the fluorine substituents. Some increase in potential energy is to be expected from such an arrangement, particularly as this cannot be offset, as in vinylidine chloride, by any appreciable mesomerism to polar forms. Alternative ionic forms might then make some larger contribution than normal to the final structure. In the absence of adequate ionization potential data

VOL. 13 1958/5

it is not possible to evaluate the energy difference between $F_2C{=}CH_2$ and $F^-[FC{=}CH_2]^+$, but a certain amount of indirect evidence is available from other sources. Thus, the FCF angle of $CF_2{=}CH_2$ closes down [29] by as much as 10° to 110°; this would be expected if the carbon orbital directed towards the CH_2 carbon atom were taking on an increased *s* character. The chemical behaviour of compounds of this type also supports this concept [30]. C_2H_5OH adds in such a way that the negative OR residue is attached to the carbon atom carrying the fluorine substituents.

$$C_2H_5OH + CF_2{=}CCl_2 \rightarrow C_2H_5O{-}\overset{\displaystyle F}{\underset{\displaystyle F}{C}}{-}CHCl_2$$

This behaviour is difficult to explain on any basis other than by contribution of forms such as $F^-[FC{=}CCl_2]^+$. Finally, there is supporting evidence from reactivity data. It has already been noted that the C=C frequencies of normal olefines are directly related to the enthalpies of hydrogenation and the frequencies fall as the reactivity rises. This situation has been shown to reverse [10] for fluorinated olefines and for frequencies above 1675 cm^{-1}, the reactivity rises steadily with the frequency. This is consistent with the idea of ionic contributions which would lead to more reactive double bonds. It is not necessary to postulate the existence of triple bonded structures to account for the high C=C frequencies, as the orbital of the fluorinated carbon atom which forms the C—C σ bond in $^-F[\dot{F}\dot{C}{=}CH_2]$ must have a bigger proportion of *s* character than in the normal trigonal state, and this will result in a shorter C—C distance and a higher frequency.

Although no final conclusions are possible, this data coupled with the evidence for related ionic forms in aluminium trihalide complexes and in nitrosyl chloride therefore suggests strongly that the abnormal frequencies found in this series are due to contributions from ionic canonical forms.

Acknowledgements—Thanks are offered to Professor C. A. Coulson for a helpful discussion and for his kindness in reading and commenting upon the manuscript.

References

[1] Hartwell E. J., Richards R. E. and Thompson H. W., *J. Chem. Soc.* 1948 1436.
[2] Bellamy L. J., *J. Chem. Soc.* 1955 4221.
[3] Lord R. C. and Miller F. A., *Appl. Spectroscopy* 1956 **10** 115.
[4] Jones R. N. and Sandorfy C., *Chemical Applications of Spectroscopy* p. 473. Interscience, New York 1956.
[5] Bellamy L. J., *J. Chem. Soc.* 1955 2818.
[6] Flett M. St. C., *Trans. Faraday Soc.* 1948 **44** 767.
[7] Fuson N., Josien M. L. and Shelton E. M., *J. Amer. Chem. Soc.* 1954 **76** 2526.
[8] Goulden J. D. S., *Spectrochim. Acta* 1954 **6** 129.
[9] Bell J. V., Heisler J., Tannenbaum M. and Goldenson, J. *J. Amer. Chem. Soc.* 1954 **76** 5185.
[10] Bellamy L. J. and Williams R. L., *J. Chem. Soc.* 1958 In press.
[11] Ketelaar J. A. A., *Chemical Constitution* p. 218 Elsevier, Amsterdam 1953

[12] Otting W., *Chem. Ber.* 1956 **89** 1940.
[13] Staab H. A., Otting W. and Ueberle A., *Z. Electrochem.* 1957 **61** 1000.
[14] Tanner E. M., *Spectrochim. Acta* 1957 **9** 282.
[15] Lorenz L. and Sternitzke, H. *Z. Electrochem.* 1934 **40** 501.
[16] Sheinker Yu. N. and Pomevantsev I. Ya., *Zh. fiz. khim.* 1956 **30** 79.
[17] Tarbell R. S. and Hoffman P., *J. Amer. Chem. Soc.* 1954 **76** 2451.
[18] Braude E. A. and Timmons C. J., *J. Chem. Soc.* 1955 3766.
[19] Huisgen R., Ugi I., Brade H. and Ravenbusch E., *Liebigs Ann.* 1956 **586** 30.
[20] White E. M., *J. Amer. Chem. Soc.* 1955 **77** 6008.
[21] Susz B. P. and Wuhrmann J. J., *Helv. Chim. Acta* 1957 **40** 971.
[22] Gerding H. and Houtgraaf M., *Rec. Trav. Chim.* 1953 **72** 21.
[23] Ketelaar J. A. A., *Chemical Constitution* p. 229 Elsevier, Amsterdam 1953.
[24] Lewis J. and Sowerby D. A., *J. Chem. Soc.* 1957 1617.
[25] Bellamy L. J. and Williams R. L., *J. Chem. Soc.* 1957 863.
[26] Kagarise R. E., *J. Amer. Soc.* 1955 **77** 1377.
[27] Smith D. C., Nielsen J. R. and Claasen, H. H. *J. Chem. Phys.* 1950 **18** 326.
[28] Smith D. C., Nielsen J. R. and Claasen, H. H. *J. Chem. Phys.* 1950 **18** 812.
[29] Gordy W., Smith W. V. and Trambarulo R. F., *Microwave Spectroscopy* p. 373 Wiley, New York 1953.
[30] Simons J. N. and Brice T. J., *Fluorine Chemistry* Vol. II, p. 376 Academic Press, New York 1954.

VOL.
13
1958/5

Spectrochimica Acta, 1958, Vol. 13, pp. 69 to 74. Pergamon Press Ltd., London

Infrared spectra and vibrational frequencies of co-ordinated ethylene

D. B. Powell and N. Sheppard
The University Chemical Laboratory, Cambridge

(*Received* 14 *May* 1958)

Abstract—A comparison has been made of the infrared spectrum of a number of complexes in which ethylene is co-ordinated to platinum and palladium. A fairly complete assignment has been made of the fundamental vibration frequencies of the bonded ethylene molecule.

Introduction

A number of authors [1, 2] have recorded infrared spectra of platinum–ethylene complexes. However, there has been little detailed discussion of the vibrational assignment of the absorption frequencies observed, with the exception of the band near 1500 cm^{-1}, which has been ascribed to the $\nu C{=}C$ vibration by Chatt and Duncanson [1].

In the present work the infrared spectra of a number of such complexes have been examined in detail. The frequency range has in most cases been extended to 400 cm^{-1} by use of a potassium bromide prism.

Experimental

The absorption frequencies observed for these compounds are shown in Table 1, the figures for $[Pt(C_2H_4)Cl_2]_2$ being taken from the paper by Chatt and Duncanson [1]. Typical spectra are shown in Fig. 1. The spectrum of Zeise's salt, $K[Pt(C_2H_4)Cl_3]H_2O$ shows a marked change on dehydration in a vacuum desiccator over calcium chloride; the frequencies of most of the absorption bands change by about 10 cm^{-1} and a new absorption band appeared at 840 cm^{-1}. This compound has a very strong absorption band near 500 cm^{-1}, due to the water of crystallization, which is difficult to remove entirely by dehydration. In order to examine the spectrum in this region, the compound was converted to the deuterium oxide derivative $K[Pt(C_2H_4)Cl_3] \cdot D_2O$. A sample of this derivative was stored in a sealed tube with excess D_2O to determine whether any of the hydrogen atoms of the C_2H_4 group exchanged with the D_2O. Examination of the spectrum after three months showed that no exchange had taken place.

Discussion

The spectra of all the platinum complexes show a marked similarity in their main features, and the frequencies observed for the palladium complex vary only slightly from those of the platinum derivatives, although the intensities of some of the absorption bands are somewhat different. For example, the frequency near 1500 cm^{-1} ascribed to the $\nu C{=}C$ vibration is considerably stronger in $[Pd(C_2H_4)Cl_2]_2$ than in the platinum counterpart. It is noteworthy that the frequency found for the $\nu C{=}C$ vibration of palladium and platinum complexes is similar in each case.

Table 1. Absorption frequencies of ethylene complexes of palladium^{II} and platinum^{II}*

$[Pd(C_2H_4)Cl_2]_2$	$[Pt(C_2H_4)Cl_2]_2$	$K[Pt(C_2H_4)Cl_3]$ H_2O Zeise's salt	Dehydrated Zeise's salt	*trans* $[Pt(C_2H_4)Cl_2(NH_3)]$
3063 vw 3013 vw 2919 vw	3088 m 3072 w 3010 w 2979 vw 2956 vw	3085 vw 3020 vw 2990 vw	Not investigated	
2044 w		2018 w	2047 w	2045 w
1525 w	1506 w	1516 vw	1516 vw	1520 w
1438 s 1421 m	1428 s 1416 m	1428 s 1402 vw	1420 s 1400 w	1430 w 1422 s
1259 w	1236 w	1241 w	1253 w	
1202 vw	1217 w	—	—	
1162 vw	1175 w	1181 vw	1192 vw	—
1027 1021 vs	1027 vs	1022 s 1010 s	1032 s 1024 s	1023 s 1010 s
974 vw	971 vw	974 vw	976 vw	980 vw
827 w	818 m	—	841 w	816 m
680 w	715 m† 722	714 m	734 m	691 m
415 w	Not investigated in potassium bromide region	405 vw?	—	—
—	—	3540 3480 s (H_2O) 1611 s (H_2O) near 500 vs (H_2O)	1613 m (H_2O) near 500 m (H_2O)	1610 s 1265 1255 s 735 m 480 w } NH_3

* Spectra of dispersions in nujol and hexachlorobutadiene, using rocksalt and potassium bromide prisms.

† These figures taken from Ref. [2].

In order to assist in the assignment of the observed absorption bands to fundamental vibrations of the co-ordinated ethylene molecule, comparison was made with the spectrum of ethylene sulphide for which a fairly complete assignment of the

VOL. 13 1958/5

absorption frequencies has been made by THOMPSON and CAVE [3]. The general symmetry of the platinum–ethylene complex resembles that of ethylene sulphide as shown below:

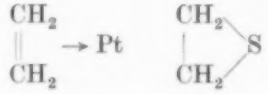

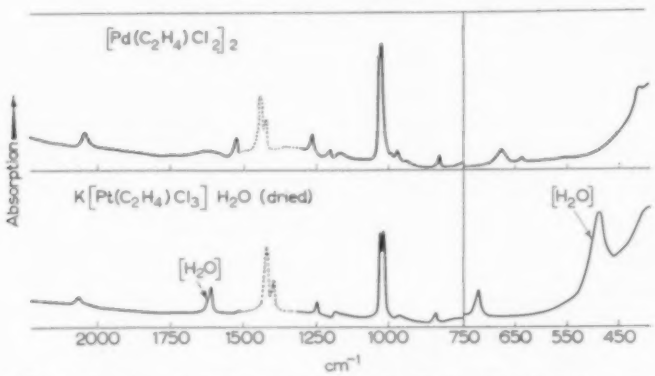

Fig. 1. Spectra of ethylene complexes of palladium^{II} and platinum^{II}.
(———) Nujol mull; (. . . . .) Hexachlorobutadiene mull.

and it was considered not unlikely that the frequencies of ethylene co-ordinated to platinum might be intermediate between those of the free molecule and the strongly "bound" ethylene molecule in ethylene sulphide.

An interpolation diagram connecting the corresponding frequencies of ethylene and ethylene sulphide is shown in Fig. 2 and has been used to make a number of assignments of the observed frequencies of the complex. The symmetry of a free ethylene molecule is V_h and this becomes C_{2v} for the coordinated or bonded ethylene molecule. The correspondences between the symmetry classes and selection rules for these two symmetries are given below [4]:

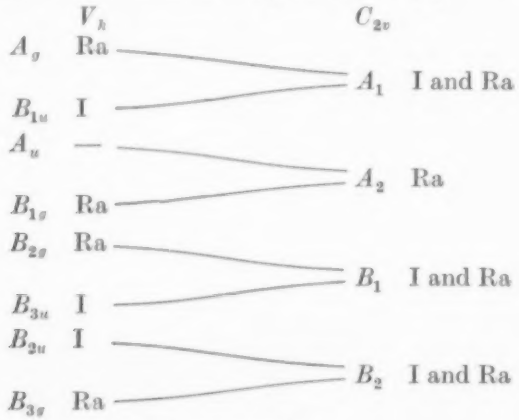

Ra = Raman active
I = Infrared active

The frequency assignments for the ethylene complexes are considered in detail below (the numbering of frequencies follows that given by Herzberg [5] for ethylene).

C—H *stretching* (νC—H). The absorption bands near 3000 cm^{-1} due to this vibration are generally weak and poorly defined. It is however noteworthy that the frequencies observed are closer to those for ethylene itself than to those observed for a CH_2 group in a saturated molecule [6].

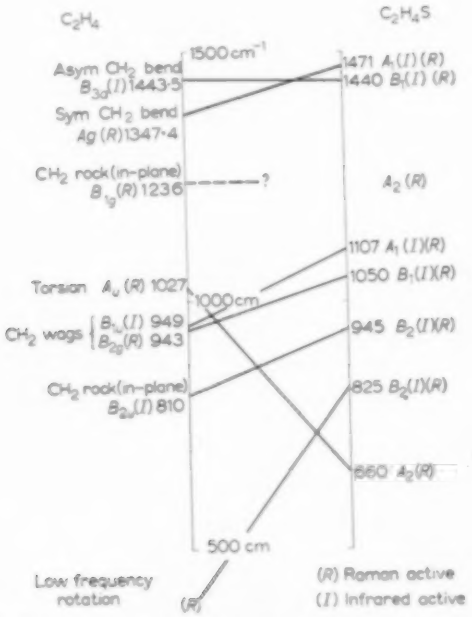

Fig. 2. Interpolation diagram relating vibration frequencies of ethylene and ethylene sulphide.

νC=C *stretching* (ν_2). This vibration is not infrared active in ethylene itself, but co-ordination to platinum causes it to become active, giving rise to a weak band near 1500 cm^{-1}. The frequencies observed for this band have been compared by Chatt and Duncanson [1] with the Raman data for ethylene and the olefine–silver perchlorate complex [7], and it is concluded that the order of frequencies observed (C_2H_4—1623 cm^{-1}; olefine–Ag, 1550 cm^{-1}; C_2H_4–Pt, 1505—1515 cm^{-1}) gives an indication of the degree of co-ordination of the ethylene to the metal. In this connexion it is interesting to note that the C_2H_4–Pd complex has an absorption frequency (1525 cm^{-1}) slightly greater than that for platinum; this therefore indicates slightly weaker co-ordination of the ethylene group.

CH_2 *bending* (ν_3 *and* ν_{12}). These vibrations are similar in frequency for ethylene and ethylene sulphide, but the symmetrical and asymmetrical frequencies are reversed in value; the vibrations for the ethylene–platinum complexes would therefore be expected to be close in frequency. The absorption found for these complexes near 1400 cm^{-1} is sometimes resolved into two peaks, but only one

VOL. 13 1958/5

distinct peak is observed in others. This absorption can therefore be ascribed to the vibrations ν_3 and ν_{12}, both of which become infrared active in the complex.

CH_2 *wagging* (ν_7 *and* ν_8). The two vibration frequencies of ethylene are narrowly separated, one being Raman active, the other infrared active (Fig. 2); both become infrared active in ethylene sulphide and in the complexes. Two absorption bands are observed for the ethylene complexes near 1000 cm^{-1} and can clearly be assigned to these vibrations.

Other fundamental vibration frequencies. There remain only two fundamental frequencies of the ethylene part of the complex which are expected to be infrared active, namely ν_{10} (an in-plane CH_2 rocking vibration) and ν_T (in the complex this is a CH_2 twisting vibration and is the analogue of the rotation of the free ethylene molecule about the C=C axis). ν_{10} has the frequency of 810 cm^{-1} in ethylene and 945 cm^{-1} in ethylene sulphide; in the spectra of the complexes it seems reasonable therefore to assign a band of rather variable intensity occurring near 820 cm^{-1} to this vibration. Another band of medium strength occurs consistently in the spectra of the complexes between 680 and 740 cm^{-1} and may be provisionally assigned to ν_T.

There remain a few more weak but consistent frequencies in the spectra, near 2000 cm^{-1} (w), 1250 cm^{-1} (w), 1190 cm^{-1} (vw) and 975 cm^{-1} (vw). The 2000 cm^{-1} band is analogous to a strong combination frequency of ethylene and can be assigned to $\nu_7 + \nu_8$. On account of its proximity to the analogous frequency of ethylene, the band near 1250 cm^{-1} can be tentatively assigned to the formally infrared inactive fundamental ν_4. The much weaker band near 975 cm^{-1} may likewise be the infrared inactive fundamental ν_4. These absorption bands may be enhanced in intensity by intermolecular forces within the lattice. However some of the weak lines may alternatively represent combination frequencies of certain of the identified fundamentals with the lower frequency skeletal modes. In this connexion it should be recorded that occasionally very weak bands have been found at the limit of the potassium bromide prism, near 400 cm^{-1}, which might possibly be due to a stretching vibration associated with the Pt–ethylene bond. With the palladium complex $[Pd(C_2H_4)Cl_2]_2$, a much more clearly defined band is observed near 410 cm^{-1} which might be assigned similarly. It is possible that the 1250 cm^{-1} band mentioned above is a combination of the fundamental near 400 cm^{-1} with ν_{10}.

General conclusions

It has been possible to suggest virtually a complete assignment of fundamental infrared absorption frequencies for co-ordinated ethylene. It is interesting to note that the fundamental frequencies of ethylene change only slightly on coordination. This is shown by the following list of fundamentals of co-ordinated ethylene in which the corresponding frequencies of ethylene itself are shown in brackets [6]. The data are those obtained with Zeise's salt:

3085(3106); 3020(3019); 2990(2990); 1516(1623); 1428(1444); 1402(1342); 1241(1236); 1022(949); 1010(943); 975?(1027); 841(810).

Acknowledgements—We should like to thank I.C.I. Ltd. and the Hydrocarbon Research Group of the Institute of Petroleum for financial assistance.

References

[1] Chatt J. and Duncanson L. A., *J. Chem. Soc.* 1953 2939.
[2] Jonassen H. B. and Field J. E., *J. Amer. Chem. Soc.* 1957 **79** 1275.
[3] Thompson H. W. and Cave W. T., *Trans. Faraday Soc.* 1951 946.
[4] Herzberg G., *Infrared and Raman Spectra of Polyatomic Molecules* p. 237. Van Nostrand 1946.
[5] Herzberg G., *Infrared and Raman Spectra of Polyatomic Molecules* p. 107. Van Nostrand 1946.
[6] Sheppard N. and Simpson D. M., *Quart. Revs.* 1953 **7** 21.
[7] Taufen H. W., Murray M. J. and Cleveland F. F., *J. Amer. Chem. Soc.*, 1941 **63** 3500.

VOL.
13
1958/5

Spectrochimica Acta, 1958, Vol. 13, pp. 75 to 79. Pergamon Press Ltd., London

Infrared absorption spectra of α-halogenated keto-steroids

FRANCESCO MEDA
Research Laboratories of S. A. Farmitalia, Milan

(*Received* 25 *May* 1958)

Abstract—The effect of the introduction of halogen in the 3-keto-Δ^4 system present in the steroids of progesterone, testosterone, deoxycorticosterone and cortisone series has been studied. The infrared absorption band linked to the carbonyl group is shifted toward higher wave numbers, with a decreasing effect in the F > Cl > Br order. The band assigned to the C=C unsaturated system falls from its normal position, about 1613 cm^{-1}, up to 1585–1570 cm^{-1}, with a considerable intensity increase. In this case the halogen series acts in the contrary order, i.e. F < Cl < Br. In derivatives containing fluorine, however, the perturbing action of halogen is either non-existent or nearly nil. Such effects are referred to steric factors: this enables the distinction between axial or equatorial configuration of epimer couples.

THE influence of α-halogen substituents on the position of the infrared absorption bands of the carbonyl group and conjugated double bond in an alicyclic ring was first pointed out by MCBEE, SMITH and UNGNADE [1]. For the carbonyl bands of conjugated *cyclo*pentenones they found a shift of over 10 cm^{-1} towards higher wave numbers; meanwhile the conjugated C=C band became localized in the 1587–1565 cm^{-1} region.

JONES, RAMSAY, HERLING and DOBRINER [2] had already shown that, for α-brominated keto-steroids, displacement of the carbonyl band is in direct relation to the steric arrangements of the C—Br linkage. The subsequent developments of COREY, TOPIE and WEZNIAK [3, 4] established correlations, for *cyclo*hexane ring systems, which enabled axial and equatorial orientations to be differentiated [5, 6]. The effects of Cl and Br substituents in the axial position were much less than in the equatorial position. Furthermore, for axial halogens, the effect on the carbonyl increased in the order I < Br < Cl. Little or nothing was known, however, about compounds containing fluorine atoms.

In a previous paper [7] data were given on some 3-keto-4-halogen-Δ^4 steroids, in which the halogen must necessarily occupy an equatorial configuration. These showed that the effects of the halogen upon the carbonyl and double linkage bands were in opposite directions and additive. A more complete series of such compounds has now been studied, including some with fluorine substitution, and the results are reported below.

Experimental and results

The spectra were run on a Beckman IR/2 spectrometer with a sodium chloride prism, using nujol mulls. The series of compounds examined and compared with the non-halogenated materials were progesterone, testosterone, deoxycorticosterone and cortisone, all containing the 3-keto-Δ^4 system in the *A* ring.

Frequencies of the infrared absorption bands of the keto groups and double bond are listed in Table 1. Their shifts from the basic position in the non-halogenated compounds are listed and compared in Table 2.

Table 1. Infrared frequencies (in nujol) of α-halogenated keto-steroids in the carbonyl and double bond region (cm^{-1})

Steroid	Ref.	20 ketone	11 ketone	3 ketone conjugated	4 : 5 C=C conjugated
Fluorinated					
4-Fluoro-progesterone	a	1689		1689	(1639), 1613
4-Fluoro-testosterone acetate	b			1689	1637, 1613
4-Fluoro-deoxycorticosterone acetate	a	1715		1686	1634, 1613
4-Fluoro-cortisone acetate	a	1724	1701	1701,1664*f*	1639, 1615
Chlorinated					
4-Chloro-progesterone	c	1698		1683	1631, 1575
4-Chloro-testosterone acetate	c			1683	(1642,1621),1585
4-Chloro-19-nor-testosterone acetate	c			1686	(1647), 1585
4-Chloro-17α-methyl-testosterone	a			1681	(1645*f*), 1580
4-Chloro-cortisone acetate	a	1701	1701	1701,1664*f*	1626, 1580
Brominated					
4-Bromo-progesterone	c	1698		1681	(1631*f*), 1570
4-Bromo-testosterone acetate	b			1681	1623, 1577
4-Bromo-deoxycorticosterone acetate	c	1715		1683	1631, 1572

Notes (1) *f* after the frequency refers to a shoulder.
(2) The frequencies in parentheses refers to the weak bands.

References (a) CAMERINO, MODELLI and PATELLI, *Il Farmaco* (*Sci. Ed.*) 1958 **13** 52.
(b) CAMERINO, PATELLI and VERCELLONE, *J. Amer. Chem. Soc.* 1956. **78** 3540
(c) CAMERINO, PATELLI, VERCELLONE and MEDA, *Il Farmaco* (*Sci. Ed.*) 1956 **11** 586.

Table 2. Infrared frequencies (in nujol) of α-halogenated keto-steroids and frequency shift on halogenation (cm^{-1})

Steroid	3 ketone conjugated	Shift $\Delta\nu$	4 : 5 C=C conjugated	Shift $\Delta\nu$
Progesterone	1661		1615	
4-Fluoro-progesterone	1689	+28	1613	−2
4-Chloro-progesterone	1683	+22	1575	−40
4-Bromo-progesterone	1681	+20	1570	−45
Testosterone propionate	1669		1613	
4-Fluoro-testosterone acetate	1689	+20	1613	0
4-Chloro-testosterone acetate	1683	+14	1585	−28
4-Bromo-testosterone acetate	1681	+12	1577	−36
17α-Methyl-testosterone	1661		1610	
4-Chloro-17α-methyl-testosterone	1681	+20	1580	−30
Deoxycorticosterone acetate	1667		1608	
4-Fluoro-deoxycorticosterone acetate	1686	+19	1613	+5
4-Bromo-deoxycorticosterone acetate	1683	+16	1572	−36
Cortisone acetate	1675,1653		1613	
4-Fluoro-cortisone acetate	1701,1664*f*	+26	1615	+2
4-Chloro-cortisone acetate	1701,1664*f*	+26	1580	−33

Note: *f* after the frequency refers to a shoulder.

VOL. 13 1958/59

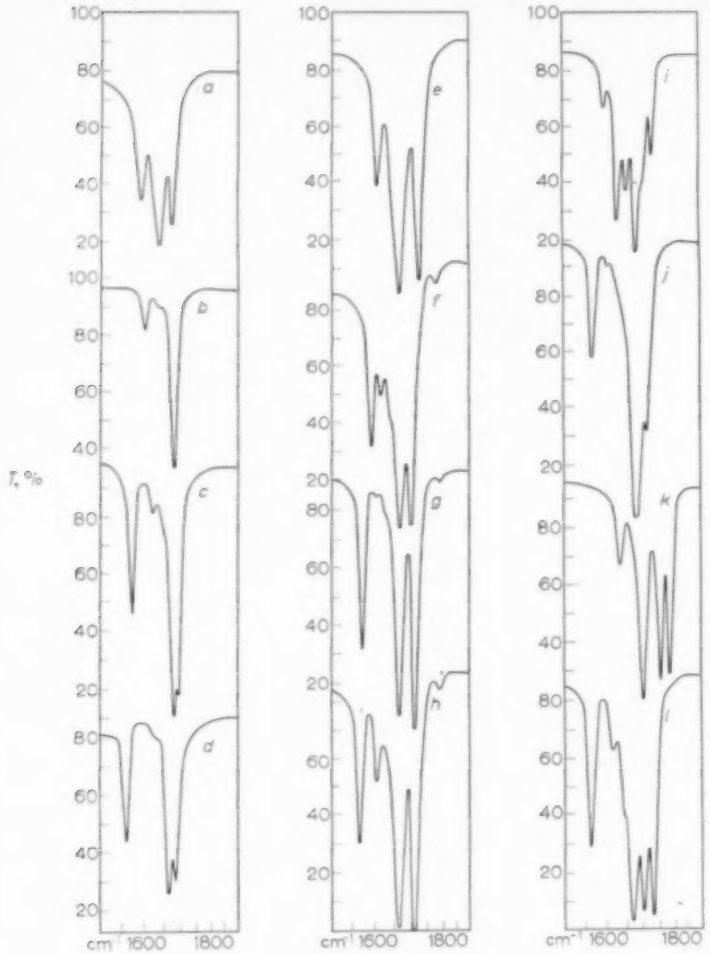

Fig. 1.

A: Progesterone
B: 4-Fluoro-progesterone
C: 4-Chloro-progesterone
D: 4-Bromo-progesterone
E: Testosterone
F: 4-Fluoro-testosterone acetate
G: 4-Chloro-testosterone acetate
H: 4-Bromo-testosterone acetate
I: Cortisone acetate
J: 4-Chloro-cortisone acetate
K: Deoxycorticosterone acetate
L: 4-Bromo-deoxycorticosterone acetate

With regard to the progesterone series, it can be seen that the introduction of an α-halogen atom raises the conjugated 3-ketone band (normal position 1661cm^{-1}) to 1689–1683–1681 cm^{-1} for derivatives containing F, Cl and Br respectively. The shifts toward higher wave numbers are therefore 28–22–20 cm^{-1}. The testosterone and 17 α-methyl-testosterone series behave similarly although the shifts are smaller. This is true also of the deoxycorticosterone and cortisone series.

The influence of the halogen substituent upon the $\diagdown\!\!\diagup C{=}C\diagdown\!\!\diagup$ frequencies has

also been studied. It will be seen from Table 2 that this is in the opposite direction to the effect upon the carbonyl group and leads to lower frequencies. The greatest frequency shift was produced by bromine and the least by fluorine. This parallels the behaviour of the C=C frequencies of the vinyl halides in which the greatest shift is shown by vinyl iodide whereas the frequency of vinyl fluoride is close to that of propene.

The absorption curves of the compounds examined in the spectral region from 1890 to 1540 cm^{-1} appears in Fig. 1, which has the percentage transmission values on the ordinate; for the sake of convenience the curves have been shifted one in relation to the other in the vertical direction. In the first column from the left we have the progesterone derivatives spectra, in the second column those of testosterone derivatives, and in the third one those of cortisone and of deoxycorticosterone derivatives.

Attention should be paid to the high intensity increase that accompanies the frequency shift of the double linkage band due to the introduction of halogen. This variation is very much less for the fluorinated derivatives (curves B and F), in which the frequency shifts are also small. Beside the very strong band of the double bond in the 1585–1570 cm^{-1} region for the chloro- and bromo-derivatives there is a weak band (or shoulder) about 1647–1626 cm^{-1}, corresponding to the unconjugated double bond.

Discussion

A theoretical interpretation of the effect induced by halogen on the carbonyl band has already been given by Bellamy [8, 9]. When the vibrational frequencies are not mass sensitive, displacements generally occur under the influence of the inductive or mesomeric effects of the substituents, however the different action according to the spatial orientation of the substituent cannot be explained in this way, as an inductive effect should be independent of steric factors and a mesomeric effect would cause a fall instead of a rise in frequency. The introduction of the concept of intramolecular dipolar effects [9, 11] explains these findings. When in a molecule a charged atom is near in space to another readily polarizable atom (carbonyl-oxygen), it is likely that a mutual action of charges will occur, which alters the bond polarity and consequently the absorption frequency. In this case, negative halogen, if equatorially oriented, comes near to the carbonyl-oxygen; the induced charge will diminish the C=O bond polarity and thus the frequency will increase.

The more the distance between the interacting atoms, the smaller the shift will be; the amount would depend only on the steric arrangement of the molecule.

The 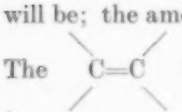 frequency is reduced due to contributions from forms such as

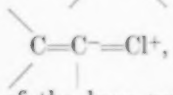 , and the extent to which this occurs depends upon the availability of the lone pair electrons of the halogen atom. It therefore follows the order I > Br > Cl > F which is that to be expected from a consideration of the ionization potential.

VOL. 13 1958/5

Apart from its theoretical importance, the analytical interest of this work should be emphasized, as it permits the characterization and differentiation of epimer steroids according to the frequency shifts induced by substituents in equatorial or axial position.

The regularities pointed out enable the forecast of shift amount to be expected for a specific steric model; the agreement with the experimental data confirms the aposite molecular structure.

Acknowledgement—The author wishes to thank the Director of S. A. Farmaceutici Italia in Milan for permission to publish this work and Professor B. CAMERINO, Chief of Chemical Division of Research Laboratories, for specimens. He wishes to acknowledge the helpful suggestions and criticism of Dr. L. J. BELLAMY.

References

[1] MCBEE E. T., SMITH D. K. and UNGNADE H. E. *J. Amer. Chem. Soc.* 1955 **77** 559.
[2] JONES R. N., RAMSAY D. A., HERLING F. and DOBRINER K. *J. Amer. Chem. Soc.* 1952 **74** 2828.
[3] COREY E. J., TOPIE T. H. and WOZNIAK W. A. *J. Amer. Chem. Soc.* 1955 **77** 5415.
[4] COREY E. J. and BURKE H. J. *J. Amer. Chem Soc.* 1955 **77** 5418.
[5] BARTON D. H. R., PAGE J. E. and SHOPPEE C. W. *J. Chem. Soc.* 1956 331.
[6] CUMMINS E. G. and PAGE J. E. *J. Chem. Soc.* 1957 3847.
[7] CAMERINO B., PATELLI B., VERCELLONE A. and MEDA F. *Il Farmaco* (*Ed. Sci.*) 1956 **11** 586.
[8] BELLAMY L. J., THOMAS L. C. and WILLIAMS R. L. *J. Chem. Soc.* 1956 3704.
[9] BELLAMY L. J. and WILLIAMS R. L. *J. Chem. Soc.* 1957 4294.
[10] BELLAMY L. J. and WILLIAMS R. L. *J. Chem. Soc.* 1957 861.
[11] JONES R. N. and SANDORFY C. *Chemical Application of Spectroscopy* p. 479. Interscience, New York 1956.

Spectrochimica Acta, 1958, Vol. 13, pp. 80 to 92. Pergamon Press Ltd., London

Analysis of P- and R-branches of the 950 cm^{-1} band of $^{14}NH_3$

M. Tsuboi, T. Shimanouchi and S. Mizushima
Chemical Laboratory, Faculty of Science, Tokyo University, Hongo, Tokyo, Japan

(*Received* 31 *March* 1958)

Abstract—The vibration-rotation spectrum of $^{14}NH_3$ were measured with a grating spectrophotometer in the region from 730 to 1200 cm^{-1} with a resolution of 0·4 cm^{-1}. The frequencies of 131 lines belonging to the P- and R-branches of the symmetric deformation vibration band were determined. The values are believed accurate to ±0·03 cm^{-1}. From these eighteen molecular constants were calculated.

Introduction

The vibration–rotation spectrum of $^{14}NH_3$ was observed and analysed by Barker, Dennison, and their collaborators in the period from 1929 to 1941. [1–6]. Recent progress in the infrared techniques has enabled us to observe the spectrum with a higher resolving power and to determine the positions of the lines more precisely than they did. In 1950, Wood, Bell, and Nielsen [7] obtained the infrared absorption curves of $^{14}HN_3$ with a higher resolving power, but they did not give exact positions of the lines, nor derived any molecular constant. In 1955, Cumming [8] made an analysis of the fundamental band arising from the doubly degenerate N—H stretching vibration of $^{14}NH_3$. However, no other bands have been studied since 1950.

In view of the situation, the present authors made a series of precise measurements on the vibration–rotation spectrum of $^{14}NH_3$, together with that of $^{15}NH_3$. The result gave detailed information on the molecular structure and the intramolecular potential of ammonia. In this paper are reported the frequencies determined for 131 lines in the P- and R-branches of the fundamental band of the symmetric deformation vibration of $^{14}NH_3$ (in the region from 730 to 1200 cm^{-1}), and the values of eighteen molecular constants calculated from these frequencies.

Experimental

The band was observed in absorption using a Perkin–Elmer 112G spectrometer with a 75 lines/mm grating blazed at 12 μ and a KBr fore-prism. The practical resolution of the spectrometer at 10 μ was about 0·4 cm^{-1}. In the observation, gas cells with optical path lengths of 5, 10 and 12 cm were used. The pressure of the gas cells was kept less than 50 mm Hg throughout the measurements, so that the pressure broadening of ammonia might not affect the results. The calibration [9] of the micrometer scale of the wavelength drive of the grating monochromator was made with known frequencies of 296 lines, namely, 20 lines of HCl [10] (observed in the third order diffraction), 69 lines in the 1600 cm^{-1} band of H_2O [11] (second order), 57 lines in the 2350 cm^{-1} band of CO_2 [12] (third order), 37 lines in the 670 cm^{-1} band of CO_2 [13] (first order), 44 lines of CO [14] (third order) and 69 lines of in the band of N_2O [15] (first order). The frequency values determined for any sharp line are believed accurate to ±0·03 cm^{-1}, except for few lines in a region of the R-branch where we have no standard lines to compare with.

VOL. 13 1958/5

Results of the measurements

Figure 1 is a reproduction of a curve recorded for the purpose of giving a general idea of the feature of the band. For the actual determination of the position of a line, the curve was recorded on much elongated scale of wave-number and with higher resolution. The observed frequencies, corrected to vacuum, are listed in the fourth and ninth columns of Table 1.

Formulation and the assignments for the lines

In a close approximation, the rotation-vibration energy levels of a symmetric top molecule, such as ammonia molecule, are expressed as:

$$T = G(v) + F_v(J, K) \tag{1}$$

where, $G(v)$ is the energy of vibration with quantum number v and $F_v(J, K)$ is the energy of rotation. This is expressed as:

$$F_v(J, K) = B_v J(J+1) + (A_v - B_v)K^2 + D_v^J J^2(J+1)^2 + D_v^{JK} J(J+1)K^2 + D_v^K K^4 \tag{2}$$

where

$$J = 0, 1, 2, \ldots \quad \text{and} \quad K = J, J-1, \ldots, 1, 0, -1, \ldots, -J \tag{3}$$

are rotational quantum numbers. Furthermore,

$$A = h/8\pi^2 c I_A, \qquad B = h/8\pi^2 c I_B \tag{4}$$

and D's are rotational constants, and I_A and I_B are the moments of inertia for axis parallel and perpendicular to the symmetry axis, respectively. The last three terms in equation (2) represent the influence of the centrifugal force. The subscript v is added to the constants, A, B, I_A, I_B, and D's, since they are functions of the vibrational quantum numbers, but they do not depend upon the values of J and K.

In this vibration the change of the electric moment takes place along the symmetry axis, and the selection rules for the rotational quantum numbers are:

$$J = 0, \pm 1 \quad \text{and} \quad K = 0 \tag{5}$$

As pointed out by Sheng, Barker, and Dennison [6], the problem of double minimum potential has to be taken into account. This gives rise to a splitting of the energy level into two sub-levels. The wave functions characterizing these two states are either *symmetric* or *antisymmetric* with respect to the inversion on the plane of the hydrogen atoms, the lower levels being symmetric. Thus, there are four, instead of two, vibrational levels with quantum numbers:

$$v = 0^s, 0^a, 1^s, \text{ and } 1^a \tag{6}$$

Here superscripts, s and a, refer to the *symmetric* and *antisymmetric* levels respectively. Two of the allowed transitions:

$$S\text{: } 0^s \rightarrow 1^a \quad \text{and} \quad A\text{: } 0^a \rightarrow 1^s \tag{7}$$

were observed in the region measured in the present research.

The frequencies of the lines which belong to the $P\,(\Delta J = -1)$ and $R\,(\Delta J = +1)$

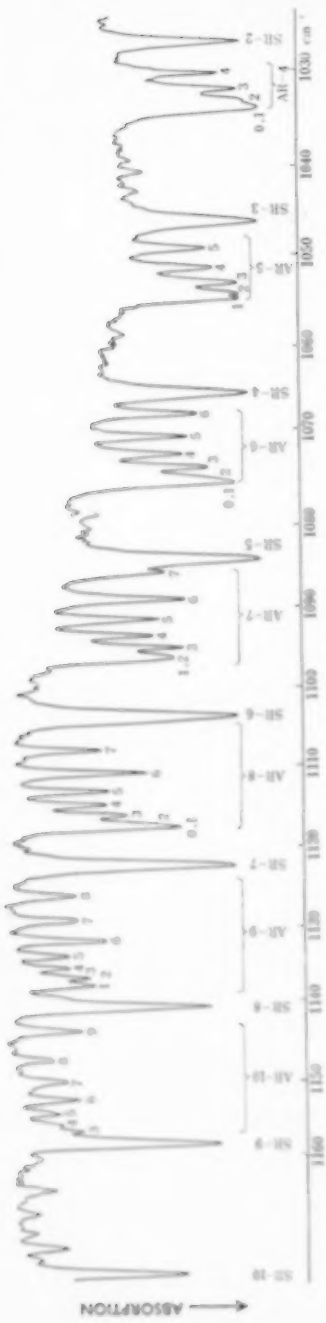

Fig. 1 A.

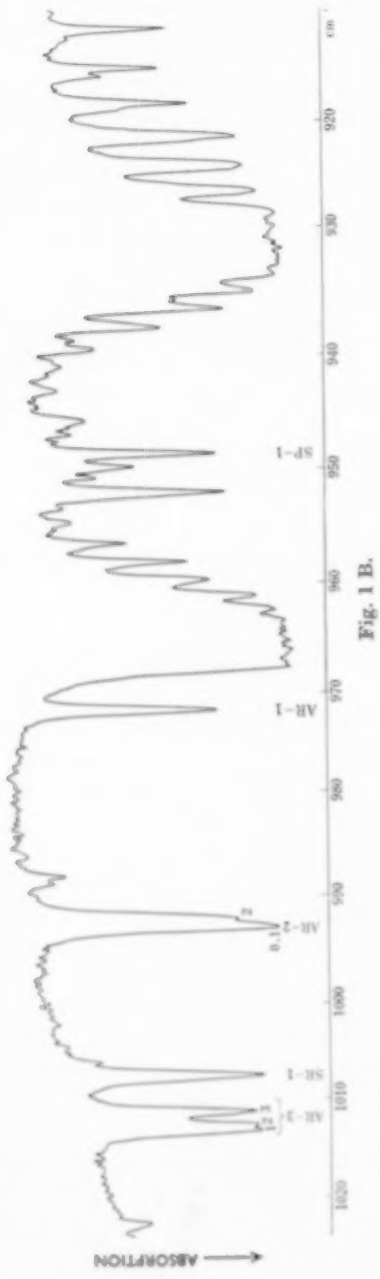

Fig. 1 B.

VOL. 13 1958/5

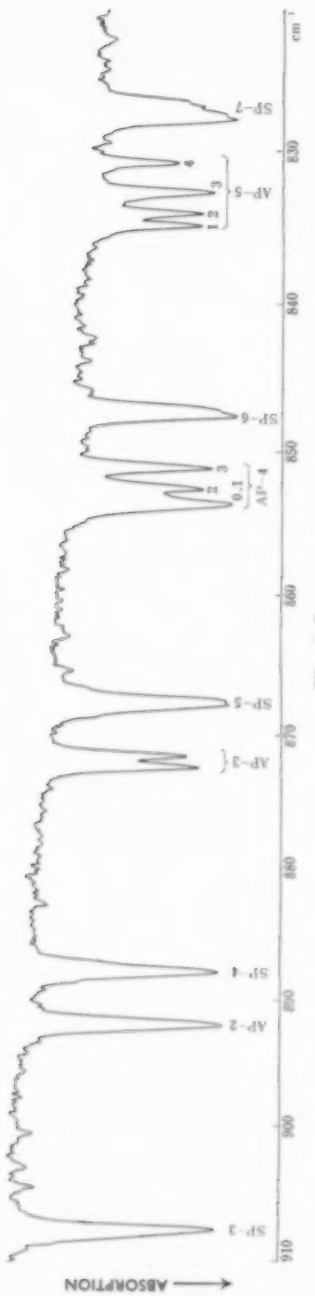

Fig. 1 C.

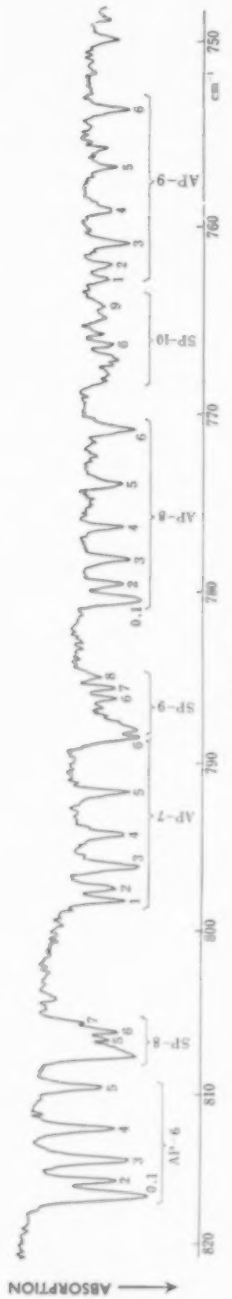

Fig. 1 D.

Fig. 1. Infrared absorption spectrum of $^{14}NH_3$ in the 1170–750 cm^{-1} region.

Table 1. Observed and calculated frequencies of the lines

Transition	*R*-branch					*P*-branch				
	J	*K*	$\nu_{obs.}$	$\nu_{calc.}$	$\Delta\nu$	*J*	*K*	$\nu_{obs.}$	$\nu_{calc.}$	$\Delta\nu$
	1 → 2	1	971·90	971·93	+0·03					
	2 → 3	0, 1	992·64	992·62	−0·02	2 → 1	0, 1	892·10	892·08	−0·02
		2	991·84	991·72	−0·12					
	3 → 4	1	1031·17	1031·20	+0·03	3 → 2	1	872·58	872·61	+0·03
		2	1012·47	1012·46	−0·01		2	871·79	871·77	−0·02
		3	1011·24	1011·19	−0·05					
	4 → 5	0, 1	1034·08	1034·14	+0·06	4 → 3	0, 1	853·83	853·71	−0·12
		2	1033·39	1033·31	−0·08		2	852·73	852·74	+0·01
		3	1032·12	1032·11	−0·01		3	851·32	851·33	+0·01
		4	1030·36	1030·37	+0·01					
	5 → 6	1	1054·88	1054·90	+0·02	5 → 4	1	834·83	834·83	0
		2	1054·29	1054·24	−0·05		2	834·02	834·02	0
		3	1053·14	1053·10	−0·04		3	832·65	832·63	−0·02
		4	1051·45	1051·46	+0·01		4	830·67	830·64	−0·03
		5	1049·25	1049·25	0					
$0^s \rightarrow 1^s$	6 → 7	0, 1	1075·77	1075·89	+0·12	6 → 5	0, 1	816·53	816·52	−0·01
		2	1075·33	1075·17	−0·16		2	815·63	815·59	−0·04
		3	1074·13	1074·11	−0·02		3	814·24	814·24	0
		4	1072·57	1072·58	+0·01		4	812·33	812·28	−0·05
		5	1070·53	1070·51	−0·02		5	809·74	809·68	−0·06
		6	1067·86	1067·84	−0·02					
	7 → 8	1	1096·60	1096·63	+0·03	7 → 6	1	798·24	798·23	−0·01
		2	1096·21	1096·06	−0·15		2	797·47	797·46	−0·01
		3	1095·15	1095·09	−0·06		3	796·15	796·14	−0·01
		4	1093·70	1093·67	−0·03		4	794·26	794·24	−0·02
		5	1091·78	1091·76	−0·02		5	791·75	791·71	−0·04
		6	1089·31	1089·28	−0·03		6	788·49	788·48	−0·01
		7	1086·19	1086·14	−0·05					
	8 → 9	0, 1	1117·41	1117·44	+0·03	8 → 7	0, 1	780·51	780·47	−0·04
		2	1116·80	1116·84	+0·04		2	779·60	779·60	0
		3	1115·97	1115·96	−0·01		3	778·33	778·33	0
		4	1114·69	1114·67	−0·02		4	776·50	776·50	0
		5	1112·91	1112·93	+0·02		5	774·05	774·06	+0·01
		6	1110·67	1110·65	−0·02		6	770·96	770·93	−0·03
		7	1107·80	1107·77	−0·03		7	767·02*	767·03	+0·01
		8	1104·13	1104·17	+0·04					
	9 → 10	1	1137·74	1137·88	+0·14	9 → 8	1	762·68*	762·71	+0·03
		2	—	1137·43	—		2	761·97*	762·00	+0·03
		3	1136·72	1136·65	−0·07		3	760·70*	760·78	+0·08
		4	1135·54	1135·51	−0·03		4	758·95*	759·04	+0·09
		5	1133·88	1133·95	+0·07		5	756·62*	756·69	+0·07
		6	1131·82	1131·90	+0·08		6	753·62*	753·69	+0·07
		7	1129·21	1129·28	+0·07		7	749·85*	749·94	+0·09
		8	1125·97	1125·99	+0·02		8	745·33*	745·35	+0·02
		9	—	1121·91	—					
	10 → 11	0	—	1158·26	—	10 → 9	0	—	745·51	—
		1	—	1158·13	—		1	—	745·29	—
		2	—	1157·75	—		2	744·49*	744·62	+0·13
		3	1157·29	1157·09*	−0·20		3	743·29*	743·48	+0·19

VOL. 13 1958/5

Table 1.—(*contd.*)

Transition	R-branch					P-branch				
	J	K	$\nu_{obs.}$	$\nu_{calc.}$	$\Delta\nu$	J	K	$\nu_{obs.}$	$\nu_{calc.}$	$\Delta\nu$
$0^a \rightarrow 1^s$		4	1156·26*	1156·10	−0·16		4	741·60*	741·82	+0·22
		5	1154·67*	1154·74	+0·07		5	739·38*	739·60	+0·22
		6	1152·80*	1152·94	+0·14		6	736·88*	736·74	−0·14
		7	1150·41*	1150·61	+0·20		7	—	733·16	—
		8	1147·45*	1147·66	+0·21		8	—	728·77	—
		9	1143·83*	1143·96	+0·13		9	—	723·44	—
		10	1139·50*	1139·39	−0·11					
	1 → 2	0,1	1007·48	1007·48	0	1 → 0	0	948·27	948·21	−0·06
	2 → 3	1,2	1026·92	1026·97	+0·05	2 → 1	1	—	928·22	—
	3 → 4	0∼3	1046·27	1046·32	+0·05	3 → 2	0∼2	908·24	908·17	−0·07
	4 → 5	1∼4	1065·46	1065·51	+0·05	4 → 3	1∼3	887·96	888·00	+0·04
	5 → 6	0∼5	1084·56	1084·55	−0·01	5 → 4	0∼4	867·82	867·86	+0·04
	6 → 7	1∼6	1103·44	1103·40	−0·04	6 → 5	1∼5	847·51	847·61	+0·10
	7 → 8	0∼7	1122·10	1122·11	+0·01	7 → 6	6	826·56	826·50	−0·06
	8 → 9	1∼8	1140·58	1140·58	0	8 → 7	1,2	807·65	807·76	+0·11
							3	807·42	807·44	+0·02
							4	807·17	807·10	−0·07
							5	806·78	806·70	−0·08
							6	806·29	806·25	−0·04
							7	805·82	805·77	−0·05
$0^s \rightarrow 1^a$	9 → 10	0∼9	1158·90	1158·95	+0·05	9 → 8	0∼2	788·06	787·95	−0·11
							3	787·67	787·51	−0·16
							4	787·22	787·12	−0·10
							5	786·74	786·63	−0·11
							6	786·20	786·08	−0·12
							7	785·61	785·49	−0·12
							8	784·97	784·89	−0·08
	10 → 11	1∼10	1177·08	1177·05	−0·03	10 → 9	1,2	768·18	768·19	+0·01
							3	767·83*	767·75	−0·08
							4	767·41*	767·28	−0·13
							5	—	766·71	—
							6	766·29	766·06	−0·23
							7	765·61	765·34	−0·27
							8	764·78	764·59	−0·19
							9	764·10	763·85	−0·25
	11 → 12	0∼11	1195·02*	1195·01	−0·01					
	12 → 13	1∼12	1212·70*	1212·64	−0·06					
	13 → 14	0∼13	1230·24*	1230·13	−0·11					

* These lines were not used for the calculation of the molecular constants because of the weak intensity or the overlapping by other lines.

branches of the bands corresponding to the S and A transitions are derived from equations (1) and (2) as

$$SP(J, K) = \{G(1^a) - G(0^s)\} + \{B_{1^a}(J-1)J - B_{0^s}J(J+1)\} + \{A_{1^a} - B_{1^a} - A_{0^s} + B_{0^s}\}K^2 + \{D^J_{1^a}(J-1)^2J^2 - D^J_{0^s}J^2(J+1)^2\} + \{D^{JK}_{1^a}(J-1)J - D^{JK}_{0^s}J(J+1)\}K^2 + (D^K_{1^a} - D^K_{0^s})K^4 \quad (8)$$

$$SR(J, K) = \{G(1^a) - G(0^s)\} + \{B_{1^a}(J+1)(J+2) - B_{0^s}J(J+1)\} + \{A_{1^a} - B_{1^a} - A_{0^s} + B_{0^s}\}K^2 + \{D^J_{1^a}(J+1)^2(J+2)^2 - D^J_{0^s}J^2(J+1)^2\} + \{D^{JK}_{1^a}(J+1)(J+2) - D^{JK}_{0^s}J(J+1)\}K^2 + (D^K_{1^a} - D^K_{0^s})K^4 \quad (9)$$

$$AP(J, K) = \{G(1^s) - G(0^a)\} + \{B_{1^s}(J-1)J - B_{0^a}J(J+1)\} + \{A_{1^s} - B_{1^s} - A_{0^a} + B_{0^a}\}K^2 + \{D^J_{1^s}(J-1)^2J^2 - D^J_{0^a}J^2(J+1)^2\} + \{D^{JK}_{1^s}(J-1)J - D^{JK}_{0^a}J(J+1)\}K^2 + (D^K_{1^s} - D^K_{0^a})K^4 \quad (10)$$

$$AR(J, K) = \{G(1^s) - G(0^a)\} + \{B_{1^s}(J+1)(J+2) - B_{0^a}J(J+1)\} + \{A_{1^s} - B_{1^s} - A_{0^a} + B_{0^a}\}K^2 + \{D^J_{1^s}(J+1)^2(J+2)^2 - D^J_{0^a}J^2(J+1)^2\} + D^{JK}_{1^s}(J+1)(J+2) - D^{JK}_{0^a}J(J+1)\}K^2 + (D^K_{1^s} - D^K_{0^a})K^4 \quad (11)$$

where J and K represent the rotational quantum numbers of the lower levels in both transitions.

The assignments of the lines with relatively low values of J and K have been made by Sheng, Barker, and Dennison [6]. As they pointed out, when K is a multiple of three the line in question should be enhanced by the factor two, because of the proton spin. The state with $K = 0$, J even and the vibration superscript s, does not exist and consequently a line arising from a transition involving such a state is absent. Furthermore, the state with $K = 0$, J odd and the superscript a does not exist. With these in mind, the assignments of the observed lines are made as shown in Fig. 1 and Table 1.

Analysis of the $0^a \rightarrow 1^s$ *band*

From equations (10) and (11), we have:

$$\frac{AR(J, K) - AP(J, K)}{4J + 2} = B_{1^s} + 2D^J_{1^s}(J^2 + J + 1) + D^{JK}_{1^s}K^2 \quad (12)$$

$$\frac{AR(J-1, K) - AP(J+1, K)}{4J + 2} = B_{0^a} + 2D^J_{0^a}(J^2 + J + 1) + D^{JK}_{0^a}K^2 \quad (13)$$

In Figs. 2 and 3, the observed values corresponding to the left sides of these equations are plotted versus K^2. Here, every set of points with the same J-value fall on a single straight line just as is expected from equations (12) and (13). In Figs. 4 and 5 these values are plotted versus $J^2 + J + 1$. Again straight lines resulted as is expected. The values of B_{1^s}, B_{0^a}, $D^J_{1^s}$, $D^J_{0^a}$, $D^{JK}_{1^s}$, and $D^{JK}_{0^a}$ in equations (12) and (13) are calculated from these observed values by the method of least squares, where a weight of $(4J + 2)^2$ was assigned to each observed value of $\{AR(J, K) - AP(J, K)\}/(4J + 2)$ or $\{AR(J-1, K) - AP(J+1, K)\}/(4J + 2)$. The values

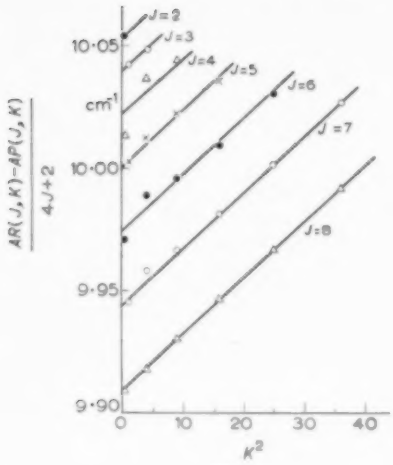

Fig. 2

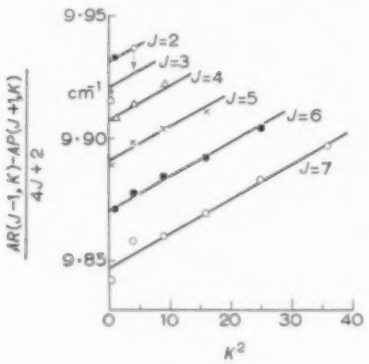

Fig. 3.

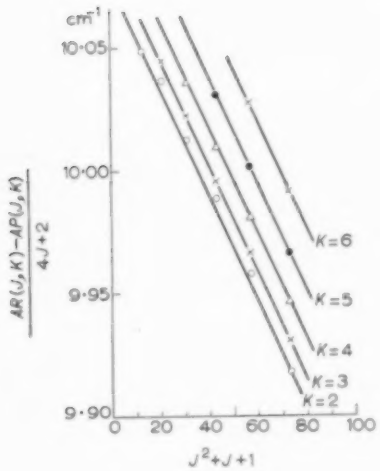

Fig. 4.

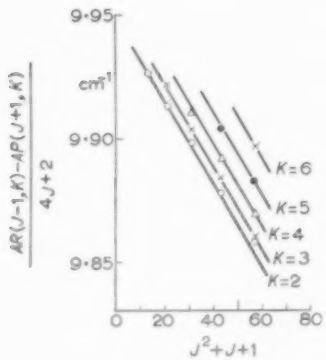

Fig. 5.

obtained are listed in Table II with probable errors, which are also calculated from the distribution of the observed values.

Equations (10) and (11) yields:

$$\frac{AR(J, K+1) - AR(J, K)}{2K+1} = \{A_{1^e} - B_{1^e} - A_{0^e} + B_{0^e}\}$$
$$+\{D_{1^e}^{JK}(J+1)(J+2) - D_{0^e}^{JK}J(J+1)\} + (D_{1^e}^{K} - D_{0^e}^{K})(2K^2+2K+1) \qquad (14)$$

$$\frac{AP(J, K+1) - AP(J, K)}{2K+1} = \{A_{1^e} - B_{1^e} - A_{0^e} + B_{0^e}\}$$
$$+\{D_{1^e}^{JK}(J-1)J - D_{0^e}^{JK}J(J+1)\} + (D_{1^e}^{K} - D_{0^e}^{K})(2K^2+2K+1) \qquad (15)$$

Plotting the observed values of the left sides of these equations versus $2K^2 + 2K + 1$, a single straight line was obtained, as is expected from the equations (see Fig. 6.) From these observed values, to each of which the weight $(2K + 1)^2$ was assigned, the values of $A_{1^s} - B_{1^s} - A_{0^s} + B_{0^s}$ and $D^K_{1^s} - D^K_{0^s}$ were calculated by the method of least squares. The results are shown in Table 2.

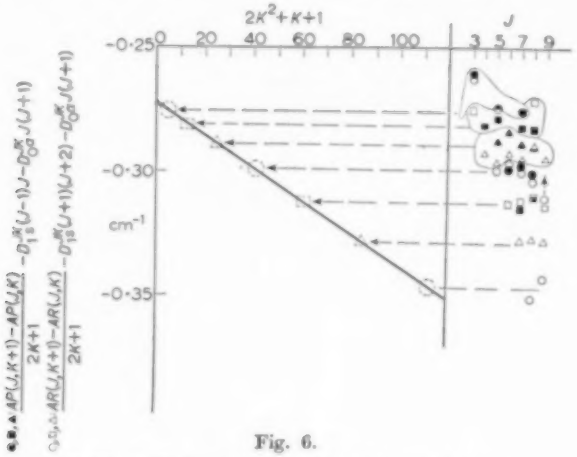

Fig. 6.

Table 2. Values of the molecular constants

Constant	Values obtained by the authors	Values given by previous investigators	Constant	Values obtained by the authors	Values given by previous investigators
$G(1^s) - G(0^s)$	931·71	931·58 [6]	$G(1^a) - G(0^s)$	968·08	968·08 [6]
B_{1^s}	10·0679 ±0·0010	10·060 [6]	B_{1^a}	9·8828 ±0·0023	9·887 [6]
B_{0^s}	9·9430 ±0·0015	9·9385 [6] 9·94 − 0·00505 [17]	B_{0^s}	9·9386 ±0·0021	9·944 [6] 9·94 [17]
$A_{1^s} - B_{1^s} - A_{0^s} + B_{0^s}$	−0·27292 ±0·00086	−0·254 [6]	$A_{1^a} - B_{1^a} - A_{0^s} + B_{0^s}$	−0·0086 ±0·0051	−0·021 [6]
$D^J_{1^s}$	−0·001084 ±0·000010		$D^J_{1^a}$	−0·000623 ±0·000014	
$D^J_{0^s}$	−0·000843 ±0·000018	−0·00081 [17]	$D^J_{0^s}$	−0·000755 ±0·000016	−0·00081 [17]
$D^{JK}_{1^s}$	+0·002286 ±0·000029		$D^{JK}_{1^a}$	+0·001060 ±0·000086	
$D^{JK}_{0^s}$	+0·001395 ±0·000046	+0·00155 [17]	$D^{JK}_{0^s}$	+0·001437 ±0·000046	+0·00155 [17]
$D^K_{1^s} - D^K_{0^s}$	−0·000641 ±0·000013		$D^K_{1^a} - D^K_{0^s}$	+0·000190 ±0·000033	

Finally, the centre of the band was located. The mean value of $G(1^s) - G(0^a)$ was determined by substituting the calculated values of the constants into the right side of equations (10) or (11) and the observed frequencies of the lines in question into the left side.

Analysis of the $0^s \rightarrow 1^a$ *band*

In this band, because of the small value of $A_{1^a} - B_{1^a} - A_{0^s} + B_{0^s}$, the lines with the same J and different K-values were not separated from one another, except those in the P-branch and with J-values greater than 7. Hence, in the analysis, procedures a little different from those given above were followed.

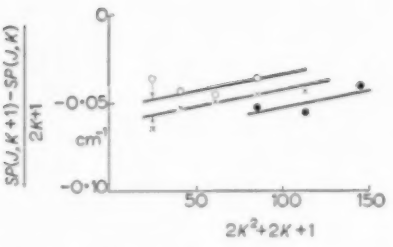

Fig. 7. ○○ J = 8; ×× J = 9; ●● J = 10.

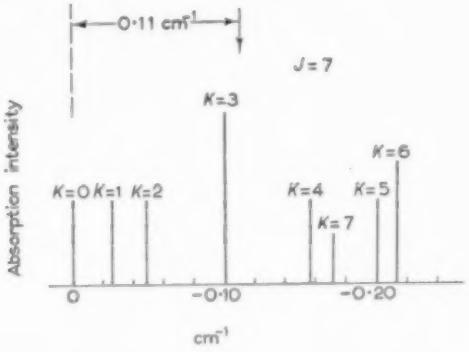

Fig. 8.

First, the values of $A_{1^a} - B_{1^a} - A_{0^s} + B_{0^s}$, $D_{1^a}^{JK}$, and $D_{1^a}^{K} - D_{0^s}^{K}$ were calculated from the observed values of $\{SP(J, K+1) - SP(J, K)\}/(2K+1)$ (given in Fig. 7) by the equation;

$$\frac{SP(J, K+1) - SP(J, K)}{2K+1} = \{A_{1^a} - B_{1^a} - A_{0^s} + B_{0^s}\} + \{D_{1^a}^{JK}(J-1)J - D_{0^s}^{JK}J(J+1)\} + (D_{1^a}^{K} - D_{0^s}^{K})(2K^2 + 2K + 1) \qquad (16)$$

Unfortunately, the intervals between the two lines $SP(J, K+1)$ and $SP(J, K)$ are very small, and the error of the observation is relatively large. The points plotted in Fig. 7 are not sufficient in number and do not fall well on straight lines. Accordingly, the probable errors of the calculated values are rather large as shown in Table 2. Here, the value of $D_{0^s}^{JK}$ in equation (16) is assumed to be 0·001437, since $D_{0^a}^{JK} - D_{0^s}^{JK} = -0{\cdot}00004260$ according to a study by Good [16] of the inversion spectrum of ammonia in the microwave region, and $D_{0^a}^{JK} = 0{\cdot}001394$, as given above.

In the second place, using the calculated values of these constants, the relative positions and relative intensities were estimated for the overlapped lines which have the same J- but different K-values and which could not be observed separately. As an example, the result obtained for the lines with $J = 7$ in the R-branch is illustrated in Fig. 8. The arrow in the figure indicates the "centre of mass" of the

calculated spectrum, which is situated at the distance of 0·11 cm^{-1} the line for $K = 0$ towards lower frequency. It was assumed that the apparent absorption peak of this bundle of lines corresponds to this "centre of mass." If so, the line for $K = 0$ should be situated at the distance of 0·11 cm^{-1} from the observed absorption peak towards higher frequency. For the multiplet corresponding to the $SP(J = 7)$, the line for $K = 6$ was observed clearly although the line for $K = 0$

Table 3. Estimated frequencies of the lines of $K = 0$ or 1

Transition	*R*-branch			*P*-branch		
	J	*K*		*J*	*K*	
$0^g \rightarrow 1^u$	1 → 2	0	1007·48	1 → 0	0	948·27
	2 → 3	1	1026·92	2 → 1	1	—
	3 → 4	0	1046·28	3 → 2	0	908·27
	4 → 5	1	1065·48	4 → 3	1	888·05
	5 → 6	0	1084·59	5 → 4	0	867·97
	6 → 7	1	1103·50	6 → 5	1	847·78
	7 → 8	0	1122·21	7 → 6	0	827·92
	8 → 9	1	1140·80	8 → 7	1	807·73
	9 → 10	0	1159·24	9 → 8	0	788·16
	10 → 11	1	1177·65	10 → 9	1	768·29
	11 → 12	0	1195·91			
	12 → 13	1	1214·09			
	13 → 14	0	1232·29			

was not observed separately. In such a case, the spacing between these two lines was calculated and the position of the line for $K = 0$ was determined. In this way, the position of the line for $K = 0$ or 1 was predicted in every case where it could not be actually observed. The results are shown in Table 3.

In the next step, using the values listed in Table 3, the values of the constants, B_{1^u}, B_{0^g}, $D^J_{1^u}$, and $D^J_{0^g}$, were calculated by the equations;

$$\frac{SR(J, K) - SP(J, K)}{4J + 2} - D^{JK}_{1^u}K^2 = B_{1^u} + 2D^J_{1^u}(J^2 + J + 1) \qquad (17)$$

$$\frac{SR(J - 1, K) - SP(J + 1, K)}{4J + 2} - D^{JK}_{0^g}K^2 = B_{0^g} + 2D^J_{0^g}(J^2 + J + 1) \qquad (18)$$

In Figs. 9 and 10, the left side values of these equations are plotted versus $J^2 + J + 1$. The points fall on a single straight line in each case as is expected. The calculation of the constants was carried out by the method of least squares in which a weight, $(4J + 2)^2$, was assigned to each of the $\{SR(J, K) - SP(J, K)\}/(4J + 2)$ or $\{SR(J - 1, K) - SP(J + 1, K)\}/(4J + 2)$ values.

Finally, the centre of the band was located by the same method as above.

Molecular constants

The values of all the molecular constants obtained here are listed in the second and fifth columns of Table 2. In the fifth and the tenth columns of Table 1 are

VOL. 13 1958/5

shown the frequencies of the lines calculated by equations (8), (9), (10) and (11) with these values of the constants. The agreement between the observed and calculated frequencies is good. In the third and sixth columns of Table 2 are given the values of the molecular constants obtained by some previous investigators.

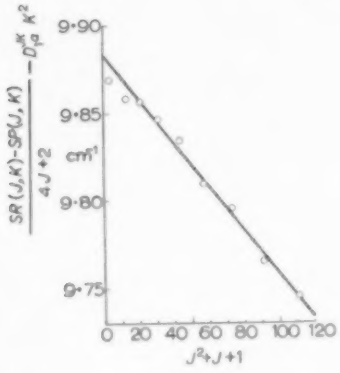

Fig. 9.

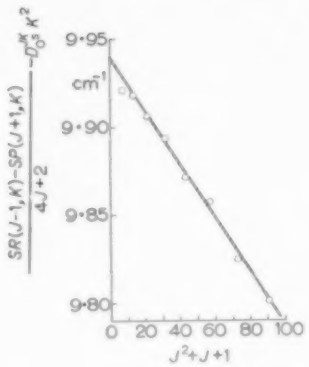

Fig. 10.

Sheng, Barker and Dennison [6] used an approximate expression:

$$D(J, K) - D(J - 1, K) = -0{\cdot}00294J^3 + 0{\cdot}00279JK^2$$

for the effect of the centrifugal distortion on the frequency of each line, instead of the last three terms of equations (8), (9), (10) and (11). According to this expression, the values of $A(J,K+1) - A(J, K)/(2K+1)$, for example, should not depend

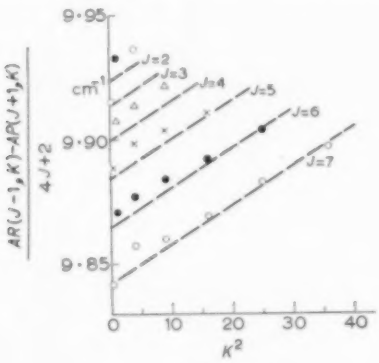

Fig. 11.

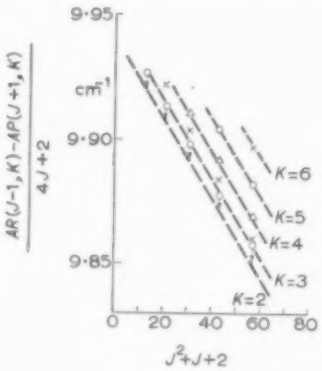

Fig. 12.

upon the K-value in contradiction to what is actually observed (see Fig. 6). Therefore, the approximation higher than that they used must be taken into account in explaining the results of the present experiments.

Values of the molecular constants for $v = 0^s$ and 0^a have been estimated by Hansler and Oetjen [17] in their study of far infrared spectrum of $^{14}NH_3$. Their value for $B_{0^s} - B_{0^a}$ should be much more reliable than that of the present authors.

In this study we cannot definitely tell even the sign of this, as may be seen from the probable errors given for the values of B's. While, the absolute values of the present authors for B's and D's at $v = 0^{e}$ and 0^{a} are better than theirs for explaining

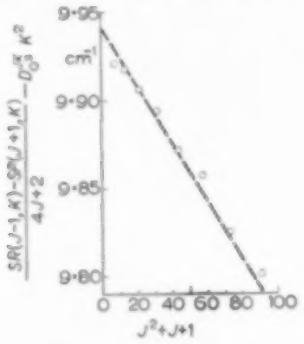

Fig. 13.

the results of the present experiment. This may be seen by comparing Figs. 3, 5 and 10 with Figs. 11, 12 and 13, respectively. In Figs. 11, 12 and 13, the dotted lines were drawn after Hansler and Oetjen's values of the constants.

Discussions of the values of the constants in relation to the molecular structure and the internal force field will be given in coming papers of the present authors.

References

[1] Stinchcomb G. A. and Barker E. F., *Phys. Rev.* 1929 **33** 305.
[2] Barker E. F., *Phys. Rev.*, 1929 **33** 684.
[3] Dennison D. M. and Hardy J. D., *Phys. Rev.* 1932 **39** 938.
[4] Barker E. F., *Phys. Rev.* 1939 **55** 657.
[5] Dennison D. M., *Rev. Mod. Phys.* 1940 **12** 175.
[6] Sheng H. Y., Barker E. F. and Dennison D. M., *Phys. Rev.* 1941 **60** 786.
[7] Wood D. L., Bell E. E. and Nielsen H. H., *Proc. Nat. Acad. Sci. Wash.* 1950 **36** 497.
[8] Cumming C., *Canad. J. Phys.* 1955 **33** 635.
[9] Mizushima S. *et al.*, To be published elsewhere.
[10] Mills I. M. and Thompson H. W., *Proc. Roy. Soc.* A 1953 **218** 29.
[11] Dalby F. W. and Nielsen H. H., *J. Chem. Phys.* 1956 **25** 934.
[12] Nielsen A. H. and Yao Y. T., *Phys. Rev.* 1945 **68** 173; 1947 **71** 825
[13] Rossmann K., Rao K. N. and Nielsen H. H., *J. Chem. Phys.* 1956 **24** 103
[14] Plyler E. K., Blain L. R. and Connor W. S., *J. Opt. Soc. Amer.* 1955 **45** 102.
[15] Lakshmi K., Rao K. N. and Nielsen H. H., *J. Chem. Phys.* 1956 **24** 811.
[16] Good W. E., *Phys. Rev.* 1946 **70** 213.
[17] Hansler R. L. and Oetjen R. A., *J. Chem. Phys.* 1953 **21** 1340.

VOL.
13
1958/5

Spectrochimica Acta, 1958, Vol. 13, pp. 93 to 98. Pergamon Press Ltd., London

The infrared spectra and the structure of some homophthalimides*

A. L. Bluhm
Pioneering Research Division, Quartermaster Research and Engineering Command, Natick, Massachusetts

(*Received* 27 *February* 1958)

Abstract—The spectra of NH and NCH_3 homophthalimides in the solid and solution phase have been observed and the various absorption bands have been correlated with functional groupings in the compounds. In the solid state and in concentrated solution, the NH homophthalimides are associated by intermolecular hydrogen bonds between the 1-carbonyl and imide groups. The assignment of a di-keto configuration to the structure of homophthalimides is most consistent with the observed spectra.

Introduction

The infrared absorption spectra of homophthalimides† as a group have not been treated previously, although some references to the spectra of certain homophthalimides have been made [1, 2, 3]. The homophthalimides present an interesting problem because of the various tautomers which can exist, e.g. (I)–(Id).

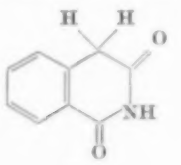

(I)

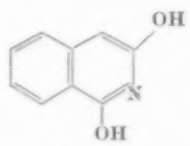

(Ia)

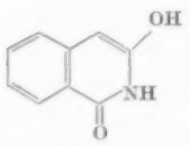

(Ib)

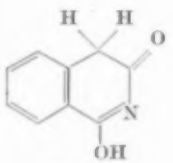

(Ic)

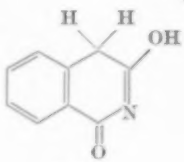

(Id)

Previous investigations have not arrived at an unambiguous structural assignment [1, 2, 4, 5, 6].

* Presented before the "Symposium on Molecular Structure and Spectroscopy" at the Ohio State University, Columbus, 10–14 June 1957.

† According to I.U.C. nomenclature, homophthalimides are named as 1:3-dioxo-2:4:4-trihydroisoquinolines. In this report they are named as substituted homophthalimides and the ring atoms are numbered as follows:

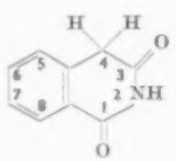

The problem of elucidating structure where a number of tautomers is possible is common also to other compounds containing the —CONHCO— group, e.g. phthalimides, succinimides, uracils, hydroxyprimidines and related compounds. Infrared absorption studies on some of these compounds have enabled structural assignments to be made [7, 8].

The present work describes the spectra of seven homophthalimides. The changes observed when comparing spectra obtained in the solid phase and in solution are useful in the elucidation of the structure of this group of compounds.

Experimental

The infrared spectra were determined on a Beckman Infrared Spectrophotometer, Model IR-3, equipped with lithium fluoride or sodium chloride optics and on a Baird, Model A, spectrometer. A polystyrene film was used to calibrate the instruments. Samples were measured either as solid dispersions in pressed potassium bromide pellets against a pure potassium bromide pellet or as solutions

Table 1. Infrared spectra of some homophthalimides (cm^{-1}). Pressed KBr dispersions

(I) Homophthalimide	(II) 7:8-Dimethoxyhomophthalimide	(III) 4-(3′:4′-Methylenedioxyphenylethyl)-7:8-dimethoxyhomophthalimide	(IV) 4:4-Dimethylhomophthalimide	(V) 2-Methyl homophthalimide	(VI) 2-Methyl-7:8-dimethoxyhomophthalimide	(VII) 2:4:4-Trimethylhomophthalimide
3175	3194	3175	3215	2882	2950	2949
3077	3086	3086	3096	1718 s	2849	2915
2950	2950	2941	2985	1667 s	1712 s	2857
2857	2841	2849	2941	1610	1675 s	1712 s
1706 s	1704 s	1704 s	2865	1590	1603	1667
1684 s	1684 s,sh	1678 s	1709 s	1495	1585	1608
1610	1605	1608	1692 s	1473	1497 s	1493
1490	1587	1580	1605	1427	1456	1471
1466	1493	1504	1471	1385	1433	1466
1445	1445	1493 s	1458	1368	1408	1456
1370	1420	1453	1385	1346	1391	1422
1339	1351	1429	1368	1309	1353 s	1389
1287 s	1326	1351	1353	1297	1338	1362 s
1189 w	1293	1333	1294	1247	1314	1307 s
1139	1271	1299	1266	1195	1279 s	1290 s
1031 w	1218	1266 s	1247	1126	1239	1259
922 w	1195	1236	1174	1086	1205	1248
879	1168	1174	1145	1003	1124	1215
806	1149	1151	1038	928	1080	1179
759	1062	1064 sh	969 w	804	1062	1159
740	1050	1052	925	742	1007	1092
682	958	1034	842	686	966	1058
	935 w	1020 sh	820		934	1038
	922 w	985	799		931	990
	876	932	769		832	969
	829	857	756		803	879 w
	801	836	707		792	869 w
	770 w	818	680		738 w	802
	739	792	667		690	771 s
	703	699				700
						679

s = strong; w = weak; sh = shoulder

VOL. 13 1958/5

against the pure solvent as a reference. Harshaw Chemical Co. powdered potassium bromide, infrared quality, was used for the preparation of pressed pellets. Eastman Kodak "Spectro Grade" solvents were used for preparing solutions for infrared examination.

The compounds were obtained from the Chemical Laboratories of Boston University.* Purity was established by comparison of the melting points with reported values from the literature and/or by elementary analyses.

Results and discussion

In Table 1 the frequencies of the absorption bands for the series of compounds are listed. Significant differences can be seen in that compounds (I)–(IV) each show two absorption bands at c. 3077 and 3175 cm^{-1}, whereas compounds (V)–(VII) lack these absorption bands. Thus, if we assume the di-keto structure, e.g. (I), it is convenient to divide the homophthalimides into two groups, based upon the substituent on the 2 (the nitrogen) atom. One group then contains the NH compounds and the other group contains the NCH_3 compounds.

Table 2. NH and C—O stretching frequencies of homophthalimides (cm^{-1})

Compound No.	NH frequencies		C=O frequencies			
			Solid		Solution‡	
	Solid	Solution‡	1C=O	3C=O	1C=O	3C=O
(I)	3077,* 3175*	3378	1684*	1706	1704	1721
(II)	3086,* 3195*	3378	1684*	1704	1704	1715
(III)	3086,* 3175*	3378	1678*	1704	1704	1715
(IV)	3096,* 3215*	3390	1692*	1709	1709	1718
		3086,*† 3215,*† 3390†			1698,*† 1709,† 1718†	
(V)			1667	1718	1681	1727
(VI)			1675	1712	1684	1727
(VII)			1667	1712	1678	1721

* These frequencies are perturbed by intermolecular hydrogen bonding.
† Concentrated solution.
‡ Compounds (I)–(III) were studied in $CHCl_3$ solutions; compounds (IV)–(VII) in CCl_4 solutions.

NH *homophthalimides.* In Table 2 the pertinent absorption frequencies in solid and solution phase are compared. The solutions are dilute enough so that there is no intermolecular hydrogen bonding. The absorption bands in the 3070–3390 cm^{-1} region are assigned to NH stretching modes. The one absorption band at about 3390 cm^{-1} in the spectra of dilute solutions is due to NH stretching in unassociated molecules. The possibility that this band is due to an OH stretching vibration is highly unlikely, as the lower limit for free OH stretching has been generally defined at 3509 cm^{-1}, and 3610 cm^{-1} is the usual assignment for unbonded enolic OH [9, 10]. Figure 1 demonstrates the shifts which occur in the 3070–3400 cm^{-1} region for 4:4-dimethylhomophthalimide when comparing the spectrum of the compound in the solid phase to spectra of solutions of decreasing concentration. The appearance of two broader bands at lower frequencies (c.

* The samples were kindly provided by Professor W. J. Gensler and Mrs. N. Wang.

3077 cm^{-1}, 3175 cm^{-1}) which are found in the solid phase and the concentrated solution spectra are characteristic of hydrogen bonded NH groups in secondary amides [11]. In a study of peptide linkages Darmon and Sutherland [12] and Darmon [13] have observed two absorption bands at 3058 and 3175 cm^{-1}. The band at 3175 cm^{-1} was attributed to associated NH in the *cis*- form of —CONH—. In the non-cyclic amides the 3175 cm^{-1} band is replaced by an absorption at

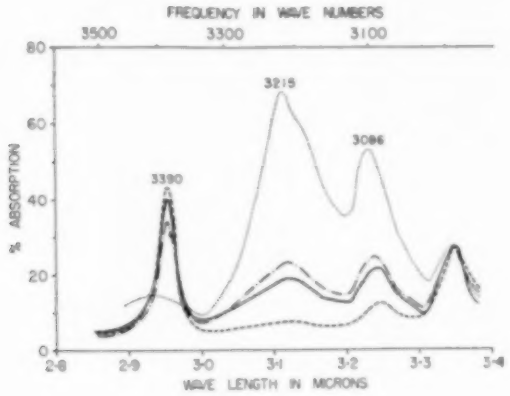

Fig. 1.

3279 cm^{-1}, which has been attributed to associated NH in the *trans*-configuration [12, 13, 14]. The appearance of a bonded NH vibration at 3155–3215 cm^{-1} in the homophthalimides in which the —CONH— configuration must be *cis*, is in agreement with the above reports.

On dilution, the hydrogen bonds are broken as indicated by the disappearance of the absorptions at 3077 and 3175 cm^{-1}, and the appearance of only one absorption at 3378 cm^{-1}. From the band shifts observed in the 1667–1754 cm^{-1} region it is apparent that a carbonyl group is taking part in this association. Assuming a di-keto configuration, the 1- and 3-carbonyl positions are not equivalent and as pointed out later, non-coplanar. Therefore, two absorptions little affected by coupling would be expected. In the homophthalimides, two very intense bands are found in this region. Since the 1-carbonyl position is conjugated with the phenyl ring, the absorption band at the lower frequency (c. 1706 cm^{-1} for dilute solutions) can be assigned to that group. The band at c. 1721 cm^{-1} may be assigned to the absorption of the carbonyl in the 3-position.

Comparison of the carbonyl group band shifts in Table 2 indicates that only the 1-carbonyl group of the NH homophthalimides is involved in the intermolecular bonding. In the NCH_3 compounds, which are not involved in any bonding (discussed further on), the band shifts of the 1- and 3-carbonyl groups on going from the solid to solution phase are from 9–15 cm^{-1} (mean value is 11 cm^{-1}). These shifts are attributed to phase change. Miyazawa, Shimanouchi and Mizushima [15] have recently reported that the carbonyl absorption band in amides shifts to lower frequencies on passing from solution to the crystalline state. In the NH homophthalimides the shifts for the 3-carbonyl absorption band are

VOL. 13 1958/5

about the same as found in the NCH_3 compounds. However, the 1-carbonyl group bands shift to a lower frequency by larger amounts (mean value is 21 cm^{-1}). This shift is attributed to the change in phase plus the effect of intermolecular hydrogen bonding. It is expected that the 1-carbonyl group which is made more electronegative by the conjugative effect of the aromatic nucleus, would be involved almost exclusively (over the 3-carbonyl position) in hydrogen bonding.

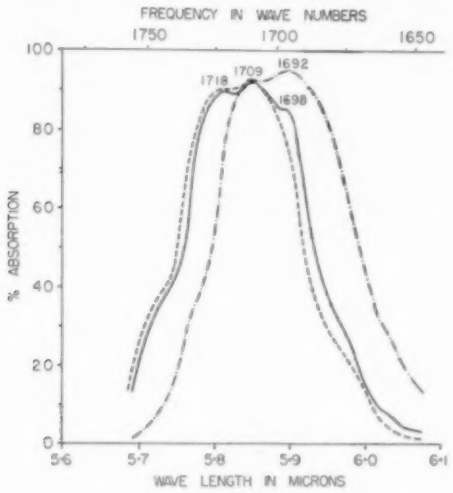

Fig. 2.

This interpretation is substantiated by the data from the studies on 4:4-dimethyl homophthalimide, (IV) (see Table 2 and Fig. 2). The spectrum of a dilute solution shows two bands at 1709 and 1718 cm^{-1} which are assigned to the unassociated carbonyl groups at the 1- and 3-positions respectively. In a concentrated solution some of the molecules are in the associated form and the appearance of the band at 1698 cm^{-1}, since there is no phase change, can be due only to hydrogen bonding involving the 1-carbonyl group.

NCH_3 *homophthalimides.* Interpretation of the infrared spectra of the NCH_3 homophthalimides is simplified by the absence of any absorption bands in the 3070–3390 cm^{-1} region. The presence of an OH group and, therefore, tautomers such as (Va) are eliminated. Compound (VII) is uncomplicated since it cannot

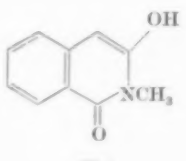

(Va)

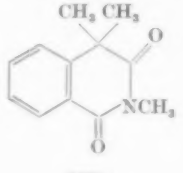

(VII)

exist in any other tautomeric form as there are no hydrogen atoms available. There is no possibility of intermolecular association by hydrogen bonding in the NCH_3 homophthalimides. Two bands, which arise from carbonyl stretching

vibrations, are found in the 1667–1718 cm^{-1} region. The bands are sharper than those observed in the case of the NH homophthalimides and are insensitive to concentration changes. The 1-carbonyl group absorptions are found at slightly lower frequencies than in the case of the 1-carbonyl groups in unassociated NH homophthalimides. The lowering of the frequency is probably due to the effect of the N-methyl group on the resonance configurations of the molecule. Resonance form (A) would tend to make the 1-carbonyl oxygen more electronegative. Resonance form (B) would also tend to shift the 3-carbonyl group absorption to a lower

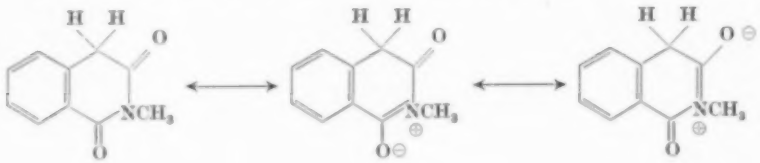

(V) (A) (B)

frequency. However, this is not observed and probably indicates that resonance form (B) makes no significant contribution. This is further suggested by the observation that the 3-carbonyl group is non-coplanar with the remainder of the molecule, as demonstrated by molecular models.

References

[1] Buu-Hoi, *Bull. Soc. Chim. Fr.* 1945 **12** 313.
[2] Ames D. E. and Grey T. F., *J. Chem. Soc.* 1955 3518.
[3] Bailey A. S. and Swallow D. L., *J. Chem. Soc.* 1956 2477.
[4] Gabriel S., *Ber. Dtsch. Chem. Ger.* 1886 **19** 1653 2354; 1887 **20** 2499.
[5] Herzog W., *Ber. Dtsch. Chem. Ger.* 1920 **53** 564.
[6] Gensler W. J. In Elderfield R. C., *Heterocyclic Compounds* Vol. IV, pp. 436–442. John Wiley, New York 1952.
[7] Bellamy L. J., *The Infra-red Spectra of Complex Molecules* pp. 236–238. John Wiley, New York 1954.
[8] Tanner E. M., *Spectrochim. Acta* 1956 **8** 9.
[9] Bellamy L. J., *The Infra-red Spectra of Complex Molecules* pp. 85–86. John Wiley, New York 1954.
[10] Jones R. N. and Sandorfy C. In Weissberger A., *Techniques of Organic Chemistry* Vol. IX, pp. 417-430. Interscience, New York 1956.
[11] Bellamy L. J., *The Infra-red Spectra of Complex Molecules* pp. 178–180. John Wiley, New York 1954.
[12] Darmon S. E. and Sutherland G. B. B. M., *Nature Lond.* 1949 **164** 440.
[13] Darmon S. E., *Disc. Faraday Soc.* 1950 **9** 325.
[14] Mizushima S. *et. al.*, *J. Amer. Chem. Soc.* 1950 **72** 3490.
[15] Miyazawa T., Shimanouchi T. and Mizushima S., *J. Chem. Phys.* 1956 **24** 408.

VOL.
13
1958/5

Spectrochimica Acta, 1958, Vol. 13, pp. 99 to 106. Pergamon Press Ltd., London

Spectral character as a function of spark source parameters

T. P SCHREIBER and D. L. FRY
Research Staff, General Motors Corp., Warren, Michigan

(*Received* 12 *December* 1957)

Abstract—The possibility of specifying high voltage spark source conditions on the basis of only two parameters, the average (rectified) current and the intensity ratio of an FeI to an FeIII line, has been investigated and found feasible.

Because of difficulties encountered in measuring the average current directly, a method was developed whereby a good approximation of it can be computed from the root-mean-square current, as measured by a radio-frequency meter, and the circuit parameters, using the equation:

$$I_{av} = \frac{2{\cdot}09\, I^2}{V}\sqrt{\frac{L}{C}}$$

The spectral character as measured by the FeI/FeIII intensity ratio was found to have the following relationship to source parameters:

$$\frac{\text{FeI } 3016{\cdot}2}{\text{FeIII } 3013{\cdot}1} \propto \frac{L^{1/2}}{CV^{4/3}}$$

Introduction

OF basic importance to spectrochemical analysis is the specification of spark source parameters and their correlation with spectral character. The specification of spark source conditions by means of the circuit constants is not completely satisfactory because the circuit constants are not uniquely related to the spectrochemical character of the discharge. There are also circuit variables which are difficult or impossible to specify. The work of KAISER [1], ENNS [2] and others has led to a better understanding of the mechanisms of spark excitation but quantitative application of this information has not been realized. The work of LAQUA [3] in which spectral character is related to the average (rectified) current and the duration of the discharge indicates that source specification by means of a few critical parameters may be possible.

This paper covers an investigation of LAQUA's ideas as applied to the point-to-plane spark excitation of low alloy steels with a high voltage spark source.

Average current—theory

The usefulness of average current in calculating the power dissipated in the analytical gap is based upon KAISER's [1] finding that after the initial breakdown the spark gap assumes the character of an arc. The voltage drop across the gap is independent of current and is determined by gap length and electrode material. Thus the average power dissipated can be computed with the equation:

$$\text{Power} = \frac{1}{T}\int_0^T i(t)v_g(t)\,dt \qquad (1)$$

where T is the period, $i(t)$ is the instantaneous current and $v_g(t)$ is the voltage

across the gap. In an oscillatory discharge $v_g(t)$ is constant except that its sign varies as $i(t)$ varies so that the product, $i(t)v_g$, is always positive. Equation (1) can thus be rewritten:

$$\text{Power} = \frac{v_g}{T}\int_0^T i(t)\,dt = v_g I_{av} \tag{2}$$

Attempts to measure the average current with a rectifying ammeter device such as that described by LAQUA failed because of the frequency sensitivity of the shunt resistor. (This work was performed at higher frequencies than those encountered by LAQUA.) Several shunt designs were tried but none was found satisfactory. Because of these difficulties, three methods of calculating I_{av} from measurable parameter were developed.

Figure 1 is a condenser voltage oscilloscope trace obtained with an air inter-

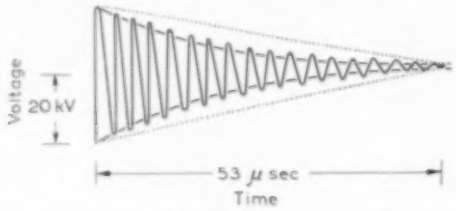

Fig. 1. Voltage oscillograph trace of transient discharge. Source conditions—$C = 0{\cdot}0080\ \mu F$; $L = 29\ \mu H$; R (added) $= 0$; $V = 20$ kV; $B = 3$ discharges/half cycle.

VOL. 13 1958/5

rupted source under standard conditions for analysing steel. The current trace, which is much more difficult to obtain, appears much the same since it is the first derivative of the voltage curve. The envelope of the curve lies between an exponential decay, which would be the case if all the resistance in the circuit were ohmic, and a linear decay, which would hold if only the voltage drops across the gaps were deducted on each half cycle. With this curve shape in mind three different approaches in calculating average current were tried.

(1) In the first method linear damping was assumed and θ was measured with an oscilloscope. The calculation takes the form:

$$I_{av} = \frac{1}{2}\left(\frac{2}{\pi} J_0 N \theta\right) \tag{3}$$

where J_0 is the first current peak ($J_0 = V\sqrt{(C/L)}$ if R is small) and $2/\pi$ is the form factor for obtaining the average of a sine wave. N is the number of discharges per sec and θ is the transient duration in seconds. For a 60 c/s supply and with B as the number of discharges per half cycle the equation becomes:

$$I_{av} = 38{\cdot}1 J_0 B \theta \tag{4}$$

(2) The second method of computing I_{av} involved the determination of θ in terms of the normally measured or known circuit parameters.

The general solution for an oscillatory discharge is given by

$$i(t) = J_0 \exp\left(-\frac{R}{2L}t\right) \sin \frac{t}{\sqrt{(LC)}} \tag{5}$$

If a linear decay is assumed, than R must be a function of t if equation (5) is applicable. The function $R(t)$ can be obtained by equating the decay portion of equation (5), exp $(-R/2L\,t)$, to a linear function with a slope of $-1/\theta$ and an intercept of 1

$$\exp\left(-\frac{R(t)}{2L}t\right) = -\frac{t}{\theta} + 1 \tag{6}$$

Solving for $R(t)$:

$$R(t) = -\frac{2L}{t}\ln\left(1 - \frac{t}{\theta}\right)$$

The average resistance, $\bar{R}$, can then be obtained from the following:

$$\bar{R} = \frac{1}{\theta}\int_0^{\theta} R(t)\,dt = \frac{2L}{\theta}\int_0^{\theta} -\frac{1}{t}\ln\left(1 - t/\theta\right)dt \tag{7}$$

This can be integrated to give:

$$\bar{R} = \frac{\pi^2 L}{3\theta} \tag{8}$$

Experimentally, it has been established that $\bar{R}$ is very nearly equal to the effective resistance of the circuit.

$$R_{\text{eff}} = \frac{NCV^2}{2{I_{\text{rf}}}^2} = \frac{60BCV^2}{{I_{\text{rf}}}^2} \tag{9}$$

where I_{rf} is the radio frequency or root mean square current as measured on a thermocouple-type meter. Equating $\bar{R}$ and R_{eff} the following relationship for θ is obtained:

$$\theta = \frac{\pi^2 L\,{I_{\text{rf}}}^2}{180BCV^2} \tag{10}$$

Substituting θ of equation (10) into equation (4):

$$I_{\text{av}} = \frac{2{\cdot}09\,{I_{\text{rf}}}^2}{V}\sqrt{\left(\frac{L}{C}\right)} = \frac{2{\cdot}09\,{I_{\text{rf}}}^2}{J_0} \tag{11}$$

With this equation I_{av} can be computed from the easily measured source parameters C, L, and V and the almost universally measured variable I_{rf}.

(3) The third method used in computing I_{av} was based on the assumption of an exponential decay [see equation (5)]. Integrating the transient for each half cycle by substituting equation (5) into equation (12) leads to the expression for the average current given by equation (13).

$$I_{\text{av}} = \frac{1}{T}\int_0^{T} |i(t)|\,dt \tag{12}$$

$$I_{\text{av}} = 120BCV\left[\frac{1 + \exp\left(-\dfrac{\pi RJ_0}{2V}\right)}{1 - \exp\left(-\dfrac{\pi RJ_0}{2V}\right)}\right] \tag{13}$$

R in this equation was assumed to be R_{eff} [see equation (9)].

Experimental

Because average current could not be measured directly, the most reliable values were obtained by method (1) above. Since this procedure requires equipment not normally found in a spectrographic laboratory, experiments were undertaken to check the usefulness of methods (2) and (3). Average current values were obtained by the three methods for forty-five different source conditions in which parameters were varied individually. Methods (1) and (2) gave values which agreed within ± 10 per cent. Method (3), however, averaged 10 per cent higher than (1) or (2).

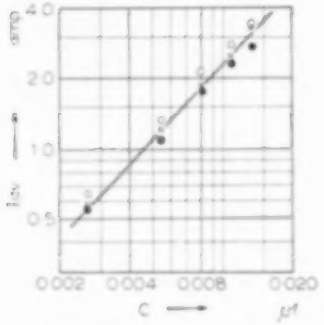

Fig. 2. Variations of average current with capacitance. Average current computed by (×) Method 1; (●) Method 2; (○) Method 3. Other source settings $L = 56$ μH, $V = 13{\cdot}5$ kV, $B = 5$ breaks/half cycle, and R (added) = 0.

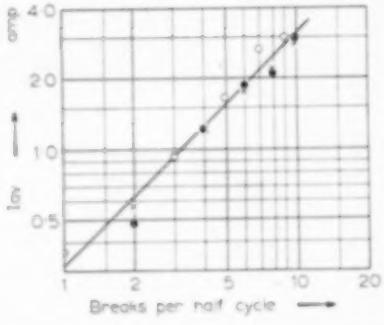

Fig. 3. Average current obtained by method (2) as a function of breaks per half cycle for three different inductance settings; 29 μH (●), 56 μH (×), and 115 μH (○). Other parameters $C = 0{\cdot}0080$ μF, $V = 12$ kV, and R (added) = 0.

To obtain accurate values for the above data it was necessary to calibrate the radio-frequency ammeter and the oscilloscope used to measure breakdown voltage. The radio-frequency current reading is especially critical when method (2) is used since it appears as the square in equation (11) and its per cent error is thus doubled. Errors in breakdown voltage cause difficulty in comparing methods (1) and (2) since the resultant errors in the average current values are in opposite directions.

Average current as a function of capacitance, breaks per half cycle, voltage and resistance is shown in Figs. 2, 3, 4 and 5. Average current was found to be independent of inductance. The fact that equations (4), (11) and (13) show a relationship between I_{av} and J_θ might lead one to believe that I_{av} is not independent of inductance ($J_\theta = V\sqrt{C/L}$). This can be explained by the fact that other variables, e.g. θ in (4), I_{rf} in (11), and R_{eff} in (13), are dependent upon inductance. From the slopes of these curves the following relationship can be obtained:

$$I_{av} \propto \frac{BCV^{3/2}}{R} \tag{14}$$

Laqua [3] found a correlation between average current and the total intensity of the spark as measured with a phototube. These measurements were not made, but an attempt was made to correlate the intensity of the 3016·2 Å FeI line with average current. Good correlation was obtained for conditions in which capacitance, voltage and breaks per half cycle were varied but inductance variations

VOL. 13 1958/5

caused some peculiar effects. When samples were sparked in air, the intensity decreased as inductance was added, but when a nitrogen atmosphere was used the intensity was much more constant and showed no specific trend except that it increased for the first few inductance steps. These variations indicate that spectral

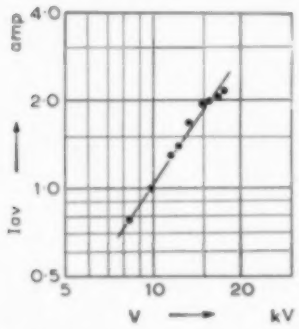

Fig. 4. Average current obtained by method (2) as a function of breakdown voltage. Other parameters, $C = 0{\cdot}0080\ \mu F$, $L = 56\ \mu H$, $B = 5$ breaks/half cycle and R (added) $= 0$.

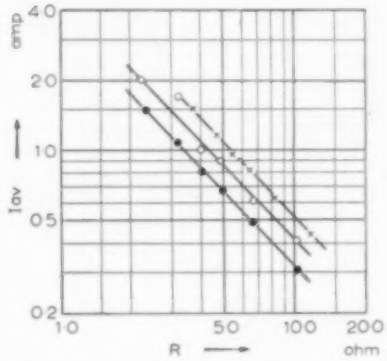

Fig. 5. Average current obtained by method (2) as a function of R for three different conditions. The R value used here is R (added) + R (residual). R (residual) was obtained by plotting R (added) vs. $1/I_{rt}^2$ and extrapolating to obtain the R at $1/I_{rt}^2 = 0$. The other parameters were (●) $C = 0{\cdot}0080\ \mu F$, $L = 56\ \mu H$; (×) $C = 0{\cdot}0080\ \mu F$, $L = 115\ \mu H$; (○) $C = 0{\cdot}0107\ \mu F$, $L = 56\ \mu H$. For all conditions $V = 12$ kV and $B = 5$ breaks/half cycle.

intensity is a function of more than just electrical source parameters. Other work performed in this laboratory [4] has shown considerable dependence of spectral intensity upon oxidation of the metal in the spark area.

Spectral character

Spectral character was measured by the ratio of an iron arc line (FeI 3016·18 Å) to a doubly-ionized iron line (FeIII 3013·12 Å). Lines from singly-ionized atoms were investigated but the iron-III line was found to be more sensitive to source parameter changes.

Figures 6 through 9 show how the ratio of the FeI 3016·18 Å (excitation potential 5·10 eV) to the FeIII 3013·12 Å (excitation potential 38·8 eV) varies with different parameters. These curves indicate that the intensity ratio of:

$$\frac{\text{FeI } 3016{\cdot}2\text{ Å}}{\text{FeIII } 3016{\cdot}1\text{ Å}} \propto \frac{L^{1/2}}{CV^{4/3}} \tag{15}$$

Figure 9 indicates that the FeI/FeIII intensity ratio is roughly proportional to the inverse of the peak current squared. The FeI/FeIII intensity ratio is substantially independent of breaks per half cycle and resistance.

Laqua [3] claimed that spectral quality, e.g. the ratio of an arc to a spark line, is a function of transient duration time. Figures 6, 7 and 8 indicate that this is

not true. The transient duration time increases as capacitance, voltage and inductance increase, while the FeI/FeIII intensity ratio increases with inductance but decreases with capacitance and voltage.

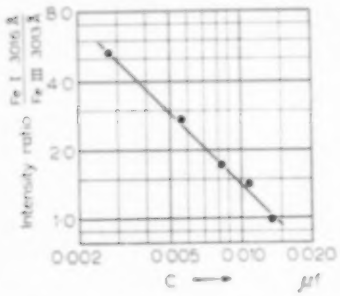

Fig. 6. FeI/FeIII intensity ratio as a function of capacitance. Other parameters $L = 56$ μH, $V = 13{\cdot}5$ kV, $B = 5$ breaks/half cycle and R (added) $= 0$.

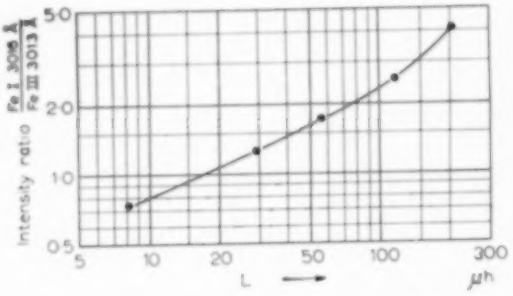

Fig. 7. FeI/FeIII intensity ratio as a function of inductance. Other parameters $C = 0{\cdot}0080$ μF, $V = 13{\cdot}0$ kV, $B = 5$ breaks/half cycle and R (added) $= 0$.

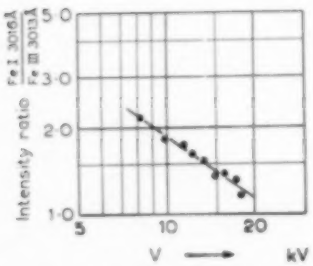

Fig. 8. FeI/FeIII intensity ratio as a function of breakdown voltage. Other parameters $C = 0{\cdot}0080$ μF, $L = 56$ μH, $B = 5$ breaks/half cycle, R (added) $= 0$.

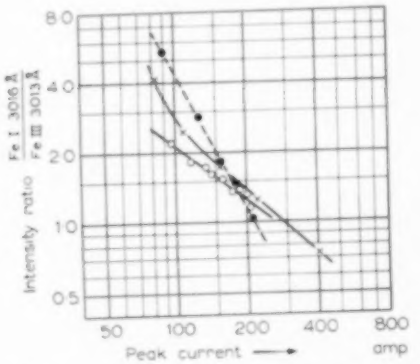

Fig. 9. FeI/FeIII ratio as a function of peak current ($J_s = V\sqrt{(C/L)}$) for conditions with C varying (●), L varying (×) and V varying (○). Other parameters as indicated in Figs. 6, 7 and 8.

Specification of source conditions

Since average current gives a measure of a very basic quantity, the energy dissipated in the analytical gap, it should be useful in the specification of source parameters. This study shows that spectral character is best specified by means of the FeI/FeIII intensity ratio. Application of this intensity ratio has the disadvantage that the FeIII line disappears with very arc-like conditions. Arc-like conditions, however, are not as critical to parameter settings as the spark-like conditions.

To test the validity of this approach, three source conditions with widely different source settings but giving the same FeI/FeIII intensity ratio and average current (see conditions 1, 2 and 3 in Table 1) were examined. Equations (14) and

VOL. 13 1958/5

(15) were very helpful in selecting suitable source parameters. Analytical curves for low alloy steel obtained with these conditions were compared with conditions which gave varying FeI/FeIII intensity ratios (conditions 4 and 5) and average current (conditions 6 and 7). Both air and nitrogen atmospheres were employed.

Table 1

Condition	C (μF)	L (μH)	V (kV)	Breaks per half cycle	I_{rf}	I_{av}	Intensity ratio $\frac{\text{FeI 3016·2}}{\text{FeIII 3013·1 (Å)}}$
1	0·0027	9 (22)	11·5	10	10·0 (7·9)	1·0	1·1 (1·65)
2	0·0078	22 (22)	10·0	4	9·6 (9·6)	1·0	1·0 (1·65)
3	0·0155	89 (38)	19·0	1	11·8 (14·4)	1·0	1·1 (1·65)
4	0·0078	9	10·0	10	11·8	1·0	0·8 (1·0)
5	0·0078	38	10·0	10	8·2	1·0	1·9 (3·0)
6	0·0078	22	10·0	2	6·6	0·5	1·1 (2·1)
7	0·0078	22	10·0	8	14·4	2·3	1·1 (1·3)

Preburn : 60 sec
Exposure : 30 sec
Analytical gap : 3 mm
Counter electrode : 120° pointed graphite

(The values in parentheses refer to the tests run with a nitrogen atmosphere.)

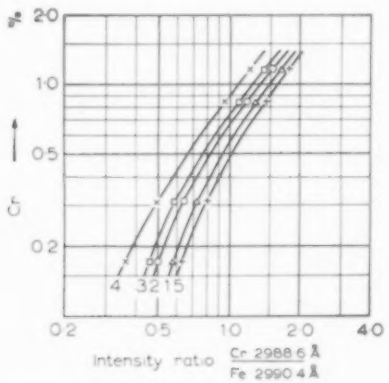

Fig. 10. Analytical curves obtained for different source conditions using a nitrogen atmosphere. The numbers indicate the source conditions as specified in Table 1.

Since the nitrogen caused a mismatch of the FeI/FeIII intensity ratio it was found necessary to vary the conditions slightly. The analytical lines used for these experiments were carefully matched in excitation potential and wavelength [5].

Figure 10 is an example of the type of curves obtained. The curve shifts shown are somewhat larger than the average for all elements. In general, the greatest

curve shifts were observed when the FeI/FeIII intensity ratio varied rather than when the average current changed.

The interesting feature of the curves is that conditions 1, 2 and 3 gave similar analytical curves and produced the same spectral intensity while 4 and 5 showed larger curve shifts. Conditions 6 and 7 showed curve shifts comparable to 1 and 3 and as expected the intensities varied as the average current.

These results indicate that average current and the FeI/FeIII intensity ratio are more unique parameters for specifying a spark source condition than are capacitance, inductance, voltage, radio frequency (r.m.s.) current, etc. The average current determines the power dissipated in the analytical gap and the general spectral intensity. The FeI/FeIII intensity ratio (or similar lines of other elements) determines the type of analytical curves obtained. Repeatability is not directly related to these two parameters so that the best combination of the other parameters must be determined experimentally. Equations (14) and (15) can be used to maintain the average current and FeI/FeIII intensity ratio constant while doing this.

References

[1] Kaiser H. and Wallraff A., *Ann. Phys.* 1939 **34,** 297.
[2] Enns J. H. and Wolfe R. A., *Special Tech. Publication No.* 76. Amer. Soc. for Testing Materials 1948.
[3] Laqua K., *Spectrochim. Acta* 1952 **4,** 446.
[4] Majkowski R. F. and Schreiber T. P. To be published.
[5] Fry D. L. and Schreiber T. P., *J. Opt. Soc. Amer.* 1954 **44,** 159.

VOL.
13
1958/5

Spectrochimica Acta, 1958, Vol. 13, pp. 107 to 119. Pergamon Press Ltd., London

Recherches sur les fréquences de déformation OH—I

Spectre infrarouge des sels basiques de cuivre*

P. Tarte
Université de Liège, Service de Chimie Générale

(*Received* 21 *June* 1958)

Abstract—The infrared spectra of a series of basic copper salts and the corresponding deuterated compounds have been studied between 4000 and 270 cm^{-1} in order to examine the behaviour of the valency and deformation vibrations of the OH groups. The torsional vibration of the OH group has not been observed and its frequency is therefore assumed to be below 270 cm^{-1}. The planar deformation frequencies of the OH group have been observed in the region 600–1050 cm^{-1}. A relationship exists between the deformation frequency and stretching frequency but it is not very exact and cannot be applied to all systems containing hydrogen bonds. The spectra are usually complex and this may be due to the irregular geometric configuration in the octahedral co-ordination to copper.

Introduction

On sait que l'existence de ponts hydrogène (O—H– – – –O) ou (N—H– – – –O), etc., est fréquente dans les substances en phase condensée. D'autre part, il est maintenant bien établi qu'il existe une relation générale entre la fréquence de valence ν_{OH} et la longueur du pont O– – – – – –O [1–6].

Par contre, on ne possède pas encore de données systématiques sur les vibrations de déformation plane δ_{OH} et de torsion τ_{OH} (déformation hors du plan), et l'on peut se demander s'il existe, pour ces vibrations, une relation générale fréquence-distance O– – – – –O analogue à celle observée pour la fréquence de valence.

Il nous est apparu assez rapidement qu'une telle relation n'existait pas et ne pouvait effectivement pas exister. Si l'on compare les spectres I.R. de l'acide borique [7–9], du bicarbonate de sodium [9] de l'hydroxyde de cuivre [9, 10] et des alcools [11] (pour ne prendre que quelques exemples), on constate qu'il n'existe aucune relation entre les fréquences ν_{OH}, δ_{OH} et τ_{OH}.

Un examen d'ensemble du problème montre d'ailleurs qu'une telle relation ne peut exister, par suite de la multiplicité des facteurs qui déterminent les fréquences δ_{OH} et τ_{OH}.

En effet, alors que la fréquence ν_{OH} ne dépend pratiquement que de la distance O– – – – –O (plus la distance totale O– – – – –O est courte, plus la distance O—H est allongée et plus la fréquence ν_{OH} est basse), la fréquence de déformation δ_{OH} doit dépendre d'au moins trois facteurs:

(1) La longueur du pont hydrogène O– – – – –O: plus cette distance est courte, plus la force de rappel est grande, plus la fréquence de déformation est élevée.

(2) Le caractère plus ou moins ionique des liaisons en cause. Si dans une substance R—O—H, la liaison R^+—$(OH)^-$ est totalement ionique (ce qui est évidemment une cas extrême exceptionnel), la fréquence de déformation sera voisine de zéro.

* Communication présentée au Congrès de Spectroscopie moléculaire de Freiburg-i-Br.

(3) La nature et la distance des atomes immédiatement voisins du groupe O—H– – – –O. En effet, au cours du mouvement de déformation OH, la distance entre l'atome de H et les atomes voisins (autres que les atomes d'oxygène participant directement au pont) varie, et l'on ne peut négliger la possibilité de l'existence d'interactions autres que celles existant dans le groupe O—H– – –O lui-même. Il est probable que ce dernier facteur ne produit que des effets secondaires, les deux facteurs déterminants étant la distance O– – – –O et le caractère plus ou moins ionique des liaisons en cause.

HARTERT et GLEMSER [8] ont récemment étudié une série d'hydroxydes et de sels basiques, et montré qu'il existait effectivement une relation bien déterminée entre ν_{OH} (elle-même fonction de la distance O– – – –O), δ_{OH} et le "rayon OH" (qui constitue une mesure du caractère ionique de la liaison R^+—$(OH)^-$).

Nous avons nous-même abordé ce problème sous un angle un peu différent, consistant à étudier une série de composés où le caractère ionique des liaisons R—OH peut être considéré comme constant (en première approximation du moins), ce qui élimine l'un des facteurs considérés plus haut: on doit alors trouver qu'il existe une relation entre ν_{OH} et δ_{OH}. Nous avons pour cela étudié la spectre I.R. (entre 4000 et 270 cm^{-1}) d'une série de sels basiques de cuivre; l'attribution des fréquences OH a pu être faite sans ambigüité grâce à l'étude systématique des composés deutérés correspondants.

Partie expérimentale

Prise des spectres

Les spectres ont été pris au moyen d'appareils Perkin–Elmer équipés de prismes de LiF, NaCl, KBr ou CsBr suivant la région étudiée. La méthode des pastilles de KBr a été utilisée d'une façon générale, et nous avons vérifié dans la plupart des cas (par la méthode de dispersion dans la paraffine) que cette méthode ne provoquait aucune altération du spectre. Dans un seul cas (Cu(OH)Cl), il y a eu réaction manifeste entre la substance et le support de KBr; cet inconvénient a été éliminé en utilisant KCl (au lieu de KBr) comme support.

Préparation des sels basiques de cuivre

(1) Cu(OH)F.—Par hydrolyse à chaud de CuF_2 (à 110°C pendant 3 jours dans un tube scellé) [12].

(2) Cu(OH)Cl.—Action de $CuCl_2 \cdot 2H_2O$ sur CuO (1 semaine à 110°C en tube scellé) [13, 14].

(3) $Cu_2(OH)_3Cl$.—Action d'une solution moyennement concentrée de $CuCl_2$ sur CuO (1 semaine à 110°C en tube scellé) [14, 15].

(4) $Cu_2(OH)_3Br$.—Action d'une solution moyennement concentrée de $CuBr_2$ sur CuO (1 semaine à 110°C en tube scellé).

(5) $CuSO_4 \cdot 3Cu(OH)_2$.—Deux méthodes ont été utilisées: (a) précipitation d'une solution de $CuSO_4$ par NH_4OH; (b) précipitation d'une solution de $CuSO_4$ par NaOH en défaut.

(6) $CuSO_4 \cdot 2Cu(OH)_2$.—Action d'une solution moyennement concentrée de $CuSO_4$ sur CuO (1 semaine en tube scellé à 110°C) [17].

VOL. 13 1958/5

(7) $Cu(NO_3)_2 \cdot 3Cu(OH)_2$.—Action d'une solution moyennement concentrée de $Cu(NO_3)_2$ sur CuO (1 semaine en tube scellé à 110°) [15].

(8) Formiate basique.—Précipitation d'une solution de formiate par NaOH en défaut.

(9) Hydroxyde.—Précipitation d'une solution de $CuSO_4$ par NH_4OH d'abord, et NaOH ensuite [16].

La purification a été effectuée, soit par lavage à l'eau bouillie et décantation, soit—lorsqu'une hydrolyse était à craindre—par lavage et décantation à l'acétone.

Les composés deutérés ont été préparés par les mêmes méthodes, en remplaçant H_2O par D_2O et NaOH par NaOD. Une petite quantité seulement (quelques centigrammes à quelques décigrammes) de ces composés a été préparée, de façon à simplifier le problème du lavage.

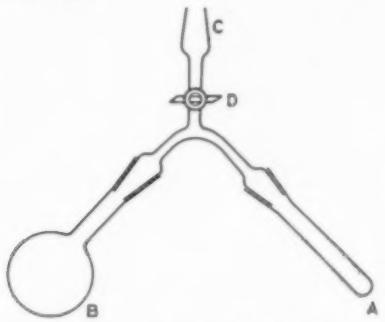

Fig. 1. Dispositif utilisé pour la préparation et la purification des sels basiques deutérés.

On ne peut en effet laver ces composés à l'eau ordinaire, de crainte d'un échange H—D. Nous avons donc effectué le lavage à l'eau lourde, en opérant en cycle fermé, sous vide, de façon à utiliser seulement une faible quantité d'eau lourde et à éviter la contamination de cette dernière par l'humidité atmosphérique.

Nous avons utilisé le montage suivant (Fig. 1). Le précipité à laver est introduit en *A*; on raccorde le tout par l'intermédiaire du rodage *C* à une installation à vide; le vide étant réalisé dans l'appareil, on distille en *A* quelques centimètres cubes de D_2O, on ferme D et, sans laisser rentrer d'air, on détache l'appareil de l'installation à vide. On procède alors, dans l'ordre, aux opérations suivantes: (a) agiter pour mettre le précipité en suspension dans D_2O; (b) laisser le précipité se déposer convenablement; (c) incliner l'appareil pour décanter vers *B* le liquide surnageant; (d) refroidir *A* dans l'air liquide; l'appareil étant toujours sous vide, l'eau lourde distille en *A*, abandonnant en *B* les sels qu'elle a dissous.

Ce cycle d'opération est répété autant de fois qu'il est nécessaire pour assurer un lavage complet de la substance à purifier. L'eau lourde ayant servi au lavage est récupérée par distillation sous vide. Les précipités ont été séchés en les soumettant, pendant 10 à 24 heures, à un vide de l'ordre de 0·01 à 0·001 mm.

Résultats

La Figure 2 montre sous forme graphique les spectres des substances étudiées.

Trois régions d'absorption sont communes à tous les composés étudiés: 3000–3600 cm^{-1}; 600–1000 cm^{-1}; 300–550 cm^{-1}. Les bandes des deux premières régions

sont fortement décalées lorsque l'on passe aux composés deutérés correspondants (on les retrouve alors dans les régions 2250–2650 cm^{-1}, et 400–800 cm^{-1} respectivement); il est donc certain qu'elles correspondent à des vibrations OH. Les positions

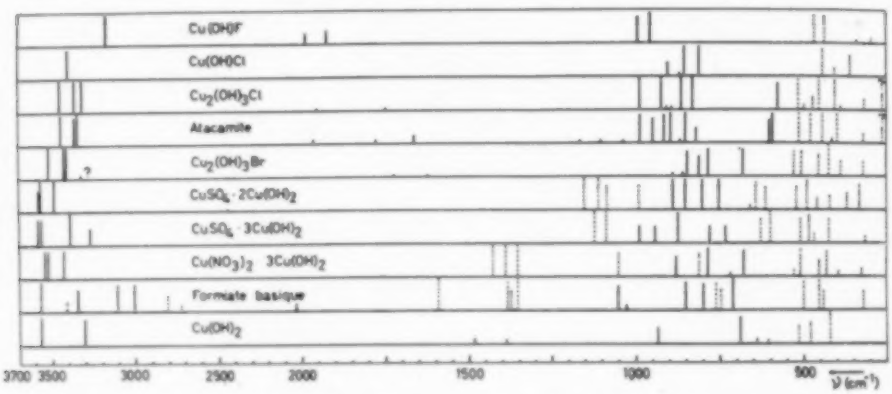

Fig. 2. Représentation schématique des spectres observés. Les traits pleins correspondent aux bandes OH; les traits interrompus, aux bandes qui ne sont que faiblement déplacées par deutération.

de ces bandes (et des bandes OD correspondantes) sont reprises dans le Tableau 1, qui donne en outre pour chaque paire la valeur du rapport $(\sqrt{\nu_{OH}/\nu_{OD}})$.

Par contre, les bandes situées dans la région 300–550 cm^{-1} ne sont que faiblement affectées par la deutération. Comme d'autre part cette région d'absorption est commune à tous les composés étudiés (y compris l'hydroxyde et l'oxyde de cuivre), on doit obligatoirement l'attribuer aux liaisons Cu—O.

Région 3000–3600

Cette région a été étudiée en utilisant un prisme de LiF, qui donne une résolution suffisante pour séparer des bandes très voisines et mesurer la position des bandes avec une bonne précision.

Parmi ces composés, trois avaient déjà été étudiés en I.R., $Cu(OH)_2$ par CABANNES-OTT [10], l'atacamite ($Cu_2(OH)_3Cl$) et $Cu_2(OH)_3Br$ par HARTERT et GLEMSER [8]. La concordance entre nos valeurs et celles proposées par ces auteurs peut être considérée comme satisfaisante, surtout si l'on tient compte du fait que HARTERT et GLEMSER ont travaillé avec un prisme de NaCl, ce qui ne leur a pas permis de séparer les bandes très proches l'une de l'autre.

On remarquera de suite que, dans deux cas seulement, Cu(OH)Cl et Cu(OH)F, il n'existe qu'une seule bande ν_{OH}. Dans tous les autres cas, l'absorption due aux vibrations de valence ν_{OH} est multiple, le nombre de bandes variant de deux ($Cu(OH)_2$) à cinq (formiate basique); le cas le plus fréquent correspond à trois bandes ν_{OH}.

Cette multiplicité constitue donc la règle plutôt que l'exception; elle peut être la conséquence de deux causes indépendantes, mais susceptibles d'intervenir simultanément: (a) l'existence de deux vibrations ν_{OH}, l'une symétrique et l'autre antisymétrique (b) la présence de ponts hydrogène O—H– – –O de longueurs différentes.

VOL. 13 1958/5

Tableau 1

Substance	Frequences OH	Frequences OD	$\sqrt{(\nu_{OH}/\nu_{OD})}$
$Cu(OH)F$	3185	2394	1·33
	1970	1457	1·36
	1905	1415	1·35
	997	~745	1·34
	962	710	1·35
$Cu(OH)Cl$	3400	2520	1·35
	1615 f	~1210	1·34
	905	676	1·34
	~870 f		
	857	650	1·32
	813	614	1·32
$Cu_2(OH)_3Cl$ (entre parenthèses, valeurs observées pour l'atacamite naturelle)	(3443) 3448	2558	1·35
	(~3360) 3360	2494	1·35
	(3343) 3317	2469	1·34
	(1950)f ~ 1940 f	~1480	1·32
	(~1775)f ~ 1745 f	~1330	1·31
	(~1660)f ~ 1660 f		
	~ 1630 f		
	(~1038)f		
	(~1104)f		
	(~1165)f		
	(988) 990	752	1·32
	(951) 925	693	1·33
	(917) ~ 910 f		
	(897) ~ 895 f		
	(868)f 866	645	1·34
	(852) 832	618	1·35
	(823)		
	(~604)		
	(594) 579	~416 ?	1·39 ?
$Cu_2(OH)_3Br$	3516	2602	1·35
	3424	2538	1·35
	~3410	2524	1·35
	~3320 ?	~2470 ?	1·34
	888 f		
	~860 f		
	848	661	1·28
	814	644	1·26
	787	610	1·29
	684	?	
$CuSO_4 \cdot 2\,Cu(OH)_2$	~3578	2643	1·35
	3570	2636	1·35
	3486	2578	1·35
	889	691	1·29
	853	~655	1·30
	805	590	1·36
	756	567	1·33

Tableau 1 (*suite*)

Substance	Frequences OH	Frequences OD	$\sqrt{(\nu_{OH}/\nu_{OD})}$
$CuSO_4 \cdot 3\,Cu(OH)_2$	3586	2646	1·36
	3564	2632	1·35
	3390	2519	1·35
	~3270	~2440	1·34
	989	737	1·34
	945	690	1·37
	874	~657	1·33
	782	~627 ?	1·25
	736	~578	1·27
Formiate basique	3570	2635	1·35
	~3410 f		
	3345	2495	1·34
	~3100	~2410	1·29
	~3000	2275	1·32
	~2005	~1485	~1·35
	1050	759	1·38
	1026 ?		
	853	679 ?	1·26
	797	634	1·26
	712	545	1·31
$Cu(NO_3)_2 \cdot 3\,Cu(OH)_2$	3543	2618	1·35
	3522		
	3428	2541	1·35
	880	663	1·33
	785	604	1·30
	677	527	1·28

Le premier facteur ne nous paraît pas devoir être retenu; en effet, l'existence de deux vibrations de valence, l'une symétrique et l'autre antisymétrique (et susceptibles de donner naissance à des fréquences nettement différentes) n'est guère concevable que dans les cas de groupements du type XY_2. Ici, les groupes OH sont séparés par un atome de cuivre, et, de surcroît, les liaisons Cu—O possèdent un caractère partiellement ionique (ce qui réduit pratiquement à zéro le couplage mécanique qui aurait pu exister entre deux groupes OH).

Par contre, la présence de ponts O—H– – – –O de longueurs différentes permet, à elle seule, d'expliquer la multiplicité des bandes ν_{OH}. Nous n'avons malheureusement aucune preuve directe de l'existence de ponts hydrogène (l'étude cristallographique détaillée des sels basiques de Cu est encore à faire dans la plupart des cas); mais l'existence de liaisons H du type "long" est tout à fait courante chez les hydroxydes et les sels basiques; de plus, la présence, dans un même composé, de ponts O—H– – – –O de longueurs différentes s'accorderait bien avec ce que l'on connaît actuellement de la stéréochimie très particulière du cuivre [19]: au lieu d'un octaèdre régulier, le cuivre s'entoure d'un octaèdre déformé (caractérisé

VOL. 13 1958/5

essentiellement par quatre liaisons courtes et deux liaisons longues); ceci introduit dans la structure un élément d'asymétrie favorisant l'existence de ponts H de longueurs différentes.

Région 2000–1500 cm^{-1}

On observe assez fréquemment une ou plusieurs bandes faibles dans cette région, ces bandes sont fortement décalées par deutération et, dans tous les cas, on peut les interpréter comme correspondant à une harmonique ou à une combinaison de fréquences de déformation δ_{OH}. Il est pas inutile de noter que la présence de bandes correspondant à des harmoniques ou des combinaisons des fréquences δ_{OH}, et possédant parfois une intensité intrinsèque relativement grande (voir par exemple Cu(OH)F), est assez fréquente, non seulement chez les sels basiques de cuivre, mais également chez les hydroxydes et les sels basiques d'autres métaux: nous avons observé de telles bandes dans les cas de αAlO(OH) (diaspore), MnO(OH) (manganite), αFeO(OH) (goethite), ε-$Zn(OH)_2$ [20].

Région 1100–600 cm^{-1}

Cette région contient toujours une série de bandes intenses, fortement décalées vers les basses fréquences lors de la deutération; leur attribution à des vibrations δ_{OH} est donc pratiquement immédiate. L'établissement d'une relation entre les fréquences δ_{OH} et ν_{OH} se heurte toutefois à une sérieuse difficulté: dans deux cas seulement ($Cu(OH)_2$ et $Cu(NO_3)_2 \cdot 3Cu(OH)_2$), le nombre des bandes δ_{OH} est égal à celui des bandes ν_{OH}; chez les autres composés étudiés, le nombre des bandes δ_{OH} est supérieur à celui des bandes ν_{OH}, de sorte qu'il est impossible d'établir une corrélation unique $\nu_{OH} \leftrightarrow \delta_{OH}$.

Comme l'ont proposé Hartert et Glemser [8], cette complication est certainement due à l'existence de plusieurs distances Cu—O: si nous considérons par exemple l'existence, dans le cristal, de deux groupes Cu—O—H- - - -O, pour lesquels les ponts hydrogène O—H- - - -O ont même longueur, mais où les distances Cu—O sont différentes, on observera une seule bande ν_{OH} (la fréquence de valence étant essentiellement déterminée par la longueur du pont H), mais deux bandes δ_{OH} (leur fréquence étant fonction, à la fois de la longueur du pont H, et de la distance Cu—O).

Toutefois cette complication ne constitue pas un obstacle insurmontable à l'établissement d'une relation $\delta_{OH} \leftrightarrow \nu_{OH}$; en effet, sauf dans quelques cas particuliers que nous discuterons plus loin, la distance Cu—O ne s'écarte guère d'une valeur moyenne de 2·0 Å, de sorte que ce facteur n'intervient que d'une façon secondaire pour déterminer la valeur de δ_{OH}.

Nous avons donc porté dans un diagramme δ_{OH} en fonction de ν_{OH} mais étant donné la présence quasi systématique de plusieurs bandes ν_{OH} et δ_{OH} pour un composé donné, il a été nécessaire de procéder comme suit:

(1) A la fréquence ν_{OH} la plus basse, on fait correspondre la fréquence δ_{OH} la plus élevée, et inversément. Cette façon de procéder n'est pas arbitraire, mais repose sur le fait—maintenant bien établi—qu'à une diminution de la longueur du pont hydrogène correspond une élévation de la fréquence de déformation.

(2) Lorsque le nombre de bandes δ_{OH} est plus élevé que celui des bandes ν_{OH},

on est bien obligé de faire correspondre deux bandes δ_{OH} de fréquences voisines à une seule bande ν_{OH}. Ici, le choix est arbitraire, mais il est impossible de procéder autrement (il faudrait en effet, pour établir une concordance rigoureuse, connaître à la fois, pour chaque groupe Cu—O—H– – – –O, la distance Cu—O et la longueur du pont HO—H– – – –O; or, la connaissance simultanée de ces deux données fait défaut).

On obtient ainsi le diagramme reproduit Fig. 3. Malgré une certaine dispersion des points, inévitable puisque l'on a négligé l'influence de petites variations de la distance Cu—O, l'existence d'une relation $\nu_{OH} \leftrightarrow \delta_{OH}$ est évidente.

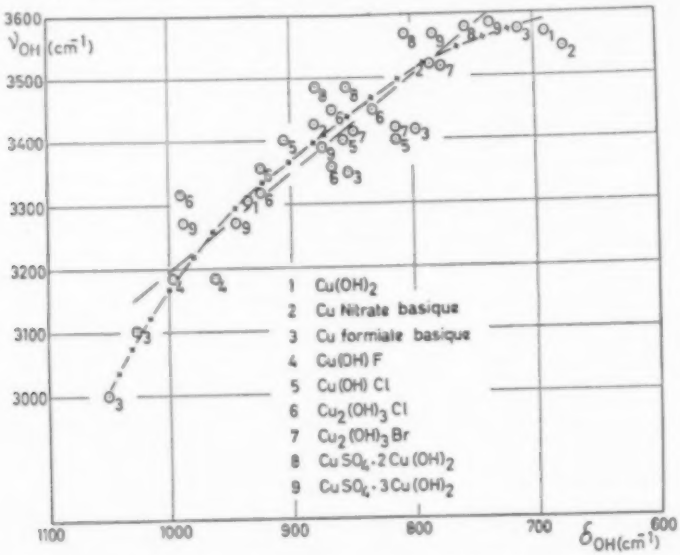

Fig. 3. Relation entre les valeurs de ν_{OH} et δ_{OH}. La droite en traits interrompus correspond à la relation proposée par HARTERT et GLEMSER.

Nous avons d'autre part tracé en traits interrompus une droite dont la pente correspond au rapport $\Delta\delta/\Delta\nu = 0{\cdot}66$ calculé par HARTERT et GLEMSER [8]. Cette droite semble représenter un bon tracé moyen de l'ensemble de nos résultats, sauf peut-être dans le domaine des liaisons H relativement courtes, où semble apparaître une certaine courbure.

Il nous semble toutefois qu'une courbe continue, telle que celle qui est tracée sur la Fig. 3, représente mieux l'allure générale du comportement des vibrations δ_{OH}: cette courbe signifierait que, dans le domaine des liaisons hydrogène très longues, δ_{OH} varie très rapidement pour une faible variation de ν_{OH} (c'est-à-dire de la longueur du pont hydrogène); cette variation devient de moins en moins importante lorsque le pont hydrogène devient plus court.

La dispersion des points expérimentaux ne permet pas de faire un choix définitif entre la droite proposée par HARTERT et GLEMSER (droite qui implique une valeur constante du rapport $\Delta\delta/\Delta\nu$, quelle que soit la longueur du pont hydrogène), et la courbe que nous proposons (avec une variation du rapport $\Delta\delta/\Delta\nu$ en fonction de la longueur du pont hydrogène).

VOL. 13 1958/5

Toutefois, d'autres résultats expérimentaux s'accordent bien avec notre hypothèse: l'étude spectroscopique d'une série d'hydroxydes contenant des liaisons hydrogène moyennes ou relativement courtes [20] et de bicarbonates à liaisons courtes [18] a montré, pour tous ces composés, une valeur du rapport $\Delta\delta/\Delta\nu$ très inférieure à la valeur 0·66 proposée par HARTERT et GLEMSER (chez les bicarbonates, nous avons trouvé $\Delta\delta/\Delta\nu \simeq 0{\cdot}24$). Ces résultats indiquent que la valeur de ce rapport est fonction de la longueur du pont hydrogène. D'autres expériences sont actuellement en cours pour préciser l'allure de cette relation.

Nous avons négligé, pour l'établissement de la Fig. 3 quelques bandes dont le comportement semblait aberrant, mais, comme nous allons le montrer, cette façon de procéder est tout à fait justifiée dans le cas envisagé ici.

Dans le spectre I.R. de l'atacamite artificielle, il apparaît dans la région 580 cm^{-1} une bande intense (il y en a deux dans l'atacamite naturelle) fortement décalée par deutération, donc attribuable à une vibration de déformation δ_{OH}. La Fig. 2 montre clairement que cette bande—et les deux bandes correspondantes de l'atacamite naturelle-paraissent posséder une fréquence anormalement basse par rapport aux autres fréquences δ_{OH}. Il est d'ailleurs évident qu'elles s'écartent considérablement du tracé moyen de la Fig. 3.

Or, la structure de l'atacamite a été étudiée par WELLS [21], qui a pu mettre en évidence l'existence de cinq distances Cu—O différentes; quatre de ces distances sont très semblables (1·94, 2·00, 2·04, et 2·07 Å) et correspondent aux distances Cu—O généralement observées ($\sim$2·0 Å), mais la cinquième est nettement plus grande (2·36 Å). La même particularité doit exister chez l'atacamite artificielle, dont la structure est presque identique à celle de l'atacamite naturelle.

La comparaison des données X et I.R. montre donc que l'anomalie signalée chez les fréquences δ_{OH} n'est qu'apparente: la fréquence I.R. très basse correspond à l'existence d'une liaison Cu—O exceptionnellement longue. Nous ne pouvions toutefois inclure les points correspondants dans notre diagramme Fig. 3, puisque ce dernier n'est valable que pour des liaisons Cu—O de longueur normale.

Des phénomènes du même genre se rencontrent peut-être chez le composé parent $Cu_2(OH)_3Br$, mais ici les choses sont beaucoup moins claires. On observe en effet chez ce composé une bande δ_{OH} de fréquence nettement plus basse (684 cm^{-1}) que les autres (l'écart est toutefois plus faible que chez l'atacamite); de plus, HARTERT et GLEMSER [8] signalent que cette bande ne s'intègre pas dans leur relation générale. Il se pourrait donc bien que cette basse fréquence δ_{OH} corresponde ici encore à une distance Cu—O plus longue que la normale. Cette hypothèse est toutefois en contradiction avec les résultats de l'étude cristallographique faite par AEBI [22] qui ne trouve dans $Cu_2(OH)_3Br$ que trois distances Cu—O tout à fait normales (1·92, 1·98 et 2·00 Å).

La question se pose donc de savoir si les résultats et les conclusions de AEBI sont tout à fait corrects. Ce doute repose, non seulement sur la contradiction que nous venons de relever, mais également sur le fait que la similitude des spectre I.R. de $Cu_2(OH)_3Br$ et $Cu_2(OH)_3Cl$ suggère des structures similaires, alors que les résultats de AEBI conduisent à des structures dissemblables.

La détermination correcte de la structure des sels basiques de Cu est d'ailleurs malaisée: cela résulte, comme nous l'avons déjà signalé plus haut, de la forme

généralement irrégulière de l'octaèdre de coordination du cuivre. Quoi qu'il en soit, une redétermination de la structure de $Cu_2(OH)_3Br$ serait souhaitable.

Pour en terminer avec la question des vibrations OH, notons immédiatement que, dans le domaine spectral couvert par ce travail (jusque $\nu = 270$ cm^{-1}), et pour les substances étudiées ici, nous n'avons jamais observé de bandes qui puissent être attribuées à la torsion (déformation hors plan) OH: aucune des bandes situées dans la région 550–270 cm^{-1} (où la présence de bandes τ_{OH} n'apparaissait pas impossible *à priori*) n'est affectée d'une manière importante par la deutération. A ce mode de vibration doit donc correspondre une fréquence relativement très basse ($\nu < 270$ cm^{-1}); cette conclusion apparaît d'ailleurs comme très raisonnable si l'on se rappelle que, dans le groupe O—Cu—O—H (en effet, un groupe d'au moins quatre atomes est indispensable pour que l'on puisse observer une vibration de torsion) les deux liaisons Cu—O ont un caractère partiellement ionique et contribuent donc à abaisser de façon notable la fréquence de torsion de l'ensemble.

Il paraît d'ailleurs impossible de prévoir, même grossièrement, l'ordre de grandeur de cette fréquence de torsion. En effet, ce mode de vibration est très sensible aux influences structurales, et sa fréquence varie dans de larges limites, même lorsque l'on s'adresse à des substances en phase gazeuse, où n'interviennent pas les complications provenant, soit de l'existence de ponts H, soit du caractère plus ou moins ionique des liaisons (par exemple, dans CH_3OH, cette fréquence de torsion est de l'ordre de 250 cm^{-1} [23]; dans l'acide nitreux gazeux, 545 cm^{-1} pour la forme *trans* [24]).

Dès lors, si l'on s'adresse à un solide, dans lequel il faut encore tenir compte d'influences diverses et parfois opposées (longueur des ponts H, caractère plus ou moins ionique des liaisons, interactions du réseau cristallin), la situation devient inextricable et aucune prévision n'est possible.

CABANNES-OTT [10] croit avoir mis en évidence l'existence d'une fréquence de torsion OH chez $Cu(OH)_2$ et d'autres hydroxydes: cette vibration se situerait dans la région 400–500 cm^{-1}. Nos résultats ne s'accordent pas avec cette conclusion, qui nous paraît un peu hâtive: en effet, elle a été tirée de l'étude d'hydroxydes partiellement deutérés seulement (la préparation d'hydroxydes totalement ou très fortement deutérés est beaucoup moins aisée que la préparation de sels basiques), et, dans le cas de $Cu(OH)_2$, les bandes en cause sont situées dans une région spectrale assez encombrée: les conditions expérimentales sont donc défavorables et, à notre avis, ne permettent guère de tirer des conclusions rigoureuses.

Toujours à propos de l'hydroxyde de cuivre, signalons que les échantillons de cette substance préparés par diverses méthodes, nous ont donné des spectres identiques, dans la mesure où la méthode utilisée conduit effectivement à l'hydroxyde. En effet, certains réactifs, généralement considérés comme donnant des hydroxydes, peuvent conduire, dans le cas du cuivre, à des sels basiques. C'est le cas notamment de l'ammoniaque: une solution de $CuSO_4$ traitée par NH_4OH donne un précipité, non pas de $Cu(OH)_2$, mais de sulfate basique $CuSO_4 \cdot 3\,Cu(OH)_2$, même lorsque NH_4OH est en excès (c'est-à-dire lorsqu'il y a redissolution partielle du précipité sous forme de $[Cu(NH_3)_4]SO_4$).

Ceci explique les divergences observées par OTT dans une première publication [25] sur le spectre I.R. de l'hydroxyde de cuivre: dans certains cas, la substance

VOL. 13 1958/5

étudiée était certainement, non pas $Cu(OH)_2$, mais un sel basique. Le même auteur a d'ailleurs constaté ultérieurement [26] que l'on obtenait toujours le même spectre, quel que soit le sel de départ, si l'on effectuait la précipitation par un excès de KOH.

Région 300–550 cm^{-1}

Cette région est caractérisée par la présence constante d'une série de bandes intenses (Fig. 1), ne subissant qu'un décalage faible ou négligeable par deutération.

Cette région d'absorption est commune à tous les sels basiques, et également à $Cu(OH)_2$ et CuO. Son attribution aux fréquences de valence CuO peut donc être considérée comme certaine.

La structure est fréquemment complexe, avec recouvrement partiel des bandes. Cette complexité est évidemment en rapport avec l'existence de plusieurs distances Cu—O, qui est elle-même la conséquence du caractère irrégulier de l'octaèdre de coordination du cuivre. Un seul composé échappe à cette complexité: c'est le fluorure basique Cu(OH)F: son spectre ne compte que cinq bandes intenses: une bande ν_{OH}, deux bandes δ_{OH} et deux bandes ν_{Cu-O}. Il est donc fort probable que sa structure possède une symétrie plus élevée que celle des autres sels basiques de cuivre; on ne possède malheureusement pas d'étude par rayons-X qui permette de vérifier notre hypothèse (une étude détaillée serait probablement malaisée, étant donné la difficulté de distinguer entre $(OH)^-$ et F^- par rayons-X). La nature même des liaisons hydrogène existant dans ce composé n'est d'ailleurs pas connue avec certitude: on ne sait pas en effet s'il s'agit de liaisons O—H-----O ou O—H------F. Toutes ces inconnues font de Cu(OH)F un composé dont l'étude structurale vaudrait la peine d'être abordée par des techniques appropriées.

Note sur la position des bandes OH *dans les composés deutérés*

Lorsque l'on prépare une substance deutérée, on n'obtient évidemment pas une deutération à 100%: à moins de prendre des précautions exceptionnelles, la substance contient toujours 1 à quelques % d'hydrogène. Il peut donc subsister dans le spectre des bandes OH faibles et, dans la mesure où ces bandes ne sont pas masquées par d'autres bandes intenses, nous avons observé ces bandes résiduelles OH dans certains des composés deutérés.

Il n'est pas sans intérêt de noter que la position de ces bandes OH résiduelles ne coïncide pas exactement avec la position des bandes OH du composé non deutéré. Ce décalage a déjà été observé dans d'autres cas: il résulte du couplage qui existe entre les vibrations de deux groupements géométriquement voisins et possédant des fréquences de vibration semblables.

Par exemple, dans un sel basique non deutéré, il y aura couplage entre les vibrations des groupements OH géométriquement voisins (et dont les fréquences de vibration seront presque toujours comparables): ce que l'on observe, ce sont les fréquences OH perturbées par ces couplages. Au contraire, dans un composé fortement (mais non totalement) deutéré, les groupements OH sont "isolés" au milieu de groupements OD, dont les fréquences sont nettement différentes: il ne peut y avoir couplage, et l'on observe des fréquences OH non perturbées.

Il résulte de ceci que, si l'on désirait étudier les fréquences OH (ou OD) non

perturbées, il faudrait assez paradoxalement mesurer les fréquences OH chez un composé fortement deutéré, et les fréquences OD chez un composé faiblement deutéré. En gros, ce problème se ramène à l'étude, dans un solide, du spectre d'une impureté présente à raison de quelques %. Ce problème n'est soluble que dans certains cas particuliers favorables: c'est pourquoi nous n'avons pas utilisé cette technique pour l'étude générale que nous venons de rapporter.

Résumé

On a étudié entre 4000 et 270 cm^{-1} le spectre I.R. d'une série de sels basiques de cuivre et des composés deutérés correspondants, de façon à mettre en évidence le comportement spectroscopique des fréquences de valence et de déformation OH. La vibration de torsion OH n'a pas été observée: sa fréquence est donc inférieure à 270 cm^{-1}. Les fréquences de déformation plane OH ont été observées dans le domaine 600–1050 cm^{-1}; il existe une relation entre la fréquence de déformation et la fréquence de valence (c'est-à-dire la longueur de la liaison hydrogène), mais cette relation n'est pas rigoureuse, et elle ne peut être étendue telle quelle à tous les systèmes contenant des liaisons hydrogène.

Le spectre est généralement complexe: cette complexité est due à la géométrie irrégulière de l'octaèdre de coordination du cuivre.

Remerciements—Nous remercions M. BOUILLON, Chef de Travaux á l'U.L.B., pour l'envoi d'échantillons d'hydroxyde, de sulfate et de nitrate basique de cuivre: ces substances ont permis d'utiles comparaisons avec nos propres échantillons. Nous remercions également Mme. MARTIN pour l'aide technique qu'elle nous a apportée. Nous remercions enfin l'Union Minière du Haut Katanga, l'Institut Interuniversitaire des Sciences Nucléaires et le Centre National Belge de Chimie Physique Moléculaire pour l'aide apportée á notre laboratoire.

VOL.
13
1958/5

Bibliographie

[1] RUNDLE R. E. et PARASOL M. *J. Chem. Phys.* 1952 **20** 1487.
[2] LORD R. C. et MERRIFIELD R. E. *J. Chem. Phys.* 1953 **21** 166.
[3] HARTERT E. et GLEMSER O. *Naturwissenschaft* 1953 **40** 199.
[4] NAKAMOTO K., MARGOSHES M. et RUNDLE, R. *J. Amer. Chem. Soc.* 1955 **77** 6480.
[5] LIPPINCOTT E. R. et SCHROEDER R. *J. Chem. Phys.* 1955 **23** 1099.
[6] PIMENTEL G. C. et SEDERHOLM C. H. *J. Chem. Phys.* 1956 **24** 639.
[7] BETHELL D. E. et SHEPPARD N. *Trans. Faraday Soc.* 1955 **51** 9.
[8] HARTERT E. et GLEMSER O. *Z. Elektrochem.* 1956 **60** 746.
[9] TARTE P. Résultats non publiés ou en cours de publication.
[10] CABANNES-OTT C. *C.R. Acad. Sci., Paris* 1956 **242** 2825.
[11] STUART A. et SUTHERLAND G. B. B. M. *J. Chem. Phys.* 1952 **20** 1977.
[12] GMELIN *Handbuch der anorganischen chemie* 1958.
[13] HAYEK E. *Z. anorg. Chem.* 1933 **210** 241.
[14] FEITKNECHT W. et MAGET K. *Helv. Chim. Acta* 1949 **32** 1639.
[15] GAUTHIER J. *Bull. Soc. Chim. Fr.* 1956 661.
[16] BRAUER G. *Handbuch der präparativen anorganischen Chemie.*
[17] POSNJAK E. et TUNELL G. *Amer. J. Sci.* 1929 (5) **18** 1.
[18] TARTE P. *Communication présentée au Ier Congrès International sur les liaisons hydrogène, Ljubljana* 1957.
[19] ORGEL L. E. et DUNITZ J. D. *Nature, Lond.* 1957 **179** 462.
[20] TARTE P. Résultats non publiés.
[21] WELLS A. F. *Acta Cryst.* 1949 **2** 175.

[22] Aebi F. *Helv. Chim. Acta* 1948 **31** 369.
[23] Hadni A. *Thèse de doctorat.* Paris 1955.
[24] D'Or L. et Tarte P. *Bull. Soc. Roy. Sci. Liège* 1951 478.
[25] Ott C. *C.R. Acad. Sci., Paris* 1953 **236** 2224; 1954 **238** 1111.
[26] Cabannes-Ott C. *C.R. Acad. Sci., Paris* 1956 **242** 355.

L.
3
/59

Spectrochimica Acta, 1958, Vol. 13, pp. 120 to 124. Pergamon Press Ltd., London

The structure of vinyl fluoride

B. Bak, D. Christensen, L. Hansen-Nygaard and J. Rastrup-Andersen
Chemical Laboratory of the University of Copenhagen, Copenhagen, Denmark

(*Received* 28 *June* 1958)

Abstract—By means of microwave spectra of vinyl fluoride and five of its deuterated species the most probable structure of vinyl fluoride has been evaluated. This structure has C(1), F = 1·348 Å; C(1), H(1) = 1·073 Å; C(2), H(2) = 1·080 Å; C(2), H(3) = 1·080 Å; C(1), C(2) (double bond distance) = 1·333 Å. ∠FC(1)H(1) = 115·4°; ∠H(1)C(1)C(2) = 123·7°; ∠H(2)C(2)C(1) = 121·1°; ∠H(3)C(2)C(1) = 118·5°. The C = C distance (1·333 Å) is probably very close to the "unperturbed" C = C distance in ethylene.

Introduction

So far no serious attempts have been made to determine the structure of the comparatively small molecule vinyl fluoride, CH_2=CHF (hereafter written CH_2CHF). From the infra-red spectrum of vinyl fluoride Cole and Thompson [1] calculated the difference between the two large rotational constants of the ground level, $A'' - B'' = 1{\cdot}816$ cm^{-1}. This does not, of course, fix the structure. Also, no electron-diffraction studies have been made. Such studies would be complicated by the fact that the expected C=C and C—F distances are about equal ($\sim$1·34 Å). Therefore, a microwave investigation seemed valuable although a determination of the structure by this method is complicated by the fact that one of the rotational constants of the molecule (A) cannot be measured with high precision, since vinyl fluoride and its deuterated species are near-prolate tops (see below).

A more general reason for studying vinyl fluoride is that probably the C=C distance found in this molecule would form an upper limit to the ethylene C=C distance which is so important in all semi-empirical bond-order considerations. Hitherto, two inconsistent values of this distance have been published, i.e. Thompson's value 1·331 Å [2] and Gallaway and Barker's 1·353 Å [3], both based on infra-red measurements. During the present work, Bartell and Bonham [4] have published the preliminary result of an electron-diffraction determination of the structure of ethylene. They found $r_m = 1{\cdot}330 \pm 0{\cdot}003$ Å (from the *radial* distribution curve) and $r_g = 1{\cdot}334$ Å (from the *probability* distribution curve), i.e. largely in agreement with Thompson's work. As will be shown, the result of the present investigation is that a probable upper limit to the C=C distance is 1·333 Å, the C=C distance found in vinyl fluoride being of this magnitude.

The idea of investigating vinyl fluoride by microwave technique was first suggested by Morgan and Goldstein, U.S.A., who reported on some of their results in Columbus, Ohio, in 1955. The present authors were unaware of this, but after discussions with them it was agreed that the group in Copenhagen should continue its work which was scheduled to include not only vinyl fluoride but also several isotopic species.

VOL. 13 1958/5

Experimental

The preparation of vinyl fluoride, CH_2CHF, CH_2CDF, the *cis-trans* mixture CHDCHF, and the *cis–trans* mixture CHDCDF is described elsewhere [5]. All samples were purified gas-chromatographically on dry silica-gel and the purity checked by infra-red spectra [6] which showed that no impurities other than 5–10 per cent isotopic species were present.

Table 1. Measured and calculated (in parentheses) microwave absorption frequencies in MHz* of vinyl fluoride, five deuterated species, and ^{13}C-containing species; *cis* and *trans* refer to the mutual position of fluorine and the "lone" hydrogen isotope.

	$0_{00} \rightarrow 1_{01}$	$1_{11} \rightarrow 2_{12}$	$1_{01} \rightarrow 2_{02}$	$1_{10} \rightarrow 2_{11}$	$4_{14} \rightarrow 4_{13}$	$5_{15} \rightarrow 5_{14}$	$6_{16} \rightarrow 6_{15}$
CH_2CHF	19,755·01 (19,754·98)	37,991·27 (37,991·36)	39,477·97 (39,478·01)	41,028·57 (41,028·56)		22,765·2 (22,767·3)	
$^{13}CH_2CHF$†	19,153·4						
$CH_2{}^{13}CHF$†	19,717·0						
CH_2CDF	19,388·1 (19,388·9)	36,895·8 (36,895·4)	38,710·6 (38,710·1)	40,660·7 (40,660·1)	18,810·9 (18,812·7)	28,189·7 (28,192·5)	
$^{13}CH_2CDF$†	18,806·0						
$CH_2{}^{13}CDF$†	19,358·0						
CHDCHF (*cis*)	18,888·8 (18,888·7)	36,109·5 (36,109·6)	37,729·8 (37,729·9)	39,445·0 (39,445·1)		24,990·6 (24,992·1)	
CHDCHF (*trans*)	18,052·0 (18,052·2)	34,820·3 (34,820·2)	36,081·3 (36,081·2)	37,388·6 (37,388·5)		19,253·7 (19,254·4)	26,942·9 (26,944·4)
CHDCDF (*cis*)	17,743·8 (17,744·1)	33,898·3 (33,898·1)	35,441·4 (35,441·2)	37,078·4 (37,078·2)		23,826·7 (23,826·6)	
CHDCDF (*trans*)	18,547·0 (18,546·9)	35,091·6 (35,091·7)	37,003·9 (37,003·9)	39,096·0 (39,096·1)	20,004·8 (20,004·5)		

* The great majority of lines were identified by their Stark effect. Up to 30,000 MHz all frequencies are measured to $\pm 0{\cdot}1$ MHz. At higher frequency $\Delta\nu = \pm 0{\cdot}2$–$0{\cdot}3$ MHz

† Occurring in natural abundance.

The conventional Stark-modulated spectrograph applied operating in the 17000–30000 MHz region has been described earlier [7]. The frequencies of the three $1 \rightarrow 2$ transitions in vinyl fluoride, given in Table 1 with the rest of the experimental frequencies, are MORGAN and GOLDSTEIN's measurements (unpublished). The corresponding transitions in the spectra of the deuterated species were measured by one of us (D. C.) by kind assistance from Dr. H. SELÉN, the University of Stockholm.

Calculation of rotational constants

The measured microwave transitions were formulated as functions of $B + C$, $2A - B - C$, and $b\{= b_p = (C - B)/(2A - B - C)\}$ [8]. From these, the best possible set of the parameters was calculated. The rotational constants are given in Table 2. The frequencies calculated from the rotational constants in Table 2 are given in Table 1 (in parentheses).

It is seen from Table 2 that the inertial defect, I.D., is sometimes found to be positive, sometimes negative. No conclusions can be drawn from this since the cause is that I_a is determined with less accuracy from the experimental data than I_b and I_c. We have taken the small numerical values of the I.D.'s found as indicating a planar structure. In the following we have *assumed* the structure to

Table 2. Calculated rotational constants A, B, and C (MHz), asymmetry parameter b, and principal moments of inertia I_a, I_b, and I_c (a.m.u. Å^2) of vinyl fluoride and five deuterated species. The inertial defect I.D. [$= I_c - (I_a + I_b)$] is given in the last column but one.

	A	B	C	b	I_c	I_b	I_a	I.D.	$I_c - I_b$
CH_2CHF	63,997	10,636·79	9118·19	−0·01403	7·8985	47·5219	55·4364	0·0160	7·9145
CH_2CDF	48,960	10,635·60	8753·27	−0·02397	10·3246	47·5272	57·7476	−0·1042	10·2204
CHDCHF (*cis*)	53,400	10,278·20	8610·48	−0·01897	9·4657	49·1798	58·7052	0·0597	9·5254
CHDCHF (*trans*)	62,440	9668·14	8384·03	−0·01202	8·0952	52·2831	60·2908	−0·0875	8·0077
CHDCDF (*cis*)	49,250	9667·07	8077·02	−0·01969	10·2637	52·2889	62·5825	0·0299	10·2936
CHDCDF (*trans*)	42,700	10,274·57	8272·36	−0·02995	11·8381	49·1972	61·1047	0·0694	11·9075

be planar, so that the I_a used in the structure calculation was taken as $I_a = I_c - I_b$ (I.D. = 0). However, in order to estimate the importance of this assumption, a model for which I_a was taken as $I_a = I_c - I_b - 0{\cdot}06$ (I.D. = 0·06) was also considered, since an experimental I.D. of this order of magnitude is not unusual.

Also, the microwave frequencies were calculated using I.D. = 0. In no case do they deviate significantly from the observed values.

Molecular models

Fig. 1 shows the approximate position of the molecule with its principal inertial axes (a and b; c perpendicular to paper) and the numbering of the atoms. First, the hydrogen positions were calculated using the I_c, I_b and $I_a = I_c - I_b$ values of Table 2 for the isotopic species in rows 1, 2, 3, and 4. The contributions of the hydrogen atoms to I_a and I_b were now subtracted. Together with the centre of mass relations, $\Sigma m_i a_i = 0$ and $\Sigma m_i b_i = 0$, this imposes four conditions on the six co-ordinates of the C=C—F skeleton. Therefore, two further data are needed for the calculation of a definite structure. One we shall take as being the frequencies of the $0_{0\cdot0} \rightarrow 1_{0\cdot1}$ transitions in the spectra of the $^{13}CH_2CHF$ and $^{13}CH_2CDF$ species (Table 1). Since the experimental data are then exhausted we shall tentatively assume that the C(2),H(2) and C(2),H(3) distances are equal (model I). The validity of this assumption is verified by the fact (see Table 3), that the calculated C(2),H(2) = C(2),H(3) distance falls within the expected 1·075–1·085 Å range.

Slight deviations from equality of the distances C(2),H(2) and C(2),H(3)

VOL. 13 1958/59

proved to have almost no effect on the calculated C(1),H(1) distance. In subsequent model calculations (models II and III) the C(1),H(1) distance was varied $\pm$ 0·0005 Å. Now, the calculated C(2),H(2) and C(2),H(3) distances became unequal *but* still within the expected range. As is seen from Table 3 all these

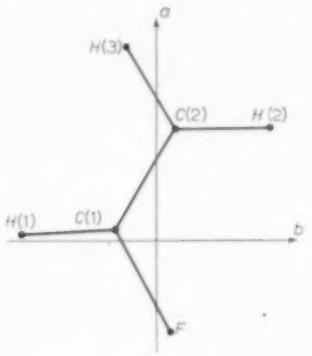

Fig. 1. Numbering of atoms in vinyl fluoride; *a* and *b* are principal axes (*c*-axis perpendicular to paper).

Table 3. Molecular models of vinyl fluoride in consistence with the microwave spectra of vinyl fluoride and some isotopic species. Distances in Å units. Concerning the numbering of models, see text.

Model no.	I	II	III	IV	V
C(1), H(1)	1·0725	1·0720†	1·0730†	1·0716	1·0765
C(2), H(2)	1·0800*	1·0874	1·0756	1·0798*	1·0800*
C(2), H(3)	1·0800*	1·0761	1·0831	1·0798*	1·0800*
C(1), C(2)	1·3328	1·3309	1·3342	1·3332	1·3308
C(1), F	1·3479	1·3491	1·3470	1·3476	1·3449

* C(2), H(2) = C(2), H(3) assumed
† Assumed.

manipulations were of almost no effect on the C=C and C—F distances. C=C and C—F distances, deviating radically from the values in Table 3, would imply C(2),H(2) respectively C(2),H(3) distances lying wide outside the usual interval.

Since a number of deuterated species greater than that which is strictly necessary (3) was investigated, the calculation of the structure was repeated using the data in columns 1, 2, 5, and 6 of Table 2. As a necessary assumption, the equality of the C(2),H(2) and C(2),H(3) distances was again used (model IV). Model IV deviates insignificantly from model I.

In a final model calculation the importance of the assumed I.D. (= 0) was tested. Taking I.D. = 0·06 a.m.u. Å^2 and assuming C(2),H(2) = C(2),H(3), model V was obtained (Table 3) which is in satisfactory agreement with models I–IV.

Acknowledgements—We are grateful to Dr. GOLDSTEIN and Dr. MORGAN, Oak Ridge, Tennessee, for permission to use some of their measurements, and to Dr. SELÉN, Stockholm for kind assistance with the measurements in the 33,000–41,000 MHz region.

References

[1] Cole A. R. H. and Thompson H. W., *Proc. Roy. Soc.* A 1951 **206** 17.
[2] Thompson H. W., *Trans. Faraday Soc.* 1939 **35** 697.
[3] Gallaway W. S. and Barker E. F., *J. Chem. Phys.* 1942 **10** 88.
[4] Bartell L. S. and Bonham R. A., *J. Chem. Phys.* 1957 **27** 1414.
[5] Bak B. and Christensen D., *Acta Chem. Scand.* 1958 **12** 1147.
[6] Bak B. and Christensen D., *Spectrochim. Acta* 1958 **12** 355.
[7] Bak B., Hansen L. and Rastrup-Andersen J., *J. Chem. Phys.* 1954 **22** 2013.
[8] Townes C. H. and Schawlow A. L., *Microwave Spectroscopy* p. 522. McGraw-Hill 1955.

VOL.
13
1958/5

Spectrochimica Acta, 1958, Vol. 13, pp. 125 to 138. Pergamon Press Ltd., London

The variation of infra-red vibration frequencies with solvent

A. D. E. Pullin
Chemistry Department, The Queen's University of Belfast

(*Received* 11 *July* 1958)

Abstract—The change of vibration frequency of a solute molecule with the nature of the solvent is considered from the standpoint of simple dielectric theory. The theory should apply as a limiting case to solutes in non-polar solvents where also specific solute–solvent interactions are absent. The theory suggests the following generalizations. For *non-polar* solutes the vibration frequency should always shift to lower frequencies with increasing dielectric constant of the solvent medium. The shift will be greater the greater the intensity of the band. For *polar* solutes several effects are superimposed and the vibration frequency may either decrease or increase with increasing dielectric constant of the solvent and this is irrespective of whether the transition moment of the band has a direction the same as, or different from, that of the permanent moment. Both static and high frequency dielectric constants of the solvent are involved for polar solutes, and for these, constants are required for evaluating the frequency shifts which are not usually available. Some experimental evidence is noted which suggests that the cavity radius present as an integral part of the theory in some cases may be determined by the solvent, rather than the solute, molecular volume. An immediate consequence of this is that the order of frequency shifts shown by a solute in a series of solvents may depend upon both the dielectric constants and the molecular volumes of the solvents. Though the theory cannot be expected to be quantitatively useful in cases where localized solvent–solute interaction is taking place, nevertheless many of the same factors should still be operative in these cases.

Introduction

The information that can be deduced from spectroscopic measurements concerning intramolecular forces is extremely detailed while that concerning intermolecular forces is at present comparatively meagre, though in the case of interaction between molecules via hydrogen bonds considerable information can be obtained from vibrational spectra. The infra-red and Raman spectra of liquids and solutions show however a number of features which, if examined carefully, should be capable of yielding useful information about interaction in solution. For infra-red spectra these features are: (a) the changes of frequency of the various bands in solution relative to the vapour phase; (b) the half-intensity band width; (c) the band shape, i.e. the existence of shoulders, general asymmetry, etc.; and (d) the variation in integrated extinction coefficient with varying solvent. Except where hydrogen bonding is present these effects are usually small and careful measurements are needed.

In general in all solutions the vibration frequency will differ from the vapour phase values because of the electrostatic interaction of the solute molecule with the solvent functioning as a continuous dielectric medium, although the frequency shift from this cause may be small compared with that arising from more specific interactions such as hydrogen bonding, dipole–dipole interactions, etc. However it is useful to consider the idealized case of the solvent functioning as a dielectric medium in some detail, first because this effect will always be present and may in

certain cases be an adequate approximation, and secondly because many of the consequences of the interaction found in the ideal case will, with modifications, apply to cases of more specific interaction and may indicate interpretations of frequency shifts occurring where quite specific interactions are present such as ion–dipole interactions [1].

This paper discusses the change of frequency of a solute band with the change of dielectric constant of the solvent, considered as a continuous dielectric medium: the effects of several approximations usually necessary in this type of treatment are considered. Basically, the treatment is the same as in the early paper on this subject by BAUER and MAGAT [2] though certain additional factors are taken into account and the treatment is later extended to include polyatomic molecules. The approximation used is that of a point dipole within, but not necessarily at the centre of, a spherical cavity in a continuous dielectric medium. The terms solute dipole and solvent refer, unless otherwise stated, to the point dipole and the continuous medium.

Frequency shifts in diatomic solutes

The vibrational frequency of a solute molecule in a dielectric is altered because of the interaction of the instantaneous molecular dipole with the surrounding dielectric. This interaction includes [3] the work required to polarize the dielectric, the energy of the interaction of the dipole with its own reaction field, and, since the molecule is polarizable, the work required to polarize it. It is shown (ref. [3], p. 134) that the work W required to bring a non-polarizable point dipole of moment μ from an infinite distance outside the dielectric to the centre of a spherical cavity inside the dielectric is given by:

$$W = -\tfrac{1}{2}\mu R \tag{1}$$

where R is the reaction field of the dipole. For this case of a point dipole at the centre of a spherical cavity of radius a the reaction field R is given by $f\mu$ where:

$$f = \frac{2\varepsilon - 2}{(2\varepsilon + 1)a^3} \tag{2}$$

ε being the dielectric constant of the medium. The vapour phase dipole moment μ of a diatomic solute molecule will be assumed to be given by:

$$\mu(x) = \mu_0 + M'x + M''x^2 \tag{3}$$

for small values of x, where x is the extension from the vapour phase equilibrium length. The vapour phase potential energy function for the molecule will be assumed to be:

$$V(x) = \tfrac{1}{2}kx^2 - bx^3 + cx^4 \tag{4}$$

Then in solution its potential energy $V_s = V + W$ will be given by:

$$V_s(x) = V(x) - \tfrac{1}{2}f\mu^2(x) \tag{5}$$

Expanding (5) one obtains:

$$V_s(x) = \tfrac{1}{2}kx^2 - bx^3 + cx^4 - \tfrac{1}{2}f\mu_0^2 - f\mu_0 M'x - \tfrac{1}{2}fM'^2x^2 - f\mu_0 M''x^2 - fM'M''x^3 - \tfrac{1}{2}fM''^2x^4 \tag{5a}$$

It is useful at this point to consider the effect of the terms in (5a) and their likely order of magnitude. Terms independent of x will not affect the vibration frequency. The term linear in x indicates that in solution the molecule will show a value of x different from zero, that is the molecule will be longer or shorter in solution. With sufficient accuracy this change of length will be determined by the quotient of the term $f\mu_0 M'x$ and the primary force constant k and the molecule will be longer or shorter in solution depending on whether or not μ_0 and M' have the same sign. At this new length in solution the value of d^2V/dx^2 is different from that at the vapour phase equilibrium length because of the mechanical anharmonicity of the molecule, so that the vibration frequency is changed. For most polar solutes this will be a significant effect. Also in equation (5a) there are two quadratic terms additional to the vapour phase quadratic term. The first, $-\frac{1}{2}fM'^2x^2$ must always cause a lowering of the vibration frequency and this effect is greater the greater the intensity of the band and the second, $-f\mu_0 M''x^2$ may operate either to raise or lower vibration frequencies. To exemplify these effects their magnitude for reasonable, arbitrary molecular constants may be calculated. Thus, for a hypothetical diatomic molecule for which the constants k, b and c of equation (4) are respectively 10^6 ergs-cm^{-2}, 10^{14} ergs-cm^{-3} and 10^{22} ergs-cm^{-4}, and the constants μ_0, M' and M'' of equation (3) are respectively $+3 \times 10^{-18}$ e.s.u.-cm, $+3 \times 10^{-10}$ e.s.u., and -3×10^{-2} e.s.u.-cm^{-1} and the solvent constant f defined by equation (2) is taken to be 2×10^{22} cm^{-3}, it is found that the additional terms in x^2 are of comparable importance, though of opposite sign and are of the order of one-thousandth of k, whilst the extra cubic and quartic terms are of the order of one-thousandth of b and c and are also of opposite sign. The effect of these additional cubic and quartic terms on vibration frequencies should always be very small and they will not be considered further. The term cx^4 in equation (4) will also be ignored in the subsequent development. Fig. 1 shows the shape of the potential function of this hypothetical molecule in the region of the potential minimum. The term $-\frac{1}{2}fM'^2x^2$ (curve c) when added to the vapour phase potential function decreases the curvature at the potential minimum and so decreases the vibration frequency, whilst in this example the term $-f\mu_0 M''x^2$ (curve d) increases the curvature and thus the frequency. As described above, the effect of the linear term (line b) is to give a slightly different equilibrium length and correspondingly, because of the anharmonicity, a slightly changed curvature. In the case being considered there is an increase in equilibrium length which can be calculated to be approximately 2×10^{-11} cm.

The above treatment assumes that the dielectric constant of the solution is the same for an oscillating as for a static electric field. This in general will not be so even for non-polar solvents, so that it is necessary to consider which values of the dielectric constant to use for the calculation of the f-factors for the various terms in equation (5a). The changed equilibrium length in solution arising from the linear term in equation (5a) is not time dependent and so the static dielectric constant must be used to calculate the f-value for this term. The f-term so calculated will be denoted by f_0 Let the dipole moment at the new equilibrium length in solution be μ, the reaction field R and the interaction energy W as in (1). Because of the vibrational motion, at any instant the dipole moment may have a value of

$\mu + \delta\mu$, the reaction field a value $R + \delta R$, and the interaction energy a value $W + \delta W$. The reaction field is not simply given by $f(\mu + \delta\mu)$ since the part $\delta\mu$ is oscillating with the frequency of the vibration (and more generally contains components oscillating at overtone frequencies of the vibration) so that the appropriate frequency dependent value of the dielectric constant has to be used.

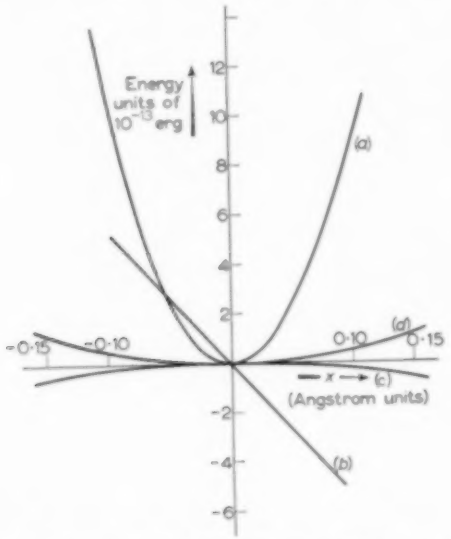

Fig. 1. Representation of (a) the potential energy curve of a hypothetical molecule in the vapour state and (b, c, and d) the additional energy terms in solution. The vertical scale of (b, c, and d) has been exaggerated thirty-fold. For the equations to curves and molecular constants employed, see text.

Further complications arise if the solvent is not transparent at these frequencies. If f_0 is the factor calculated using the static dielectric constant ε_0 and f_ν that using the value ε_ν for the frequency ν of the vibration, then the equation corresponding to (1) is:

$$\begin{aligned} W + \delta W &= -\tfrac{1}{2}(\mu_0 + \delta\mu)(f_0\mu_0 + f_\nu\delta\mu) \\ &= -\tfrac{1}{2}f_0\mu_0^2 - \tfrac{1}{2}(f_0 + f_\nu)\mu_0\delta\mu - \tfrac{1}{2}f_\nu\delta\mu^2 \end{aligned}$$

During the vibration the part of the change of dipole moment corresponding to the term $M'x$ in equation (3) gives rise to an oscillating moment of the frequency ν of the vibration so that the factor $\frac{1}{2}(f_0 + f_\nu)$ as derived above is involved: however, the part corresponding to the term $M''x^2$ of equation (3) gives rise to a changing moment at twice the frequency of the vibration (ref. [4], p. 241) so that the f-factor for the corresponding quadratic term in x in equation (5a) is similarly $\frac{1}{2}(f_0 + f_{2\nu})$. At this stage a further correction can be applied to correct for the non-centrality of the dipole in the cavity. This correction (ref. [3], p. 137) is fairly insensitive to the precise value of the dielectric constant. Values of f so corrected will be distinguished by primes.

As well as changes of internuclear distance in solution, the molecule will be polarized electronically, that is, at identical internuclear distances in the vapour

VOL. 13 1958/5

and solution phases the electron distribution will, in general, differ. It is necessary to consider the effect of this on vibration frequencies. BÖTTCHER (ref. [2], p. 138) derives the expression $-2f\mu^2/(1-f\alpha)$ for the interaction energy of a polarizable point dipole with the surrounding dielectric. By writing the dipole moment and energy explicitly as functions of x, as in equation (3) and (4) the atomic polarization has been taken into account so that, to allow for the increased interaction resulting from allowing electronic polarization equation (5) must be modified by writing:

$$V_s = V - \tfrac{1}{2}f\mu(x)^2/\{1 - f(\alpha_0 + \alpha' x)\} \tag{6}$$

where the required electronic polarizability α is assumed given by $\alpha = \alpha_0 + \alpha' x$. Equation (6) may be rewritten:

$$V_s = V - \phi(x)/\{1 - (A + Bx)\} \tag{6a}$$

so that, remembering that the term cx^4 of equation (4) is being neglected:

$$\frac{dV_s}{dx} = kx - 3bx^2 - \left[\frac{\phi'(x)}{1 - (A + Bx)} + \frac{B\phi(x)}{\{1 - (A + Bx)\}^2}\right] \tag{7}$$

where $\phi' = d\phi/dx$.

The change of equilibrium length x' in solution is then given by the appropriate solution of:

$$kx - 3bx^2 = \left[\frac{(\phi' x)}{1 - (A + Bx)} + \frac{B\phi(x)}{\{1 - (A + Bx)\}^2}\right] \tag{8}$$

and

$$\frac{d^2V_s}{dx^2} = k - 6bx - \left[\frac{\phi''(x)}{1 - (A + Bx)} + \frac{B\phi'(x)}{\{1 - (A + Bx)\}^2} + \frac{B\phi'(x)}{\{1 - (A + Bx)\}^2} + \frac{2B^2\phi(x)}{\{1 - (A + Bx)\}^3}\right] \tag{9}$$

The frequency of vibration in solution is determined by the value d^2V_s/dx^2 at the value x' of x given by equation (8), so substituting partially for x:

$$\frac{d^2V_s}{dx^2} = k - 6bx - \frac{\phi''(x)}{1 - (A + Bx)} - \frac{2B(kx - 3bx^2)}{1 - (A + Bx)} \tag{10}$$

Trial calculations show that most of the terms in equation (8) are quite unimportant in determining the equilibrium length in solution and that this is given with sufficient accuracy by:*

$$kx' = f_0'\mu_0 M'/\{1 - (A + Bx)\} \tag{11}$$

The value of d^2V_s/dx^2 at the new equilibrium length in solution can now be obtained by putting $x = x'$ in equation (10) and then substituting for x' from equation (11). At the same time the expression may be simplified without appreciable error by neglecting $3bx^2$ in comparison with kx and Bx in comparison with A.

The required value of d^2V_s/dx^2 is then given by:*

$$\frac{d^2V_s}{dx^2} = k - \frac{6f_0'b\mu_0M'}{k(1-A)} - \frac{2f_0'B\mu_0M'}{(1-A)} - \frac{f_r'M'^2}{(1-A)} - (f_0' + f_{2r}')\frac{\mu_0M''}{(1-A)} \quad (12)$$

or

$$\frac{d^2V_s}{dx^2} = k\left[1 - \frac{1}{k(1-A)}\left\{\frac{6f_0'b_0\mu M'}{k} + 2f_r'B\mu_0M' + f_r'M'^2 + (f_0' + f_{2r}')\mu_0M''\right\}\right] \quad (13)$$

which is of the form $k[1 - \Delta]$. Since the reduced mass of the molecule is the same in solution as in the vapour phase, the change in frequency is then given by:

$$\frac{\nu_{\text{vap.}} - \nu_{\text{soln.}}}{\nu_{\text{vap.}}} = \frac{\Delta\nu}{\nu} = \left\{\frac{k - k[1-\Delta]}{k}\right\}^{\frac{1}{2}} \simeq \Delta/2$$

or

$$\frac{\Delta\nu}{\nu} \simeq \frac{1}{k(1-A)}\left\{\frac{3f_0'b\mu_0M'}{k} + f_r'B\mu_0M' + \frac{f_r'M'^2}{2} + \tfrac{1}{2}(f_0' + f_{2r}')\mu_0M''\right\} \quad (14)$$

The first term in equations (14) involving the anharmonic potential constant b accounts for the change in vibration frequency resulting from the change of equilibrium length in solution as discussed above and the third and fourth terms in equation (14) correspond to the terms in (5a) also involving the products M'^2 and μ_0M''. If the factor $(1 - A)$ is omitted from equation (14) then the first and third terms are equivalent to the equation derived by Bauer and Magat [2] for $\Delta\nu/\nu$ and the third and fourth terms equivalent to the equation for $\Delta\nu/\nu$ employed by West and Edwards [5] and stated by them to have been derived by Kirkwood, though it appears that the moment of inertia I appearing in the numerator of their equation should be replaced by the reduced mass as otherwise their constant C is not dimensionless as it should be.†

The only new features in equation (14) not implicit in equations (5a) come from the inclusion in the derivation of equation (14) of the electronic part of the polarization of the molecule by its own reaction field. This gives rise to the overall multiplying factor $1/(1 - A)$ which allows for the increased values of the dipole moment in solution compared with the vapour phase values for the same bond lengths and also to the term $f'B\mu_0M'$ depending on α', the rate of change of the electronic polarizability of the molecule with bond length. Calculations show that this term will usually be unimportant. Frequently, in cases where this theory is applicable A $(= f'\alpha)$ will be small compared with unity (e.g. 0·05–0·2) so that in these cases it is unimportant whether f_0' or f_r' is used to calculate A, especially in view of the uncertainty in the choice of cavity radius: detailed and rather cumbrous calculations show that strictly the $1/(1 - A)$ factor should be calculated separately for each of the four terms, using in each case the same f' value as appears in the

* In this and in the following equations the appropriate f-value has been used, in accordance with the previous discussion.

† Alternatively, instead of the quantities $\partial\mu/\partial r$ and $\partial^2\mu/\partial r^2$ the quantities $\partial\mu/\partial\xi$ and $\partial^2\mu/\partial\xi^2$ could be used, where $\xi = (r - r_e)/r_e$, and I retained.

VOL. 13 1958/59

numerator. Similarly it is found that no one choice of f or f' is correct for calculating B; the best approximation is probably given by $B = f_v'\alpha'$, the error so introduced is negligible since the term involving B is always small.

All the parameters f' involve the cube of the radius a of the cavity so that the value of a assumed has a very large effect on the frequency shifts predicted. Some experiments suggest that this cavity radius is more correctly derived from the solvent than the solute molecular volume: this and similar points are discussed below after having generalized the previous type of treatment to include polyatomic solutes.

Frequency shifts in polyatomic solutes

The same treatment can be extended to polyatomic solutes. The potential energy of the molecule in the vapour phase ([4], p. 204) is given with sufficient accuracy for our purpose by:

$$V = \tfrac{1}{2}\sum_i \lambda_i \eta_i^2 + \sum_i \sum_j \sum_k \alpha_{ijk}\eta_i\eta_j\eta_k \tag{15}$$

where η are normal co-ordinates.

Since the potential function must have the symmetry of the molecule some of the cubic coefficients will be zero. The dipole moment of the molecule may be similarly expressed as:

$$\boldsymbol{\mu} = \boldsymbol{\mu}_0 + \sum_i \boldsymbol{M}_i'\eta_i + \sum_i \sum_j \boldsymbol{M}_{ij}''\eta_i\eta_j$$

where
$$\boldsymbol{M}'_i = \frac{\partial \boldsymbol{\mu}}{\partial \eta_i} \quad \text{and} \quad \boldsymbol{M}''_{ij} = \frac{\partial^2 \boldsymbol{\mu}}{\partial \eta_i \partial \eta_j} \tag{16}$$

As for the diatomic case, the equilibrium bond lengths in solution differ from those in the vapour phase, that is, in solution the molecule is distorted from the vapour phase equilibrium configuration. It follows from the assumptions of this treatment that the reaction field has the symmetry of the solute molecule so that the distortion in solution can be expressed in terms of the normal co-ordinates of the vibrations in A, the totally symmetric class of vibrations.

Thus, omitting cubic and fourth power contributions to V_s from the reaction field:

$$V_s = V - \frac{\frac{1}{2}f}{1 - f\alpha}\left(\boldsymbol{\mu}_0^2 + 2\boldsymbol{\mu}_0 \sum_A \boldsymbol{M}_i\eta_i + \sum_i \sum_j \boldsymbol{M}_i' \cdot \boldsymbol{M}_j'\eta_i\eta_j + 2\boldsymbol{\mu}_0 \cdot \sum_i \sum_j \boldsymbol{M}_{ij}''\eta_i\eta_j\right) \tag{17}$$

in which the double summation need only include products of terms of the same symmetry class. In the diatomic case writing $\alpha = \alpha_0 + \alpha' x$ resulted in a term ($f_v' B\boldsymbol{\mu}_0\boldsymbol{M}'$ in equation (14)) involving α' in the final expression for the frequency shift in solution. This term should always be small and considerable complexity is avoided in the polyatomic case by treating α as a constant. For compactness of expression the distinction between f_0 and f_v will be ignored and the factor $\frac{1}{2}f/(1 - f\alpha)$ rewritten $S/2$. In applications to specific cases the necessary changes resulting from using the appropriate f values can be made easily. With these

changes, the equation analogous to (7) becomes:

$$\frac{\partial V_s}{\partial \eta_r} = \lambda_r \eta_r + \sum_j \sum_k \alpha_{rjk} \eta_j \eta_k + \sum_i \sum_k \alpha_{irk} \eta_i \eta_k + \sum_i \sum_j \alpha_{ijr} \eta_i \eta_j - S \boldsymbol{\mu}_0 \cdot \boldsymbol{M}_r' - S \boldsymbol{M}_r' \cdot \sum_i \boldsymbol{M}_r' \eta_i - 2S \boldsymbol{\mu}_0 \cdot \sum_i \boldsymbol{M}_{ri}'' \eta_i \quad (18)$$

and

$$\frac{\partial^2 V_s}{\partial \eta_r^2} = \lambda_r + 2 \sum_k \alpha_{rrk} \eta_k + 2 \sum_i \alpha_{irr} \eta_i + 2 \sum_j \alpha_{rjr} \eta_j - S \boldsymbol{M}_r'^2 - 2S \boldsymbol{\mu}_0 \cdot \boldsymbol{M}_{rr}'' \quad (19)$$

Similar approximations may be made as in the diatomic case (cf. [11]) and the distortion in solution is then given with sufficient accuracy by the set of equations:

$$\eta_r = S \boldsymbol{\mu}_0 \cdot \boldsymbol{M}_r' / \lambda_r \quad (20)$$

η_r being normal co-ordinates belonging to the totally symmetric class, since there is no reduction of molecular symmetry.

Substituting equation (20) into equation (19) the value of $\partial^2 V_s / \partial \eta_r^2$ for the equilibrium configuration in solution is given by:

$$\frac{\partial^2 V_s}{\partial \eta_r^2} = \lambda_r + 2S \boldsymbol{\mu}_0 \cdot \sum_A \frac{\boldsymbol{M}_i'}{\lambda_i} (\alpha_{irr} + \alpha_{rir} + \alpha_{rri}) - S \boldsymbol{M}_r' - 2S \boldsymbol{\mu}_0 \cdot \boldsymbol{M}_{rr}'' \quad (21)$$

where i belongs to A, the totally symmetric class.

From equation (21) the fractional decrease of frequency for the change from vapour to solution phase is obtained by the same procedure as for the diatomic case (cf. equations (13) and (14)) and is:

$$\frac{\Delta \nu_r}{\nu_r} = \frac{S}{\lambda_r} \left(\frac{\boldsymbol{M}_r'^2}{2} - 3 \boldsymbol{\mu}_0 \cdot \sum_A \frac{\boldsymbol{M}_i'}{\lambda_i} \alpha_{irr} + \boldsymbol{\mu}_0 \cdot \boldsymbol{M}_{rr}'' \right) \quad (22)$$

Equation (22) may be checked by applying it to a diatomic molecule. For a diatomic molecule $\lambda_r = 4\pi^2 \nu_r^2 = k/m^*$ where m^* is the reduced mass, and $\eta_r = m^{*\frac{1}{2}} x$ so that equation (22) reduces as it should to equation (14), less the second term involving α', if S is appropriately interpreted.

Some simplifications of equation (22) may be possible in particular instances. As an example an XYZ_2 molecule of C_{2v} symmetry will be considered and this will be used as a basis for examining some frequency shifts of the skeletal modes of acetone. Using the designation of symmetry classes and normal modes given by HERZBERG ([4] pp. 65, 106) it is apparent from symmetry considerations that the only cubic coefficients which are non-zero are the α_{irr} where both i and r are of the A_1-class and α_{irr} where i is an A_1 mode and r is one of the B_1- or B_2-classes (there are no genuine vibrations in the A_2-class for this model). The physical interpretation of the contributions from the several terms involving α_{irr} is clear: since the cavity is assumed spherical and the dielectric medium is isotropic the distortion of the molecule in solution is totally symmetric so that it can be expressed as a linear combination of displacements in the totally symmetric normal modes, the degree of displacement in each of these being proportionately larger the larger the corresponding value of $\partial \boldsymbol{\mu} / \partial \eta$ and proportionately smaller the larger the restoring force called into play for a displacement in that mode.

VOL. 13 1958/5

In the case of acetone if a skeletal model is assumed to be adequate for a discussion of some of the vibrations considerable simplification results from the fact that the intensity of ν_2 (the "carbonyl stretching" vibration) has very much greater intensity than the other totally symmetric vibrations so that unless one of the other α_{irr} is unusually large, the relative decrease of frequencies $\Delta\nu_2/\nu_2$ of the A_1-class and (say) $\Delta\nu_4/\nu_4$ of the B_1-class are given by equations (23) and (24).

$$\frac{\Delta\nu_2}{\nu_2} \simeq \frac{S}{\lambda_2}\left(\frac{\boldsymbol{M}_2'^2}{2} - 3\boldsymbol{\mu}_0 \cdot \frac{\boldsymbol{M}_2'}{\lambda_2}\alpha_{222} + \boldsymbol{\mu}_0 \cdot \boldsymbol{M}_{22}''\right) \tag{23}$$

$$\frac{\Delta\nu_4}{\nu_4} \simeq \frac{S}{\lambda_4}\left(\frac{\boldsymbol{M}_4'^2}{2} - 3\boldsymbol{\mu}_0 \cdot \frac{\boldsymbol{M}_2'}{\lambda_2}\alpha_{244} + \boldsymbol{\mu}_0 \cdot \boldsymbol{M}_{44}''\right) \tag{24}$$

Physically it is clear that in the case of ν_4 the unharmonicity effect must operate through the cross term in the potential energy since $\boldsymbol{\mu}_0 \cdot \boldsymbol{M}_4 = 0$ from symmetry, and there are no terms in the potential function of odd powers of the displacement in a non-totally symmetric mode. As in all cases, there is a term in $\boldsymbol{M}'^2$ which can only operate to decrease frequencies with increasing dielectric constant.

Numerical calculations of frequency shifts

Unfortunately there are few molecules for which there are sufficient data to test either equations (14) or (22). Possible molecules are diatomic halides and pseudo-diatomic systems such as >NH and —OH groups, but there is much evidence that in many cases the hydrogen atom is subject to localized interaction with oxygen or nitrogen atoms, double bonds, etc., so that these do not provide a fair test of a theory derived for a solvent considered as a continuous dielectric medium. In the case of solutions of HCl calculations have been made by West and Edwards [5] using Kirkwood's equation which omits what proves to be the most important term in this case, namely the term depending on the anharmonicity (the first term in equation (14)). By using a large correction factor for the non-centrality of the point dipole in the cavity West and Edwards obtained reasonable concordance between their calculated and observed frequency shifts. Reasonable concordance with the observed frequency shifts for HCl between the vapour and solution phases in carbon tetrachloride and benzene have been reported by Galatry and Schuller [6] who used the Bauer–Magat theory [2] but inserted into it a more complicated expression for the reaction field. This work is referred to again later.

Calculations were carried out to find the relative contributions of the different terms in equation (14) for the decrease in frequency of HCl in passing from the vapour phase to a dilute solution in carbon tetrachloride. Constants used were: k, $5{\cdot}17 \cdot 10^5$ ergs-cm^{-2}; b, $4{\cdot}49 \cdot 10^{13}$ ergs-cm^{-3}; μ_0, $1{\cdot}092 \cdot 10^{-18}$ e.s.u.-cm; M', $0{\cdot}952 \cdot 10^{-10}$ e.s.u. [7]; M'', $-0{\cdot}275 \cdot 10^{-2}$ e.s.u.-cm^{-1} [7]; α, $2{\cdot}69 \times 10^{-24}$ cm^3 [8]; α', $1{\cdot}0 \cdot 10^{-16}$ cm^2 [8]. The cavity radius was assumed to be 1·70 Å and the centre of the point dipole was arbitrarily taken as four-tenths along the radius from the centre of the cavity. The static dielectric constant of carbon tetrachloride ($\varepsilon = 2{\cdot}234$) was used throughout. As a result of the small size of the cavity and the appreciable correction to f arising from the assumed non-centrality of the point dipole ($f' = 1{\cdot}85\,f$) the factor $1/(1 - A)$ is large (1·84) and the B term appreciable.

With these values the contributions in order to $10^2\Delta\nu/\nu$ from the four terms in equation (14) are 1·64, 0·12, 0·28 and −0·18 giving the result $\Delta\nu/\nu = 1{\cdot}86 \cdot 10^{-2}$, almost identical with the observed fractional decrease. The agreement is probably largely fortuitous. The cavity radius chosen is rather small and could reasonably be taken as large as 2·0 Å, which would decrease $\Delta\nu/\nu$ to about 60 per cent of that calculated, also the correction for non-centrality of the assumed point dipole is problematical: placing the point dipole two-tenths of the way along the cavity radius would make $f' = 1{\cdot}16\,f$ which would also decrease the value of $\Delta\nu/\nu$ to about 60 per cent of that calculated.

A large amount of data is required to test the applicability of equation (22) to frequency shifts of polyatomic molecules. The simplified equations (23) and (24) should apply to the skeletal modes of acetone but there is not sufficient known of the constants for acetone to test these equations quantitatively, since in particular the values of M_{22}'' and M_{44}'' are not known. If the very drastic assumption that ν_2 can be treated as the vibration of a diatomic molecule is made then equation (14) can be applied and the contribution of the first three terms calculated. Calculations were made on this basis, using a reduced mass of $11{\cdot}38 \cdot 10^{-24}$ g, equal to that of the carbonyl group combined with potential constants derived from the Morse potential function for this reduced mass and $\omega_e = 1756\ \text{cm}^{-1}$, $x_e\omega_e = 9\ \text{cm}^{-1}$. These constants were k, $12{\cdot}45 \cdot 10^5$ ergs-cm^{-2}; b, $11{\cdot}90 \cdot 10^{13}$ ergs-cm^{-3}; and c, $1{\cdot}33 \cdot 10^{22}$ ergs-cm^{-4}. Other constants used were: μ_0, $1{\cdot}76 \cdot 10^{-18}$ e.s.u.-cm; M', $4{\cdot}26 \cdot 10^{-10}$ e.s.u. calculated from a molar integrated intensity value $\int\varepsilon\,d\nu = 5000$ mole^{-1} l.-cm^{-1} (cf. solution values of $\int\varepsilon\,d\nu$ for the carbonyl vibration of acetone [9]; α, $7{\cdot}0 \cdot 10^{-24}$ cm^3; α', $2{\cdot}6 \cdot 10^{-16}$ cm^2 [10]. The point dipole was assumed to be one-quarter of the way along the radius of the cavity from the centre, which corresponds approximately to midway along the carbonyl bond. This gives $f' = 1{\cdot}27\,f$. Solvent dielectric constants were either as used previously by ARCHIBALD and PULLIN [11] or from standard sources. The cavity radius was determined from a relation of the type $\frac{4}{3}\pi a^3 = V/N$ but three different ways were used to obtain V. These were:

(a) V equal to the molecular volume of acetone;

(b) V equal to the mean molecular volume of acetone and the solvent;

(c) V equal to the molecular volume of the solvent.

Molecular volumes at 25°C were used. CS_2 has a molecular volume of 60·2 cm^3 at 25°C compared with 73·4 cm^3 for acetone. If the solvent plays a part in determining the cavity size then it could be argued that in CS_2 solutions more than one CS_2 molecule would have to be displaced to make room for an acetone molecule, so that twice the molecular volume of CS_2 should be taken. Calculations were made using both the molecular volume and twice the molecular volume of CS_2.

The results of the calculations, for the three ways of choosing V and the two choices for CS_2 are given in Table 1. The relative contributions of the three terms in equation (14) to the frequency shifts are not detailed since they vary only slightly with solvent. In all cases the first term depending on the mechanical anharmonicity was found to be responsible for 69–75 per cent of the frequency shift from the vapour phase, the B term for 0·6–1·4 per cent and the third term necessarily for the remainder. It is seen from Table 1 that the calculated frequency

VOL. 13 1958/5

shifts are only one-third to one-half the observed shifts. This disagreement could arise from a number of causes such as the neglect of the fourth term in equation (14), the several approximations introduced in treating ν_2 as the vibration of a diatomic molecule or from the approximations of basing the calculation on the idealizations of a point dipole and its derivatives.* It is also probable that other than dipole–dipole forces may make an appreciable contribution to the frequency shift since

Table 1. Lowering of frequency of carbonyl vibration of acetone by various solvents: calculated and observed values

Solvent	$\Delta\nu$ (cm^{-1}) Frequency decrease from vapour phase			
	(a)	(b)	(c)	Observed
n-Hexane	8·0	5·5	4·2	14
*cyclo*Hexane	8·7	7·2	6·1	14·5
Decalin	9·8	6·0	4·2	15
Tetrachloroethylene	10·2	8·3	7·0	17·5
Carbon tetrachloride	9·6	8·1	7·0	18·5
Carbon disulphide I	11·1	12·3	14·1	20·0
Carbon disulphide II*		8·2	6·5	
Benzene	9·7	8·7	7·7	20·5
Dioxane	9·5	8·7	8·0	22·5

* Twice the molecular volume of CS_2 used.

liquid H_2 shows a ν_0 value 10 cm^{-1} lower than the vapour [12]. If attention is directed in Table 1 to the relative $\Delta\nu$ values for the different solvents then it seems that best agreement is obtained using a cavity radius determined by the solvent though in the previously discussed case of HCl this procedure would result in a much too small predicted frequency shift. There is independent experimental support for the procedure of calculating the cavity size from the molecular volume of the solvent. POWLING and BERNSTEIN measured the solvent dependence of the equilibrium between *gauche* and *trans* forms of substituted ethanes [13] and of tautomeric equilibria [14]. They found that agreement between the observed dependence of the equilibrium position with solvent with that predicted by the same basic dielectric theory embodied in equations (1) and (2) of this paper could only be obtained if the solvent molecular volume was used to calculate the cavity radius. There is no indication, however, in the data reproduced [13] that the molecular volume used for CS_2 should be other than the normal value.

It was noted above that for a molecule possessing a permanent dipole moment the frequency shifts can be in either direction. Acetone is such a case. A series of solvents arranged to give a decreasing value of the ν_2 vibration of acetone is also the order of increasing ν_4 [1]. This could arise from a positive value of α_{244} in

* The approximation of a point dipole is inherent in the quantities $\boldsymbol{M}'$ and $\boldsymbol{M}''$ as well as μ_0, and may well be a good approximation for (say) μ_0 and a bad approximation for (say) $\boldsymbol{M}'$.

equation (24) ($\Delta\nu$ has been defined as $\nu_{gas}-\nu_{sol.}$). A positive value of α_{244} results in the restoring forces resisting displacement in the mode ν_4 being greater if the molecule is simultaneously displaced in the mode ν_2 (cf. equations (15) and (19)). Consistent with this is the supposition [1] that the C—C bonds in acetone acquire some double bond character as the carbonyl bond is elongated.

Discussion

The points discussed below concern firstly the approximations made in the above treatment and their bearing on the interpretation of observed frequency shifts and secondly some consequences of the change of equilibrium configuration of molecules on solution.

Many of the approximations stemming from the idealized model assumed are sufficiently obvious; clearly errors are introduced by assuming a continuous dielectric medium, a spherical cavity, a point dipole and dipole moment derivatives. One approximation has not been mentioned, it is that in the treatment of polyatomic molecules it was tacitly assumed that the geometrical form of the normal modes remained unaltered from vapour to solution phase. This will not be exactly true as some bonds will be weakened more than others in solution, depending on the products $\boldsymbol{\mu}_0 \cdot \boldsymbol{M}'$ and the anharmonic terms of the potential function. Probably the effect of this on the frequency shifts is quite unimportant compared with the other approximations made, at least for vibrations differing considerably in frequency from other vibrations of the molecule.

VOL. 13 1958/5

It has been noted that there is some evidence that the use of the solvent molecular volume to define the radius of the cavity gives better correlation with the order of observed frequency shifts for different solvents, than the use of the solute molecular volume. In view of the idealized character of the model used it is probably not justifiable to infer therefrom that the solute molecules actually occupy cavities roughly determined in size by the size of the solvent molecules. It has been noted [11] that a number of ketones and secondary amides show the same solvent order for increasing $\Delta\nu$ values as acetone though these compounds vary in size from acetaldehyde to diphenylacetamide and would require cavities one-half to three times the volume of the solvent molecules. It does not appear possible to explain the apparent dependence of the cavity size on the solvent molecular volume by employing the expression for the reaction field of a dipole recently derived by Galatry and Schuller [6]. By dropping the assumption of the continuity of the dielectric they obtain in addition to the term for the reaction field used in this paper an extra term. The contribution of this extra term to the reaction field is directly proportional to the solvent molecular volume rather than inversely proportional as would be required to explain the results quoted above.

The change of equilibrium configuration of the molecule on solution is given by equation (11) for diatomic molecules and by equation (20) for polyatomic molecules. Unless the value of $\partial^2\boldsymbol{\mu}/\partial x^2$ (or values of $\partial^2\boldsymbol{\mu}/\partial\eta_l^2$ for polyatomic molecules) are zero the change of equilibrium configuration contributes to the change of band intensity on solution. It is easily shown that, for diatomic molecules, the fractional change of intensity from this cause is given by $(4f\boldsymbol{\mu}_0 \cdot \boldsymbol{M}'')/k$. This factor will generally be

very small. Thus for the hypothetical situation considered previously (p. 127) the fractional increase of intensity resulting from the process of solution is −0·7 per cent. However this same mechanism will also be operative in cases of local interaction that could cause larger changes of bond lengths.

It has been noted that about 70 per cent of the calculated decrease of the frequency of ν_2 of acetone on solution arises from the first term in equation (14): that is, it is due to the changed value of the effective force constant consequent on the change of bond length on solution. It is of interest to see whether the change of carbonyl frequency between one compound and another can also be interpreted in similar terms. From equation (4) one obtains:

$$\frac{d^2V}{dx^2} = k - 6bx + 12cx^2$$

or

$$k' = k - 6bx + 12cx^2$$

where k' is the effective force constant at the new bond length in solution. Using the same potential constants as previously for the carbonyl bond of acetone it is found that an increase of $0{\cdot}02_1$ Å in the bond length would decrease k' from $12{\cdot}45 \cdot 10^5$ ergs-cm^{-2} to $11{\cdot}0 \cdot 10^5$ ergs-cm^{-2}, that is sufficiently to decrease the carbonyl frequency by about 100 cm^{-1}. This relation between bond length and frequency is similar to that found by Layton, Kross and Fassel [15]. These authors plotted the stretching frequencies attributable to C—O bonds against the corresponding bond lengths and found that the points, though quite widely scattered, lay near a smooth curve. In the region 1600–1700 cm^{-1} this curve has a slope of approximately −100 cm^{-1}/$0{\cdot}02_7$ Å. That the bond length–frequency relations should be similar is not surprising since the process of solution is in some respects similar to the process of substitution, particularly in molecules RY, where Y is a group having a characteristic frequency and a high group dipole moment and the size or polarizability of the residue R can be increased by substitution. In this case when the polarizability of R is increased by substitution the moment induced in R by Y is increased and Y in turn can take up a more polar configuration by virtue of the increased reaction field emanating from R, in the same way that the reaction field in solution enables the molecule to assume a more polar configuration.

Finally it may be useful to stress that the above treatment is concerned only with dipole-induced dipole forces and takes no cognisance of Van der Waals forces. It is also limited in application to non-polar solvents and assumes that polarization is proportional to field strength. Being a general treatment it necessarily ignores special effects such as, for instance, the possibility [16] that in some highly flexible molecules, the paraffin chain may coil back around the polar group when the molecule is removed from solution, so tending to maintain the solvated state of the polar group in the vapour phase.

References

[1] Pullin A. D. E. and Pollock J. M., *Trans. Faraday Soc.* 1958 **54** 11.
[2] Bauer E. and Magat M., *J. de Physique* 1938 (VII) **9** 329.
[3] Böttcher C. J. F., *Theory of Electric Polarisation* Sections 24 and 25. Elsevier Publishing Co., Amsterdam, Houston, London and New York 1952.

[4] HERZBERG G., *Infrared and Raman Spectra*. Van Nostrand, New York 1945.
[5] WEST W. and EDWARDS R. T., *J. Chem. Phys.* 1937 **5** 14.
[6] GALATRY L. and SCHULLER F. G., *C. R. Acad. Sci., Paris* 1957 **244** 1749.
[7] LEGAY F., *C. R. Acad. Sci., Paris* 1956 **242** 1593.
[8] STANSBURY E. J., CRAWFORD M. F. and WELSH H. L., *Canad. J. Phys.* 1953 **31** 960.
[9] BAYLISS N. S., COLE A. R. H. and LITTLE L. H., *Austr. J. Chem.* 1955 **8** 26.
[10] SHORYGIN P. P., *Uspekhi Khimii* 1950 **19** 419 (National Research Council of Canada Technical translation TT-228).
[11] ARCHIBALD L. B. and PULLIN A. D. E., *Spectrochim. Acta* 1958 **12** 34.
[12] ALLIN E. J., FELDMAN T. and WELSH H. L., *J. Chem. Phys.* 1956 **24** 1116.
[13] POWLING J. and BERNSTEIN H. J., *J. Amer. Chem. Soc.* 1951 **73** 1815.
[14] POWLING J. and BERNSTEIN H. J., *J. Amer. Chem. Soc.* 1951 **73** 4353.
[15] LAYTON E. M., JR., KROSS R. D. and FASSEL V. A., *J. Chem. Phys.* 1957 **25** 135.
[16] LASCOMBE J., GRANGES P. and JOSIEN M-L., *Bull. Soc. Chim. France* 1957 773.

Note added in proof

THE author is grateful to Dr. Jaffe and Dr. Oppenheim for drawing his attention to their recent determination of several refractive indices in the 1–6 μ region. (JAFFE J. H. and OPPENHEIM U., *J. Opt. Soc. Amer.* 1957 **47** 782.) Use of their refractive index values for *cyclo*hexane, tetrachloroethylene and benzene does not significantly affect the results obtained except for benzene solutions for which the calculated $\Delta\nu$ values given in Table 1 are all increased by 0·2 cm^{-1}.

VOL. 13 1958/5

Spectrochimica Acta, 1958, Vol. 13, pp. 139 to 149. Pergamon Press Ltd., London

Quantitative analysis, by a spectrographic method, of the isotopic composition of hydrogen, deuterium and tritium mixtures*

M. N. Oganov and A. R. Striganov
Translated by L. Bovey

Abstract—Detailed investigations of calibration graphs for spectroscopic sources excited by a 10 Mc/s electrodeless discharge in the concentration range from 0·7 to 97 per cent H_2 in D_2 were made. The results agreed well with theory. The possibility of tritium analysis in a H_2 and D_2 mixture is pointed out. The effect of pressure in the discharge tube on the relative line intensities was investigated.

Introduction

Attempts to use spectroscopic methods in the analysis of hydrogen isotopes have been made several times. However it was only in 1952 that a thorough investigation of the problem was made. Broida *et al.* [1] developed a photoelectric method to analyse spectroscopically hydrogen and deuterium mixtures in the 85–99 per cent deuterium range.† Also at this time, Veinberg *et al.* [3] and ourselves had independently developed a photographic method applicable over a wider range. Our investigations were carried out on hydrogen and deuterium but tritium analysis was also attempted.

1. Experimental details

An auto-collimating three prism glass spectrograph ISP-51 with a camera lens of focal length 1300 mm was used. The dispersion in the 6500 Å region was 9·5 Å/mm and was fully adequate to resolve the H_α and D_α lines. It was not sufficient to resolve D_α from T_α but the possibility of tritium analysis could still be studied with this spectrograph. A platinized three-step filter was used so that lines of markedly different intensities could be compared. This had transmission of 100, 46·2 and 11·8 per cent in the 6500 Å region (these steps are subsequently designated as 1, 2 and 3). In some cases an additional gelatine filter was put over one of the lines in front of the plate. This gave 25·8 per cent transmission.

A quartz tube with a capillary 1–1·5 mm diameter and 50 mm long was the light source. The light was excited by an electrodeless discharge from an oscillator with power 800 W and frequency 10 Mc/s. A 400 mA current maintained the discharge. A variable condenser was used to match the circuit and oscillator.

The standard hydrogen and deuterium mixtures were prepared in a special vacuum apparatus based on the principle of partial pressure at constant volume. The arrangement is shown in Fig. 1.

* This communication appeared in Russian in *Atomnaya Energiya* 1957 **2**, 112–119, and was translated for publication in English because of its special interest to spectroscopists.

† This work is fully discussed in the review by Striganov [2].

2. Sample preparation

The deuterium was led into the storage vessel [(8) in Fig. 1]. After this it was passed through two liquid air traps and the palladium tube into the evacuated vessel (1), where its pressure was measured on the manometer (2).

The hydrogen passed from the cylinder (9) through the liquid nitrogen trap and the palladium tube as far as the stop-cock k_1; its pressure was measured on manometer (5). Hydrogen was added to the mixture in small amounts until the necessary pressure was reached. After a 10 hr

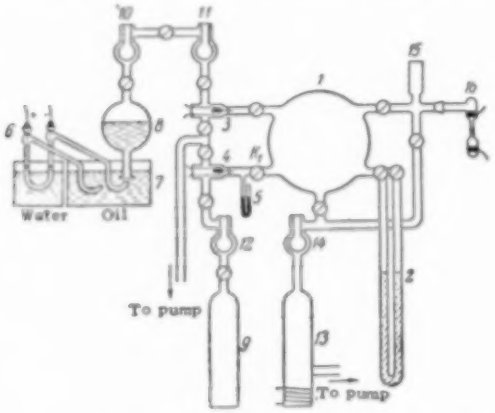

Fig. 1. Vacuum apparatus used in the preparation of the standard mixtures.
(1) vessel; (2) large oil U-tube manometer; (3, 4) two palladium tubes for hydrogen and deuterium purification; (5) mercury U-tube manometer to measure hydrogen pressure; (6, 7, 8) electrolysis apparatus for deuterium preparation from heavy water; (9) gas cylinder containing ordinary hydrogen; (10, 11, 12) liquid nitrogen traps to retain water vapour; (13) diffusion pump; (14) liquid air trap; (15) thermocouple pressure gauge; (16) quartz discharge tube.

interval for thorough mixing, the mixture was lead into the discharge tube. The accurate preparation of standards by this method depends on both the purity of the initial gases and the exact pressure measurement in the mixing vessel.

The deuterium was prepared from heavy water with 99·5 per cent D_2O content. About 8 cm^3 of a 10 per cent alkaline solution of heavy water (LiOD) were placed in the U-shaped electrolyser, which was cooled by water. It had been shown by a spectroscopic method that the isotopic content of both the alkaline solution and the heavy water was the same. The vessel (7) and the gas container (8) were filled by a vacuum type oil. Water vapour was removed from the gases by the liquid air traps; this removal took less than 20 min. The palladium tube gave a means of purification from other gases.

Pressure in the mixing vessel was measured on a 1000 mm long oil manometer with a cathetometer and a vernier attachment. This allowed measurement to 0·1 mm accuracy. Special tests showed that the oil did not affect the isotopic composition in the sample. Since the standard samples depend on the partial pressures of hydrogen and deuterium (P_H and P_D) one can express the atomic concentration in the following manner:

$$C_H = \frac{P_H}{P_H + P_D} \times 100 \tag{1}$$

The relative error in preparation will be given by:

$$\frac{\Delta C_H}{C_H} = \frac{\Delta P_H}{P_H} + \frac{\Delta P_H + \Delta P_D}{P_H + P_D} \tag{2}$$

VOL. 13 1958/5

Because the pressure is measured on the same manometer $\Delta P_H = \Delta P_D$ and therefore

$$\frac{\Delta C_H}{C_H} = \frac{\Delta P_H}{P_H} + \frac{2\Delta P_H}{P_H + P_D} \tag{3}$$

With small concentrations (up to 10 per cent) and $P_H \ll P_D$

$$\frac{\Delta C_H}{C_H} \sim \frac{\Delta P_H}{P_H} \tag{4}$$

and in the middle of the average concentrations (10–90 per cent) with $P_H \sim P_D$

$$\frac{\Delta C_H}{C_H} \sim \frac{2\Delta P_H}{P_H} \tag{5}$$

It therefore follows that in the sample preparation with low hydrogen concentration, the relative error $\Delta P_H/P_H$ in the pressure measurement must not exceed the fixed relative error in the standard $\Delta C_H/C_H$ and in the case of average concentrations must be half as big.

Since the absolute measurement error is now given, the lowest pressure which can be used to reach the required accuracy can be calculated. From equations (4) and (5) it follows that at small concentrations:

$$P_H = \frac{\Delta P_H}{\Delta C_H/C_H} \tag{6}$$

and at average concentrations:

$$P_H = \frac{2\Delta P_H}{\Delta C_H/C_H} \tag{7}$$

From equation (1) the other component can be calculated:

$$P_D = \frac{100 - C_H}{C_H} P_H \tag{8}$$

In the calculation of standards it is necessary to take into consideration the accuracy requirement in relation to concentrations (see Table 1).

It must be noted that the calculated data to give the composition of the gas mixture standards are only approximate guides because it is not possible to control the hydrogen and deuterium flow into the vessel accurately enough. Therefore the percentage composition in the standard follows equation (1) based on H_2 and D_2 pressures obtained practically.

The arrangement gives the possibility of using considerably higher pressures which correspondingly increases the accuracy in the standards preparations. There is a reduced error from gas absorption on the glass walls when standards are made up at higher pressures.

Table 1.

Concentration H_2, %	1	5	10	20	30	50	70	80
Maximum error in composition $\frac{\Delta C_H}{C_H}$, %	2	1	0·5	0·4	0·3	0·2	0·1	0·1

3. Choice of spectral line

The line H_α in the Balmer series seems the most suitable. It is ten times more intense than H_γ and, unlike H_β, occurs in a region free from molecular bands. There is the disadvantage that the line occurs in the red region where the dispersion of the instrument is small.

In Fig. 2 are shown microphotometer traces of a photographic plate taken on the ISP-51 spectrograph. A sample containing the three hydrogen isotopes was examined. It is seen that H_α and D_α are completely resolved but that there is partial overlap between D_α and T_α.

An instrument with higher dispersion (approximately 5 Å/mm) was preferred for the analysis of $D_2 + T_2$ mixtures. As an example of resolution with a 2·8 Å/mm, in Fig. 3 is given the microphotometer record of the mixture and this shows the complete isotopic line resolution.

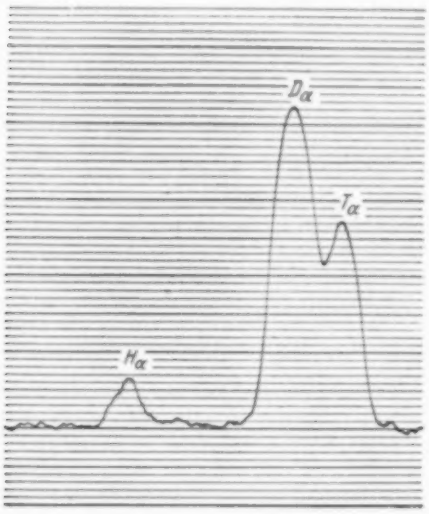

Fig. 2. Microphotometer trace of the H_α line in a three-component mixture.

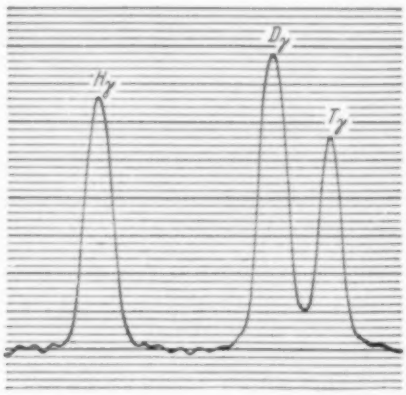

Fig. 3. Microphotometer trace of the H_γ line in the three-component mixture.

VOL. 13 1958/5

4. Spectra recording and plate calibration

The discharge tube was thoroughly outgassed by heating under vacuum. After this it was flushed out several times with the mixture under investigation and a conditioning discharge run five times for 30 min each time. In Fig. 4 the effect of the conditioning discharge is shown.

The discharge tube was filled with the gas mixture at 0·4 mm (Hg) pressure. In the case of the standards, the spectra from five gas fillings were photographed. Three fillings were used for the sample under investigation. The discharge tube was cooled by an air jet. The spectra were recorded on panchromatic plates using exposures of 3 sec in the central range, 20–80 per cent, and up to 6 sec for other concentrations (1–20 per cent and 80–95 per cent).

The ratio $\log I_H/I_D$ was determined by means of the step filter. Steps 1/1, 1/3 and 3/1 were used for the central, low and high concentrations respectively. From the relationship:

$$\log I_H/I_D = (W_H - W_D)/\gamma_w \qquad (9)$$

the ratio is found where W_H and W_D are the respective H_α and D_α line densities obtained from the microphotometer records. The contrast factor γ_w was determined

from the photometer records of lines photographed with 1/2 and 2/3 stepped filters.

5. Calibration graphs

In Fig. 5 are shown the calibration graphs based on twenty standard $H_2 + D_2$ mixtures and divided into four groups corresponding to the concentration ranges. $\log I_H/I_D$ is plotted against $\log C_H/C_D$. For conversion from the reduced ratio

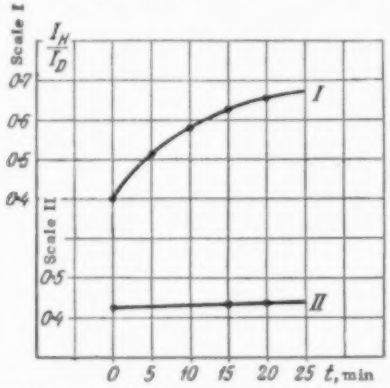

Fig. 4. The effect of conditioning a discharge tube. I. Relative intensity change in the case of an unconditioned tube. II. The change in a conditioned tube.

C_H/C_D to the usual atomic concentration C_H one can use either the auxiliary C_H percentage scale on the ordinate axis or develop separate tables. The conversion is given by:

$$C_H = \frac{C_H/C_D}{1 + C_H/C_D} \times 100 \tag{10}$$

Curve I shows the lowest hydrogen concentrations (0·7–3·5 per cent) obtained with the 1/1 step filter and the additional filter (with 25·8 per cent transmission) on the deuterium line. Curves II, III and IV correspond to concentrations 3·5–25 per cent, 25–75 per cent and 75–97 per cent and were obtained with filters 1/3, 1/1 and 3/1 respectively.

If the last three graphs are superimposed then it is found that for the 5–95 per cent hydrogen concentration they can be represented by a straight line passing at 44·6° to the ordinate axis, curved at both ends and cutting the abscissa at a point given by $\log I_H/I_D = -0{\cdot}055$. This displacement shows that when $C_H = C_D = 50$ per cent, the intensities of the hydrogen and deuterium lines are not equal. With an equal number of H_2 and D_2 molecules in the discharge tube the ratio of the hydrogen and deuterium line intensities is 0·88. From this figure it is seen that the intensities become equal when the number of hydrogen molecules in the mixture is 1·13 times that of deuterium.

The apparent reasons for the discrepancy are the different Doppler widths of the lines and the different molecular dissociation energies (4·47 and 4·53 eV respectively, for H_2 and D_2). Actually the relative intensities of the H and D lines is given by:

$$\frac{I_H}{I_D} = \frac{\alpha_H}{\alpha_D}\frac{C_H}{C_D}\sqrt{\left(\frac{A_H}{A_D}\right)} \tag{11}$$

where α_H, α_D are proportionality constants, determined by the isotopes' physical properties; $\sqrt{(A_H/A_D)}$ represents the Doppler correction factor.

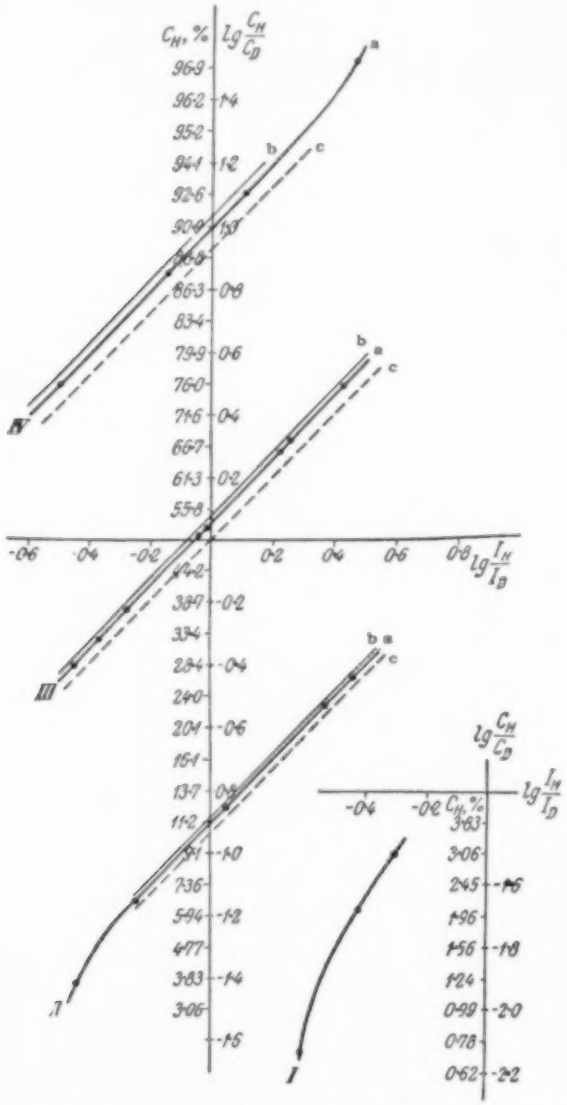

Fig. 5. Calibration graphs. (a) Experimental graph used to determine H_2 in D_2. (b) Auxiliary graph used to determine H_2 in T_2. (c) Graph corresponding to the relation $I_H/I_D = C_H/C_D$.

In the hydrogen and deuterium case $\sqrt{(A_H/A_D)} = 0{\cdot}71$. It therefore follows that the Doppler effect will decrease the normal intensity ratio by 0·71. The ratio α_H/α_D can be calculated from the difference in dissociation energies. Since the

hydrogen dissociation energy is less there will be more dissociated molecules in the tube. The number of dissociated molecules is given by

$$N = N_0 \exp(-E/kT) \tag{12}$$

where N_0 is the total number of molecules,
E is the dissociation energy,
k is the Boltzmann constant,
T is the absolute temperature.

From this

$$\alpha_H/\alpha_D \sim \exp(E_H - E_D)/kT \tag{13}$$

where E_H and E_D are the hydrogen and deuterium dissociation energies. If the temperature is assumed to be 2500°K then $\alpha_H/\alpha_D = 1{\cdot}30$. This shows that the normal intensity ratio should be increased by 1·30. Both effects give a factor $0{\cdot}71 \times 1{\cdot}30 = 0{\cdot}92$. This value is greater than that found experimentally (0·88). These correction factors are only of a general nature but a full calculation would be difficult.

All the points noted here about the form of the calibration graphs completely confirm the relationship obtained theoretically between the relative line intensity and concentration [5]. The departure of the straight line calibration graph from 45° and likewise the curving at the ends are explained by a small background effect in the spectra.

6. Pressure effect

During the work it was noticed that I_H/I_D changed according to the gas pressure in the tube. In Fig. 6 are shown the change in the ratios for different concentrations with different gas pressures. The results show that whilst with concentrations around 10·2 per cent the intensity ratio remains roughly constant above and below, it increases with higher pressure. It was shown by Broida *et al.* that for pressures below 0·4 mm the increase was approximately inversely proportional to the pressure; with higher pressures, as in our case the relationship is linear. From recent results it seems that the D_α absolute line intensity decreases more quickly in comparison to the H_α line with increase in pressure.

A full theoretical treatment of the relation between the ratio I_H/I_D and the pressure has not been possible so far. Broida *et al.* pointed out that a basic factor influencing the ratio was the fractionation in the gas flow through the capillary tubes of the system. However in our arrangement there are no capillaries and therefore this fractionation cannot influence the gas composition of the mixture in the closed tube.

It seems that both Doppler width and differences in dissociation energies play their part here. It is obvious that increased pressure decreases the kinetic energy of the molecules and lowers the temperature in the discharge canal. The Doppler width correction remains constant because the ratio does not depend on temperature. In contrast to this the error depending on the dissociation energy difference will increase with decreasing temperature because of the relationship given in equation (13). From the combined effect it can be seen that the intensity ratio will increase with increased pressure. Since these effects act on the intensity ratio in different ways, for some pressure they will compensate each other. In this case the ratio will equal that obtained by neglect of these factors (i.e. at a 50·8 per cent concentration and 1·6 mm pressure it can be seen in Fig. 6 that $I_H/I_D = 1$).

It is probable that other factors exist which compensate the different dissociation energies. For example at 10 per cent concentration the ratio does not change appreciably with pressure.

From the practical point of view the variation of the ratio with pressure means that in the analysis the pressure must be maintained constant.

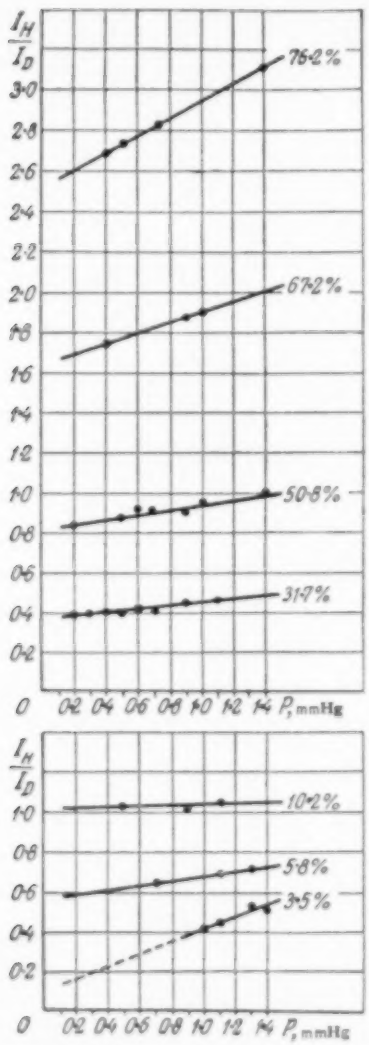

Fig. 6. The relationship between relative intensity and pressure.

7. Analysis of two and three component samples

The apparatus shown in Fig. 7 was used in the analyses. It consists of a quartz tube (1), an oil manometer (2) for pressure measurement, a flask (3) with tap, a tube with two-way taps (4), a thermocouple pressure gauge (5) and liquid nitrogen trap (6). The discharge tube had the same size as that used in the standardizing method. The gas under investigation in the flask was passed to the tube through two- or three-way taps. After a thorough outgassing and conditioning of the system (see Section 4) the gas was passed in small amounts to the discharge tube at 0·4 mm pressure and the spectrum was photographed.

For the analysis the calibration graphs were used. Those for the mixture $H_2 + D_2$ are shown in Fig. 5. As already pointed out, the graph is displaced relative to the orign by an amount $\log I_H/I_D = -0{\cdot}055$. Based on this in the determination of both H_2 and T_2 and D_2 and T_2 mixtures calibration graphs were used in which the displacement $\log I_H/I_D$ corresponded to the different mass numbers. The respective displacements were $-0{\cdot}08$ and $-0{\cdot}04$.

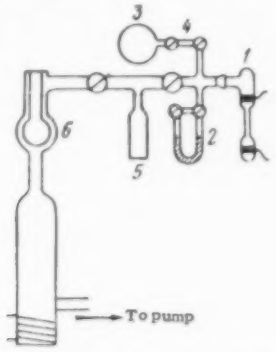

Fig. 7. Diagram of apparatus used to analyse the isotopic composition in the H_2, D_2 and T_2 mixture.

The spectrographic method allows the quick determination of the reduced relative concentrations which by equation (10) can be transformed into percentage composition relative to the sum of the two isotopes. However the expression to give the concentration relative to the sum of the three components has not yet been derived. Below it is shown how from the reduced relative concentrations, the percentage composition relative to the three components may be found.

If the partial pressure of each isotope be denoted by P_H, P_D and P_T then the reduced relative intensity will be expressed as:

$$C'_H = P_H/P_D \quad \text{and} \quad C''_H = P_H/P_T \tag{14}$$

The concentrations, relating to the sum of three components will be given by

$$C_H = \frac{P_H \times 100}{P_H + P_D + P_T}$$

$$C_D = \frac{P_D \times 100}{P_H + P_D + P_T} \tag{15}$$

and

$$C_T = \frac{P_T \times 100}{P_H + P_D + P_T}$$

The relationship between the reduced concentration C'_H, $C''_H$and the concentrations C_H, C_D and C_T relating to the sum of three components have the form:

$$C'_H = C_H/C_D, \qquad C''_H = C_H/C_T \tag{16}$$

If to these two equations is added a third:

$$C_{\mathrm{H}} + C_{\mathrm{D}} + C_{\mathrm{T}} = 100(\%) \tag{17}$$

then it can be shown that:

$$C_{\mathrm{H}} = \frac{100}{[1 + (1/C'_{\mathrm{H}}) + (1/C''_{\mathrm{H}})]}$$

$$C_{\mathrm{D}} = \frac{100}{C'_{\mathrm{H}}[1 + (1/C'_{\mathrm{H}}) + (1/C''_{\mathrm{H}})]} \tag{18}$$

$$C_{\mathrm{T}} = \frac{100}{C''_{\mathrm{H}}[1 + (1/C'_{\mathrm{H}}) + (1/C''_{\mathrm{H}})]}$$

These show that in order to have percentage composition in a three component mixture it is necessary to know the reduced concentration C'_{H} and C''_{H}. Both these quantities can be found by means of the calibration graph. To reduce calculation, equation (18) need only be used for C_{H} and two other concentrations can be determined from the formulae:

$$C_{\mathrm{D}} = C_{\mathrm{H}}/C'_{\mathrm{H}} \quad \text{and} \quad C_{\mathrm{T}} = C_{\mathrm{H}}/C''_{\mathrm{H}} \tag{19}$$

The accuracy was determined by repeated analyses with 14 gaseous $H_2 + D_2$ samples.

In Table 2 is shown the root mean square error in four concentration ranges.

Table 2.

H_2 Concentration %	Root mean square error, %	
	Absolute	Relative
4–5·5	±0·25	±5·5
18–30	±0·77	±3·5
38–61	±0·33	±0·6
71–89	±0·50	±0·6

The change in error according to the concentration range supports the theoretical investigation (2).

Summary

It is shown that under the condition of our experiments there is no simple general relationship between $I_{\mathrm{H}}/I_{\mathrm{D}}$ and $C_{\mathrm{H}}/C_{\mathrm{D}}$. A simple relationship between pressure and concentration is given only at certain pressures whose values depend on the concentration. Therefore in order to avoid systematic error it is necessary to calibrate a method with the aim of determining the relationship between $I_{\mathrm{H}}/I_{\mathrm{D}}$ and $C_{\mathrm{H}}/C_{\mathrm{D}}$. However by suitable choice of conditions it is possible to make the factor $\alpha_{\mathrm{H}}/\alpha_{\mathrm{D}} \times \sqrt{(A_{\mathrm{H}}/A_{\mathrm{D}})}$ in equation (11) nearly equal to one; in this case the ratio $I_{\mathrm{H}}/I_{\mathrm{D}}$ directly gives the relative concentration $C_{\mathrm{H}}/C_{\mathrm{D}}$ in the sample being investigated.

VOL. 13 1958/5

For completeness, of course, the method requires full preliminary investigation with standard mixtures.

References

[1] Broida H. P. and Moyer I. W., *J. Opt. Soc. Amer.* 1952 **42**, 37;
Broida H. P. and Morgan G. H., *Analyt. Chem.* 1952 **24**, 799.
[2] Striganov A. R., *Usp. Fiz. Nauk* 1956 **58**, 365.
[3] Veinberg G. V., Zaidel' A. N. and Petrov A. A., *Optika i Spektrosk.* 1956 **1**, 972.
[4] Dontsov Yu. P. and Striganov A. R., *Analitcheskaya Khim.* 1957 **12**, 5.
[5] Striganov A. R., *Zavodskaya Lab.* 1955 **12**, 1476.

OL.
13
8/59

Spectrochimica Acta, 1958, Vol. 13, pp. 150 to 153. Pergamon Press Ltd., London

RESEARCH NOTES

Application of the vacuum sliding spark to spectrochemical analysis in the far ultraviolet

(*Received* 31 *May* 1958)

It is usually stated that only seventy of the known elements can be detected spectrographically by the standard methods [1]. The other twenty elements are the simple gases, the halogens, and some metalloids such as sulphur, phosphorus and carbon. They have ionization potentials above 10 V and they are difficult to excite by using the common sources. Moreover, the sensitive lines of the neutral atom generally lie in the vacuum ultraviolet [2], for instance — C_I : 1657 Å; P_I : 1774·9 Å; S_I : 1807·3 Å. The use of these lines for spectrochemical analysis has been proposed [1, 3], but experimental tests have been performed only very recently [4, 5, 6]. It is possible to excite these lines with a normal spark, but, of course, the gas used must be transparent in that spectral region (nitrogen, argon), and it is necessary to interpose a transparent window between the spark chamber and the spectrograph in which a sufficient vacuum is maintained.

Another method has been developed in our laboratory, in which are used the sensitive lines of highly ionized atoms produced in a vacuum spark of a special type ("sliding vacuum spark"). In this paper is briefly summarized the work performed on this subject since 1954.

The most general source of line spectrum of ionized atoms is the Millikan "hot spark". The disadvantages of this spark are well known: high breakdown field and consequently a very small gap between the electrodes and a pronounced instability. On the other hand it was known that at atmospheric pressure the breakdown was helped by the presence of an insulating or semiconducting solid between the electrodes. It was found [7] that in vacuum the aspect of the discharges is changed but the main advantages remain, that is, the breakdown potential is much lower for the same distance between the electrodes. With a gap of a few millimetres one can run such a spark at voltage of 15 kV. The stability in space and the constancy of light output in time are reasonably good [7, 8]. As shown later by Bockasten [9], the lines in a vacuum sliding spark are less broadened by Stark effect than in the Millikan spark. The spectrum is essentially composed of the lines from the metals of the electrodes, with a few lines from the elements of the insulator. Aluminium oxide is commonly used for this material because it is hard and because the aluminium spectrum exhibits a small number of lines. Different mountings of the electrodes are possible [10, 11]; for instance, in the best arrangement the electrodes are cylindrically shaped and are pressed against an insulating ring, provided with one radial opening.

Like the Millikan spark, this light source emits the spectrum of highly ionized atoms. Very sensitive lines have been found in the far ultraviolet region. These lines are produced by the ion having only one *s*-electron on the outer shell, and the most sensitive are those due to the transition of this electron from the *s*-level to the *p*-level [12]. This result constitutes an extension of the well known Meggers' rule. To mention only a few examples, these lines are doublets of hydrogen-like atoms, analogous for C_{IV}, N_V, O_{VI} to the doublet of ultimate lines of neutral Li, for Si_{IV}, P_V, S_{VI} to the doublet of neutral Na, etc., and this explains

their high sensitivity. In the particular case of phosphorus, sulphur and carbon, it is possible to use for detection and quantitative analysis the lines 1118 Å of P_V, 950·7 Å of P_{IV}, 933·4 and 944·5 Å of S_{VI}, 977 and 1176 Å of C_{III}, 1548 Å of C_{IV}. For instance by this method, a limit of sensitivity was obtained of 50 p.p.m. for sulphur and phosphorus in steel [13] and of a few p.p.m. of phosphorus in aluminium alloys [14]. By using pure aluminium electrodes with an axial hole in which a powder is compressed, it is possible to study non-conducting materials as ceramics, or materials which are only available as powders; for instance the sensitivity presently obtainable is of a few p.p.m. of sulphur and phosphorus in aluminium oxide powders.

This method seems to be of general interest, because for the shortest wavelengths of the far ultraviolet the matrix spectrum is not so rich as in the range 1500–2000 Å, and also because there is no limitation of the spectral region studied. Consequently the method is potentially applicable to the study of other non-metallic elements (e.g. simple gases), the sensitive lines of which are in the region of the shortest wavelengths.

Laboratoire des Hautes Pressions
Bellevue
France

J. Romand
Germaine Balloffet
B. Vodar

References

[1] Harrison G. R., *Metals & Alloys* 1936 **7** 290.
[2] Meggers W. F., *J. Opt. Soc. Amer.* 1941 **31** 39.
[3] McNally J. R., Harrison G. R. and Rowe E., *J. Opt. Soc. Amer.* 1947 **37** 93.
[4] Bills K. M., *Öst.ChemZtg.* 1954 **55** 73.
[5] Lüscher E., *La Metallurgia Italiana* 1956 IV *Seminaria Spettrochimica* p. 48.
[6] *Hilger J.* 1957 **4** 19.
[7] Vodar B. and Astoin N., *Nature, Lond.* 1950 **166** 1029.
[8] Astoin N. and Vodar B., *J. Phys. Radium* 1953 **14** 494.
[9] Bockasten K., *Ark. Fys.* 1955 **9** 457.
[10] Romand J. and Balloffet G., *J. Phys. Radium* 1955 **16** 489.
[11] Romand J., Balloffet G. and Vodar B., *Proceedings of the Sixth International Conference on Spectroscopy (Amsterdam* 1956), p. 269. Pergamon Press, London 1957.
[12] Balloffet G. and Romand J., *C.R. Acad. Sci., Paris* 1956 **242** 1964.
[13] Balloffet G. and Romand J., *J. Phys. Radium* 1955 **16** 490.
[14] Romand J. and Balloffet G., *J. Phys. Radium* 1957 **18** 641.

An infrared absorption study of *n*-alkyl malonic acids and their diethyl esters

(*Received* 27 *May* 1958)

In continuation of the earlier work [1], a study of the infrared absorption spectra of a homologous series of *n*-alkyl malonic acids [$CH_3(CH_2)_xCH(COOH)_2$, where $x = 1$–11, 13, 15 and 17] and of their diethyl esters between the range 4000 and 700 cm^{-1} has been undertaken. It seems worthwhile to report some of the preliminary observations at this stage.

The spectra were recorded in a Grubb–Parsons double beam spectrometer provided with LiF and NaCl optics. All the compounds used were of a purity better than 99·8 per cent. The acids were run both as thin solid films and as mulls in nujol and the esters as liquid films, between two rocksalt plates. As an illustration, the spectra of amyl malonic acid and its ester are presented in Fig. 1.

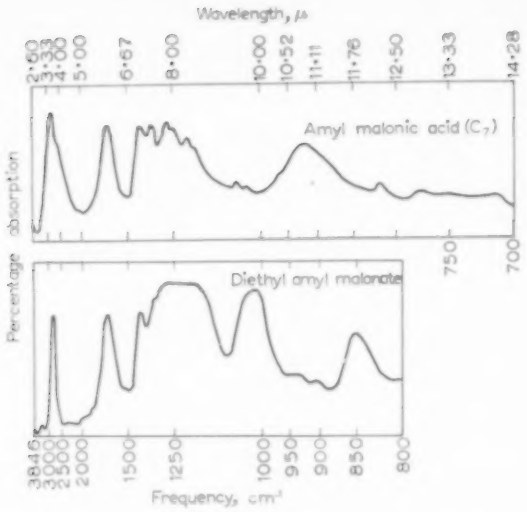

Fig. 1

Table 1

No. of carbon atoms	Saturated fatty acids		*n*-Alkyl malonic acids	
C_n*	Melting point (°C)	$C{=}O_\gamma$[2] (cm^{-1})	Melting point [1] (°C)	$C{=}O_\gamma$ (cm^{-1})
4	−5·5†	—	111·5	1647
5	−34·5†	—	96·0	1658
6	−3·9†	—	101·5	1650
7	−7·5†	—	81·0	1661
8	16·5	—	103·5	1650
9	12·4	—	95·5	1658
10	31·3	—	115·0	1653
11	28·1	—	103·5	1660
12	44·0	—	117·5	1653
13	41·1	—	108·5	1658
14	54·0	1701	120·0	1653
15	52·1	—	113·3	—
16	62·8	1701	120·6	1653
17	61·18	1705	117·9	—
18	69·6	1698	121·5	1653
19	—	1706	—	—
20	76·2	1698	120·4	1653
21	—	1705	—	—

* C_n (in the case of alkyl malonic acids) = (actual number of carbon atoms) −1.
† Freezing point.

VOL. 13 1958/5

Comparing the general appearance of the spectra there is observed quite a good resemblance among the members of the same homologous series, but significant differences are noticed between the two. Thus, in the lower frequency range some of the bands, for example, around 920 cm^{-1} in the acid, and around 850 cm^{-1} and 1025 cm^{-1} in the ester spectra, afford an opportunity to distinguish between the two series.

The appearance of a strong and broad absorption in the 3400–3000 cm^{-1} region is an evidence for the presence of molecular hydrogen bonding in the acids. It is interesting to note in Table 1 that the frequency of the C—O stretching vibrations in the spectra of the acid series alternates between the odd and even members, which is similarly exhibited in their X-ray long spacings [1]. Similar alternations were observed also in the case of saturated long chain fatty acids [2]. Further, it seems possible to correlate the frequency of this band, varying characteristically with the chain length, with the corresponding melting point of these compounds; the seventh member, viz. amyl malonic acid exhibiting the highest C—O frequency possesses the lowest melting point (81·0°C). This frequency seems to be appreciably influenced by the strength of intermolecular interactions. It is suggested that the intermolecular binding through this group, presumably by the hydrogen bond formation, is stronger in these than in the corresponding saturated fatty acids, the absorption frequency being appreciably lower in the former series. It is also noted that the influence of the length of the chain diminishes progressively in a series, and the frequency changes like their melting points [1] and ultimately reaches a constant value. On the other hand, in the case of the corresponding C_{14} to C_{21} fatty acids the respective absorption frequencies are more or less the same in the odd or the even group, even though their melting points differ appreciably.

A detailed report of these data and their spectrostructural discussions will be presented in a forthcoming communication.

Acknowledgements—We wish to record our thanks to Dr. (Mrs.) S. Dasgupta, Dr. B. D. Sharma and Dr. (Miss) S. B. Kulkarni for their help in this investigation.

National Chemical Laboratory,
Poona, 8, India

K. Nagaraja Rao and A. B. Biswas

References

[1] Sharma B. D. and Biswas A. B., *Analyt. Chem.* 1958 **30** 1356.
[2] Sinclair R. G., McKay A. F. and Norman Jones R., *J. Amer. Chem. Soc.* 1952 **74** 2570.

Spectrochimica Acta, 1958, Vol. 13, pp. 154 to 158. Pergamon Press Ltd., London

REPORT OF MEETING

THE Ninth Annual Symposium on Spectroscopy, sponsored by the American Association of Spectrographers, was held in Chicago on June 9 to 11. In addition to contributed papers presented at the meeting, seminars and "Ask the Experts" sessions were also held. The topics discussed at this year's seminars included "Application of Out-of-Plane Hydrogen Deformation Vibrations to Chemical Analysis" by W. J. Potts (Dow Chemical Company); Emission Spectrographic Determination of Gases in Metals" by V. A. Fassel (Iowa State College); "Near-Infrared Spectroscopy" by Scott Anderson (Anderson Physical Laboratory); and "X-Ray Spectrography" by L. S. Birks (Naval Research Laboratory). "Ask the Experts" sessions were held in emission, infrared and x-ray fluorescence spectroscopy. The titles and abstracts of contributed papers presented at the meeting were as follows:

EMISSION SPECTROSCOPY

Spectrographic investigation of non-metallic elements: CHARLES E. HARVEY and JAMES W. MELLICHAMP, C. E. Harvey Associates and U.S. Army Signal Engineering Laboratory, Chicago, Illinois.

A discussion of apparatus and techniques for the detection of the halogens, carbon, sulfur and selenium using spark discharges at reduced pressure. Non-conducting materials are pressed into pellets with silver powder for a binder and a silver rod used for counter electrode. Sensitivities of 0·1% or less were obtained for most elements.

The plasma jet as a spectroscopic source: MARVIN MARGOSHES and BOURDON F. SCRIBNER, National Bureau of Standards, Washington, D.C.

The temperatures of the usual flame sources are limited to about 2000°C when the fuel is burned with air and to about 3000°C when burned with oxygen. Higher temperatures are often desired to allow detection of elements not excited in the cooler flames, to permit more effective excitation of others and to reduce certain matrix effects. Spark-in-flame techniques have been applied to develop higher excitation temperatures. More recently, hydrogen-fluorine and cyanogen-oxygen have been used to reach temperatures of nearly 5000°C.

The plasma jet produces a flame-like cone consisting of the arc plasma, with temperatures of 5000 to 15,000°C or higher. A plasma jet has been designed to operate with moderate currents obtained from an ordinary d.c. arc supply. Solutions in the form of a fine spray are introduced into the "flame". Some of the properties of this source were described.

Performance patterns of a.c. arc excitation: J. T. ROZSA, National Spectrographic Laboratories, Cleveland, Ohio.

While the information on d.c. arc excitation is quite bulky, little is known of its new competitor, the a.c. arc excitation. After five years of use in a commercial laboratory, the sustaining arc has developed its own performance patterns. In general, the a.c. arc is especially suited to total energy method determinations on a wide variety of materials with improvement in reproducibility, sensitivity and reduction of mineralogical effects. The latter item has had particular significance for semi-quantitative analysis. Alternation of parameters to improve repetition rate has been unrewarding.

VOL. 13 1958/59

A dual photographic–direct reading attachment for the Jarrell-Ash Ebert spectrograph: R. K. Brehm and G. Benzie, Jarrell-Ash Company, Newtonville, Mass.

A direct reading attachment for the Jarrell-Ash 3·4 meter convertible Ebert Spectrograph was discussed. The attachment consists of a housing containing exit slits and multiplier phototubes on special focal curves mounted permanently in the instrument. To make photographic work compatible with the direct reading assembly, a movable 30″ × 2″ 45° reflecting mirror is provided. The camera track and slide, normally located at the primary focus, is relocated on the side of the instrument. The direct reading attachment incorporates standard Jarrell-Ash "Atomcounter" electronics. Data on precision of alignment and instrumental stability were given.

Concentration of trace elements by extraction technique prior to spectrographic determination: S. R. Koirtyohann and E. E. Pickett, University of Missouri, Columbia, Missouri.

The Mitchell precipitation method for concentration of the biologically important trace elements has certain limitations; very high iron and calcium phosphate contents lead to line interferences or poor spectroscopic buffering. An extraction procedure employing dithizone for the elements Cu, Co and Zn, and alpha benzoin oxime for Mo, was developed and the efficiencies checked by means of radioisotopes. A novel method was devised for bringing the extracted trace elements into an alumina matrix suitable for arcing.

Some aids in spectrochemical calculations: E. S. Hodge, Mellon Institute, Pittsburgh, Pa.

A large scale Seidel function for preliminary curve plot and similar paper for emulsion curve plot have been prepared. A table of Seidel function transmission valves vs. relative exposure is taken from each emulsion curve and used to prepare a circular intensity calculator. The latter is facilitated through the use of an enlarged two-cycle circular log scale. The design and use of a "working curve shifter" has eliminated the need of a calculating board in non-routine work.

The determination of trace impurities in zirconium metal by a point to plane spectrochemical procedure: Raymond F. Farrell, G. Jane Harte and Ralph M. Jacobs, Westinghouse Company, Pittsburgh, Pennsylvania.

The wide applicability of zirconium metal to the nuclear reactor program necessitated the development of a rapid spectrochemical method for the production control analysis of impurities in this metal. The purpose of this paper was to describe a method of direct excitation of zirconium metal for the determination of aluminum, cobalt, chromium, copper, iron, magnesium, manganese, molybdenum, nickel, lead, silicon, titanium, vanadium, tungsten and hafnium in the parts per million range.

The required spectral sensitivity and reproducibility are obtained by excitation of the sample with an ignited alternating current arc. Compared to other applicable methods, the time for analysis and the opportunity for sample contamination are both considerably reduced by this method. Standard spectrochemical procedures are used for the recording and computation of results. With some changes in analytical lines and with adequate solid standards, the method can be extended to the analysis of impurities and alloying elements in Zircaloy.

The use of hydrogen as an internal standard in analysis of additives and wear metals in lube oils by direct reading methods: R. R. Thieme, Jarrell-Ash Company, Newtonville, Massachusetts.

A method was developed using the hydrogen line at 4816A as internal standard in analysis of additives and wear metals in lubricating oils by Direct Reading Methods. The elements determined are Ag, Al, B, Cr, Cu, Fe, Pb, Si, Sn, Ba, Ca, Zn, in a range dependent on elements from 1 p.p.m. to 3,000 p.p.m.

Application of percentage ratio technique to analysis of cast and wrought copper-nickel-zinc alloys: Dana J. Roberts, Revere Copper and Brass, Dallas Division, Chicago, Illinois.

A spectrographic method of analysis of copper-nickel-zinc alloys was described. Precision and sensitivity are obtained by use of an underdamped multisource discharge. Compensation

for percentage variation of matrix element is made by plotting intensity ratio vs. % zinc/% copper and % nickel/% copper. A single set of working curves apply to any alloy with composition 50–70% copper and 10–20% nickel. Consideration is given to variables which could prevent application of working curves to full range of alloys such as background variations with composition, metallurgical phase changes, and enhancement of zinc and copper lines due to variations in % nickel.

Flame photometry of strontium: C. E. Moore and A. H. Maas, Loyola University, Chicago, Illinois.

Eight emission lines of strontium have been studied for possible analytical usage. Of these the lines 4077·7 Å, 4607·3 Å and the bands in region 5300 Å to 7000 Å show the greatest possibilities. Data on enhancement and depressant effects of various ions will be given.

Determination of the metal content of driers by flame photometry: P. J. Secrest, The Sherwin-Williams Company, Chicago, Illinois.

A method for determining the metal content of calcium, cobalt, lead and manganese paint driers by means of flame photometry was described. The drier is dissolved directly in a benzene-acetone-alcohol solvent. The metal concentration is obtained by comparing the emission of the solution with the emission of a standard solution. Duplicate determinations require about thirty minutes. The standard deviation of the method varies from 0·60% (of the total metal found) for lead to 0·85% for calcium. Agreement with chemical method is within about one per cent.

INFRARED SPECTROSCOPY

Micro infrared analyses as applied to gas chromatography fractions: J. E. Stewart and W. S. Gallaway, Scientific Instruments Division, Beckman Instruments, Inc., Fullerton, California.

Numerous applications of infrared spectrophotometry require greater sensitivity than can be obtained by conventional operation of commercial spectrophotometers. The analysis of very small samples is of considerable importance, particularly when infrared is utilized in conjunction with gas chromatography. For these analyses the area of the beam is reduced in the sampling area which in effect increases the number of absorbing particles per unit area of beam. However, for this technique to be practical the beam condensing system should be easily mounted and dismounted in the spectrophotometer, should include a simple, reliable means of handling small specimens, and should accept gas, liquid, and solid samples. The design and use of such a system was described. Its performance was illustrated by studies on major and minor constituents isolated from diverse mixtures by gas chromatography. The technique conveniently handles liquid samples of 0·2 microliter volume, solid samples weighing as little as 10 micrograms and gas samples of 22 ml volume. Applications other than those involving gas chromatography were also described.

Recent developments in infrared instrumentation: John W. Huley, Perkin-Elmer Corporation Cleveland, Ohio.

The broadening scope of infrared application has been coupled with extensions in relative instrumentation. This paper discusses some recent advances made by the Perkin-Elmer Corporation in this field.

Application of infrared analysis to air separation unit control: R. A. Hagstrom and P. A. Demkovich, Standard Oil Company (Indiana), Whiting, Indiana.

Existing chemical procedures used for the detection and measurement of trace hydrocarbon contaminants in air-liquefaction process streams are lengthy and provide inadequate information. A modified Perkin-Elmer Model 21 infrared spectrophotometer, in conjunction with a special sampling system, permits rapid and accurate routine analyses of both gaseous and liquid air samples from streams leading to nitrogen production.

Polarized infrared spectroscopy: Aaron Bluhm, Quartermaster, Research and Development Center, U.S. Army, Natick, Mass.

The theory and techniques employed in the propagation of polarized infrared radiation were discussed, along with the methods of sample preparation and spectral measurement. The

VOL. 13 1958/5

application of polarized infrared spectra to the determination of the structure of inorganic and organic molecules and polymeric materials was demonstrated. Some recent applications and results were reviewed.

SPECTROPHOTOMETRY

The evaluation of colorants by spectrophotometric methods: W. F. Ulrich, F. Kelley and D. C. Nelson, Scientific Instr. Div., Beckman Instruments, Inc., Fullerton, California.

The diverse problems encountered in the production and control of colorants require the use of many different analytical techniques. Of these, spectrometric measurements in the visible region are among the most useful because of their relationship to the color response of the human eye. However, factors other than color are also important. It is frequently necessary to establish the identity of a pigment or dye, and its concentration. The effect of optical brightening agents is also of current interest. These and other problems are discussed in relation to instrumental requirements. In some instances, ultraviolet and near-infrared data are employed to supplement the visual information obtained by absorptiometric, reflectance and fluorescence techniques.

Some new developments in the spectrophotometric field: E. Leurches, Lausanne, Switzerland.

OPTICAL FLUORESCENCE SPECTROSCOPY

Determination and identification of polycyclic, aromatic hydrocarbons in paraffins, waxes and fats using fluorescence spectra: Hans J. Eichoff, Anorganic Chem. Inst. University Mainz, Germany, and Georg Titschak, Hamburg 1, Germany.

The determination and identification of polycyclic, aromatic hydrocarbons in paraffins, waxes and fats using fluorescence spectra requires dispersion of the fluorescent light and the measuring of intensities in the spectral regions in question. This is done because in such products a fluorescence can appear which is uncharacteristic and of indefinite structure; this then would render the judgment of such products under an analysis quartz lamp impossible.

The paper will show by means of a number of typical fluorescence spectra that polycyclic aromatics such as benzpyrene, methyl-chloranthrene and anthracene can be determined to 10^{-5} to 10^{-4}% with an adequate accuracy. The behavior of polycyclic aromatics in the refinement of paraffins is investigated by means of models.

X-RAY SPECTROGRAPHY

X-ray absorption as a tool in valence state determination: R. A. van Nostrand, Sinclair Research Laboratories, Incorporated, Harvey, Illinois.

Fine structure at the X-ray K-absorption edge provides a new approach to certain problems of chemistry. Absorption curves will be shown and discussed for manganese, cobalt and chromium compounds. The interpretation of these curves involves concepts familiar in ultraviolet spectroscopy and in electron diffraction. Factors which are evident in the curves include valence state of the element, separation between the Fermi level and the conduction band, and proximity and nature of atoms within the first co-ordination sphere. Utility of this technique to the chemist was shown in applications to fundamental structure problems and to identification of the variety of electronic states which an element may assume. Evidence that oxygen forms double bonds in the permanganate, manganate and chromate ions was presented.

Determination of sulfur and chlorine in petroleum by X-ray fluorescence: T. C. Yao, Standard Oil Company (Indiana), Whiting, Indiana.

X-ray fluorescence can determine sulfur and chlorine in such petroleum stocks as gasolines, distillate fuels, residual fuels, lube-oil additives and insecticides. A commercial spectrometer, equipped with a rock-salt crystal, helium path, flow-proportional counter, and pulse-height analyzer, is used. The minimum concentrations for analysis are 0·005 weight per cent sulfur and 0·002 weight per cent chlorine. With single calibrations for each element, the X-ray

methods are as accurate as the ASTM methods of analysis. Moreover, the X-ray methods are much faster, the elapsed time per analysis being five to ten minutes.

X-ray spectrographic analysis of lignites: G. L. Clark and Raymond Hunt, University of Illinois, Urbana, Illinois.

The present theory, instrumentation and applications of X-ray fluorescence spectrometry were concisely reviewed including a critical listing of the advantages and disadvantages in comparison with optical spectrographic and other instrumental and purely chemical methods of analysis of ores and minerals particularly. The experiences in the analysis of 35 specimens of lignites from South Dakota for uranium, molybdenum, iron and other elements are illustrated, and the results were compared with the values obtained by accepted chemical methods of analysis depending upon separations, which, of course, were not required in X-ray spectrometry. A comparison of results was also given for the original lignite specimen and the ashed specimen in each instance. The control of instrumental variables which will assure reproducible results were critically considered.

Practical application and operational factors of fluorescent X-ray spectrography, a review: Merlyn L. Salmon.

Recent advances in the detection of light elements by X-ray spectroscopy: William R. Kiley, Philips Electronics, Inc., Mt. Vernon, New York.

Instrumental factors used in the determination of the light atomic number elements were discussed. Data were presented for the determination of S, P and Cl in petroleum products and the determination of Al and Si in high Ni–Cr alloys and low alloy steels.

VOL.
13
1958/5

The production X-ray quantometer, a direct reading X-ray polychromator: H. T. Dryer, Applied Research Laboratories, Dearborn, Michigan.

A Production control X-ray Quantometer has been designed for the rapid and accurate determination of all elements with atomic number 12 and above. Simultaneous determinations of as many as 22 elements, compared to a common standard, can readily be achieved.

This instrument has been designed to incorporate the current crystal optics with the inherent advantages in resolution and sensitivity and the standard ARL Recording Console utilizing a full null system. Special emphasis has been placed on instrumental stability, unitized design and versatility of application. Optimum conditions for any particular problem can be obtained through the various combinations of slit widths, crystals, detectors and optical paths. Analytical data were presented.

Analysis of thin films of iron-nickel alloy on glass: T. C. Loomis, Bell Telephone Laboratories, Inc., Murray Hill, New Jersey.

Thin films of iron-nickel alloy deposited on glass slides by evaporation at reduced pressure under the influence of a magnetic field show promise for use in memory storage devices. This paper described a procedure for the non-destructive analysis of such films by X-ray spectroscopy.

A single pair of linear calibration curves is sufficient to allow quantitative determination of both composition (15 to 20% iron) and thickness (250 to 2000 angstroms). A precision of about 1% of the amount present is obtained on a slide one-fourth inch long by one inch long. X-ray fluorescence measurements on solutions were used for the analysis of the standard reference samples employed in the preparation of the calibration curves.

Spectrochimica Acta, 1959, Vol. 13, p. 159. Pergamon Press Ltd., London

Book review

G. F. LOTHIAN: **Absorption Spectrophotometry** Second Edition. Hilger and Watts Ltd., London, 1958. viii + 246 pp., 52s.

THIS book contains an account of the basic principles of the theory and practice of absorption spectrophotometry both in the ultra-violet and infra-red regions. It is divided into three parts, the first of which deals with the absorption laws, factors limiting their application, optimum conditions for accurate measurement, calculation of the composition of multicomponent mixtures, etc. The second part is concerned with the relation of spectra to chemical structure and analysis and though very brief it is illustrated by a variety of applications from widely differing fields. The third section of the book deals with techniques. It contains chapters on spectrophotometers both ultra-violet and infra-red, with descriptions of most of the types now in common use. Associated equipment such as cells, sources, detectors and amplifiers are dealt with and there is a section on standards and solvents.

The aim of the book appears to be to provide a background of information for the increasing number of workers who use spectrophotometry as a tool, to give them basic knowledge about their instruments and to help them to avoid the pitfalls of the subject. It contains a large number of useful diagrams though the examples chosen to illustrate various topics are not always the best available. It concludes with a brief guide to the literature on the treatment of more specialized branches of what has now become a vast subject.

W. C. PRICE

Department of Physics
University of London
King's College, Strand, W.C.2

OL.
13
8/59

Papers to be published in future issues

A. MIYAKE, I. NAKAGAWA, T. MIYAZAWA, I. ICHISHIMA, T. SHIMANOUCHI and S. MIZUSHIMA: Infrared and Raman spectra of dichloroacetyl chloride in relation to rotational isomerism

P. TARTE: Réchérches sur les frequences de déformation OH—I. Spectra infra-rouge des sels basiques de cuivre

D. A. SINCLAIR and R. N. WHITTEM: Apparent rectification in Tesla sparks

A. DANTI and R. C. LORD: Rotational analysis and upper-stage transitions of parallel absorption bands in benzene, Sym-benzene-d_3, benzene-d_6 and pyridine

B. BAK, D. CHRISTENSEN, L. HANSEN-NYGAARD and J. RASTRUP-ANDERSEN: The structure of vinyl fluoride

H. STAMMREICH, D. BASSI, O. SALA and H. SIEBERT: The vibrational spectrum of the dichromate ion

D. M. SHAW, O. WICKREMASINGHE and C. YIP: A simple device for the spectrochemical analysis of minerals in an inert atmosphere using the Stallwood jet

A. D. E. PULLIN: The variation of infrared vibration frequencies with solvent

E. A. V. EBSWORTH, J. R. HALL, M. J. MACKILLOP, D. C. MCKEAN, N. SHEPPARD and L. A. WOODWARD: Vibrational spectra and structure of trisilylamine and trisilylamine-d_9

E. A. V. EBSWORTH and N. SHEPPARD: The infra-red spectra of some methylammonium iodides: angle deformation frequencies of $\overset{+}{N}H$ and $\overset{+}{N}H_2$ groups

K. LAQUA and U. LUOTO: Ein thyratrongesteuertes Schaltgerat für Wechselstromabreissbögen

G. L. Caldow and H. W. Thompson: Vibrational bands of isothiocyanates, thiocyanates and isocyanates

J. P. Jesson and H. W. Thompson: Vibrational band intensities of the C≡N group in aliphatic nitriles

P. E. B. Butler, D. R. Eaton and H. W. Thompson: Vibration–rotation bands of keten

H. W. Thompson and D. A. Jameson: Vibrational frequency and band intensity of the carbonyl group

R. G. Snyder and J. C. Decius: The infrared spectra of $N_2H_6Cl_2$ and $N_2H_6F_2$

H. Rosenkratz and C. Gaul: The infrared absorption spectra of ring *D* steroid lactones—II

E. Lieber, C. N. R. Rao and J. Ramachandran: The infrared spectra of organic thiocyanates and isothiocyanates

R. N. Kniseley, V. A. Fassel, R. W. Tabeling, B. G. Hurd and B. B. Quinney: Quantitative spectrographic analysis of the rare earth elements—X

L. H. Ahrens and R. A. Edge: Observations on the use of L and O bands for d.c. arc spectrochemical analysis

N. S. Bayliss, A. R. H. Cole and L. H. Little: Solvent effects on the infrared frequency and intensity of the nitrile vibration in aceto-, propio-, benzo- and phthalo-nitriles

L. A. Duncanson, J. W. Edell, M. B. Lloyd and W. T. Moore: Diffration gratings for the measurement of spectra in the 20–100 μ region

H. F. Hazebroek: Electrostatic sample preparator for infrared spectroscopy of powders

Z. Hainski and P. Herman: Essais d'enregistrements à energie d'émission controlée

J. Charette and Ph. Teyssié: Infrared study of heterocyclic compounds carrying a conjugation substituent—I

A. R. H. Cole and F. Macritchie: The energy of a hydrogen bond by infrared spectroscopy

E. M. Tanner: The infrared absorption spectra of some -phenyl-hydrazonoketones and alcohols

D. A. Dows: Torsional vibrations in CO_2 and N_2O crystals

W. E. Ohnesorge and L. B. Rogers: Fluorescence of some metal cholate compounds of 8-quinolinal—I

W. E. Ohnesorge and L. B. Rogers: Fluorescence of some metal cholate compounds of 8-quinolinal—II

G. F. G. Knipe: The spectrographic analysis of antimony and antimony sulphide for heavy metals

S. J. Cyvin: An approximate method for calculating mean amplitudes of vibration from spectroscopic data—I

R. R. Patty and R. T. Lagemann: The infrared spectrum and molecular structure of carbonyl-bromofluoride

VOL.
13
1958/5

Spectrochimica Acta, 1958, Vol. 13, pp. 161 to 167. Pergamon Press Ltd., London. Printed in Northern Ireland

Infra-red and Raman spectra of dichloroacetyl chloride in relation to rotational isomerism

A. Miyake, I. Nakagawa, T. Miyazawa, I. Ichishima,
T. Shimanouchi and S. Mizushima
Chemical Laboratory, Faculty of Science, Tokyo University,
Hongo, Tokyo, Japan

(*Received* 11 *June* 1958)

Abstract—Vibration spectra of dichloroacetyl chloride have been measured in the gaseous, liquid and solid states and also in solutions. From the experimental result it was concluded that in the gaseous and liquid states there exist two molecular forms, of which only the more polar form persists in the solid state. The energy difference between these two forms is almost zero in the liquid state and amounts to about 200 cal/mole in the gaseous state, the less polar form being more stable. In this form the oxygen atom is in the *cis*-position with respect to the hydrogen atom. The more polar form is obtained from this form by an internal rotation about the C—C axis by about 90°.

Introduction

The investigation of the internal rotation in the molecule of the type 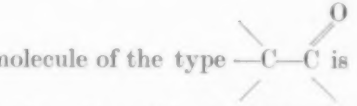 is important for the determination of the configuration of a polypeptide chain [1]. Of molecules of this type we have studied $ClCH_2COCl$, $BrCH_2COCl$, $BrCH_2COBr$ and $ClCH_2COCH_3$ [2], [3]. In this paper we shall discuss the molecular structure of dichloroacetyl chloride $CHCl_2COCl$ based on the measurement of the infrared and Raman spectra.

Experimental

Dichloroacetyl chloride was prepared according to the following reactions [4, 5]:

$$2CCl_3CH(OH)_2 + 2CaCO_3 \xrightarrow{NaCN} (CHCl_2CO_2)_2Ca + 2CO_2 + 2H_2O + CaCl_2$$

$$(CHCl_2CO_2)_2Ca + 2HCl \longrightarrow CaCl_2 + 2CHCl_2CO_2H$$

$$CHCl_2CO_2H + SOCl_2 \longrightarrow CHCl_2COCl + HCl + SO_2$$

The sample was distilled three times (b.p. 107°–107·5°C).

The Raman spectra were measured in the liquid and solid states and in solutions. In the liquid state the measurements were made at ordinary temperature and also at −45°C, 65°C and 80°C. The solid spectrum was taken at liquid air temperature, using aqueous solution of praseodymium nitrate as a filter. In the measurements of solutions benzene and acetonitrile were used as solvents. The Raman spectrum of the liquid at room temperature was also reported by Cheng [6].

The infrared spectra were measured in the gaseous, liquid and solid state and in solutions. The solvents used are carbon disulphide and carbon tetrachloride

(non-polar) and acetone, acetonitrile and nitrobenzene (polar). The measurements in the liquid state were made at different temperatures.

The infrared and Raman spectra obtained are listed in Table 1 and Fig. 1.

Table 1. Vibration spectra of $CHCl_2COCl$

Solid		Liquid		Assignment*	
R.	I.R.	R.	I.R.		
2986 (4)		3002 (5b)	3000 (m)	M,L.	ν(C—H)
			1936 (w)		
		1808 (5)	1799 (s)	M	ν(C=O)
		1772 (5)	1783 (s)	L	
		1592 (0)			
		1262 (4)	1256 (m)	M	δ(C—H)
		1233 (2)	1232 (m)	L	
		1211 (?)	1215 (m)	L	
1198 (2)		1201 (5)	1202 (m)	M	
		1073 (2)	1069 (s)	L	ν(C—C)
	997	988 (3)	987 (s)	M	
		974 (0)?			
808 (3)	819	808 (6b)	800 (s)	M	ν(C—Cl_2)
		782 (4b)	784 (s)	L	
753 (4)	756	754 (8)	751 (s)	M	
		734 (3b)	734 (v.s.)	L	
		631 (1)	637 (w)	L	ν((O)C—Cl)
577 (6)		580 (5vb)	578 (m)	M	
		503 (7)		L	δ(C—Cl) and δ(C=O)
464 (4)		461 (9)		M	
		409 (7)		L	
336 (5)		338 (10)		M	
268 (2)		264 (7)		L,M	
243 (3)		237 (6)		M	
		176 (8)		L	

* M denotes the more polar form and L the less polar form.

Result and discussion

The normal vibrations of one form of this molecule are fifteen in number and all of them are active in both the infrared and Raman spectra. In our measurements in the gaseous and liquid states the number of bands observed amounts to more than twenty. In the C=O frequency region (ca. 1800 cm^{-1}) two bands were observed and in the C—Cl frequency region five or six bands. This leads to the conclusion that at least two molecular forms exist in these states. This is confirmed by the experimental result obtained in solutions where one group of bands increase in intensity with respect to the other in a polar solvent. Therefore, according to our previous researches [1, 7, 8], the former group of bands can be assigned to the more polar form (i.e. the form with larger dipole moment) and the latter to the less polar form.

Thus the first member of each of the following pairs of frequencies (in cm^{-1}) is

VOL. 13 1958/5

assigned to the more polar form, whereas the second member to the less polar form: (754, 782); (808, 734); (988, 1073); (1201, 1215); (1262, 1233); (1808, 1772). In the lower frequency region, we have grouped the observed frequencies according to the solvent effect of the Raman spectra. From this we can assign the frequencies of 237, 338 and 461 cm^{-1} to the more polar form and those of 176, 264, 409 and 503 cm^{-1} to the less polar form.

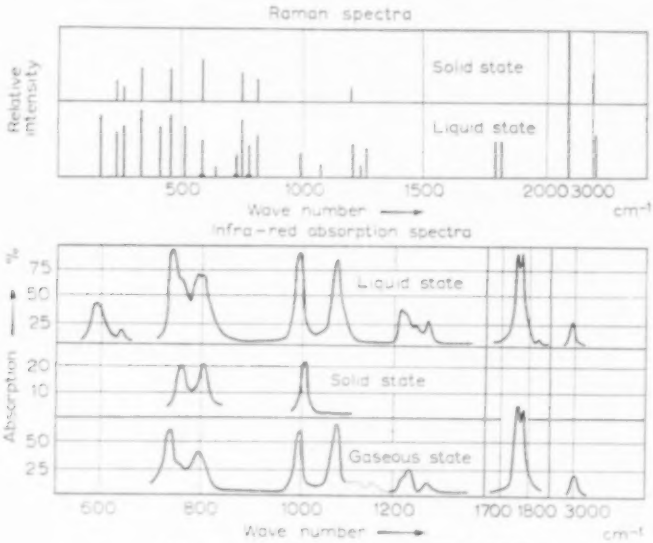

Fig. 1. Vibration spectra of $CHCl_2COCl$.

Of the observed frequencies mentioned above, only those assigned to the more polar form persist in the solid state (see Fig. 1). Therefore, only one of the two molecular forms is stable in this state, just as we have seen in many other substances showing rotational isomerism [1]. The Raman line at 261 cm^{-1} which persists in the solid state but decreases in relative intensity considerably, may be assigned to both of the two isomers in the liquid state.

The energy difference between the two isomers in the gaseous state were determined according to the method described in our previous papers [1, 9]. The absorption band at 988 cm^{-1} was chosen as a characteristic band of the more polar form and the band at 1073 cm^{-1} as that of the less polar form. The intensity ratio of the two bands was measured at different temperatures and from the result the energy difference was determined. It was found that the less polar form is more stable than the more polar form by about 200 cal/mole.

In the liquid state the relative intensity of the Raman lines remained almost constant in the temperature range from $-45°C$ up to $+80°C$ and that of the infra-red bands from room temperature down to $-150°C$. This shows that the energy difference in the liquid state is negligibly small.

We are now interested in the determination of the configurations of the two molecules which is by no means easy, since the molecular forms have no pronounced symmetry. In the first place the dipole moment of the molecule was

calculated by the vector addition of bond moments as a function of azimuthal angle of internal rotation. The moments of the bonds C—Cl, H—C and C=O were taken as 1·56, 0·3 and 2·5 $\times$ 10^{-18} e.s.u. respectively, and the origin of the azimuthal angle was taken at the *cis* position with respect to the O and H atoms. In the

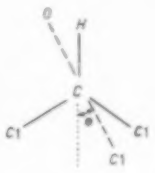

Fig. 2.

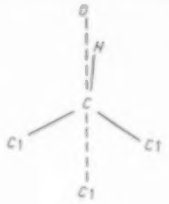

Fig. 3.

second place the normal vibrations of the molecule were calculated on the basis of the Urey–Bradley potential function [1, 10]:

$$V = \sum_i \tfrac{1}{2} K_i (\Delta r_i)^2 + \sum_{ij} \tfrac{1}{2} H_{ij} r_i^0 r_j^0 (\Delta \alpha_{ij})^2 + \sum_{ij} \tfrac{1}{2} F_{ij} (\Delta q_{ij})^2 + \text{linear terms}$$

where r_i and r_j are bond lengths with equilibrium values r_i^0 and r_j^0; α_{ij} bond angles and q_{ij} distances between non-bonded atoms. In addition K, H and F represent

Table 2. Calculated dipole moment μ of $CHCl_2COCl$

Azimuthal angle (°)	μ (10^{-18} e.s.u.)
0	1·43
30	1·50
60	1·68
90	1·86
120	2·80
150	2·21
180	2·26

stretching bending and repulsive force constants, respectively. The values of these constants are shown in Table 3 together with the equilibrium values of bond distances and bond angles.

The calculation was made for molecular forms with azimuthal angles of 0°, 90° and 180°, and the result is shown in Table 4. It is seen that the frequencies calculated for the molecular form with azimuthal angle 0° agree with those observed for the less polar form and, furthermore, the calculated dipole moment (shown in Table 2) is less in this position. Therefore, it can be concluded that the less polar form is not much different from the *cis*-form, even it it is not exactly so.

In order to determine the configuration of the more polar form, we made use of the sum and product rules of rotational isomers derived in our previous papers [1, 2]. The former is expressed as:

$$\sum r_{\mathrm{LP}}^2 = \sum r_{\mathrm{MP}}^2 \qquad (1)$$

VOL. 13 1958/5

Table 3. Values of force constants and molecular constants

Force constant (mdyn/Å)	Bond distance (Å)	Bond angle
K(C—Cl) = 1·75	r(C—Cl) = 1·76	α(∠Cl—C—O) = 125°
K(C=O) = 11·0	r(C—H) = 1·09	α(∠Cl—C(O)—C) = 110°
K(C—H) = 3·9	r(C—C) = 1·54	α(∠O—C—C) = 125°
K(C—C) = 2·8	r(C=O) = 1·22	other angles = 109° 28′
H(H—C—Cl) = 0·05		
H(Cl—C—Cl) = 0·1		
H(Cl—C—C) = 0·2		
H(H—C—C) = 0·15		
H(Cl—C=O) = 0·3		
H(C—C=O) = 0·4		
H(C—CO—Cl) = 0·1		
F(Cl . . . H) = 0·8		
F(Cl . . . Cl) = 0·65		
F(Cl . . . C) = 0·6		
F(C . . . . H) = 0·4		
F(Cl . . . O) = 1·0		
F(O . . . . C) = 0·4		
$F' = -\frac{1}{10} F$		
κ = 0·1 mdyn/Å		

Table 4. Calculated and observed frequencies (cm^{-1}) of $CHCl_2COCl$

Observed		Calculated		
More polar form	Less polar form	$\theta = 0°$	$\theta = 90°$	$\theta = 180°$
3002	3002	2937	2935	2936
1808	1772	1743	1750	1745
1262	1233	1250	1253	1250
1201	1215	1181	1187	1193
988	1037	1088	1081	1043
808	782	794	837	765
754	734	761	722	761
580	631	595	649	727
461	503	529	516	491
	409	396	371	383
338	(406)	383	310	339
264	264	264	258	242
237	176	161	155	212

and the latter as

$$|G(\theta)|/|G(0^\circ)| = \Pi\nu_{\mathrm{MP}}^2/\Pi\nu_{\mathrm{LP}}^2 \qquad (2)$$

Here ν_{LP} and ν_{MP} denote the normal frequencies of the less polar and more polar forms, respectively and G the kinetic energy matrix. G is calculated from the geometrical form of the molecule and consequently depends on the azimuthal angle θ of internal rotation. In Table 5 are shown the values of the ratio $|G(\theta)|/|G(0^\circ)|$, or the left-hand side of equation (2), calculated for different θ.

Table 5. Ratio of G-matrices on azimuthal angle

θ	$\lvert G(\theta)\rvert/\lvert G(0^\circ)\rvert$
0°	1·000
30°	1·011
90°	0·570
120°	0·755
150°	0·761
180°	1·197

For the evaluation of right-hand side of the equation, all the normal frequencies must be known. Actually, however, one frequency of the more polar form remains undetermined. Since this is the only unknown frequency, this can be determined by the use of the sum rule of equation (1). Thus the frequency is found to lie in the region from 300 to 450 cm^{-1}.

There is no reason to believe that the corresponding Raman line is so weak as to escape detection. Therefore, it is probable that this and one of the observed lines overlap each other. There are two lines 338 and 461 cm^{-1} in the above-mentioned region observed in the solid spectrum which is assigned to the more polar form. If we take the line at 338 cm^{-1}, the right hand side of equation (2) is calculated as 0·611 and the azimuthal angle θ is found to be 90°. If however, we take the line at 461 cm^{-1}, the right-hand side of equation (2) is calculated as 1·136 and θ is found to be 180°.

Of the two forms with $\theta = 90^\circ$ and 180°, the former is more probable as the more polar form, because in the form with $\theta = 180^\circ$, the H atom is in the *cis*-position with respect to one of the Cl atoms. Such a form has not been found to be stable for the molecules so far studied in this laboratory.

Recently Morino, Kuchitsu and Hirota have made electron diffraction investigation on gaseous dichloroacetyl chloride [12]. The result can also be accounted for by the coexistence of two forms with $\theta = 0^\circ$ and 90°.

References

[1] Mizushima S., *Internal Rotation*. Academic Press, New York 1954.
[2] Nakagawa I., Ichishima I., Kuratani K., Miyazawa T., Shimanouchi T. and Mizushima S., *J. Chem. Phys.* 1952 **20** 1720.
[3] Mizushima S., Shimanouchi T., Miyazawa T. and Shido N., *J. Chem. Phys.* 1953 **21** 815.
[4] *Organic Synthesis* (Collective Volume) 1948 181.

VOL.
13
1958/5

[5] Boesken M. J., *Rec. Trav. Chim.* 1910 **29** 85.
[6] Cheng H. C., *Z. phys. Chem.* 1934 **B26** 288.
[7] Watanabe I., Mizushima S. and Mashiko Y., *Sci. Pap. Inst. Phys. Chem. Res. Tokyo* 1943 **40** 425.
[8] Mizushima S. and Okazaki H., *J. Amer. Chem. Soc.* 1949 **71** 3411.
[9] Shimanouchi T., Tsuruta H. and Mizushima S., *Sci. Pap. Inst. Phys. Chem. Res. Tokyo* 1946 **42** 165.
[10] Shimanouchi T., *J. Chem. Phys.* 1949 **17** 245.
[11] Mizushima S., Shimanouchi T., Nakagawa I. and Miyake A., *J. Chem. Phys.* 1953 **21** 215.
[12] Morino Y., Kuchitsu K. and Hirota E., Private communication.

OL.
13
8/59

Spectrochimica Acta, 1958, Vol. 13, pp. 168 to 179. Pergamon Press Ltd., London. Printed in Northern Ireland

Apparent rectification in Tesla sparks

D. A. Sinclair and R. N. Whittem
Australian Defence Scientific Service, Defence Standards Laboratories,
Department of Supply, Sydney, Australia

(*Received* 23 *April* 1958)

Abstract—Pulses of electric current and vapour ejection in the secondary gap of a Tesla spark system are found to be asymmetric to a degree far greater than is commonly observed in simple sparks. The magnitude and direction of the apparent rectification varies with the setting of the gap width. A satisfactory explanation can be derived from elementary circuit analysis. It is shown that over 50 per cent of the original energy in the primary condenser may appear as non-oscillatory current in the secondary circuit. The conditions that favour the appearance of a large d.c. component are delineated.

The coupling system of Fig. 1 shows a well-known method of introducing a trigger spark into an arc circuit for the purpose of igniting a low-voltage arc discharge. While experimenting with a system of this kind we found that, with the trigger spark only being energized and sparks occurring fifty times per sec, an abnormally bright flash occurred at S_2 every 2–3 sec. Investigation showed that condenser C_4 was being charged in accumulative small steps until it reached a potential of about 100 V, whereupon it discharged through S_2. If the resistance R_1 were increased to about 50 Ω, the charging steps were reduced in size, but the ultimate voltage attained by C_4 was raised to about 400 V. The rate of charging of C_4, and even the direction of charging, could be varied merely by making small adjustments to the width of the gap S_2. As S_2 was progressively widened from zero the charging first increased then decreased and finally reversed direction just before maximum sparking length was reached.

Photographs taken through a rotating mirror showed marked asymmetry in the ejection of luminous vapour from the electrodes of the gap S_2. Examples are shown in Fig. 2. For these photographs C_3 was short-circuited. As gap S_2 was widened the extent and direction of bias passed through a sequence of variation analogous to that observed in the charge transfers.

Since under the conditions of the experiment the polarity of C_1 was the same at every spark initiation one might expect a net transfer of charge in the secondary circuit owing to the transfer in the primary. We found, however, that the amounts of charge being transferred in the secondary circuit were as much as fifteen times as great as that calculated from this consideration and moreover the direction of transfer was often opposite to that predicted.

Asymmetry and some degree of rectification may sometimes be observed when the two electrodes of a spark differ in composition or in shape. Experiment with different electrodes showed that these factors had no significant bearing on our observations.

Oscilloscope observations on the rectifying sparks indicated that the current pulse in the secondary winding consisted of a rapidly damped oscillation lasting

VOL.
13
1958/5

about 2 μsec superposed on a unidirectional component, the latter persisting for several times the duration of the oscillatory current and decaying in linear fashion at a rate corresponding to a constant damping voltage of the order of 50–100 V. Unfortunately we were not able to photograph oscillograms from this circuit in which the frequency of oscillation was about 5 Mc/s. However, we have since

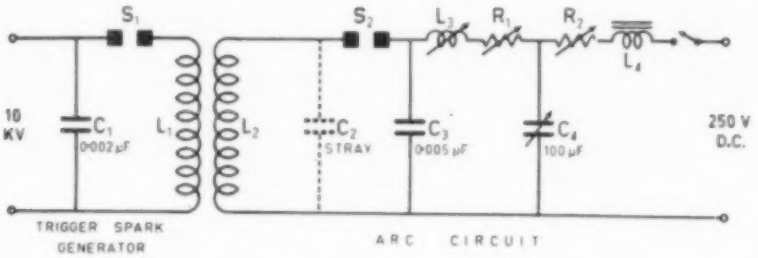

Fig. 1. Circuit of a spark-triggered pulsed-arc source.

obtained clearer oscillograms from a lower-frequency circuit in which the main elements of the phenomenon were reproduced. Examples are given in Figs. 4 and 5.

The experimental low-frequency circuit was as shown in Fig. 3 with the addition of small resistances between L_2 and C_2 and between L_1 and C_1 to provide C.R.O. tappings. Values of the circuit components were C_1, 0·03 μF, L_1, 80 μH,

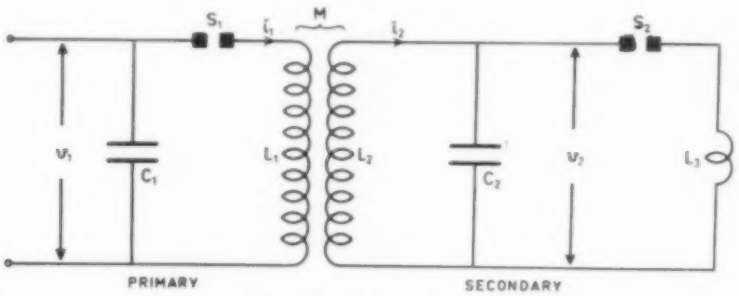

Fig. 3. Basic Tesla circuit.

L_2, 1100 μH, M and C_2 variable. The condenser C_2 in this circuit corresponds to the stray capacitance (also labelled C_2) in Fig. 1. With this circuit primary spark oscillations had a frequency of the order of 100 kc/s.

The oscillograms shown are all single sweep traces triggered by the breakdown at S_1. Because of an instrumental fault the trace in the first few microseconds is distorted and again when S_2 breaks down the trace is obscured for short periods by the reaction from the discharge of C_2 through S_2. In general, however, the following four phases in the secondary current pulse are clearly discernible:

(a) Between the breakdowns of S_1 and S_2 the current follows a two-frequency wave form;

(b) After breakdown of S_2 there follows: (i) A short-lived, high-frequency oscillatory pulse corresponding to the discharge of C_2 through S_2 reacting slightly

on the tapped loop; (ii) A longer-lived, lower-frequency, oscillatory pulse of single-frequency wave form similar to that obtained when S_2 is initially closed, obviously induced from the residual oscillations in the primary circuit; (iii) A unidirectional current commencing at the same time as (b, i) and (b, ii) and decaying linearly to zero.

The oscillograms in Fig. 4 are from sparks of five different kinds obtained by varying the length of S_2 using a circuit with moderate coupling. No spark occurs at S_2 in the top and bottom rows. In the other three the non-oscillatory current is in the same direction despite the different directions of i_2 and of v_2 at the instant of S_2 breakdown. In the middle row phase (b, ii) is absent; this is a special case to be commented on later.

The oscillograms in Fig. 5 are from a loosely coupled combination. They illustrate reversal of the non-oscillatory current as S_2 is widened and also that, with a fixed setting of S_2 near the limit (2·6 mm), the variation in the sparking point is accompanied by considerable variation in the non-oscillatory current without much variation in the other phases.

Theoretical analysis

It is remarkable that although the Tesla spark system has been in use for nearly 70 years we have not been able to find a thorough analysis of it in the literature. References to early work are given by Boynton [1]. Among later contributors are Drude [2], Pernot [3], Taylor-Jones [4], Calvert and Llewellyn Jones [5]. A short summary is given by Robinson [6]. Practically all workers have been interested mainly in the voltage attainable in the secondary circuit and have concentrated on that aspect. Very little attention has been given to the currents flowing after the breakdown of the secondary gap, despite the fact that, almost invariably, a substantial proportion of the energy available remains after the discharge of the secondary condenser.

The only reference we have seen to a non-oscillatory component in the Tesla spark current is by Boynton [1], who made passing reference to it, but did not develop an adequate analysis. He was probably correct in attributing the blurring of his spark photographs to a persisting current, but apparently did not realize how it may also have explained a puzzling feature of his measurements of secondary current. Further analysis would have shown that with the initial conditions as stated in his theoretical treatment the non-oscillatory current would have been zero.

A non-oscillatory component is well-known in the closely similar system known as the induction coil which differs from the Tesla in that the initial energy is in the form of a d.c. current in the primary circuit and, in general, operates at lower oscillation frequencies and lower secondary current—usually below stable arc current. Observations on secondary currents in an induction coil were made by Colley [7] and recently oscillograms were published by Kimura and Kumagai [8]. Llewellyn Jones [9, 10] qualitatively described the prolongation of arcing that sometimes occurs after the condenser discharge in a magneto-charged or a transformer-charged spark system. The current in this arcing may be unidirectional, but is not regarded as non-oscillatory current as it is part of a cycle of

VOL. 13 1958/5

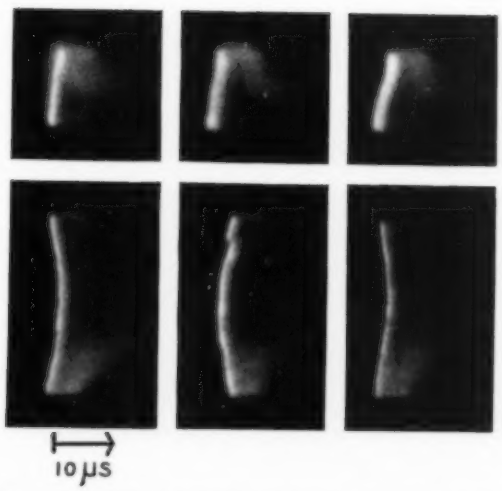

Fig. 2. Rotating-mirror photographs of sparks at secondary gap. Polarity of charging and all settings are identical except length of S_2, which for top row was 2·5 mm and for bottom row 5·5 mm.

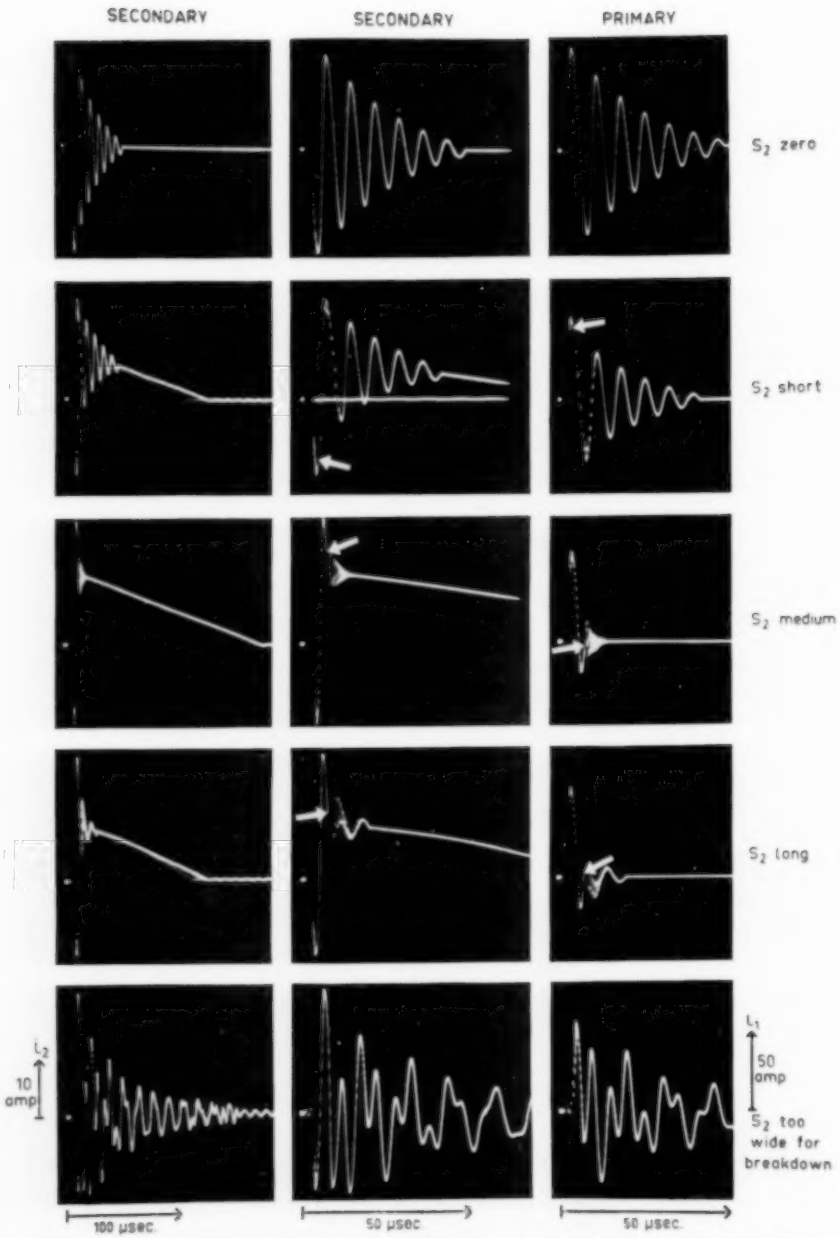

Fig. 4. Current–time oscillograms from experimental Tesla circuit with moderate coupling ($M^2/L_1L_2 = 0{\cdot}53$ and $C_2L_2/C_1L_1 = 0{\cdot}83$). Each row of three is from substantially the same discharge. Sweep starts when S_1 breaks down and arrow indicates point on trace where breakdown of S_2 occurs.

VOL. 13 1958/5

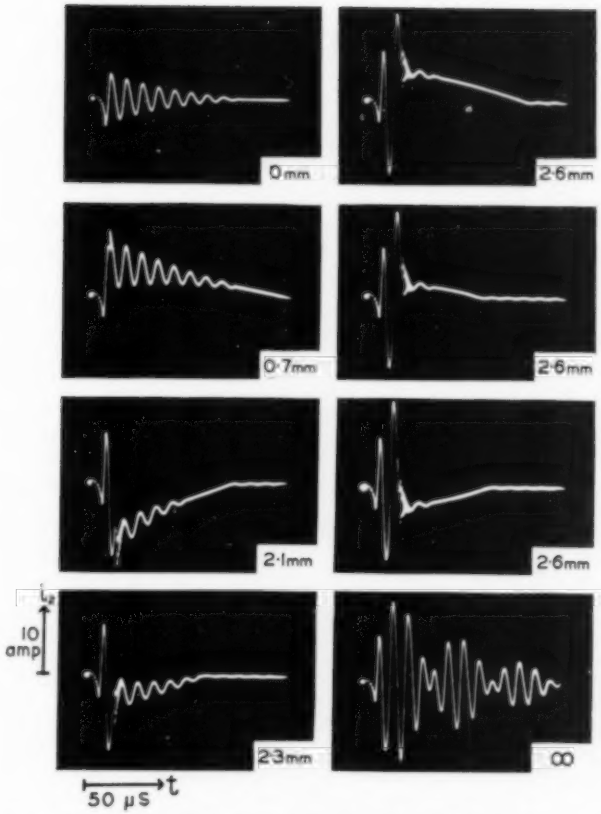

Fig. 5. Current–time oscillograms from experimental Tesla circuit with loose coupling ($M^2/L_1L_2 = 0{\cdot}055$ and $C_2L_2/C_1L_1 = 0{\cdot}83$). Frame labels indicate lengths of S_2.

VOL.
13
1958/5

low-frequency oscillatory current that is cut off as the wave passes through zero. (It will be clear later that these "arc phase" currents also contain a small non-oscillatory component.) In a Tesla system, however, the frequencies of oscillation are of a higher order and arcing usually proceeds until virtually the whole of the energy in the system is dissipated. One does not expect a non-oscillatory component in it, and in fact there is none if the secondary gap is very short or if it breaks down instantaneously with the primary gap, as might happen if the secondary capacitance were negligibly small.

The natural evolution of thinking about the currents in a Tesla secondary discharge is then somewhat as follows. First, ignoring stray capacity in the wiring the secondary current is pictured as a simple damped oscillation—a reduced replica of that in the primary circuit. Second stage, stray capacity is taken into account and the current is pictured as two damped oscillations superposed, (a) that originating from the discharge of C_2 and (b) that induced by the residual oscillation in the primary circuit. For an adequate picture one must proceed to a third stage and take into consideration energy which, at the instant when S_2 breaks down, is resident in the inductance L_2 and is not reflected back to the primary circuit, but appears as a non-oscillatory component of the secondary discharge current. This energy is commonly of major proportions and, as will be shown, may be greater than the combined energies residing in C_2 and in the primary circuit.

In this discussion we shall use symbols as indicated in Fig. 3, neglect damping and regard the spark gaps as equivalent to perfect switches.

As has been shown by many previous workers (and derived more simply in the Appendix), immediately after the breakdown of S_1 the currents i_1, i_2 in the coils of a Tesla transformer follow a two-frequency wave form as expressed in the following equations:

$$i_1 = A_1 \sin \alpha t + B_1 \sin \beta t \tag{1}$$

$$i_2 = A_2 \sin \alpha t + B_2 \sin \beta t \tag{2}$$

where t is the time after breakdown of S_1; $\pm j\alpha$, $\pm j\beta$ are the roots of the auxiliary equation to the controlling differential equation; A_1, A_2, B_1, B_2 are constants determined by circuit values and initial conditions.

When S_2 breaks down C_2 ceases to react on the rest of the system. (It is immaterial whether one regards the voltage across C_2 as dropping immediately to zero or as commencing to oscillate at a higher order of frequency about a mid-point of zero.) Distinguishing by dash marks the currents after S_2 breaks down, i_1' and i_2' take up a single-frequency wave form expressible thus:

$$i_1' = V_1 C_1 \gamma \sin \gamma(t - T) + I_1 \cos \gamma(t - T) \tag{3}$$

$$i_2' = i_1' \, \mathrm{M/L_2} + Y \tag{4}$$

where $$\gamma = [C_1 L_1 (1 - M^2/L_1 L_2)]^{-1/2}$$

and $$Y = I_2 - I_1 M/L_2 \tag{5}$$

The constants V_1, I_1, I_2, T are the respective values of v_1, i_1, i_2, t at the instant when S_2 breaks down. The constant Y represents a non-oscillatory component in

i_2'; but no such component appears in i_1'. In the equation (5) the negative sign applies only if the convention is adopted that a positive change in i_1 tends to produce a positive change in i_2.

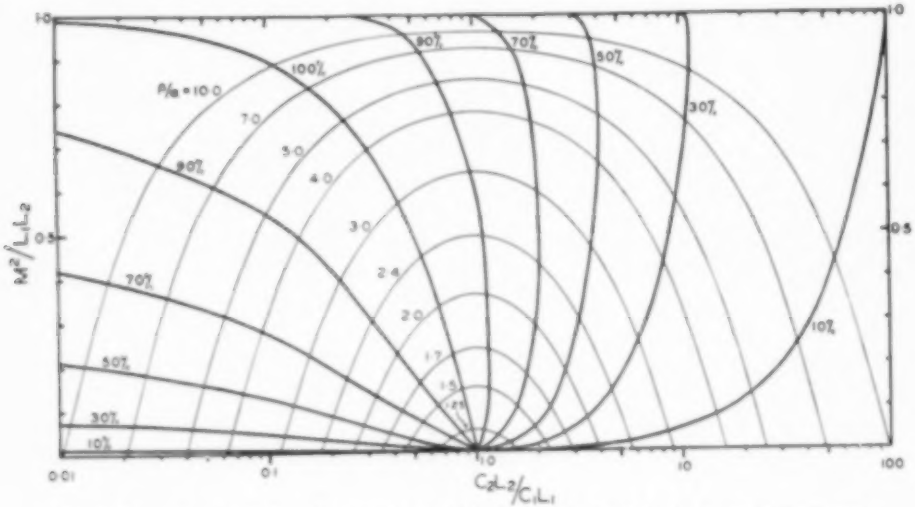

Fig. 6. Curves showing the relationship to M^2/L_1L_2 and C_2L_2/C_1L_1 of β/α (thin lines) and amplitude of y (thick lines), the latter being expressed as a percentage of $V_0C_1^{1/2}/L_2^{1/2}$ in the curve labels.

For further analysis it is helpful to define a variable y, representing the potential value of Y at time t (that is, the value Y would have if S_2 broke down at time t). y varies with t according to the equation:

$$y = i_2 - i_1 M/L_2$$
$$= (A_2 - A_1 M/L_2) \sin \alpha t + (B_2 - B_1 M/L_2) \sin \beta t$$

By inserting the values of A_1, A_2, B_1, B_2 derived in the Appendix and rearranging, this equation can be written:

$$y = UX[(\beta \sin \alpha t - \alpha \sin \beta t)/(\alpha + \beta)] \qquad (6)$$

where $U = V_0C_1^{1/2}/L_2^{1/2}$, the maximum value of y set by energy limitations:

$$X = K/[1 + H^2 - 2H(1-K^2)^{1/2}]^{1/2}$$

where $K^2 = M^2/L_1L_2$ and $H^2 = C_2L_2/C_1L_1$. X represents the relative amplitude of y, (relative to U), while the square brackets in equation (6) enclose an oscillating factor of amplitude unity. It is clear that the wave form is determined solely by β/α, though the frequencies are dependent on the absolute values of α and β.

Figure 6 shows the relationship between β/α and the circuit parameters K^2 and H^2. The value of β/α is conveniently derived from the identity:

$$\beta^2/\alpha^2 = (1 + N)/(1 - N)$$
$$\text{where } N^2 = 1 - 4H^2(1 - K^2)/(1 + H^2)^2$$

Figure 6 also includes curves showing the values of X at various combinations of K^2 and H^2.

VOL. 13 1958/5

Obviously X can not be greater than unity; it equals unity when $H^2 = 1 - K^2$. If this latter condition is met then it appears that all of the energy originally present in C_1 can be converted to a non-oscillatory current in the secondary circuit which may be only loosely coupled with the primary. This would be possible only if S_2 were closed at a time when, *inter alia*, the voltage across C_2 was zero. That is to say, it could not happen in a spontaneously sparking system; a switching device would be required. Oscillations would cease forthwith in both primary and secondary loops. Though in a spontaneously sparking system some energy must reside in C_2 when S_2 breaks down it is possible, with an appropriate combination of circuit values, to achieve a somewhat similar effect, i.e. immediate cessation of oscillations in primary and secondary windings when S_2 breaks down. An example is shown in Fig. 4 ("S_2 medium"). The condition for this to happen is that S_2 breaks down when all of the energy in the system is located in C_2 and L_2. To put it in another way, when I_1 and V_1 are both zero it will be seen from equations (3) and (4) that i_1' must also be zero and i_2' will equal I_2 and contain no oscillatory component.

Further exploration of the possibilities in a spontaneously sparking system can be made by comparing graphically equation (6) with that for v_2 which is:

$$v_2 = WZ\,[\tfrac{1}{2}(\cos \alpha t - \cos \beta t)] \tag{7}$$

where

$$W = V_0\, C_1^{1/2}/C_2^{1/2}$$
$$Z = [1 + (1 - H^2)^2/4H^2K^2]^{-1/2}$$

Analogously with equation (6), W is the value v_2 would have if all the energy in the system were located in C^2, Z represents the relative amplitude factor and the square bracketed factor in equation (7) gives the wave form, again determined solely by β/α.

In Fig. 7 are shown the wave forms of y and v_2 for three values of β/α. (The relative amplitudes, 1 and 2, are arbitrarily chosen for convenience of display.) The rippled long wave forms are typical of high values of β/α while the beat-type forms are typical of low values of β/α.

The thickened portions of the y curves correspond to those regions where spontaneous breakdown of S_2 may normally be expected, that is, where the magnitude of v_2 is greater than at any earlier point. The actual point of breakdown is primarily determined by the relative gap settings, but because of variations in surface conditions and in gas-ionization the spark point with any particular gap setting is liable to considerable meandering from its mean position and indeed it may occasionally go beyond the regions marked, i.e. to where the voltage is lower than at some earlier time. This erratic behaviour is particularly marked when S_2 is near the limit as is illustrated in the 2·6 mm settings of Fig. 5. Subject to those qualifying remarks, however, the regions marked on Fig. 7 are for most practical purposes the significant ones in a spontaneously sparking system and values of y inside these regions will be called the realizable or attainable values of Y.

The curves show that as S_2 is widened from zero y increases very slowly at first and then more steeply as v_2 approaches its first maximum. When the sparking

point jumps to the reverse polarity y is still in the same sense as before, but falling. In the example where $\beta/\alpha = 1{\cdot}33$, y passes through zero and reverses sign, while v_2 is still rising to its second numerical maximum. It is not universal for the realizable Y to reverse sign and sometimes, even when the undamped curves indicate that

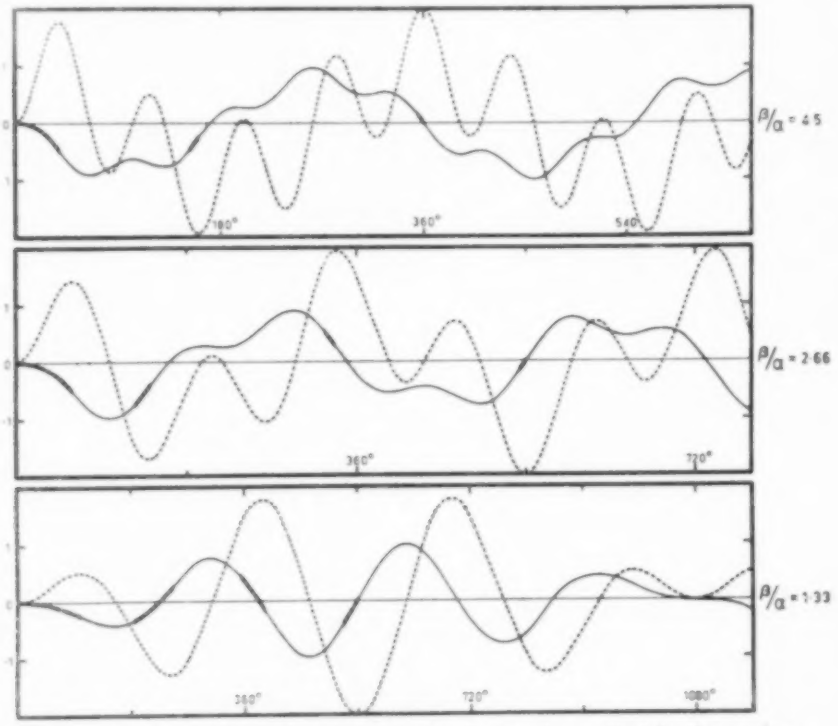

Fig. 7. Examples of wave-forms of v_2 (dotted line) and y (continuous line) for three values of β/α. Amplitudes are arbitrary and abscissae are marked in degrees of the longer cycles. Thickened portions of the y curves indicate the normal sparking regions.

it should do so, a small appearance (as in the last spark region in the example where $\beta/\alpha = 4{\cdot}5$) would probably be eliminated in practice by damping.

It is of interest to determine under what circumstances Y attains its highest relative value in a spontaneously sparking system. We have already shown that the amplitude of y is highest when $C_2L_2/C_1L_1 = 1 - M^2/L_1L_2$. It remains to establish what shape of curve (or value of β/α) is the optimum and at what point in the curve the highest fraction of the amplitude is attained by any portion of the sparking regions. By inspection we find that the highest value of y in any sparking region is always at either the end or the beginning, that is, either at a maximum value of v_2 or at a point where the next sparking region begins. In Fig. 8 are drawn curves plotting against β/α the relative value of y at the limits of sparking regions. The curve A, referring to the first maximum of v_2 has a simple form with a single maximum where $\beta/\alpha = 2{\cdot}9$. The other curves, however, consist of a series of disjointed sections, the pairs B–C, D–E and F–G forming loops of complex shape.

Only the first members of numerous D–E and F–G loops are drawn. Succeeding members are of academic interest only since they correspond to late sparking points which would not be attained in practical circuits and in any case at no point do they exceed the highest point of curve B.

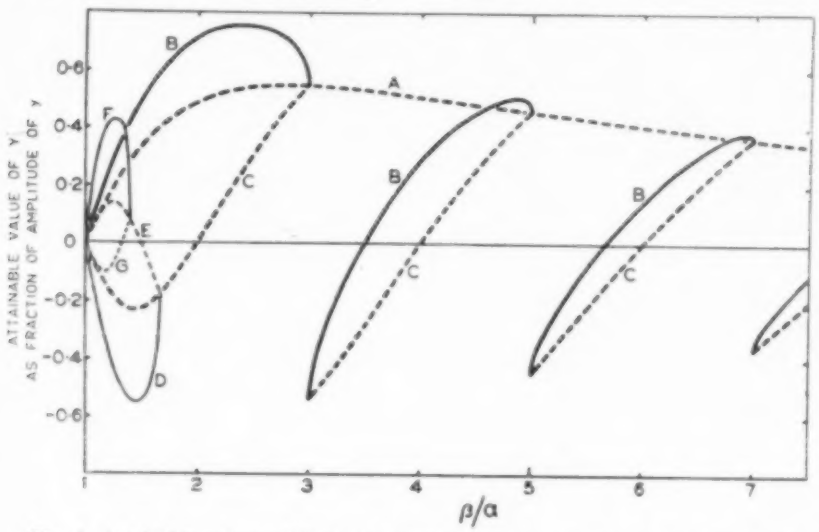

Fig. 8. Attainable values of Y at the boundaries of spark regions; A at end of first, B beginning of second, C end of second, D beginning of third and so on.

It is clear from Fig. 8 that the highest relative value of Y is obtained when β/α has a value near 2·4 and when sparking occurs at the beginning of the second region, i.e. when S_2 breaks down at a voltage just exceeding the first numerical maximum of v_2. Y then has a value 0·75 of the amplitude of y. Combining this condition with the criterion for maximum amplitude of y we find that the optimum combination is $M^2/L_1L_2 = 0{\cdot}45$ and $C_2L_2/C_1L_1 = 0{\cdot}55$ (i.e. where, in Fig. 6, the 2·4 β/α curve intersects the 100 per cent y amplitude curve). With such a combination the fraction of the original energy in C_1 that may appear as non-oscillatory current in L_2 is $0{\cdot}75^2$, or 56 per cent.

Figure 8 was used further in conjunction with the curves in Fig. 6 to produce contour lines as in Fig. 9 showing the general features of a diagram relating the parameters M^2/L_1L_2 and C_2L_2/C_1L_1 to the limits of realizable conversion of energy to d.c. current in the secondary circuit. The discontinuities in these contour lines correspond to transitions from curve A to curve B in Fig. 8. The broken-line appendages to the 25 per cent and 10 per cent contour lines apply if spark points corresponding to curves D and F in Fig. 8 are taken into account.

General discussion

The effects of damping on the individual voltage and current curves are readily pictured. It is not quite so obvious how it would affect the complex structure of curves that have been derived in this paper from considering sparking regions only, because phase changes are involved as well as two exponential decay factors.

However, in a few theoretical curves allowing for resistive damping we have not found any spectacular changes in, for instance, the energy conversion to d.c. current at points of most interest.

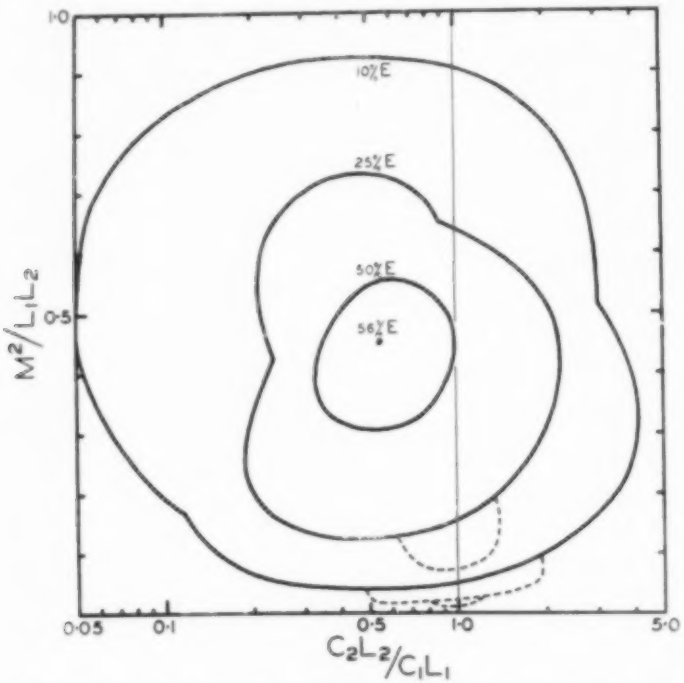

Fig. 9. Contour lines of a diagram showing the relationship of the highest attainable values of y in a spontaneously sparking system to the parameters M^2/L_1L_2 and C_2L_2/C_1L_1. Line labels indicate the percentage of the total energy in the system which can appear as non-oscillatory current in $L_3(=100Y^2/U^2)$.

This, together with the fact that we are concerned mainly with spark points early in the oscillatory train, makes us confident that the simple theory outlined gives a fairly adequate guide to the significant features of the phenomena discussed. We have at least found it successful in predicting the appropriate combination of circuit elements required to secure the oscillogram types shown in Figs. 4 and 5.

It is clear that in a Tesla spark system a substantial fraction of the energy is likely to be dissipated in the form of a non-oscillatory current in the secondary circuit. This is particularly so with a coupling coefficient of the order of 55–75 per cent (i.e. $K^2 = 0{\cdot}3$ to $0{\cdot}55$) and with the secondary capacitance of about 30–100 per cent of tuning value. Values in these ranges are quite commonly encountered in practical constructions, intentionally or otherwise.

For spectrographic purposes a Tesla spark source must be used with caution because of the pronounced effects which the asymmetry of current can have on the emission from electrodes of different materials.

Other observations which the recognition of the d.c. component has helped us to explain are:

VOL. 13 1958/5

(a) Ignition of an arc discharge using a circuit of Fig. 1 type has been found sometimes to fail at moderate gap settings though ignition was readily effected at both shorter and longer settings of the secondary gap. This effect disappeared when the polarity of either the arc or the trigger spark was reversed. The explanation is that the d.c. tail was in the first place opposite in direction to that of the arc current to be established.

(b) By-pass condensers in situations corresponding to C_3 in Fig. 1 have been found to fail unexpectedly. It has been found that C_3 attains much higher voltages than calculated from the oscillatory currents alone. Obviously the energy in the non-oscillatory component can lead to substantial charging of C_3.

(c) Shocks received from a Tesla circuit have been greater than expected and were found to vary in a mysterious way when gap-lengths were changed. The mystery vanishes when changes in the non-oscillatory component are recognized. This will be discussed elsewhere.

It should be recognised too that a non-oscillatory component of current is likely to be encountered whenever a spark gap is bridged by an inductive impedance as, for example, in a series-gap circuit of the type described by LEVY [11] and others. In these circuits, however, the proportionate amount of energy in the non-oscillatory component should be quite small because the coupling and stray capacitance are likely to be remote from optimum values. Another example of interest is WALSH's [12] trigger circuit in which the blocking condenser in the secondary appears at first sight to block the d.c. component. It does block that arising in the secondary of the HF transformer, but it must be realized that the arc gap is effectively bridged by another inductance with its stray capacitance and hence an asymmetric trigger spark is possible in that circuit also, though probably less pronounced than in our Fig. 1 circuit.

Acknowledgements—We are grateful to Mr. W. M. HARPER for assistance with the mathematics and to Professors C. J. MILNER and F. LLEWELLYN JONES for criticism. The paper is published with the permission of the Chief Scientist, Australian Defence Scientific Service, Department of Supply, Melbourne, Australia.

Appendix

Short derivation of equations relating to Tesla circuit

Using the symbols of Fig. 3 to denote circuit values in any self-consistent fundamental units and t for the time after closing S_1 (S_2 remaining open) one obtains by successive differentiation of the basic simple equation relating the circuit values the following fourth order differential equation:

$$(1 - M^2/L_1L_2)D^4i_1 + (1/C_1L_1 + 1/C_2L_2)D^2i_1 + i_1/C_1L_1C_2L_2 = 0 \qquad \text{(I)}$$

where D^ni_1 represents the nth differential coefficient of i_1 with respect to t. An exactly similar equation is obtained for any of the variables i_2, v_1, v_2 in place of i_1. If resistances are taken into account Di_1 and D^3i_1 would appear in the equation.

The general solution of (I) can be written in the form:

$$i_1 = A \sin \alpha t + B \sin \beta t + F \cos \alpha t + G \cos \beta t \qquad \text{(II)}$$

where A, B, F, G are constants and $\pm j\alpha$, $\pm j\beta$ are the roots of the auxiliary equation to (I).
If we write for abbreviation:

$$m = 1 - M^2/L_1L_2$$
$$p = (1/C_1L_1 + 1/C_2L_2)/m$$
$$q = (p^2 - 4/C_1L_1C_2L_2m)^{1/2}$$

then $2\alpha^2 = p - q$ and $2\beta^2 = p + q$.

By differentiating (II) to the third stage and substituting values holding when $t = 0$, viz. $v_1 = V_0$, $v_2 = 0$, $i_1 = 0$, $i_2 = 0$ and derivatives $Di_1 = V_0/L_1m$, $D^2i_1 = 0$, $D^3i_1 = (1/C_2L_2 - p)V_0/L_1$ we obtain:

$$A = V_0(1/C_2L_2 - \alpha^2)/\alpha L_1qm$$
$$B = V_0(\beta^2 - 1/C_2L_2)/\beta L_1qm$$
$$F = 0 \text{ and } G = 0$$

Similarly the equations for i_2, v_1, v_2 may be derived and the values of the corresponding constants are

for i_2: $A = -V_0M\alpha/L_1L_2qm$
$B = -A\beta/\alpha$
$F = 0$ and $G = 0$

for v_1: $A = 0$ and $B = 0$
$F = V_0(\beta^2 - 1/C_1L_1m)/q$
$G = V_0(1/C_1L_1m - \alpha^2)/q$

for v_2: $A = 0$ and $B = 0$
$F = -G = V_0M/L_1L_2C_2qm$

The foregoing equations hold while S_1 is closed and S_2 is open. After S_2 is closed at a time when $t = T$ the variables will be distinguished by dash marks. The values of i_1, i_2, v_1 at time T (or $t' = 0$) will be designated I_1, I_2, V_1 respectively. The secondary circuit becomes a slave loop in which the driving voltage is Mdi_1'/dt' acting upon the reactance L_2. Therefore $di_2'/dt' = (M/L_2)di_1'/dt'$ from which one immediately obtains by integration the relation:

$$i_2' = i_1'M/L_2 + Y$$

where Y is a constant which, from the values of i_2' and i_1' at the time when $t' = 0$, is equatable to $(I_2 - I_1M/L_2)$.

It is readily shown that the primary loop behaves as though L_1 were replaced by an inductance of value $L_1(1 - M^2/L_1L_2)$ and the equation for i_1' becomes:

$$i_1' = P \sin \gamma t' + Q \cos \gamma t'$$

where

$$\gamma = (C_1L_1m)^{-1/2}$$

VOL. 13 1958/5

and by considering values of i_1' and di_1'/dt' when $t' = 0$ the constants P and Q may be evaluated as:

$$P = V_1 C_1 \gamma \quad \text{and} \quad Q = \mathrm{I}_1$$

t' may be written as $(t - T)$ as in equation (3) in the main text.

References

[1] Boynton W. P., *Phil. Mag.* 1898 **46** 312.
[2] Drude P., *Ann. Phys., Lpz.* 1904 **13** 512.
[3] Pernot F. E., *Univ. Calif. Publ. Engng.* 1916 **1** 8 161.
[4] Taylor-Jones E., *The Theory of the Induction Coil.* Pitman, London 1921.
[5] Calvert W. J. R. and Llewellyn Jones F., *Report No.* EL. 1339. Royal Aircraft Establishment, Farnborough 1944.
[6] Robinson A. W., *Electr. Engng. Trans.* 1944 **63** 916.
[7] Colley R., *Ann. Phys. Chem.* 1891 **44** 109.
[8] Kimura I. and Kumagai S., *J. Phys. Soc. Japan* 1956 **11** 599.
[9] Llewellyn Jones F., *Report No.* EL. 1336. Royal Aircraft Establishment, Farnborough, 1945.
[10] Llewellyn Jones F., *J. Soc. Chem. Ind.* 1945 **64** 317.
[11] Levy S., *J. Opt. Soc. Amer.* 1945 **35** 221.
[12] Walsh A., *Metal Industry* 1946 **68** 243.

OL.
3
3/59

Spectrochimica Acta, 1958, Vol. 13, pp. 180 to 191. Pergamon Press Ltd., London. Printed in Northern Ireland

Rotational analysis and upper-stage transitions of parallel absorption bands in benzene, *sym*-benzene-d_3, benzene-d_6 and pyridine

A. Danti and R. C. Lord
Spectroscopy Laboratory, Massachusetts Institute of Technology, Cambridge 29, Mass., U.S.A.

(*Received* 26 *May* 1958)

Abstract—Parallel bands in the infrared spectra of benzene, *sym*-benzene-d_3, benzene-d_6 and pyridine have been studied at a resolution of 0·3 cm^{-1} or slightly better. The rotational lines were readily resolved for the bands of benzene and pyridine and measured with a precision of about $\pm$0·04 cm^{-1}. Analysis of the data leads to values for the rotational constant B'' of 0·18965 $\pm$ 0·00010 and 0·19676 $\pm$ 0·00012 cm^{-1} for benzene and pyridine, respectively, and for the distortion constant D_J of 1·2 and 0·5, both times 10^{-6} cm^{-1}. These are in good agreement with values obtained from Raman and microwave spectra except for D_J in pyridine, for which the infrared value is believed to be more nearly correct. The bands in *sym*-benzene-d_3 and benzene-d_6 were less cleanly resolved, but a value for B'' of 0·1733 $\pm$ 0·001 cm^{-1} for the former agrees reasonably well with the Raman value. The Q-branches of these bands have extensive structure due to upper-stage vibrational transitions ("hot bands"). The components of the Q-branches have been assigned in a plausible fashion on the basis of the observed intensities and those expected from the Boltzmann factors. A symmetrical grouping of certain of these components about the principal Q-branch is also pointed out.

VOL. 13 1958/5

Introduction

The infrared absorption of the parallel vibration in benzene (ν_{11} in the notation of Wilson [1] and of many other investigators of the spectra of benzene and derivatives) was originally studied by us [2] to see whether the rotational fine structure could be resolved. When this study succeeded, *sym*-benzene-d_3 and benzene-d_6 were also investigated, as well as pyridine. In addition to the rotational fine structure, a wealth of coarser structure of the Q-branches was uncovered. Our interpretation of this structure is not entirely satisfactory, but we wish to report the results at this time both for their own sake and as a further example of the effectiveness of the small grating spectrometer.

Spectroscopic results and rotational analyses

Table 1 gives the results of measurements on the rotational structure of the parallel band in benzene, together with the analysis thereof, and Table 2 gives the same information for the analogous band in pyridine. These measurements are believed to have a precision of $\pm$0·04 cm^{-1}. Since benzene and pyridine are readily available, these bands are convenient for testing instrumental performance in this region of the spectrum.

On the other hand, results with *sym*-benzene-d_3 (Table 3) and benzene-d_6 were much less satisfactory. For *sym*-benzene-d_3, all possible combinations of component parts, such as single or double-pass operation and off-blaze use of gratings normally available for use in the 530 cm^{-1} region, proved to be rather disappointing. With

the instrumental conditions given under Fig. 2 (see reference [2] for details) it was possible to obtain measurable fine structure for *sym*-benzene-d_3, but the rotational analysis gave results considerably inferior, as the estimate of precision shows, to those for benzene (see Table 4). In the case of benzene-d_6, some of the upper-stage bands can be readily resolved out of the Q-branch by prism instrumentation, and their number and intensity are such as to make the resolution of rotational structure impossible with our spectrometer. We suspect that considerably higher resolution, of the order of 0·1 cm^{-1} or better, is needed for this purpose.

The inferior results achieved with *sym*-benzene-d_3 and benzene-d_6 are a consequence both of the smaller rotational spacings, which are not much above the limit of resolution of the instrument, and also of the increased intensity of bands whose transitions begin on excited vibrational levels ("hot bands"). The latter factor is probably the more important, and is less harmful in benzene because of smaller Boltzmann factors and a favorable accident in the frequency shifts from the fundamental to the hot bands. OVEREND and THOMPSON [3] have pointed out that the effect of this shift on the frequency of a given line in the R-branch is given by:

$$R_h(J) - R(J) = \nu_{0,h} - \nu_0 + (B_h' - B')(J+1)(J+2) - (B_h'' - B'')J(J+1) \quad (1)$$

The quantities marked with the subscript h belong to a given hot band, while the others relate to the fundamental band (the symbols have their usual significance) [6]. The differences in the rotational constants cancel to such an extent that only the difference in the ν_0's is of importance. In the benzene molecule (and also in pyridine) this difference for the major hot bands is practically an integral multiple of the rotational spacing, $2B$ (see Table 5). Thus in benzene, rotational lines in the two strongest hot bands are within 0·05 cm^{-1} of superposition on those of the fundamental. In *sym*-benzene-d_3, however, the shifts are not integral multiples of $2B$, but rather are close to half-integral multiples. The rather ill-defined P-branch of *sym*-benzene-d_3 is probably the result of this half-integral factor. A higher resolving power would undoubtedly reveal a complex rotational structure with hot-band satellites.

In this work, two separate samples of *sym*-benzene-d_3 were used. The first sample was prepared in this laboratory by following the procedure outlined by BRODERSEN and LANGSETH [4]. A second sample was obtained from Professor A. LANGSETH.* No difference in resolution was observed for the bands of the two samples, both of which contained less than 2 mole per cent of isotopic impurity.

Rotational constants

The rotational constants obtained in the present work are given in Table 4 and compared with values obtained by other methods. The analysis of rotational structure followed the usual procedure [6]. The center of the band was determined rather closely from the Q-branch component exhibiting the greatest optical density in scans at reduced pressure. This value of ν_0 was later confirmed by the difference plot which was used to obtain $B' - B''$. For all ν_0 plots, slight curvature at high J

* The kindness of Professor LANGSETH in furnishing this sample is gratefully acknowledged.

Table 1. Rotational analysis of the benzene band at 674 cm^{-1}

J	$R(J-1)$ (cm^{-1} (vac))	$P(J+1)$ (cm^{-1} (vac))	$\Delta_2 F''/2(2J+1)$
7	676·66		
8	677·02		
9	677·38		
10	677·77	669·78	0·19024
11	678·17	669·40	0·18956
12	678·54	669·03	0·19020
13	678·92	668·65	0·19000
14	679·28	668·27	0·19000
15	679·67	667·88	0·19016
16	680·04	667·50	0·19015
17	680·41	667·11	0·19014
18	680·90	666·72	0·19162
19	681·16	666·33	0·19000
20	681·54	665·96	0·19000
21	681·90	665·55	0·19012
22	682·28	665·17	0·19011
23	682·65	664·80	0·18989
24	683·02	664·40	0·19000
25	683·38	664·01	0·18990
26	683·76	663·63	0·19000
27	684·14	663·23	0·19009
28	684·53	662·85	0·19018
29	684·90	662·47	0·19008
30	685·28	662·10	0·19000
31	685·65	661·69	0·19016
32	686·02	661·31	0·19015
33	686·40	660·92	0·19015
34	686·76	660·54	0·19000
35	687·15	660·16	0·19007
36	687·51	659·78	0·18993
37	687·87	659·39	0·18987
38	688·25	659·00	0·18994
39	688·61	658·63	0·18975
40	688·97	658·23	0·18975
41	689·36	657·86	0·18976
42	689·71	657·45	0·18976
43	690·07	657·07	0·18966
44	690·43	656·70	0·18949
45	690·80	656·30	0·18962
46	691·15	655·91	0·18946
47	691·52	655·53	0·18942
48	691·91	655·14	0·18954
49	692·25	654·74	0·18950
50	692·63	654·34	0·18955
51	692·97	653·96	0·18937
52	693·36	653·56	0·18952
53	693·72	653·19	0·18935
54	694·10	652·79	0·18954
55	694·48	652·41	0·18950

VOL. 13 1958/5

Table 1—*continued*

J	$R(J-1)$ (cm^{-1} (vac))	$P(J+1)$ (cm^{-1} (vac))	$\Delta_2F''/2(2J+1)$
56	694·84	651·97	0·18969
57	695·20	651·62	0·18948
58	695·61	651·21	0·18974
59	695·91	650·85	0·18933
60	696·26	650·44	0·18934
61	696·62	650·03	0·18939
62	697·00	649·64	0·18944
63	697·35	649·18	0·18965
64	697·70	648·79	0·18957
65	698·01	648·38	0·18943
66	698·38	647·97	0·18951
67	698·73	647·55	0·18956
68	699·11	647·13	0·18971
69	699·47		
70	699·87		
71	700·20		
72	700·52		
73	700·87		
74	701·25		
75	701·59		
76	701·99		

suggests that $D_J' - D_J''$, though very small, differs from zero. Pyridine was treated as a quasi-symmetrical top with $\tilde{B} = (B + C)/2$. All combination plots exhibited the typical deviations at low and very high J. The experimental error quoted was determined from straight lines which just failed to give a reasonable fit for the more heavily weighted J-values.

Pyridine. The results of the rotational analysis on the pyridine band confirm the microwave results of Bak and co-workers [7] and of McCulloh and Pollnow [8] (see Table 4). It is clear from the infrared data that at least one moment of inertia is considerably smaller in the excited state ($v = 1$) which leads to a positive value of $\tilde{B}' - \tilde{B}''$. The rotational spacing is greater in the R-branch, and the P-branch is convergent.

The dimensions of pyridine, as determined by Bak *et al.* [7d] indicate that the molecule is narrower than benzene and tapered toward the nitrogen end. The value of D_J obtained in this work differs considerably from that reported by McCulloh and Pollnow. In the light of the agreement of our value of D_J for benzene with that of Stoicheff, added to the fact that the microwave data are less amenable to the determination of this constant, we prefer our result.

Several comments are to be made regarding the appearance of the pyridine bands illustrated in Fig. 1. The band at 744 cm^{-1}, ν_4 in the assignment of Wilmshurst and Bernstein [9], overlaps part of the R-branch but does not interfere seriously with the resolution and measurement of ν_{11}, causing only a

Table 2. Rotational analysis of the pyridine band at 700 cm^{-1}

J	$R(J-1)$ (cm^{-1} (vac))	$P(J+1)$ (cm^{-1} (vac))	$\Delta_2F''/2(2J+1)$
5	702·19		
6	702·61		
7			
8	703·32		
9	703·71	696·28	0·19553
10	704·13	695·87	0·19667
11	704·59	695·51	0·19739
12	704·92	695·07	0·19700
13	705·32	694·67	0·19722
14		694·27	
15		693·87	
16	706·47	693·45	0·19727
17	706·88	693·05	0·19757
18	707·32	692·67	0·19797
19	707·72	692·27	0·19808
20	708·14	691·88	0·19829
21	708·54	691·50	0·19814
22	708·90	691·16	0·19711
23	709·32	690·75	0·19755
24	709·71	690·36	0·19745
25	710·12	689·97	0·19755
26	710·51	689·59	0·19736
27	710·91	689·21	0·19727
28	711·32	688·81	0·19746
29	711·73	688·45	0·19729
30	712·11	688·04	0·19730
31	712·50	687·66	0·19714
32	712·88	687·28	0·19692
33	713·25	686·89	0·19672
34	713·65	686·51	0·19667
35	714·04	686·09	0·19683
36	714·40	685·72	0·19644
37	714·81	685·32	0·19660
38	715·20	684·90	0·19675
39	715·59	684·50	0·19677
40	715·97	684·08	0·19685
41	716·37	683·70	0·19681
42	716·75	683·30	0·19676
43	717·15	682·91	0·19678
44	717·53	682·54	0·19657
45	717·96	682·15	0·19676
46	718·33	681·75	0·19667
47	718·73	681·35	0·19674
48	719·14	680·95	0·19686
49	719·53	680·58	0·19672
50	719·92	680·20	0·19663
51	720·34	679·82	0·19670
52	720·76	679·42	0·19686
53	721·14	679·04	0·19673

VOL. 13 1958/5

Table 2—*continued*

J	$R(J-1)$ (cm^{-1} (vac))	$P(J+1)$ (cm^{-1} (vac))	$\Delta_2 F''/2(2J+1)$
54	721·54	678·64	0·19679
55	721·95	678·30	0·19662
56	722·36	677·90	0·19673
57	722·75	677·52	0·19661
58	723·16	677·10	0·19684
59	723·58	676·71	0·19693
60	724·01	676·31	0·19711
61	724·40	675·93	0·19703
62	724·79	675·54	0·19700
63	725·20	675·11	0·19720
64	725·60	674·72	0·19721
65	726·01	674·34	0·19721
66	726·39	673·94	0·19718
67	726·77	673·59	0·19696
68	727·16	673·21	0·19690
69	727·53	672·85	0·19669
70	727·92	672·54	0·19638
71		672·11	
72		671·70	
73		671·29	
74		670·91	
75		670·52	
76		670·15	

smearing-out of some of the higher J-transitions in the R-branch. Between 750 and 760 cm^{-1} in the R-branch of ν_4, 26 rotational lines could be identified. The average spacing is somewhat less than that obtained in the R-branch of ν_{11}. Although confirming evidence from the P-branch of this band is lacking, it appears that for this parallel band [9, 10] (whose assignment to species-B_2 is incidentally confirmed by the rotational spacing), we have the more usual case of a convergent R-branch and therefore a greater moment of inertia in the excited state. The anomaly at about 679 cm^{-1} in the P-branch of ν_{11} represents the absorption band usually given at 675 cm^{-1} in the pyridine spectrum. In our spectrum this absorption cannot be attributed to impurities such as benzene or CO_2. Its assignment as a difference tone ($\nu_{18a} - \nu_{16b} = 663$ cm^{-1}) by Wilmshurst and Bernstein [9] appears doubtful.

Upper-stage transitions

Table 5 lists the observed frequencies of the various components of the Q-branches of these molecules. The absorption maxima are given in the order of ascending frequency and any component given in the second column may be easily found on the respective spectral illustration (Figs. 1–3 and Ref. [2], Fig. 8). In the case of benzene, the stronger components occur on the lower frequency side of ν_0,

Table 3. Rotational analysis of the *sym*-benzene-d_3 band at 531 cm^{-1}

J	$R(J-1)$ (cm^{-1} (vac))	$P(J+1)$ (cm^{-1} (vac))	$\Delta_2F''/2(2J+1)$
8		527·98	
9		527·56	
10		527·22	
11	534·95	526·86	0·1759
12	535·30	526·48	0·1763
13	535·63	526·10	0·1765
14	535·99	525·75	0·1765
15	536·33	525·42	0·1760
16	536·68	525·09	0·1755
17	537·00	524·72	0·1755
18	537·35	524·36	0·1756
19	537·70	524·03	0·1753
20	538·04	523·68	0·1751
21	538·39	523·28	0·1756
22	538·71	522·92	0·1755
23	539·05	522·57	0·1753
24	539·38	522·20	0·1752
25	539·77	521·84	0·1758
26	540·12	521·49	0·1758
27	540·45	521·13	0·1756
28	540·79	520·75	0·1758
29	541·15	520·45	0·1754
30	541·48	520·16	0·1748
31	541·81	519·82	0·1745
32	542·15	519·44	0·1747
33	542·48	519·10	0·1744
34	542·81	518·70	0·1748
35	543·12	518·33	0·1746
36	543·46	518·00	0·1744
37	543·75	517·66	0·1740
38	544·11	517·26	0·1744
39	544·40	516·88	0·1742
40	544·68	516·58	0·1735
41	544·99	516·22	0·1733
42	545·28	515·90	0·1728
43	545·56	515·53	0·1726
44	545·93	515·12	0·1731
45	546·23	514·68	0·1733
46	546·56	514·24	0·1738
47	546·89	513·87	0·1738
48	547·19	513·51	0·1736
49	547·58	513·17	0·1738
50	547·91	512·80	0·1738
51	548·27		
52	548·66		
53	549·02		
54	549·38		
55	549·70		
56	550·00		
57	550·31		
58	550·59		
59	550·89		
60	551·18		
61	551·49		
62	551·76		
63	552·10		

VOL. 13 1958/5

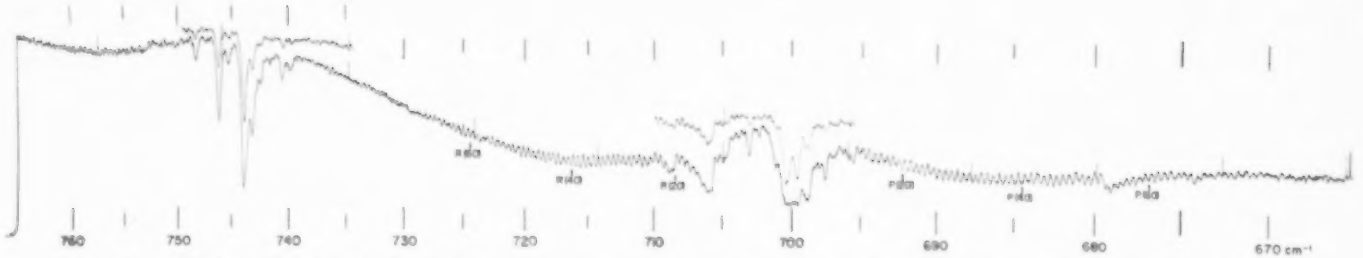

Fig. 1. Parallel absorption bands of pyridine, ν_{11} at 700 cm^{-1} and ν_4 at 744 cm^{-1}. Reproduction of the original tracing recorded in the third order of a 40 line/mm grati g used on the short side of the grooves; 10 cm path at 4 cm pressure.

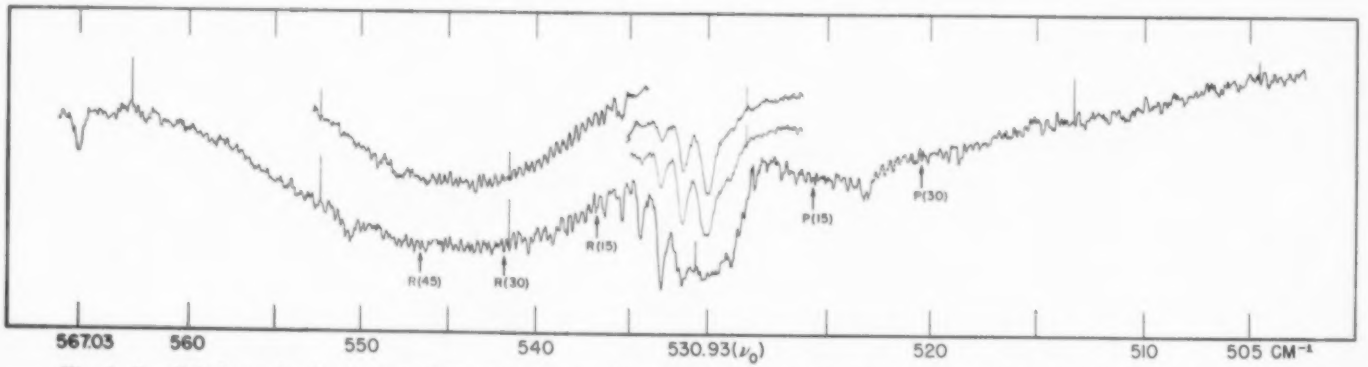

Fig. 2. Parallel absorption band of *sym*-benzene-d_3. Reproduction of the original tracing recorded in the second order of a 40 line/mm grating used on the short side of the grooves; 10 cm path at 4 cm pressure.

Table 4. Rotational constants in cm^{-1}

Constant	Molecule	This work	Reference
	Benzene		[5a]
B''		0·18965 ± 0·00010	0·18960 ± 0·00005
$B' - B''$		$-1·22 \times 10^{-4}$	
B'		0·18953	
D_J		$1·2 \times 10^{-8}$	$(2·2 \pm 1·0) \times 10^{-8}$
	sym-Benzene-d_3		[5b]
B''		0·1733 ± 0·001	0·17165 ± 0·0001
$B' - B''$		$-1·62 \times 10^{-4}$	
B'		0·1731	
D_J		(~0)	$1·3 \times 10^{-8}$
	Benzene-d_6		[5a]
B''			0·15681 ± 0·00008
D_J			$(0·8 \pm 1) \times 10^{-8}$
	Pyridine		[7, 8]
B''			0·193573
C''			0·201391
$\tilde{B}'' = (B'' + C'')/2$		0·19676 ± 0·00012	(0·197482)
$\tilde{B}' - \tilde{B}''$		$+2·91 \times 10^{-5}$	
$\tilde{B}'$		0·19679	
D_J		$0·5 \times 10^{-8}$	$-1·19 \times 10^{-7}$

while in *sym*-benzene-d_3 the reverse is true. Both kinds of behavior are reported in the literature. Hot bands in acetylene-d_2 [3] and *cyclo*propane [11], for example, occur on the low-frequency side while they are found on the high-frequency side in methyl *iso*cyanide [12] and methyl acetylene [13]. The two pyridine bands of Fig. 1 show hot bands on both sides of the band center, and the benzene-d_6 band of Fig. 3 displays a particularly large collection of components.

In the absence of an *a priori* knowledge of the anharmonic coefficients, it is usually possible to ascribe such magnitude and sign to these coefficients as to "explain" the observed separations of the components from the main Q-branch. Only in the instance of transitions arising from successively higher levels of the same mode of vibration is there an opportunity to check the observed spacings.

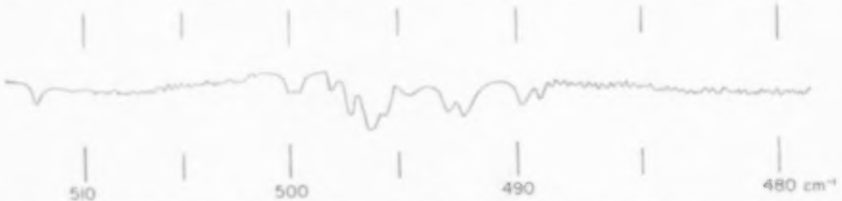

Fig. 3. Parallel absorption band of benzene-d_6 illustrating "hot band" structure. Various pressures were used to record all of the details.

VOL. 13 1958/5

Table 5. Vibrational fine structure of parallel bands and possible assignments

Molecule		Frequency in (cm^{-1} (vac))	Peak absorbance ($\times 10^2$)	Possible assignment	Boltzmann factor for assignment
	A	670·70	8	11 + 3(16) − 3(16)	1·5
	B	671·75	29	11 + 2(16) − 2(16)	7·3
	C	672·53	10	11 + 4 − 4	3·7
C_6H_6*	*D*	672·83	67	11 + 16 − 16	31·6
	E	673·49	24	11 + 6 − 6 (^{13}C band?)	11·8
	F	673·99	140	11 (ν_0)	100·0
	G	675·24	6	2(11) − 11	4·3
	H	676·10	4	11 + 10 − 10	3·8
	A	528·59	2	11 + 2(6) − 2(6)	1·2
	B	529·82	10	11 + 6 − 6	12·5
sym-	*C*	530·93	83	11 (ν_0)	100·0
$C_6H_3D_3$*	*D*	532·15	61	11 + (16) − (16)	35·9
	E	533·31	16	11 + 2(16) − 2(16)	9·7
	F	534·41	7	11 + 3(16) − 3(16)	2·3
	G	535·48	2	11 + 4(16) − 4(16)	0·52
	A	489·09	12	11 + 18 − 18	4·5
	B	489·79	22	11 + 17 − 17	5·1
	C	492·11	26	11 + 11 − 11	9·9
	D	492·78	22	11 + 10 − 10	9·2
	E	494·46	8	11 + 2(6) − 2(6)	1·3
C_6D_6*	*F*	495·62	28	11 + 6 − 6	13·4
	G	496·21	57	11 (ν_0)	100·0
	H	497·11	34	11 + 16 − 16	39·9
	I	497·95	9	11 + 2(16) − 2(16)	12·0
	J	499·73	7	11 + 9 − 9	3·5
	K	512·56	0·6	11 + 15 − 15	2·1
	A	697·50	11	11 + 6*a* − 6*a*	5·9
	B	698·83	26	11 + 2(16*a*) − 2(16*a*)	3·0
	C	699·52	86	11 + 16*a* − 16*a*	17·4
	D	700·22	123	11 (ν_0)	100·0
	E	701·02	6	11 + 6*b* − 6*b*	4·8
	F	702·94	6	11 + 11 − 11	3·8
	G	704·80	−2	11 + 4 − 4	3·0
	H	705·96	20	(11 + 16*b* − 16*b*) or ($\nu_{18b} - \nu_{16a}$)?	15·1
C_5H_5N†	*A*	739·76	2	4 + 4 − 4	3·0
	B	740·49	5	4 + 6*a* − 6*a*	5·9
	C	742·44	4	4 + 2(16*b*) − 2(16*b*)	2·3
	D	743·19	16	4 + 16*b* − 16*b*	15·1
	E	744·00	65	4 (ν_0)	100·0
	F	745·31	4	4 + 6*b* − 6*b*	4·8
	G	746·26	17	4 + 16*a* − 16*a*	17·4
	H	748·35	4	4 + 2(16*a*) − 2(16*a*) or 4 + 11 − 11	3·0 3·8

* Following the assignment of reference [4] and others.
† Following the assignment of reference [9].
The numbers in column 4 are the frequency numbers of references [4] and [9].

A number of such cases are to be noted in Table 5. For example, the lowest vibrational frequency in benzene (the doubly degenerate ν_{16} at 400 cm^{-1}) is assumed to produce components arising from its first, second and third excited levels. The positions of the components, calculated from an average value of the anharmonic coefficient, agree with the observed positions within 0·05 cm^{-1}. Unfortunately the difficulty of making accurate measurements of intensities of closely spaced satellites makes an assignment by means of Boltzmann factors unreliable. Within the rather

Table 6. Paired frequencies in the hot band systems

Molecule	Vib.	Paired lines	Mean freq. ν_m	$\nu_m - \nu_0$
C_6H_6	ν_{11}	*B* and *H*	673·92	−0·07
		D and *G*	674·03	0·04
$C_6H_3D_3$	ν_{11}	*A* and *E*	530·95	0·02
		B and *D*	530·98	0·05
C_6D_6	ν_{11}	*D* and *J*	496·26	0·05
		E and *I*	496·20	−0·01
C_5H_5N	ν_{11}	*C* and *E*	700·27	0·05
	ν_4	*A* and *H*	744·06	0·06
	ν_4	*C* and *F*	743·88	−0·12
		Molecules studied by other investigators		
*cyclo*Propane [11]	ν_2		~3101·47	
*cyclo*Propane-d_6 [11]	ν_6		No pairs	
Methyl acetylene [13a,b]	$2\nu_9$	1250·0, 1258·2	1254·1	~−0·9
	ν_3	2135, 2145	2140	~−2·0
Methyl acetylene-*d* [14]	ν_1	2613·5, 2623·5	2618·5	~+1·5
Methyl *iso*cyanide [12]	ν_2	2150·6, 2179	2164·8	−0·9
		2158, 2172·5	2165·2	−0·5
Allene [15]	ν_5		~3006	
Allene-d_4 [15]	ν_6	1916·2, 1922·6	1919·4	−1·1

wide limits of error of the measurements, the Boltzmann factors are believed to be consistent with the assignments of Table 5.

There is a feature of the hot-band structure which suggests that the above interpretation may need to be revised for certain components. A total of eighteen components, out of the thirty-seven hot bands listed in Table 5, occur as nine pairs of lines equally spaced about ν_0 with an average deviation of 0·05 cm^{-1}. This suggests a symmetrical splitting of certain levels, as though by Fermi resonance or by release of degeneracy. However, there seems to be no reason for such a splitting in the benzene derivatives, and in pyridine there are no degenerate vibrations. No satisfactory explanation has been thought of, and therefore the assignments of Table 5 are preferred at the present time. The paired absorptions are listed in Table 6. For cases where the vibration is degenerate, a pair would have the same assignment as its stronger component listed in Table 5.

It is of interest to examine the results of similar high-dispersion studies on

VOL. 13 1958/5

related molecules. Parallel bands are more suited for comparisons of this kind, since in perpendicular bands the hot band structure is more easily lost in the more widely spaced Q-branches. Some cases of paired components are listed at the bottom of Table 6. As high-dispersion instrumentation and techniques are applied to larger molecules, more examples of this type will doubtless appear and may suggest some explanation of this phenomenon.

Acknowledgements—This work was undertaken when Dr. T. K. McCubbin, Jr., was a member of the Spectroscopy Laboratory staff, and we thank him for help with the early studies on benzene. Financial support of the work by the Engineer Research and Development Laboratories, U.S. Army (Contract DA-44-009-eng-3126) and by the National Science Foundation (Grant G-1892) is also gratefully acknowledged.

References

[1] Wilson E. B., Jr., *Phys. Rev.* 1934 **45** 706.
[2] Lord R. C. and McCubbin T. K., Jr., *J. Opt. Soc. Amer.* 1957 **47** 689.
[3] Overend J. and Thompson H. W., *Proc. Roy. Soc.* A 1955 **232** 291.
[4] Brodersen S. and Langseth A., *Mat. Fys. Skr. Dan. Vid. Selsk.* 1956 **1** No. 1.
[5a] Stoicheff B. P., *Canad. J. Phys.* 1954 **32** 339.
[5b] Langseth A. and Stoicheff B. P., *Canad. J. Phys.* 1956 **34** 350.
[6] Herzberg G., *Infrared and Raman Spectra* p. 390 *et seq.* Van Nostrand, New York 1945.
[7a] Bak B. and Rastrup-Andersen J., *J. Chem. Phys.* 1953 **21** 1305.
[7b] Bak B., Hansen L. and Rastrup-Andersen J., *J. Chem. Phys.* 1954 **22** 565.
[7c] Bak B., Hansen L. and Rastrup-Andersen J., *J. Chem. Phys.* 1954 **22** 2013.
[7d] Bak B., Hansen-Nygaard L. and Rastrup-Andersen J., *J. Molec. Spectrosc.* 1958 **2** 361.
[8a] McCulloh K. E. and Pollnow G. F., *J. Chem. Phys.* 1953 **21** 2082.
[8b] McCulloh K. E. and Pollnow G. F., *J. Chem. Phys.* 1954 **22** 681.
[9] Wilmshurst J. K. and Bernstein H. J., *Canad. J. Chem.* 1957 **35** 1183.
[10] Corrsin L., Fax B. J. and Lord R. C., *J. Chem. Phys.* 1953 **21** 1170.
[11] Gunthard H. H., Lord R. C. and McCubbin T. K., Jr., *J. Chem. Phys.* 1956 **25** 768.
[12] Thompson H. W. and Williams R. L., *Trans. Faraday Soc.* 1952 **48** 502.
[13a] Boyd D. R. J. and Thompson H. W., *Trans. Faraday Soc.* 1952 **48** 493.
[13b] Boyd D. R. J. and Thompson H. W., *Trans. Faraday Soc.* 1953 **49** 141.
[14] Grisenthwaite R. J. and Thompson H. W., *Trans. Faraday Soc.* 1954 **50** 212.
[15] Overend J. and Thompson H. W., *J. Opt. Soc. Amer.* 1953 **43** 1065.

Spectrochimica Acta, 1958, Vol. 13, pp. 192 to 196. Pergamon Press Ltd., London. Printed in Northern Ireland

The vibrational spectrum of the dichromate ion

H. Stammreich,* D. Bassi,* O. Sala* and H. Siebert†

(*Received* 10 *June* 1958)

Abstract—The infra-red and Raman spectra of the dichromate ion are described. The observed spectra are consistent with a C_{2v}-structure of the ion containing one bridging oxygen atom bound to the two chromium atoms. The secular equations for a simplified model $O_3Cr—O'$ have been calculated and the principal force constants of this model are given.

Experimental and results

Employing an experimental technique previously reported by one of us [1] we obtained the Raman spectrum of the dichromate ion. The samples consisted of aqueous solutions of sodium and potassium dichromate in concentrations ranging from 5 per cent to saturation. The Raman spectra were excited by He 5875·6 Å and in some cases by He 6678·1 Å. The following shifts (in cm^{-1}) were observed: 220 (4); 365 (5b); 558 (2) P; 772 (0); 904 (10) P; 946 (3b).

The number of observed Raman lines is surprisingly small for a nine-atomic molecule, but we are not able to detect additional shifts even in strongly over-exposed spectra (up to 24 hr whereas the normal exposures ranged from 5 to 60 min). The extremely weak shift 772 cm^{-1} was recorded only with long exposures and was initially considered as uncertain; the infra-red spectrum, however, supports its identification.

Our excitation unit consists of a helium discharge tube helicoidally wound around the Raman tube. The direction of incidence of the exciting radiation is therefore insufficiently defined to permit correct quantitative measurements of the state of polarization of the Raman shifts and to distinguish weakly polarized from depolarized lines. The arrangement enables us, however, to recognize with certainty depolarization factors $<0{\cdot}4$; such strongly polarized shifts are indicated above by P.

The infra-red spectra of solid $(NH_4)_2Cr_2O_7$, $Na_2Cr_2O_7{\cdot}2H_2O$ and $K_2Cr_2O_7$ were obtained in the 400–1200 cm^{-1} region using a Perkin–Elmer Model 21 spectrometer with NaCl and KBr prisms. The finely powdered materials were mixed with potassium bromide and pressed into disks.

Table 1 presents the observed infra-red spectra of the three dichromates in the solid state as compared with the Raman spectrum of aqueous solutions. Infra-red spectra of these compounds have been reported previously by Miller and Wilkins [2]. Their results agree satisfactorily with our work; our spectra, however, seem to be better resolved.

* Department of Physics, University of São Paulo, São Paulo, Brazil
† Institute of Chemistry, Academy of Mining, Clausthal-Zellerfeld, Germany

VOL. 13 1958/5

Table 1. Vibrational spectra of dichromates (cm^{-1})

Raman* (aq. sol.)	Infra-red (solid)†			Species (C_{2v})	Approximate description‡
	$(NH_4)_2Cr_2O_7$	$Na_2Cr_2O_7 \cdot 2H_2O$	$K_2Cr_2O_7$		
220 (4)				A_1	δ (CrOCr)
365 (5b)				A_1; A_2	δ (CrO_3)
				B_1; B_2	
		557 (w) sh	556 (w)		
558 (2)P	567 (w)			A_1	ν_s (CrOCr)
		566 (w)	566 (w)		
	762 (s)	771 (s)	764 (vs)		
772 (0)				B_1	ν_{as} (CrOCr)
	795 (w) sh	799 (m)	796 (ms)		
		885 (ms)	885 (s)		
—	884 (ms)	890 sh	891 (ms)	B_1	ν_s (CrO_3)
		903 (ms)	902 (ms)		
904 (10)P	906 (ms)			A_1	ν_s (CrO_3)
		906 sh	908 (m)		
		925 (s)	924 (s)		
		935 (vs) sh	934 (vs)		
		939 (vs)	940 (vs)	A_1; A_2	
	937 (vs)				
946 (3b)		947 (vs) sh	946 (vs) sh		ν_{as} (CrO_3)
	955 (vs)			B_1; B_2	
		950 (vs)	950 (vs)		
		956 (vs)	956 (vs)		
		966 (s)	966 (s)		

* Estimated intensities in parentheses; b = broad; P = polarized shifts $\rho < 0{\cdot}4$.
† w = weak; m = medium; s = strong; v = very; sh = shoulder.
‡ ν = stretching vibration; δ = bending or rocking vibration; s = symmetric, as = antisymmetric.

Assignment

The $(Cr_2O_7)^{=}$ ion can be assumed to have the bridged structure $O_3Cr—O—CrO_3$. At first sight the small number of Raman shifts seems to indicate a highly symmetrical configuration as represented by the point groups D_{3d} or D_{3h}, which would suggest the occurrence of six or ten Raman-active fundamentals, respectively. Obviously these structures are to be rejected because they presume the improbable angle of 180° between the Cr—O—Cr bonds.

Assuming a normal valence angle of the bridging oxygen atom, the expected structure of the ion should belong to the C_{2v}, C_s or C_i point groups depending on the positions of the outer oxygen atoms. The selection rules predict for all of these cases twenty-one fundamental vibrations belonging to nondegenerate species

active both in Raman and IR, except in the case of C_{2v} symmetry, where only seventeen fundamentals should be infra-red active.

The analysis of the observed spectra is greatly facilitated by a comparison with the Raman spectrum of the chromate ion reported in a previous paper [3]. Considering the dichromate ion as (CrO_3)—O—(CrO_3) we may try to identify separately the vibrations belonging to the nonlinear Cr—O—Cr skeleton and the "internal" vibrations of the trigonal pyramidal CrO_3 groups. The frequencies of the latter are expected to lie near those of the corresponding modes of vibration of the tetrahedral $(CrO_4)^=$ ion. Of course, this approach is to be regarded only as a roughly approximate description of the real vibrational motions of the $(Cr_2O_7)^=$ ion, since the skeleton and internal vibrations are expected to couple.

However, in this way three of the observed frequencies can be assigned immediately to the Cr—O—Cr skeleton vibrations. The 220 cm^{-1} Raman line corresponds to the bending frequency, the frequencies observed in the 560 and 770 cm^{-1} region belong to the symmetric and antisymmetric stretching mode of vibration, respectively. This assignment is supported by the opposite intensity ratio of the latter bands in the Raman and IR spectra and by the state of polarization of the Raman line 558 cm^{-1}.

In the cases of $K_2Cr_2O_7$ and $Na_2Cr_2O_7 \cdot 2H_2O$ the corresponding absorption bands appear doubled, and the splitting may be explained by the possibility of various non-equivalent arrangements of the $(Cr_2O_7)^=$ ions in the crystal lattice.

The broad Raman shift observed at 365 cm^{-1} corresponds to the bending and rocking modes of vibration of the $(Cr_2O_7)^=$ ion, except the Cr—O—Cr bending motion already assigned to 220 cm^{-1}. Ten vibrations of this type are to be expected; their frequencies lie very close together or are accidentally degenerate. The fact, that the frequencies of the two corresponding bending vibrations of the $(CrO_4)^=$ ion are nearly equal, supports this assumption. We were not able to resolve the diffuse Raman band 365 cm^{-1} into separate components, although some spectra were taken with a fairly high dispersion of 9 Å/mm, corresponding to 25 wavenumbers/mm in the 6000 Å region.

For the assignment of the remaining frequencies we can use the above simplified approach. The outer CrO_3 groups of the dichromate ion are regarded as symmetric (point group C_{3v}). Then each of these groups will possess a symmetric and an antisymmetric stretching mode of vibration. The symmetric vibrations are easily recognized by the very strong and polarized Raman line 904 cm^{-1} and by the intensity ratio of the infra-red bands 885 and 905 cm^{-1}, which are again split into two components in the sodium and potassium salt.

The bands 937 and 955 cm^{-1} found in the infra-red spectrum of $(NH_4)_2Cr_2O_7$ have to be assigned to the antisymmetric CrO_3 stretching vibrations. They are not resolved or are accidentally degenerate in the Raman spectrum. The corresponding absorption bands of the sodium and potassium salts show a complicated structure.

The last columns of Table 1 summarizes our assignment of the observed frequencies to the species of the C_{2v} model and gives the approximate description of the vibrational motions involved.

VOL. 13 1958/5

Force constants

It does not seem desirable to carry out a normal co-ordinate treatment for the $(Cr_2O_7)^{=}$ ion, since we have only a limited number of observed frequencies which can be assigned to the twenty-one vibrational degrees of freedom of the molecule. It is possible, however, to obtain approximate values of the most interesting force constants in a simple way. Neglecting the bending motion of the Cr—O—Cr skeleton, we may regard the dichromate ion as a pentatomic molecule $O_3Cr—O'$ belonging to the C_{3v} point group. This simplification seems to be admissible because of low value of the Cr—O—Cr bending frequency. Furthermore we have to use the average value of the frequencies ν_s (Cr—O—Cr) and ν_{as} (Cr—O—Cr), namely 670 cm^{-1}, in order to obtain the probable stretching frequency of the hypothetical Cr—O′ bond in the simplified model.

The model molecule O_3CrO' has six fundamental vibrations, three of species A_1 and three of species E. All Cr—O distances are taken as equal and the angles as tetrehadrals. Since all bending and rocking modes of vibration have the same frequency, namely 365 cm^{-1}, we assume the bending constants of the OCrO and OCrO′ angles to be identical. The mean value 895 cm^{-1} of the two infra-red bands 884 and 906 cm^{-1} is taken as the symmetric stretching frequency of the Cr—O bonds.

Under these simplifying conditions we obtain for the model the secular equations:

$$\sum_{i=1}^{3} \lambda_i = f_1(\mu_1 + \mu_2) + (f_2 + 2f')(\tfrac{1}{3}\mu_1 + \mu_2) + 2d(\tfrac{5}{3}\mu_1 + \mu_2)$$

$$\sum_{\substack{i,k=1 \\ (i \neq k)}}^{3} \lambda_i\lambda_k = f_1(f_2 + 2f')\mu_2(\tfrac{4}{3}\mu_1 + \mu_2) + 2f_1 d\mu_2(\tfrac{14}{3}\mu_1 + \mu_2) + 2(f_2 + 2f')d\mu_2(3\mu_1 + \mu_2)$$

$$\prod_{i=1}^{3} \lambda_i = 2f_1(f_2 + 2f')d\mu_2{}^2(4\mu_1 + \mu_2)$$

$$\lambda_4 + \lambda_5 = (f_2 - f')(\tfrac{4}{3}\mu_1 + \mu_2) + 2d(\tfrac{8}{3}\mu_1 + \mu_2)$$

$$\lambda_4\lambda_5 = 2(f_2 - f')d\mu_2(4\mu_1 + \mu_2)$$

$$\lambda_6 = 3d\mu_2$$

In the expression above μ_1 and μ_2 are the reciprocal masses (in atomic weight units) of chromium and oxygen, respectively; f_1 and f_2 are the stretching force constants of the Cr—O′ and Cr—O bonds, respectively; f' is an interaction constant for the Cr—O bonds, d is the sole bending force constant: $\lambda_i = 0{\cdot}05889\ \nu_i{}^2$ (ν in cm^{-1}).

The calculated force constants of the O_3CrO' model are given in Table 2.

Using these constants we recalculated from the above equations the frequency values of the six fundamentals of our model. The results are in excellent agreement with the observed frequencies as shown in Table 3.

It seems of interest to compare the force constants obtained with those of the chromate ion [3]: f_1 is considerably smaller and f_2 is larger than the corresponding

f_d of the $(CrO_4)^=$ ion. A mesomerism between six canonic structures may be assumed in the case of the chromate ion, each having two single and two double bonds. In the dichromate ion the mesomerism is restricted to the outer CrO_3 groups since the Cr—O—Cr bridge is formed by single bonds. Consequently the

Table 2. Force constants of the O_3CrO' model (mdyn/Å)

f_1	f_2	f'	d
3·27	6·07	0·25	0·42

Table 3. Calculated and observed frequencies of the O_3CrO' model (cm^{-1}).

Frequency	ν_1	ν_2	ν_3	ν_4	ν_5	ν_6
Calc.	895	670	365	947	370	365
Obs.	895	670	365	946	365	365

bond order of the bridging bonds decreases and that of the outer bonds increases as compared with the $(CrO_4)^=$ ion. Being approximately proportional to the bond orders, the force constants behave in the same way. The stretching force constant of the bridging Cr—O bonds (3·27 mdyn/Å) is in good agreement with that predicted previously (3·41 mdyn/Å) for a single Cr—O bond [4].

Acknowledgement—This work has been supported by the Conselho Nacional de Pesquisas, Rio de Janeiro, by the Deutsche Forschungsgemeinschaft, Bonn, and by the Verband der Chemischen Industrie, Düsseldorf. The authors wish to express their gratitude for the facilities created by the aid of these organizations.

References

[1] STAMMREICH H., *Spectrochim. Acta* 1956 **8** 41.
[2] MILLER F. A. and WILKINS C. H., *Analyt. Chem.* 1952 **24** 1253.
[3] STAMMREICH H., BASSI D. and SALA O., *Spectrochim. Acta*. In press.
[4] SIEBERT H. *Z. anorg. Chem.* 1954 **275** 225.

VOL. 13 1958/5

Spectrochimica Acta, 1958, Vol. 13, pp. 197 to 201. Pergamon Press Ltd., London. Printed in Northern Ireland

A simple device for the spectrochemical analysis of minerals in an inert atmosphere using the Stallwood jet

D. M. Shaw, O. Wickremasinghe and C. Yip
Department of Geology, McMaster University, Hamilton, Ontario, Canada

(*Received* 30 *May* 1958)

Abstract—A Pyrex glass partially closed chamber for d.c. excitation of minerals in a controlled atmosphere in conjunction with the Stallwood jet is described. The chamber is easily prepared, cheap and expendable and easy to clean. Its use with a 1 : 1 argon–oxygen mixture gives satisfactory sensitivity and precision for trace elements in geological materials.

Introduction

Many methods have been introduced during the last 15 years for improving the sensitivity, precision and accuracy of d.c. arc spectrochemical analysis of minerals. One of the most valuable inventions has been B. J. Stallwood's [1] device for cooling the lower electrode and stabilizing the arc by a concentric flow of air. The device is commonly referred to as the Stallwood air-jet and is now in use in several laboratories on the North American continent and elsewhere. Its particular advantage is to stabilize the arc and to reduce matrix effects.

A modified air-jet has been in use in this laboratory for the last 5 years for the determination of minor elements in geological materials. Its use has resulted in notable improvements in accuracy and reproducibility but for most elements the sensitivity is not adequate to determine figures of the order of a few parts per million. In discussing this matter with Dr. G. D. Nicholls, Department of Geology, University of Manchester, he suggested that the use of carbon dioxide in the place of air might materially improve sensitivity, by reducing cyanogen band spectra. Experiments showed, however, that the force of the carbon dioxide stream was inadequate to prevent all air from reaching the arc and it became obvious that it was necessary to isolate the arc in some kind of closed chamber.

Various chambers for excitation in a controlled atmosphere have been described in the literature [2, 3, 4, 5, 6, 9]. Most of these are somewhat elaborate and difficult to clean out and in any case not designed for use with the Stallwood jet. Moreover, if the chamber is to be completely enclosed a quartz window is necessary to pass ultra-violet light. A suitable chamber was therefore devised with a view to simplicity of construction, cheapness of materials and consequent expendability, and ready accessibility for cleaning. The chamber has proved very successful and its construction and use are described in the following sections.

Description

The components of the assembly are shown in Fig. 1 and their preparation requires only the services of a glass-blowing shop and a lathe for turning graphite. The chamber consists of a piece of $\frac{3}{4}$ in. Pyrex tube about 3 in. long to which has been attached a piece of $\frac{1}{4}$ in. Pyrex tube in a T-join. The chamber rests on the

upper surface of the Stallwood jet and is closed at its upper end by a plug turned from 1 in. graphite rod. The centre of the T-tube is approximately $\frac{1}{2}$ in. above the surface of the jet and the tube is therefore aligned to allow light to pass from a 5 mm arc to the spectrograph. The lower electrode projects 5 mm above the chimney of the jet and the upper electrode is carried in a $\frac{3}{8}$ in. graphite holder which passes through a hole bored in the graphite plug. The chamber is supported by the jet assembly which was devised in this laboratory to allow three-dimensional adjustment of the position of the jet and electrodes. A Hilger arc-spark stand is

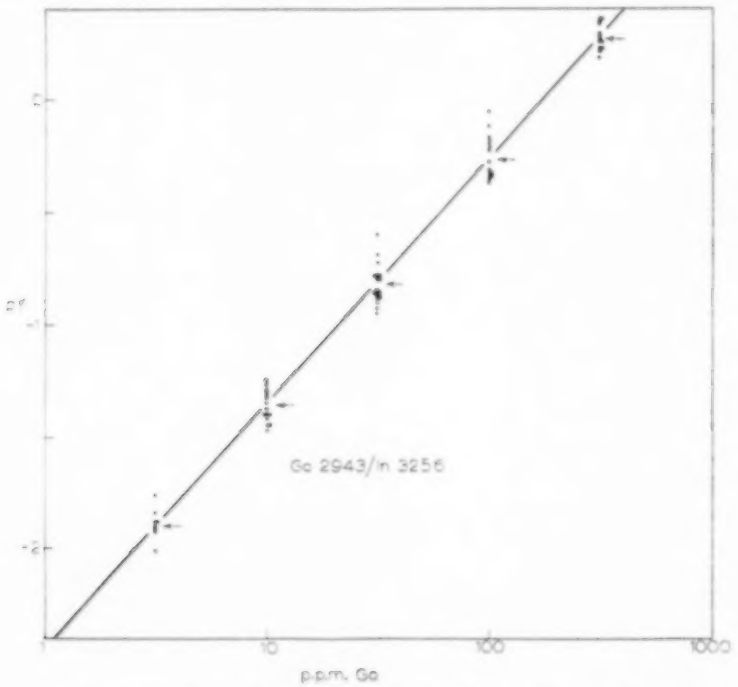

Fig. 4. Working-curve showing the log intensity ratio Ga 2943/In 3256 (dY) plotted against log concentration for seventy-one standards. The line was drawn through the averages, indicated by arrows.

used and the whole assembly is shown in Fig. 2. The gas mixture for the jet enters through a hole drilled in one of the supporting rods. Using a total gas flow rate of about 5 litres/min it is found that air can be excluded completely and cyanogen bands eliminated from the spectra (Fig. 3).

Experiments were carried out initially using carbon dioxide or argon. Carbon dioxide was found not to give adequate improvement of sensitivity. Argon prolonged the burning time to an inordinate degree, as has been reported [1, 8, 9], and sensitivity was still not adequate. To reduce the burning time various argon–oxygen mixtures were tried and a 1 : 1 mixture was found most suitable. All the work reported in the following paragraphs was carried out using this mixture. By comparison with methods using air the sensitivity is notably enhanced and

VOL. 13 1958/5

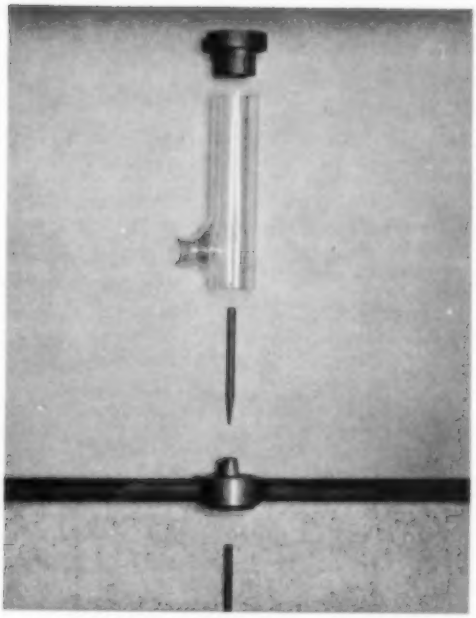

Fig. 1. Expanded view of the chamber components. The chamber is 3 in. long.

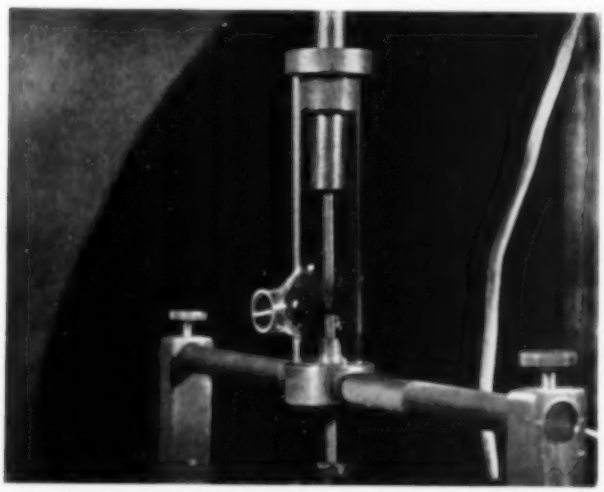

Fig. 2. Chamber supported in position for arcing on the jet assembly.

Fig. 3. Upper spectrum of a silicate taken with an argon–oxygen mixture, showing the absence of CN band-lines. Lower spectrum of graphite in air.

VOL.
13
1958/5

Table 1. Details of the argon–oxygen method

Spectrograph	JACO 21 ft grating, Wadsworth mount, first order dispersion 5 Å/mm.
Condensing optics	25 cm focal length cylindrical lens (horizontal axis) at the slit; 6·7 cm focal length cylindrical lens (vertical axis) 16·1 cm from the slit; diaphragm with 5 mm aperture 27·5 cm from the slit; 10 cm focal length spherical lens 58·1 cm from the slit; arc located 72·5 cm from the slit.
Slit width	30 μ.
Intensity calibration	Seven-step sector at the slit, log intensity ratio = 0·2.
Slit length	4 mm; sector height adjusted for steps 4, 5, 6.
Electrodes	National Carbon Co. graphite ("Special" grade); sample (anode), $\frac{1}{8}$ in. rod, plain crater $\frac{1}{16}$ in. × $\frac{3}{8}$ in.; counter electrode, $\frac{1}{8}$ in. rod.
Emulsion and range	Eastman–Kodak Type S.A.1 plate, 2900–4250 Å.
Processing	3 min development in D19 developer at 20·C; 15 sec stop-bath; 20 min acid fix; 20 min wash.
Voltage	220 V d.c. on open-circuit.
Exposure	90–100 sec (completion of alkalies).
Current	6 A.
Atmosphere	Argon and oxygen 1 : 1 at total flow-rate of 5 litres/min.
Sample	5 parts mineral, 1 part graphite and 4 parts KCl containing 0·025% In_2O_3.
Synthetic standards	Prepared from Johnson–Matthey "Specpure" compounds; matrix of: SiO_2, 45%, Al_2O_3, 23%, $CaCO_3$, 22%, NaCl, 9%, Fe_2O_3, 1%; Li, Cu, Ag, Pb, Sn and Ga were mixed (as oxides) with this matrix and diluted to give standards ranging from 3·16–1000 p.p.m.
Photometry	ARL photodensitometer used; galvanometer readings between 1·0 and 95 were used and background corrections applied in all cases; clear-plate reading adjusted to 100 before each measurement; readings made on step 4 (steps numbered 0 to 8) where possible.
Exposure sequence	At least one standard exposed on each sample plate, recording seven steps in order to check calibration curves and minimize working-curve drift; samples analyzed in triplicate, one on each of three plates.
Spectral lines	Ga 2943·637 In 3256·090 (internal standard). Sn 3175·019 Li 3232·61 Cu 3273·962 Pb 3683·471 Pb 4057·820 Ga 4172·056

the authors confirm the findings of THIERS and VALLEE [8] that argon (a) reduces the overall background and (b) selectively enhances certain spectral lines.

Using this chamber the arc is a narrow confined column, with none of the flame-like characteristics of the ordinary d.c. arc, and there is no tendency for gas pressure to bow out the arc toward the T-tube. At the close of the burn the chamber and plug are coated with graphite and oxide powders but can readily be cleaned. For a sequence of exposures a number of chambers and plugs can be prepared and changed at the end of each arcing. In spite of the powder deposited and occasional globules of molten material which adhere permanently to the glass

of the chamber no contamination problems have been experienced. The gas flow maintains the surroundings of the arc at a relatively low temperature and only occasional breakages due to uneven glass expansion have been found to occur.

Discussion

The chamber has been used in a method to determine lead, gallium, copper, tin and lithium in silicate minerals, using indium as internal standard. Details of the method are given in Table 1. Diminution in the overall background and

Table 2. Replicate analyses on *G*1 and *W*1

Analysis Number	*G*1 (p.p.m.)					*W*1 (p.p.m.)	
	Ga 2943	Ga 4172	Pb 3683	Pb 4057	Cu 3273	Ga 2943	Ga 4172
1	38	32	51	60	14	41	42
2	38	30	56	60	17	35	34
3	42	37	65	69	16	27	27
4	30	27	48	61	11	27	24
5	34	28	58	58	15	21	22
6	43	36	63	72	16	38	35
7	28	20	43	49	20	23	31
8	37	27	52	61	21	23	28
9	41	32	56	55	13	17	22
10	45	35	57	58	14	31	43
11	32	26	45	47	12	21	25
12						21	26

Pb too weak to measure in *W*1.
Cu too strong to measure in *W*1.

elimination of CN bands permitted the use of Ga 4172, Pb 4057 and Pb 3683. The arc burn is continued until the volatiles have been completely consumed. The working curve for Ga 2943, constructed by arcing seventy-one synthetic standards, is shown in Fig. 4 to illustrate the sensitivity and precision of the method. Table 2 includes some replicate determinations on the well-known standard samples *G*1 and *W*1. It is seen that the reproducibility of analyses (made on different plates) is entirely adequate for the determination of volatile trace elements in rocks and minerals. Additional work suggests that non-volatile trace elements can also be determined with adequate sensitivity and precision.

The absolute accuracy of the method established is open to question however, as may be seen from Table 3, which compares the average gallium, lead and copper content of *G*1 and *W*1 with figures from the literature. The synthetic standards used to establish the working curves were low in Mg and Fe, by comparison with *G*1 and *W*1, and it is possible that a matrix effect has been operating. Further work is however being carried out to resolve this problem of systematic bias which is of course one of the plagues of d.c. arc methods. This paper, however, is

VOL. 13 1958/5

primarily concerned with the development of a chamber suitable to allow the use of an atmosphere other than air with the Stallwood jet.

Table 3. Results of analysis of *G*1 and *W*1

Element	Result	Number of replicates	Probable absolute value†
*G*1 (p.p.m.)			
Pb*	56	11	50
Ga*	33	11	20
Cu	15	11	9·5
*W*1 (p.p.m.)			
Ga*	28	12	15

* Average of determinations on two spectral lines.
† Chosen by authors from a compilation of published and unpublished determinations made by Dr. M. FLEISCHER, U.S. Geological Survey (private communication).

References

[1] ADELSTEIN, S. J. and VALLEE B. L., *Spectrochim. Acta* 1954 **6** 134.
[2] EMERY R. ST. J., *Spectrochim. Acta* 1952 **4** 513.
[3] KINGSBURY G. W. J. and TEMPLE R. B., *Spectrochim. Acta* 1952 **4** 473.
[4] MARKS G. W. and GARDNER M., *Rev. Sci. Instrum.* 1947 **18** 370.
[5] OWEN L. E., *J. Opt. Soc. Amer.* 1951 **41** 139.
[6] SMITH D. M. and WIGGINS G. M., *Analyst* 1949 **74** 95.
[7] STALLWOOD B. J., *J. Opt. Soc. Amer.* 1954 **44** 171.
[8] THIERS R. E. and VALLEE B. L., *Spectrochim. Acta* 1958 **11**
[9] VALLEE B. L., REIMER C. B. and LOOFBOUROW J. R., *J. Opt. Soc. Amer.* 1950 **40** 751.

Spectrochimica Acta, 1958, Vol. 13, pp. 202 to 211. Pergamon Press Ltd., London. Printed in Northern Ireland

Vibrational spectra and structure of trisilylamine and trisilylamine-d_9

E. A. V. Ebsworth.* J. R. Hall.‡ M. J. Mackillop.† D. C. McKean.†
N. Sheppard* and L. A. Woodward‡

(*Received* 14 *July* 1958)

Abstract—The infra-red spectra of $N(SiH_3)_3$ and $N(SiD_3)_3$ have been obtained in the gas phase over the region 400—4000 cm^{-1}. The Raman spectrum of liquid $N(SiH_3)_3$ has also been measured. The combined results provide strong evidence that the NSi_3 skeleton of these molecules is planar. The observed skeletal vibration frequencies are used to derive the approximate value $4{\cdot}0 \times 10^5$ dyn/cm for the N—Si stretching force constant.

One of the more striking contrasts in the chemistry of carbon and silicon is the disappearance of the usual donor properties of an ether or amine when several silyl groups are attached to the oxygen or nitrogen atoms [1]. This is considered to be due to the ability of silicon to form bonds involving *d*-orbitals [1, 2] and is accompanied by marked changes of structure.

A recent electron diffraction study of disilyl ether indicates[3] that the Si—O—Si angle is approximately 140°. Previously, spectroscopic evidence had been interpreted [4] as showing it to be 180°. According to recent electron diffraction measurements [5], the molecular skeleton NSi_3 of trisilylamine is planar, in contrast to the pyramidal structure of trimethylamine. In the present paper the vibrational spectra of trisilylamine and trisilylamine-d_9 are observed; the results also provide strong evidence for a planar skeleton.

Experimental

Preparation of compounds. Samples of trisilylamine were prepared by mixing ammonia with excess of silyl chloride in the vapour phase [6]. Silane was first obtained by reacting silicon tetrachloride in diethyl ether with lithium aluminium hydride, and then converted to silyl chloride or iodide by treatment with the appropriate hydrogen and aluminium halides. Where silyl iodide was prepared, conversion to the chloride was achieved by passing its vapour over mercuric chloride. Lithium aluminium deuteride and deuterium chloride were used in the two corresponding stages in the preparation of $N(SiD_3)_3$. Formation of silylene chloride-d_2 was almost completely prevented by using excess of silane-d_4 and heating the reaction mixture for 2–4 hr. In the reaction between silyl chloride-d_3 and ammonia no exchange of hydrogen between the species SiD_3Cl and NH_3 was observed. The isotopic purity of the deuterated materials was estimated from the intensity of infra-red absorption bands due to the Si—H stretching vibrations.

* University Chemistry Laboratory, Cambridge
† Chemistry Department, University of Aberdeen
‡ Inorganic Chemistry Laboratory, Oxford.

VOL. 13 1958/5

The purity of all samples was checked by vapour-pressure measurements. The $N(SiH_3)_3$ used to obtain the Raman spectrum contained a very small amount of a more volatile CH-containing impurity, possibly diethyl ether. The infra-red spectrum of this sample was identical with that of independently prepared samples except for the presence of a weak C—H stretching band near 2950 cm^{-1}, a weak band at 1131 cm^{-1} and two very weak bands at approximately 503 and 446 cm^{-1}. On fractionation the 2950 cm^{-1} band was reduced in intensity relative to the rest of the spectrum, the other three bands being unaffected. It is therefore assumed that the latter are not due to impurity.

Infra-red spectra. These were obtained either with a Perkin–Elmer Model 21 or a Hilger H.800 double-beam spectrometer, both fitted with sodium chloride and potassium bromide prisms. For calibration, carbon monoxide, water and ammonia frequencies were recorded between 750 and 2200 cm^{-1}, while methyl alcohol or water frequencies were used in the region 400–750 cm^{-1}.

Cells 10 cm or 50 cm long were used. They had potassium bromide windows attached by glyptal or beeswax–rosin mixture.

Raman spectra. When the liquid sample (volume 1 ml) was first transferred to the Raman vessel by distillation *in vacuo*, a very slight solid deposit was formed on the walls and window. Consequently the quality of the spectra obtained was poor. It was found, however, that the deposit could be removed by transferring the sample to an auxiliary vessel *in vacuo* and then heating the empty Raman tube. Repetition of this procedure eventually made it possible to photograph spectra of very satisfactory quality. Most of the results were obtained with the apparatus (Toronto arc excitation, Hilger E.518 spectrograph) previously described [7]. Some spectra were also photographed with a Hilger E.612 spectrograph, which has a greater dispersion and resolving power, but no additional information was thereby obtained.

The principal exciting line was the mercury blue line (4358 Å), a filter (*m*-dinitrobenzene in benzene) being used to reduce the intensity of primary lines of lower wavelength. An attempt to excite the whole spectrum by the violet line (4046 Å) resulted in a rather rapid deterioration of the sample with formation of a fine white suspension.

Qualitative information on the states of polarization of the Raman lines was obtained by the method of polarized incident light, using suitably oriented polaroid cylinders surrounding the Raman tube. Copper or iron arc spectra were used as standards for the measurement of the frequencies. The limits of error are approximately ± 2 cm^{-1} for lines that are not very weak or diffuse.

During all exposures the temperature of the sample was maintained at approximately 0°C. Exposure times varied from 1 min to $1\frac{1}{4}$ hr, using Kodak Special Scientific plates (Oa, G).

Fig. 1 shows the infra-red spectra of trisilylamine and its completely deuterated derivative. A microphotometer trace of the Raman spectrum is reproduced in Fig. 2.

The observed frequencies for $N(SiH_3)_3$ are given in Table 1, with qualitative intensities and, for the Raman lines, an indication of appearances and states of polarization. A notable feature of the Raman spectrum is the very high intensity of

the frequency 2168 cm^{-1}, which is evidently to be attributed to Si—H stretching. Despite the use of the primary filter which greatly reduced the intensity of the violet mercury lines 4046 and 4077 Å, this Raman frequency was excited by both

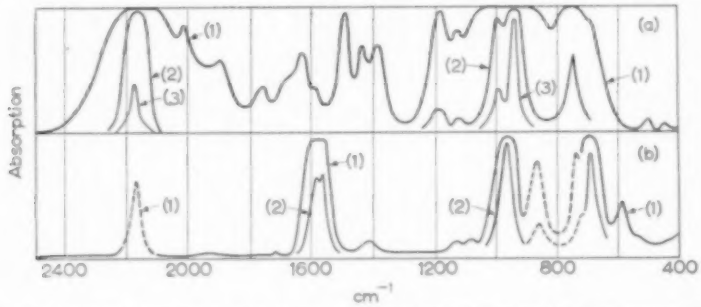

Fig. 1. The infra-red spectra of trisilylamine (A) and trisilylamine-d_9 (B) vapours. Trisilylamine: (1) 50 cm cell, 60 mm pressure; (2) 50 cm, 2 mm; (3) 5 cm, 2 mm; Trisilylamine-d_9: (1) 10 cm cell, 25 mm; (2) 10 cm. 2·5 mm (dashed curves indicate bands due to SiH impurity).

and appeared on the Stokes side of the blue line 4358 Å. That the Raman lines in question were indeed excited by 4046 and 4077 Å was easily verified by short exposures without the filter. In the longer exposures $\Delta\nu = 2168$ cm^{-1} was also

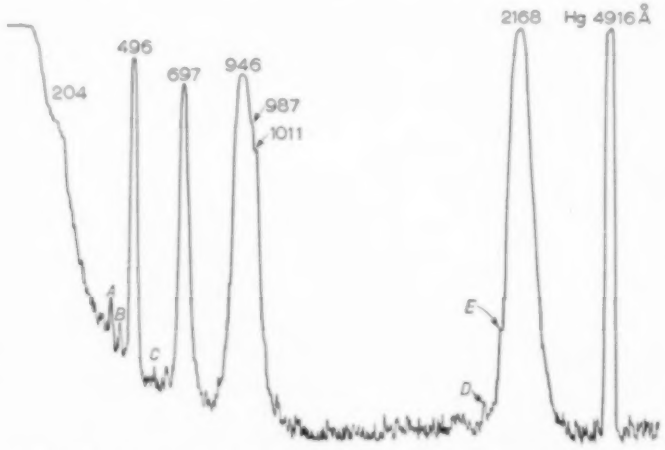

Fig. 2. A microphotometer tracing of the Raman spectrum excited by Hg 4358 Å. of a liquid sample of trisilylamine
A: 2168 excited by Hg 4046 Å
B: 496 excited by Hg 4346 Å
C: 2168 excited by Hg 4077 Å
D: 2168 excited by Hg 4339 Å
E: 2168 excited by Hg 4346 Å
Numbers ($\Delta\nu$) in cm^{-1}.

observed to be excited by the relatively weak mercury blue lines 4339 and 4346 Å. The strong Raman frequency 496 cm^{-1} was likewise excited by 4346 Å.

The infra-red measurements for trisilylamine-d_9 are given in Table 2. The bands at 2170, 865 and 735 cm^{-1} are regarded as due to residual traces of

VOL. 13 1958/5

Table 1. Infra-red and Raman spectra of trisilylamine

Infra-red (vapour)* ν (cm^{-1})	Intensity, etc.	Raman (liquid) $\Delta\nu$ (cm^{-1})	Intensity, etc.
446	vvw	204	w, br, depol.
		496	s, sp, pol.
503	vvw		
695	w, sh	697	s, br, depol.
748	vs		
941 }	vs	946	s, br, depol.
947 }			
996	vs	987	m, br, depol.
		1011	w, sp, depol.(?)
1131	w		
1186	m		
1388	w		
1436	w		
1489	m		
1590	sh		
1635	w		
1687	sh		
1760	vw		
1898	w		
2010	mw		
2165	vs	2168	vs, sp, pol.
3110	w		
3170	w		
4335	vw		

vvw = very weak indeed; vw = very weak; w = weak; mw = medium weak; m = medium intensity; s = strong; vs = very strong; sh = shoulder; br = broad; sp = sharp; pol. = polarized; depol. = depolarized.

* Not studied below 400 cm^{-1}.

Table 2. Infra-red spectrum of trisilylamine-d_9

ν(cm^{-1})	Intensity, etc.	Remarks
587	m	Analogous to 748 of $N(SiH_3)_3$
698	vs	Analogous to 941, 947 of $N(SiH_3)_3$
(735)	m	Residual SiH
(865)	m	Residual SiH
964	vs	Analogous to 996 of $N(SiH_3)_3$
(1095)	w	SiOSi impurity
1130	w	Analogous to 1186 of $N(SiH_3)_3$
1427	w	Analogous to 1489 of $N(SiH_3)_3$
1568 }	vs	Analogous to 2165 of $N(SiH_3)_3$
1583 }		
1723	w	964 + 698?
1930	w	2 × 964
(2170)	mw	Residual SiH

compounds containing Si–H as they increased in intensity together in a sample of slightly higher hydrogen content. The band at 1095 cm^{-1} is attributed to a small amount of disilyl ether impurity. It appears that the pair of bands at 1583 and 1568 cm^{-1} is analogous to that of $N(SiH_3)_2$ at 2165 cm^{-1}, and so must be due to Si—D stretching. The 996 cm^{-1} frequency of $N(SiH_3)_3$ appears only relatively little shifted (to 964 cm^{-1}) for the deuterated compound; but the features of $N(SiH_3)_3$ near 945 and at 748 cm^{-1} move respectively to 698 and 587 cm^{-1} on deuteration.

Discussion of results

Assignments and structure of the NSi_3 *skeleton.* The overall symmetry of the $N(SiH_3)_3$ molecule will depend upon the "rest" orientations (or possibly the free motion) of the hydrogen atoms with respect to rotation of the silyl groups about the N—Si bonds. It is reasonable to suppose, however, that the vibrations of the NSi_3 skeleton will be little affected by the configuration of the hydrogen atoms, and that therefore the interesting question of the shape of the skeleton can be discussed without reference to the overall symmetry of the whole molecule.

Table 3. Selection rules for planar and pyramidal NSi_3 skeletons

Planar			Pyramidal		
Mode	Activity infra-red	Raman	Mode	Activity infra-red	Raman
N—Si sym. stretch	—	pol.	N—Si sym. stretch	active	pol.
NSi_3 out-of-plane deformation	active	—	NSi_3 sym. deformation	active	pol.
N—Si asym. stretch	active	depol.	N—Si asym. stretch	active	depol.
NSi_3 in-plane deformation	active	depol.	NSi_3 asym. deformation	active	depol.

The rules of selection and polarization (see Table 3) offer the possibility of deciding whether the NSi_3 skeleton is planar (as indicated by the electron diffraction evidence [5]) or pyramidal (like $N(CH_3)_3$). The planar skeleton should give only one polarized Raman line with no counterpart in the infra-red, whereas the pyramidal structure should give two polarized Raman lines, both with coincidences in the infra-red.

By analogy with BCl_3 the skeletal frequences are expected to occur below 1000 cm^{-1}. As is seen from Table 1, only one polarized Raman line (and that of high intensity) is observed in this region. Its frequency, 496 cm^{-1}, is attributed to the symmetrical stretching mode of the NSi_3 skeleton. The extremely weak infra-red absorption at 503 cm^{-1} may possibly be due to the same mode of a slightly non-planar configuration; it might alternatively be attributed to a "hot" transition of this forbidden fundamental, made weakly active by the excitation of the lowest-frequency skeletal bending mode in the lower and upper states; or it might be assigned as the difference frequency 996–496 = 500 cm^{-1}. The very low intensity of

VOL. 13 1958/5

the symmetrical stretching mode of the skeleton in the infra-red (or its absence therefrom) provides strong evidence for the planar structure. Only one Raman frequency below 496 cm^{-1} is observed, i.e. 204 cm^{-1}, and by analogy with BCl_3 this can be assigned with confidence to the skeletal in-plane deformation. The infra-red active out-of-plane deformation might very well lie below 400 cm^{-1} and so have escaped observation in the present work. Its absence from the Raman spectrum provides further strong evidence in favour of the planar-skeleton model. The assignment of a frequency to the asymmetric stretching mode of NSi_3 is not quite so straightforward, as it is expected to lie near to 1000 cm^{-1}, i.e. in the region where silyl deformation frequencies may also occur. It is here that recourse may be made to the infra-red data for the deuterated compound. Of the frequencies in the region in question, 996 cm^{-1} of $N(SiH_3)_3$ moves only relatively little to 964 cm^{-1} for $N(SiD_3)_3$, whereas the other strong features near 945 and 748 move to 698 and 587 cm^{-1} respectively. Thus 996 (infra-red) and the nearly equal 987 cm^{-1} (Raman) are assigned to the skeletal mode. It is possible that the bands at 996 and near 945 cm^{-1} may involve some mixing of Si—N stretching and SiH_3 deformation vibrations. In Table 4 the fundamentals of the NSi_3 skeleton are compared with those of the planar BCl_3 molecule [8]. The parallelism is obvious.

Table 4. Fundamental frequencies of BCl_3 and NSi_3

Mode	BCl_3[8]	NSi_3
sym. stretch	471	496
out-of-plane deformation	462	<400?
asym. stretch	958	987
in-plane deformation	243	204

Assignments for the $N(SiH_3)_3$ *molecule as a whole.* As already mentioned, the overall symmetry of the molecule will depend on the "rest" configuration (or possible free rotation) of the hydrogen atoms. The NSi_3 skeleton being planar, the effective point group for free silyl rotation would be D_{3h}; with different "rest" configurations it might be C_{3h}, C_{3v}, C_3, C_s or C_1. In each case the rules of selection and polarization would be different, and in principle a discrimination is possible. In practice, however, it is found that the numbers of observed Raman and infra-red frequencies, of polarized Raman lines and of coincidences, are too few to permit any definite conclusions; they would be consistent even with D_{3h} symmetry. The paucity of the experimental evidence makes low symmetries, such as C_3, C_s or C_1, very improbable. On the other hand owing to the partial double-bond character of the N—Si bonds, due to d–p π-bond formation, it may be that the silyl groups cannot rotate freely. Unfortunately no thermodynamic data are available to check on this. Of the remaining point groups C_{3h} and C_{3v}, the former appears more plausible on general steric grounds (see Fig. 3); we therefore choose it as the basis for a formal assignment of the observed frequencies. (Alternative formal assignments could, of course, be made on the basis of D_{3h} or C_{3v}.)

For C_{3h} the twenty-two distinct fundamentals are distributed as follows amongst the symmetry species: $6A' + 5A'' + 7E' + 4E''$. Modes of species A' are active only in the Raman spectrum, where they give polarized lines; those of species A'' are active only in the infra-red; those of species E' are active in both spectra, while those of E'' are active only in the Raman spectrum, giving depolar-

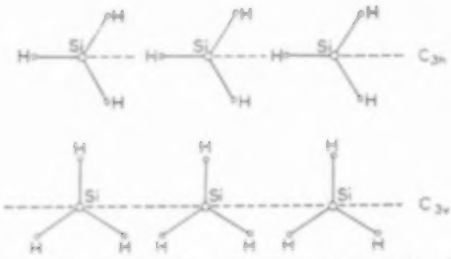

Fig. 3. Silyl group orientation for possible point groups C_{3h} and C_{3v}. For clarity the circle upon which the three Si atoms lie is shown opened out into a straight line (dotted).

ized lines. The numbering of the fundamentals and an approximate description of the predominant type of motion involved in each mode is given in Table 5. It should be borne in mind that modes of not very different frequencies which belong to the same symmetry class may be subject to considerable mixing.

The frequencies 204, 496 and 987 cm^{-1} have alrady been assigned to skeletal vibrations. With the enumeration for point group C_{3h} they become ν_{18}, ν_6 and ν_{16} respectively. The other skeletal frequency ν_{10} probably lies below 400 cm^{-1}. The Raman frequency 2168 cm^{-1} is presumed to be largely due to ν_1 in view of its polarization. The other Si—H stretching frequencies will lie close to this value: even with the considerable resolving power of the Hilger 2-prism E.612 instrument they could not be resolved in the Raman spectrum. The infra-red band at 2165 cm^{-1} is clearly to be ascribed to overlapping ν_7, ν_{12} and ν_{13}. In the deuterated compound it suffers a large displacement and appears as the two frequencies 1568 and 1583 cm^{-1}.

The silyl deformation and rocking frequencies are expected to lie in the neighbourhood of 1000 and 700–760 cm^{-1} respectively. There is no definitely polarized Raman line which can be ascribed to ν_3 or ν_4. The symmetrical silyl deformation of $O(SiH_3)_2$, analogous to ν_3, occurs at 1009 cm^{-1} [4], and it seems reasonable to suggest that the apparently depolarized but sharp Raman line at 1011 cm^{-1} may in fact contain ν_3. Its degree of polarization may be small on account of its being nearly coincident with the depolarized ν_{20}, to which this frequency is also assigned. The Raman line at 946 cm^{-1} is ascribed to ν_{14} and ν_{15} on account of its practical coincidence with the infra-red frequencies 941 and 947 cm^{-1}. It is suggested that ν_4 has approximately the same value. In accordance with the assignment of 941 and 947 to silyl vibrational modes, these infra-red features (unlike the skeletal frequency 996) suffer a large displacement (to 698 cm^{-1}) on deuteration. The same is true of the infra-red band at 748 cm^{-1}, which moves to 587 cm^{-1} on deuteration; and in view of the absence of a Raman line at 748 cm^{-1}, this frequency is assigned specifically to ν_9, the out-of plane silyl rocking mode. It

VOL. 13 1958/5

Table 5. Assignment of fundamentals of $N(SiH_3)_3$ on the basis of point group C_{3h}

Symmetry species	No. of frequency and approximate type of vibration	Assignment	
		infra-red (vapour) ν (cm^{-1})	Raman (liquid) $\Delta\nu$ (cm^{-1})
A'	ν_1 Si—H stretch		2168
	ν_2 Si—H stretch		2168
	ν_3 SiH_3 deformation		1011
	ν_4 SiH_3 deformation		946
	ν_5 SiH_3 rock		697
	ν_6 N—Si stretch		496
A''	ν_7 Si—H stretch	2165	
	ν_8 SiH_3 deformation	~945	
	ν_9 SiH_3 rock	748	
	ν_{10} NSi_3 out-of-plane deformation	(<400)	
	ν_{11} SiH_3 torsion	—	
E'	ν_{12} Si—H stretch	2165	2168
	ν_{13} Si—H stretch	2165	2168
	ν_{14} SiH_3 deformation	947	946
	ν_{15} SiH_3 deformation	941	946
	ν_{16} N—Si stretch	996	987
	ν_{17} SiH_3 rock	695	697
	ν_{18} NSi_3 in-plane deformation	—	204
E''	ν_{19} Si—H stretch		2168
	ν_{20} SiH_3 deformation		1011
	ν_{21} SiH_3 rock		697
	ν_{22} SiH_3 torsion		—

is observed to have something of a type-C contour, in agreement with this assignment. The Raman line at 697 cm^{-1} is ascribed to ν_{17}, in view of its coincidence with the weak infra-red shoulder at 695 cm^{-1}. The remaining silyl rocking frequencies ν_5 and ν_{21} presumably lie at approximately the same frequency. We thus arrive at the formal assignment of fundamentals in terms of point group C_{3h}, as given in Table 5. This is complete except for the two torsional frequencies.

The remaining bands in the infra-red spectrum, all relatively weak, are nearly all assignable as first overtones or binary combinations belonging to active symmetry species (see Table 6). The band at 1590 cm^{-1} has to be explained as at least a ternary combination. The frequency 1131 cm^{-1}, if due to trisilylamine, is unexplained.

Stretching force constant of the N—Si *bond.* The planarity of the NSi_3 skeleton is evidence that d–p π-bonding occurs, but it does not give any quantitive information about its strength. It is therefore of considerable interest to calculate an approximate stretching force constant for the Si—N bond. This may be done very simply on the assumption that there is negligible coupling between the skeletal and silyl

modes. Using a value of 31 atomic units as the effective mass of the silyl group and adopting a valency type of force field with interactions [9], the observed frequencies 496, 996 and 204 cm^{-1} of the planar NSi_3 skeleton lead to the value $k_1 = 4{\cdot}1 \times 10^5$

Table 6. Assignment of overtones and combinations for $N(SiH_3)_3$

Observed infra-red frequency (cm^{-1})	Assignment (cf. Table 5)
446	941 − 496 = 445
503	996 − 496 = 500
1131	?
1186	695 + 496 = 1191
	or 996 + 204 = 1200
1388	2 × 695 = 1390
1436	941 + 496 = 1437
1489	996 + 496 = 1492
1590	2 × 695 + 204 = 1594
1635	941 + 695 = 1636
1687	996 + 695 = 1691
1760	1011 + 748 = 1759
1898	2 × 947 = 1894
2010	1011 + 996 = 2007
3110	2165 + 947 = 3112
3170	2165 + 996 = 3161
4335	2 × 2165 = 4330

dyn/cm for the bond-stretching force constant and $k_1' = 0{\cdot}20 \times 10^5$ dyn/cm for the stretch–stretch interaction force constant. If the N—Si asymmetric stretching frequency for the deuterated trisilylamine (964 cm^{-1}) is employed, the corresponding results are $k_1 = 3{\cdot}9$ and $k_1' = 0{\cdot}27$ in the same units. We may adopt the approximate value 4·0 for k_1. This is near to the corresponding value 3·8 calculated by Kriegsmann [10] from the vibrational frequencies of $NH(SiMe_3)_2$; but the agreement may be partly fortuitous, since Kriegsmann used only a simple valency force field with an effective point mass for each $Si(CH_3)_3$ group.

The value 4·0 for the stretching force constant of the N—Si bond in trisilylamine is within what is commonly regarded as the single-bond range, and so indicates that the degree of π-bonding (although sufficient to cause the NSi_3 skeleton to be planar) is not in fact very large. In this connexion it is interesting to compare the force constants for analogous compounds involving respectively methyl and silyl groups (see Table 7). In making the comparisons the approximations underlying the derivations of the calculated values should be borne in mind. For $O(SiH_3)_2$, $O(CH_3)_2$, $N(CH_3)_3$, $C(CH_3)_4$ and $Si(CH_3)_4$ valency type force fields with interaction terms were used. Less strictly comparable are the values for $O(SiMe_3)_2$, $NH(SiMe_3)_2$ and $CH_2(SiMe_3)_2$, as they are based upon a simple valency force field, the $SiMe_3$ groups being regarded as point masses. As no force constant is available for a C—(SiH_3) bond analogous to the C—(CH_3) bonds in $C(CH_3)_4$, Table 7 quotes the value for Si—(CH_3) in $Si(CH_3)_4$. Despite these considerations,

VOL. 13 1958/5

however, Table 7 suggests that there is a more marked increase of k_1 in passing from the single bond C—Si to N—Si and O—Si than there is in the series C—C, N—C, O—C where all three bonds are single. This is as expected on the view that the N—Si and O—Si bonds have some double-bond character on account of d–p-π-bond formation.

Table 7. Stretching force constants for bonds involving either silicon or carbon

Bond	Molecule	k_1 (10^5 dyn/cm)	Reference
O—Si	$O(SiH_3)_2$	5·0	[11]
	$O(SiMe_3)_2$	4·7	[10]
N—Si	$N(SiH_3)_3$	4·0	present work
	$HN(SiMe_3)_2$	3·8	[10]
C—Si	$H_2C(SiMe_3)_2$	2·8	[10]
	$Si(CH_3)_4$	2·9	[12]
O—C	$O(CH_3)_2$	5·2	[12]
N—C	$N(CH_3)_3$	4·7	[12]
C—C	$C(CH_3)_4$	4·2	[12]

Acknowledgements—Our thanks are due to Dr. B. J. Aylett for helpful advice and loan of apparatus for the preparation of some of the samples of trisilylamine; Miss M. J. Mackillop is indebted to the Carnegie Trust, and J. R. Hall to the University of Queensland, for Research Scholarships.

References

[1] MacDiarmid A. G. *Quart. Rev. Chem. Soc., Lond.* 1956. **10** 208
[2] Aylett B. J. *J. Inorg. Nuclear Chem.* 1956 **2** 325.
[3] Ewing V. and Sutton L. E. Private communication.
[4] Lord R. C., Robinson D. W. and Schumb W. C. *J. Amer. Chem. Soc.* 1956 **78** 1327.
[5] Hedberg, K., *J. Amer. Chem. Soc.* 1955 **77** 6491.
[6] Stock A. and Somieski K., *Ber. dtsch. chem. Ges.* 1921 **54** 740.
[7] Rolfe J. A. and Woodward L. A. *Trans. Faraday Soc.* 1954 **50** 1030.
[8] Herzberg G. *Infrared and Raman Spectra* p. 178. Van Nostrand, New York 1945.
[9] Herzberg G. *Infrared and Raman Spectra* p. 188. Van Nostrand, New York 1945.
[10] Kriegsmann H. *Z. Elektrochem.* 1957 **61** 1088.
[11] McKean D. C. Unpublished calculation.
[12] Siebert H., *Z. anorg. Chem.* 1953 **273** 170.

Spectrochimica Acta, 1958, Vol. 13, pp. 212 to 216. Pergamon Press Ltd., London. Printed in Northern Ireland

Vibrational bands of isothiocyanates, thiocyanates and isocyanates

G. L. Caldow and H. W. Thompson
The Physical Chemistry Laboratory, Oxford

(*Received* 10 *July* 1958)

Abstract—Vibrational absorption bands of some isothiocyanates, thiocyanates and isocyanates in the region 2000–2300 cm^{-1} have been measured, using dilute solutions in carbon tetrachloride or chloroform. In many cases the bands are not single, but no explanation can be given for their complexity. The variation of the main vibrational frequency and band intensity of the chromophoric group with different aromatic ring substituents has been examined. With isothiocyanates the vibration frequencies are higher in chloroform than in carbon tetrachloride, but with thiocyanates there is no such solvent effect.

Recent papers from this laboratory have reported data on the effect of substituents in an aromatic ring upon the vibration frequency and band intensity of a chromophoric group attached to the ring. Interesting empirical relationships have been discovered with nitriles [1], anilines [2], phenols [3] and other compounds [4] and an interpretation has recently been suggested in terms of the electronic effects of the substituent groups [5]. This paper describes results with aryl isothiocyanates, thiocyanates and isocyanates, each of which has strong absorption between 2000 and 2200 cm^{-1}. Alkyl isothiocyanates have also been measured for comparison. Little has been reported previously about the characteristic frequencies of these compounds.

A Perkin–Elmer 21 spectrometer with rock-salt prism was used, the effective slit width being about 8 cm^{-1}. In estimating the intensities the bands were recorded for solutions of different concentration and path length, and extrapolation was carried out by the usual Wilson–Wells method. In the tables below, the intensity A is given in absolute units, molecules, cm, c/s, $\log_e$. The solutes were either special preparations or commercial products, repurified before use.

The aryl isothiocyanates have an intense band in the range 2000–2200 cm^{-1}, but there are other bands or shoulders, and the main band is very broad ($\Delta\nu_{1/2}{}^a \sim$ 100 cm^{-1}). Some examples are shown in Fig. 1, and the results are given in Table 1, the value of A referring to the total absorption in this region. The significance of the large band width, and of the multiple bands is not yet clear. It may be noted that the frequencies are higher in chloroform than in carbon tetrachloride, which is the converse of the results with many other solutes. Change of solvent has little effect upon the observed band intensity.

The results for aryl thiocyanates are given in Table 2. The apparent half band widths are about 15 cm^{-1} and the intensities are much lower than those of the isothiocyanates, and of about the same magnitude as those for the C≡N group in nitriles. The vibration frequencies are not significantly altered on passing from carbon tetrachloride to chloroform, as with the substituted benzonitriles [6].

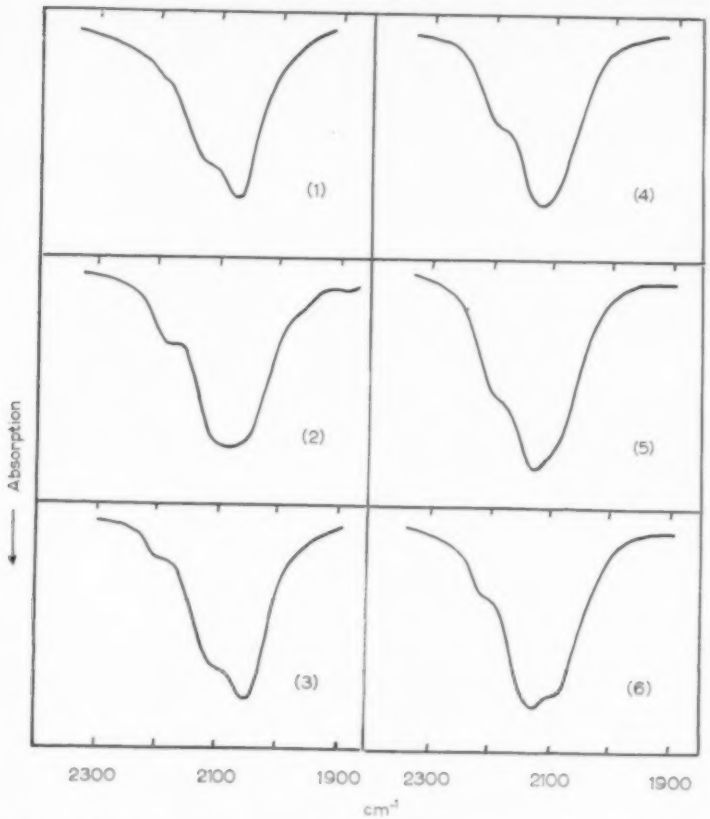

Fig. 1. Phenyl isothiocyanates. (1), (2), (3): Phenyl, *p*-ethoxyphenyl and *p*-chloro in carbon tetrachloride. (4), (5), (6): As above in chloroform.

Table 1. Phenyl isothiocyanates

Substituent	σ	Carbon tetrachloride		Chloroform	
		ν (cm^{-1})	(10^6 Å)	ν (cm^{-1})	(10^6 Å)
p-CH_3O	−0·268	2087	7·4	2130	7·5
p-C_2H_5O	−0·25	2080	7·6	2120	7·9
2·5 diC_2H_5O	−0·20	2040	8·1	2050	7·9
3COOH—4OH	−0·002			2132	7·6
—	0	2065	7·8	2112	7·7
p-Cl	+0·227	2052	8·9	2112	8·8
m-COOH	+0·355			2115	8·4
p-NO_2	+0·78			2045	10·4
2·3 $(CH)_4$		2085	8·4		

Table 2. Phenyl thiocyanates

Substituent	σ	Carbon tetrachloride ν (cm^{-1})	Chloroform	
			ν (cm^{-1})	(10^7 Å)
p-$N(CH_3)_2$	−0·73	2164	2161	2·6
p-NH_2	−0·66	2166	2161	2·4
p-OH	−0·357	2168	2164	2·0
p-$CH_3CO{\cdot}NH$	−0·015	2167	2168	2·0
$3NO_2{\cdot}4NH_2$	+0·05		2167	1·8
p-COOH	+0·245		2169	
m-COOH	+0·355		2170	
p-NO_2	+0·778	2174	2175	1·4
2·4 diNO_2	+1·578	2173	2174	

Table 3. Phenyl isocyanates

Substituent	σ	Carbon tetrachloride	
		ν (cm^{-1})	(10^6 Å)
p-CH_3	−0·17	2280	7·1
o-CH_3	−0·17	2282	7·3
m-CH_3	−0·069	2273	7·4
—	0	2267	7·0
p-C_6H_5	+0·009	2272	8·4
$3{\cdot}4(CH)_4$	+0·17	2273	8·4
p-Cl	+0·227	2275	7·1
p-Br	+0·232	2269	7·4
m-NO_2	+0·71	2272	7·7
p-NO_2	+0·778	2269	8·5
o-NO_2	+0·8	2271	7·8
o-CH_2O	−0·39	2243/2257	7·8
$2{\cdot}3(CH)_4$		2277	7·8

Table 4. Alkyl isothiocyanates, R·NCS

R	Carbon tetrachloride		Chloroform	
	ν (cm^{-1})	(10^6 Å)	ν (cm^{-1})	(10^6 Å)
CH_3	2113	2·0	2137	1·9
C_2H_5	2103	5·9	2130	4·8
$CH_2{=}CH{\cdot}CH_2$	2100	5·2	2113	5·3
n-C_3H_7	2085	3·6	2110	3·7
iso-C_3H_7	2083	6·0	2094	5·5
C_6H_5CO	1990	9·7	2000	9·8
p-$CH_3O{\cdot}C_6H_4{\cdot}CO$			1998	8·8

VOL. 13 1958/5

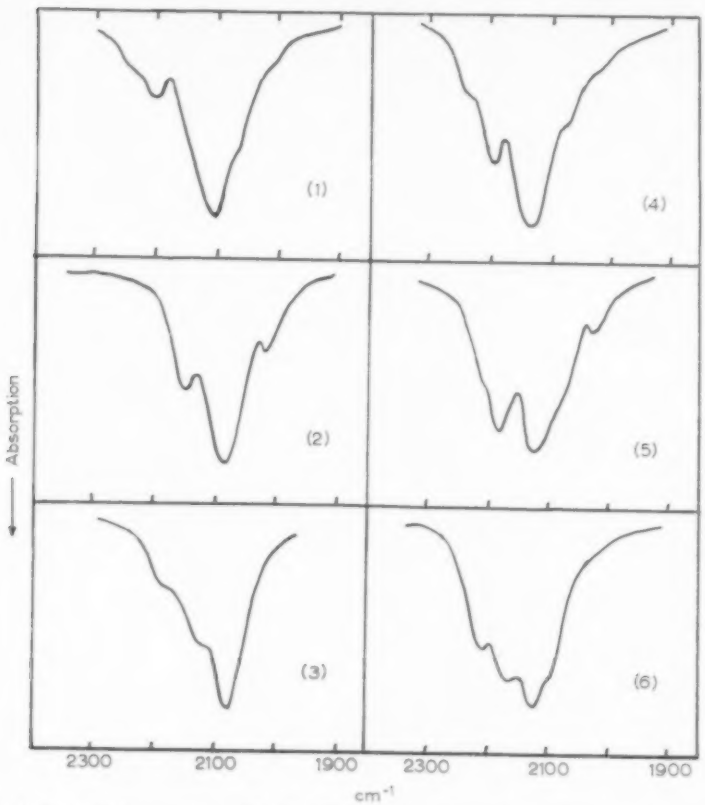

Fig. 2. Alkyl isothiocyanates. (1), (2), (3): Ethyl, *iso*propyl, *n*-propyl in carbon tetrachloride. (4), (5), (6): As above in chloroform.

The aryl isocyanates, which polymerize easily, were all redistilled under reduced pressure just before use. The intense absorption occurs in the range 2200–2300 cm^{-1}, and there are shoulders to the main bands, whose half width is 25–35 cm^{-1}. Table 3 gives the results, which agree satisfactorily with earlier data of DAVISON [7] and also with measurements in this laboratory by MIDDLETON [8]. Some liquid isocyanates were studied by HOYER [9].

A number of aliphatic isothiocyanates were also measured. These have an intense absorption near 2100 cm^{-1}, but the band splitting is more marked than with the compounds discussed above. Fig. 2 shows some typical examples, and the results are summarized in Table 4 where the intensity A again refers to the total absorption in this region. It is impossible to interpret the band splitting. In some cases rotational isomerism could occur, but this explanation could not apply to the multiple band structure found with the aromatic derivatives above.

The results for the aryl compounds listed in Tables 1–3 have been considered from the standpoint of the relationships found with other series. With aryl isothiocyanates and isocyanates the plots of ν against σ, the Hammett constant of the substituent, show scatter although with aryl thiocyanates this plot is roughly

linear with a small positive slope. The plots of log A against σ are roughly linear for isothiocyanates and thiocyanates, with small positive and negative slopes respectively. With aryl isocyanates the band intensity is essentially independent of σ. However, the occurrence of shoulders, and the broad nature of some bands complicates the problem as regards both frequency and intensity plots. On the other hand, the small slope of the log A/σ plot is consistent with the value now found for the —SCN substituent [10] if the general arguments recently suggested by Krueger and Thompson are valid [5].

Acknowledgements—Many of the compounds used were kindly supplied by Imperial Chemical Industries, Dyestuffs Division, to whom we express our thanks. We are also grateful to the Hydrocarbon Research Group for financial help, and to the board of electors for the award of a Shell Postgraduate Scholarship to one of us (G. L. C.).

References

[1] Thompson H. W. and Steel G., *Trans. Faraday Soc.* 1956 **52** 1451.
[2] Krueger P. J. and Thompson H. W., *Proc. Roy. Soc.* A 1957 **243** 143.
[3] Stone P. J. and Thompson H. W., *Spectrochim. Acta* 1957 **10** 17.
[4] Thompson H. W., *Molecular Spectroscopy Symposium.* Institute of Petroleum 1958.
[5] Krueger P. J. and Thompson H. W., *Proc. Roy. Soc.* 1958. In press.
[6] Mander M. R. and Thompson H. W., *Trans. Faraday Soc.* 1957 **52** 1451.
[7] Davison W. H. T., *J. Chem. Soc.* 1953 3712.
[8] Middleton R. D., Dissertation, Oxford 1956.
[9] Hoyer H., *Chem. Ber.* 1956 **89** 2677.
[10] McDaniel D. H. and Brown H. C., *J. Org. Chem.* 1958 **23** 420.

VOL. 13 1958/5

Spectrochimica Acta, 1958, Vol. 13, pp. 217 to 222. Pergamon Press Ltd., London. Printed in Northern Ireland

Vibrational band intensities of the C≡N group in aliphatic nitriles

J. P. Jesson and H. W. Thompson
The Physical Chemistry Laboratory, Oxford

(*Received* 10 *July* 1958)

Abstract—The vibrational frequency and band intensity of the C≡N group in a large number of aliphatic nitriles have been measured. In most cases the substances were studied in carbon tetrachloride and in chloroform, but some were also measured in the vapour state. The results have been discussed in relation to the detailed molecular structure of the molecules concerned. Some important variations of band intensity have been found between the vapour and solutions.

Some recent measurements on the frequency and intensity of the C≡N group stretching vibration band have revealed interesting correlations between spectral characteristics and molecular structural factors. Substituted benzonitriles have been studied in some detail [1] and the results suggested that it might be profitable to examine a larger variety of aliphatic compounds containing the C≡N group than was measured previously [2]. Also, the changes in the spectral properties which occur with these substances on passing from the vapour phase to solutions in solvents of different character may provide important information about intermolecular forces. This paper describes such measurements on a number of simple and substituted aliphatic nitriles.

Experimental method

A Perkin–Elmer 12C spectrometer was used, with lithium fluoride prism, and the effective slit width was about 5 cm^{-1}. Carbon tetrachloride and chloroform were washed, dried and redistilled. The nitriles used were commercial products repurified by standard methods. Dichloroacetonitrile was prepared from ethyl dichloroacetate through the amide. Gas phase measurements were made in a 1 m path length multireflection cell, both before and after adding air up to one atmosphere as a pressure broadener. Determinations were made using a number of partial pressures of each compound. Solutions were studied in a variable path length cell, with thickness 0·05–0·125 cm. Concentrations were usually in the range 0·2–0·6 molar, but much higher concentrations were needed for chloroacetonitrile and much lower ones for the cyanamides. The apparent intensities were measured by direct graphical integration for a series of different path lengths and concentrations, and extrapolated to zero absorbance by the usual Wilson–Wells method. All intensities are given in absolute units, cm^2 $molecule^{-1}$ sec^{-1}, $\log_e$. It may be noted that the Ramsay constant K calculated from the observed intensities and half band widths was uniformly about 20 per cent lower than the value expected. This discrepancy has also been noticed in other cases and may arise because the band contour does not follow a Lorentz function.

Results

The results are summarized in Tables 1 and 2. Preliminary data on some of the compounds [2] have been revised. Where comparisons are possible, the present results agree well with those of Sensi and Gallo [3]. For example, the band intensities in chloroform for acetonitrile and chloracetonitrile are now found to be 4·3 and 0·45 $\times 10^{-8}$, against 4·0 and 0·46 $\times 10^{-8}$ given by them.

Table 1. C≡N group vibration in alkyl cyanides and dicyanides

Substance	Vapour			Carbon tetrachloride			Chloroform		
	ν (cm^{-1})	(10^8 Å)	($\Delta\nu^0_{1/2}$)	ν (cm^{-1})	(10^8 Å)	($\Delta\nu^0_{1/2}$)	ν (cm^{-1})	(10^8 Å)	($\Delta\nu^0_{1/2}$)
Alkyl cyanides									
CH_3CN	2267	0·72	—	2255	2·1	9·2	2255	4·3	9·7
C_2H_5CN	2259	0·7	—	2249	2·6	8·4	2249	5·6	9·8
n-C_3H_7CN	2260·5	0·92	—	2253	3·3	—	2253	6·3	—
n-$C_5H_{11}CN$				2248	3·6	11	2249	6·8	12·5
iso$C_5H_{11}CN$				2253	4·0	—	2253	6·8	—
n-$C_{11}H_{23}CN$				2247·5	3·7	12·5	2248	6·7	13·8
n-$C_{16}H_{33}CN$				2248	3·5	12·4	2248	6·5	13·4
n-$C_{17}H_{35}CN$				2248	3·6	12	2249	6·8	13·6
Dicyanides									
$CH_2(CN)_2$							2273	1·7*	12·3
$(CH_2)_2(CN)_2$							2256	4·8*	12·0
$(CH_2)_3(CN)_2$							2255	7·6*	12·7
$(CH_2)_4(CN)_2$				2250	4·9*	11·3	2251	9·9*	13·2
$(CH_2)_5(CN)_2$				2248	6·7*	14·3	2249	11·7*	16
$(CH_2)_{10}(CN)_2$				2249	7·3*	12	2249	13·2*	13·5

* This value includes two C≡N groups.

The vibration frequency of the C≡N group in aliphatic nitriles in a given solvent is not much affected by changes in molecular structure unless there is direct conjugation or the possibility of a marked resonance effect. Also, although with any given compound the frequency is lowered slightly on passing from the vapour to solutions in carbon tetrachloride, it is almost unchanged on going from carbon tetrachloride to chloroform. Since no frequency shift occurs it might be inferred that there can be little hydrogen bond formation in chloroform. On the other hand there are changes of band intensity and the possibility of weak hydrogen bond formation cannot be ruled out.

The C≡N group band intensity appears to be more susceptible than its frequency to structural influences and other factors. For measurements in the vapour state, if "mass" effects and Fermi resonance can be ignored, the main factors affecting the band intensity will be inductive and resonance effects of attached groups or the occurrence of hyperconjugation. Unfortunately few of the compounds are sufficiently volatile to make the vapour phase intensities conveniently measurable. The results with chloro-acetonitriles illustrated in Fig. 1 suggest that at least two influences come into play when chlorine atoms are substituted

VOL. 13 1958/5

Table 2. C≡N group vibration in substituted alkyl cyanides and cyanamides

Substance	Vapour			Carbon tetrachloride			Chloroform		
	ν (cm^{-1})	(10^5 Å)	($\Delta\nu_{1/2}^{\circ}$)	ν (cm^{-1})	(10^5 Å)	($\Delta\nu_{1/2}^{\circ}$)	ν (cm^{-1})	(10^5 Å)	($\Delta\nu_{1/2}^{\circ}$)
α-substituted									
$CN{\cdot}CH_2CN$							2273	1·7*	12·5
$CO_2C_2H_5{\cdot}CH_2CN$				2265	2·2	17	2268	3·45	17·5
$Cl{\cdot}CH_2CN$	2266	0·39	—	2260	0·38	11·5	2261	0·45	11·5
$Cl_2CH{\cdot}CN$	2261	3·1	—	2259	1·1	—	2260	0·54	—
$Cl_3C{\cdot}CN$	2256	5·3	—	2249	3·2	9·5	2250	2·4	10·5
$CH_2{=}CH{\cdot}CH_2CN$				2253	2·6	18·5	2253	4·5	19
$C_6H_5{\cdot}CH_2CN$				2253	2·6	13	2253	4·8	14
$(C_6H_5)_2CHCN$				2246	2·8	12	2245	4·9	13
$CH_3CH(OH)CN$							2249	1·2	20·5
$(CH_3)_2C(OH)CN$				2243	1·6	16·5	2240	1·5	18·5
$N(C_2H_5)_2{\cdot}CH_2CN$				2232	0·57	10	2233	1·2	11·5
$CH_2{=}CH{\cdot}CN$	2241	0·3	—	2230	2·4	9	2231	5·5	10
β-substituted									
$Cl(CH_2)_2CN$				2259	2·5	—	2259	3·1	—
$OH(CH_2)_2CN$							2255	5·7	14·5
$N(CH_3)_2(CH_2)_2CN$							2252	6·1	16·5
$Br(CH_2)_2CN$				2256	2·0	10·5	2257	3·2	11·0
$CH_3O(CH_2)_2CN$				2254	3·3	13·5	2255	5·6	14·8
γ-substituted									
$Cl(CH_2)_3CN$				2252	2·94	12·5			
$Br(CH_2)_3CN$				2250	3·2	12·8	2251	5·6	13·5
$C_6H_5(CH_2)_3CN$				2249	3·6	10·3	2250	6·3	12
$C_6H_5O(CH_2)_3CN$				2251	3·76	17·5	2253	6·2	18
Cyanamides									
$N(C_2H_5)_2CN$	2227·5			2214	83	17·5	2209	115	23·5
$(CH_2{:}CH{\cdot}CH_2)_2CN$				2217	82	14·5	2215	110	16·5
$N(CH_3)_2CN$	2235			2221	83	11·0	2218	110	14

* This value includes two C≡N groups.

In some cases values of the apparent half band width are not given, owing to complications caused by shoulders.

successively into the methyl group, for the C≡N band intensity first falls and then rises. It is possible that inductive and hyperconjugative effects could operate. An alternative description of the trend would be to suppose that as chlorine atoms are successively substituted, there is a gradual alteration of the C≡N bond length, causing the r_e value to move along the curve which expresses the dipole moment as a function of r. If the equilibrium distance lies near to that corresponding to the maximum of this dipole function, it might be possible to get a large variation of $\partial\mu/\partial r$ for fairly small changes of r_e.

With solutions, factors other than internal molecular structure may affect the vibrational bands of the solute. These include the effect of the solvent dielectric, specific dipolar interaction between solute and solvent, and hydrogen bridge interaction. As more data accumulate it becomes more obvious that specific effects

between the solute and solvent are very important, even when the solvent is non-polar and "inert." Moreover, different vibrations, of a given solute may be affected by a particular solvent in different ways. It is reasonable, however, as a first step to compare molecules of a related series in the same solvent. With simple

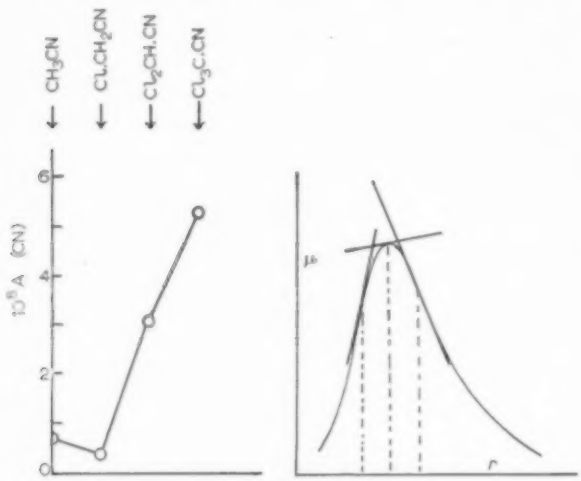

Fig. 1.

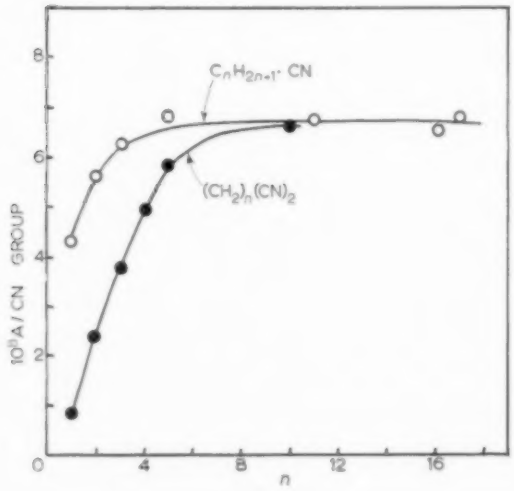

Fig. 2.

alkyl cyanides, as shown in Fig. 2, the C≡N group band intensity rises to a limiting value as the chain length increases, either in carbon tetrachloride or in chloroform. With the di-nitriles, the intensity per C≡N group rises to the same limiting value as the chain lengthens. Any inductive effect of one end group upon the other is gradually eliminated as the methylene chain is lengthened. These results show clearly that the inductive effect of groups attached to the C≡N

VOL. 13 1958/5

vibrational chromophore is such that no "standard" value can be adopted for its band intensity in different molecules. It is possible, however, that a C≡N group at the end of a long hydrocarbon chain will have a reliably fixed vibrational intensity, such as might be used in counting end groups of a polymer.

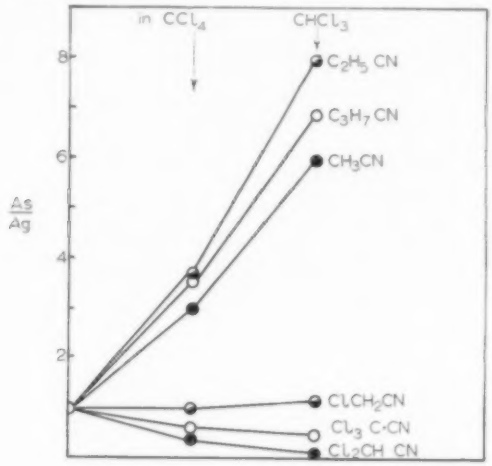

Fig. 3.

TAFT [4] has recently proposed a set of values for σ^*, the inductive power of different groups, on the basis of kinetic data, and we have examined how far these values of σ^* can be correlated with the changes of band intensity. With simple alkyl cyanides and a number of β-substituted propio-nitriles, for which the appropriate σ^* values are known, there is a regular trend of the intensity A (in chloroform) with σ^*, and the plot of log A against σ^* is roughly linear. If the value for malononitrile is included, this linear plot appears to hold over a range of σ^* from $-0{\cdot}1$ to $+1{\cdot}3$, and a sevenfold change in A. Values for σ^* in the γ-substituted butyronitriles are not known, and their computation by repeated application of the Taft reduction factor is not satisfactory. The results for the α-substituted aceto-nitriles are not in accord with the above linear plot, presumably because more powerful electronic influences occur which are not adequately described by the inductive effect alone. The deviations for α-substituents such as $N(C_2H_5)_2$, NH_2, OH, $CO_2C_2H_5$, appear in most cases to be roughly proportional to the resonance effect of the group concerned when it is present in an aromatic ring [4]. In this respect the group CH_2CN has a small resonance factor, and for this reason the intensity in malononitriles may appear to fit the linear relationship just mentioned. On the other hand, the results with several of the halogenated acetonitriles suggest the interplay of several influences upon the band intensity.

With substituted cyanamides, in which the participation of charge separated forms such as $R_2\overset{+}{N}{=}C{=}\overset{-}{N}$ is much more likely, there is a considerable increase of intensity of the C≡N group vibration band, and a marked fall in its frequency. In the case of vinyl cyanide, conjugation lowers the frequency markedly but the band intensity is not much affected.

The change of band intensity on passing from the vapour to solutions in carbon tetrachloride or chloroform seems to depend very much upon the exact nature of the solute, as illustrated in Fig. 3. With alkyl cyanides, the intensity in carbon tetrachloride is greater than that in the vapour state, but with chloracetonitriles it is less. Some intermolecular interaction must occur between solute and solvent involving mutual polarization or dipolar effects. It is possible that stearic factors introduced by the large halogen atoms may also play a part. The band intensity found with most of the compounds in chloroform is almost double that in carbon tetrachloride, but this ratio is much lower in the case of the chloracetonitriles and falls below unity. It is also relatively low in the case of the substituted cyanamides.

All these results emphasize the need for more measurements on solvent–solute interactions through studies on band intensities. At the same time, if suitable series of molecules can be chosen as solutes, correlations between the spectral features and the detailed electronic structural properties may be worked out.

The C≡N group vibration frequency of three dialkyl cyanamides in a number of solvents was also measured, and the results are given in Table 3. The data are not in good accord with the Kirkwood–Bauer–Magat relation, but will be discussed in more detail in a later paper together with other measurements in solvent effects.

Table 3. $\nu_{C\equiv N}$ in different solvents

Solvent	$(CH_3)_2N{\cdot}CN$	$(C_2H_5)_2N{\cdot}CN$	$(CH_2{:}CH{\cdot}CH_2)_2N{\cdot}CN$
Vapour	2235	2227·5	
Carbon tetrachloride	2221	2214	2217
Chloroform	2218	2209	2215
*cyclo*Hexane	2224	2217	2218·5
Carbon disulphide	2218	2213	2215
Acetonitrile	2216·5	2208·5	2214
Hexane	2223·7	2218·5	2220·5
Benzene	2219	2211	2215
Methylene chloride	2217	2210	2215
*trans*Dichloroethylene	2220·5	2214·5	2217
Ethylene dichloride	2216	2209·5	2213·5
Pyridine	2215	2210	2213
Bromoform	2215	2206	
Methyl chloroform	2220	2213	2216
Tetrachloroethylene	2221·5	2216	2218
Nitrobenzene	2215	2209·5	

Acknowledgement—We thank the Hydrocarbon Research Group of the Institute of Petroleum for financial help.

References

[1] KRUEGER P. J. and THOMPSON H. W., *Proc. Roy. Soc.* In press.
[2] THOMPSON H. W. and STEEL G., *Trans. Faraday Soc.* 1956 **52** 1451.
[3] SENSI P. and GALLO G. G., *Gazz. Chim. Ital.* 1955 **85** 224.
[4] TAFT R., *Steric Effects in Organic Chemistry*, Chap. 13. Wiley; New York 1956.

VOL. 13 1958/5

Spectrochimica Acta, 1958, Vol. 13, pp. 223 to 235. Pergamon Press Ltd., London. Printed in Northern Ireland

Vibration–rotation bands of keten

P. E. B. Butler, D. R. Eaton and H. W. Thompson
The Physical Chemistry Laboratory, Oxford

(*Received* 10 *July* 1958)

Abstract—The rotational structure of a number of vibrational bands of keten has been analysed, and values have been derived for some of the rotational constants. Several parallel type bands give a value of B_0 close to that obtained from the microwave spectrum (0·3371 cm^{-1}). Two other bands, associated with stretching modes of the C=C=O chain, give values much higher than this. Examination of other published data on this molecule, and also of results on the related molecules diazomethane and allene-d_2 suggest that a similar anomaly may occur in these cases. One perpendicular type band which is free from interactions has been analysed, and the value 9·34 cm^{-1} has been obtained for A_0. Using the measured values for A_0 and B_0, the following geometrical parameters have been derived:

$$r_0^{CH} = 1{\cdot}075\ \text{Å}, \qquad r_0^{CC} = 1{\cdot}31\ \text{Å}, \qquad r_0^{CO} = 1{\cdot}17\ \text{Å} \quad \text{and} \quad \widehat{HCH} = 123{\cdot}5^\circ.$$

The infra-red spectrum of keten has been measured by a number of workers. Although there is agreement about the frequencies of the stretching vibrational modes, the values for the skeletal bending vibrations are still not definitely settled. Arendale and Fletcher [1] have described a rotation analysis of one band of keten, and also of another band of dideutero-keten. For keten itself, Arendale and Fletcher's analysis gave a rotational constant $B_0 = 0{\cdot}3403$ cm^{-1}, which they regarded as being in satisfactory agreement with the microwave spectrum value of 0·3371 reported by Johnson and Strandberg [2]. With the dideutero derivative, B_0 was found to be 0·2952, which is very close to the microwave value of 0·2948 cm^{-1}. The discrepancy in the values of B_0 for the case of keten was specially interesting to us, since several years ago a rotational analysis of several keten bands had been made in this laboratory [3], and it had been found that in some cases there was close agreement with the microwave spectral data whilst in other cases there was a discrepancy of about the same magnitude and in the same sense as that reported by Arendale and Fletcher. It seemed desirable therefore to examine this problem again more critically. The present paper summarizes results on a number of parallel type bands of keten and on one perpendicular type band which is free from complications. We hope shortly to report an analysis of other perpendicular bands lying at longer wavelengths, in which special Coriolis interactions are involved.

Experimental method

Keten was prepared by the pyrolysis of acetone vapour on a heated nichrome wire. The mixture of products was passed through a series of traps and separated by vacuum distillation. Silicone tap grease was used throughout, and a check on the removal of ethylene and other likely impurities was made by repeated measurement of the entire spectrum using a Perkin–Elmer 21 spectrometer (rock salt). Although acetylene could not be removed by fractional distillation, a mass spectrometric check on purity suggested that little (<1%) was present and this amount was too small to interfere with the bands described below. Our

samples did not show the band at 2966 cm^{-1} reported by Arendale and Fletcher [4].

The spectrum was measured under high resolution with a grating spectrometer described in earlier papers from this laboratory, using a lead telluride detector for the range 3–5·5 μ and a Schwarz thermocouple at longer wavelengths. For the former region a grating with 7200 lines/in. blazed near 3·5 μ was used, giving a resolution of about 0·15 cm^{-1}. At longer wavelengths a large Sayce grating with 2500 lines/in. and blazed at 9 μ was used. The perpendicular band lying around 6100 cm^{-1} was measured with a small grating spectrometer fitted with a replica grating having 7500 lines/in., blazed at 3·5 μ and used in the second order. A lead suplhide cell was the detector and the resolution was about 1·5 cm^{-1}. As a rule, the absorption cell was a glass tube 10 cm in length with rock-salt end plates, but some measurements were made with a multireflection long path cell using paths up to several metres, and a few others with a low temperature gas cell using solid carbon dioxide–acetone as cooling bath.

Results

Keten has four fundamental vibrational modes which give rise to parallel type bands, namely the CH_2-symmetrical stretching mode, the CH_2-group deformation, and two stretching vibrations of the C=C=O chain. It is a planar molecule with symmetry C_{2v}, and approximates closely to a symmetrical top with moments of inertia about 3×10^{-40} g cm^2 and 85 g cm^2. The slight asymmetry is too small, as far as these measurements are concerned, to cause appreciable deviations from symmetrical top behaviour and we can expect to derive two main rotational constants A and B, although the latter should really be written as $\bar{B} = \frac{1}{2}(B + C)$. The parallel bands should consist of P, Q, R branches with sub-bands corresponding to different K-values. The extent to which overlapping of sub-bands will complicate the simple appearance in any particular case will be determined by the relative values of A' and A''. It is doubtful whether the present results justify any attempt to determine the very small centrifugal stretching constant D.

Band ν_1

This band is associated with the stretching of C—H bonds and has well resolved P- and R-"lines". Near the centre of the band there are some stronger absorption peaks, alternating in intensity and presumably corresponding to the Q-branches with different K-value. Wavelength calibration was carried out using standard lines of hydrogen chloride [5] and of water vapour. The band was recorded in a 10 cm path with pressures around 50 mm, and also in the cooled cell (30 mm) with 15 mm pressure. The positions of the absorption lines are given in Table 1.

The data were analysed using the usual combination difference and sum plots. In the P and R "lines":

$$\frac{\Delta_2 F''(J)}{(J + \frac{1}{2})} = (4B'' - 6D_J'') - 8D_J''(J + \tfrac{1}{2})^2$$

VOL. 13 1958/5

Table 1. Band ν_1 (positions in cm^{-1})

J	$R(J)$	$P(J)$	J	$R(J)$	$P(J)$
1	3071·88		26	3088·41	3052·81
2	72·52		27	89·15	52·09
3	73·15		28	89·75	51·47
4	73·85		29	90·38	50·81
5	74·44		30	91·04	50·09
6	75·13		31	91·69	49·17
7	75·78		32	92·35	48·62
8	76·46		33	92·98	47·95
9	77·06		34	93·64	47·29
10	77·82	3063·60	35	94·24	46·57
11	78·45		36	3094·95	45·85
12	79·15	62·28	37		45·22
13	79·75	61·55	38		44·50
14	80·46	60·88	39	3096·80	43·78
15	81·15	60·21	40	97·50	43·12
16	81·80	59·57	41	98·10	42·34
17	82·51	58·93	42	3098·78	41·71
18	83·08	58·17	43		41·02
19	83·76	57·56	44		40·31
20	84·48	56·86	45		39·68
21	85·10	56·33	46		38·96
22	85·79	55·49	47		38·28
23	86·41	54·82	48		37·63
24	87·13	54·12	49		3036·94
25	3087·79	3053·46			
Q_2	3069·94	w	Q_5	3066·57	s
Q_3	3069·04	s	Q_6	3064·98	w
Q_4	3067·75	w	Q_7	3063·04	s

and

$$R(J-1)+P(J)=2\nu_0+2(B'-B'')J^2$$

The value both expected and estimated for the centrifugal stretching constant D_J'' is small, so that is seems justifiable to ignore other terms in these equations until still higher resolution and precision can be obtained. The combination plot leading to B'' is shown in Fig. 1, and the sum plot giving ν_0 in Fig. 2. The plot of ν^Q against K^2, according to the relation for sub-band origins, namely:

$$\nu=\nu_0+[(A'-A'')-(B'-B'')]K^2$$

is shown in Fig. 3 and leads to a value for ν_0 which agrees with that obtained from the combination sum plot. The superposition of the sub-bands associated with different K-values seems in this case to leave the set of P- and R-"lines" clearly resolved, although a definite K-value cannot be assigned to them. This

should not, however, much affect the value of B_0 determined. The following constants are thus obtained (cm^{-1}):

$$B'' = B_0 = 0{\cdot}3370 \qquad \nu_0 = 3070{\cdot}45$$
$$\alpha_1{}^B = B'' - B' = +0{\cdot}0003$$
$$D_J{}' \sim D_J{}'' \sim 2 \times 10^{-7}$$
$$\alpha_1{}^A = (A'' - A') = +0{\cdot}15$$

Johnson and Strandberg [2] have found $B_0 = 0{\cdot}3371$ from the microwave spectrum.

Band $(\nu_3 + \nu_4)$

This combination band consists of well resolved P- and R-"lines" and a weak central Q-branch. There are other lines interspersed among the P- and R-lines, which may arise from one or more overlapping "hot" transitions. Lines of hydrogen bromide [6] were used for calibration, and the best measurements on this band were obtained in the long path cell using 2 m and 20 mm pressure. At higher pressures there appeared to be excessive broadening.

There is some ambiguity in the choice of the band origin and in the J numbering of the P- and R-lines, but the α-value is so small that any plausible error in this assignment of J-values will not seriously affect the value derived for B''. The assignments listed in Table 2, which seemed also the most likely on other grounds, lead to a value of B'' in close agreement with that already found for the band ν_1. The combination difference and sum plots leading to B'', ν_0 and α are shown in Figs. 1 and 2. The following constants were derived:

$$\nu_0 = 2513{\cdot}65 \qquad B'' = B_0 = 0{\cdot}3368$$
$$\alpha = B'' - B' = +0{\cdot}00007_5$$
$$D_J{}' \sim D_J{}'' \sim 1{\cdot}5 \times 10^{-7}$$

Band $2\nu_6$

This parallel type band is associated with the overtone of a CH_2-group rocking mode. P- and R-"lines" are well resolved and can be measured satisfactorily up to about $J = 40$ in each branch, but there are other lines at each extremity which have not been explained. There is a weak central Q-branch. The band was calibrated against lines of deuterium chloride [7], and also using lines of water vapour and carbon dioxide near 2·8 μ in the second order. For measuring the band a pressure of 150 mm was used in a 10 cm path. The results are collected in Table 3 and the combination plots are shown in Figs. 1 and 2. The following values were obtained:

$$\nu_0 = 1962{\cdot}9 \qquad B'' = 0{\cdot}3367 \qquad \alpha = -0{\cdot}0002$$

The data on this band are somewhat unsatisfactory in one respect, in that the combination difference plot for B'' seems to have zero slope, implying a negligible value of D''. No explanation can be given for this at present.

VOL. 13 1958/5

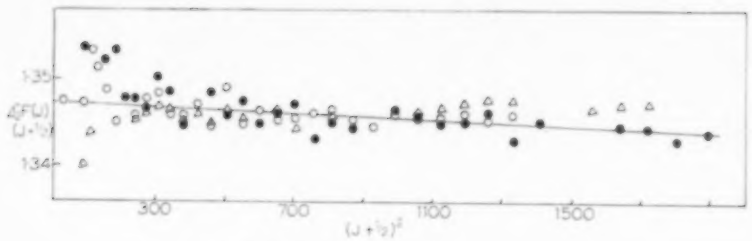

Fig. 1. Plots of $\frac{\Delta_2 F''(J,K)}{(J+\frac{1}{2})}$ against $(J+\frac{1}{2})^2$. ● ν_1; ○ $(\nu_3+\nu_4)$; △ $2\nu_6$.

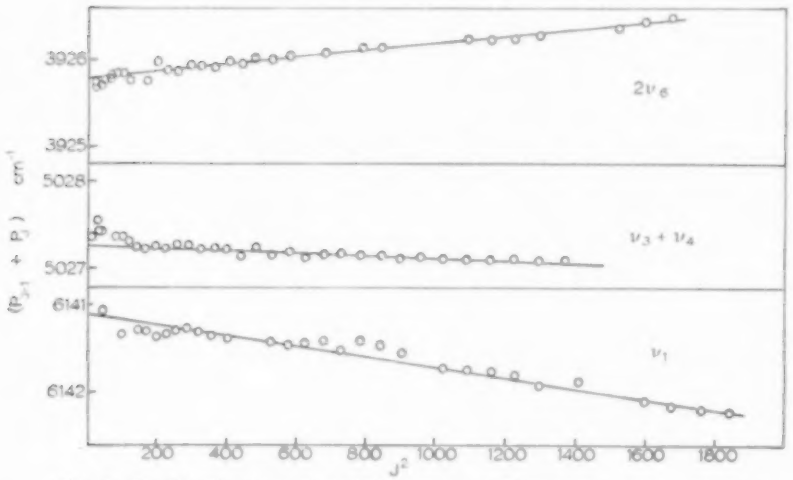

Fig. 2. Combination sum plots $[R(J-1)+P(J)]$ against J^2 for $2\nu_6$,$(\nu_3+\nu_4)$,ν_1.

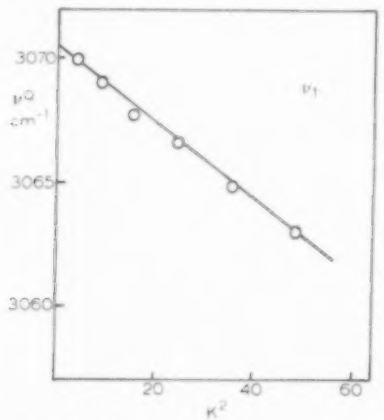

Fig. 3. Band ν_1. Plot of ν_Q against K^2.

Table 2. Band ($\nu_3 + \nu_4$)

J	$R(J)$	$P(J)$	J	$R(J)$	$P(J)$
0	2514·31		28	2533·08	2494·75
1	15·01	2513·04	29	33·75	94·09
2	15·65	12·37	30	34·43	93·39
3	16·35	11·71	31	35·09	92·74
4	17·14	11·12	32	35·76	92·03
5	2517·71	10·43	33	36·46	91·35
6		9·73	34	37·11	90·68
7		9·02	35	37·71	90·02
8	2519·75	8·32	36	38·45	89·34
9	20·43	7·64	37	2539·11	88·66
10	21·10	6·95	38		88·00
11	21·72	6·22	39		87·37
12	22·38	5·56	40		86·67
13	23·06	4·86	41		85·99
14	23·73	4·22	42		85·29
15	24·43	3·52	43		84·74
16	25·10	2·87	44		84·08
17	25·75	2·19	45		83·42
18	26·41	1·50	46		82·76
19	27·09	2500·85	47		82·07
20	27·70	2500·16	48		81·33
21	28·47	2499·47	49		80·67
22	29·07	98·79	50		80·02
23	29·75	98·11	51		79·40
24	30·40	97·47	52		78·63
25	31·09	96·76	53		77·98
26	31·77	96·09	54		2477·35
27	2532·47	2495·43			

Band ν_4

This band is associated with a stretching vibration of the C=C=O skeleton. It has been measured by Arendale and Fletcher [1], and was also studied previously by Eaton. For our present purpose the main point is that these earlier analyses suggested a value for B_0 which is substantially greater than those obtained from the bands described above, or from the microwave spectrum. The band has now been measured using 50 mm pressure in a 10 cm path length, and calibrated against lines of deuterium cyanide [8]. It shows clear series of P- and R-"lines", more than fifty being measurable in each branch, as listed in Table 4. Near the centre, between 1115–1140 cm^{-1}, some additional stronger lines occur, which have the appearance of Q-branches of the sub-bands in a parallel band. Some of these lines are discernible in the record shown by Arendale and Fletcher. They also alternate in intensity and a plausible assignment of K-values can be made. When the frequencies of these supposed Q-branches are plotted against K^2, a good straight line is found, which extrapolates to a band

VOL. 13 1958/5

Table 3. Band $2\nu_6$

J	$R(J)$	$P(J)$	J	$R(J)$	$P(J)$
0	1963·42		21	1977·83	1948·86
1	64·23	1962·16	22	78·48	48·19
2	64·89	61·47	23	79·18	47·54
3	1965·56	60·84	24	79·87	1946·87
4		60·16	25	1980·54	
5	1966·88	59·54	26		1945·54
6		58·84	27	1981·91	44·92
7	1968·23	58·20	28	82·60	44·24
8	68·94	57·56	29	83·30	1943·56
9	69·63	56·90	30	84·00	
10	1970·25	56·21	31	84·65	
11		1955·52	32	85·34	
12	1971·59		33	86·02	1940·90
13	72·29	1954·17	34	86·71	40·22
14	73·01	53·70	35	1987·42	39·54
15	73·72	52·87	36		38·86
16	74·41	52·16	37		38·22
17	75·07	51·51	38	1989·48	37·55
18	75·74	50·84	39	90·18	36·90
19	76·45	50·16	40	1990·88	36·28
20	1977·10	1949·52	41		1935·62

origin ν_0 at 1117·8 cm^{-1}. However, the slope of this plot, namely $[(A' - A'') - (B' - B'')]$, is surprisingly large, namely +0·36. Since $(B' - B'')$ is very small we should conclude that $(A' - A'') = +0{\cdot}36$, and such a change in A between the two states seems rather large. Also, it would imply a decrease in I_A with vibrational excitation. While it might be possible to interpret such a change in terms of changed orbital hybridization of the carbon atom in the CH_2-group during the vibration of the main skeleton, it may be better to leave this matter unsettled.

If the band centre is taken as 1117·8 cm^{-1}, a numbering of the P- and R-lines follows. Fig. 4 shows the usual combination plots, and the following results are obtained:

$$B'' = B_0 = 0{\cdot}3412$$
$$\alpha = (B'' - B') = -0{\cdot}00015$$
$$D_J'' \sim 2 \times 10^{-7}$$

If the band origin is moved somewhat, and the J-numbering altered accordingly, the value derived for B_0 is not greatly affected because of the small value of α. Arendale and Fletcher found $\nu_0 = 1120{\cdot}8$, and $B'' = 0{\cdot}3403$. (Their value of $\alpha = -0{\cdot}0003$ is quoted wrongly, a factor two having been omitted, as their results show.) The previous analysis by Eaton in this laboratory gave $\nu_0 = 1122{\cdot}6$ $B'' = 0{\cdot}3418$. It is quite clear that the value for B_0 derived from this band is greater than that determined from the microwave spectrum (0·3371) or from the

Table 4. Band ν_4

J	$R(J)$	$P(J)$	J	$R(J)$	$P(J)$
0	1118·21		31	1139·76	1096·75
1	19·06	1117·05	32	40·46	96·09
2	1119·77	16·30	33	41·14	95·43
3		15·69	34	41·84	94·77
4		15·02	35	42·51	94·10
5		14·36	36	43·20	93·45
6	(1122·73)	13·71	37	43·87	92·80
7		13·07	38	44·61	92·12
8	1124·04	12·47	39	45·29	91·40
9	24·76	11·81	40	45·94	90·74
10	25·41	11·17	41	46·61	90·08
11	1126·01	10·47	42	47·31	89·45
12		9·77	43	47·99	88·80
13		9·12	44	48·76	88·13
14	1128·18	8·52	45	49·45	87·38
15	28·85	7·81	46	50·09	86·75
16	29·58	7·16	47	50·75	86·08
17	30·41	6·50	48	51·52	85·36
18	30·97	5·83	49	52·31	84·86
19	31·65	5·10	50	53·01	84·25
20	32·32	4·37	51	53·76	1083·65
21	(1133·04)	3·60	52	54·42	
22	(1133·73)	2·92	53	55·10	
23	34·37	2·23	54	55·79	
24	35·05	1·57	55	56·40	
25	35·72	1100·95	56	57·13	
26	36·32	1100·25	57	57·82	
27	37·04	1099·64	58	58·49	
28	37·72	98·80	59	59·17	
29	38·42	98·07	60	1159·99	
30	1139·08	1097·40			

other parallel bands described above, and the discrepancy is outside possible experimental error.

Band ν_2

This band is connected with the other stretching vibration of the C=C=O skeleton. It is intense, and was measured at 5 mm pressure in a 10 cm path, and calibrated against lines of carbon monoxide [9]. There is a central Q-branch, in which some splitting corresponding to different K-values is noticeable, but this is not large enough to enable us to assign K-numbers and thus to estimate $[(A' - A'') - (B' - B'')]$. The P- and R-lines are well resolved, but on both sides of the band there are many complicating features which make it impossible to fix J-numbers convincingly. Among the P- and R-lines there are many other irregularly spaced lines with peculiar variations of intensity. Up to about $J = 25$ on each side of the band the P- and R-lines can be measured and assigned with reasonable certainty,

VOL. 13 1958/59

and these are listed in Table 5. The reason for the complexity elsewhere is uncertain, but is may arise from irregular overlapping of lines in the different K-sub-bands.

Since the assignments at high J-values cannot be made, it is not satisfactory to use the standard combination plot for determining B''. The combination sum $(R_{J-1} + P_J)$ has been plotted against J^2 to obtain $\nu_0 = 2151{\cdot}8\ \mathrm{cm}^{-1}$ and

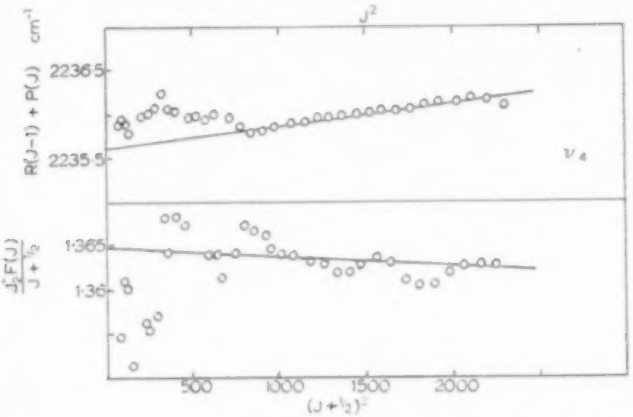

Fig. 4. Band ν_4. Plot of $[R(J-1) + P(J)]$ against J^2 and of $\dfrac{\Delta_2{}'F(J,K)}{(J+\frac{1}{2})}$ against $(J+\frac{1}{2})^2$.

Table 5. Band ν_2

J	$R(J)$	$P(J)$	J	$R(J)$	$P(J)$
0	2152·50		13	2160·76	2142·61
1	53·23		14	61·41	41·78
2	53·80	2150·48	15	62·08	41·08
3	54·46	49·78	16	62·72	40·26
4	55·11	49·06	17	63·35	39·62
5	55·73	48·35	18	63·93	38·72
6	56·44	47·66	19	64·52	37·98
7	57·07	46·96	20	65·11	2137·17
8	57·71	46·34	21	65·69	
9	58·35	45·49	22	66·27	
10	59·00	44·79	23	66·86	
11	59·63	44·05	24	2167·41	
12	2160·22	2143·29			

$\alpha = +0{\cdot}0024$. Assuming this value for ν_0, the quantities $(R_{J-1} - \nu_0)/J$ and $(\nu_0 - P_J)/J$ were plotted against J (Fig. 5), the intercept in each case being $(B' + B'')$. Combining this value with α, we obtain $B'' = B_0 = 0{\cdot}3405 \pm 0{\cdot}001$, which is again anomalously high by an amount roughly equal to the discrepancy found with ν_4.

Other parallel bands

A weak band lies on the lower frequency side of ν_2, with a clear series of P-"lines", but the R-lines are submerged in ν_2. There is a weak central Q-branch which suggests the probable position of the band origin and an assignment of

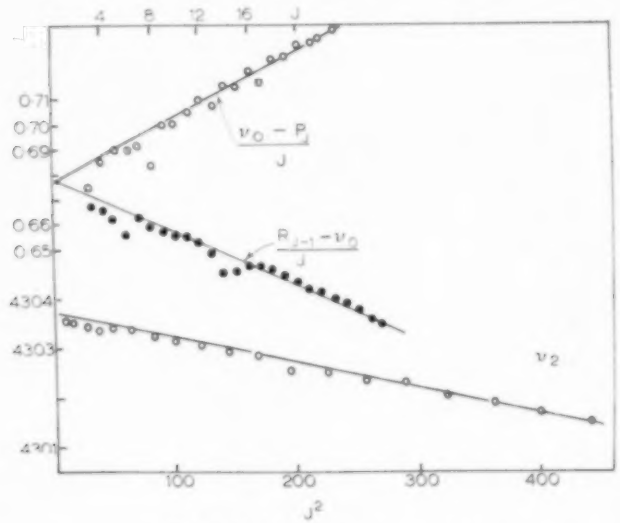

Fig. 5. Band ν_2. Plots of $\frac{R(J-1)-\nu_0}{J}$ against J, and of $[R(J-1)+P(J)]$ against J^2.

J-values to the P-lines. The band was measured using 50 mm pressure in a 10 cm path length and calibrated against standard lines of carbon monoxide, the positions of lines being given in Table 6.

This band cannot be interpreted as any obvious overtone or combination, and the shift of about 56 cm^{-1} from ν_2 is much larger than would arise if it were a "hot" band associated with ν_2. Rough calculations using plausible force constants for the C=C and C=O bonds suggest that the band can be assigned to an isotopic species with main skeleton $^{12}C{=}^{13}C{=}^{16}O$, and the intensity relative to that of ν_2 would be in accordance with this. The P-"lines" have been fitted by least-squares to a function:

$$[\nu_0 - (B' + B'')m + (B' - B'')m^2]$$

and $(\nu_0 - P_J)/J$ has been plotted against J, with the following conclusions:

$$\nu_0 = 2095{\cdot}9\ cm^{-1} \qquad B'' = B_0 = 0{\cdot}3425 \qquad \alpha = +0{\cdot}0021$$

It is to be noted that this value of α agrees fairly well with that obtained from ν_2 of the normal keten molecule.

Other parallel type bands have been measured with centres near 1060, 1176 2190 and 2186 cm^{-1}. In each case the P- and R-branches have been partially resolved, but it was impossible to carry out any detailed analysis.

VOL. 13 1958/5

Table 6. Isotope band ν_4

J	$P(J)$	J	$P(J)$	J	$P(J)$
2	2094·58	15	2085·20	28	2075·15
3	93·95	16	84·41	29	74·36
4	93·16	17	83·69	30	73·54
5	92·49	18	82·94	31	72·74
6	91·75	19	82·16	32	71·94
7	2091·04	20	81·41	33	71·10
8		21	80·65	34	70·28
9	2089·62	22	79·87	35	69·46
10	88·86	23	79·09	36	68·62
11	88·12	24	78·31	37	67·80
12	87·38	25	77·52	38	2066·94
13	86·66	26	76·76	39	
14	2085·94	27	2075·93	40	2065·24
				41	
				42	2063·53
				43	62·64
				44	2061·73

Perpendicular band ($\nu_1 + \nu_5$)

This band was measured using 600 mm pressure in a 20 m path length, and calibrated against standard argon emission lines [10]. There is a clearly defined series of Q-branches, which are overlapped by several unresolved parallel type bands. The positions of the Q-branches are given in Table 7.

The following combination relationships apply:

$$^{R}Q_{K-1} - {}^{P}Q_{K-1} = 4(A'' - B'')K$$

$$^{R}Q_{K} - {}^{P}Q_{K} = 4(A' - B')K$$

$$^{R}Q_{K} + {}^{P}Q_{K} = 2\nu_0 + 2(A' - B') + 2[(A' - A'') - (B' - B'')]K^2$$

Table 7. Band ($\nu_1 + \nu_5$)

$^{P}Q_9$	5943·86	s	$^{R}Q_0$	6123·26	w
$^{P}Q_8$	—		$^{R}Q_1$	6139·93	s
$^{P}Q_7$	5986·11	s	$^{R}Q_2$	6156·02	w
$^{P}Q_6$	6008·51	w	$^{R}Q_3$	6172·13	s
$^{P}Q_5$	6027·43	s	$^{R}Q_4$	6188·86	w
$^{P}Q_4$	6047·44	w	$^{R}Q_5$	6202·64	s
$^{P}Q_3$	6066·41	s	$^{R}Q_6$	6217·09	w
$^{P}Q_2$	—		$^{R}Q_7$	6230·99	s
$^{P}Q_1$	6103·34	s			

s = strong, w = wesk

From the appropriate plots, two of which are shown in Fig. 6, the following values are obtained:

$$(A'' - B'') = 9{\cdot}00 \text{ cm}^{-1}$$
$$\nu_0 = 6113{\cdot}31 \text{ cm}^{-1}$$
$$(A' - A'') - (B' - B'') = -0{\cdot}27 \text{ cm}^{-1}$$

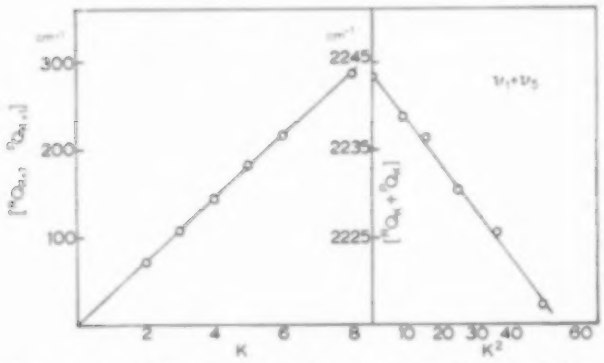

Fig. 6. Band $(\nu_1 + \nu_5)$. Plots of $[{}^{R}Q_{K-1} - {}^{P}Q_{K+1}]$ against K, and of $[{}^{R}Q_{K} + {}^{P}Q_{K}]$ against K^2.

Discussion

Three of the parallel bands of keten described above lead to a rotational constant B_0 close to 0·3370, agreeing with the value obtained from the microwave spectrum. Two other bands lead to a much higher value around 0·3410 cm^{-1}. The discrepancy seems definite enough to imply that some factor has been ignored in dealing with these two bands, each of which is connected with a stretching of the C=C=O chain. It is interesting to note that Arendale and Fletcher obtained a value $B_0 = 0{\cdot}2952$ from the CD_2 deformation band of dideuteroketen, which agreed with the microwave spectrum value 0·2948 cm^{-1}. This emphasizes the point that the discrepancy found with the two bands of keten may not be due to any experimental error. It may be noted, too, that a similar anomaly may occur with the band which was assigned above to the ^{13}C isotopic species.

It may also be worth noting that the data on diazomethane suggest a similar peculiarity, for diazomethane and keten are structurally isoelectronic and almost identical. Fletcher and Garrett [11] found that the two stretching vibrations of the chain C=N=N in diazomethane give B_0 values 0·3724 and 0·3726, whereas the CH_2 deformation band gives a value 0·3698 cm^{-1}. A value of about 0·369 was reported previously by Mills and Thompson [12] for the CH_2 group symmetrical stretching vibration band. We have also recently analysed a number of bands of dideuteroallene, and preliminary results appear to suggest a similar anomaly with the C=C=C skeletal stretching vibrations. No satisfactory interpretation of this peculiarity can be suggested at present, but none of the usual deviations caused by asymmetry seem responsible.

From the results on the perpendicular type band $(\nu_3 + \nu_5)$, and assuming that $B_0 = 0{\cdot}3371$, it follows that $A_0 = 9{\cdot}34$ cm^{-1}. These two values for the rotational

VOL. 13 1958/5

constants together with B_0 for dideuteroketen [2] are most satisfactorily fitted by the following geometrical parameters:

$$r_0^{C=C} = 1{\cdot}31 \text{ Å} \qquad r_0^{CH} = 1{\cdot}075 \text{ Å}$$

$$r_0^{C=O} = 1{\cdot}17 \text{ Å} \qquad \widehat{HCH} = 123{\cdot}5^\circ$$

It would, however, be valuable to determine A_0 for dideuteroketen from its infrared bands.

Acknowledgements—We again express appreciation of financial help from the Hydrocarbon Research Group of the Institute of Petroleum, and one of us (D. R. E.) is grateful to the Department of Scientific and Industrial Research for a maintenance grant.

References

[1] Arendale W. F. and Fletcher W. H., *J. Chem. Phys.* 1956 **24** 581.
[2] Johnson H. R. and Strandberg M. W. P., *J. Chem. Phys.* 1952 **20** 687.
[3] Eaton D. R. Dissertation, Oxford 1956.
[4] Arendale W. F. and Fletcher W. H., *J. Chem. Phys.* 1957 **26** 793.
[5] Mills I. M., Thompson H. W. and Williams R. L., *Proc. Roy. Soc.* A 1953 **218** 29.
[6] Thompson H. W., Williams R. L. and Callomon H. J., *Spectrochim. Acta* 1952 **5** 313.
[7] Pickworth J. and Thompson H. W., *Proc. Roy. Soc.* A 1953 **218** 37.
[8] Checkland P. B. and Thompson H. W., *Trans. Faraday Soc.* 1955 **51** 1.
[9] Plyler E. K., Bendict W. S. and Silverman S., *J. Chem. Phys.* 1952 **20** 175.
[10] *Spectroscopic Wavelength Standard* Lofthus, Oslo 1956.
[11] Fletcher W. H. and Garrett T. P., *J. Chem. Phys.* 1956 **25** 50.
[12] Mills I. M. and Thompson H. W. *Trans. Faraday Soc.* 1954 **50** 1270.

Spectrochimica Acta, 1958, Vol. 12, pp. 236 to 247. Pergamon Press Ltd., London. Printed in Northern Ireland.

Vibrational frequency and band intensity of the carbonyl group

H. W. Thompson and D. A. Jameson
The Physical Chemistry Laboratory, Oxford

(*Received* 10 *July* 1958)

Abstract—The frequencies and intensities of the fundamental and overtone bands of the carbonyl group vibration in a large number of compounds have been measured. The results suggest that data on the band intensities can help to resolve ambiguities in structural determinations where groups of different character have the same vibration frequency. The variations in both frequency and intensity have been considered in relation to the inductive and resonance properties of the attached groups. The results suggest that inductive effects largely control the variation of vibration frequency in different compounds, but the intensity is more dependent upon mesomeric effects. Rough correlations can be established using the known inductive and mesomeric factors for the groups concerned. The relative intensity of fundamental and overtone bands found for different structural types reveals differences in their electrical anharmonicity.

Data are also given on the C=O and N—H group vibrations in ring-substituted N-methyl benzamides and acetanilides.

VOL. 13 1958/5

It has long been known that the vibrational frequency of a carbonyl group varies according to the class of compound in which it occurs [1], and at the start an interpretation was suggested which is based upon the differing extents to which ionic forms participate as the radicals R_1 and R_2 in R_1R_2CO are changed. These variations in the group frequency have been applied in structural diagnosis, but a discrimination between types is not always unambiguous. Attempts have therefore been made to correlate the frequency shifts more precisely with known structural properties. Walsh [2] drew attention to the rough relationships between the vibrational frequency and bond length, force constant, ionization potential or dissociation energy, and later workers have extended these considerations. There is a regular trend of ν_{CO} with bond length in many compounds over a wide range of frequency and length [3, 4], but the bond lengths are not known precisely enough to bring out the details in the frequency range 1600–1800 cm^{-1}. Kagarise [5] tried to correlate frequency shifts with the electronegativities of R_1 and R_2, using Gordy's values for the latter, and noticed regularities among some aliphatic compounds, especially halogenated acyl halides and esters. Cook [6] examined the correlation between vibration frequency and ionization potential in greater detail and found a regular trend in each of two groups, namely the non-conjugated and conjugated compounds. Lord and Miller [7] have discussed the frequency shifts in general, and concluded that in the absence of special influences such as ring strain or hydrogen bonding, the main factors are the inductive and resonance effects of R_1 and R_2, as originally supposed.

Hartwell, Richards and Thompson [1] suggested that the variation of intrinsic band intensity of different types of carbonyl group might prove illuminating, and recent results have confirmed this. Richards and Burton [8], Francis [9] and Jones and Dobriner [10] have found significant differences of

the intensity among bond types which are often useful in structural determination [11]. BARROW [12] has shown that the intensity of the fundamental band can be related to the resonance energy of the group.

It seemed profitable to reconsider this matter in terms of newer ideas about the inductive and mesomeric properties of different groups which have been used in the interpretation of other spectroscopic data [13]. The intensities of overtone bands are also important. We have therefore measured the frequencies and intensities of the fundamental and overtone bands for a large number of substances containing the carbonyl group, dissolved in carbon tetrachloride or chloroform. Where direct comparisons are possible, our results usually agree satisfactorily with those reported by other workers.

Experimental method

The fundamental bands near 6 μ were measured on a Perkin–Elmer 21 (rock salt) instrument using effective slit widths of about 6 cm^{-1}. The carbonyl overtone bands, and also some NH group bands in the substituted N-methyl benzamides, were measured on a Perkin–Elmer 12C spectrometer with lithium fluoride prism ($s_{eff} \sim 8\,cm^{-1}$) and in a few cases also on a small grating spectrometer ($s_{eff} \sim 2\,cm^{-1}$). The compounds used were either standard commercial products or laboratory preparations, all repurified before use.

Integrated band areas were determined in each case for several concentrations and path lengths, and extrapolated by the usual Wilson–Wells method. With some compounds complications arose due to doubling of bands, and these were not studied further. In some other cases, the bands were unsymmetrical or had shoulders. Although it was hoped to fix the intensities to 5 per cent, various small difficulties may make the results less accurate in some cases, although they appear in general to agree well with values previously recorded. They are given in absolute units, cm, c/s, molecule, $\log_e$.

Results and discussion

Table 1 summarizes the results on the fundamental and overtone bands for different classes of carbonyl groups in carbon tetrachloride. The C=O and N—H group stretching vibrations of some ring substituted N-methyl banzamides, and of the C=O group vibration in substituted acetanilides, dissolved in chloroform were also measured, the results being given in Table 2. Data for the N—H stretching vibration in substituted acetanilides were reported previously [14].

From the point of view of empirical structural diagnosis, where it is required to distinguish between different kinds of carbonyl group, some interesting conclusions can be drawn from the present results. In some cases, the value of the fundamental frequency ν_{01} does not provide a clear differentiation between structural types, but the intensities of both fundamental and overtone bands A_{01} and A_{02} can be applied to resolve the ambiguities. Fig. 1 shows the relation between A_{01} and ν_{01}, and also that between A_{02} and ν_{02}. In each of these plots, structural classes can be segregated. Fig. 2 shows another such plot of the ratio A_{01}/A_{02} against ν_{01}. The limits of the classifications indicated in Figs. 1 and 2 cannot be taken as entirely infallible, and a few exceptions may occur. For example, some formates and vinyl esters

Table 1. Carbonyl group vibration, in carbon tetrachloride

Compound	ν_{01}	ν_{02}	$10^7 A_{01}$	$10^9 A_{02}$	$\frac{A_{01}}{A_{02}}$	$10^2 x$	$\Delta\nu_{\frac{1}{2}}^{e}$ (0–1)	$\Delta\nu_{\frac{1}{2}}^{e}$ (0–2)
Acetone	1715	3419	8·6	16·4	52	3·2	16·5	22
Methyl ethyl ketone	1722	3423	8·5	17·7	48	6	18	30
Diethyl ketone	1720	3421	8·6	15·4	56	8·3	17	29
*cyclo*Pentanone	1750	3470	12·3	28·8	43	8·4	20	39
*cyclo*Hexanone	1717	3418	12·8	21·4	60	4·6	21	30
*cyclo*Heptanone	1704	3387	10·5	20·5	51	3·2	15	32
Benzaldehyde	1710	3404	13·2	16·3	81	4·6	13	19
Acetophenone	1690	3367	10·8	17·5	62	3·8	11	22
Benzophenone	1666	3316	10·9	16·0	68	4·8	11	23
Methyl formate	1735	3453	11·8	15·2	77	4·9	15	25
Ethyl formate	1734	3443	14·7	19·6	75	7·1	12	24·5
n-Butyl formate	1730		19·6				12	
*iso*Butyl formate	1731		17·3				13·5	
*cyclo*Hexyl formate	1728		13·9				16·5	
Alkyl formate	1732		15·2				15	
Methyl acetate	1750		18·1				17	
Ethyl acetate	1742	3465	17·6	15·6	113	5·4	15·5	30
n-Butyl acetate	1743		15·0				18·5	
*iso*Butyl acetate	1742		14·0				28·5	
*cyclo*Hexyl acetate	1738		13·5				15·5	
Alkyl acetate	1746		15·4				18	
Vinyl acetate	1763	3508	13·8	16·0	86	5·1	14	28
Phenyl acetate	1769		13·4				16	
Methyl propionate	1745	3474	14·5	16·3	89	4·5	18	37
Ethyl propionate	1736	3459	14·0	13·2	106	3·7	18	35
Phenyl propionate	1767		12·7				16·5	
Methyl benzoate	1727	3440	17·7	13·3	133	4·0	12	27
Ethyl benzoate	1720	3426	16·1	13·0	124	4·0	15	30
n-Butyl benzoate	1726		13·9				14	
*iso*Butyl benzoate	1726		15·5				14·5	
Phenyl benzoate	1743	3465	14·6	13·9	105	6·0	17	38
Methyl chloroformate	1786	3535	19·6	17·9	109	8·5	30	39
Ethyl chloroformate	1779	3533	20·8	16·2	128	6·9	16	29
n-Butyl chloroformate	1779		18·6				18·5	
*iso*Butyl chloroformate	1780		21·1				20·5	
Methyl acrylate	1734	3451	12·9	12·9	100	4·8	16	28
Ethyl acrylate	1730		13·1				15·5	
n-Butyl acrylate	1728		13·7				16·5	
Methyl methacrylate	1727	3439	12·4	12·2	102	4·3	14	33
Ethyl methacrylate	1722		12·9				16·5	
n-Butyl methacrylate	1721		13·6				15·5	
*iso*Butyl methacrylate	1722		13·2				15	
Methyl pivelate	1736	3447	12·5	12·4	101	7·1	18	31
Ethyl cyanoacetate	1755		16·9				20	
Methyl cinnamate	1724		16·6				17	
Dimethyl carbonate	1758	3496	18·7	10·8	173	5·6	17	39
Diethyl carbonate	1748	3483	21·1	8·8	239	3·7	18	32
Di-*n*-butyl carbonate	1746	3471	20·3	9·8	207	5·9	18	33

VOL. 13 1958/5

Table 1 *continued*.

Compound	ν_{01}	ν_{02}	$10^7 A_{01}$	$10^9 A_{02}$	$\frac{A_{01}}{A_{02}}$	$10^2 x$	$\Delta\nu_{\frac{1}{2}}^a$ (0–1)	$\Delta\nu^{1a}$ (0–2)
Di-*iso*butyl carbonate	1749	3472	18·2	8·4	216	7·3	20	38·5
Diphenyl carbonate	1786	3548	19·2	(7·0)	(274)	6·6	17	
Di-*p*-tolyl carbonate	1774	3533	18·0	10·1	178	4·2	15	30
Di-*m*-tolyl carbonate	1774	3540	20·1	11·6	173	2·2	21	46
N:N-Dimethyl formamide	1688	3358	31·4	20·5	153	5·3	13	28
N:N-diethyl formamide	1684	3347	36·8	20·0	184	6·2	14	28·5
N:N-Dimethyl acetamide	1653	3300	22·5	16·2	138	1·8	24	43
N:N-Dibutyl acetamide	1647	3284	19·8	15·3	129	3·0	20	40
N:N-Diphenyl acetamide	1679	3346	20·6	18·7	110	3·5	20	36
N-N-Diethyl diphenyl urea	1654	3297	27·2	22·8	119	3·3	23	51
Methylphenyl urethane	1707	3400	24·6	18·2	135	4·1	21	51
Ethylphenyl urethane	1704	3394	26·7	15·3	175	4·1	20	41
Trichloroacetyl chloride	1805		7·9				14	

Table 2. Solutions in chloroform

	Substituent	ν	$10^7 A$	$\Delta\nu_{\frac{1}{2}}$	σ (HAMMETT)
(a) ν_{CO} in *N*-methyl benzamides	*p*-NO_2	1671	17·3	20	0·778
	m-NO_2	1672	17·3	26	0·71
	p-Br	1661	15·8	23	0·232
	H	1660	17·3	27	0
	p-CH_3	1657	17·3	25	−0·17
	p-C_2H_5O	1655	16·7	28	−0·25
(b) ν_{NH} in *N*-methyl benzamides	*p*-NO_2	3463	3·7	27	0·778
	m-NO_2	3464	3·75	28·5	0·71
	p-Br	3465	3·6	28	0·232
	H	3468	3·6	27	0
	p-CH_3	3467	3·2	27·5	−0·17
	p-C_2H_5O	3472	3·25	25·5	−0·25
(c) ν_{CO} in acetanilides	*p*-NO_2	1710	11·6	22	0·778
	m-NO_2	1707	13	24	0·71
	p-Br	1693	14·8	24·5	0·232
	p-Cl	1695	14·7	25	0·227
	H	1691	15·1	24	0
	m-CH_3	1688	15·8	23	−0·069
	p-C_2H_5O	1681	16·9	27·5	−0·25
	p-CH_3O	1683	16·8	27	−0·268
	p-NH_2	1681	20·1	30	−0·66

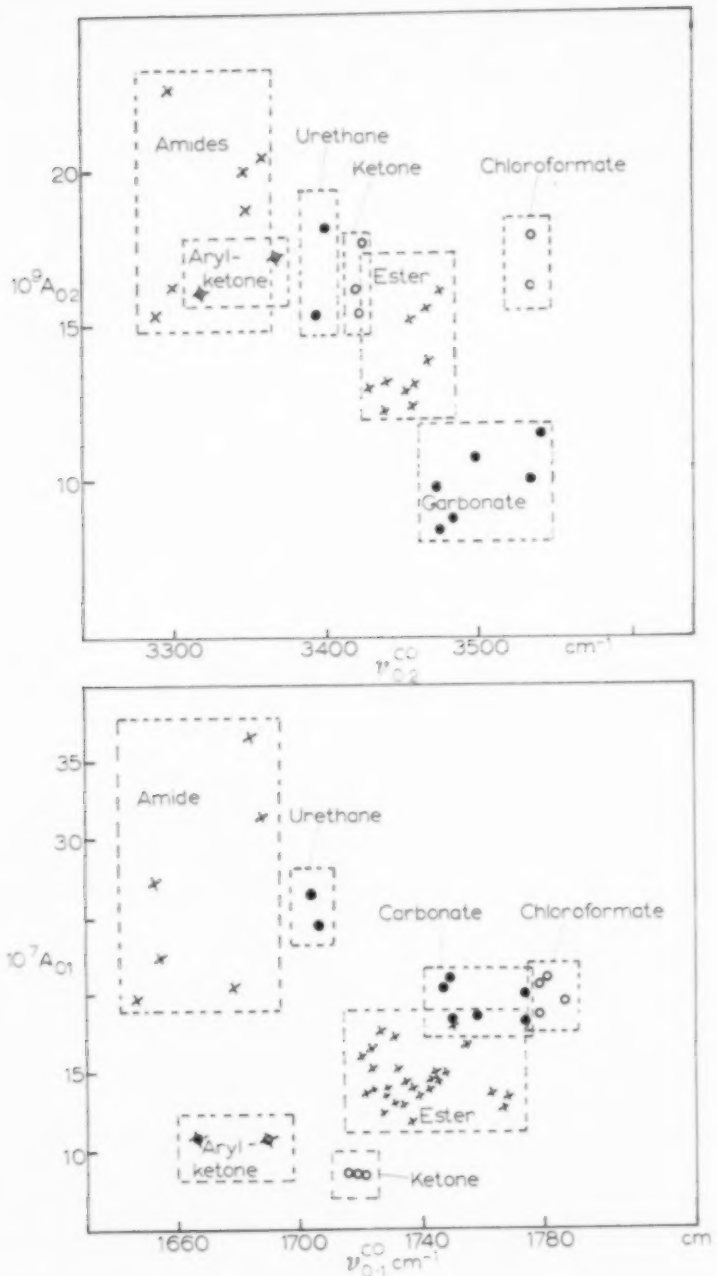

Fig. 1. Diagram of relation between frequency and band intensity for fundamental and first overtone of carbonyl group vibrations.

VOL. 13 1958/5

appear somewhat irregular. However, there is no doubt that the data on the band intensities are helpful in many cases, for example with amides and aryl ketones, or with esters and carbonates, where the fundamental frequencies lie in the same range.

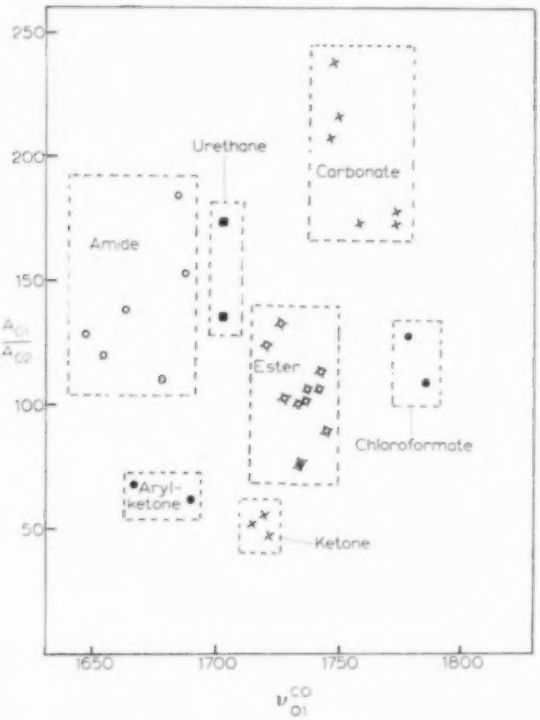

Fig. 2. Relation between ν_{10} and ratio $\frac{A_{01}}{A_{02}}$ for different classes of carbonyl compound.

It is desirable, of course, to correlate the variations of frequency and intensity with differences of electronic structure more explicitly, and none of the attempts so far made is completely satisfactory. The frequency ν_{01} is determined essentially by the bond force constant, and the intensity A_{01} by $\delta\mu/\delta r$ for the bond. In principle therefore no direct connexion can be expected between ν_{01} and A_{01}, and indeed none exists. The effects of the attached groups R_1 and R_2 in $R_1R_2C{=}O$ upon ν_{01} and A_{01} will be a combination of inductive and mesomeric influences, together with hyperconjugative, steric and spatial field effects. Recent work has shown, too, that even in an "inert" solvent the solute–solvent interactions may be important, but at present there is no alternative but to use the same inert solvent throughout and make comparative measurements. It is unlikely that all the structural factors just mentioned will be disentangled by a study of only two properties (ν and A), even by a careful choice of the compounds measured. On the other hand, many recent results suggest that the inductive and mesomeric effects as a rule outweigh others in importance.

Our present data suggest that there is a regular trend of ν_{01} with bond length, and also that the intensity—or some simple function of it—varies roughly with the estimated resonance energy, as suggested by Barrow. We can now explore another approach, namely the correlation of ν and A with what is known about the specific inductive and mesomeric influences of the attached groups. Taft [15] has

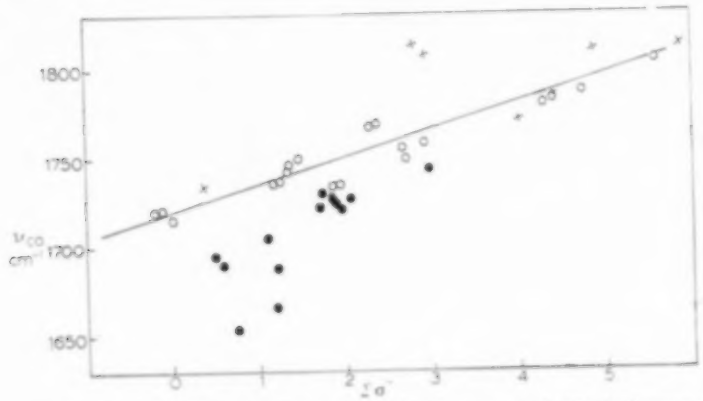

Fig. 3. Relation between ν_{CO} and inductive power of attached groups.

derived measures of these σ factors in aliphatic and aromatic compounds, corresponding to the Hammett σ factors for substituents in an aromatic ring which affect the properties of an attached functional group. For several aromatic series, such as the anilines, benzonitriles or phenols, the spectral characteristics of the vibration bands of the functional group —NH_2, —CN or —OH have been found to be related to the Hammett value σ of ring substituents [16, 17, 18]. Recently, these correlations have been refined by splitting up the σ values into their inductive and resonance parts [13]. For aliphatic compounds, inductive factors σ^* have been suggested by Taft, but the problem is less easily examined since no corresponding measures of the resonance factors have been derived. However, some data on the OH group vibration band in substituted aliphatic acids and benzoic acids [13], and on that of the C≡N group in substituted aliphatic nitriles [19], suggest that this kind of analysis may be extended.

Indeed, O'Sullivan and Sadler [20] have proposed relations between ν_{CO} and σ^*, the Taft polar factor of attached groups, in some compounds R·CO·CH_3, namely:

$$\nu_{CO}\text{ (vapour)} = 1690 + 52{\cdot}56\sigma^*$$

and

$$\nu_{CO}\text{ (condensed state of solution)} = 1655 + 53{\cdot}71\sigma^*$$

These particular equations are not satisfactory since they do not take into account the full details. Thus, of the six compounds used by O'Sullivan and Sadler, two involve a conjugation of the radical R with the carbonyl group, and two others will later be shown to be "abnormal" in this connexion. In Fig. 3, ν_{01} is plotted against $\Sigma\sigma^*$ for compounds $R_1R_2C{=}O$, using the values of σ^* given in Table 3. This plot

VOL. 13 1958/5

also includes data for a few compounds listed by Cook [6]. Most of the results agree satisfactorily with the equation:

$$\nu_{CO} = 1720 + 15\Sigma\sigma^*$$

but significant deviations occur with three classes, namely (a) compounds in which one or both of the attached groups R_1, R_2 are conjugated with the carbonyl group, (b) amides, and probably also the substituted ureas and urethanes for which σ^*

Table 3

Group	σ^*	σ_I	σ_R
CH_3	0	−0·05	−0·13
C_2H_5	0·1	−0·05	−0·10
C_6H_5	+0·6	+0·10	−0·09 | −0·2
H	+0·49	0	0
CH_2O	+1·46*	+0·23	−0·5
C_2H_5O	+1·35†	+0·21	−0·46
C_6H_5O	+2·38*	+0·38	−0·41
Cl	+2·94*	+0·47	−0·24
$CH_3CH{=}CH$	+0·36		
$CH_2{=}C(CH_3)$	+0·36‡		
$CH_2{=}CH$	+0·36‡		
$C(CH_3)_3$	−0·3	−0·07	−0·12
CH_2CN	+1·3	−0·3	−0·19
$C_6H_5CH{:}CH$	+0·41		
CCl_3	+2·65	−0·4	
$N(CH_3)_2$	+0·65§	+0·1	−0·83
OH	+1·55*	+0·25	−0·61
n-C_3H_7	−0·11	−0·05	−0·10
CH_2Cl	+1·05		
$CHCl_2$	+1·94		

* Using the relation $\sigma^*(X) = 2{\cdot}8\sigma^*(CH_2X)$.

† Using the relation $\sigma^*(C_2H_5O) = \sigma^*(CH_2O)\left[\frac{\sigma^*(CH_3OCH_2)}{\sigma^*(CH_2OH)}\right]$

‡ Assumed equal to Taft value for $CH_3CH{=}CH$.

§ Using $\sigma = +0{\cdot}10$ for $N(CH_3)_2$ given by Taft, and then $\sigma^*(N(CH_3)_2) = 2{\cdot}8\sigma^*(CH_2N(CH_3)_2)$.

is not known exactly, (c) acetyl halides such as CH_3COCl and CH_3COBr. For the classes (a) and (b) it is reasonable to suppose that the deviations arise because of the greater mesomeric influences of the groups concerned, although no very clear quantitative relation can be deduced between these mesomeric effects and the extent of the deviation. Similar irregularities were found by Cook with the conjugated ketones in plots involving the ionization potentials, and they arise in the plots of ν_{OH} of carboxylic acids or ν_{CN} of nitriles against σ^* for the attached groups. As regards the acetyl halides, the anomaly probably arises as a result of some interaction between the hydrogen atoms of the methyl group and the halogen atom near to it, which disturbs the normal inductive effects of these two groups

upon the carbonyl group. It should be noted that with trichloroacetyl chloride or carbonyl chloride, the carbonyl frequency is in satisfactory accord with the σ^* values, and in dichloroacetyl chloride the deviation is small.

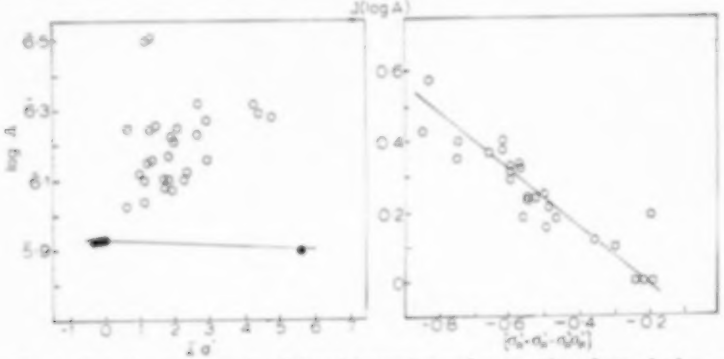

Fig. 4. Relation between C=O band intensity and properties of attached groups.

In considering the variations of band intensity of functional groups attached to an aromatic ring, it has been found that a roughly linear relation exists between log A and the Hammett factor σ of the ring substituent [16, 17, 18, 21]. This resembles the original Hammett equation. In deriving values for the polar substituent constants σ^* in aliphatic compounds Taft has used an analogous equation, and it is therefore reasonable to examine the present results by a plot of log A_{01} against σ^*. This is shown in Fig. 4. At first sight the data suggest a completely random variation of A, and it is obvious that some factor other than the simple inductive effect of attached groups is mainly responsible for the differences in band intensity. That this is the mesomeric effect is suggested by the following considerations.

It is generally accepted that little resonance hybridization occurs in simple aliphatic ketones, and all these compounds have about the same band intensity A_{01} [22, 8]. In carbonyl chloride and trichloroacetyl chloride, too, the estimated resonance energy is probably very small. Using the methods described by Wheland [23], the calculated and measured heats of combustion of methyl chloride agree closely, implying no resonance energy. With methylene chloride and chloroform, there are small discrepancies which probably arise because the spatially close halogen atoms exert a mutual electrostatic interaction. A similar small discrepancy is found between the measured and calculated heats of combustion of carbonyl chloride, and it can be explained in the same way. Now, as explained above, the variation of carbonyl group frequency in aliphatic ketones, trichloroacetyl chloride and carbonyl chloride is adequately accounted for by the σ^* inductive parameter. Also, incidentally, A_{01} is about the same in aliphatic ketones and in trichloroacetyle chloride. It can therefore be assumed as a first approximation that in the simple aliphatic ketones and in trichloroacetyl chloride the main operative effect is inductive. It may be noted that in other cases where resonance is inhibited, band intensities are almost unaffected by substituents. For example, with ortho substituted ethyl benzoates, in which the ortho group (NH_2, Br, I, NO_2, CH_3O

inhibits resonance by steric effects, the carbonyl group band intensity is roughly constant [13]. The inductive effects of these substituents must also be small in these cases.

In Fig. 4 a line has therefore been drawn between the log A_{01} values for the aliphatic ketones and trichloroacetyl chloride, and deviations from this line have been read off for each of the other compounds measured. In analysing the spectral data for several series of aromatic compounds [13], this procedure was followed, log A_{01} being plotted against σ_I for the substituent. It was then found that $\Delta(\log A_{01})$ was related to σ_R, the factor estimated by TAFT to represent the resonance effect of the substituent.

In the present case, we do not know the factors σ_R for the groups concerned in this particular series of carbonyl compounds. Indeed, as regards absolute magnitude, σ_R for a given group will vary according to the functional group to which it is attached, and the variations may be greater among series of aliphatic compounds than in the case of different aromatic series like anilines or benzonitriles in which the substituent works through the aromatic nucleus. However, as a first approximation, it may be fair to assume that in the aliphatic carbonyl compounds σ_R for an attached group will be roughly proportional to its value in the aromatic series. We have therefore compiled values of σ_R listed in Table 3. In some cases, values of σ_I and σ_R have already been given by TAFT. In other cases, σ_I can be determined using the linear relation established by TAFT between σ^* for a group CH_2X and σ_I for X, and assuming that $\sigma^*(X) = 2{\cdot}8\,.\,\sigma^*(CH_2X)$, σ_R can then be obtained by subtracting σ_I from the Hammett σ^{para} value of the group concerned.

If now the deviations $\Delta(\log A_{01})$ are plotted against $\Sigma\sigma_R$ for the attached groups, an essentially linear plot is obtained, which justifies the conclusion that mesomeric factors are dominant in fixing the band intensities. The results can be refined further by studying the plots of $\Delta(\log A_{01})$ against ${\sigma_R}^X$ for a number of series Y·CO·X. Each of these is roughly linear, and the slopes and intercepts are dependent upon ${\sigma_R}^Y$. In this way it is found that the results can be fitted best by an equation of the form:

$$\log A = \log A_0 + \alpha\,.\,\Sigma\sigma^* + \beta({\sigma_R}^X + {\sigma_R}^Y) - \gamma({\sigma_R}^X\,.\,{\sigma_R}^Y).$$

In this equation, σ^* might be replaced by $\cdot\sigma_I$, with an appropriate change of the constant α. The presence of the interaction term $({\sigma_R}^X \cdot {\sigma_R}^Y)$ is noteworthy, and this seems reasonable, for the mesomeric effect of one attached group may be expected to depend to some extent upon the nature of the other. The coefficients β and γ will depend upon the particular vibrational chromophore concerned, and probably also upon the solvent. In the present case the data do not seem sufficiently uniform to enable us to derive precise values, but if $\beta = \gamma = 0{\cdot}8$ there is reasonable agreement. In accordance with the above, α is very small. In Fig. 5, $\Delta(\log A_{01})$ is plotted against $({\sigma_R}^X + {\sigma_R}^Y - {\sigma_R}^X\,.\,{\sigma_R}^Y)$. There is no doubt about the essential linearity of this plot, and the deviations could well arise from experimental errors in determining the intensity, from hyperconjugation effects, or from steric or specific field effects. The resonance factor used for the phenyl group also requires comment. TAFT gave a value $\sigma_R = -0{\cdot}09$ for the phenyl group when used as a substituent on the aromatic nucleus in aromatic compounds. If this value is used

in the present series of carbonyl compounds, the results for all the compounds containing one or more phenyl groups appear anomalous. Using a value $\sigma_R = -0{\cdot}2$ they are more satisfactorily in accord, and this value was used in the plot of Fig. 5. This peculiarity is not surprising, since the Hammett factor usually adopted for the phenyl group has already been found to lead to anomalies in interpreting the

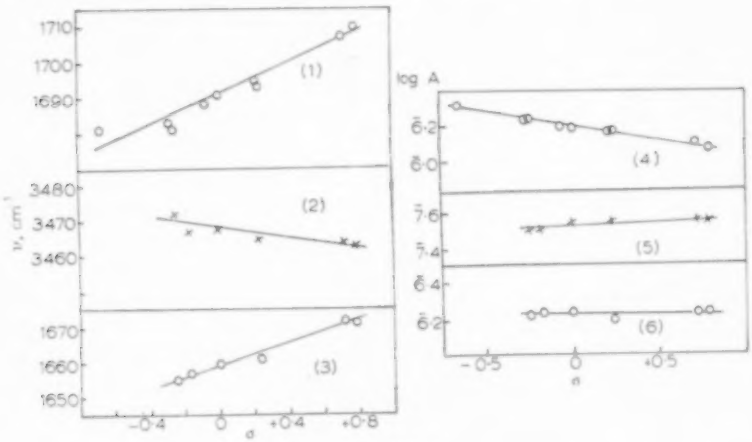

Fig. 5.

(a) Plots of frequency against σ (Hammett) (1) ν_{CO} in acetanilides, (2) ν_{NH} in N-methyl benzamides, (3) ν_{CO} in N-methyl benzamides.

(b) Plots of log A against σ (Hammett) (1) C=O in acetanilides, (2) N—H in N-methyl benzamides, (3) C=O in N-methyl benzamides.

All solutions in chloroform.

spectral data for other series. Also, the special conjugative properties of the phenyl group may make it less satisfactory to assume the rough proportionality between its resonance effect upon aromatic systems and upon the carbonyl group directly. The present interpretation of these effects appears not only to show the correlation between band intensity and resonance structure, but also conversely to provide another justification for the significance of the Taft structural parameters.

As regards the overtone bands, the observed values of ν_{01} and ν_{02} have been used to compute the mechanical anharmonicity factors using the expression for the vibrational energy of a diatomic oscillator:

$$E_v = (v + \tfrac{1}{2})\omega - (v + \tfrac{1}{2})^2 x\omega$$

The values of x are very small, and are very sensitive to small errors in either ν_{01} or ν_{02}. It is clear, however, that the mechanical anharmonicity is about the same in all classes of carbonyl compounds. The variation in relative intensity of fundamental and overtone must therefore be due to differences in electrical anharmonicity. In some other series where the vibrational chromophore can be treated as a diatomic molecule, such as N—H or O—H compounds [24, 25], attempts have been made to compute the functions expressing the dipole moment in terms of the bond length, and thus to estimate the coefficients which express the electrical anharmonicity. Such calculations are quantitatively less satisfactory with these carbonyl groups.

VOL. 13 1958/5

The results obtained with the substituted benzamides and acetanilides have been analysed in the way used for other aromatic compounds. Fig. 6 shows the plots of the frequency of the functional group against Hammett factor σ of the aromatic ring substituent, and of log A against σ. It may be more appropriate to consider these elsewhere in connexion with other related series.

Acknowledgements—We are grateful to the Hydrocarbon Research Group of the Institute of Petroleum for financial help, and for the award of a D.S.I.R. maintenance grant to one of us (D. A. J.).

References

[1] Hartwell E. J., Richards R. E. and Thompson H. W., *J. Chem. Soc.* 1948 1436.
[2] Walsh A. D., *Trans. Faraday Soc.* 1946 **42** 561; 1947 **43** 158.
[3] Margoshes M., Filtwalk F., Fassel V. A. and Rundle R. E., *J. Chem. Phys.* 1954 **22** 381.
[4] Layton E. M., Kross R. D. and Fassel V. A., *J. Chem. Phys.* 1956 **25** 135.
[5] Kagarise R. E., *J. Amer. Chem. Soc.* 1955 **77** 137.
[6] Cook D., *J. Amer. Chem. Soc.* 1958 **80** 49.
[7] Lord R. C. and Miller F. A., *Appl. Spectrosc.* 1956 **10** 115.
[8] Richards R. E. and Burton W. R., *Trans. Faraday Soc.* 1949 **45** 874.
[9] Francis S. A., *J. Chem. Phys.* 1950 **18** 861; 1951 **19** 942.
[10] Jones R. N. and Dobriner K., *J. Amer. Chem. Soc.* 1952 **74** 80.
[11] Thompson H. W., *Molecular Spectroscopy.* Institute of Petroleum 1955.
[12] Barrow G. M., *J. Chem. Phys.* 1953 **21** 2008.
[13] Krueger P. J. and Thompson H. W., *Proc. Roy. Soc.* In press.
[14] Moccia R. A. and Thompson H. W., *Spectrochim. Acta.* 1957 **10** 240.
[15] Taft R., *Steric Effects in Organic Chemistry* Chap. 13. Wiley, New York 1956; *J. Chem. Phys.* 1957 **26** 93.
[16] Krueger P. J. and Thompson H. W., *Proc. Roy. Soc.* A 1957 **243** 143.
[17] Thompson H. W. and Steel G., *Trans. Faraday Soc.* 1956 **52** 1451.
[18] Stone P. J. and Thompson H. A., *Spectrochim. Acta.* 1957 **10** 17.
[19] Jesson J. P. and Thompson H. W., *Spectrochim. Acta.* In press.
[20] O'Sullivan D. G. and Sadler P. W., *J. Chem. Soc.* 1957 4144.
[21] Thompson H. W., *Molecular Spectroscopy.* Institute of Petroleum 1958.
[22] Thompson H. W., Needham R. W. and Jameson D., *Spectrochim. Acta* 1957 **9** 208.
[23] Wheland G. W., *Resonance in Organic Chemistry.* Wiley, New York 1955.
[24] Russell R. A. and Thompson H. W., *Proc. Roy. Soc.* A 1956 **234** 318.
[25] Moccia R. A. and Thompson H. W., *Proc. Roy. Soc.* A 1957 **243** 154.

Spectrochimica Acta, 1958, Vol. 13, pp. 248 to 252. Pergamon Press Ltd., London. Printed in Northern Ireland

The infrared absorption spectra of ring-D steroid lactones—I

Intense hydrogen bonding in estrololactone*

C. Gual, R. I. Dorfman and H. Rosenkrantz
Worcester Foundation for Experimental Biology, Shrewsbury, Massachusetts

(*Received* 23 *June* 1958)

Abstract—It has been observed that an unusual tendency for hydrogen bonding occurred in the estrololactone molecule. Marked displacements of the hydroxyl vibrations from approximately 3500 to 3200 cm^{-1} and of the lactone carbonyl absorption from approximately 1740 to 1677 cm^{-1} took place. Comparison of the infrared spectra of other ring-D steroid lactones indicated that the hydrogen bonding was of an intermolecular nature and required the presence of the 3-hydroxyl attached to a benzenoid ring-A and a 17a-ketone carbonyl associated with a lactone unit in a homo ring-D. Alteration of these structural requirements restored the displaced maxima to higher frequencies.

As early as 1946 Furchgott *et al.* [1] found that infrared analysis of steroid compounds prepared as films or melts became involved in hydrogen bonding. Recently Rosenkrantz [2] has reviewed this subject for steroid molecules and has extended this discussion to include vitamins and hormones analyzed by dispersal in potassium bromide [3]. Hydrogen bonding is evident because of displacement of the hydroxyl stretching vibration from the non-bonded frequency near 3640 (2·75) to one nearer 3330 cm^{-1} (3 μ). In most instances it has been demonstrated that the hydrogen bonding was of an intermolecular nature since serial dilution of the compound restored the hydroxyl absorption band to the higher frequency.

When the other functional group involved in the hydrogen bonding was a carbonyl, little alteration in the absorption of the latter was observed. On the other hand shifts in the carbonyl band to higher frequencies suggested vicinal effects which have been observed in solution and solid state spectra [2]. Splitting of the carbonyl maximum and the appearance of both a bonded and unbonded hydroxyl band has been assigned to intramolecular hydrogen bonding when the doublet in the 3 μ region did not respond to dilution [4]. An unusual example of intermolecular hydrogen bonding has been reported for 7-keto-cholesterol [5]. The spectra of this steroid contained a hydroxyl doublet in the 3 μ region which was not influenced by dilution and the carbonyl absorption band was not significantly displaced.

In the present investigation a marked displacement of the lactone carbonyl stretching vibrations of estrololactone was observed. There was a shift of approximately 50 cm^{-1} to a lower frequency. Since a few ring-D steroid lactones have become available recently, it was of interest to investigate the cause of the shift. In a second paper in this series the characteristic structure–absorption relationships of this group of steroids will be discussed.

* This investigation was supported in part by the Research and Development Division, Office of Surgeon General, Department of the Army, under Contract No. DA-49-007-MD-184 and by U.S. Public Health Service Grants No. A-1207 and C-2207.

VOL. 13 1958/5

Methods and experimental

All samples were dispersed in potassium bromide according to the method of ROSENKRANTZ *et al.* [6] and the rectangular prisms were studied in a Perkin–Elmer Infracord. Infrared spectra were recorded on estrololactone, its acetate, *iso*androlololactone, its acetate, 5-chloro*iso*androlololactone acetate, 1-dehydrotestololactone, and testololactone.* Some of the spectra of the non-hydroxylated steroids showed

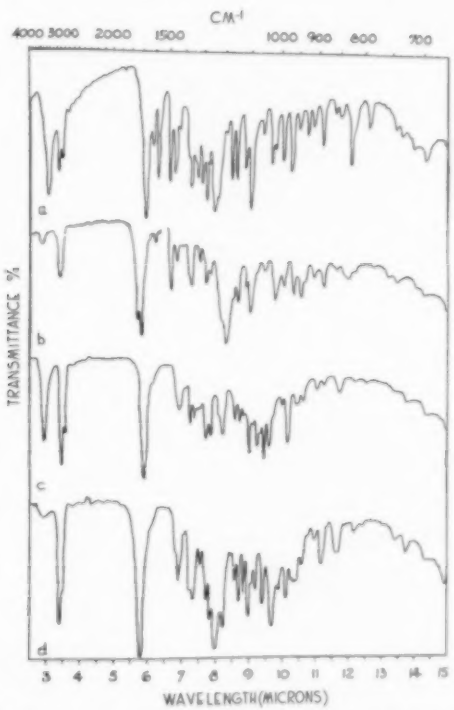

Fig. 1. The infrared absorption spectra of: (a) estrololactone (17a-oxa-17-oxo-D-homoestra-1:3:5(10)-trien-3-ol); (b) estrololactone acetate; (c) *iso*androlololactone (17a-oxa-17-oxo-D-homoepiandrostan-3β-ol) and (d) *iso*androlololactone acetate.

an absorption band near 3 μ which had arisen from adsorbed water in some of the preparations of potassium bromide. This artifact was easily recognized and no alterations of the other portions of the spectra due to adsorbed water were encountered.

Additional spectra of ring-D steroid lactones were available for inspection in the recently published steroid atlas of ROBERTS *et al.* [7].

Estrololactone was obtained from an incubation of 19-norprogesterone with *Streptomyces lavendulae* and the details of this work will be presented in another paper.† The acetoxy derivative of estrololactone was formed in the usual manner

* We wish to express our thanks to Dr. D. A. SHEPHERD and the Upjohn Research Division for generously donating samples of *iso*androlololactone acetate, 5-chloro*iso*androlololactone acetate, testololactone and 1-dehydrotestololactone.

† GUAL C. and DORFMAN R. I., manuscript in preparation.

with pyridine and acetic anhydride. Free *iso*andrololactone was generated from its acetate by the procedure of Levy and Jacobsen [8].

Results and discussion

The infrared absorption spectra of the steroid lactones recorded in this investigation are shown in Figs. 1 and 2 and some of the pertinent chemical structures are given in Fig. 3. The remarkable shifts of the hydroxyl and lactone carbonyl vibrations are quite evident in the spectrum of estrololactone (17a-oxa-17-oxo-D-homoestra-1:3:5(10)-trien-3-ol). The stretching vibrations of the hydroxyl

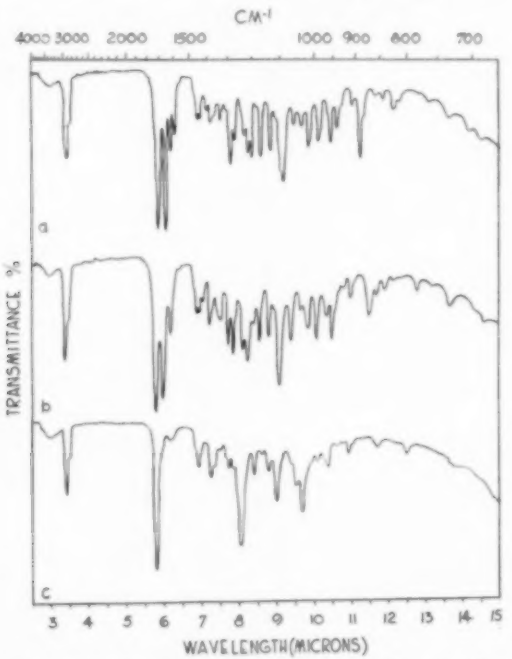

Fig. 2. The infrared absorption spectra of: (a) 1-dehydrotestololactone (17a-oxa-17-oxo-D-homoandrosta-1:4-dien-3-one); (b) testololactone (17a-oxa-17-oxo-D-homoandrost-4-en-3-one) and (c) 5-chloro*iso*andrololactone acetate.

group occurred near 3219 cm^{-1} (3·11 μ) which is characteristic of intense hydrogen bonding. The corresponding absorption band in the solid state spectrum of estrone appeared near 3483 cm^{-1} (2·87 μ) in the deposited film [9] and in a KBr preparation (unpublished spectrum). The location of the absorption band of the phenolic hydroxyl group in the latter compound fits the expected intensity of hydrogen bonding usually found in steroids in the solid state. In contrast the estrololactone molecule appeared to have a greater opportunity for hydrogen bonding. That this bonding was in part dependent on the benzenoid ring was revealed by the smaller change in frequency in the spectrum of *iso*andrololactone (17a-oxa-17-oxo-D-homoepiandrostan-3β-ol). For this compound the hydroxyl absorption occurred near 3470 cm^{-1} (2·88 μ).

VOL. 13 1958/5

The marked displacement of the hydroxyl maximum in the estrogenic ring-D lactone suggested an unusual structural feature in this molecule which initiated hydrogen bonding. Further evidence for such an interpretation was gathered from an examination of the carbonyl region of the spectra. It can be seen in Fig. 1 that the vibrations of the lactone carbonyls in the 3-hydroxy steroids were found near

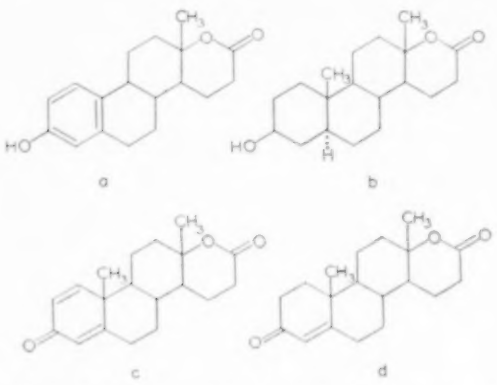

Fig. 3. The chemical structures of (a) estrololactone; (b) *iso*androlololactone; (c) 1-dehydrotestololactone and (d) testololactone.

1677 cm^{-1} (5·97 μ) for estrololactone and near 1690 cm^{-1} (5·91 μ) for *iso*androlololactone. The normal location of the absorption of a lactone carbonyl in a solid state spectrum is shown by the corresponding bands near 1720 cm^{-1} (5·82 μ) and 1725 cm^{-1} (5·80 μ) in the spectra of 1-dehydrotestololactone (17a-oxa-17-oxo-D-homoandrosta-1:4-dien-3-one) and testololactone (17a-oxa-17-oxo-D-homoandrost-4-en-3-one), respectively. This is confirmed by the spectra of the acetates of *iso*androlololactone, 1732 cm^{-1} (5·77 μ), and estrololactone, 1729 cm^{-1} (5·78 μ); in the latter curve the acetoxy absorption does not obliterate the absorption band of the lactone carbonyl. These results establish the necessity of the 3-hydroxy group in explaining the unusually intense hydrogen bonding in estrololactone.

That the lactone structure is required for interpreting the hydrogen bonding of estrololactone and *iso*androlololactone may be deduced from the spectrum of 3β-hydroxy-D-homoandrostan-17a-one. This steroid has the enlarged ring-D without the oxygen atom and no interaction between its 3-hydroxyl group and the ring-D ketone group could be discerned in the carbonyl region (chart 654, ref. [7]).

Investigations in the conversions of androgens to estrogens, microbial transformations of the types of steroids discussed here and isolation studies may find these observations helpful in the identification of related steroid lactones. The spectral changes induced by hydrogen bonding may be of aid in studies on protein-steroid interactions.

References

[1] Furchgott R. F., Rosenkrantz H. and Shorr E., *J. Biol. Chem.* 1946 **163** 375.
[2] Rosenkrantz H., *Glick's Methods of Biochemical Analysis*, Vol. II, p. 1. Interscience, New York 1955.

[3] Rosenkrantz H., *Glick's Methods of Biochemical Analysis* Vol. V, p. 407. Interscience, New York 1957.
[4] Jones R. N., Humphries P., Herling F. and Dobriner K., *J. Amer. Chem. Soc.* 1952 **74** 2820.
[5] Rosenkrantz H. and Gut M., *Science* 1954 **120** 1035.
[6] Rosenkrantz H., Potvin P. and Skogstrom P., *Analyt. Chem.* 1958 **30** 975.
[7] Roberts G., Gallagher B. S. and Jones R. N., *Infrared Absorption Spectra of Steroids—An Atlas* Vol. II. Interscience, New York 1958.
[8] Levy H. and Jacobsen R. P., *J. Biol. Chem.* 1947 **171** 71.
[9] Furchgott R. F., Rosenkrantz H. and Shorr E., *J. Biol. Chem.* 1946 **164** 621.

VOL.
13
1958/5

Spectrochimica Acta, 1958, Vol. 13, pp. 253 to 260. Pergamon Press Ltd., London. Printed in Northern Ireland

RESEARCH NOTES

νOH of trifluoroethanol and the Kirkwood-Bauer relation

(*Received* 25 *July* 1958)

STUDIES of the effect of solvents on infra-red frequencies have shown marked deviations from the Kirkwood–Bauer theory [1, 2] which relates the frequency shift to the polarization of the solvent medium by the vibrating solute dipole. Observed shifts are almost always larger than the theory predicts.

We have recently recorded the OH frequencies of ethanol and trifluoroethanol (CF_3CH_2OH) on a Perkin–Elmer 12C spectrometer equipped with a lithium fluoride prism and slit drive. The frequencies are compared in the table.

State	C_2H_5OH (cm^{-1})	CF_3CH_2OH (cm^{-1})	Assignment
Vapour—10 cm cell at 25°C	3673	3656	Free OH stretch
0·5% v/v in perfluorocarbon	3655	3644	
Pure liquid—capillary layer	—	3628	
0·1% v/v in CCl_4—1 cm cell	3629	3617	
Higher conc. in perfluorocarbon	3520	3530	"Dimer" OH
Higher conc. in CCl_4	3507	3505	
Higher conc. in perfluorocarbon	3353	3363	"Polymer" OH
Higher conc. in CCl_4	3363	3371	
Pure liquid—cap.	3340	3355	

Trifluoroethanol is of particular interest as it shows a weak "free" OH stretching band at 3628 cm^{-1} in the pure liquid, in common with several polyhalogenated alcohols investigated by HASZELDINE [3]. He suggested that this "free" OH frequency might arise from OH groups intramolecularly hydrogen bonded to a halogen atom. Our investigation does not support this suggestion.

On progressive dilution in CCl_4 trifluoroethanol exactly parallels ethanol in the behaviour of the OH stretching frequencies. Three distinct bands are resolved which are commonly assigned to monomer, dimer and higher polymer species. The band assigned by HASZELDINE to intramolecular OH – – – X (X = F or Cl) groups is clearly the usual intermolecular "dimer" band in trifluoroethanol. This conclusion is fully confirmed by the frequencies observed. The free OH band in trifluoroethanol is at a *higher* frequency in the pure liquid than in dilute solution in CCl_4. In a perfluorocarbon (b.p. 150°–200°C) frequencies very close to the vapour values were recorded for the free OH of both alcohols. The ethanol and trifluoroethanol frequencies given in the table lie on a good straight line when plotted against each other, showing that the change in solvent environment or degree of association produces proportional shifts in the OH frequency of both alcohols.

We have tried to relate the observed frequency shifts of the free OH of both alcohols to the electronic polarizability of the environment, calculated from the refractive indices of the solvents using the Kirkwood–Bauer function [1, 2]. Compared with CCl_4, which previous work has shown is similar to non polar hydrocarbons, the shifts in perfluorocarbon were much smaller than the K–B line would predict even though, by using the refractive

index rather than the dielectric constant of the solvent, the contribution of orientation polarization was neglected. The free OH frequency shift in liquid trifluoroethanol lies on the K–B line.

The infra-red frequencies in solution appear to be determined partly by the bulk polarizability of the medium and partly by the polarity and polarizability of the solvent cage surrounding the solute molecules. The high frequency of the "free" OH band in liquid trifluoroethanol is consistent with the OH groups being in essentially a $-CF_3$ environment.

Research Department
British Nylon Spinners Ltd.
Pontypool, S. Wales

C. G. Cannon
B. C. Stace

References

[1] Bayliss N. S., Cole A. R. H. and Little L. H., *Aust. J. Chem.* 1955 **8** 26.
[2] Josien M. L. and Fuson N., *J. Chem. Phys.* 1954 **22** 1169 and 1264.
[3] Haszeldine R. N., *J. Chem. Soc.* 1953 1757.

Effect of solvent upon vibration bands

(*Received* 25 *July* 1958)

Abstract—Data are reported for the frequency and intensity of the carbonyl band of acetone when measured in different solvents. The results have been correlated with similar data on other solutes containing the C=O group in series of current ideas about frequency shifts. Comparisons are also made with some recent data on the C≡N group vibration.

VOL. 13 1958/5

Data have been reported recently on the vibration band of the carbonyl group in several molecules when measured in different solvents [1, 2, 3, 4]. We have measured the frequency and intensity of this band in acetone in twenty-five solvents, the results being given in Table 1. A Perkin–Elmer 21 spectrometer (rock salt) was used, and the intensities were determined by Wilson–Wells extrapolation of data obtained by direct graphical integration of the absorption curves using a series of path lengths and concentrations. In all cases, compensation for any solvent absorption was arranged by using a second cell in the blank beam. Our results are generally in good agreement with those of previous workers where comparisons are possible, but extend the data to other solvents.

It is evident that no simple relation exists between ν_{CO} and the dielectric constant of the solvent medium. If, according to the Kirkwood–Bauer–Magat equation, $\Delta\nu/\nu$ is plotted against $(D-1)/(2D+1)$, a straight line can be drawn through the origin which passes satisfactorily through the points corresponding to non-polar solvents, but the results for nearly all other solvents deviate markedly from this line. The deviations do not seem to arise from hydrogen bonding, since this should lower ν and increase $\Delta\nu$, whereas the converse is found.

Using some earlier data [5] on the shift of several C=O bands in different solvents, we have plotted (Fig. 1) $\Delta\nu/\nu$ for acetone against the same ratio for other solutes in the same solvents as suggested by Bellamy [6, 7]. The data on N-N-diethyl acetamide given by Archibald and Pullin [4] were used, and all frequency values listed by Hartwell, Richards and Thompson [5] were reduced by 5 cm^{-1} to bring them into line with more recent results. The plot for benzophenone has been transferred from that recently recorded by Bellamy [6]. The plots are satisfactorily linear, as found by Bellamy for a set of X—H vibrations, and for other C=O vibrations. Data on *cyclo*hexanone [8] also give a linear plot when plotted against those for acetone, but it does not pass through the origin.

Table 1. ν_{CO} of acetone

Solvent	ν (cm^{-1})	$10^7 A_{01}$	$\Delta\nu_{\frac{1}{2}}$[a]
Vapour	1737	6·5	
n-hexane	1722·5	6·7	19
*Cyclo*Hexane	1722·5	7·2	17·5
Methyl *cyclo*hexane	1722	7·7	18
Benzene	1716·5	7·9	17
Toluene	1717·5	7·6	17·5
Chlorobenzene	1713·5	7·8	18
Carbon tetrachloride	1719	8·2	17·5
Chlorform	1712·5	10·3	15
Methyl chlorform	1715	7·0	19·5
1:2 Dichloro-ethane	1714	10·5	13·5
Pentachloroethane	1712	10·8	15
trans-1:2-Dichloroethylene	1716	9·4	17
Tetrachloroethylene	1721	7·1	15·5
Bromoform	1708	10·5	15·5
Nitromethane	1712·5	9·8	14·5
Nitroethane	1712	9·7	
Methyliodide	1714	10·3	13·5
Methylene dichloride	1714	9·5	13
Methylene debromide	1711	8·2	14
Methylene di-iodide	1707	8·4	16
Acetonitrile	1713	10·1	16·5
Pyridine	1712·5	9·3	17
Tetrahydrofuran	1716·5	8·1	16·5
Carbon disulphide	1716·5	7·5	19·5

There is no doubt that the slope of the lines is related to the polar character of the carbonyl group concerned, and although insufficient data are yet available to show the precise functional relationship, these slopes can be correlated with the inductive and mesomeric powers of the attached groups.

In Fig. 2, using $\Delta\nu/\nu$ for dimethyl cyanamide as a standard, similar plots are shown for other compounds containing the C≡N group [9], and also for acetone and N-N-diethyl acetamide. As expected, the slope for the plot of diethyl cyanamide is about unity, and in general the slopes are related to the nature of the groups attached to the chromophore. The plots show that the functional groups C=O and C≡N behave similarly, and are affected by attached groups in parallel fashion.

It is impossible at present to correlate the variation of band intensity in different solvents quantitatively with the properties of the solvents. It is usually increased in those solvents where hydrogen bonding might be possible, but the biggest variation found with acetone in different solvents is much smaller than those which occur between different kinds of carbonyl group in the same solvent [10]. More data of this kind on different vibrational chromophores is needed before any current theories of the solute–solvent interactions can be tested satisfactorily.

Acknowledgement—Our thanks are due to the Hydrocarbon Research Group of the Institute of Petroleum for a grant.

Physical Chemistry Laboratory
Oxford

H. W. Thompson
D. J. Jewell

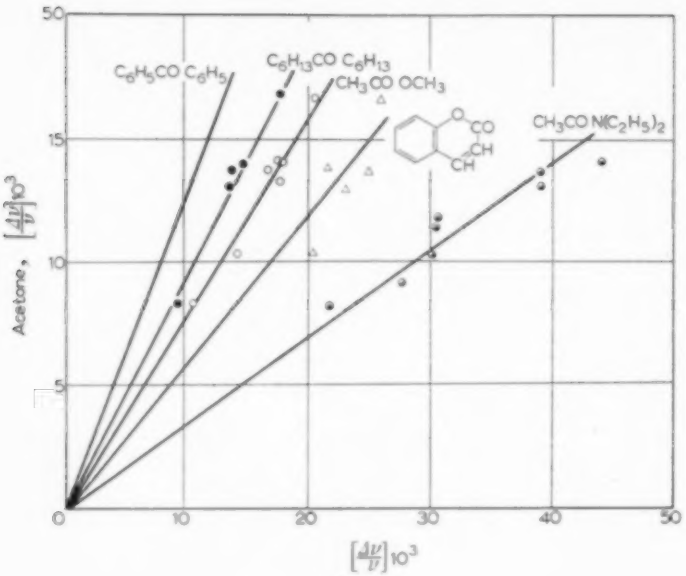

Fig. 1.

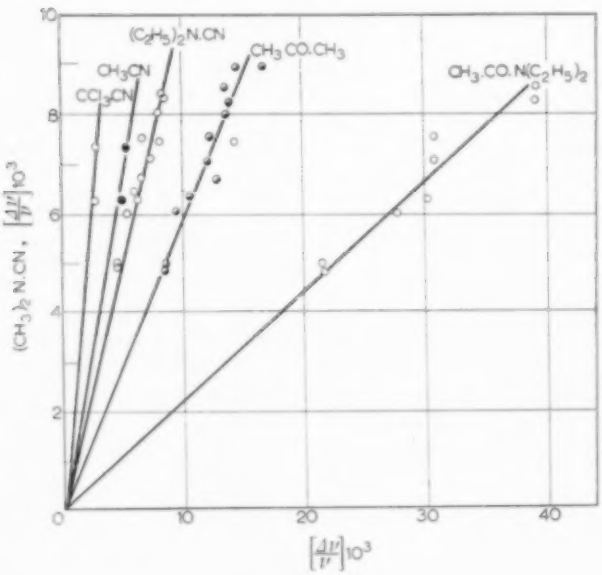

Fig. 2.

References

[1] Bayliss N. S., Cole A. R. H. and Little L. H., *Aust. J. Chem.* 1955 **8** 26.
[2] Chulanowsky V. M., *Dokl. Akad. Nauk SSSR* 1955 101.
[3] Barrow G. M., *J. Chem. Phys.* 1953 **21** 2008.
[4] Archibald L. B. and Pullin A. D. E., *Spectrochim. Acta* 1958 **12** 34.
[5] Hartwell E. J., Richards R. E. and Thompson H. W., *J. Chem. Soc.* 1948 1436.

VOL. 13 1958/5

[6] BELLAMY L. J., *Symposium on Molecular Spectroscopy*. Institute of Petroleum 1958
[7] BELLAMY L. J., HALLAM H. E. and WILLIAMS R. L., *Trans. Faraday Soc.* 1858 **54** 1120.
[8] JOSIEN M. L. and LASCOMBE J., *J. Chim. Phys.* 1955 **52** 162.
[9] JESSON J. P. and THOMPSON H. W., *Spectrochim. Acta*. This issue, p. 217.
[10] THOMPSON H. W. and JAMESON D. A., *Spectrochim. Acta*. This issue, p. 236.

Infrared group frequencies vs. electronegativity

(*Received* 4 *August* 1958)

IT has been evident for some time that the well known characteristic group frequencies of the infrared spectrum actually fall within a range of frequencies rather than at one particular frequency. Within the last several years investigators have found that the frequency of the absorption within this range can in some instances be related to the inductive and mesomeric effects within the molecule [1–8]. More particularly, the frequency can sometimes be related to the electronegativities of the other substituents in the molecule. A linear relationship between the frequency and the sum of the electronegativities is indicated for the P—O [2], C—O [3], CH_2 [4, 7], C—C [5] and S—H [8] frequencies.

The purpose of this note is to point out that such a relationship is also indicated for the asymmetric and symmetric stretching vibrations of the SO_2 group, the asymmetric stretching vibration of the NO_2 group, the stretching vibration of the C—S group and perhaps also for the stretching vibration of the SeO, SO and NO groups. Data collected from numerous sources in the literature are presented in Fig. 1 as plots of assigned group frequencies vs. the sum of the electronegativities of the attached groups. Horizontal lines indicate the spread of values for various compounds having the general formula given on the graphs. The atomic electronegativities are those of PAULING [9], while the electronegativities for the polyatomic groups are those derived from the study of P—O group [2].

Certain limitations of the data should be mentioned. (a) The slopes of the lines are not so well established that a claim for high accuracy in their use can be made. For example, the data for the P—O bond, although voluminous, is still heavily weighted with compounds in which the summed electronegativity of the substituents covers a shorter span than is desirable. As a result, one can pivot the straight line somewhat and not unduly affect the mean deviation. As a matter of fact, the author finds the best fit for the data on this particular group is obtained with a quadratic function. (b) The plots are formed from data on samples in the gas, liquid and solid states and the shifts in groups frequencies which follow changes in state will introduce additional error. (c) It shoud be remembered that electronegativity is a measure of the inductive effect and has no direct relationship to mesomerism, the other generally recognized form of intramolecular electronic interaction. Therefore, one would expect a correlation only in those cases where the inductive effect is the major factor contributing to the change in group frequency. (d) Furthermore it has become increasingly evident that the electronegativity of an atom has constancy only when referred to the same state of hybridization.

Knowing these limitations, certain practical uses of the data are clearly suggested. (1) One can predict the approximate absorption frequency for certain vibrations of the groups. The use of this sort of information in qualitative analyses and vibrational assignments is obvious. (2) It seems possible to use some of the empirical polyatomic group electronegativities in the same manner as atomic electronegativities, that is, they may be

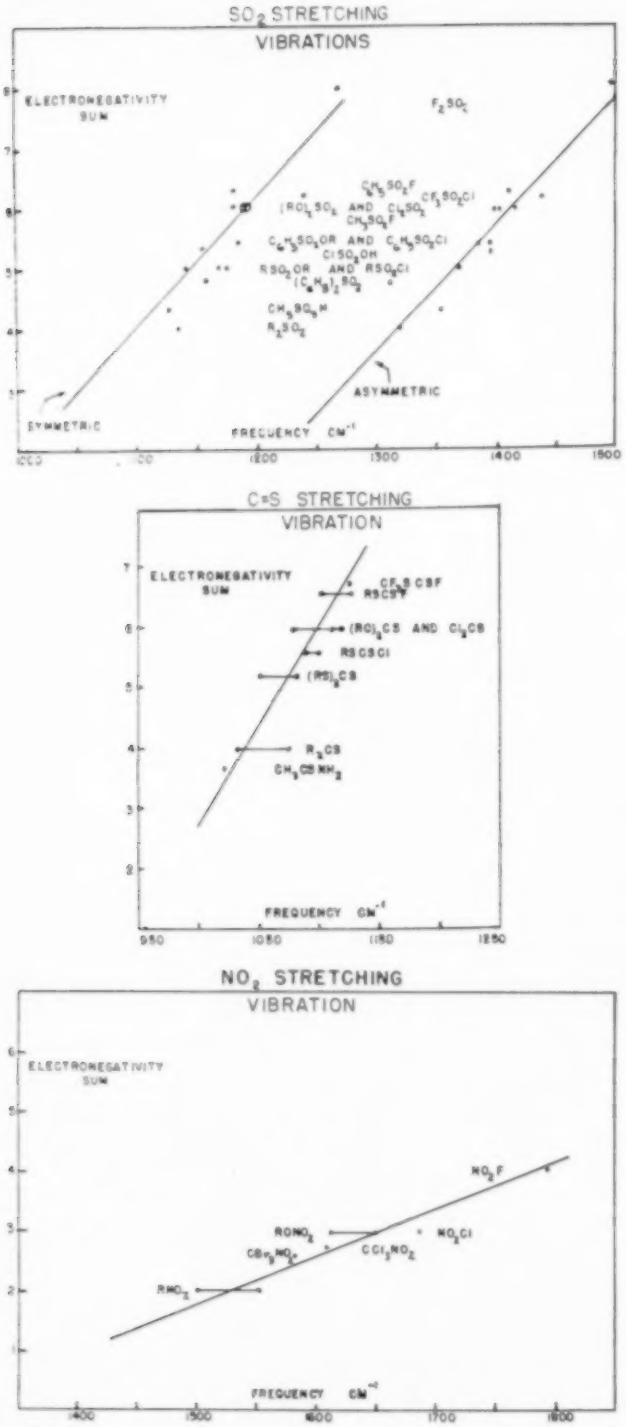

Fig. 1.

VOL. 13 1958/5

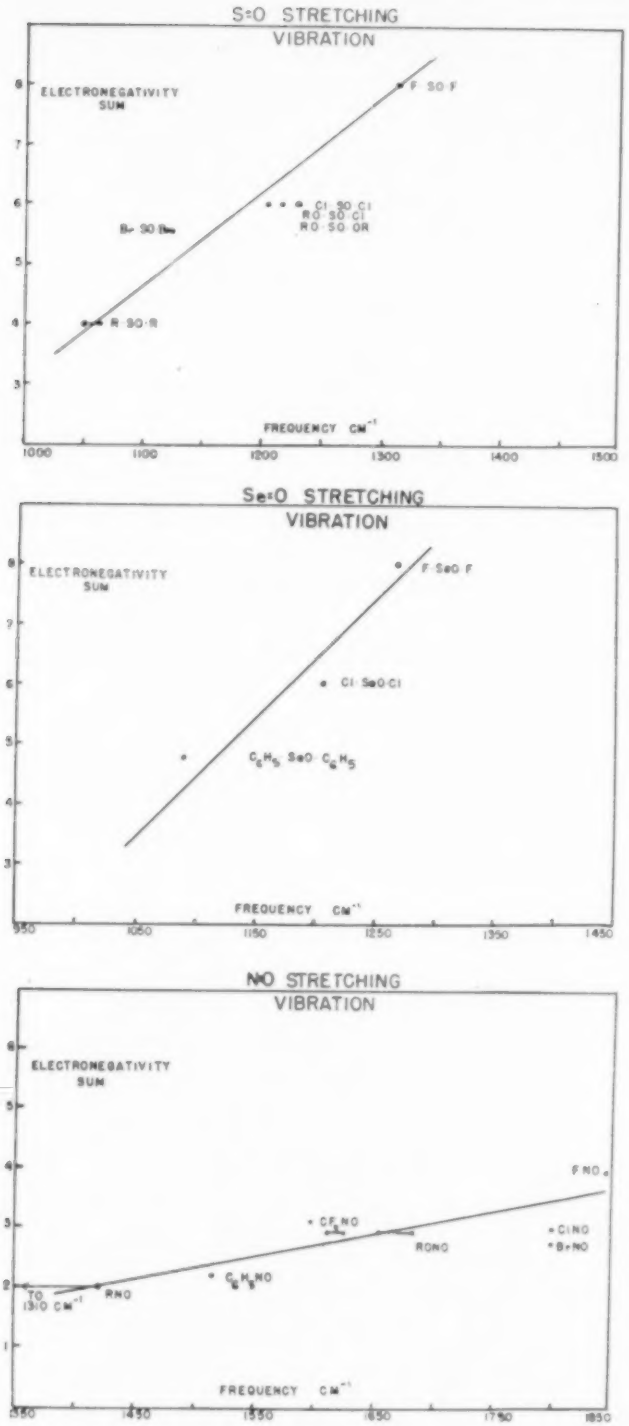

Fig. 1 (*continued*)

transferred from one set of data to another. (3) It is suggested that a refinement and enlargement of the data will be sufficient to assign values for the electronegativity of atoms and perhaps establish a scale of relative values for polyatomic groups.

L. W. Daasch

U.S. Naval Research Laboratory
Washington 25, D.C.

References

[1] Daasch L. W., *Analyt. Chem.* 1951 **23**, 853.
[2] Bell J. V., Heisler J., Tannenbaum H. and Goldenson J., *J. Amer. Chem. Soc.* 1954 **76** 5185.
[3] Kagarise R. E., *J. Amer. Chem. Soc.* 1955 **77** 1377.
[4] Bellamy L. J., *J. Chem. Soc.* 1955 863.
[5] Halpern E. and Goldenson J., *Report* CRLR642. Army Chemical Center 1956.
[6] Bellamy L. J. and Williams R. L., *J. Chem. Soc.* 1957 863.
[7] Wilmhurst J. K., *J. Chem. Phys.* 1957 **26** 426; *J. Chem. Phys.* 1958 **28**.
[8] Nebergall W. H. and Prake J. S., *Final Report on Reactions of Silanes*. ONR Contract No. 908 (02) 1957.
[9] Pauling L., *Nature of the Chemical Bond*. Cornell University Press, New York, 1948.

Erratum

R. Andrisano and G. Pappalardo:

Absorption spectra in the near ultraviolet of some α- and β-monosubstituted derivatives of thiophene

Spectrochim. Acta 1958 **12** 350

Formulae Ia and IIa were unfortunately omitted from this article and are reproduced here. They were referred to on p. 354 of the article.

Ia

IIa

MEETING ANNOUNCEMENT

The Tenth Annual Symposium on Spectroscopy of the American Association of Spectrographers is to be held at the Conrad Hilton Hotel in Chicago, Illinois, on June 1–3, 1959.

An increasing emphasis is being placed on international co-operation. Original papers in the fields of emission, X-ray, infrared, near infrared, Raman spectrometry and flame photometry are invited.

Authors living in the U.S.A. are requested to submit titles to G. W. Bailey, Program Chairman, Borg-Warner Research Center, Des Plaines, Illinois.

All international correspondence should be directed to Theodore H. Zink, International Activities Chairman, c/o Armour Research Foundation of Illinois Institute of Technology, 10 West 35th Street, Chicago 16, Illinois.

Submitted and accepted papers may be given by proxy; the author and/or the American Association of Spectrographers will supply a person well qualified to present the work.

Spectrochimica Acta, 1959, Vol. 13, pp. 261 to 270. Pergamon Press Ltd. Printed in Northern Ireland

The infra-red spectra of some methylammonium iodides: angle deformation frequencies of $\overset{+}{N}H$ and $\overset{+}{N}H_2$ groups

E. A. V. Ebsworth and N. Sheppard
University Chemical Laboratories, Lensfield Road, Cambridge, England

(*Received* 14 *July* 1958)

Abstract—The infra-red spectra of di-, tri- and tetramethylammonium iodides have been determined and interpreted in terms of the vibrations of the cations. The frequencies of the infra-red active deformation modes of the $\overset{+}{N}H_2$ and $\overset{+}{N}H$ groups have been identified with the help of the spectra of deuterated samples. The values observed are compared with those for analogous vibrations of the isoelectronic hydrocarbons propane, *iso*butane and neopentane.

Introduction

Several papers have been published that deal with the infra-red or Raman vibrational spectra of the simple methylated ammonium ions. The infra-red spectra of methyl, dimethyl and trimethylammonium chlorides have recently been studied by Bellanato and Barceló [1] and that of the monomethylammonium ion has been analysed in detail by Waldron [2] with the help of data on $CH_3ND_3^+$. Raman spectra of the series of methylammonium chlorides have been studied in aqueous solution by Edsall [3]. However there remain a number of uncertainties in the assignment of frequencies for the dimethyl and trimethyl derivatives, particularly with respect to the external angle deformation modes of $\overset{+}{N}H$ and $\overset{+}{N}H_2$ groups. It was therefore considered worthwhile to reinvestigate the spectra of these ions in the form of the iodides and at the same time to measure the spectra of the N-deutero derivatives. In addition the spectrum of tetramethylammonium iodide was recorded as no detailed assignment of the frequencies of the cation appears to have been made. The iodides are less hygroscopic than the chlorides studied previously [1].

Experimental

Di- and trimethylammonium iodides were prepared from aqueous solutions of the amines and hydrogen iodide: tetramethylammonium iodide was made from trimethylamine and methyl iodide. Each compound was purified by recrystallization, and its purity was confirmed by analysis and by rapid determinations of its melting-point (For C_2H_8IN: found, C, 13·6, H, 4·4 per cent, mp. 153°C; expected, C, 13·8, H, 4·6 per cent, mp. 155°C. For $C_3H_{10}IN$: found, C, 19·0, H, 5·3 per cent, mp. 260°C; expected, C, 19·2, H, 5·4 per cent, mp. 263°C. For $C_4H_{12}IN$: found, I, 63·4 per cent; expected, I, 63·1 per cent). N-Deutero samples of di- and trimethylammonium iodides were prepared by dissolving pure samples of the normal salts in heavy water (99·9 per cent) and pumping away the excess of solvent; the process was repeated twice. The deuterated salts were stored *in vacuo* and handled in a dry-box.

The spectra were recorded in the range 4000–400 cm^{-1}, using a Perkin-Elmer model 21 double-beam spectrometer, fitted with sodium chloride and potassium bromide prisms. The compounds were examined as finely-ground solids mulled with nujol and hexachlorobutadiene. The nujol spectra obtained for the di- and trimethylammonium salts were in general in good agreement with those given by Bellanato and Barceló for the hydrochlorides in KBr discs [1], although there

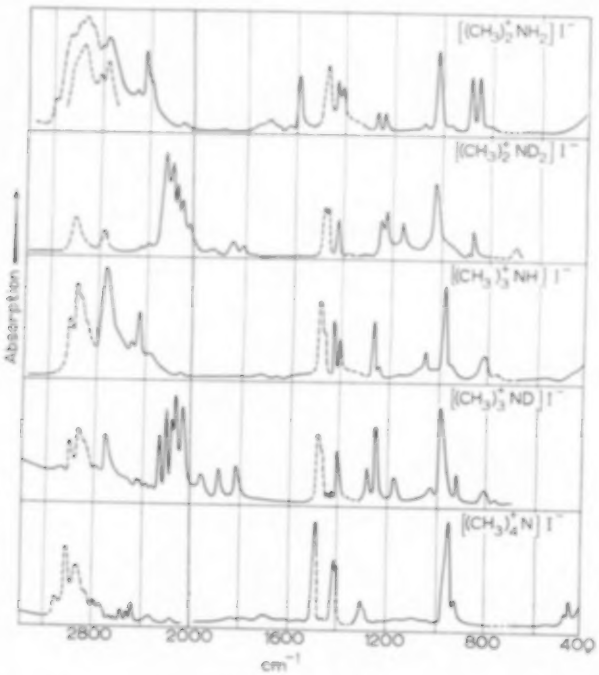

Fig. 1. The infra-red spectra of $[(CH_3)_2\overset{+}{N}H_2]I^-$; $[(CH_3)_2\overset{+}{N}D_2]I^-$; $[(CH_3)_3\overset{+}{N}H]I^-$; $[(CH_3)_3\overset{+}{N}D]I^-$ and $[(CH_3)_4\overset{+}{N}]I^-$, as nujol (———) and hexachlorobutadiene (· · · · · ·) mulls.

are some differences; their nujol spectra were much less well defined, possibly because of the considerably greater hygroscopicity of their salts. The spectra obtained in the present work are illustrated in Fig. 1.

Interpretation of the spectra

The vibrational degrees of freedom of the cations with $\overset{+}{N}H$ groups are enumerated in Tables 1 and 3 where they are classified in terms of symmetry properties and vibrational selection rules. The infra-red absorption frequencies, together with those of the Raman lines observed in water solution by Edsall [3] are set out in Tables 2 and 4 where they are assigned to the various fundamental modes of vibration.

Many of the assignments follow well established lines and need not be discussed

VOL. 13 1958/5

in detail. These include the CH stretching frequencies, the symmetrical and asymmetrical angle deformation modes of the CH_3 groups [4] and the $\overset{+}{N}H$ stretching and $\overset{+}{N}H_2$ bending (scissors) frequencies which have been identified in earlier work [5–10]; all of these are internal vibrations of the groups concerned. The symmetrical C—$\overset{+}{N}$ stretching vibrations are also readily assigned by virtue of their strong and polarized Raman lines, and most of the skeletal bending modes can be easily chosen from the few frequencies observed below 600 cm^{-1}. There remain to be identified the external angle deformation vibrations of the $\overset{+}{N}H$ and $\overset{+}{N}H_2$ groups, and the coupled CH_3 rocking and asymmetrical $\nu C\overset{+}{N}$ vibrations, all of which occur in the range 1600–600 cm^{-1}. It was found that the $\overset{+}{N}H$ deformation frequencies were readily established with the help of the spectra of the deuterated ions. As in the spectra of the corresponding hydrocarbons the actual normal modes involving some of the methyl rocking and skeletal stretching vibrations are mixtures of these two types; in such cases only the numbers of the fundamentals are given. Some specific points in the assignments are discussed below.

(a) *The* $(CH_3)_2\overset{+}{N}H_2$ *ion* (*Tables* 1 *and* 2)

The $\overset{+}{N}H_2$ bending (scissors) vibration clearly corresponds to the band at

Table 1. Vibrations of the ion $(CH_3)_2\overset{+}{N}H_2$ of assumed overall symmetry C_{2v}

Vibration	Symmetry class			
	A_1	A_2	B_1	B_2
νCH_3 asymm.	ν_1	ν_{10}	ν_{15}	ν_{22}
νCH_3 symm.	ν_2		ν_{16}	
$\nu\overset{+}{N}H$	ν_3			ν_{23}
$\overset{+}{N}H_2$ bend (scissors)	ν_4			
δCH_3 asymm.	ν_5	ν_{11}	ν_{17}	ν_{24}
$\overset{+}{N}H_2$ wag			ν_{18}	
δCH_3 symm.	ν_6		ν_{19}	
$\overset{+}{N}H_2$ twist		ν_{12}		
CH_3 rock.	ν_7	ν_{13}	ν_{20}	ν_{25}
$\nu C\overset{+}{N}$	ν_8		ν_{21}	
$\overset{+}{N}H_2$ rock.				ν_{26}
$\delta C_2\overset{+}{N}$	ν_9			
CH_3 torsion		ν_{14}		ν_{27}
Activity	I,R(p)	R(dp)	I,R(dp)	I,R(dp)

I: infra-red active; R: Raman active; (p): polarized; (dp): depolarized.

Table 2. Vibrational assignments to the observed frequencies (cm^{-1}) in the spectra of the ions $(CH_3)_2\overset{+}{N}H_2$ and $(CH_3)_2\overset{+}{N}D_2$

$(CH_3)_2\overset{+}{N}H_2\ I^-$			$(CH_3)_2\overset{+}{N}D_2\ I^-$	
Raman [3] (H_2O solution)	Assignment	Infra-red (crystalline)	Infra-red (crystalline)	Assignment
3048 (4) (dp)	νCH_3 asymm.	3010 (m)	3020 (m)	νCH_3 asymm.
2990 (5) (p)	νCH_3 symm. + $\nu\overset{+}{N}H$, ν_{23}	~2965 (s)	2980 (m)	νCH_3 symm.
2940 ($\frac{1}{2}$)				
2883 (1)	$2\nu_6$?	2800 (m)		
2839 (1)	$\nu\overset{+}{N}H$, ν_3	2745 (s)	[2755 (m)]	residual $\overset{+}{N}H$
		2490 (w)		
	$\nu_{18} + \nu_{21}$	2412 (m)	[2430 (vw)]	residual $\overset{+}{N}H$
			2245 (s)	$\nu\overset{+}{N}D$
			2190 (s)	$\overset{+}{N}D_2$ bend. + $\overset{+}{N}D_2$ wag?
			2135 (s)	$\nu\overset{+}{N}D$
			2100 (s)	$2 \times \overset{+}{N}D_2$ wag?
			2060 (m)	$\overset{+}{N}D_2$ wag + $\nu\overset{+}{C}N$?
	$\overset{+}{N}H_2$ bend., ν_4	1582 (m)		
1481 (4) (dp)	δCH_3 asymm.	1472 (s)	1474 (m)	δCH_3 asymm.
		1464 (vs)	1463 (m)	
	$\overset{+}{N}H_2$ wag., ν_{18}	1421 (s)		
	δCH_3 symm.	1407 (s)	1409 (m)	δCH_3 symm.
			1380 (vw)	
1240 ($\frac{1}{2}$b) (dp)	CH_3 ν_7 rocks. ν_{25}	1258 (m)	1228 (m)	CH_3 rocks.
		1233 (w)	1217 (m)	
			1157 (m)	$\overset{+}{N}D_2$ bend.
1099 (1) (dp)	ν_{20}	~1077 (vw)	~1055 (vw)	$\overset{+}{N}D_2$ wag.
1029 (2) (dp)	ν_{21}	1016 (s)	1021 (2)	$\nu\overset{+}{C}N$
	$\overset{+}{N}H_2$ rock., ν_{26}	878 (s)	[878 (vw)]	residual $\overset{+}{N}H$
895 (4) (p)	$\nu\overset{+}{C}N$, ν_8	853 (s)	868 (m)	$\nu\overset{+}{C}N$
			689 (mw)	$\overset{+}{N}D_2$ rock.
412 (2) (p)	$\delta\overset{+}{N}C_2$, ν_9	420 (w)?		

(vs): very strong; (s): strong; (m): medium; (w): weak; (vw): very weak; (p): polarized; (dp): depolarized.

1582 cm^{-1}; this assignment is in agreement with earlier work by Heacock and Marion [8], Nakanishi *et al.* [9] and Stone *et al.* [10] based upon the spectra of more complex ions containing the $\overset{+}{N}H_2$ group. Infra-red active $\overset{+}{N}H_2$ wagging and

VOL. 13 1958/59

rocking modes are also expected in the observed spectra. The former, ν_{18}, is identified with the band at 1421 cm^{-1} which is removed by deuteration. One of the pair of bands at 853 and 878 cm^{-1} must correspond to the rocking mode, ν_{26}, and once again deuteration identifies the higher frequency band as the $\overset{+}{N}H_2$ vibration. The analogous $\overset{+}{N}D_2$ frequencies of the deutero-ion seem to be 1157 (scissors), 1055 (wagging) and 689 cm^{-1} (rocking); the isotopic ratios range from 1·36 to 1·27 and are in reasonable agreement with the assignments. The choice of the remaining CH_3 rocking and $\nu\overset{+}{C}N$ fundamentals have been made using the analogous vibration frequencies of the isoelectronic hydrocarbon propane as a guide [4]. They differ slightly from those given previously [1].

There remains a prominent combination band in the spectrum of the parent ion at 2412 cm^{-1}. Deuteration-sensitive bands in this region are found consistently in the spectrum of compounds containing the $\overset{+}{N}H_2$ groups [10]. In this case an acceptable assignment of this band appears to be $\nu_{18}(\overset{+}{N}H_2$ wag) + $\nu_{21}(\nu\overset{+}{C}N)$, with $\nu_4(\overset{+}{N}H_2$ bend) + $\nu_{26}(\overset{+}{N}H_2$ rock) as an alternative.

(b) *The* $(CH_3)_3\overset{+}{N}H$ *ion* (*Tables* 3 *and* 4)

The assignment of frequencies given in Table 4 for $[(CH_3)_3\overset{+}{N}H]$ seems fairly straightforward. The $\nu\overset{+}{N}H$ and $\delta\overset{+}{N}H$ vibrations are identified easily with the help of the changes observed on isotopic substitution. The unassigned bands between 2800 and 2900 cm^{-1} undoubtedly represent overtones and combinations of δCH_3

Table 3. Vibrations of the $(CH_3)_3\overset{+}{N}H$ ion assumed to be of symmetry class C_3

Vibration	Symmetry class		
	A_1	A_2	E
νCH_3 (asymm.)	ν_1	ν_9	ν_{13}, ν_{14}
νCH_3 (symm.)	ν_2		ν_{15}
$\nu\overset{+}{N}H$	ν_3		
δCH_3 (asymm.)	ν_4	ν_{10}	ν_{16}, ν_{17}
$\delta\overset{+}{N}H$			ν_{18}
δCH_3 (symm.)	ν_5		ν_{19}
CH_3 rock.	ν_6	ν_{11}	ν_{20}, ν_{21}
$\nu\overset{+}{C}N$	ν_7		ν_{22}
$\delta C_3\overset{+}{N}$	ν_8		ν_{23}
CH_3 torsion		ν_{12}	ν_{24}
Activity	I,R(p)		I,R(dp)

Table 4. Vibrational assignments in the spectra of the $[(CH_3)_3\overset{+}{N}H]$ and $[(CH_3)_2\overset{+}{N}D]$ ions

$[(CH_3)_3\overset{+}{N}H]I^-$			$[(CH_3)_3\overset{+}{N}D]I^-$	
Raman [3] (H_2O solution)	Assignment	Infra-red (crystalline)	Infra-red (crystalline)	Assignment
3030 (5b) (dp)	νCH_3 asymm.	3015 (s)	2990 (m)	νCH_3 asymm.
2969 (6 vb) (p)	νCH_3 symm.	2955 (vs)	2930 (m)	νCH_3 symm.
2894 (3) (p)		2865 (s)	2850 (m)	
2822 (3)				
	$\nu\overset{+}{N}H$, ν_3	2725 (vs)	[2720 (m)]	residual $\overset{+}{N}H$
			2250 (s)	1455 + 802
			2200 (s)	1403 + 802
			2155 (m)	1167 + 983,
				or 1241 + 915
			2125 (vs)	$\nu\overset{+}{N}D$
			2070 (s)	1167 + 915
			1961 (w)	2 × 983
			1885 (m)	983 + 915
			1813 (s)	2 × 915
1464 (5) (dp)	δCH_3 asymm.	1476 (s) 1460 (s)	1471 (s) 1455 (m)	δCH_3 asymm.
			1435 (w)	
	$\delta\overset{+}{N}H$, ν_{18}	1418 (s)	[1418 (w)]	residual $\overset{+}{N}H$
	δCH_3 symm.	1401 (m)	1403 (s)	δCH_3 symm.
	ν_6	1256 (s)	1272 (m)	802 + 460?
1248 (1) (dp)	ν_{20}?	1241 (w)	1241 (s)	e-fundamental
			1167 (m)	e-fundamental
1067 (1) (dp)	ν_{21}	1052 (m)		
		1020 (w)	1017 (w)	
987 (4) (dp)	ν_{22}	980 (vs)	983 (vs)	e-fundamental
	$2\nu_8$?	947 (w)	915 (m)	e-fundamental
821 (5) (p)	$\nu\overset{+}{C}N$, ν_7	810 (m)	802 (m)	$\nu\overset{+}{C}N$
468 ($\frac{1}{2}$) (p)	$\delta\overset{+}{C_2}N$, ν_8	460 (w)		
406 (1) (dp)	$\delta\overset{+}{C_2}N$, ν_{23}			

asymm. and δCH_3 symm. fundamentals. The assignments of $[(CH_3)_3\overset{+}{N}D)]$ are less certain in the regions 2300 to 1800 cm^{-1}, where there is a surprising multiplicity of strong absorption bands near the $\nu\overset{+}{N}D$ fundamental, and in the region 1300–900 cm^{-1} where deuteration of the $\overset{+}{N}H$ group has resulted in several smaller band shifts rather than a single large one. However, in the latter region it seems very probable that the frequencies 1241, 1167, 983 and 915 cm^{-1} represent the set of e-fundamentals, although they cannot be assigned to separate group motions. The many bands in the 2000 cm^{-1} region can be plausibly accounted for, as shown in

VOL. 13 1958/5

Table 4, as overtone and summation bands which interact with $\nu\overset{+}{N}D$ by Fermi resonance. They might alternatively result from interaction of the $\nu\overset{+}{N}D$ frequency with low frequency lattice modes [11] caused by the hydrogen bond between $\overset{+}{N}D$ and I^-. However, this explanation seems less probable as the $\nu\overset{+}{N}H$ band does not have a comparable amount of structure.

In the present work the $\delta\overset{+}{N}H$ vibration has been given a much higher frequency than previously [1].

(c) *The* $(CH_3)_4\overset{+}{N}$ *ion*

Because of the high symmetry of this ion (effectively T_d) only a few of its vibrational degrees of freedom—those of symmetry f_2—are infra-red active. The few strong bands observed are listed below together with their straightforward assignments:

3005 (s)νCH_3 asymm.; 2925 (s)νCH_3 symm.; 1483 (s)δCH_3 asymm.; 1403 + 1397 (s)δCH_3 symm.; 1294 (m)$\nu\overset{+}{C}N$; 946 (vs), CH_3 rocking; 917 (m), 2x451?; 451 (m)$\delta\overset{+}{N}C_4$.

The respective assignments of the 1294 and 946 cm^{-1} frequencies are made by analogy with the corresponding bands of neopentane [12]. A number of other weak bands in the region 2800–2400 cm^{-1} are undoubtedly combination frequencies involving probably both infra-red and Raman active fundamentals.

The main Raman frequencies of this ion observed in water solution [3] are: 3037 (8, dp) 2991 (3, dp) 2967 (3, p) 2930 (5, p) 2828 (4) 1455 (5, dp) 1418 (1) 1289 (3) 1173 (3) 1047 (1) 955 (6, dp) 752 (6, p) 455 (2, dp) 372 (2, dp). Those at 2991, 1289, 955 and 455 cm^{-1} are clearly counterparts of infra-red active f_2-frequencies listed above; the 2930 (νCH_3 symm.), 1418 (δCH_3 symm.) and 752 cm^{-1} ($\nu\overset{+}{C}N$) lines are probably the a_1 Raman active fundamentals, and those at 3037 (νCH_3 asymm.), 1455 (δCH_3 asymm.), 1047 (CH_3 rocking) and 372 cm^{-1} ($\delta\overset{+}{N}C_4$) are probably the Raman active e-class fundamentals. The remaining frequencies at 2967 and 2828 cm^{-1} are presumably overtone or combination frequencies involving δCH_3 fundamentals (the former of symmetry A_1) and the 1173 cm^{-1} band might correspond to the combination 752 + 455 brought up somewhat in intensity by Fermi resonance with the nearby f_2-class fundamental. Alternatively this might correspond to the e-class CH_3 rocking frequency, in which case the 1047 cm^{-1} frequency could be the formally forbidden f_1-CH_3 rocking mode.

Discussion

As might be anticipated there are a number of similarities between the fundamental frequencies of these ions and those of the analogous isoelectronic hydrocarbons propane, *iso*butane and *neo*pentane. In Table 5 the analogous frequencies of $\overset{+}{N}H_3$ and CH_3, $\overset{+}{N}H_2$ and CH_2, and $\overset{+}{N}H$ and CH groups are collected together, with some of the skeletal frequencies of the ions and hydrocarbons.

Table 5. A comparison of frequencies (cm^{-1}) of the methylammonium ions and the analogous isoelectronic hydrocarbons

$CH_3\overset{+}{N}H_3$ [2]		CH_3CH_3* [13]	
$\nu\overset{+}{N}H_3$ asymm.	~3080	νCH_3 asymm.	2965
$\nu\overset{+}{N}H_3$ symm.	2980	νCH_3 symm.	2915
$\delta\overset{+}{N}H_3$ asymm.	1580	δCH_3 asymm.	1466
$\delta\overset{+}{N}H_3$ symm.	1538	δCH_3 symm.	~1390
$\overset{+}{N}H_3$ rock.†	1265	CH_3 rock.	1006
$\nu C—\overset{+}{N}$	1003	$\nu C—C$	993
$(CH_3)_2\overset{+}{N}H_2$		$(CH_3)_2CH_2$ [4]	
$\nu\overset{+}{N}H_2$ asymm.	~2965	νCH_2 asymm.	~2930
$\nu\overset{+}{N}H_2$ symm.	2745	νCH_2 symm.	~2850
$\overset{+}{N}H_2$ scissors	1582	CH_2 scissors	1460
$\overset{+}{N}H_2$ wag.	1421	CH_2 wag.	1336
$\overset{+}{N}H_2$ rock.	878	CH_2 rock.	748
$\nu\overset{+}{C}N$ symm.	895‡	$\nu C—C$ symm.	870
$\delta\overset{+}{N}C_2$	412‡	δC_3	372
$(CH_3)_3\overset{+}{N}H$		$(CH_3)_3CH$ [14]	
$\nu\overset{+}{N}H$	2725	νCH	2880
$\delta\overset{+}{N}H$	1418	δCH	1330
$\nu\overset{+}{C}N$ symm.	821‡	$\nu C—C$ symm.	799
$\delta\overset{+}{N}C_3$	468‡ 406‡	δC_4	433 367
$(CH_3)_4\overset{+}{N}$		$(CH_3)_4C$ [12]	
$\nu\overset{+}{C}N$ symm.	752‡	$\nu C—C$ symm.	733
$\delta\overset{+}{C}N$	455‡ 372‡	δCC	418 335

* These are mean values of the pairs of coupled frequencies of ethane of symmetries a_{1g} and a_{2u}, and e_g and e_u respectively.

† This value may be somewhat high due to coupling of $\overset{+}{N}H_3$ and CH_3 rocking vibrations.

‡ Raman data [3].

VOL. 13 1958/5

The hydrocarbon data for ethane, isobutane and neopentane are taken from the work of HANSEN and DENNISON [13], EVANS and BERNSTEIN [14] and SHIMIZU and MURATA [12] respectively.

It can be seen from the Table that all the $\overset{+}{N}H$ angle deformation frequencies are greater than their δCH counterparts, and that the pattern of such frequencies is closely similar for the two classes of compound. The $C\overset{+}{N}$ skeletal stretching vibrations also have consistently higher values than the C—C vibrations. The behaviour of the $\overset{+}{N}H$ and CH bond stretching frequencies is less regular: thus the $\nu\overset{+}{N}H$ vibrations of the $\overset{+}{N}H_3$ and $\overset{+}{N}H$ groups are respectively higher and lower in frequency than the analogous νCH vibrations. However, these latter variations are most probably caused by hydrogen-bonding, as is suggested by the considerable breadth of the $\nu\overset{+}{N}H$ band [6]. In connexion with other work it was observed that the $\nu\overset{+}{N}H$ frequency of a salt of a complex tertiary amine varied in value from $\sim$2600 cm^{-1} to $\sim$2800 to $\sim$3100 cm^{-1} as the anion, A^-, to which the $\overset{+}{N}H$ group was hydrogen-bonded changed from Cl^- to Br^- to ClO_4^- [15]. This is obviously caused by hydrogen-bonding effects; somewhat similar results have been reported previously by NAKANISHI *et al.* [9]. The fact that the $\nu\overset{+}{N}H$ frequency of a given cation can vary so widely in value is of some importance in structural diagnosis work. It seems likely that under conditions of weak hydrogen-bonding most stretching frequencies of $\overset{+}{N}H_3$, $\overset{+}{N}H_2$ and $\overset{+}{N}H$ groups would lie in the region 3100–3000 cm^{-1}. The particularly marked lowering of the frequency of the lone $\overset{+}{N}H$ group is probably caused by the absence of other such bonds to share in hydrogen-bonding with the anion.

After allowance is made for these hydrogen-bonding anomalies, it is seen that the general effect of the extra positive charge on the nucleus of the nitrogen atom is to cause a tightening of the $\overset{+}{N}H$ and $C\overset{+}{N}$ bonds as compared with analogous CH and CC groups.

Acknowledgements—One of us (E. A. V. E.) is indebted to the Department of Scientific and Industrial Research for a maintenance grant and to King's College, Cambridge, for a Harold Fry Studentship. We wish to thank the Hydrocarbon Research Group of the Institute of Petroleum for financial assistance in the purchase of materials.

References

[1] BELLANATO J. and BARCELÓ J. R. *An. Fis. Quim.* B 1956 **52** 469.
[2] WALDRON R. D. *J. Chem. Phys.* 1953 **21** 734.
[3] EDSALL J. T., *J. Chem. Phys.* 1936 **4** 1; 1937 **5** 225.
[4] SHEPPARD N. and SIMPSON D. M. *Quart. Rev., Chem. Soc., Lond.* 1953 **7** 19.
[5] WITKOP B., PATRICK J. B. and KISSMAN H. M., *Chem. Ber.* 1952 **85** 949.
[6] LORD R. C. and MERRIFIELD R. E. *J. Chem. Phys.* 1953 **21** 166.
[7] WITKOP B., *Experientia* 1954 **10** 420.
[8] HEACOCK R. A. and MARION L., *Canad. J. Chem.* 1956 **34** 1782.
[9] NAKANISHI K., GOTO T. and OHASHI M., *Bull. Chem. Soc. Japan* 1957 **30** 403.

[10] Stone P. J., Craig J. C. and Thompson H. W., *J. Chem. Soc.* **1958** 52.
[11] Bratož S., Hadži D. and Sheppard N., *Spectrochim. Acta* **1956** **8** 249.
[12] Shimizu K. and Murata H., *Bull. Chem. Soc. Japan* **1957** **30** 487.
[13] Hansen G. E. and Dennison D. M., *J. Chem. Phys.* **1952** **20** 313.
[14] Evans J. C. and Bernstein H. J., *Canad. J. Chem.* **1956** **34** 1037.
[15] Hinton I. C., Mann F. G. and Sheppard N. Unpublished work.

VOL.
13
1958/5

Spectrochimica Acta, 1959, Vol. 13, pp. 271 to 279. Pergamon Press Ltd. Printed in Northern Ireland

Ein thyratrongesteuertes Schaltgerät für Wechselstromabreissbögen

K. Laqua* und U. Luoto†
National Physical Research Laboratory, Council for Scientific and Industrial Research, Pretoria

(*Received* 7 *April* 1958)

Abstract—A thyratron regulated device is described for attachment to an arc or spark service, which provides convenient control and stability, and which also allows variation of the operating conditions.

I. Einleitung

Es soll im folgenden ein Wechselstromabreissbogen-Zusatzgerät mit elektronischer Schaltung der Brenn- und Pausenzeiten beschrieben werden. Zur Erzeugung der Zündimpulse wird ein im Laboratorium vorhandener gesteuerter Funkenerzeuger verwandt, die Einspeisung der Zündimpulse in den Bogenstromkreis geschieht in herkömmlicher Weise über einen Teslatransformator.

Das Kernstück des Gerätes ist ein einpoliger elektronischer Schalter, der den Primärstromkreis des Funkenerzeugers periodisch unterbricht und damit die Zündfolge und den Brennrhythmus des Abreissbogens bestimmt. Durch den Einbau dieses Schalters können ältere Wechselstromabreissbogengeräte mit mechanischer Steuerung, wie sie zuerst von Pfeilsticker [1] angegeben worden sind, wesentlich verbessert werden.

Bardócz [3] hat die Vorteile der elektronischen gegenüber einer mechanischen Steuerung der Schaltzeiten eingehend erörtert. Das von uns gebaute und seit mehreren Jahren in Betrieb befindliche Gerät unterscheidet sich von den beiden von Bardócz unlängst beschriebenen Geräten [2, 3] in wesentlichen Punkten. Da der gesamte Aufwand so niedrig wie möglich gehalten werden sollte, lag es nahe, nur ein Zusatzgerät zu bauen und im übrigen von bereits vorhandenen Einrichtungen Gebrauch zu machen. Durch Verwendung von Gasentladungsröhren konnte der die Schaltvorgänge steuernde Impulsgenerator recht einfach und störunanfällig gestaltet werden. Dieser Impulsgenerator ist, wie nach Erscheinen der Bardócz' schen Arbeiten festgestellt wurde, übrigens auch zur Steuerung von elektronischen Zündimpulserzeugern geeignet.

Das hier gebaute Gerät entspricht, ebenso wie die zweite Anlage von Bardócz, folgenden Bedingungen:

(1) Die Schaltzeiten: Brenn- und Pausenzeit sind mit der Netzfrequenz synchronisiert, damit stets ganzzahlige Vielfache einer Wechselspannungsperiode.

(2) Auch die den Bogen in jeder Halbwelle zündenden Hochspannungsimpulse sind synchron mit der Netzfrequenz, die Zündung erfolgt also stets in der gleichen Phase der den Bogen treibenden Wechselspannung. Die Phasenlage der Zündung kann in weiten Grenzen verändert und damit die Brenndauer des Bogens pro Halbwelle eingestellt werden.

* jetzt: Institut für spektrochemie und angewandte spektroskopie, Dortmund-Aplerbeck, Deutschland.
† jetzt: EKONO, Association for Power and Fuel Economy, Helsinki, Finland.

(3) Die beiden Schaltparameter Brenndauer und Pause können kontinuierlich und unabhängig voneinander eingestellt werden. Das Gerät schaltet innerhalb des von uns erprobten Bereiches absolut genau. Die Schaltzeiten sind aus wenigen elektrischen Parametern leicht errechenbar. Die Schaltbereiche lassen sich leicht erweitern.

(4) Wirkungsweise und Eichung des Gerätes werden durch etwa erforderlichen Röhrenwechsel kaum beeinträchtigt.

(5) Es können mit dem Gerät auch pulsierende Gleichstromabreissbögen, wie sie etwa zur Analyse von Ölrückständen empfohlen werden, hergestellt werden.

II. Konstruktionsprinzipien

Abb. 1 zeigt die Prinzipschaltbilder zweier hier erprobter Anlangen, die sich

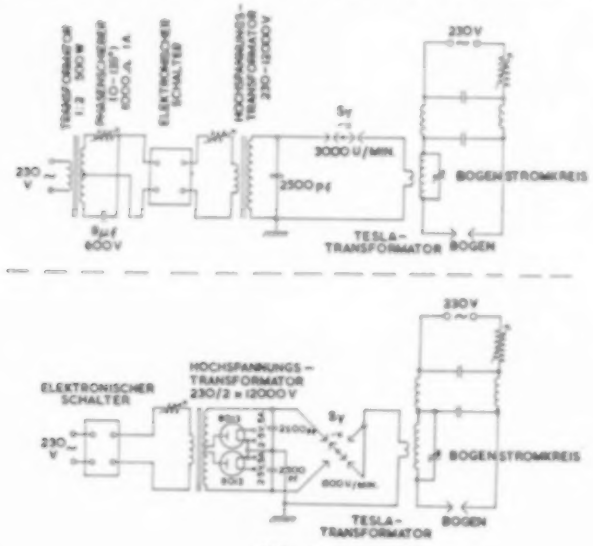

Abb. 1.

hauptsächlich in der Art der Phasenjustierung unterscheiden. Oben ist ein Phasenschieber auf der Primärseite eines Feussnerschen Funkenerzeugers eingebaut, der zusammen mit einer Verdrehung der festen Elektroden des rotierenden Synchronschalters Sy eine Verschiebung der Zündimpulse gegenüber der Bogenwechselspannung erlaubt. Unten wird ein selbstgebauter Funkenerzeuger der High Precision Source Type (Applied Research Laboratories) verwandt, bei dem die Phasenschiebung lediglich durch Verdrehen der feststehenden Elektroden des rotierenden Synchronschalters vorgenommen wird.

Abb. 2 zeigt das Prinzipschaltbild des elektronischen Schalters. Es wurde eine von H. L. Palmer und anderen in einer Serie von Artikeln über elektronisch gesteuerte Schweissgeräte angegebene Schaltung benutzt [4] und zweckentsprechend umgeändert.

Der dick ausgezogene Teil ist der eigentliche Schalter, im Prinzip ein durch die beiden Thyratrons V_1 und V_2 gebildeter Einpolschalter. Nur V_1 wird durch den

VOL. 13 1958/5

darunter gezeichneten Schaltmechanismus gesteuert. V_2 folgt jeweils V_1 nach, d.h. lässt V_1 eine Halbwelle durch, dann lässt auch V_2 die nachfolgende Halbwelle entgengesetzter Polarität durch. Dies wird auf folgende Weise bewirkt: Solange V_1 nicht leitet, liegt über dem Transformator T_2 eine gegenphasige Wechselspannung so am Gitter von V_2, dass das Gitter immer dann negativ wird, sobald die Anode positiv ist. V_2 kann also nicht zünden. Leitet dagegen V_1, dann liegt die

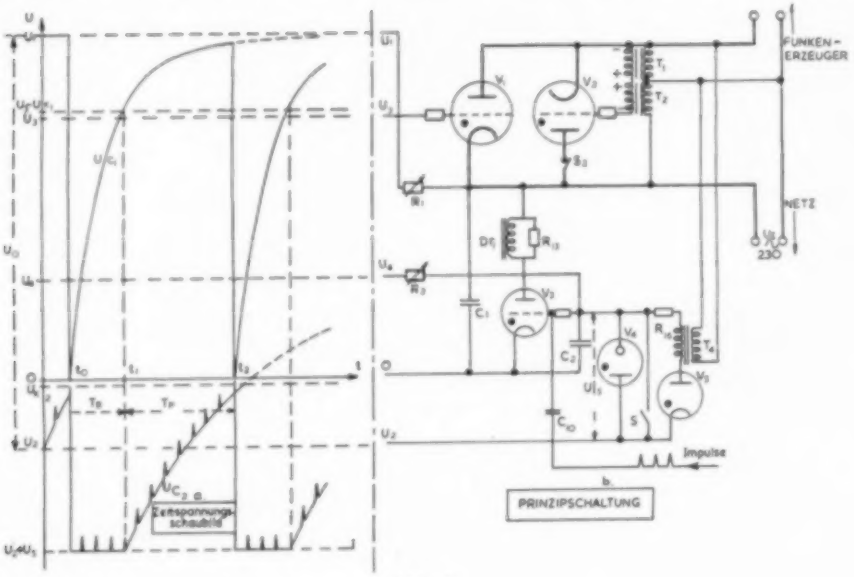

Abb. 2.

volle Netzspannung über der Primärseite des Transformators T_1, dessen Sekundärseite so geschaltet ist, dass hierdurch eine gleichphasige Spannung von grösserem Absolutbetrag als die gegenphasige Spannung an das Gitter von V_2 gelegt wird. Da diese Spannungen durch die Induktivitäten von T_1 bzw. T_2 genügend in der Phase verzögert sind, kann V_2 zünden.

Die Steuerung von V_1 wird hauptsächlich durch die beiden Zeitkreise R_1C_1 und R_2C_2 im Anoden-bzw. Steuergitterkreis des Thyratrons V_3 bewirkt. Sie bestimmen die Zeiten, in denen V_1 und damit V_2 leiten können oder nicht und damit die Brenn- und Pausenzeiten des Abreissbogens. Die Steuerung arbeitet folgendermassen:

(a) *Anlaufzeit.* Die Gleichspannung U_0, aufgeteilt in die Spannungen U_1 bis U_4 sei angelegt, der Hauptschalter S in der Stellung "Aus", d.h. kurzgeschlossen. Dann ist der Kondensator C_1 auf die Spannung U_1 aufgeladen und die Kathode von V_1 positiv gegenüber dem Steuergitter. V_1 kann nicht leiten. Der Kondensator C_2 und damit das Steuergitter von V_3 ist über den kurzgeschlossenen Schalter S mit der negativen Spannung U_2 verbunden. V_3 kann also auch nicht leiten und etwa C_1 entladen. Dieser Zustand ist im Zeit-Spannungsschaubild auf der linken Seite von Abb. 2 zur Zeit $t = 0$ aufgetragen. U_{C_1} bzw. U_{C_2} geben den jeweiligen

Ladezustand der beiden Kondensatoren an. Die der Spannung U_{C_2} überlagerten Impulse sollen zunächst vernachlässigt werden.

Nun wird, um die Schaltvorgänge einzuleiten, der Hauptschalter S auf "Ein" geschaltet, d.h. geöffnet. Damit wird C_2 und natürlich auch das Gitter von V_3 von dem negativen Potential U_2 abgeschaltet. Mit der nun folgenden Aufladung des Kondensators C_2 über den Ladewiderstand R_2 steigt auch das Gitterpotential von V_3 bis die kritische Gitterspannung U_{k_2}, bei der V_3 zünden kann, erreicht ist. V_3 zündet und entlädt über die mit R_{13} bedämpfte Drossel Dr_1 in sehr kurzer Zeit den Kondensator C_1. Damit sinkt aber gleichzeitig das Kathodenpotential von V_1, V_1 feuert in der nächsten über V_1 liegenden positiven Halbwelle der zu schaltenden Wechselspannung U_1. Dieser Zustand ist im Diagram der Abb. 2 zur Zeit $t = t_0$ angegeben.

V_2 folgt in der schon beschriebenen Weise V_1 nach. Der aus V_1 und V_2 gebildete elektronische Schalter ist bis auf weiteres geschlossen, der Bogen brennt.

(b) *Brennzeit.* Wichtig für die weiteren Vorgänge ist, dass V_3 unmittelbar nach dem Entladen von C_2 löscht. Dies geschieht mit Hilfe der Drossel Dr_1. Beim Entladen von C_1 wird durch die Trägheit von Dr_1 der Spannungsnullpunkt kurzzeitig unterschritten, V_3 damit sicher gelöscht.

Sobald nun V_1 und V_2 leiten, liegt die volle Netzspannung U_1 über der Primärseite des Transformators T_4 und erzeugt eine durch die Gasgleichrichterröhre V_5 gleichgerichtete und durch die Glimmstabilisatorröhre V_4 stabilisierte Spannung U_5, so dass der Kondensator C_2 und damit das Gitter von V_3 sehr schnell auf das negative Potential $U_2 + U_5$ gebracht und dort gehalten wird. V_3 kann somit vorläufig nicht wieder zünden. (Zu beachten ist, dass V_4 gleichzeitig als Gleichrichter und als Schalter benutzt wird, also eine Gasentladungsröhre mit einer Zündspannung grösser als $U_4 - U_2$ sein muss, sodass sie nur über T_4 gezündet werden kann.) Nach dem Löschen von V_3 hat die Wiederaufladung von C_1 über den Ladewiderstand R_1 begonnen. Während also V_1 und V_2 leiten, steigt die Kathodenspannung von V_1 an, bis die kritische Gitterspannung U_{k1} von V_1 erreicht ist. Das ist bei $U_{C_1} = U_3 - U_{k_1}$ der Fall. V_1 kann dann nach dem nächsten Nulldurchgang der Wechselspannung nicht wieder zünden, auch V_2 anschliessend nicht mehr leiten, der elektronische Schalter ist wieder offen. Dieser Zustand ist zur Zeit $t = t_1$ erreicht.

(c) *Pausenzeit.* Mit dem Erlöschen von V_1 und V_2 wird auch die Wechselspannung U_1 vom Transformator T_4 abgeschaltet, V_4 und V_5 löschen und schalten damit den Kondensator C_2 von dem negativen Potential $U_2 + U_5$ ab. Die Wiederaufladung von C_2 über R_2 bis zur kritischen Gitterspannung U_{k_2} von V_3 bestimmt die Pausenlänge. Beim Erreichen dieser Spannung zündet V_3, C_1 wird entladen und damit V_1 ebenfalls gezündet, die nächste Brennphase beginnt. Dieser Zustand ist im Zeit-Spannungsdiagramm zur Zeit $t = t_2$ erreicht.

(d) *Abschalten.* Die unter (b) und (c) beschriebenen Vorgänge wiederholen sich, bis der Schalter S auf "Aus" geschaltet, d.h. kurzgeschlossen wird. Damit wird das Gitter von V_3 wieder an die negative Spannung U_2 gelegt. Geschieht dies während einer Pause, dann kann V_3 nicht wieder zünden, der elektronische Schalter ist endgültig offen. Geschieht dies während der Brennzeit, dann öffnet. der elektronische Schalter nach Ablauf dieser Brennperiode endültig.

VOL. 13 1958/5

Aus dem Diagramm der Abb. 2 können leicht die quantitativen Beziehungen für die Brennzeit T_B und die Pausenzeit T_P abgeleitet werden:

Brennzeit:

Eine Brennperiode starte zur Zeit $t = t_0$. Dann gilt

$$(U_{C_1})_{t_0} = 0$$

und

$$(U_{C_1})_{t\infty} = U_1$$

also kann die Spannung über dem Kondensator C_1 zur Zeit t angegeben werden durch:

$$U_{C_1} = U_1 \left\{1 - \exp\left(-\frac{t - t_0}{R_1 C_1}\right)\right\}$$

Die Brennzeit ist nach der Zeit T_B beendet. Hierfür gilt:

$$(U_{C_1})_{t_0 + T_B} = U_3 - U_{k_1} = U_1 \left\{1 - \exp\left(-\frac{T_B}{R_1 C_1}\right)\right\}$$

Hieraus folgt:

$$T_B = R_1 C_1 \quad \ln \quad \frac{U_1}{U_1 - U_3 + U_{k_1}} \tag{1a}$$

Pausenzeit:

Eine Pausenperiode starte zur Zeit $t = t_1$. Dann gilt

$$(U_{C_2})_{t_1} = U_2 + U_5$$

ausserdem

$$(U_{C_2})_{t\infty} = U_4$$

Der Ladevorgang von C_2 kann somit beschrieben werden durch

$$U_{C_2} = (U_4 - U_2 + U_5)\left\{1 - \exp\left(-\frac{t - t_1}{R_2 C_2}\right)\right\} + (U_2 + U_5)$$

Die Pause ist nach der Zeit $t = T_P$ beendet, nämlich dann, wenn

$$(U_{C_2})_{t_1 + T_P} = U_{k_2} = (U_4 - U_2 + U_5)\left\{1 - \exp\left(-\frac{T_P}{R_2 C_2}\right)\right\} + (U_2 + U_5)$$

Hieraus folgt:

$$T_P = R_2 C_2 \left(\ln \frac{U_4 - U_2 + U_5}{U_4 - U_{k_2}}\right) \tag{2a}$$

Um der in der Einleitung genannten Bedingung, dass die Schaltzeiten ganzzahlige Vielfache einer Wechselspannungsperiode sein sollen, zu genügen, werden der Kondensatorspannung U_{C_2} Impulse der Höhe U_P und der Frequenz 50 Hz überlagert. Damit wird erreicht ,dass stets ein derartiger Impuls die Röhre V_3 zündet. Durch richtige Einstellung der Phase dieser Impulse kann erreicht werden, dass die Brennzeit stets mit einer vollen Halbperiode der über V_1 liegenden Wechselspannung beginnt. V_3 zündet dann also, sobald:

$$(U_{C_2})_{t_1 + T_P} + U_P = U_{k_2}$$

Hieraus folgt für die Pausendauer

$$T_P = R_2 C_2 \left(\ln \frac{U_4 - U_2 + U_5}{U_4 - U_{k_2} - U_P} \right) \tag{2b}$$

Wie man aus den Formeln (1a) und (2b) für Brenn- und Pausendauer entnehmen kann, sind diese beiden Parameter unabhängig voneinander.

Schaltet man V_2 aus durch Öffnen des Schalters S_2, dann werden durch den elektronischen Schalter nur Halbwellen einer Polarität durchgelassen, man kann so leicht einen pulsierenden Gleichstromabreissbogen herstellen.

III. Praktische Ausführung des Gerätes

Die Abbildung 3 zeigt das vollständige Schaltbild des elektronischen Schalters. Die Spannungen U_1 bis U_4 werden einem von einem üblichen Netzteil gespeisten

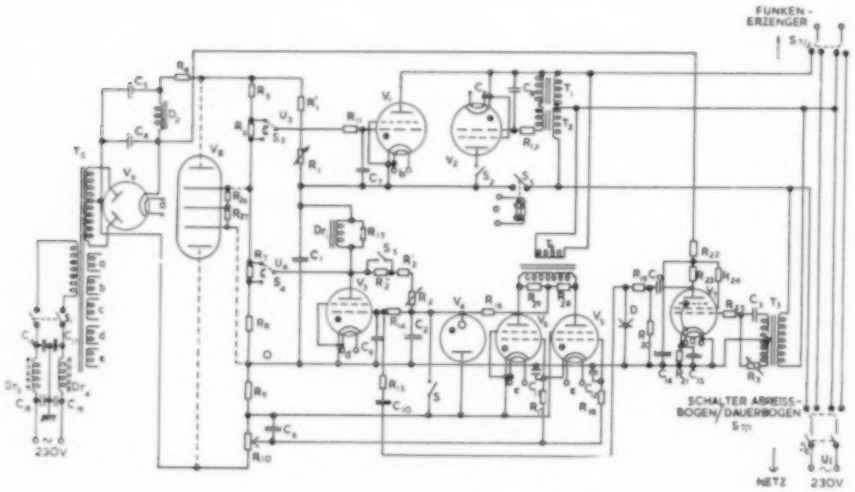

Abb. 3.

R_1 Pot. 200 kΩ, 20 W, Draht.
R_1' 18 kΩ, 5 W, Draht
R_2 Pot. 200 kΩ, 20 W, Draht
R_2' 23 kΩ, 5 W, Draht
R_2'' 200 kΩ, 1 W, Draht
R_3 Pot. 200 kΩ
R_4 1,5 kΩ, 10 W, Draht
R_5 500Ω, 5 W, Draht
R_6 1 kΩ, 5 W, Draht
R_7 2 kΩ, 10 W, Draht
R_8 800 Ω, 5 W, Draht
R_9 1,2 kΩ, 5 W, Draht
R_{10} Pot. 200 Ω, 1 W, Draht

$R_{11,12,17,18}$ 500 kΩ
R_{13} 100 Ω, 1 W
R_{15} 10 kΩ
R_{16} 4 kΩ, 10 W, Draht
$R_{19,28,29}$ 25 kΩ, 3 W
$R_{20,22,25,26,27}$ 200 kΩ
R_{21} 10 kΩ
R_{23} 30 kΩ
R_{24} 1 MΩ

$V_{1,2}$ Thyratron 3 D 22
$V_{3,5,6}$ Thyratron 2 D 21
V_4 Stabilisatorröhre 0 D 3
V_7 6 A G 5
V_8 Stabilovolt 280/40
V_9 6 x 4
D Germaniumdiode 1 N 34

C_1 1 μF, Papier
C_2 2 μF, Papier
C_3 0,1 μF, Papier
$C_{4,5,14}$ 16 μF, 450 V, Elektrolyt
$C_{6,15}$ 50 μF, 25 V, Elektrolyt
$C_{7,8,9,11,12}$ 50 pF, keramisch
$C_{10,13}$ 1000 pF
$C_{16,17,18,19}$ 0,05 μF

Dr_1 Drossel 100 mH, 10 Ω
Dr_2 Drossel 5 H, 100 mA
$Dr_{3,4}$ Drossel 1 mH, 500 mA

T_1 Transformator 230/8 V (Klingeltransformator)
T_2 Transformator 230/5 V (Klingeltransformator)
T_3 Transformator 230/6,3—0—6,3 V, 50 mA
T_4 230/265—0—265 V, 60 mA
T_5 230 V/
375—0—375 V, 60 mA
6,3 V, 1 A
2 × 6,3 V, 2 A
2 × 6,3 V, 3 A

$S_{1,6}$ Netzschalter, 2—polig
S_2, S_3 Netzschalter, 1—polig
$S_{3,4}$ Schalter 1 Arm, 2 Stellungen
S_5 Schalter 4 Arme, 2 Stellungen
S_7 Thermorelais, 60 Sek. Verzögerung

Spannungsteiler R_5 bis R_{10} entnommen, der verhältnismässig niederohmig ausgelegt ist, um die Spannungen unabhängig von den stossweisen Belastungen zu halten. Bei stark schwankender Netzspannung kann es zweckmässig sein, diese Spannungen zu stabilisieren. Die Verwendung eines Glimmstreckenstabilisators für diesen Zweck ist angedeutet.

Die Brennzeit wird durch den Ladewiderstand R_1 und die Spannung U_3, die Pausenzeit durch den Ladewiderstand R_2, den ausschaltbaren Vorwiderstand R_2 und die Spannung U_4 eingestellt. Natürlich könnten auch C_1 und C_2 veränderlich gemacht werden.

Die Gewinnung von U_5 durch Doppelweggleichrichtung verbesserte die Stabilität des Gerätes bei kurzen Schaltzeiten erheblich. Nach anfänglichen Versuchen mit gasgefüllten Kaltkathodentrioden wurden schliesslich für V_5 und V_6 Thyratrons gewählt. Sie sind zuverlässiger (keine Gefahr von Rückzündungen!) und ihre Zündspannung lässt sich in weiten Grenzen durch Verändern der Gittervorspannung einstellen. Die günstigste Grösse dieser Vorspannung muss durch Versuche ermittelt werden. Einerseits sollen V_5 und V_6 auch bei sehr kurzen Brennzeiten (bis zu einer Periode!) sicher zünden und C_2 auf das Potential $U_2 + U_5$ umladen, andererseits dürfen sie nicht vorzeitig durch die über ihnen liegende positive Spannung U_{C_2}–U_2 gezündet werden. In unserem Gerät wurde eine durch R_{10} eingestellte Gittervorspannung $U_g = -1{,}6$ V als günstig gefunden.

Die bereits erwähnten 50 Hz Impulse werden aus der Netzspannung U_1 gewonnen. Nach Passieren des aus T_3, R_3, C_3 gebildeten Phasenschiebers wird die ursprünglich sinusförmige Spannung durch die mit stark negativer Gittervorspannung arbeitende Röhre V_7 verstärkt und begrenzt. Durch Differentiation (C_{13}, R_{20}) entstehen dann Impulse. Die Diode D sperrt für die negativen Impulse, sodass nur die positiven durchgelassen und über den Kondensator C_{10} eingekoppelt werden.

IV. Ergebnisse

Mit den gemessenen Werten:

$U_1 = 197$ V $U_g = -1{,}6$ V
$U_2 = -60$ V $U_{k_1} = -3{,}5$ V
$U_3 = 124$ bis 173 V $U_{k_2} = -2{,}2$ V
$U_4 = 36$ bis 124 V $U_p = 10{,}7$ V
$U_5 = -150$ V

sollte sich theoretisch ein Einstellbereich der Brennzeit von 1 Periode ($2 \cdot 10^{-2}$ Sek) bis 20 Perioden ($5 \cdot 10^{-1}$ Sek) und der Pause von 2 Perioden ($4 \cdot 10^{-2}$ Sek) bis 75 Perioden (1,5 Sek) ergeben. In der Tabelle 1 sind berechnete und gemessene Schaltzeiten vergleichsweise aufgeführt. Es konnte nicht eindeutig geklärt werden, wodurch die Abweichungen der gemessenen von den berechneten Schaltzeiten hervorgerufen werden. Ursachen, wie endliche Entladezeiten der Kondensatoren C_1 und C_2, Schwingungen der Drossel Dr_1 und eingestreute Brummspannungen kommen in Frage. Durch Zufügung von Korrekturspannungen $U_{z_1} = 10$ V bzw. $U_{z_2} = 7$ V in den Formeln (1a) und (2b) kann eine bessere Übereinstimmung der

Tabelle 1. Vergleich von gemessenen (M) und berechneten (R) Brennzeiten T_B und Pausenzeiten T_P (Werte mit' sind nach den korrigierten Formeln (1b) bzw. (2c) berechnet)

Nr.	U_3 (V)	R_1 (kΩ)	T_{B_M} (Perioden)	T_{B_R} (Perioden)	T'_{B_R} (Perioden)	U_4 (V)	R_2 (kΩ)	R'_2 (kΩ)	T_{P_M} (Perioden)	T_{P_R} (Perioden)	T'_{P_R} (Perioden)
1	124	0	1	1	1	124	0	0	3	2	2
2	124	0	1	1	1	36	0	0	5	4	4
3	124	0	1	1	1	124	200	0	22	20	21
4	124	0	1	1	1	36	200	0	40	36	40
5	124	0	1	1	1	36	200	200	74	68	75
6	173	0	2	2	2	124	0	0	3	2	2
7	173	0	2	2	2	36	0	0	5	4	4
8	173	0	2	2	2	124	200	0	23	20	21
9	173	0	2	2	2	36	200	0	40	36	40
10	173	0	2	2	2	36	200	200	75	68	75
11	124	200	9	11	10	124	0	0	3	2	2
12	124	200	9	11	10	36	0	0	5	4	4
13	124	200	9	11	10	124	200	0	23	20	21
14	124	200	9	11	10	36	200	0	41	36	40
15	124	200	9	11	10	36	200	200	77	68	75
16	173	200	20	25	20	124	0	0	3	2	2
17	173	200	20	25	20	36	0	0	5	4	4
18	173	200	20	25	20	124	200	0	23	20	21
19	173	200	20	25	20	36	200	0	42	36	40
20	173	200	20	25	20	36	200	200	78	68	75

Rechnung mit den Messungen erreicht werden. Die endgültigen Formeln lauten dann:

$$T_B = R_1 C_1 \left(\ln \frac{U_1}{U_1 - U_3 + U_{k_1} + U_{z_1}} \right) \tag{1b}$$

$$T_P = R_2 C_2 \left(\ln \frac{U_4}{U_4 - U_{k_2} + U_{z_2}} \right) \tag{2c}$$

Die hiernach berechneten Werte sind in der Tabelle mit einem Strich versehen.

Die gegenseitige Beeinflussung von Brenn- und Pausenzeiten ist gering. Wie man aus der Tabelle ersieht, wachsen mit längeren Brennzeiten auch die Pausenzeiten etwas an. Wahrscheinlich ist der Spannungsteiler hierfür verantwortlich.

Aus den Formeln (1b) und 2c) ist ersichtlich, in wie geringem Masse die Röhrendaten U_{k_1} und U_{k_2} (sie gehen als einzige in die Formeln ein) die Schaltzeiten bestimmen. Alterungserscheinungen und Röhrenwechsel haben praktisch keinen Einfluss auf die Eichung des Gerätes.

V. Anhang: Verwendung des Gerätes als Steuerteil eines rein elektronischen Abreissbogengerätes

Wie bereits in der Einleitung angedeutet, kann der oben beschriebene elektronische Schalter leicht zur Steuerung der Bardócz schen Geräte benutzt werden.

VOL. 13 1958/59

Abb. 4 zeigt die Schaltung einer solchen Anlage. Die Phase muss vor dem Eingang des elektronischen Schalters geregelt werden. Die am Ausgang erhältliche unterbrochene Sinusspannung wird durch einen leicht selbst herstellbaren Impulstransformator verformt. Je nach Art der Gleichrichtung sind dann die in Abb. 4 rechts

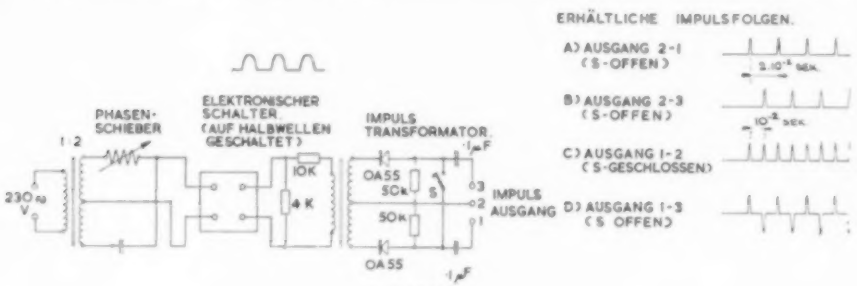

Abb. 4.

gezeichneten Impulsfolgen erhältlich. Der elektronische Schalter selbst muss dabei auf Halbwellen geschaltet sein. Das Thyratron V_2 wird dann überhaupt nicht gebraucht und für V_1 kann eine wesentlich kleinere Type, etwa die 2D21, genommen werden.

VI. Zusammenfassung

Es wird ein thyratrongesteuertes Schaltgerät beschrieben, das als Zusatz zu einem gesteuerten Funkenerzeugen oder zu einem elektronischen Zündimpulserzeuger nach Bardócz die Herstellung von Wechselstrom–Abreissbögen gestattet. Brenndauer und Pause, die Hauptparameter eines Abreissbogens neben der Stromstärke, können in weiten Grenzen kontinuierlich und unabhängig voneinander verändert werden. Sie können aus den elektrischen Grössen des Gerätes leicht angenähert berechnet werden. Das Gerät ist voll mit der Netzfrequenz synchronisiert, zeichnet sich durch hohe Konstanz der Schaltzeiten aus, unterliegt keiner mechanischen Abnutzung und kann leicht mit mässigem Aufwand selbst gebaut werden.

Anerkennung—Die Veröffentlichung erfolgt mit Genehmigung des Council for Scientific and Industrial Research, Pretoria, Union of South Africa.

Literatur

[1] Pfeilsticker K., *Z. Elektrochem.* 1937 **43** 719.
[2] Bardócz Á., *Spectrochim. Acta* 1952 **5** 397.
[3] Bardócz Á., *Spectrochim. Acta* 1956 **8** 152.
[4] Palmer H. L. *et al.*, *Electronics*—August 1942–Januar 1943. Serie von Artikeln: Electronic Resistance Welding Control.

Spectrochimica Acta, 1959, Vol. 13, pp. 280 to 290. Pergamon Press Ltd. Printed in Northern Ireland

The infrared spectra of $N_2H_6Cl_2$ and $N_2H_6F_2$

R. G. SNYDER* and J. C. DECIUS†
*Shell Development Company, Emeryville, California,
†Department of Chemistry, Oregon State College, Corvallis, Oregon

(*Received* 18 *July* 1958)

Abstract—The infrared spectra of hydrazine dihydrochloride and hydrazine dihydrofluoride, together with the spectra of their completely deuterated analogues, have been examined over the region 400–3500 cm^{-1}. In the hydrogen stretching region both salts show great breadth and complexity. Assignments of fundamental vibrations of the $N_2H_6^{2+}$ ion are discussed. For the chloride salt, the internal torsion mode was observed.

ALTHOUGH the Raman spectrum of crystalline $N_2H_6Cl_2$ has been reported [1, 2], no account of the infrared spectrum of the $N_2H_6^{2+}$ ion has, to the authors' knowledge, been published. The high symmetry D_{3d}, which the $N_2H_6^{2+}$ ion exhibits in the crystalline salts, hydrazine dihydrochloride [3], $N_2H_6Cl_2$, and hydrazine dihydrofluoride [4], $N_2H_6F_2$, makes a study of the vibrational spectra of these compounds attractive. Moreover, opportunity is afforded to compare the relative effects of hydrogen bonding upon their spectra and in turn to compare the spectra of the hydrazine salts with that of their close relatives, ammonium chloride and ammonium fluoride. The spectra of these latter salts have been reported [5, 6]. In this paper the infrared spectra of $N_2H_6Cl_2$ and $N_2H_6F_2$, together with $N_2D_6Cl_2$ and $N_2D_6F_2$, will be presented and interpretation pursued as far as the available data permit.

VOL.
13
1958/5

Experimental

Hydrazine dihydrofluoride and hydrazine dihydrochloride were prepared by titration of hydrazine monohydrate with the appropriate hydro-acid using a slight excess of acid. Purification was by recrystallization from an aqueous solution. Deuteration of the salts was readily accomplished by repeated recrystallization from excess D_2O. The slightly hydroscopic property of the salts, particularly of the difluoride made handling under anhydrous conditions necessary to prevent re-exchange with water vapour.

Films of hydrazine dihydrofluoride suitable for spectroscopic examination were obtained by sublimation of the salts onto a transparent window cooled to near liquid nitrogen temperature, using a cell of design similar to that described by WAGNER and HORNIG [5]. Because of the reactivity of this salt it was necessary to line the side arm containing the sample with platinum foil. For the same reason, silver chloride was chosen as the window material. No reaction between the window and the sample occurred even when the window was warmed to room temperature. Sublimation of the salt from the side arm to the cooled window was accelerated by warming the sample to 40–50°C. With liquid nitrogen as a refrigerant for the sample window, slow sublimation resulted in a clear film, in evidence only from interference colours of reflected light. However, a film thus deposited was

not hydrazine dihydrofluoride as shown from the infrared spectrum of the deposit. Rather, it appeared to be a solid solution of hydrogen fluoride and hydrazine, produced as a result of decomposition during sublimation. Warming the window caused the appearance of the deposition to change suddenly from clear to slightly cloudy. The film recooled to liquid nitrogen temperature then gave a spectrum which is that characteristic of $N_2H_6^{2+}$. No further significant changes were observed upon repeating the cycle of warming and recooling. The possibility of orientation of the uniaxial crystals constituting the film was examined using large polaroids. Extinction of the crystallites seemed random indicating no orientation. This is further confirmed by comparing the spectra of the dihydrofluoride and dihydrochloride, the latter of which has cubic symmetry. The relative intensities of the major absorption bands are approximately the same.

The deuterated fluoride salt was prepared by exchange with D_2O directly in the platinum lined side arm of the cell. The cell was attached to a vacuum system arranged so that D_2O could be distilled into the cooled side arm of the cell containing the salt. After warming to room temperature, the exchanged water was pumped off. This procedure was repeated several times to assure nearly complete deuteration.

Hydrazine dihydrochloride does not sublime so that samples were prepared as mulls with Nujol or perfluorokerosene as the mulling agent. A sandwich using sodium chloride salt blanks was formed which could be clamped onto the window holder of the low temperature cell and cooled to liquid nitrogen temperature.

All spectra were recorded by Perkin–Elmer Model 12-C and Beckman IR-4 spectrophotometers using LiF, NaCl and CsBr optics.

Interpretation of the spectra

In both salts, $N_2H_6Cl_2$ and $N_2H_6F_2$, the ion $N_2H_6^{2+}$ has D_{3d} symmetry [3, 4] like ethane with which it is isoelectronic. Numbering of the normal modes will follow that used for ethane [7]. In Table 1 will be found a tabulation of the fundamental vibrations of the $N_2H_6^{2+}$ and $N_2D_6^{2+}$ ions for the chloride and fluoride salts together with the assignments for ethane. These assignments will be discussed below.

Since, fortunately, X-ray crystal structure determinations have been made for both salts [3, 4], predictions based on symmetry can be made about the influence of the crystal environment upon the spectrum of the isolated ion. Some useful information regarding the crystal structure is summarized in Table 2.

A diagram showing the correlation between the factor group, the site and the molecular symmetries for the chloride salt is shown in Fig. 1.

The fact that the fluoride has only one molecule per unit cell and that the cation is in an environment which has the symmetry D_{3d}, makes a correlation of symmetries trivial. Thus, only the five vibrations allowed with infrared activity for the isolated ion $N_2H_6^{2+}$ are permitted in the crystal and all else in the spectrum must arise from combinations.

The chloride salt has a more complex crystal structure with four molecules per unit cell. However, retention of the centre of symmetry permits, in addition to the allowed modes of the isolated ion, only the torsional motion. Factor group splitting,

Table 1. Description and assignment of fundamental vibrations of ethane, $N_2H_6Cl_2$, $N_2D_6Cl_2$, $N_2H_6F_2$ and $N_2D_6F_2$

Species	Designation	Description	Frequencies* (cm^{-1})				
			C_2H_6 [7]	$N_2H_6Cl_2$	$N_2D_6Cl_2$	$N_2H_6F_2$	$N_2D_6F_2$
A_{1g}	ω_1	NH stretching	2915	~2650			
	ω_2	NH_3 deformation	~1400	1524			
	ω_3	NN stretching	993	1027			
E_g	ω_{10}	NH stretching	2955	2745			
	ω_{11}	NH_3 deformation	1460	1599			
	ω_{12}	NH_3 rocking	~1190	1105			
A_{1u}	ω_4	torsion	(290)[12]	455			
A_{2u}	ω_5	NH stretching	2915	2600	1927	~2545	~1925
	ω_6	NH_3 deformation	1379	1485	1125	1567	1184
E_u	ω_7	NH stretching	2995	2739	2060	~2545	~1925
	ω_8	NH_3 deformation	1472	1613	1198	1679	(1243)†
	ω_9	NH_3 rocking	822	1096	798	1182	858

* Frequencies for the hydrazine salts are for −180°C except for the Raman frequencies of $N_2H_6Cl_2$ which are for 23°C. For ethane, gas phase frequencies are given.
† Calculated from the product rule.

which is not expected or realized to be great, occurs for species E_u of the isolated ion. In summary it goes as

$$\begin{array}{ll} S_6 & T_h \\ A_g \rightarrow A_g + F_g & \\ E_g \rightarrow E_g + 2F_g & \\ \boldsymbol{A_u} \rightarrow A_u + \boldsymbol{F_u} & \\ \boldsymbol{E_u} \rightarrow E_u + 2\boldsymbol{F_u} & \end{array}$$

with infrared activity for bold species only.

Table 2. Crystal structure data for $N_2H_6Cl_2$ and $N_2H_6F_2$

	$N_2H_6Cl_2$	$N_2H_6F_2$	Reference
Space group	T_h^6	D_{2d}^5	[3, 4]
Molecules per unit cell	4	1	[3, 4]
Site group	S_6	D_{3d}	[3, 4, 8]
N—N distance (Å)	1·42	1·42	[3, 4]
N—H - - - X distance (Å)	3·10	2·62	[3, 4]
N—H distance (Å)	(1·045)*	1·050	[11]

* Estimated from plot of NH bond length vs. $\langle\omega_s\rangle^{-2/3}$ for NH_4Cl, NH_4F and $N_2H_6F_2$, where $\langle\omega_s\rangle$ is the weight-average stretching frequency [11].

VOL. 13 1958/5

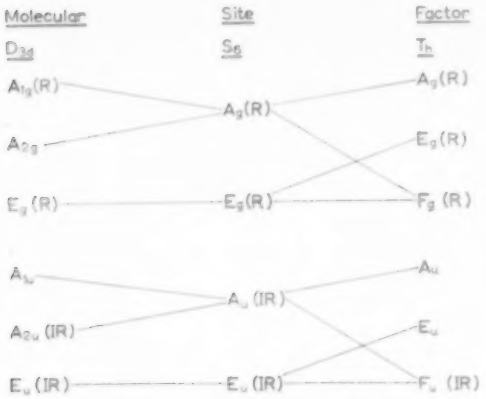

Fig. 1. Correlation of molecular, site and factor group symmetry for crystalline $N_2H_6Cl_2$.

Hydrazine dihydrochloride

The infrared spectrum of hydrazine dihydrochloride at −180°C is shown in Fig. 2 and the frequencies of the absorption maxima are listed in Table 3. The spectrum of the solid at room temperature is essentially the same. In going to the lower temperature, doubling of some of the bands becomes clearer and there is a shift in frequency, usually less than 10 cm^{-1}, towards higher frequencies.

As a guide to the assignment of the five infrared active fundamentals of the $N_2H_6^{2+}$ ion, the assignments for ethane will be used. First, the designation of the strong band at 1098 cm^{-1} to the NH_3 rocking vibration, ω_9, seems obvious by virtue of its intensity and position. It is at 821 cm^{-1} for ethane and at 958 cm^{-1} in methyl ammonium chloride [9]. The doubling of this band is consistent with the predicted factor group splitting.

Assignment of the non-degenerate and degenerate ∠HNH deformation modes presents a problem, namely that in the region 1400–1650 cm^{-1} where these are expected to occur, only one strong band is observed. The assignment of the strong band which occurs at 1485 cm^{-1} to the symmetric deformation, ω_6, is in

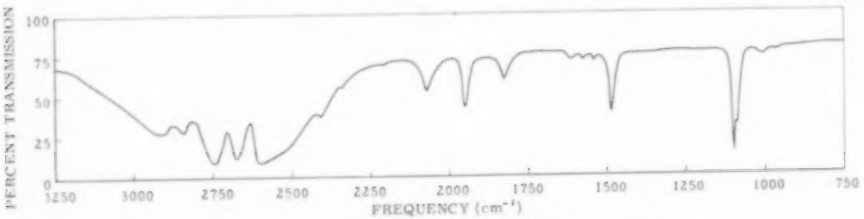

Fig. 2. Infrared spectrum of $N_2H_6Cl_2$ at −180°C.

keeping with the analogous mode in methyl ammonium chloride [9] which has been taken as 1538 cm^{-1}. For the remaining infrared active deformation mode, ω_8, one can either look for a weak band in the expected region, 1500–1650 cm^{-1}, or else assume that for some reason this mode lies at higher frequencies and is associated with some of the strong bands in the region 1800–2000 cm^{-1}.

Table 3. Frequencies and assignments of the infrared spectra* of $N_2H_6Cl_2$, $N_2D_6Cl_2$, $N_2H_6F_2$ and $N_2D_6F_2$

$N_2H_6Cl_2$			$N_2D_6Cl_2$		
ω (cm^{-1})	Relative intensity†	Assignment	ω (cm^{-1})	Relative intensity	Assignment
455‡	w	ω_4	796	s	ω_9'
1019	vw	?	800	m	
1093	s	ω_9	814	vw	
1100	s		826	vw	
1485	m	ω_6	836	m	
1536	w	$\omega_{12} + \omega_4 = 1560$	856	vw	
1570	w		876	vw	
1613	w	ω_8(?)	1019	vw	
1829	m	$\omega_8 + \omega_{L\perp} = 1843$	1123	m	ω_6'
1960	m	$\omega_2 + \omega_4 = 1979$	1128	m	
2084	m	$\omega_3 + \omega_9 = 2123$	1198	vw	ω_8' (?)
2341	w, vb	$\omega_5 - \omega_{L\perp} = 2374$	1410	m	
2404	w		1490	w	
2690	s	ω_5	1754	vw	
2674	s	$\omega_9 + \omega_{11} = 2695$	1849	w	
2739	s	ω_7	1927	m	ω_5' (?)
2841	m	$\omega_5 + \omega_{L\parallel} = 2846$	1946	m	
2908	m	$\omega_7 + \omega_{L\perp} = 2965$	2011	m	
			2060	vs, vb	ω_7' (?)
			2209	m	
			2236	m	
			2282	w	
			2442	w	
			2685	m	$N_2HD_5Cl_2$
			2795	m	

$N_2H_6F_2$			$N_2D_6F_2$		
ω (cm^{-1})	Relative intensity	Assignment	ω (cm^{-1})	Relative intensity	Assignment
1182	s	ω_9	858	s	ω_9'
1567	m	ω_6	912	w	
1679	vw	ω_8 (?)	1184	m	ω_6'
1813	w, vb		1462	vw	
2083	m		1498	w	
2208	m		1530	vw	
2328	m		1617	s, vb	
2427	m		1691	vw	
2545	vs, vb	ω_5, ω_7 (?)	1925	vs, vb	ω_5', ω_7'(?)
2820	w		2003	m, vb	
			2121	s, vb	
			2176	s, vb	
			2282	s	
			2529	m	$N_2HD_5F_2$

* The spectra were recorded with the sample at −180°C.
† s = strong, m = medium, w = weak, b = broad, v = very.
‡ Sample at 23°C.

VOL. 13 1958/5

For reasons stated below, a deformation frequency higher than 1800 cm^{-1} seems quite unreasonable. However, the considerable intensities of the three bands in this region seem rather puzzling if they are not fundamental vibrations. A similar situation exists, however, for both ammonium fluoride [6] and the low temperature forms of methyl ammonium chloride [9]. These salts exhibit strong bands in this region which have had to be assigned to combinations. It appears that in these cases combinations can gain considerable intensities presumably by interaction with the NH stretching modes even though the combinations are well out on the wings of the stretching bands.

Some idea of the expected position and relative intensities of the deformation modes can be obtained from the conclusions drawn from a study of the NH_3 deformation vibrations of solid inorganic complexes [10]. It was found that the symmetric deformation mode occurs in the region 1150–1350 cm^{-1} and is sensitive to the strength of the nitrogen–metal bond, increasing in frequency with increasing bond strength. Thus the assignment of ω_6 is not unreasonable. It was also found that the symmetric mode absorption band was much sharper and much more intense than the degenerate mode. The latter was found to occur in the comparatively narrow region 1560–1650 cm^{-1}. Further evidence that the degenerate mode is to be found within 100 cm^{-1} of 1600 cm^{-1} is that the same mode for methyl ammonium chloride is at 1580 cm^{-1}. Finally, it is to be noted that the Raman active degenerate deformation is found at 1599 cm^{-1} [2]. For these reasons, candidates for assignment to ω_8 will be looked for among the three very weak bands, 1536, 1570 and 1613 cm^{-1}. The latter of these by virtue of its being the strongest and broadest of the three and its best satisfying the product rule when $N_2D_6Cl_2$ is considered, is chosen with considerable reservation as ω_8.

The hydrogen stretching region offers no clear path for assignments since there are more strong bands than the two needed for fundamentals and these are broad and overlapping. As a guide in attempting to select these fundamentals, we use the residual N—H stretching mode in the spectra of the almost completely deuterated salt. Thus, following WALDRON [9] in his interpretation of the spectrum of methyl ammonium chloride, we use for the g-elements of the stretching modes, $\mu_H + \frac{1}{3}\mu_N$ and $\mu_H + \frac{4}{3}\mu_N$ respectively for the nondegenerate and degenerate modes whose frequencies are calculated from a force constant from the uncoupled N—H stretching frequency, whose g-element is $\mu_H + \mu_N$. Then we have:

	Calc. (cm^{-1})	Found (cm^{-1})
Uncoupled N—H stretching	(2685)	2685
Symmetric N—H stretching	2620	2600
Degenerate N—H stretching	2710	2739

Using CsBr optics, a weak and very broad band was observed at 455 cm^{-1}. This is near the expected position of the torsional mode ω_4 which is infrared active in the crystal. For methyl ammonium chloride this vibration has been observed at

487 cm^{-1} [9]. The assignment of this band to ω_4 is supported by the usefulness of this frequency in explaining combination bands in the spectrum.

The Raman spectrum of $N_2H_6Cl_2$ as recorded by COUTURE and MATHIEU [2] is reproduced in Table 4. Assignments are those given by these authors with whom we have no significant disagreement. We designate the librational modes, ω_L, as $\parallel$ or $\perp$ depending on whether the rotation axis is parallel or perpendicular to the

Table 4. Raman spectrum* of $N_2H_6Cl_2$ as observed by COUTURE and MATHIEU [2]

$\Delta\omega$ (cm^{-1})	Relative intensity†	Species‡	Assignment	$\Delta\omega$ (cm^{-1})	Relative intensity	Species	Assignment
67	w	E_g	$\omega_{T\perp}$	2613	md	F_g	ω_1 (?)
82	m	F_g		2660	wd	F_g	
				2690	wd	?	
98	s	$A_g + F_g$	$\omega_{T\parallel}$	2745	sd	F_g	ω_{10}(?)
223	s	F_g	$\omega_{L\perp}$	2872	m	F_g	$\omega_1 + \omega_{L\perp} = 2877$
230	s	E_g					
246	vs	$A_g + F_g$	$\omega_{L\parallel}$	2945	m	F_g	$\omega_{10} + \omega_{L\perp} = 2972$
				2978	w	A_g	$2\omega_6 = 2970$
1027	s	$A_g + F_g$	ω_3	3045	w	A_g	$2\omega_2 = 3048$
1105	w		ω_{12}	3085	w	A_g	$\omega_6 + \omega_8 = 3098$
1524	m	$A_g + F_g$	ω_2	3190	w	?	$\omega_7 + \omega_4 = 3194$
							$2\omega_{11} = 3198$
1599	w	$E_g + F_g$	ω_{11}				
2002	wd	F_g	$\omega_{12} + 2\omega_4 = 2015$				
2025	?		$2\omega_9 = 2054$				
2251	sd	A_g (or E_g) + F_g	$2\omega_{12} = 2210$				

* Spectrum measured for the crystal at 23°C.
† s = strong, m = medium, w = weak, d = diffuse, v = very.
‡ Based on unit cell symmetry T_h.

N—N-axis of the $N_2H_6^{2+}$ ion. Similarly for the translational modes, ω_T, of the chloride ions, the motion is designated as either parallel or perpendicular to the N—N-axis. As in the case of the infrared spectrum, the NH stretching region is rich in lines far beyond what is required for fundamentals and equally difficult to interpret.

With Raman data available, a fairly complete assignment of the vibrational spectrum has been attempted. However, in view of the complexities which can arise from lattice interaction and Fermi resonance, it is felt that many of the interpretations of the combinations and overtones are somewhat speculative.

d_6-*Hydrazine dihydrochloride*

The infrared spectrum of the salt given in Fig. 3 shows by the residual NH stretching absorption band at 2685 cm^{-1} that deuteration was not complete. Some other weak bands in the spectrum, particularly in the region near 900 cm^{-1} must be attributed to hybrid species, mostly $N_2HD_5Cl_2$.

Since all infrared active vibrations of the ion involve primarily hydrogen motion, observed shifts are not useful for identifying normal modes. However, since the ratio ω/ω' will be in the vicinity of 1·35, determining the correspondence between the spectra of $N_2H_6^{2+}$ and $N_2D_6^{2+}$ is facilitated. Thus, bands identified as ω_6' and ω_9' are found at 1125 and 798 cm^{-1} respectively. Doubling of ω_6' is

VOL. 13 1958/5

puzzling since the selection rules permit only a singlet. Possibly this doubling is caused by accidental superposition of two absorption bands, or the band really should be the two components of the degenerate deformation fundamental. More likely the weaker component arises from $N_2HD_5Cl_2$. Again the location of ω_8' is questionable. If its assignment in $N_2H_6Cl_2$ spectrum is correct, it must be identified

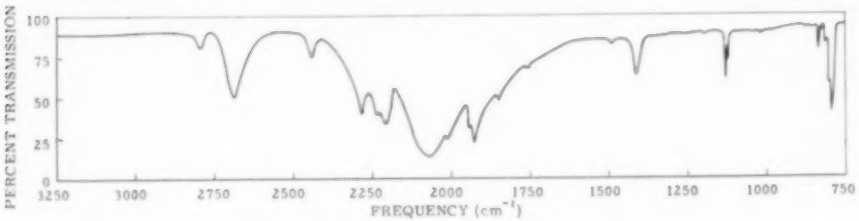

Fig. 3. Infrared spectrum of $N_2D_6Cl_2$ at $-180°C$.

as the very weak band at 1198 cm^{-1} in the spectrum of $N_2D_6Cl_2$. This leaves the strong band at 1410 cm^{-1} to be explained as a combination in the same manner as the 1960 cm^{-1} band of $N_2H_6Cl_2$ with which it is probably associated.

In the region associated with ND stretching there is no clear correspondence to the NH stretching region of $N_2H_6Cl_2$. Consequently, choice of ω_5' and ω_7' is made to accommodate the product rule. Then if ω_5' and ω_7' are taken to be 1927 and 2060 cm^{-1}, though admittedly the choice is not necessarily unique, the product rule gives

$$A_{2u}\,\frac{\omega_5\,\omega_6}{\omega_5'\,\omega_6'} = 1{\cdot}78\ (\text{exp}),\quad \text{cf. } 1{\cdot}84\ (\text{theor.})$$

$$E_u\,\frac{\omega_7\,\omega_8\,\omega_9}{\omega_7'\,\omega_8'\,\omega_9'} = 2{\cdot}46\ (\text{exp}),\quad \text{cf. } 2{\cdot}60\ (\text{theor.})$$

The experimentally found ratios differ from the theoretical values, which assume vanishing external forces, by 3 and 5 per cent respectively.

Hydrazine dihydrofluoride

In Fig. 4 is shown the infrared spectrum of $N_2H_6F_2$, at $-180°C$. It differs

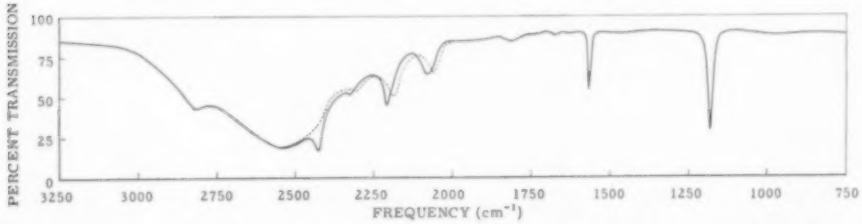

Fig. 4. Infrared spectrum of $N_2H_6F_2$ at $-180°C$. Broken line is for sample at $0°C$.

from that of the chloride salt in ways generally accepted to be the result of stronger hydrogen bonds. Hence, the NH stretching bands of $N_2H_6F_2$ are lower than those of $N_2H_6Cl_2$ and the deformation and rocking modes are higher. Also the NH

stretching band for the fluoride tends to be somewhat broader and more formless than for the chloride. The effect upon the spectrum in the broad NH stretching band of raising the temperature of the salt to 0°C is to leave the high frequency side practically unaffected but to increase slightly the intensity of the low frequency side and noticeably broaden the structure on this side. As seen in Fig. 4 the comparatively sharp band at 2427 cm^{-1} completely vanishes at 0°C. Freezing out of

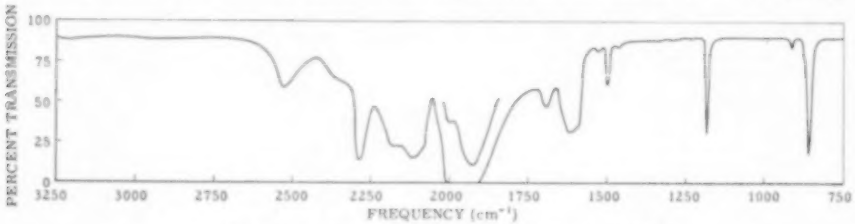

Fig. 5. Infrared spectrum of $N_2D_6F_2$ at −180°C.

excited lattice vibrations at −180°C probably accounts for the observed temperature dependence of the contour of the stretching band but no explanation is offered for changes in the finer structure of the band. Because of the large intramolecular interaction force constant between NH bonds observed for NH_4F [6] it seems doubtful whether the degenerate stretch, ω_7, could be expected to occur at a higher frequency than the symmetric stretch, ω_5, as it does when this interaction constant is small. Consequently, the maximum of the broad NH stretching band occurring in the vicinity of the residual NH stretching band at 2529 cm^{-1} in the spectrum of $N_2D_6F_2$, is taken to represent both ω_5 and ω_7. It occurs at 2545 cm^{-1}. For reasons given under the discussion of the chloride salt, ω_6, ω_8 and ω_9 are assigned to absorption bands at 1567, 1679 and 1182 cm^{-1} respectively with ω_8 again open to question.

VOL.
13
1958/5

d_6-*Hydrazine dihydrofluoride*

Nearly complete deuterium substitution is indicated from the low intensity of the NH stretching band (2529 cm^{-1}) in the spectrum of $N_2D_6F_2$ shown in Fig. 5. Yet the ND stretching region for the deuterated salt displays considerable detail little of which has any obvious correspondence to the same region in the spectrum of $N_2H_6F_2$. The strongest band has maximum intensity at 1925 cm^{-1} and it will be taken as belonging to ω_5' and ω_7'. Assignment of the 1184 and 858 cm^{-1} bands to ω_6 and ω_9 seems apparent. However, no absorption band could be found where ω_8' is to be expected. The product rule is then limited to the A_{2u} species, giving

$$\frac{\omega_5\,\omega_6}{\omega_5'\,\omega_6'} = 1{\cdot}75 \text{ (exp.)}, \quad \text{cf. } 1{\cdot}84 \text{ (theor.)}$$

Using the observed product rule ratio from the chloride salt ω_8' is calculated to be 1243 cm^{-1}.

Discussion

In comparing the NH stretching frequencies of NH_4F and $N_2H_6F_2$ it is noted that those of the latter occur at frequencies about 300 cm^{-1} lower than those of the former. Although part of this difference may be due to the increased strength of

hydrogen bonds, it is felt that most of the difference is due to simply a weaker NH bond in the $N_2H_6^{2+}$ ion itself. This situation becomes apparent in comparing NH_4Cl and $N_2H_6Cl_2$ where weaker hydrogen bonds are to be expected. Here the stretching frequencies differ in the same direction as before but the difference is about 400 cm^{-1}, being greater than for the fluoride salt and inconsistent with a picture where hydrogen bonding is used to explain these differences. Consequently, the question of whether the hydrogen bonding in $N_2H_6F_2$ is greater than in NH_4F cannot be answered by comparing the relative frequencies of the stretching modes.

Perhaps more important than hydrogen bonding on the vibrational spectrum is the role of the anharmonicity in the potential for NH stretch in determining the breadth of the NH stretching bands. It has been observed [6] that the NH stretching band in the infrared spectrum of NH_4F at $-195°C$ has a half-width of about 50 cm^{-1}. Yet $N_2H_6F_2$ which can be assumed to have hydrogen bonding of approximately the same strength has for the half width of those same bands a value roughly ten times that of NH_4F. Furthermore, $N_2H_6Cl_2$ which can be assumed to be considerably less hydrogen bonded than NH_4F has half widths of NH stretching bands probably four times greater than NH_4F. The spectrum of $N_2H_6Br_2$ also shows the same broad band. It is thought that this breadth may be related to the anharmonicity in the NH stretching modes.

Availability of Raman data giving the frequency of the librational mode, ω_L, about the N—N-axis of $N_2H_6^{2+}$ for the chloride salt together with a value for the observed frequency of the torsional mode, ω_4, for this ion in the crystal lattice, makes it possible to estimate the torsional frequency of the free $N_2H_6^{2+}$ ion. Thus, if k_1 is the intermolecular force constant for libration of a single NH_3 group, and k_2 is the force constant for internal rotation, it can be easily shown that:

$$\lambda_L = \frac{1}{I} k_1$$

$$\lambda_4 = \frac{1}{I} (k_1 + 2k_2)$$

where I is the moment of inertia of one NH_3 group about the three-fold axis. Assuming $\angle NNH = 100°$ [4], then $I = 5{\cdot}27 \times 10^{-40}$ g cm^2 gives

$$k_1 = 0{\cdot}114 \times 10^{-11} \text{ dyn-cm/rad}$$
$$k_2 = 0{\cdot}137 \times 10^{-11} \text{ dyn-cm/rad}$$

Then using k_2 to calculate the torsional frequency, ω_T, for the free ion gives

$$\omega_T = 383 \text{ cm}^{-1}$$

which is higher than the corresponding frequency, 290 cm^{-1}, found for ethane [12].

Acknowledgement—One of us (J. C. D.) is indebted to the Graduate School of Oregon State College for a grant from General Research Funds in support of the present work.

References

[1] Ananthakrishnan R., *Proc. Indian Acad. Sci.* A 1937 **5** 87.
[2] Couture L. and Mathieu J. P., *Ann. Phys., Paris* 1954 **9** 255.
[3] Donahue J. and Lipscomb W. N., *J. Chem. Phys.* 1946 **15** 115.

[4] Kronberg M. L. and Harker D., *J. Chem. Phys.* 1942 **10** 309.
[5] Wagner E. L. and Hornig D. F., *J. Chem. Phys.* 1950 **18** 296.
[6] Plumb R. C. and Hornig D. F., *J. Chem. Phys.* 1955 **23** 947.
[7] Hansen G. E. and Dennison D. M., *J. Chem. Phys.* 1952 **20** 313.
[8] Halford R. S., *J. Chem. Phys.* 1946 **14** 8.
[9] Waldron R. D., *J. Chem. Phys.* 1953 **21** 734.
[10] Svatos *et al.*, *J. Amer. Chem. Soc.* 1957 **79** 3313.
[11] Ibers J. A. and Stevenson D. P., *J. Chem. Phys.* 1958 **28** 929.
[12] Pitzer K. S., *Disc. Faraday Soc.* 1951 **10** 1.

VOL.
13
1958/5

Spectrochimica Acta, 1959, Vol. 13, pp. 291 to 295. Pergamon Press Ltd. Printed in Northern Ireland

The infrared absorption spectra of ring-*D* steroid lactones—II

Structure-absorption correlations*

H. Rosenkrantz and C. Gual
Worcester Foundation for Experimental Biology, Shrewsbury, Massachusetts

(*Received* 2 *July* 1958)

Abstract—A search of the infrared spectra of several ring–*D* steroid lactones was carried out in order to recognize characteristic frequencies of these molecules. Sufficient differences existed among the spectra to permit the identification of each compound. In addition it was found that bands of relatively strong intensity consistently occurred near 1219 (8·20), 1110 (9·00) and 989 cm^{-1} (10·11 μ). Cross-comparisons with compound absorption curves in the literature indicated that the three bands correlated with a *D*-homolactone structure. The 1219 cm^{-1} (8·20 μ) band could be assigned to the vibrations of the —C(=O)—O— unit and the 1110 cm^{-1} (9 μ) to the oscillations of the —C(—)—O grouping of the lactone structure. Although the 1219 (8·20) absorption was obliterated in the acetoxy derivatives of the ring-*D* steroid lactones, the 1110 cm^{-1} (9 μ) band appeared clearly and consistently. The present data on ten ring–*D* steroid lactones suggested that the aforementioned three maxima can be useful for identifying *D*-homolactone structures.

In a previous paper it was shown that estrololactone (17*a*-oxa-17-oxo-*D*-homoestra-1:3:5(10)-trien-3-ol) formed intense intermolecular hydrogen bonds between the 3-hydroxy and 17*a*-ketone groups [1]. Both the hydroxyl and carbonyl absorption bands were displaced to lower frequencies. This unusual tendency for hydrogen bonding was markedly noticeable in solid state spectra of estrololactone and also occurred in *iso*andrololactone (17*a*-oxa-17-oxo-*D*-homo*iso*androstan-3β-ol) although to a lesser extent.

Since the spectra of a few ring–*D* steroid lactones had become available, a search was made for characteristic frequencies which might help in identifying these steroid molecules. It was found that bands of relatively strong intensity consistently appeared near 1219 (8·20), 1110 (9·00) and 989 cm^{-1} (10·11 μ) in the spectra of the ring–*D* steroid lactones. Other bands were present which permitted the differentiation of each spectrum from the other.

Methods and experimental

The methods and instruments used were discussed in the previous communication which also contains copies of the infrared spectra of seven ring–*D* steroid lactones [1]. Pertinent absorption curves from the new steroid atlas were consulted [2].

* This investigation was supported in part by the Public Health Service Grants Nos. A-1207 and C-2207.

Results and discussion

Since the hydroxyl and carbonyl regions have been discussed in detail [1], the present paper will be concerned with the vibrations occurring at lower frequencies. Naturally the benzenoid ring of estrololactone provided several distinct oscillations which afforded easy differentiation between estrogenic and non-estrogenic steroids. The frequencies originating in the vibrations of the benzenoid ring occurred near 1619 cm^{-1} (6·18 μ) with a side inflection near 1608 cm^{-1} (6·22 μ) in the spectra of the least structurally complex estrogens, estra-1:3:5(10)-trien-3-ol and estra-1:3:5(10):16-tetraen-3-ol (charts 309 and 311 of [2]). The aromatic nature of the compounds was also revealed by the bending vibrations of the aromatic C—H groupings near 1499 cm^{-1} (6·68 μ). Addition of a ketone at position 17 like in estrone resolved the bands arising from the conjugated double bond system in ring *A* into maxima near 1620 cm^{-1} (6·17 μ) and 1580 cm^{-1} (6·34 μ) (unpublished KBr spectrum and chart 5 of [3]). These two bands occurred at approximately the same frequencies in the infrared recording of estrololactone (Fig. 1 of [1]).

Whereas enlargement of ring-*D* and formation of a lactone structure had little if any influence on the vibrations of the benzenoid ring, acetylation markedly reduced their intensity. Estrololactone acetate gave rise to a weak band near 1610 cm^{-1} (6·21 μ) (Fig. 1 of [1]) and the acetates of estrone (chart 6 of [3]) and estra-1:3:5(10)-trien-3-ol (chart 310 of [2]) gave a similar band.

In addition to the characteristic frequencies of the aromatic ring the phenolic structure of 3-hydroxy-estra-1:3:5(10)-triene compounds also contain a —C(=O)—O— unit which is known to absorb near 1250 cm^{-1} (8 μ). In the absence of acetoxy groups absorption near the latter frequency lends confirmatory evidence for a phenolic ring. In the case of steroid lactones a —C(=O)—O-grouping also exists and the ability to distinguish these vibrations from the corresponding ones in the phenolic structure could be extremely helpful in identifying steroid lactones. The data in Table 1 indicates that such characteristic frequencies do exist. It can be seen that a band near 1219 cm^{-1} (8·20 μ) consistently occurred in the spectra of the ring-*D* steroid lactones. The infrared curves recorded on KBr preparations contained the pertinent maximum near 1230 cm^{-1} (8·13 μ) for estrololactone ((I) 17*a*-oxa-17-oxo-*D*-homoestra-1:3:5(10)-trien-3-ol), near 1217 cm^{-1} (8·82 μ) for *iso*androlololactone ((II) 17*a*-oxa-17-oxo-*D*-homo*iso*androstan-3β-ol), near 1219 cm^{-1} (8·21 μ) for 1-dehydrotestololactone ((III) 17*a*-oxa-17-oxo-*D*-homoandrosta-1:4-dien-3-one) and near 1211 cm^{-1} (8·25 μ) for testololactone ((IV) 17*a*-oxa-17-oxo-*D*-homoandrost-4-en-3-one)*. The spectra of compounds (II), (III) and (IV) do not contain the intense absorption near 1250 cm^{-1} (8·00 μ) and 1241 cm^{-1} (8·05 μ) which appear in the curve of compound (I) and arose from the —C(=O)—O— linkage of the phenolic ring.

* We wish to express our thanks to Dr. D. A. Shepherd and the Upjohn Research Division for generously donating samples of *iso*androlololactone acetate, 5-chloro*iso*androlololactone acetate, testololactone and 1-dehydrotestololactone.

VOL. 13 1958/5

Table 1. Frequencies between 1250–835 cm^{-1} (8–12 μ) for ring–*D* steroid lactones*

(I)	(II)	(III)	(IV)	(V)	(VI)
1250 (8·00)s					
1241 (8·05)s		1231 (8·11)m	1240 (8·06)m		
1230 (8·13)s	1217 (8·22)m	1219 (8·21)ms	1211 (8·25)ms	Solvent interference	
		1208 (8·29)ms			
1173 (8·52)m		1168 (8·56)ms	1166 (8·58)w		
1153 (8·67)w	1162 (8·60)w				
1120 (8·93)w	1145 (8·74)w	1134 (8·81)ms	1132 (8·83)w		
1100 (9·09)s	1110 (9·01)ms	1091 (9·17)s	1099 (9·10)s	1110 (9·01)s	1112 (8·98)s
				1092 (9·15)ms	1097 (9·12)ms
	1081 (9·25)w				
1055 (9·48)w	1059 (9·45)m	1057 (9·46)w	1061 (9·41)m	1061 (9·41)ms	1066 (9·39)ms
	1041 (9·60)m	1037 (9·65)w		1041 (9·60)w	1037 (9·65)s
1030 (9·71)m					
1019 (9·82)w		1011 (9·87)ms	1012 (9·86)w	1019 (8·82)w	
	999 (10·01)w			997 (10·02)m	1005 (9·95)m
994 (10·06)m	985 (10·16)ms	988 (10·12)ms	989 (10·11)m	988 (10·12)m	992 (10·09)m
971 (10·30)ms			963 (10·39)w	975 (10·27)w	968 (10·32)m
		957 (10·44)ms		960 (10·41)ms	
950 (10·53)w	952 (10·50)w		952 (10·50)m		948 (10·56)w
	941 (10·62)w	944 (10·60)ms			
927 (10·79)w				932 (10·72)m	
910 (10·99)w	904 (11·05)w	907 (11·01)w	906 (11·03)w	905 (11·04)w	904 (11·05)w
890 (11·23)m	889 (11·25)w	891 (11·22)s			
				883 (11·32)w	
			868 (11·51)m		
860 (11·62)w		861 (11·61)w			
849 (11·79)w	853 (11·72)w				
		844 (11·85)w			

* Spectrum refers (I) to estrololactone, (II) to *iso*androlololactone, (III) to 1-dehydrotestololactone, (IV) to testololactone, (V) to androlololactone and (VI) to etiocholololactone. Spectra (I) to (IV) were recorded on KBr preparations while (V) and (VI) were obtained in chloroform. The first four spectra may be seen in Fig. 1 of [1] while the last two may be found in charts 666 and 668 of [2].
Relative intensities are designated by s = strong; ms = medium strong; m = medium and w = weak.

That the assignments of the —C(=O)—O— unit of the phenolic ring to a band near 1250 cm^{-1} (8·00 μ) and the analogous grouping of the lactone ring to a band near 1220 cm^{-1} (8·19 μ) appeared reasonable was indicated by the presence of the former band and absence of the latter band in the spectra of estra-1:3:5(10)-trien-3-ol (chart 309 of [2]) and estrone (chart 5 of [3]). Unfortunately, because of solvent interference the bands under consideration could not be examined in the published curves of androlololactone ((V) 17*a*-oxa-17-oxo-*D*-homoandrostan-3*a*-ol); (chart 666 of [2]) and etiocholololactone ((VI) 17*a*-oxa-17-oxo-*D*-homoandrostan-3*a*-ol; chart 668 of [2]). Although several ring *A* steroid lactones are known [4], they had been synthesized as acetates and prevented the interpretation of the region concerned with the —C(=O)—O— linkage of the lactone ring.

In addition to the band arising from the —C(=O)—O— unit, the lactone structure must

give rise to a band associated with the —C—O— grouping. This absorption usually occurs between 1110–1000 cm^{-1} (9–10 μ) [5]. Investigation of this region in the spectra of ring–*D* steroid lactones revealed the presence of two consistent bands. A band of strong intensity occurred near 1100 cm^{-1} (9·09 μ) for (I), near 1110 cm^{-1} (9·01 μ) for (II), near 1091 cm^{-1} (9·16 μ) for (III) and near 1099 cm^{-1} (9·10 μ) for (IV). The usual occurrence of bands at higher frequencies in solution spectra gave the corresponding band near 1110 cm^{-1} (9·01 μ) for (V) and near 1112 cm^{-1} (8·98 μ) for (VI).

The other maximum was of medium to medium strong intensity and appeared

Table 2. Frequencies between 1250–835 cm^{-1} (8–12 μ) for acetate derivatives of ring steroid *D* lactones*

(I acetate)	(II acetate)	(V acetate)	(VII acetate)
	1251 (7·99)s	1252 (7·98)ms	
		1241 (8·05)s	1243 (8·04)s
1227 (8·15)s	1218 (8·21)ms	1232 (8·11)m	1220 (8·20)m
1204 (8·30)s			
1191 (8·39)s		1189 (8·41)w	1189 (8·41)w
	1171 (8·54)w	1181 (8·46)ms	
1159 (8·63)m	1154 (8·66)m		
		1149 (8·71)m	
	1135 (8·81)w	1135 (8·81)w	1137 (9·80)w
1124 (8·90)w			
1108 (9·03)ms	1118 (8·95)s	1116 (8·96)s	1110 (9·00)ms
	1089 (9·18)w	1100 (9·09)ms	
1056 (9·47)w	1064 (9·40)m	1070 (9·35)ms	
		1045 (9·56)w	1050 (9·52)w
	1034 (9·67)s		1031 (9·69)ms
1029 (9·72)m			
	1011 (9·89)w	1020 (9·80)ms	
998 (10·01)w	991 (10·09)w	995 (10·05)w	993 (10·08)w
		988 (10·12)m	
		980 (10·21)w	
970 (10·32)m	968 (10·33)w	963 (10·39)m	966 (10·36)w
948 (10·55)m	946 (10·58)w	945 (10·59)m	
		923 (10·83)w	
916 (10·91)w	913 (10·95)w		916 (10·91)w
	899 (11·12)m		
890 (11·22)w			
	862 (11·60)m		
836 (11·97)w			855 (11·70)w

* Spectrum (I) refers to estrololactone 3-acetate, (II acetate) to *iso*androlololactone-3β-acetate, (V acetate) to androlololactone 3α-acetate and (VII) to 5-chloro*iso*androlololactone 3β-acetate. Spectra (I acetate), (II acetate) and (VII) were recorded on KBr preparations (Fig. 1 of [1]) while (V acetate) was studied in CCl_4 solution (chart 667 of [2]).

Relative intensities are designated by s, strong; ms, medium strong; m, medium and w, weak.

VOL. 13 1958/5

near 994 cm^{-1} (10·06 μ), 985 cm^{-1} (10·16 μ), 988 cm^{-1} (10·12 μ), 989 cm^{-1} (10·11 μ), 997 cm^{-1} (10·02 μ) and 1005 cm^{-1} (9·95 μ) for compounds (I), (II), (III), (IV), (V) and (VI), respectively.

It was known that the 17-ketone carbonyl and steroids with a 3α-hydroxyl *cis* to the C_5-hydrogen atom absorb near 1000 cm^{-1} (10 μ) [5, 6]; therefore, the absorption curves in the steroid atlases were primarily examined near 1110 cm^{-1} (9 μ) [2, 3]. All the free, naturally occurring steroid compounds were considered. These numbered approximately 300 and of these four absorbed significantly near 1110 cm^{-1} (9 μ) similarly to the ring–*D* steroid lactones. These steroids were pregnan-17α-ol-3:20-dione (chart 201), pregn-4-en-17α-ol-3:20-dione (chart 204, pregn-4-en-17α-ol-3:11:20-trione (chart 224) and allopregnane-3α:11β:21-triol-20-one (chart 503) [2, 3]. However none of the spectra contained all three bands near 1220 cm^{-1} (8·19 μ), 1110 cm^{-1} (9·00 μ) and 989 cm^{-1} (10·11 μ) found in the recordings of ring–*D* steroid lactones.

Additional evidence for assigning the origin of the 1110 cm^{-1} (9 μ) band to the lactone structure may be obtained from the spectra of ring–*D* steroid lactone acetates (Table 2). The infrared curve of estrololactone acetate (I acetate) had a band of relatively strong intensity near 1108 cm^{-1} (9·03 μ), *iso*androlololactone acetate (II acetate) near 1118 cm^{-1} (8·95 μ), androlololactone acetate (V acetate) near 1116 cm^{-1} (8·96 μ) and 5-chloro*iso*androlololactone acetate (VII) near 1110 cm^{-1} (9·00 μ). A band near 995 cm^{-1} (10·05 μ) existed for all the acetoxy derivatives but was of weak intensity as compared to the analogous band in the spectra of the free ring–*D* steroid lactones. Correlation of the 1220 cm^{-1} (8·19 μ) band was not possible because of interference by the absorption of the acetoxy group.

The aromatic type acetoxy maximum of estrololactone acetate absorbed, where expected, near 1204 cm^{-1} (8·30 μ). The similar grouping in estra-1:3:5(10)-trien-3-ol-3-acetate gave rise to a band near 1210 cm^{-1} (8·26 μ) (chart 310 of [2]). The aliphatic type acetoxy absorption was near 1250 cm^{-1} (8 μ) as can be seen for the (II acetate), (V acetate) and for compound (VII) in Table 2.

The infrared spectra of a few acetylated ring *A* steroid lactones associated with a double bond between position 5 and 6 were compared [4]. There was no correlation between the lactone structure and absorption near 1110 cm^{-1}. This was not too surprising since the Δ^5-double bond also contributed to a —C(=O)—O— linkage which involved the same oxygen atom as the corresponding grouping in the lactone ring. Under this situation a comparison of the ring–*A* and ring–*D* steroid lactones was less satisfactory.

References

[1] Gual C., Dorfman R. I. and Rosenkrantz H. *Spectrochim. Acta* 1958 **13** 248.

[2] Roberts L., Gallagher B. S. and Jones R. N., *Infrared Absorption Spectra of Steroids, An atlas* Vol. II. Interscience, New York 1958.

[3] Dobriner K., Katzenellenbogen E. R. and Jones R. N., *Infrared Absorption Spectra of Steroids, An atlas* Vol. I. Interscience, New York 1953.

[4] Rosenkrantz H. and Gut M., *Helv. Chim. Acta* 1953 **36** 1000.

[5] Rosenkrantz H. In Glick's *Methods of Biochemical Analysis* Vol. II, p. 1. Interscience, New York 1955.

[6] Rosenkrantz H. and Skogstrom P., *Analyt. Chem.* 1956 **28** 31.

Spectrochimica Acta, 1959, Vol. 13, pp. 296 to 299. Pergamon Press Ltd. Printed in Northern Ireland

The infrared spectra of organic thiocyanates and *iso*thiocyanates

E. LIEBER,* C. N. R. RAO and J. RAMACHANDRAN
Department of Chemistry, De Paul University, Chicago 14, Illinois, U.S.A.

(*Received* 21 *July* 1958)

Abstract—The infrared spectra of several organic thiocyanates and *iso*thiocyanates have been studied. The thiocyanates and the *iso*thiocyanates can be distinguished by their characteristic vibration frequencies around 2140 cm^{-1} and between 2060–2105 cm^{-1}, respectively. These respective frequencies serve as an analytical tool for distinguishing these isomers both singly and in mixtures.

Introduction

THERE have been several isolated reports of the infrared spectra of organic thiocyanates and *iso*thiocyanates. We have now conducted a systematic investigation of the infrared spectra of these compounds. Since thiocyanates and *iso*thiocyanates are isomeric it was considered that the infrared spectra may yield a simple analytical tool for their identification.

Experimental

The compounds used in this study were obtained commercially and when necessary purified to the constants reported for them. The spectra were recorded on a Perkin–Elmer Spectrometer, Model 21, with sodium chloride prism. The spectra of liquids, using liquid cells, and of solids in Nujol mulls, were taken. In a few cases the spectra were also taken in carbon tetrachloride solutions. The positions of the absorption maxima are listed in cm^{-1} in Tables 1 and 2, with the intensities being indicated by the symbols: (vs), very strong; (s), strong; (m), medium; (mw), medium weak; (w), weak. The infrared data on some *iso*thiocyanates from the literature [5, 10, 11] have also been included in Table 2 for purposes of comparison.

Discussion

Organic thiocyanates. The important absorption frequencies of several organic thiocyanates have been summarized in Table 1. The well known vibration frequencies (e.g. C—H, etc.) have not been tabulated. All the organic thiocyanates show a sharp strong peak due to the nitrile stretching vibration [1] around 2140

Table 1. Infrared spectra of organic thiocyanates (R—S—C≡N)

R	S—C≡N	Other bands						
CH_3	2141 s	1316 m	—	—	—	988 vw	696 w	672 w
C_2H_5	2141 s	1269 m	—	1062 s	—	968 s	772 s	683 w
n-C_4H_9	2137 s	1272 mw	1225 m	1095 w	1053 mw	916 s	742 mw	700 w
n-C_7H_{15}	2137 s	1275 m	1238 mw	1101 w	1058 w	—	722 m	—
$C_6H_5CH_2$	2141 s	—	1233 m	1072 s	—	914 w	—	—

* To whom all correspondence and requests for reprints should be addressed.

VOL. 13 1958/5

cm^{-1}. The nitrile band is observed around this region in diazoguanidine cyanide [2] and cyanogen halides [3].

Methyl thiocyanate shows a medium intensity band at 1316 cm^{-1} which can be ascribed to the CH_3 deformation [1]. The other alkyl thiocyanates also exhibit a medium intensity band around 1270 cm^{-1} which may also be due to the CH_3

Table 2. Infrared spectra of organic *iso*thiocyanates (R—N=C=S)

R	N=C=S	N=C=S	Other bands			
CH_3	2188 s	2092 vs	—	1089 w	—	—
C_2H_5	2174 s	2092 vs	1120 mw	1062 m	938 m	795 mw
n-C_4H_9	2155 s	2088 vs	1116 w	1081 w	977 mw	745 s
				1038 w	942 w	
n-C_7H_{15}	2155 s	2088 vs	1121 w	1081 w	—	725 w
CH_2=$CHCH_2$	2151 s	2079 vs	—	986 m	921 m	707 m
C_6H_5	2160 s	2060 vs	—	1067 w	926 nw	750 s
4-$NH_2C_6H_4$	2160 s	2105 vs	1172 s	1070 w	946 w	751 mw
					913 mw	
t-C_4H_9 [5]	—	2090 s	—	—	—	—
allyl carbinyl [10]	—	2105 s	—	992	—	—
trans-crotyl [10]	—	2062 s	1120	1078	887	772
cis-crotyl [10]	—	2105 s	1115	1075	955	746
					889	
methoxybenzyl [11]	—	2079 s	1153	1050	—	739

deformation frequency in these compounds. Also, one of the bands exhibited in the region of 683–722 cm^{-1} may be due to the —C—S— vibration.

Organic isothiocyanates. The infrared spectra of organic *iso*thiocyanates are listed in Table 2. The well known vibration frequencies like the CH vibrations, etc., have not been tabulated. All the organic *iso*thiocyanates exhibit a broad and very strong band centred around 2100 cm^{-1} due to the *iso*thiocyanate group. At lower concentrations (smaller layer thickness) this band shows finer resolution and gives a strong peak or shoulder between 2080–2105 cm^{-1} (Fig. 1). This is in agreement with the observation of WILLIAMS [4] on phenyl *iso*thiocyanate. However, no weak band was apparent around 1950–2000 cm^{-1} [4, 5]. The infrared spectra of organic *iso*cyanates (R—N=C=O) has been extensively studied and the characteristic *iso*cyanate band is found between 2269–2275 cm^{-1} [6, 7, 8]. It is interesting to note that the *iso*thiocyanate group shows its characteristic band at a lower frequency (2060–2190 cm^{-1}) than the *iso*cyanate groups. While going from the normal thiocyanate to the *iso*thiocyanate there is a decrease in the characteristic frequency just as in the example of nitrile to isonitrile [1, 9]. This suggests that the contribution of the resonance form:

$$R—\overset{\oplus}{N}=C—\overset{\ominus}{S}$$

is greater than that of the others [4]. All the isothiocyanates also show other bands of which the weak or medium intensity band between 1050–1089 cm^{-1} occurs

constantly in all of them. This may be due to the *iso*thiocyanate symmetric stretching vibration.

Fig. 1. Infrared spectra of methyl thiocyanate and methyl *iso*thiocyanate. (a) ——— methyl *iso*thiocyanate, – – – – methyl thiocyanate. (b) A mixture of methyl thiocyanate and methyl *iso*thiocyanate in carbon tetrachloride solution.

From the results discussed above it may be noted that the organic thiocyanates and *iso*thiocyanates can be distinguished by their characteristic vibration frequencies around 2140 cm^{-1} and between 2060 and 2105 cm^{-1} respectively. Fig. 1 also includes the infrared spectrum of a mixture of methyl thiocyanate and methyl *iso*thiocyanate in carbon tetrachloride solution. The peaks due to the thiocyanate and the *iso*thiocyanate groups are clearly distinct.

Acknowledgement—The authors gratefully acknowledge grants-in-aid from the Frederick Gardner Cottrell Program of the Research Corporation, New York, U.S.A. and the Lilly Research Laboratories, Eli Lilly and Company, Indianapolis, Indiana, U.S.A., which made this study possible.

VOL. 13 1958/5

References

[1] Bellamy L. J., *The Infrared Spectra of Complex Molecules* Methuen, London 1954.
[2] Lieber E., Levering D. R. and Patterson L., *Analyt. Chem.* 1951 **23** 1594.
[3] West W. and Farnsworth M., *J. Chem. Phys.* 1933 **1** 402.
[4] Williams D., *J. Chem. Phys.* 1940 **8** 513.
[5] Luskin L. S., Gamtert G. E. and Craig W. E., *J. Amer. Chem. Soc.* 1956 **78** 4965.
[6] Hoyer H. *Chem. Ber.* 1956 **89** 2677.
[7] Bortnick N., Luskin L. S. and Hurowitz M. D., *J. Amer. Chem. Soc.* 1956 **78** 4358.
[8] Davison W. H. T., *J. Chem. Soc.* 1953 3712.
[9] Gordy W. and Williams D., *J. Chem. Phys.* 1936 **4** 85.
[10] Ettlinger M. G. and Hodgkins J. E., *J. Amer. Chem. Soc.* 1955 **77** 1831.
[11] Ettlinger M. G. and Lundeen A. J., *J. Amer. Chem. Soc.* 1956 **78** 1952.

OL.
13
8/59

Spectrochimica Acta, 1959, Vol. 13, pp. 300 to 305. Pergamon Press Ltd. Printed in Northern Ireland

Quantitative spectrographic analysis of the rare earth elements—X

Determination of rare earth impurities commonly associated with purified thulium, ytterbium, lutetium and scandium*

R. N. Kniseley, V. A. Fassel, R. W. Tabeling, B. G. Hurd and B. B. Quinney
Institute for Atomic Research and Department of Chemistry
Iowa State College, Ames, Iowa

(*Received* 21 *August* 1958)

Abstract—Emission-spectrometric methods are described for the following quantitative determinations: yttrium, holmium, erbium, ytterbium and lutetium in thulium; samarium, yttrium, erbium, thulium, lutetium and scandium in ytterbium; yttrium, thulium, ytterbium and lutetium in scandium. The basic method involves the d.c. carbon arc excitation of rare earth oxide–graphite mixtures. In all cases the percent deviation from the mean is less than ±5 per cent.

Introduction

This article is an extension of previously published emission-spectrometric procedures for the determination of rare earth impurities in purified rare earth matrices [1–4]. In this paper the determination of rare earth impurities commonly associated with purified thulium, ytterbium, lutetium and scandium is discussed.

VOL. 13 1958/59

Experimental

The previous papers [1–4] have described in detail the apparatus and excitation conditions employed in these studies. Likewise, these papers have adequately covered the considerations involved in the selection of the line pairs. It suffices to state here that since excitation potential data were not available, each line pair selected was subjected to a variation in the excitation current covering the range from 10 to 19 A. Only those line pairs which varied less than ±5 per cent over this current range were acceptable.

Figure 1 shows the behavior of the analytical intensity ratios during the arcing cycle. It is evident that a wide range of volatilities is encountered in this group of elements. The relatively high volatility of ytterbium is particularly apparent. Because of the dissimilarities in vaporization behavior, a rather low degree of internal standardization of the excitation variables during the arcing cycle can be expected. However, the internal standard lines do provide compensation for weighing, optical and photographic photometry errors. Since none of the elements in this group are highly refractory, no difficulty is experienced in vaporizing the entire sample. Consequently, integrated intensity ratios show adequate reproducibility.

The line pairs which were selected are presented in Table 1 along with the

* Contribution No. 651. Work was performed in the Ames Laboratory of the U.S. Atomic Energy Commission.

analytical data concerning these lines. Table 1 also lists the important interferences which may cause difficulty when these line pairs are employed. In cases where background corrections were necessary, readings were restricted to those steps where the background under both lines was between 70 and 85 per cent

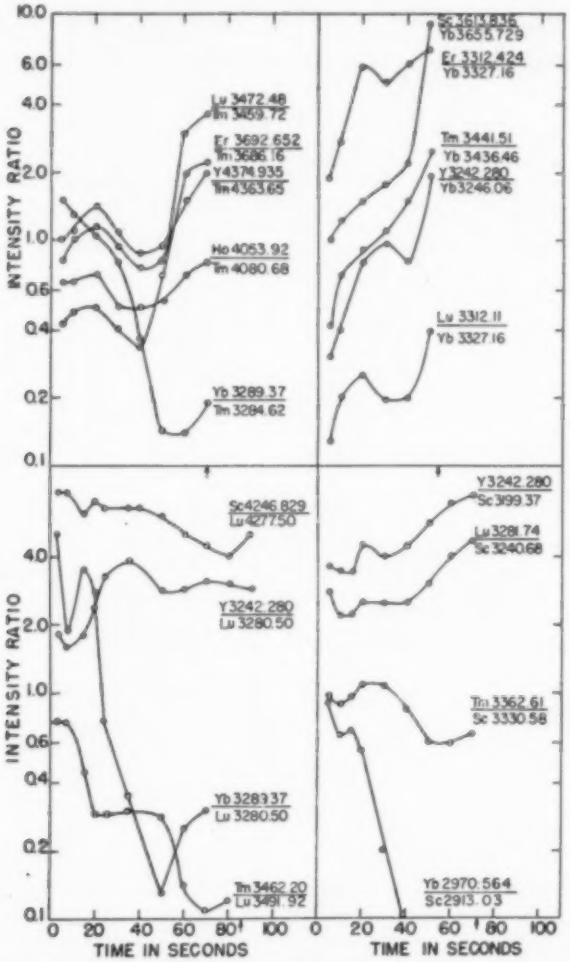

Fig. 1. Variation of analytical intensity ratio during the arcing period. Arrows indicate complete sample consumption. Wavelengths are expressed in Å.

transmission. This restriction minimized the errors inherent in making background corrections.

While no extensive precision studies were made, replicate exposures of the standards over the entire concentration range and on individual plates showed that in all cases the percent deviation from the mean did not exceed ± 5 per cent. The lack of other methods for the determination of these impurities at the concentration level involved precluded the verification of the analytical results

Table 1. Data on analytical line pairs

Matrix	Line pair* (Å)	Conc. range (%)	Conc. index (%)	Detection limit (%)	Background correction	Remarks
Tm_2O_3	Y 4374·935 Tm 4363·65	0·02–1·0	0·15	0·005	No	
	Ho 4053·92 Tm 4080·68*	0·02–1·0	0·42	0·02	Yes (below 0·1)	
	Er 3692·652 Tm 3686·16	0·02–1·0	0·35	0·005	Yes (below 0·1)	
	Yb 2970·56 Tm 2961·41	0·02–1·0	0·45	0·005	No	Fe 2970·513 Å interferes at Fe concentrations above ~0·5%
	Yb 3289·37 Tm 3284·62*	0·02–1·0	0·05	0·0002	No	
	Lu 3472·48 Tm 3459·72*	0·02–1·0	0·20	0·005	No	
Yb_2O_3	Sm 4390·865 Yb 4370·81	0·07–1·0	0·60	0·05	Yes	Fe 4390·954 A may interfere at Fe concentrations greater than 1%
	Y 3242·280 Yb 3246·06*	0·01–1·0	0·10	0·002	No	Fe 3245·984 Å may interfere at Fe concentrations greater than 0·5%
	Tm 3441·51 Yb 3436·46	0·01–1·0	0·20	0·003	No	
	Er 3312·424 Yb 3327·16*	0·01–1·0	0·17	0·005	No	
	Sc 3613·836 Yb 3655·729	0·01–1·0	0·60	0·005	No	
	Lu 3312·11 Yb 3327·16*	0·01–1·0	0·17	0·005	No	
Lu_2O_3	Tm 3462·20 Lu 3491·92	0·02–1·0	0·08	0·002	No	There is an Yb line at ~3462·4 Å which may interfere at Yb concentration greater than 0·5% unless sufficient resolving power is available
	Yb 2970·564 Lu 2931·53	0·02–1·0	0·13	0·005	No	Fe 2970·513 Å interferes at Fe concentrations above ~0·5%
	Yb 3289·37 Lu 3280·50	0·008–0·1	0·05	0·0005	No	
	Sc 4246·829 Lu 4277·50	0·02–1·0	0·10	0·001	No	
	Y 3242·280 Lu 3280·50	0·01–1·0	0·02	0·004	No	
Sc_2O_3	Y 3242·280 Sc 3199·37	0·01–1·0	0·08	0·002	No	
	Tm 3362·61 Sc 3330·58	0·01–1·0	0·25	0·005	Yes	
	Yb 2970·564 Sc 2913·03	0·01–1·0	0·20	0·004	No	Fe 2970·513 Å interferes at Fe concentrations above ~0·5%
	Lu 3281·74 Sc 3240·68*	0·01–1·0	0·14	0·005	No	
	Th 3291·743 Sc 3253·38*	0·1–1·0	0·05	0·03	No	Recommended for semiquantitative analysis only. Since ThO_2 is highly refractory, it is difficult to vaporize the thorium content in a reproducible manner. Moreover, the large difference in vaporization behavior between Th and Sc prevents adequate internal standardization.

* Wavelengths marked with an asterisk were measured by the authors; all other wavelengths were taken from the MIT Wavelength Tables.

VOL. 13 1958/5

obtained by the spectrographic methods. However, the results from a series of recovery experiments indicated that the accuracy was within the limits of the reported precision.

Acknowledgements—The authors wish to express their appreciation to Dr. F. H. SPEDDING and his associates for providing the rare earth materials used in these investigations and to Mrs. M. KIVEL for checking much of the experimental data.

References

[1] FASSEL V. A. and WILHELM H. A., *J. Opt. Soc. Amer.* 1948 **38** 518.
[2] FASSEL V. A., COOK H. D., KROTZ L. C. and KEHRES P. W., *Spectrochim. Acta* 1952 **5** 201.
[3] FASSEL V. A., QUINNEY B. B., KROTZ L. C. and LENTZ C. F., *Analyt. Chem.* 1955 **27** 1010.
[4] KNISELEY R. N., FASSEL V. A., QUINNEY B. B., TREMMEL C., GORDON W. A. and HAYLES W. J., *Spectrochim. Acta* 1958 **12** 332.

OL.
13
3/59

Spectrochimica Acta, 1959, Vol. 13, pp. 304 to 307. Pergamon Press Ltd. Printed in Northern Ireland

Observations on the use of LaO bands for d.c. arc spectrochemical analysis

L. H. AHRENS* and R. A. EDGE†

(*Received* 10 *October* 1958)

Abstract—Under certain conditions of d.c. arc excitation LaO bands with heads at λ4371·9 and λ4418·1 Å are intensely emitted and are more sensitive than the most sensitive lanthanum lines: these are normally La^{II} (ion) lines. The ratio

$$\frac{\text{LaO } 4371}{La^{II}\ 4333}$$

has been found to vary from ~0·1 to ~16–factor of more than 100—in different matrices. A comparatively cool (alkali metal rich) arc favours LaO band emission.

Introduction

UNDER certain conditions of excitation, several rare earth elements emit intense oxide bands. PICCARDI [6], PINTA [7] and ISHIDA [2] have discussed their analytical use when excited in the flame whereas JAFFE [3] and PETTERSON and JAFFE [5] describe the use of YO and LaO bands for visual (spectroscopic) analysis when excited in the d.c. arc. For the purpose of estimating Y, La and other rare elements in rocks and minerals, the combined use of ion exchange enrichment and d.c. arc spectrochemical analysis is being investigated (EDGE *et al.* [1]). The spectrograph have been used to monitor the columns in these experiments and when La and Y were added to the solutions to be eluted, intense LaO and YO bands were observed in the dried residues of some of the effluent fractions. Under certain conditions the bands were much more intense than the normally used sensitive lines. As a result, some investigations were carried out on the analytical use of LaO bands; the results of these investigations are discussed here.

The LaO bands which we shall consider are shown in Fig. 2 (a and b); these were recorded on a large Hilger Littrow Spectrograph, using quartz optics. The bands are degraded to the red. The sharply defined heads are at λ4371·9 and λ4418·1 Å.

Experimental details

Observations were made at 3 A and 7 A in a variety of matrices, namely: NaCl; NaCl + C (1 : 1); Na_2CO_3 + C (1 : 1); KCl; KCl + C (1 : 1); $CaCO_3$ + C (1 : 1); and in carbon powder alone. Lanthanum was added as La_2O_3 and also as $LaCl_3$, to give concentrations of 0·01%, 0·1% and 1% La. The charge was 25 mg in each case and was loaded into a carbon anode, 4 mm (external diameter) × 3 mm (internal diameter) × 3 mm (depth). In some experiments, the plate holder was racked down at intervals of 10 sec and in others a single exposure was made of

* University of Cape Town.
† University of Cape Town, and Government Chemical Laboratories, Cape Town.

VOL. 13 1958/5

the complete arc burn. In each of the experiments observations were made on two sensitive lanthanum lines, La^{II} 3949, often regarded as the most sensitive lanthanum line, and on La^{II} 4333 another sensitive line which is located quite close to LaO 4371 (Fig. 2 (a)). Both are ion lines.

Discussion

Two main conclusions may be drawn from the experiments:

(1) At a given concentration, the intensity of the LaO bands varies enormously in different matrices and tends to be at a maximum in the presence of an alkali metal salt. In this respect LaO emission closely resembles that of AlO, but not

Table 1. Intensity ratios of (LaO 4371/La^{II} 4333) at different Na vapour concentrations, as indicated by the intensity of Na 3302 (arranged in order of increasing intensity of Na 3302)

$\frac{LaO}{La^{II}}$	Na 3302
0·11	1·0
0·39	1·4
0·50	2·0
1·6	2·0
2·0	5·0
0·50	8·0
0·50	15·0
2·0	15·0
4·0	23·0
4·0	33·0
8·0	33·0
8·0	50·0
16·0	60·0
8·5	62·0
4·0	65·0

CN. Thus, for example, whereas LaO was not detected in a $CaCO_3$ matrix containing 1% La (added as La_2O_3) the bands were intense in NaCl and KCl matrices containing the same concentrations of lanthanum.

(2) The intensities of sensitive lanthanum lines often tend to vary inversely with that of the LaO bands.

An example of the LaO–La^{II} relationship is shown in Fig. 1 and in Fig. 2. Fig. 1 shows the variation of the intensities of LaO 4371, La 4333 and also Na 3302 with respect to time (7 A excitation of 1% La as La_2O_3 in NaCl). The intensity of LaO is decidedly greater than La 4333 during the early period of the arc burn, but after most of the sodium was distilled the reverse holds. Table 1 lists intensity ratios (LaO 4371/La 4333) and the intensity of Na 3302 (7 A excitation of 1% La as La_2O_3 in NaCl and of 1% La_2O_3 in NaCl × C(1:1)). The arrangement is in order of increasing intensity of Na 3302. Though the ratio (LaO 4371/La 4333)

varies very considerably and irregularly, a trend is apparent and this has been found to hold quite generally.

The relationship is not a simple one, however, because the presence of an alkali metal tends to depress volatilization of lanthanum in the first place but at the same time provides an excitation environment highly conducive to LaO excitation and

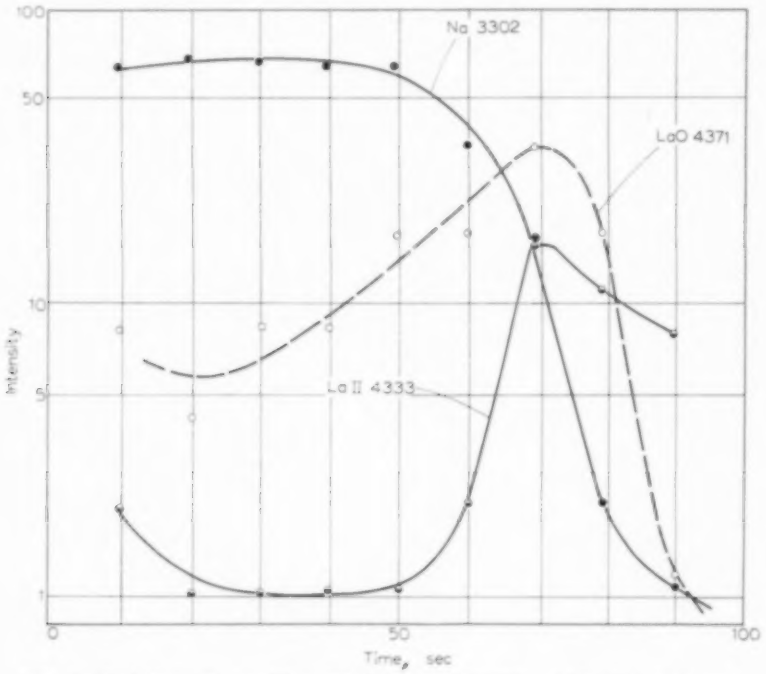

Fig. 1. Variation of intensities of LaO 4371, La^{II} 4333 and Na 3302 with time.

not La^{II} excitation. It may be noted that the magnitude of the ratio LaO band/La 4333 varies from ~0·1 to ~16; this large range of more than 100 represents the maximum which we have found in our experiments.

It is clear from Fig. 1 and from Table 1 that the sensitivity of LaO 4371 is considerably greater than La 4333 under certain conditions. This is demonstrated further in Fig. 2 (a) and (b). The LaO bands are of about equal intensity in (a) and (b) whereas La 4333 is intense only in (a) (3 A excitation of La_2O_3) and only barely visible in (b) (3 A excitation of NaCl containing 1·5% La_2O_3). La 3939 is a little more intense than La 4333 but in (b) (not shown in photograph) is far weaker than LaO 4371.

The tendency for the intensities of the LaO bands to vary inversely with La 3949, La 4333 and other lanthanum ion lines arises presumably from these facts: LaO bands are easily excited in a comparatively cool arc whereas intense La^{II} emission is only possible from a hot arc because a high temperature is required to bring about a significant degree of ionization; we may recall also that degree of ionization is very sensitive to temperature changes (Saha's equation). Accordingly,

VOL. 13 1958/5

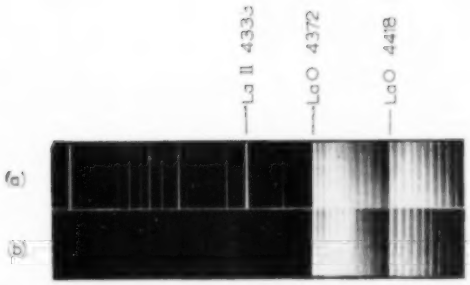

Fig. 2. D.C. arc spectra of LaO 4372 and lanthanum lines; (a) 3 A excitation of La_2O_3 and (b) 3 A excitation of 1% La (added as La_2O_3) in NaCl matrix.

DL.
13
8/59

VOL.
13
1958/5

the ratio (LaO bands/La^{II} lines) tends to a maximum in the presence of copious alkali metal vapour (low temperature arc) and a minimum in a matrix of carbon powder (high temperature arc). The absence of LaO bands in a $CaCO_3$ matrix (see above) comes, however, as some surprise because although a calcium–rich arc is hotter than arc in sodium or potassium vapour, it can hardly be regarded as a high temperature arc (first ionization potential of calcium = 6·1 V).

References

[1] Edge R. A., Brooks R. R., Ahrens L. H. and Amdurer S. *Geochim. et Cosmochim. Acta* 1959 **15** 461.

[2] Ishida R., *J. Chem. Soc. Japan* (1) 1955 **76** 60.

[3] Jaffe H. W., *Amer. Min.* 1949 **34** 667.

[4] Pearse R. W. B. and Gaydon A. G., *The Identification of Molecular Spectra*. Chapman and Hall, London 1950.

[5] Peterson M. J. and Jaffe H. W., *Visual-arc Spectroscopic Analysis*. Bulletin 524, U.S. Bureau of Mines, Washington 1953.

[6] Piccardi G., *Spectrochim. Acta* 1939 **1** 249.

[7] Pinta M., *J. Rech.* 1952 **21** 260.

OL.
13
3/59

Spectrochimica Acta, 1959, Vol. 13, pp. 308 to 310. Pergamon Press Ltd. Printed in Northern Ireland

Torsional vibrations in CO_2 and N_2O crystals*

D. A. Dows
Department of Chemistry, University of Southern California, Los Angeles 7, California

(*Received* 13 *October* 1958)

Abstract—Infra-red spectra of thick films (several hundred microns) of crystalline CO_2 and N_2O show bands in the vicinity of the bending vibrations which are attributed to combinations with several torsional frequencies. Information presently available on torsional vibrations in these crystals is summarized.

INFRA-RED spectra of crystalline CO_2 and N_2O have been reported respectively by OSBERG and HORNIG[1] and by DOWS[2] and GIGUERE and HARVEY.[3] Certain absorption bands in the spectrum of each substance are identified with transitions involving torsional motions of the molecules in the lattice. We have recently had the occasion to study the infra-red spectrum of a thick film of solid CO_2, and have found additional combinations involving torsional levels; subsequent re-examination of solid N_2O using films of much greater thickness than previously has revealed combinations analogous to the new ones found for CO_2.

VOL. 13 1958/5

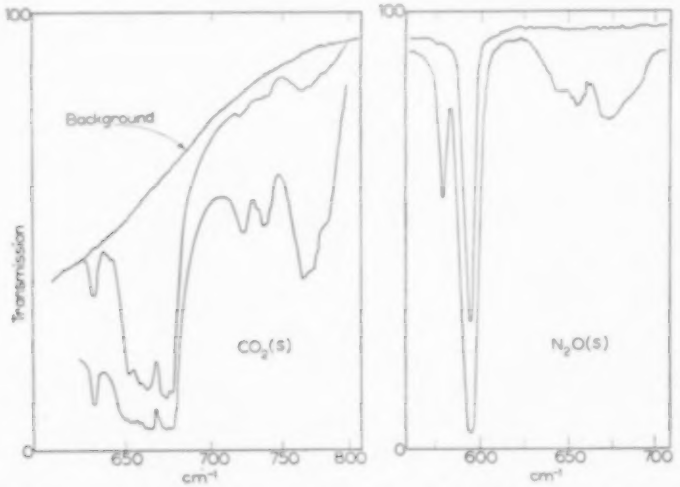

Fig. 1. Infra-red spectra of thick films of crystalline CO_2 and N_2O in the vicinity of the bending vibration.

The samples were taken from Matheson lecture bottles, distilled *in vacuo*, and condensed on a silver chloride plate cooled to 82°K in a cell similar to that used before.[2] Spectra in the vicinity of the bending fundamentals are shown in Fig. 1. NaCl optics were used for CO_2 and KBr for N_2O (the use of KBr optics with

* This work was supported by the Office of Ordnance Research, U.S. Army.

CO_2 showed only small differences attributable to lower resolution). Thin films of CO_2 gave spectra in agreement to those of OSBERG and HORNIG. Peak frequencies listed in Table 1 are believed accurate to two wavenumbers.

Table 1. Observed frequencies (cm^{-1}) in crystalline CO_2 and N_2O

CO_2			N_2O		
ν_{obs}	$\Delta\nu_{1/2}$	Assignment	ν_{obs}	$\Delta\nu_{1/2}$	Assignment
778 (sh)		$\nu_2 + 2 \times 63$	692 (sh)		$\nu_2 + 2 \times 51$
767 (sh)			675		
758		$\nu_2 + \tau$	655		$\nu_2 + \tau$
731	8		642		
718	8		590	6	ν_2
670		reflection	574	6	$\nu_2(^{14}N^{15}NO)$
660		ν_2			
653					
635	6	$\nu_2(^{13}CO_2)$			

sh = shoulder

The band seen at 667 cm^{-1} in the spectrum of CO_2 is assigned by OSBERG and HORNIG as a reflection maximum. The unusual changes in intensity of this band with sample thickness which formed the basis for their interpretation were reproduced in these experiments, using the NaCl prism, with a different sample substrate (AgCl instead of KBr). In spectra obtained with the KBr prism, no distinct peak was seen at 667 cm^{-1}, but the band broadened asymmetrically to higher frequencies as the sample was thickened.

The crystal structures of the two substances being the same except for the centre of symmetry in CO_2, the previous theoretical analysis[1] applies to both cases. Torsional oscillation falls in the class E_g of the site symmetry (drop subscripts "g" and "u" for N_2O), and consultation with the correlation diagram[1] results in a prediction of three torsional fundamentals of the unit cell ($E_g + 2F_g$). In combination with the bending vibration the torsions are symmetry allowed in the infra-red spectrum. It is realized that there are no strict selection rules for combination bands, but the lack of evidence that the usual rules for limiting modes are not obeyed makes it prudent to establish the allowedness of these transitions.

Table 2 lists the frequencies observed in combination with the bending vibrations. These are differences between the observed combination band frequencies and 590 cm^{-1} (N_2O) or 653 cm^{-1} (CO_2). The lower of the two CO_2 frequencies was arbitrarily chosen as discussed below. The Raman spectrum of crystalline CO_2 has been observed by GAIZAUSKAS and WELSH,[4] who also studied the region of the symmetric stretching vibration in very thick films in the infra-red. They obtain values for torsional frequencies which are included in Table 2.

Also listed are the values given in references 1 and 2. All entries under "other occurrence" give the band with which the lattice frequency is observed in combination and the frequency difference found (or the Raman shift).

The agreement between different observations seems quite good, and it is simply for this reason that the lower CO_2 frequency (653) was chosen as a basis for the differences in compiling Table 2; the frequencies resulting are then in close

Table 2. Torsional frequency summary

CO_2		N_2O	
Difference from ν_2	Other occurrence	Difference from ν_2	Other occurrence
125		101	
114	R*(112), ν_3†(110)	85	ν_3§(80), ν_1§(92)
105		65	
78	R*(77), ν_1‡(86)	52	
65	R*(64), ν_1‡(57)		

* Raman, ref. [4]. † Ref. [1]. ‡ Ref. [4]. § Ref. [2].

agreement with the other data. The close accord suggests that limiting modes of the librational and vibrational branches are being observed, as is suggested by usual selection rules for fundamentals. The most serious numerical disagreement is in the case of combinations with the symmetric stretching fundamental of CO_2, where combinations with the limiting modes are symmetry forbidden.

If the highest combination frequencies in each case are assigned as the bending frequency plus *twice* the lowest observed torsional frequency, then there remain three torsional frequencies for N_2O and four for CO_2. No more specific assignment, nor any reason for the appearance of an extra frequency for CO_2 will be given here. The curious preference for combining with the 653 wavenumber level of CO_2 must also go unexplained.

Acknowledgement—It is a pleasure to acknowledge an interesting discussion with Professor H. L. Welsh, and to thank him for permission to refer to the work of Gaizauskas and Welsh before its publication.

References

[1] Osberg W. E. and Hornig D. F. *J. Chem. Phys.* 1952 **20**, 1345.
[2] Dows D. A. *J. Chem. Phys.* 1957 **26**, 745.
[3] Giguere P. A. and Harvey K. B. *Spectrochim. Acta* 1957 **9**, 204.
[4] Gaizauskas V. Ph.D. Thesis, Toronto 1955; Welsh H. L. Private communication.

Spectrochimica Acta, 1959, Vol. 13, pp. 311 to 335. Pergamon Press Ltd. Printed in Northern Ireland

Essais d'enregistrements à énergie d'émission contrôlée*

Z. Hainski‡ et P. Herman§

(*Received* 21 *September* 1958)

I. Principes et méthodes

(1) *Justification*

En analyse quantitative par spectrographie d'émission à l'arc la reproductibilité dépend de facteurs qui demeurent incontrôlables malgré les meilleures mises au point. Un simple courant d'air, un défaut de centrage entre électrodes, les variations de l'état physique et de la conductibilité du milieu, provoquent des déplacements de l'arc. En d'autres moments l'arc restera fixé sur la paroi de l'électrode ou en un point déterminé de l'échantillon. D'un essai à l'autre: la chauffe, la formation d'une bille conductrice ou celle d'un revêtement réfractaire évoluent différemment. Ainsi le temps et le degré d'excitation réels de la substance analysée varient, alors que la durée d'illumination et les conditions d'excitation sont rigoureusement reproduites.

D'autre part, l'alignement imparfait de la source lumineuse sur le banc optique, les sauts d'un arc souvent instable, un pan de graphite mal consumé faisant effet d'écran, provoquent des anomalies à l'illumination de la fente.

Finalement on constate que la plaque photographique reçoit des intensités lumineuses parfois très différentes pour des conditions opératoires apparemment les mêmes.

Dès lors on ne peut espérer obtenir une bonne reproductibilité entre les valeurs absolues d'intensités telles que mesurées d'après divers enregistrements d'une émission donnée.

Les possibilités d'application des méthodes semi-quantitatives, dites par apparition de raies, sont ainsi très réduites. En opérant d'après des rapports d'intensités, avec ou sans standard interne, les variations des conditions réelles d'excitation entraîneront encore des écarts de teneurs si les réponses des éléments, à ces variations, ne sont pas exactement les mêmes.

Nous avons tenté de compenser certaines des anomalies citées en appliquant un procédé simple permettant de mesurer l'émission lumineuse et d'enregistrer jusqu'à reproduire une même énergie d'émission du produit ou d'un de ses constituants essentiels.

En essayant d'améliorer la reproductibilité des impressions photographiques nous cherchons à favoriser le développement de méthodes semi-quantitatives rapides ainsi que l'amélioration de méthodes par comparaison dans certains cas défavorables.

---

* Communication présentée au XXI^{ème} Congrès du G.A.M.S. à Paris, en Juin 1958.

‡ Laboratoires de la Société d'Etudes, de Recherches et d'Applications pour l'Industrie, S.E.R.A.I. à Bruxelles.

§ Laboratoire de Recherches Chimiques du Ministère du Congo belge et du Ruanda-Urundi à Tervuren.

(2) *Principe de fonctionnement*

Une portion de l'émission lumineuse de l'arc, captée par une cellule photoélectrique, est transmise à un intégrateur d'énergie. Le courant d'alimentation aux électrodes est coupé automatiquement dès que l'énergie ainsi accumulée atteint une certaine valeur.

L'intégrateur utilisé est l'appareil Quantex, de la firme Baldwin; son fonctionnement est décrit au chapitre suivant (II, 2). Pratiquement, avant d'enregistrer un spectre, on fixe un curseur sur un premier cadran, à la valeur choisie de la graduation, de 0 à 250, en unités conventionnelles. Puis on enregistre sans autre disposition particulière, sinon la cellule placée sur le parcours de l'émission lumineuse. Le fonctionnement de l'intégrateur est suivi grâce au mouvement d'une aiguille sur un second cadran, gradué comme le premier. Cette aiguille se déplace aussitôt que l'arc jaillit, elle parcourt l'échelle jusqu'au zéro, l'arc s'éteint et elle reprend sa position initiale; un nouveau spectre peut être enregistré.

L'opération est donc conduite comme elle le serait en utilisant un "Timer" classique. Cependant, avec le "Quantex", la durée de l'émission, c'est-à-dire de l'enregistrement, va dépendre de diverses variables.

D'abord, celles qui sont liées au comportement de la substance dans l'arc et au centrage de celui-ci vis-à-vis de l'axe optique. En fait, la méthode est mise en oeuvre en vue de compenser l'effet de ces variables.

Ensuite, celles qui dépendent essentiellement de la position de la cellule et de sa sensibilité relativement aux différentes longueurs d'ondes du rayonnement émis par la substance, par un élément standard y ajouté éventuellement et par la matière du support.

La plus grande partie de notre travail a été consacrée à la mise au point de ces conditions opératoires.

(3) *Réalisation*

Les problèmes à résoudre nous semblent pouvoir être résumés comme suit:

(a) La portion de lumière reçue par la cellule doit être représentative de celle également reçue par la plaque photographique.

(b) L'énergie accumulée par l'intégrateur doit provenir uniquement de l'émission de la substance analysée.

Ces deux conditions étant satisfaites l'enregistrement sera poursuivi, automatiquement, jusqu'à reproduire une même intensité d'éclairement de la plaque photographique par le spectre des constituants essentiels. Il peut être prévu, d'après la loi de non réciprocité, qu'à des durées d'illumination trop différentes correspondront cependant des impressions inégales de la couche sensible.

Les diverses réalisations que nous avons essayées sont exposées ci-après:

(a) *Prélèvement de la lumière.* La méthode la plus simple serait de fixer la cellule photoélectrique dans le spectrographe. Elle est à retenir si la méthode est adoptée.

Nous nous sommes heurtés à des difficultés d'exécution dues au prisme Littrow parce que nous ne voulions pas transformer le spectrographe pour de simples

VOL. 13 1958/5

essais. A ce propos, soulignons qu'il importe de limiter la réalisation à des montages faciles faute de quoi il serait préférable d'en revenir à l'enregistrement direct sur cellule.

Pour que les résultats puissent être reproductibles il convient de fixer la position de la cellule vis-à-vis de la source lumineuse et de la mettre à l'abri de toute lumière parasite. Après diverses tentatives nous avons réalisé un dispositif appelé un peu abusivement "collimateur" (voir schéma en II, 3). Posé devant la fente du spectrographe, il est garni d'un miroir réfléchissant la lumière de l'arc vers la cellule, bien isolée de toute autre radiation. Une fente percée au centre et sur toute la hauteur du miroir, permet à une partie de la lumière de l'arc de poursuivre son parcours jusqu'à la fente du spectrographe. Ce système est imparfait car il risque de provoquer l'effet inverse de celui espéré. En effet, un défaut de centrage peut entraîner une illumination accrue de la cellule. C'est pourquoi de nouveaux essais ont été effectués après avoir limité la surface réfléchissante du miroir à deux bandes étroites bordant la fente.

La cellule a ensuite été placée, sans collimateur, à l'endroit de l'écran servant au centrage des électrodes. Elle était entièrement masquée d'une cache, percée d'une fente suivant l'axe vertical. S'il est possible ainsi de faire correspondre l'illumination de la cellule à celle de la plaque, la lumière, qui est captée par une lentille auxiliaire, ne provient plus exactement de la même région de l'arc.

Enfin, pour pouvoir apprécier l'efficacité de ces montages, quelques enregistrements ont été effectués en plaçant simplement la cellule d'un côté quelconque de l'arc.

D'autres dispositifs ont été envisagés, dont un miroir tournant devant la fente et des combinaisons optiques plus complexes. Ils n'ont pas encore été réalisés.

Il est arrivé, au cours des essais que la durée maximum de réponse de l'intégrateur soit plus petite que celle d'une pose photographique normale. Dans ce cas, la quantité de lumière captée par la cellule était limitée en interposant un filtre neutre plus ou moins opaque.

(b) *Sélection des radiations.* Diverses possibilités ont été essayées également pour sélectionner les longueurs d'ondes transmises à l'intégrateur.

Si les électrodes sont façonnées dans la matière analysée, il est acceptable d'opérer avec l'entièreté des radiations émises. Mais avec des substances peu conductrices, supportées par des électrodes en graphite, l'existence d'émissions moléculaires intenses: CO–CN–CO_2, pose un premier problème. Il s'agit de sélectionner une région qui soit pauvre en émissions moléculaires et dans laquelle existe une forte émission d'un élément essentiel du mélange analysé. Autrement, la durée de fonctionnement de l'intégrateur dépend quasi uniquement de l'émission moléculaire du support.

Il n'y a pas grand choix en fait de régions possibles, même en ne tenant compte que de la seule considération précédente. Les plus favorables sont celles qui correspondent aux radiations ultimes de K: $\pm$7700 Å, de Ba: $\pm$5800 Å et de Sr: $\pm$4600 Å. Pour Na, $\pm$5900 Å il existe une bande CN intense et pour Ca: $\pm$6150 Å des bandes de Swan et CN. Quant aux régions de plus petites longueurs d'ondes elles sont infestées d'émissions moléculaires.

Mais il n'est pas que cette seule considération, il faut pouvoir isoler la région

choisie et la cellule doit y être sensible. A cet égard, nos essais ont été limités à 7500 Å, vers les grandes longueurs d'ondes, la sensibilité de la cellule normale livrée avec le Quantex n'allant pas au-delà. Nous avons reçu une seconde cellule à enveloppe de quartz dont la sensibilité maximum est 3700 Å. Il existe une troisième au Cs dont le maximum de sensibilité est 8400 Å, elle n'a pas encore été essayée.

La sensibilité relative des cellules peut aider à sélectionner grossièrement les longueurs d'ondes enregistrées mais d'autres moyens sont nécessaires pour les isoler convenablement.

Nous avons utilisé un petit spectrographe auxiliaire avec écran et fente fixés au châssis, placé avant la cellule. Le centrage est difficile; cette solution est peu pratique.

D'autres essais ont été effectués avec des filtres "Chance" devant la cellule. La sélection reste peu précise même en combinant plusieurs filtres.

Nous avons alors utilisé des filtres interférentiels Iena qui permettent d'isoler une étroite gamme spectrale. La transmission est réduite à 50% à une dizaine de mμ de part et d'autre de la longueur d'onde à transmission maximum. Pour une installation définitive il serait intéressant de monter un filtre Iena continu, à dispersion linéaire de 0,63 mm/mμ et largeur de demi-bande (50% T_{max}) d'environ 10 mμ (1).

Enfin il nous a paru intéressant d'effectuer quelques enregistrements de silicates sur électrodes en métal au lieu de graphite.

(c) *Standard interne.* Les substances à analyser ne contiennent pas souvent un élément essentiel émettant intensément dans une région favorable. Nous avons tenté de pallier cet inconvénient en incorporant un standard interne approprié au produit spectrographié. Non seulement l'élément standard doit répondre aux nécessités d'émission dans une région favorable mais son comportement dans l'arc doit aussi être semblable à celui des éléments essentiels du produit.

Les résultats des différents essais décrits dans ce paragraphe font l'objet de la troisième partie de cet exposé.

(4) *Comparaisons*

L'essai de chaque variante de la méthode a été répété huit à douze fois, toujours en notant la durée de l'enregistrement. D'autre part, pour chaque produit différent, on a effectué une série de spectrographies, en utilisant un "Timer" pendant une durée constante égale à la moyenne de celles observées lors des enregistrements du même produit, avec le Quantex. Il est donc toujours possible de comparer entre eux les résultats des essais à durée constante et à énergie constante.

Notre but étant l'amélioration en reproductibilité des valeurs absolues d'intensités, la comparaison entre séries a porté sur les écarts relatifs moyens et maxima d'un résultat à la moyenne arithmétique des intensités de la série. Pratiquement, une raie caractéristique par constituant a été photométrée sur chaque enregistrement et les résultats traduits en intensités d'après la courbe caractéristique de l'émulsion photographique.

Le grand nombre d'essais effectués et surtout la variété des constituants

VOL. 13 1958/5

enregistrés ne nous ont pas permis de choisir les conditions de travail les plus favorables à chaque cas. Ainsi, la reproductibilité est généralement faible. Rappelons que le caractère comparatif des essais nous préoccupait avant toute autre chose.

Partant d'un produit bien déterminé il sera intéressant de confronter les meilleurs résultats obtenus par application soit de méthodes éprouvées, à durée constante, soit d'une méthode bien mise au point, à énergie constante.

Ceci sera l'objet d'une prochaine publication.

II. Equipement

(1) *Appareillage classique*

Les essais ont été effectués au Laboratoire de Recherches Chimiques du Ministère du Congo belge et du Ruanda-Urundi. L'installation de spectrographie optique d'émission comprend l'équipement suivant:

(a) Un grand spectrographe, Hilger–E742, à systèmes optiques interchangeables dont seul le prisme Littrow Quartz-30° a été utilisé, dans la position assurant l'étalement des spectres, de 2500 à 3600 Å, sur les 25,4 cm de longueur des plaques photographiques. Le règlage de la fente, à 8 μ de largeur et 1 mm de haut, a permis l'enregistrement et l'interprétation faciles de nombreux spectres sur une même plaque. Le banc optique avec porte-électrodes classique, arc placé à 38 cm de la fente, était garni d'une lentille F.S. 15, projetant l'image des électrodes sur l'écran auxiliaire (centrage), et d'un condensateur sphérique:

soit le F.958, focalisant l'image des électrodes sur la fente, distante de 28 cm.

soit le E.1083, à 2 cm de la fente, focalisant l'image sur le système optique du spectrographe.

(b) Une multisource universelle Philips, telle que mise au point par le Professeur Breckpot, permettant un travail reproductible: à l'étincelle, à l'arc intermittent ou enfin à l'arc continu, amorcé par une étincelle unidirectionnelle, entre 2 et 15 Å. Tantôt la source était commandée par une minuterie, tantôt par le Quantex auquel cas les durées d'enregistrements étaient chronométrées par deux observateurs.

(c) Un spectroprojecteur photométrique Fuess dont la lampe de projection de 100 W est alimentée par le réseau, après stabilisation. Devant la cellule est placé un filtre protecteur garni de trois fentes; seule celle de 8 μ de largeur a été employée.

Nous nous sommes servis de plaques Gevaert Scientia 35–D–65 et des bains Rév. G 201, pendant 5 min à $\pm 21°C$, eau acétique 10 sec et Fix. G 301 A–15 min.

Enfin les substances spectrographiées étaient posées sur anode en graphite National Carbide, dans une cuvette cylindrique de 10 × 1,5 mm (int.) et 13 × 1,8 mm (ext.), la contre électrode de 6 mm de ϕ étant taillée en pointe.

Quantex

(1) On suppose la photocellule complètement occultée.

(a) Les points A, B et D sont pratiquement au même potentiel et le micro-ampèremètre est au zéro.

(b) On ferme l'interrupteur S. Condensateur C_1 se charge et les points A et D sont à -20 V par rapport à B. Le micro-ampèremètre dévie vers le $+$.

(c) Si on ouvre S, C ne se décharge pratiquement pas car: la résistance entre A et D est extrêmement élevée; la résistance diélectrique du condensateur C est pratiquement infinie; la photocellule ne conduit pas.

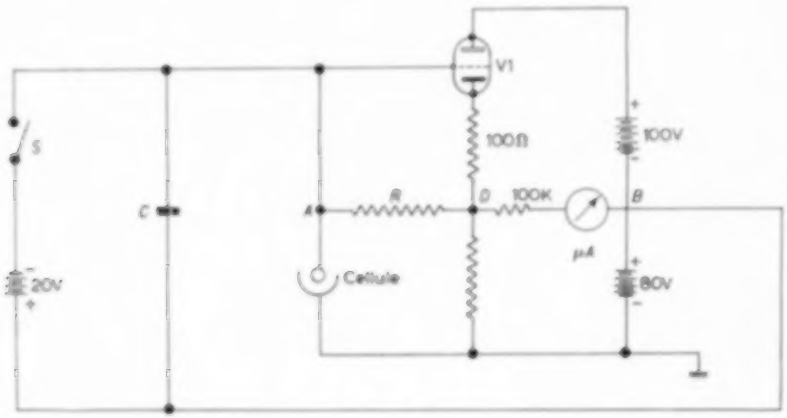

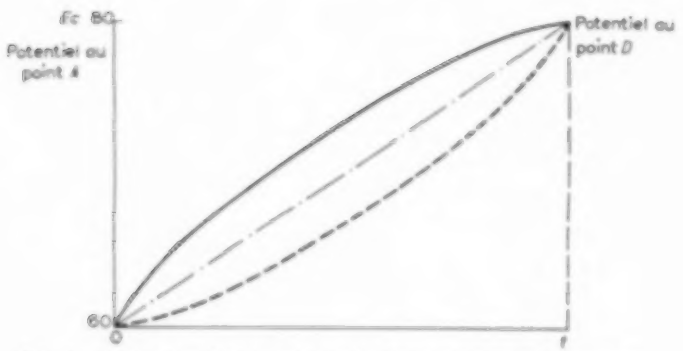

Fig. 2. Schéma simplifié et principe de fonctionnement du Quantex.

(2) On illumine la photocellule. C se décharge par la photocellule et d'autant plus rapidement que l'illumination est intense (courant photo-électrique).

Au fur et à mesure que C se décharge, l'aiguille du micro-ampèremètre revient vers le zéro. Si C se déchargeait suivant une loi linéaire, le potentiel au point D suivrait la courbe en pointillé, à cause de la courbure de la caractéristique (courant/potentiel à la grille) du tube V_1 qui travaille dans une région très négative. La résultante de la courbure de la décharge du condensateur et de la courbure de la caractéristique courant/tension du tube V_1 est une droite. En résumé: la décharge du condensateur au travers de la photocellule, vue sur le micro-ampèremètre est une fonction linéaire du temps. La décharge sera d'autant plus courte que: (1) l'intensité lumineuse incidente sur la photocellule est forte; (2) la tension de charge du condensateur est faible.

En pratique la tension de charge du condensateur est prélevée à partir d'un

VOL. 13 1958/5

OL.
13
8/59

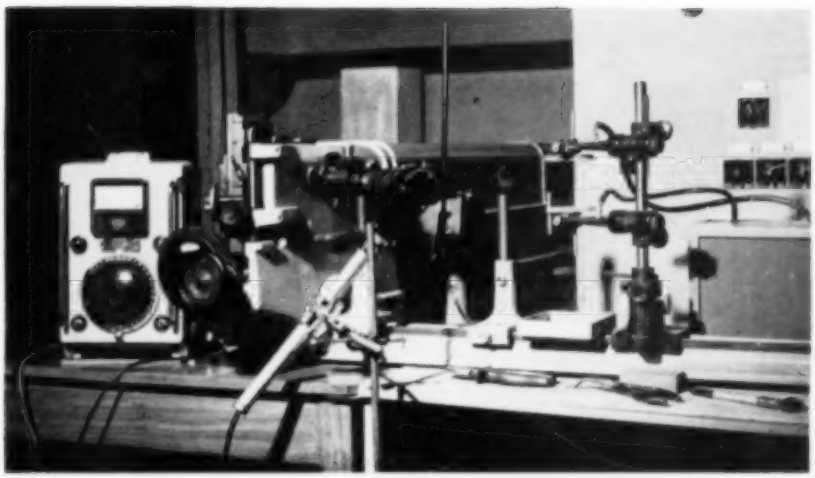

Fig. 1.

VOL.
13
1958/5

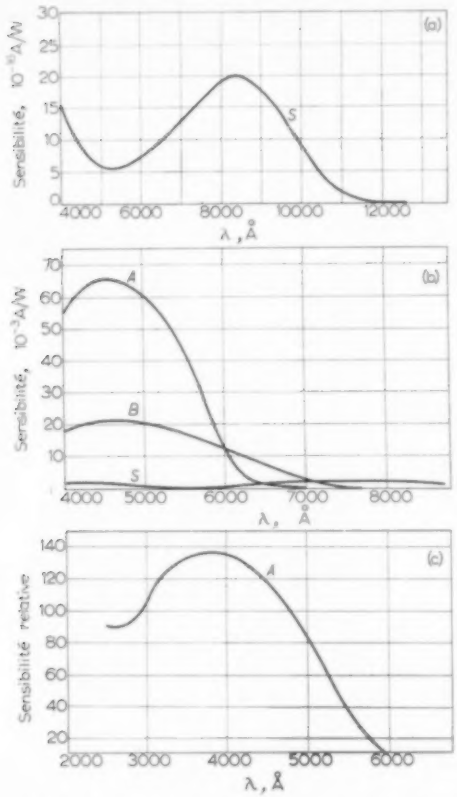

Fig. 3. Courbes de sensibilité spectrale: (a) type S (caesium) cathode; (b) courbe A, type A cathode; courbe B, type B cathode; S, type S (caesium) cathode; (c) type A cathode á enveloppe en quartz.

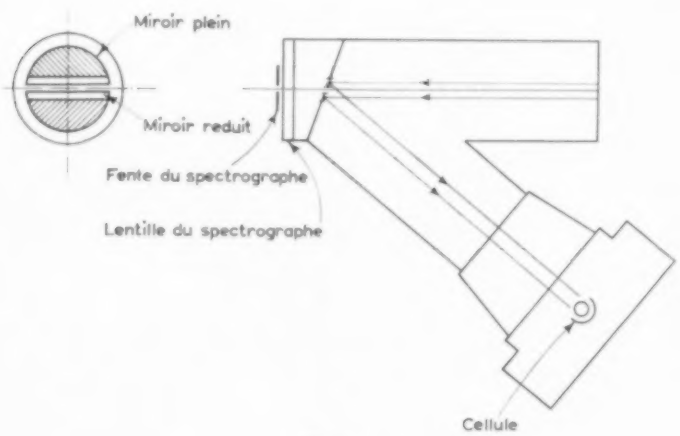

Fig. 4.

potentiomètre R_{16} et le curseur de ce potentiomètre est couplé mécaniquement à un cadran gradué en unités arbitraires. Dès que l'aiguille du micro-ampèremètre atteint le zéro, un relais est déclenché qui coupe la source d'émission.

III. Essais et résultats

(1) *Mode d'illumination*

Essai I

But. Étude préliminaire des conditions de travail.

Résultats. La cellule étant placée aux environs de l'arc la durée de fonctionnement du Quantex est excessivement courte. Elle est influencée par l'entièreté de l'émission lumineuse.

La cellule est alors mise dans un tube ce qui permet de lui faire recueillir la lumière émise seulement par la région visée de l'arc. La durée de fonctionnement du Quantex est ramenée à des valeurs acceptables en plaçant un filtre neutre devant la cellule. Aucune différence n'est constatée, que les essais soient effectués avec ou sans substance sur les électrodes en graphite.

Conclusions. Il y a lieu d'assurer le prélèvement de la lumière et la protection de la cellule; le collimateur à miroir est construit dans ce but. Il faut aussi se débarrasser des émissions moléculaires ce qui est tenté en employant des filtres sélectifs.

Essai II

But. Apprécier l'intensité relative des émissions recueillies par le Quantex, en fonction du filtre placé devant la cellule et des produits spectrographiés.

(a) *Avec filtres d'absorption*

Conditions. Arc continu à 10 A commandé par le Quantex toujours réglé à la même valeur. Les durées sont chronométrées. Pas d'enregistrement photographique. Cellule insérée dans le collimateur.

Résultats. Voir Tableau 1.

Tableau 1

Filtres utilisés "Chance"	λ Transmis en (Å) de - à	T_{max}	Durées fonctionnement Quantex (sec)	
ON. 30 + 0 Gr. 1	4300/6300	5300(12%)	graphite/graphite :	22 et 24
			graphite/graphite + $CaCO_3$:	30 et 29
OY. 3 + 0 Gr. 1	5000/6300	5300(39%)	graphite/graphite:	5
			graphite/graphite + $CaCO_3$:	5
ON. 13 + 0 Gr. 1	4300/6300	5300(37%)	graphite/graphite:	2
			graphite/graphite + $CaCO_3$:	2
id. ON. 16 + OY. 2	5200/5700	5500(9,3%)	graphite/graphite:	13
	et 5900/6300	6000(1,1%)	graphite/graphite + $CaCO_3$:	17
OR. 2 + 0. Gr. 1	4300/6300	5900(1,2%)	graphite/graphite:	30,5
			graphite/graphite + NaCl:	32

VOL. 13 1958/5

Conclusions. Émissions plus intenses avec électrodes en graphite sans substance.

(b) *Filtres interférentiels*

Conditions. Identiques à Tableau 2 mais à intensités variables.

Tableau 2

Int. Arc (A)	Valeur Quantex (unités conventionnelles)	Durées de fonctionnement (sec)		Rapports des durées
		avec filtre DIL. Ca. T_{max}: 6190 Å		
11	50	graphite/graphite:	90	3,0
		graphite/graphite + $CaCO^3$:	30	
		avec filtre DIL. Na T_{max}: 5890 Å		
10	200	graphite/graphite:	252	7,7
		graphite/graphite + Na_2CO_3:	33	
10	200	graphite/graphite (B):	252 (A)	1
9		graphite/graphite/roche silicatée.	292	att. A.
10	200	graphite/graphite:	(252)	7,9
9	200	graph./graph. + roche sil. + 50% de Na_2CO_3	32	att. A.
9	200	graphite/graphite/roche silicatée:	(292)	9,1
		graph./graph. + roche sil. + 50% de Na_2CO_3:	(32)	
9	100	graphite/graphite + roche silicatée:	142	
		graph./graph. + roche sil. + 50% de Na_2CO_3:	(C)	
		premier essai 16 4/10 / deuxième essai 19 2/10	17 8/10	8,0
5 pdt. 1' puis 9	100	laiton/laiton:	auc. div.	
		laiton/laiton + Na_2CO_3:	112	
5	100	fer/fer:	390	

Résultats. (i) Les résultats entre parenthèses sont ceux d'essais précédents.

(ii) A cette mention (roche silicatée) correspond l'échantillon "Flint Clay standard sample no. 97. Bureau of Standards U.S.A." Sa composition, simplifiée est la suivante: 42,9% SiO_2, 38,8% Al_2O_3, 13,3% perte au feu, 0,4% CaO + MgO, 0,9% K_2O + Na_2O, 3,8% autres oxydes (principalement TiO_2 et Fe_2O_3).

(iii) On a modifié la position du miroir entre ces deux essais.

Conclusions. Avec filtre Ca l'enregistrement est trois fois plus rapide quand on ajoute $CaCO_3$ à la roche posée sur graphite et huit à neuf fois plus rapide, avec filtre Na, quand on ajoute Na_2CO_3.

Avec des électrodes en laiton seul le Na ajouté fait fonctionner le Quantex.

(c) *Evolution du phénomène*

En spectrographiant la roche silicatée, à 9 A, sur électrodes en graphite, nous avons chronométré les durées correspondantes au passage de l'aiguille du Quantex (départ à 200) à 150 (82 sec) à 100 (146 sec) et à 0 (292 sec).

Comme on peut le voir ci-contre, l'évolution en fonction du temps se traduit graphiquement par une droite.

En fait, dans d'autres cas, cette évolution se fait par à-coups et même, en présence de standard interne ou d'élément essentiel particulièrement volatils, elle ralentit considérablement après une certaine période.

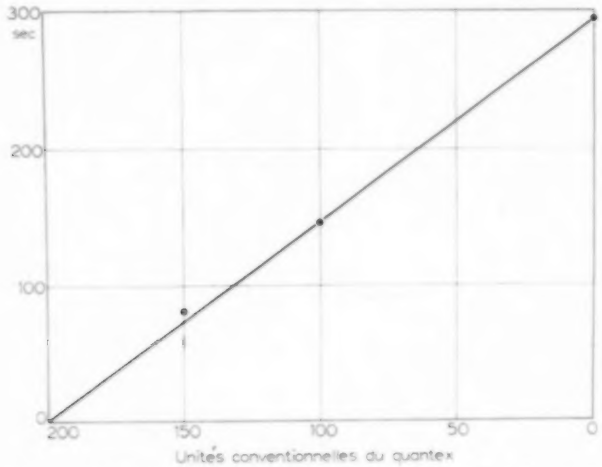

Fig. 5. Réponse du quantex en fonction du temps: roche silicatée sur graphite à 9 A.

C'est pourquoi nous croyons que ce procédé constitue un excellent moyen facile et rapide pour apprécier la régularité d'une émission ou l'effet de l'addition d'un standard interne. Il permet notamment d'éviter les nombreux enregistrements effectués habituellement lors de l'élaboration d'une méthode spectrographique. A ce titre, quelles que soient ses possibilités d'application en analyse systématique, le Quantex nous paraît être un instrument très précieux dans le domaine des études et des mises au point.

Essai III

But. Mettre au point la position de la cellule et l'emploi du collimateur en comparant la reproductibilité des intensités.

Conditions générales. Presque tous les essais sont effectués avec une roche correspondant à l'échantillon: "Argillaceous limestone—standard sample no. 1 A—Bureau of Standards U.S.A." Sa composition simplifiée est la suivante: 41,3 % CaO, 2,2 % MgO, 34,6 % perte au feu, 14,1 % SiO_2, 4,2 % Al_2O_3, 1,1 % $Na_2O + K_2O$, 2,1 % autres oxydes (principalement Fe_2O_3). Chaque essai est enregistré et les raies citées sont photométrées.

(a) *Emploi du collimateur devant la fente*

Conditions particulières. Arc continu à 8 A, roche carbonatée sur électrodes en graphite. Devant la cellule se trouve un filtre neutre ON30: 2,4 % transmission de 3650 à 8000 Å.

Premier cas. Spectres 1–10, dix essais, le collimateur à miroir plein est placé devant la fente. Le Quantex est réglé à 150.

VOL. 13 1958/5

Deuxième cas. Spectres 17–22, six essais, le collimateur est placé sur le côté, la fente du spectrographe est illuminée librement. Le Quantex est réglé à 250.

Résultats. Voir Tableau 3.

Tableau 3. Reproductibilité de la durée des enregistrements

Cas	Durées moyennes (sec)	Ecarts moyens abs. (sec)	Ecarts moyens rel. (%)	Ecarts maximum en +		Ecarts maximum en −	
				sec.	spectre	sec.	spec.
1 collim./fente	27,4	1,2	4,4	1,3	9	4,1	3
2 fente libre	38,9	2,5	6,5	2,9	18 et 20	3,7	17

Reproductibilité des intensités

Radiations	cas	Intensités moyennes	Ecart relatif moyen (%)	Ecart relatif max. (%)	No. des spectres (a) + grande I 9–18 et 20	No. des spectres (a) − grande I 3–17
Si^{I} 2987,65(100/100)	1	24,6	40	103	1(103)	4(34)
	2	59,3	44,4	68	20(68)	17(64)
Al^{I} 2652,49(150R/60)	1	19,4	28	79,5	1(79,5)	10(25,3)
	2	46,4	46,2	72,5	20(72,5)	17(62,5)
Fe^{II} 2621,67(200/400)	1	11,0	24,2	59,0	6(59,0)	4(29,0)
	2	14,7	29,2	48,5	20(48,5)	17(36,8)
Mn 2933,06(80/15)	1	15,5	42,2	146	6(146)	4(42,7)
	2	28,5	54,0	61	18–22(58)	17(61)
Ti^{I} 2646,64(20/15)	1	7,3	16,5	39,7	1(39,7)	7(23,2)
	2	10,0	19,2	35,0	18(35,0)	17(25,0)
Ca^{I} 2721,65(20/2)	1	10,7	33,6	120	1(120)	2(29,9)
	2	18,7	33,8	61	20(61)	17(52,4)
Mg^{I} 3091,08(80/10)	1	28,4	44	141	6(141)	4(41,6)
	2	63,1	49,6	65	18(58,3)	17(65)
Fond continu près 2722	1	3,8	6,3	15,8	5(15,8)	7(10,5)
	2	4,8	6,7	10,4	18(8,3)	22(10,4)

(i) Dans cette colonne sont inscrits les numéros des spectres correspondant aux intensités les plus hautes ou les plus basses; entre parenthèses l'écart relatif entre cette intensité et la moyenne. Les numéros des spectres correspondant aux durées maxima (voir Tableau 3) et minima figurent à l'en-tête.

Conclusions. Avec le collimateur devant la fente, l'écart moyen est plus faible mais l'écart maximum est plus grand. Lorsque le collimateur ne commande pas la fente il y a toujours une relation directe entre la durée de l'enregistrement et l'intensité. Par contre, cette relation n'existe jamais dans le second cas et les résultats diffèrent suivant les radiations.

(b) *Réduction de la surface du miroir, première série*

Conditions particulières. Arc continu 8 A, roche carbonatée sur électrodes en graphite.

Premier cas. Voir 1er cas III (a).

Deuxième cas. Spectres 11–16, six essais. Même position du collimateur qu'en (1) mais miroir réduit à deux bandes bordant la fente. Quantex réglé à 250, filtre ON 31: 26,5 % transmission de 3650 à 8000 Å.

Résultats. Voir Tableau 4.

Tableau 4. Reproductibilité de la durée des enregistrements

Cas	Durées moyennes (sec)	Ecarts moyens abs. (sec)	Ecarts moyens rel. (%)	Ecarts maximum en +		Ecarts maximum en −	
				sec.	spect.	sec.	spect.
premier miroir plein	27,4	1,2	4,4	1,3	9	4,1	3
deuxième miroir réduit	22,1	1,0	4,5	1,1	11	2,0	16

Reproductibilité des intensités

Radiations	Cas	Intensités moyennes	Ecart relatif moyen %	Ecart relatif max %	No. des spectres + grande I 9–11	No. des spectres − grande I 3–16
Si^{I} 2987,67(100/100)	1	24,6	40	103	1(103)	4(34)
	2	16,6	16,6	45,8	14(45,8)	12(22,3)
Al^{I} 2652,49(150R/60)	1	19,4	28	79,5	1(79,5)	10(25,3)
	2	13,1	14,9	36	14(36)	12(19,1)
Fe^{II} 2621,67(220/400)	1	11,0	24,2	59,0	6(59)	4(29)
	2	6,4	13,9	25,0	14(25)	11 et 16 (18,8)
Mn 2933,06(80/15)	1	15,5	42,2	146	6(146)	4(42,7)
	2	8,2	8,0	14,6	12(12,2)	11(14,6)
Ti^{I} 2646,64(20/15)	1	7,3	16,5	39,7	1(39,7)	7(23,3)
	2	5,0	6,4	14,0	14(14)	13(10)
Ca^{I} 2721,65(20/2)	1	10,7	33,6	120	1(120)	2(29,9)
	2	7,3	20,8	45	14(45)	12(21,9)
Mg^{I} 3091,08(80/10)	1	28,4	44	141	6(141)	4(41,6)
	2	16,0	13,9	38	14(38)	12(18,7)
Fond continu	1	3,8	6,3	15,8	5(15,8)	7(10,5)
	2	2,8	6,5	14,3	14(14,3)	16(7,2)

VOL. 13 1958/5

Conclusions. Les écarts sont nettement plus petits quand le miroir du collimateur est réduit; cette fois les écarts maxima sont beaucoup plus faibles vis-à-vis de ceux enregistrés avec fente librement illuminée. Il n'y a aucune relation entre la durée des enregistrements et les intensités des raies. Les anomalies de celles-ci, d'une radiation à l'autre, marquent une tendance à apparaître aux mêmes essais (notamment pour les valeurs en excès).

Tableau 5. Reproductibilité de la durée des enregistrements

Cas	Durées moyennes (sec)	Ecarts moyens abs. (sec)	Ecarts moyens rel. (%)	Ecarts maximum en +		Ecarts maximum en −	
				sec.	spect.	sec.	spect.
premier miroir plein	48,4	8,1	16,8	10,3	38	17,1	34
deuxième miroir réduit	31,2	1,8	5,8	2,9	9	3,1	1

Reproductibilité des intensités

Radiations	Cas	Intensités moyennes	Ecart relatif moyen (%)	Ecart relatif max. (%)	No. des spectres + grande I 38–9	No. des spectres − grande I 34–1
Fe^{I} 2880,58(15/5)	1	11,5	3,4	7,0	37(4,3)	33 et 34
	2	6,6	7,7	13,7	2 et 3(13,7)	5(9,1)
Fe^{II} 2619,08(5/150)	1	10,1	7,5	20,7	35(11,8)	34(20,7)
	2	4,7	8,9	17,0	1 et 2(14,9)	10(17,0)
Mn 3258,41(75/40)	1	6,7	8,3	17,9	37(17,9)	33(10,5)
	2	4,0	13,7	22,5	1(22,5)	9(22,5)
Cr^{II} 2677,16(35/300R)	1	4,4	6,8	20,5	30(9,1)	34(20,5)
	2	1,8	4,9	11,1	6(11,1)	5,7 et 8 (5,6)
Cu^{I} 2618,37(500/100)	1	5,9	7,2	15,3	36(15,3)	34(15,3)
	2	2,4	7,0	12,5	9 et 10 (12,5)	4 et 5 (12,5)
F.C. près 3258	1	2,3	6,9	13,1	32 et 34 (13,1)	38(13,1)
	2	1,7	5,7	17,7	1(17,7)	6,8 et 9 (5,9)

(c) *Réduction de la surface du miroir, deuxième série*

Conditions particulières. Arc continu à 3 A, électrodes en fer, Quantex réglé à 250.

Premier cas. Spectres 30–38, neuf essais. Collimateur à miroir *plein* devant la fente. Cache neutre devant la cellule.

Deuxième cas. Spectres 1–10, dix essais. Collimateur à miroir *réduit* devant la fente.

Résultats. Voir Tableau 5.

Conclusions. Avec petit miroir les reproductibilités sont du même ordre ou moins bonnes. L'effet de la réduction du miroir n'est pas marqué comme il l'était avec les roches. Ceci est assez normal; l'arc beaucoup plus stable ne donne pas lieu à des anomalies accidentelles (voir notamment la diminution de l'écart maximum pour les roches).

A noter une meilleure reproductibilité des durées d'enregistrement et l'absence de relation entre durées et intensités. Enfin, les anomalies d'intensités d'une émission à l'autre ne se produisent pas aux mêmes essais.

(d) *Changement de condensateurs*

Conditions particulières. Roche carbonatée sur graphite, collimateur à miroir réduit sur la fente. Filtre ON 31, 26,5 % transmission, devant la cellule.

Premier cas. Spectres 11–16, six essais, lentille 1083 (image sur système optique). Quantex à 250, arc 8 A.

Deuxième cas. Spectres 18–22 et 26, six essais, lentille 958 (image sur fente). Quantex à 100, arc 3 A.

Résultats. Voir Tableau 6.

Conclusions. Reproductibilité meilleure en durée, du même ordre en intensités; peu ou pas de relations entre intensités et durées. Avec lentille 958, d'une émission à l'autre, les anomalies ne se représentent pas aux mêmes essais. Toujours avec la lentille 958 nous avons effectué deux enregistrements au cours desquels le centrage des électrodes a été déréglé intentionnellement:

le premier: les électrodes sont déplacées de gauche à droite;
le deuxième: idem et de bas en haut.

La comparaison des résultats est présentée comme suit:

d'abord : écarts maxima d'un résultat à la moyenne tels que constatés dans la série précédente de six essais;
ensuite : écarts entre résultats du 1er enregistrement (déréglage latéral) et moyennes de la série de six essais;
enfin : même chose pour résultats du deuxième enregistrement,
écarts relatifs en %

Cas	Si	Al	Fe	Mn	Ca	Mg	F.C.
E_{max} série de 6	21,8	29,2	35,1	34,6	42	39,2	20
Premier enr. dérégl. latéral	21,7	12,5	7,4	15,4	32	5,0	6,7
Deuxième idem en haut	43,5	50	52	56	—	44,0	20

VOL. 13 1958/5

Tableau 6. Reproductibilité de la durée des enregistrements

Cas	Durées moyennes (sec)	Ecarts moyens abs. (sec)	Ecarts moyens rel. (%)	Ecarts maximum en + sec.	Ecarts maximum en + spect.	Ecarts maximum en − sec.	Ecarts maximum en − spect.
premier lentille 1083	22,1	1.0	4,5	1,1	11	2,0	16
deuxième lentille 958	21,8	1,9	8,7	4,7	26	2,7	18

Reproductibilité des intensités

Radiations	Cas	Intensités moyennes	Ecart relatif moyen (%)	Ecart relatif max. (%)	No. des spectres + grande I 11–26	No. des spectres − grande I 16–18
Si^{I} 2987,67	1	16,6	16,6	45,8	14(45–8)	12(22,3)
	2	2,3	13,1	21,8	21(21,8)	18 et 26 (13,1)
Al^{I} 2652,49	1	13,1	14,9	36	14(36)	12(19,1)
	2	2,4	12,5	29,2	21(29,2)	26(20,8)
Fe^{II} 2621,67	1	6,4	13,9	25	14(25)	19 et 16 (18,8)
	2	5,4	18,5	35,1	20(22,2)	21(35,1)
Mn 2933,06	1	8,2	8,0	14,6	12(12,2)	11(14,6)
	2	7,8	20,5	34,6	20(27)	26(34,6)
Ti^{I} 2646,64	1	5,0	6,4	14,4	14(14)	13(10)
	2	trop faible	—	—	—	—
Ca^{I} 2721,65	1	7,3	20,8	45	14(45)	12(21,9)
	2	3,1	29	42	26(38,8)	18(42)
Mg^{I} 30191,08	1	16,0	13,9	38	14(38)	12(18,7)
	2	24,0	17,1	39,2	20(27,1)	18(39,2)
Fond continu	1	2,8	6,5	14,3	14(14,3)	16(7,2)
	2	1,5	10,7	20,0	19,20 et 26 (6,7)	21(20,0)

Les résultats obtenus quand on dérègle latéralement le centrage s'inscrivent dans la série des six essais précédents: il y a compensation. A noter que cet enregistrement a duré 23 sec ce qui est supérieur à la moyenne mais inférieur à la durée d'un des six essais.

Les résultats correspondant à un déréglage de haut en bas sont hors série. Les intensités sont plus basses; de fait, en hauteur le miroir n'a pas été limité aux dimensions de la fente. La compensation est partielle en durée: 28 sec, c'est-à-dire nettement plus que la durée de l'essai le plus long de la série.

(d) *Déplacement de la cellule*

But. Rechercher s'il est possible d'installer la cellule sur l'écran auxiliaire, qui sert à vérifier le centrage des électrodes.

Conditions particulières. Roche carbonatée sur graphite. Lentille 1083. Quantex réglé à 250.

Premier cas. Spectres 11–16, six essais. Collimateur à miroir réduit devant la fente. Filtre ON 31: 26,5 % transmission devant la cellule. Arc 8 A.

Deuxième cas. Spectres 27–32, six essais. Cellule garnie d'un écran à fente, montée devant l'écran servant au centrage, au côte du spectrographe. Arc 5,5 A.

Résultats. Voir Tableau 7.

Tableau 7. Reproductibilité de la durée des enregistrements

Cas	Durées moyennes (sec)	Ecarts moyens abs. (sec)	Ecarts moyens rel. (%)	Ecarts maximum en + sec.	en + spect.	en − sec.	en − spect.
premier collim/fente	22,1	1,0	4,5	1,1	11	2,0	16
deuxième cellule écran	16,4	1,2	7,3	1,7	32	2,3	29

Reproductibilité des intensités

Radiations	Cas	Intensités moyennes	Ecarts relatifs moyens (%)	Ecarts relatifs max. (%)	No. des spectres + grande I 11–32	No. des spectres − grande I 16–29
Si^{I} 2987,67	1	16,6	16,6	45,8	14(45,8)	12(22,3)
	2	5,5	7,0	18,2	28,31(7,3) et : 2	30(18,2)
Al^{I} 2652,49	1	13,1	14,9	36	14(36)	12(19,1)
	2	4,6	11,7	19,6	28(19,6)	30(17,4)
Fe^{II} 2621,67	1	6,4	13,9	25,0	14(25,0)	11 et 16 (18,8)
	2	2,2	23,5	59,0	28(59,0)	27(22,8)
Mn 2933,06	1	8,2	8,0	14,6	12(12,2)	11(14,6)
	2	2,8	21,0	46,5	28(46,5)	29(28,5)
Ca^{I} 2721,65	1	7,3	20,8	45	14(45)	12(21,9)
	2	2,4	15,1	29	28(29)	27,29 et 30(10,7)
Mg^{I} 3091,08	1	16,0	13,9	38	14(38)	12(18,7)
	2	5,5	13,7	36,5	28(36,5)	30(14,6)
Fond continu	1	2,8	6,5	14,3	14(14,3)	16(7,2)
	2	1,3	6,4	7,7	28 et 32 (7,7)	27,29 et 30 (7,7)

VOL. 13 1958/5

Conclusions. Reproductibilité générale à peu près du même ordre. Il n'y a pas de relation entre les durées et les intensités, mais avec la cellule sur écran, les anomalies en excès se reproduisent au même essai pour toutes les radiations mesurées.

Tableau 8

	Ecarts relatifs moyens (%)				Ecarts relatifs maximum (%)			
	Sans. coll.	Coll. mir. plein	Coll. mir. réd.	Cellule sur écran	Sans. coll.	Coll. mir. plein	Coll. mir. réd.	Cellule sur écran
Si	44,4	40	16,6	7,0	68	103	45,8	18,2
Al	46,2	28	14,9	11,7	72,5	79,5	36	19,6
Fe	29,2	24,2	13,9	23,5	48,5	59	25	59
Mn	54	42,2	8,0	21,0	61	146	14,6	46,5
Ti	19,2	16,5	6,4	—	35	39,7	14,0	—
Ca	33,8	33,6	20,8	15,1	61	120	45	29
Mg	49,6	44	13,9	13,7	65	141	38	36,5
F.C.	6,7	6,3	6,5	6,4	10,4	15,8	14,3	7,7
moyennes	35,4	29,3	12,6	14,0	52,7	88,0	29,1	30,9

OL.
13
3/59

Conclusions Générales des Essais III

L'amélioration de la reproductibilité, grâce à l'utilisation d'un collimateur à miroir réduit, est illustrée par les résultats globaux, présentés ci-après, obtenus avec la roche carbonatée.

Dans l'ensemble, vis-à-vis des résultats obtenus sans collimateur, les écarts

Tableau 9. Répétition maximum des anomalies des diverses radiations au même enregistrement (%)

Essais intensités	Cellule libre	Coll. à mir. plein		Coll. à mir. réduit			Cellule sur écran	Moyennes
		roches	Fe	roches		Fe		
				L. 1083	L. 958			
+ forte	50	50	33	88	57	50	100	61
+ faible	88	50	66	50	43	50	71	60
moyennes	69	50	49	69	50	50	85	60

moyens enregistrés avec miroir réduit sont 2,8 fois plus petits et les écarts maxima 1,8 fois. L'illumination peut se faire par lentille F.958 ou par E.1083. Quant à l'installation de la cellule devant l'écran auxiliaire, plus pratique d'ailleurs, ses résultats semblent également favorables.

Il nous a paru intéressant de fournir les résultats détaillés de ces essais car il

est ainsi possible de contrôler divers facteurs en fonction des conditions toutes particulières adoptées.

Le fait qu'il existe ou non une relation entre la durée de fonctionnement du Quantex et l'intensité des radiations sur plaque nous paraît pouvoir être interprété comme suit.

S'il y a corrélation entre l'illumination de la fente et celle de la cellule, une durée plus longue d'enregistrement peut être provoquée soit par une émission générale plus faible, soit par un mauvais éclairement de la fente. Théoriquement

Tableau 10. Reproductibilité des intensités

Radiations	Cas	Intensités moyennes	Ecarts relatifs moyens (%)	Ecarts relatifs max. (%)	No. des spectres	
					+ grande I	− grande I
Fe^{I} 2880-58	1er Q Réd.	6,6	7,7	13,7	2 et 3(13,7)	5(9,1)
	2è Q Pl.	11,5	3,4	7,0	37(4,3)	33/34(7,0)
	3è T	4,3	7,0	11,6	8(11,6)	16/17(11,6)
Fe^{II} 2619,08	1er Q Réd.	4,7	8,9	17,0	1/2(14,9)	10(17)
	2è Q Pl.	10,1	7,5	20,7	35(11,8)	34(20,7)
	3è T	3,0	7,6	16,7	8(16,7)	17(13,4)
Mn 3258,4	1er Q Réd.	4,0	13,7	22,5	1(22,5)	9(22,5)
	2è Q Pl.	6,7	8,3	17,9	37(17,9)	33(10,5)
	3è T	2,0	9,0	25,0	8(25,0)	16/17(15,0)
Cu^{I} 2618,37	1er Q Réd.	2,4	7,0	12,5	9/10(12,5)	4/5(12,5)
	2è Q Pl.	5,9	7,2	15,3	36(15,3)	34(15,3)
	3è T	1,8	2,8	11,2	8/9/12(15,6)	17(11,2)

il y aura compensation et les impressions resteront constantes. Dès lors, les anomalies en intensités d'impression photographique résulteront de l'imperfection du procédé dans son ensemble et elles ne seront pas liées à la durée des enregistrements. Par contre s'il n'y a aucune corrélation (voir deuxième cas de l'essai III, a) une durée plus longue aura comme seule cause une diminution de l'intensité d'émission dans la partie de l'arc qui fait face à la cellule. Si cette diminution ne se produit pas du côté de la fente celle-ci sera exposée plus longtemps à même intensité et l'impression résultante sera plus forte. Le raisonnement inverse peut être tenu dans le cas d'une durée d'enregistrement plus courte.

Logiquement on peut s'attendre à ce qu'une anomalie d'intensité se produise à la même occasion pour toutes les radiations. Comme ce n'est pas le cas nous avons jugé utile d'étudier la distribution des écarts maxima. Le tableau ci-après a été établi comme suit: pour chaque essai on a chiffré le pourcentage le plus grand d'anomalies se répétant au même enregistrement. Ainsi, au 1er cas de l'essai III(a) l'impression la plus intense est constatée pour Si, Al, Ti et Ca, soit quatre éléments à l'enregistrement no. 1, pour Fe, Mn et Mg au no. 6 et pour le fond continu au no. 5. Nous inscrirons une répétition maximum de 50 % (4/8) aux intensités les plus fortes.

VOL. 13 1958/5

On le voit, il n'y a pas de règle à déduire de ces valeurs. Il convient de rappeler, à propos de l'essai avec cellule libre, que les enregistrements 20 et 28 étant de durées égales, mais plus longues que les autres, les plus fortes intensités des diverses radiations se sont partagées également entre ces deux enregistrements. Nécessairement la répétition maximum est de 50 %. A part cet essai, la distribution des anomalies des diverses radiations mesurées n'est donc pas liée au montage.

Tableau 11. Reproductibilité de la durée des enregistrements au premier cas

Cas	Durées moyennes (sec)	Ecarts moyens abs. (sec)	Ecarts moyens rel. (%)	Ecarts maximum en + sec.	Ecarts maximum en + spect.	Ecarts maximum en − sec.	Ecarts maximum en − spect.
Premier Coll.	74,7	5,3	7,1	6,8	28	7,1	27

Reproductibilité des intensités

Radiations	Cas	Intensités moyennes	Ecarts relatifs moyens (%)	Ecarts relatifs max. (%)	No. des spectres + grande I 28	No. des spectres − grande I 27
Cu^{I} 2723,95	1er *Q*	3,7	6,3	13,5	24–25(8,1)	28(13,5)
	2è *T*	2,7	13,8	29,5	23(29,5)	18/20(14,8)
Cu^{I} 2998,38	1er *Q*	4,4	6,5	11,4	24–25(6,8)	28(11,4)
	2è *T*	3,1	17,7	42,0	23(42,0)	18(16,1)
Fe^{II} 2625,67	1er *Q*	5,8	2,6	3,5	23(3,5)	27/28(3,5)
	2è *T*	4,0	10,4	22,5	19(22,5)	22(15,0)
Mn 2794,82	1er *Q*	14,2	5,2	10,6	23(10,6)	26(9,9)
	2è *T*	11,1	20,5	32,5	23(32,5)	18/20(20,8)
Mg^{II} 2795,53	1er *Q*	4,1	21,0	46,5	27(46,5)	24(26,9)
	2è *T*	2,3	14,3	21,8	18/22(17,4)	20(21,8)
Sn 2813,58	1er *Q*	3,3	5,5	6,0	23/24/25 (5,5)	26/28(5,5)
	2è *T*	2,4	16,6	29,2	23(29,2)	20(20,8)

Nous avons supposé que les filtres neutres, posés devant la cellule, pouvaient avoir une influence; rien ne permet de l'affirmer.

Seul un comportement différent des éléments, suivant l'évolution de la combustion, semble en cause. A cet égard, si on relève le nombre de fois que deux ou trois éléments réagissent de la même manière, au même enregistrement, la meilleure répétition est trouvée pour la paire Si–Al. Dans ce cas les anomalies des radiations mesurées concordent 8 fois sur 10. La répétition est de 7/10 pour Si–Ca et Mn–Mg, de 6/10 pour Fe–Mn, Ca–Mg, Al–Ca et Si–Al–Ca.

A noter qu'avec électrode en fer les anomalies des radiations mesurées de Fe^{I} et Fe^{II} ne concordent qu'une fois sur quatre.

Pratiquement retenons que la meilleure solution serait d'illuminer la cellule avec de la lumière prélevée après la fente du spectrographe. A défaut, le miroir du collimateur doit correspondre, le plus étroitement possible, aux dimensions de la fente. Enfin, une autre solution, plus facile, consiste à remplacer l'écran auxiliaire, servant à centrer les électrodes, par la cellule munie d'une fente fine à l'endroit de l'axe vertical de cet écran.

Tableau 12. Reproductibilité des intensités

Radiations	Cas	Intensités moyennes	Ecarts relatifs moyens (%)	Ecarts relatifs max. (%)	No. des spectres	
					+ grande I	− grande I
Si^{I} 2987,67	1er *Q*	16,6	16,6	45,8	14(45,8)	12(22,3)
	2è *T*	9,5	12,2	21,0	6(21)	3(14,8)
Al^{I} 2652,49	1er *Q*	13,1	14,9	36,0	14(36)	12(19,1)
	2è *T*	8,9	14,9	24,8	6(24,8)	4(20,3)
Fe^{II} 2621,67	1er *Q*	6,4	13,9	25,0	14(25)	11/16(18,8)
	2è *T*	4,7	28,0	85,3	6(85,3)	3(29,9)
Mn 2933,06	1er *Q*	8,2	8,0	14,6	12(12,2)	11(14,6)
	2è *T*	5,6	30,0	87,3	6(87,3)	3(32,2)
Ti^{I} 2646,64	1er *Q*	5,0	6,4	14,0	14(14)	13(10)
	2è *T*	3,4	13,5	26,5	5(26,5)	3(26,5)
Ca^{I} 2721,65	1er *Q*	7,3	20,8	45,0	14(45)	12(21,9)
	2è *T*	4,4	20,0	31,8	5(31,8)	3(29,6)
Mg^{I} 3091,08	1er *Q*	16,0	13,9	38,0	13(38)	12(18,7)
	2è *T*	9,1	12,4	30,8	6(30,8)	3(20,9)
Fond continu	1er *Q*	2,8	6,5	14,3	14(14,3)	16,0(7,2)
± 3091	2è *T*	2,1	8,1	19,1	5(9,5)	3(19,1)

(2) *Travail avec électrodes métalliques seules*

Essai IV

But. Comparer la méthode à énergie d'émission contrôlée à celle à durée constante pour l'enregistrement de spectres d'électrodes métalliques, en ce qui concerne la reproductibilité des impressions photographiques.

(a) *Electrodes en fer*

Conditions particulières. Arc continu à 3 A entre électrodes en fer, lentille 1083.

Premier cas. Spectres 1–10, dix essais. Collimateur à *miroir réduit* devant la fente. Quantex réglé à 250, durée moyenne 31 sec (voir III (b)2, deuxième série)

Deuxième cas. Spectres 30–38, neuf essais. Collimateur à *miroir plein*. Quantex 250, durée moyenne 48 sec (voir III, (b)1, deuxième série)

Troisième cas. Spectres 8–17, dix essais. Source raccordée à la minuterie réglée à 31 sec.

Conclusions. On a déjà vu que dans le cas des électrodes en fer les résultats obtenus avec le collimateur à miroir plein sont les meilleurs. Vis-à-vis du travail

VOL. 13 1958/5

à durée constante ils sont du même ordre. A noter qu'à durée constante les anomalies se produisent toujours au même spectre. Au total des écarts moyens valent: 6,6 % (*Q* et *T*) et les écarts maxima: 10,1 % (*Q*) et 10,7 % (*T*).

(b) *Electrodes en laiton*

Conditions particulières. Arc continu à 3 A entre électrodes en laiton. Lentille 1083.

Premier cas. Spectres 23–28, six essais. Collimateur à miroir plein devant la fente. Quantex réglé à 250, durée moyenne 75 sec.

Deuxième cas. Spectres 18–23, six essais. Source raccordée à la minuterie réglée à 75 sec.

Conclusions. Sauf pour Mg, le travail à durée constante est plus reproductible. Au total, Mg y compris, les écarts moyens valent: 7,9 % (*Q*) et 15,6 % (*T*) et les écarts maxima: 15,3 % (*Q*) et 29,6 % (*T*). A énergie contrôlée il n'y a pas de relation entre la durée et l'intensité sinon tendance à ce qu'elles soient en rapport inverse pour les faibles intensités. En effet, dans quatre essais sur six elles correspondent aux enregistrements les plus longs.

La distribution des anomalies entre les divers enregistrements est semblable pour les deux cas.

(3) *Travail sur électrode en graphite*

Essai V

But. Comparer les deux méthodes appliquées à la spectrographie d'une roche sur électrodes en graphite.

Conditions particulières. Arc continu 8 A, roche carbonatée sur électrodes en graphite.

Premier cas. Six essais, à énergie contrôlée, voir essai III, (b)2, deuxième série. durée moyenne: 22,1 sec.

Deuxième cas. Spectres 1–6 (15/58), six essais. Durée constante: 22 sec.

Conclusions. Au total les écarts moyens valent: 12,6 % (*Q*) et 17,5 % (*T*) et les écarts maxima: 29,1 % (*Q*) et 40,8 % (*T*). A énergie constante il y a une répétition maximum, en moyenne de 68,7 % des anomalies dans le même enregistrement, à durée constante: 75 %.

(4) *Travail avec standard interne*

Essai VI

But. Comparer les deux méthodes appliquées à un produit dans lequel est incorporé un standard interne; à énergie contrôlée la cellule est garnie d'un filtre approprié.

(a) *Roche avec* Na *sur graphite*

Conditions particulières. Arc continu 11 A. Roche silicatée (voir note en b essais II, (b)), à laquelle on a ajouté 50 % en poids de Na_2CO_3 c.p.; sur électrodes en graphite.

Tableau 13. Reproductibilité de la durée des enregistrements au premier cas.

Cas	Durées moyennes (sec)	Ecarts moyens abs. (sec)	Ecarts moyens rel. (%)	Ecarts maximum en + sec.	Ecarts maximum en + spect.	Ecarts maximum en − sec.	Ecarts maximum en − spect.
Premier coll. à miroir plein	37,1	4,5	12,1	11,3	3	5,9	7

Reproductibilité des intensités

Radiations	Cas	Intensités moyennes	Ecarts relatifs moyens (%)	Ecarts relatifs max. (%)	No. des spectres + grande I	No. des spectres − grande I
Na^{I} 2593,83/93	1er Q	8,4	5,4	10,7	6(9,5)	5(10,7)
	2è T	7,7	13,0	30,0	18(30,0)	15(28,6)
Li^{I} 3262,61	1er Q	53,6	19,2	39,5	5/6/7(19,4)	8(39,5)
	2é T	41,2	41,5	79,8	18(79,8)	15(66,0)
Si^{I} 2987,67	1er Q	15,7	42,1	101,0	8(101)	5(42,7)
	2é T	21,2	92,8	315,0	14(315)	17(75,0)
Al 2567,99	1er Q	19,4	42,2	116,0	8(116)	5(44,4)
	2è T	37,4	104,0	389,0	14(389)	21(82,0)
Fe^{I} 2936,91	1er Q	15,0	29,3	82,0	7(82)	4(34)
	2è T	14,0	55,9	220,0	14(220)	16(58)
Ti^{I} 2646,64	1er Q	7,4	25,7	50,0	5(50)	5(33,9)
	2è T	12,6	102,0	408,0	14(408)	17(75,5)
Mn 2794,82	1er Q	4,1	24,4	56,2	7(56,2)	3/4/5(26,9)
	2è T	4,5	59,2	235,0	14(235)	17(53,5)
Ca^{II} 3179,33	1er Q	3,9	13,5	41,2	1(41,2)	8(28,2)
	2è T	3,8	30,0	84,3	14(84,3)	15(44,8)
Mg^{II} 2795,53	1er Q	23,5	39,2	83,0	7(83,0)	5(52,0)
	2è T	31,5	97,8	344,0	14(344)	19(73,3)
Cu^{I} 3273,96	1er Q	57,1	8,9	26,6	3/4/7(12,1)	6(26,6)
	2è T	42,9	35,3	49,4	16/18(49,4)	14(49,4)
Cr^{II} 2677,16	1er Q	14,9	2,8	68,5	7(68,5)	8(44,9)
	2è T	10.0	25,0	53,0	18(49,0)	15(53,0)
V^{II} 2952,08	1er Q	2,6	15,8	34,6	7(34,6)	5/8(23,1)
	2è T	2,0	15,5	40,0	14(40,0)	15/17(15,0)
C^{I} 2478,57	1er Q	49,3	35,8	129,0	8(129)	5(39,7)
	2è T	44,0	84,0	157,0	20/21(157)	14/15(45,1)
C^{II} 2836,71	1er Q	2,4	20,4	37,5	8(37,5)	4(29,2)
	2è T	2,7	20,2	40,8	20(37,0)	17(40,8)
F.C. ± 3275	1er Q	5,4	15,6	39,0	7(35.1)	8(39,0)
	2è T	4,0	32,5	72,5	18(72,5)	15/19(50,0)

VOL. 13 1958/5

Premier cas. Spectres 1–8, huit essais. Collimateur à miroir plein devant la fente. Cellule garnie d'un filtre interférentiel Iena DIL. Na, T_{max} 5890 Å. Quantex réglé à 245.

Deuxième cas. Spectres 14 à 20, huit essais. Durée constante: 30 sec.

Conclusions. Pour l'ensemble des dix constituants de la roche l'écart moyen

Tableau 14. Reproductibilité de la durée des enregistrements au 1er cas

Cas	Durées moyennes (sec)	Ecarts moyens abs. (sec)	Ecarts moyens rel. (%)	Ecarts maximum sec.	Ecarts maximum spect.	sec.	spect.
Premier coll. à miroir plein	41,6	12,4	29,8	24,8	2	13,1	4

Reproductibilité des intensités

Radiations	Cas	Intensités moyennes	Ecarts relatifs moyens (%)	Ecarts relatifs max. (%)	No. des spectres + grande I	No. des spectres − grande I
					2	4
Cu^{I} 2723,95	1er Q	7,9	43,0	86,0	2	3
	2è T	7,0	18,5	40,0	10	8
Cu^{I} 2998,38	1er Q	8,4	50,0	97,0	2	3
	2è T	7,5	14,6	32,0	10	8
Na^{I} 2680,44	1er Q	6,8	8,0	14,7	2	3/4
	2è T	5,9	11,0	17,1	9	6

vaut 24,4% à énergie contrôlée et 61,8% à durée constante, l'écart maximum: 65,9 % (Q) et 213,8 % (T).

Les rapports des écarts obtenus à durée constante à ceux obtenus avec Quantex valent successivement:

Rapports des écarts T/Q

	E_{moyens}		E_{max}	Moyennes
Standard interne	Na	2,4	2,8	2,6
Standard interne	Li	2,2	2,0	2,1
Dix éléments de la roche		2,5	3,2	2,8
Idem corrigé		1,3	1,5	1,5
Fond continu		2,1	1,9	2,0

Il n'y a aucune relation entre la durée des enregistrements et l'intensité des spectres.

A énergie constante: au plus, dans 60% des cas pour les fortes intensités et dans 53% des cas pour les faibles, les anomalies des diverses radiations se répètent au même spectre. A durée constante cette répétition se produit dans 53% des cas pour les fortes intensités et dans 47% pour les faibles.

A durée constante, l'enregistrement no. 14 est responsable d'écarts importants des éléments essentiels de la roche, mais le rapport entre ces écarts et ceux du Quantex est à peine supérieur aux rapports calculés pour les radiations non influencées par cet enregistrement.

D'ailleurs, nous avons recalculé les écarts moyens et maxima pour la série à durée constante, après avoir éliminé l'enregistrement no. 14. Le rapport moyen entre les écarts de cette nouvelle série de sept essais, de laquelle a donc été enlevé l'essai le plus mauvais, et la série de huit essais à énergie constante, inchangée, pour Si, Al, Mn, Ti, Fe et Mg, vaut 1,3 (écarts moyens) et 1,5 (écarts maxima).

Pour la seule paire Ti–Mn, les radiations mesurées ont leurs anomalies aux mêmes enregistrements. Il n'y a pas d'autre association remarquable à signaler des multiples combinaisons possibles entre éléments et endroits des anomalies.

A noter la différence qui existe entre C^{I} 2478,57, 400/(400) et C^{II} 2836, 71, -/200 (intensités arc/étincelle d'après Harrisson) tant au point de vue de la reproductibilité que de la répétition des anomalies. La première de ces émissions requiert une tension d'excitation de 7,69 eV (d'après Saidel) et la seconde de 16,34 eV. La première sera donc plus sensible aux fluctuations de l'énergie d'excitation en cours d'enregistrement et ces fluctuations seront mieux compensées par la cellule.

(b) Na *sur laiton*

Conditions particulières. Arc continu 6 A. Na_2CO_3 sur électrodes en laiton.

Premier cas. Spectres 1–4, quatre essais. Collimateur à miroir plein devant la fente. Cellule garnie d'un filtre interférentiel Na. Quantex réglé à 30.

Deuxième cas. Spectres 6–10, cinq essais. Durée constante 40 sec.

Conclusions. Nous avons voulu ajouter cet essai tout particulier puisque le spectre du laiton seul ne fait pas dévier le Quantex quand la cellule est garnie d'un filtre à Na (voir avant-dernier essai II, (b)). Ceci fait que la reproductibilité du Cu est nettement moins bonne à énergie contrôlée.

Celle à durée constante est semblable à ce qui a été enregistré aux essais IV (b). Par contre, Na donne une reproductibilité légèrement meilleure au premier cas. Elle aurait été plus favorable si le collimateur avait été garni d'un petit miroir. C'est à l'effet du miroir plein également que nous attribuons la concordance entre les grandes durées et les intensités.

Notons enfin que ces résultats correspondent à des durées ayant varié de 29,8% en moyenne et de 59,5% au maximum et ce avec un arc 6 A.

IV. Commentaires

Ces essais correspondent à une première réalisation suivant des procédés encore très imparfaits; les résultats sont nettement favorables. En effet, dans plusieurs cas l'application de la méthode permet, dans une large mesure, de compenser les

VOL. 13 1958/5

anomalies dues aux déplacements de l'arc et aux irrégularités graves de l'émission lumineuse. L'analyse semi-quantitative complète est ainsi facilitée et particulièrement en combinant l'emploi du Quantex à celui d'un standard interne bien choisi. De même, dans certains cas particuliers de dosage précis, difficiles à améliorer suivant les procédés classiques, il y a net gain de reproductibilité.

En outre, le Quantex constitue un moyen nouveau, permettant d'augmenter sérieusement les possibilités qui sont habituellement à la disposition du spectrographiste pour étudier les phénomènes qui se produisent dans l'arc et pour la mise au point des méthodes d'enregistrement. Un vaste champ d'applications est donc ouvert. Notre intention est d'étudier spécialement celles relatives à l'analyse complète et rapide des silicates et des cendres végétales.

Les méthodes élaborées feront l'objet d'une prochaine publication.

Remerciements—En terminant, nous tenons à remercier tout particulièrement Monsieur M. Lheureux, Ingénieur Technicien Chimiste au Laboratoire de Recherches chimiques à Tervuren, avec qui nous avons effectué tous les essais. Nous remercions également la firme Baldwin et Monsieur Mathys, son délégué en Belgique, qui ont bien voulu mettre à notre disposition les appareils nous ayant permis de réaliser la présente étude. Nous rendons hommage à nos directions respectives grâce auxquelles nous avons pu effectuer le travail.

L.
3
3/59

Spectrochimica Acta, 1959, Vol. 13, pp. 336 to 337. Pergamon Press Ltd. Printed in Northern Ireland

RESEARCH NOTE

Infra-red absorption spectrum of the nitrite ion in alkali halide solid solutions

(*Received* 11 *October* 1958)

SOLID solutions of sodium, potassium and silver nitrite were prepared in various alkali halide pressed disks [1]. The infra-red absorption spectra only showed one sharp strong band situated near 1270 cm^{-1} due to ν_3, the antisymmetric stretching vibration of the nitrite ion. The weak symmetric stretching and bending vibrations could not be detected because of the low concentrations employed. It appears that the upper limit for solid solution formation is ca. 0·1 per cent (w/w) nitrite in the alkali halides used.

The spectra of the various nitrites pressed into the same alkali halide are identical when solid solution formation occurred.

The values found for ν_3 are given in Table 1.

Table 1. The frequency of the antisymmetric stretching vibration (ν_3) of the nitrite ion in the alkali halides

ν_3 (cm^{-1})	ν_3 (cm^{-1})	ν_3 (cm^{-1})	ν_3 (cm^{-1})
NaCl 1302	KCl 1287	RbCl 1279	CsCl —
NaBr 1279	KBr 1273	RbBr 1267	CsBr —
NaI —	KI 1256	RbI 1250	CsI 1236

No mixed crystal formation was detected in CsCl pellets. The values found for ν_3 of the nitrites are identical with those of the pure nitrites in paraffin oil mulls between rock salt plates.*

The frequency decreases with increasing unit cell dimensions of the alkali halides although the corresponding frequency shifts are much smaller than those recorded for the bifluoride [1] and borohydride [2] ions. However, the changes for the nitrate [1] and borofluoride [3] are also comparatively small.

The frequency of the antisymmetric stretching vibration is plotted against $1/r$, where r is the dimension of the unit cell of the alkali halide in question, in Fig. 1.

It is seen that the frequency of the nitrite ion in the alkali halide solid solutions is not a simple function of the dimensions of the alkali halide unit cell. It depends also on the

* The band is, naturally, much broader than in the case of the solid solutions because of the reflection losses. Care has to be taken when the NaCl plates are rubbed together to form the mull because double decomposition occurs rather easily according to the reaction:

$$MNO_2 + NaCl = NaNO_2 + MCl$$

VOL. 13 1958/5

nature of the matrix ions. This is clearly seen in the case of KBr and RbCl where the dimensions of the unit cells are nearly identical, but where the observed frequencies differ appreciably. This indicates that the observed frequency shift is not a simple function of the Coulomb forces, which depend only on the dimensions of the unit cell.

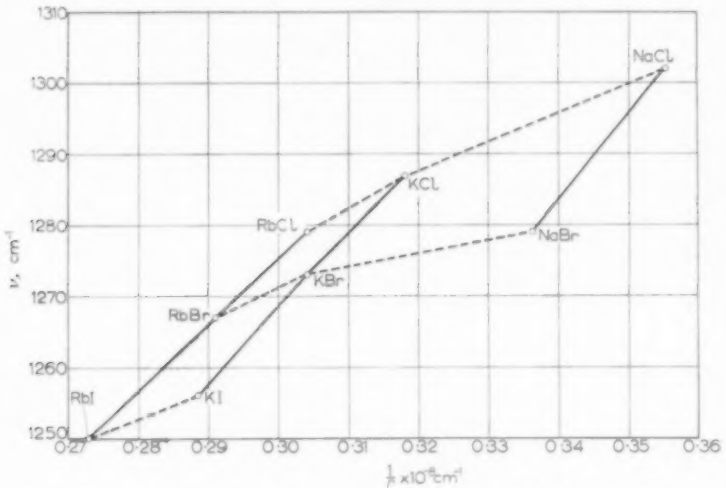

Fig. 1. Frequency of the antisymmetric stretching vibration (ν_3) of the nitrite ion plotted against $1/r$ where r is the dimension of the unit cell of the alkali halide in question.

Acknowledgements—This work is part of the research programme of the Stichting voor Fundamenteel Onderzoek der Materie (Foundation for Fundamental Research of Matter: F.O.M.) and was made possible by financial support from the Nederlandse Organisatie voor Zuiver-Wetenschappelijk Onderzoek (Netherlands Organization for Pure Research: Z.W.O.).

One of us (C. J. H. S.) received a grant from the South African Council for Scientific and Industrial Research.

Laboratory for General and Inorganic Chemistry, University of Amsterdam, Netherlands

J. A. A. Ketelaar
C. J. H. Schutte*
B. L. Schram

References

[1] Ketelaar J. A. A., Haas C. and van der Elsken J., *J. Chem. Phys.* 1956 **24** 624.
[2] Wilkinson, Private communication.
[3] Fulton R. L., University of Amsterdam, Personal communication.

* On leave of absence from Potchefstroom University for C. H. E., South Africa.

Spectrochimica Acta, 1959, Vol. 13, pp. 338 to 339. Pergamon Press Ltd. Printed in Northern Ireland

BOOK REVIEWS

L. KASHA and M. KASHA: **Molecular Electronic Bibliography. Vol. I. Molecular Quantum Mechanics and Molecular Electronic Spectroscopy. Early Workers.** Publishers Press, Tallahassee, 1958. v + 136 pp., $3.50 U.S.A., $4.50 elsewhere.

THIS bibliography should be welcomed by all readers of *Spectrochimica Acta;* this reviewer certainly will make much use of it. Given in approximate chronological order are the author(s), *Chemical Abstracts* reference, title, and journal reference for each of 1540 + papers and books by seventeen investigators which were abstracted in *Chemical Abstracts* through 1955. The investigators selected, with the numbers of their works included, are COULSON (86 +) EYRING (190), HEITLER (70), HERZBERG (119), E. HÜCKEL (35), HUND (49), HYLLERAAS (42 +), JORDON (72), LENNARD-JONES (57 +), LONDON (47), MULLIKEN (149 +), PAULING (250), PENNEY (38), SLATER (75), SPONER (79), TELLER (85) and VAN VLECK (97 +). Just a list of research papers, but what a list!

A necessary condition for inclusion in this volume was publication before 1935; additional volumes are planned. Must such books be priced so much higher elsewhere than in the U.S.A.?

To correct four minor mistakes, the publisher for COULSON's publication 64 is Oxford University Press, MULLIKEN's 23 has a second part beginning on p. 151, for MULLIKEN's 67 the volume is **4**, and MULLIKEN's 129 has a part on pp. 675–713. The reviewer also offers ten addenda:

H. EYRING

191. MUELLER C. R. and EYRING H. Chemical valence forces and binding energy calculations. *Proc. Natl. Acad. Sci.* **38,** 149–54 (1952).

J. E. LENNARD-JONES

58. JONES J. E. (*Chem. Abstr.* **17,** 1742 (1923)) The velocity distribution function and the stresses in a non-uniform rarefied monatomic gas. *Trans. Roy. Soc.* (*London*) **223,** 1–33 (1922).

59. JONES J. E. (*Chem. Abstr.* **17,** 3118 (1923)) Free paths in a non-uniform rarefied gas with an application to the escape of molecules from isothermal atmospheres. *Trans. Cambridge Phil. Soc.* **22,** 535–56 (1923).

60. JONES J. E. (*Chem. Abstr.* **19,** 196 (1925)) The equation of state of a gas. *Proc. Cambridge Phil. Soc.* **22,** 105–12 (1924).

61. JONES J. E. (*Chem. Abstr.* **19,** 756 (1925)) On the determination of molecular fields. I. From variation of viscosity of gas with temperature. II. From equation of state of gas. *Proc. Roy. Soc.* A**106,** 441–62; 463–77 (1924).

62. JONES J. E. (*Chem. Abstr.* **19,** 757 (1925)) On the determination of molecular fields. III. From crystal measurements and kinetic theory data. *Proc. Roy. Soc.* A**106,** 709–18 (1924).

63. JONES J. E. and INGHAM A. E. (*Chem. Abstr.* **19,** 1973 (1925)) On the calculation of certain crystal potential constants, and on the cubic crystal of least potential energy. *Proc. Roy. Soc.* A**107,** 636–53 (1925).

R. S. MULLIKEN

150. MULLIKEN R. S. (*Chem. Abstr.* **43,** 942c (1949)) Molecular orbital method and molecular ionization potentials. *Phys. Rev.* **74,** 736 (1948).

151. MULLIKEN R. S., RIEKE C. A., ORLOFF D. and ORLOFF H. (*Chem. Abstr.* **43,** 7762f) Overlap integrals and chemical binding. *J. Chem. Phys.* **17,** 510 (1949).

152. MULLIKEN R. S. A comparative survey of approximate ground state wave functions of helium atom and hydrogen molecule. *Proc. Natl. Acad. Sci.* **38,** 160–66 (1952).

ROBERT G. PARR

VOL. 13 1958/5

Proceedings of the Colloquium Spectroscopicum Internationale VI, edited by Prof. Dr. W. van Tongeren and F. Freese. Pergamon Press, London, 1957. ix + 663 pp. £8.8.0.

This volume contains most of the papers, their summaries and recorded discussion that were presented at the Sixth International Conference on Spectroscopy at Amsterdam, Holland, in May 1956. The papers which appear in English, French and German describe recent developments in flame, emission, absorption and infra-red spectroscopy. Most of the papers give the results of work performed on problems that arise in applied spectrometry and relatively few papers are devoted to the description of analytical procedures. Since most of the work was done in Euporean laboratories, this book is particularly useful to spectroscopists elsewhere in the world.

J. K. Hurwitz

W. Seith und K. Ruthardt: **Chemische Spektralanalyse,** Funfte Auflage von Walter Rollwagen, Springer, Berlin, 1958. viii + 162 pp. 26 D. M.

The fifth edition of this elementary text-book on emission spectrochemical analysis has been revised by Professor Rollwagen, following Professor Seith's death in 1956. Although it is essentially a student's laboratory manual, describing a series of forty-six experiments or exercises, it introduces details of many of the processes and much of the equipment normally employed in spectrochemical work, and is therefore a useful work of reference with a somewhat German bias. The emphasis throughout is on the fundamental principles of the techniques involved rather than on a detailed training in modern spectrochemical methods.

The first part of the book deals with sources, spectrographs, and photographic and photometric processes, while the second part covers qualitative and quantitative techniques. The full course should give the student a reasonable impression of what spectrochemical analysis can achieve, without making him an experienced spectrochemical analyst, as only eight of the exercises deal with quantitative methods.

The discussion of photometric evaluation is probably the most valuable part of the book, including the use of Seidel functions and the application of background correction. Such subjects as direct reading methods, preparation of metallic sample electrodes and statistical analysis of accuracy are dealt with very briefly, without any experimental instruction, in an appendix. In general, more attention is paid to methods applicable to metals and alloys than to those suitable for non-conducting powders. All the apparatus required in the experiments should be available in a reasonably equipped teaching laboratory, although not necessarily in a specialized analytical department.

A useful feature of this edition is a brief vocabulary of technical terms in German with French and English equivalents, although not all are quite exact, and the first test word sought—Niederspannungsfunke—was not included, although it occurred as a section heading only seven pages earlier.

This small book should serve a useful purpose for non-German speaking workers by providing a readily accessible means of reference to German spectrochemical usage. For German students its value is obvious from the continued demand for new editions.

R. L. Mitchell

Spectrochimica Acta, 1959, Vol. 13, p. 340. Pergamon Press Ltd. Printed in Northern Ireland

Papers to be published in future issues

N. S. Bayliss, A. R. H. Cole and L. H. Little: Solvent effects on the infrared frequency and intensity of the nitrite vibration in aceto-, propio-, benzo- and phthalo-nitriles.

L. A. Duncanson, J. W. Eddell, M. B. Lloyd and W. T. Moore: Diffraction gratings for the measurement of spectra in the 20–100 μ region.

H. F. Hazebroek: Electrostatic sample preparator for infrared spectroscopy of powders.

J. Charette and Ph. Teyssié: Infrared study of heterocyclic compounds carrying a conjugation substituent—I. Isopropenyl Pyrazoles.

A. R. H Cole and F. Macritchie: The energy of a hydrogen bond by infrared spectroscopy.

E. M. Tanner: The infra-red absorption spectra of some α-phenyl-hydrazonoketones and alcohols.

W. E. Ohnesorge and L. B. Rogers: Fluorescence of some metal chelate compounds of 8-quinolinal—I. Effect of metallic ion and solvent on spectrum and quantum yield.

W. E. Ohnesorge and L. B. Rogers: Fluorescence of some metal chelate compounds of 8-quinolinal—II. Effect of acid, alkali and ultraviolet radiation.

G. F. G. Knipe: The spectrographic analysis of antimony and antimony sulphide for heavy metals.

S. J. Cyvin: An approximate method for calculating mean amplitudes of vibration from spectroscopic data—I.

R. R. Patty and R. T. Lagemann: The infrared spectrum and molecular structure of carbonyl-bromofluoride.

Sr. M. Martinette, S. Mizushima and J. V. Quagliano: Infrared absorption spectra of inorganic co-ordination complexes—XIX. N-methylacetamide cadmium (II) chloride.

R. Blinc and D. Hadži: The in-plane normal vibrations of formic acid.

E. Spinner: The vibration spectra and structures of the hydrochlorides of urea, thiourea and acetamide. The basic properties of amides and thioamides.

A. Danielsson, F. Lundgren and G. Sundkvist: The Tape Machine—I. A new tool for spectrochemical analysis.

A. Danielsson and G. Sundkvist: The Tape Machine—II. Applications using different kinds of *iso*formations.

A. Danielsson and G. Sundkvist: The Tape Machine—III. Notes on useful corrections in spectrochemical analysis with the tape technique.

M. Margoshes and B. F. Scribner: The plasma jet as a spectroscopic source.

H. R. Linton and E. R. Nixon: Infrared spectra of methyl and silyl phosphines.

F. F. Bentley and E. F. Wolfarth: Analytical applications of far infrared spectra—II. Spectra-structure correlations for aliphatic and aromatic hydrocarbons in the cesium bromide region.

J. M. Lebas, C. Garrigou-Lagrange and M. L. Josien: Etude comparée des spectres de vibration des dérivés paradisubstitués du benzène—II. Région 3000–3200 cm^{-1}.

K. Fukushima, T. Onishi, T. Shimanouchi and S. I. Mizushima: Assignment of vibration bands of *DL*-alanine.

A. G. Moritz: Hydrogen bonding in N-2-Hydroxybenzylaniline.

L. A. Woodward, J. R. Hall, R. N. Dixon and N. Sheppard: Vibrational spectra of boron trimethyl and the question of internal rotation.

VOL. 13 1958/5

OL.
13
8/59